METEOR-Berichte

Geo Bremen South Atlantic 1996

Cruise No. M34

January 3 – April 15, 1996

Cape Town (South Africa) – Bridgetown (Barbados)

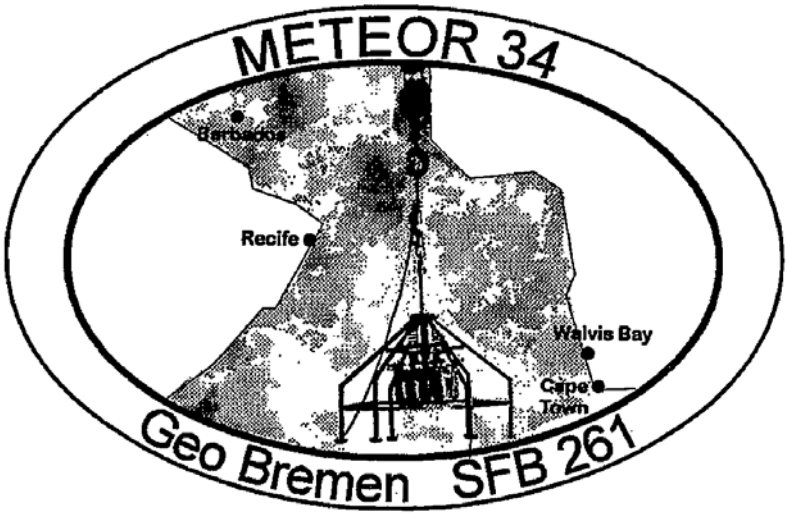

G. Wefer, U. Bleil, H. Schulz, G. Fischer

Editorial Assistance:

Sylvia Kemle-von Mücke
Universität Bremen Fachbereich Geowissenschaften

Leitstelle METEOR
Institut für Meereskunde der Universität Hamburg

1997

The METEOR-Berichte are published at irregular intervals. They are working papers for people who are occupied with the respective expedition and are intended as reports for the funding institutions. The opinions expressed in the METEOR-Berichte are only those of the authors.

The METEOR expeditions are funded by the *Deutsche Forschungsgemeinschaft (DFG)* and the *Bundesministerium für Bildung und Forschung (BMBF)*.

Editor:
DFG-Senatskommission für Ozeanographie
c/o MARUM – Zentrum für Marine Umweltwissenschaften
Universität Bremen
Leobener Strasse
28359 Bremen

Authors:

Prof. Dr. Gerold Wefer
Fachbereich Geowissenschaften
Universität Bremen
Klagenfurter Straße
28359 Bremen / Germany
Telefon: (0421) 218-3389
Telefax: (0421) 218-3116
E-Mail: gwefer@allgeo.uni-bremen.de

Prof. Dr. Ulrich Bleil
Universität Bremen
Fachbereich Geowissenschaften
Postfach 330 440
28334 Bremen / Germany
Telefon +49 421 218 3366
Telefax +49 421 218 7008
E-Mail: bleil@uni-bremen.de

Prof. Dr. Horst D. Schulz
Fachbereich Geowissenschaften
Universität Bremen
Postfach 330 440
28334 Bremen / Germany
Telefon +49 421 218 3393
Telefax +49 421 218 4321
E-Mail: hdschulz@uni-bremen.de

Dr. Gerhard Fischer
Fachbereich Geowissenschaften
Universität Bremen
Klagenfurter Straße
28359 Bremen / Germany
Telefon: (0421) 218-3588
Telefax: (0421) 218-3116
E-Mail: g05f@allgeo.uni-bremen.de

Citation: G. Wefer, U. Bleil, H. Schulz, G. Fischer (1997) Geo Bremen South Atlantic 1996 – Cruise No. M34 – January 3 – April 15, 1996 – Capetown (South Africa) – Bridgetown (Barbados). METEOR-Berichte, M34, 550 pp., DFG-Senatskommission für Ozeanographie, DOI:10.2312/cr_m34

ISSN 2195-8475

METEOR-BERICHTE

97-1

Geo Bremen South Atlantic 1996
Cruise No. 34
3 Januar - 18 February 1996
Volume I

Edited by:
Gerold Wefer, Ulrich Bleil, Horst Schulz, Gerhard Fischer

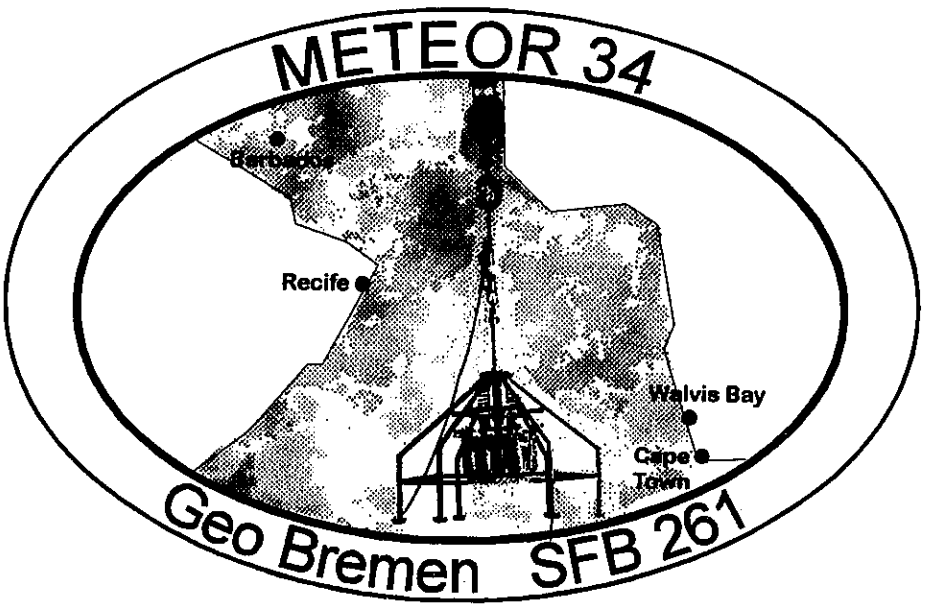

Editorial Assistauce:
Sylvia Kemle-von Mücke

Universität Bremen Fachbereich Geowissenschaften

Leitstelle METEOR
Institut für Meereskunde der Universität Hamburg

1997

Table of Contents
Volume I

Table of Contents
Volume II

Abstract

METEOR expedition M34 was carried out as part of the long-range investigations being pursued under the Special Research Project (SFB) No. 261, for the reconstruction of mass budget and current systems in the South Atlantic during the Late Quaternary. On METEOR cruise M34 samples and data were recovered from the upwelling region off Namibia, the central South Atlantic, and off North Brazil and Barbados. The cruise consisted of four legs, starting in Cape Town on January 3, 1996, and ending at Barbados on April 15, 1996.

During the first leg, seismic and echographic measurements along a series of profiles as well as the sampling of surface sediments in the Cape Basin area was performed. These investigations provide basic information for a deep coring operation by the international *Ocean Drilling Program*, which is being prepared for by the University of Bremen.

The main objective of the second leg was to investigate the biogeochemical processes in sediments of the upwelling area off Namibia. The scientific groups of the Max-Planck-Institut for Marine Microbiology and the Department of Geoscience of the University of Bremen worked closely together to produce new data for the biogeochemical reaction rates.

On the third leg sediment cores were recovered to supplement the sample material of SFB 261 in the central South Atlantic. Core-station profiles were taken from the Angola Basin to the Mid-Ocean-Ridge, and from there into the Brazil Basin. This cruise served also as a continuation of the investigations of the Institut für Meereskunde Kiel and the Traceroceanography of the University of Bremen, which are studying the spread of bottom water on the southern edge of the Brazil Basin, and determining temporal changes in the chlorofluoromethane content of the water, respectively. Three signal generator moorings were also recovered.

The main objective of the fourth leg was to determine the seasonal particle sedimentation in the western equatorial Atlantic and to extend the investigations of sediments from the Amazon Fan and the Ceara Rise.

Zusammenfassung

Für die langfristig angelegten Untersuchungen des SFB 261 zur Rekonstruktion von Stoffhaushalt und Stromsystemen im Südatlantik während des Spätquartär wurde die Meteor-Expedition M34 durchgeführt. Auf der METEOR-Fahrt M34 wurden in größerem Umfang weiteres Proben- und Datenmaterial vor allem aus dem Auftriebsgebiet vor Namibia und aus dem zentralen Südatlantik sowie vor Nordbrasilien und Barbados gewonnen. Die Fahrt bestand aus vier Abschnitten. Sie begann in Kapstadt am 3. Januar 1996 und endete am 15. April 1996 in Barbados.

Während des ersten Fahrtabschnittes wurden seismische und echographische Profilmessungen sowie Beprobungen der Oberflächensedimente im Gebiet des Kap Beckens durchgeführt. Diese Untersuchungen sollen als Grundlage für eine Bohrkampagne des internationalen *Ocean Drilling Program* dienen, die derzeit von der Universität Bremen vorbereitet wird.

Schwerpunkt des zweiten Fahrtabschnittes war die Untersuchung biogeochemischer Prozesse in den Sedimenten des Auftriebgebietes vor Namibia. Eine gemeinsame Beprobung der Sedimente durch die Wissenschaftsgruppe des Max-Planck-Instituts für Marine Mikrobiologie und dem Fachgebiet Geochemie der Universität Bremen diente der Erkundung der biogeochemischen Umsatzraten.

Auf dem dritten Fahrtabschnitt wurden zur Ergänzung des Probenmaterials des SFB 261 Sedimentkerne aus dem zentralen Südatlantik gewonnen. Es wurden Kernstationsprofile vom Angola Becken zum Mittelatlantischen Rücken und von dort in das Brasil Becken bearbeitet. Diese Reise diente auch der Fortsetzung der Untersuchungen des Instituts für Meereskunde, Kiel, und der AG Traceroceanographie der Universität Bremen zur Bodenwasserausbreitung am Südrand des Brasilianischen Beckens bzw. zur Feststellung der zeitlichen Veränderung der FCKW-Gehalte im Wasser. Desweiteren wurden drei Signalgeneratorenverankerungen geborgen.

Der Schwerpunkt des vierten Fahrtabschnittes war die Erfassung der saisonalen Partikelsedimentation im westlichen äquatorialen Atlantik und die Ergänzung und Ausweitung der bisherigen Untersuchungen an Sedimenten des Amazonasfächers und des Ceara Rückens.

1 Research Objectives

The four legs of METEOR cruise no. 34 continue a long-term geoscientific study aimed at reconstructing the mass budget and current systems of the South Atlantic during the late Quaternary. This is a Special Research Project (Sonderforschungsbereich 261 Universität Bremen), finacially supported by the German Science Foundation (Deutsche Forschungsgemeinschaft).

Prime objective of the first leg of RV METEOR cruise M34 was a pre-site survey in various parts of the Cape Basin, which had previously been identified as potential target areas for the reconstruction of the paleoceanographic evolution of the Benguela Current and related upwelling systems from the sedimentary deposits. Seismic and echographic measurements along a series of profiles combined with the sampling of surface sediments will provide further basic information for subsequent deep coring operations by the international Ocean Drilling Program. The University of Bremen is presently charged with the scientific preparation of this project entitled *"Neogene History of the Benguela Current and Angola/Namibia Upwelling System"* which is schedulded to take place as ODP Leg 175 in fall 1997. Additional sample sets to supplement presently ongoing investigations were collected at the South African and Namibian continental margin based on a complete site survey performed in the Angola Basin between 5 and 17° S during Cruise SO 86 of the RV SONNE.

During cruise M34/2 the sediments were sampled at sites along two profiles, one in a south/north direction at a constant water depth of 1300 m, and the other in an east/west direction at increasing water depths, from the African shelf down to the Cape Basin. For cruise M34/2 various geochemical, microbiological and biogeochemical methods were employed to analyze the sediment samples, which were taken with the multicorer and gravity corer. The sampling of the sediments in the upwelling area off Namibia complemented the previous METEOR cruises M6/6 (1988) and M20/2 (1992). A group of various research facilities undertook the investigation of benthic remineralisation rates of organic substance and the intensity of decomposition processes within the sediment.

The area of investigation for leg 3 extends from the Mid-Ocean Ridge at about 30° S into the Brazil Basin. Sediment sampling was performed with a multicorer and gravity corer along two depth profiles, the first going from Angola Basin to the Mid-Atlantic Ridge, the second from there to the Brazil Basin. With this material, the history of surface-water temperature distributions and former positions of the current systems in the South Atlantic will be reconstructed using a variety of methods. Among the most useful parameters are the species distributions and stable oxygen isotope compositions of planktic organisms and surface water temperatures based on the analysis of alkenones. In particular, the changes between glacial and interglacial intervals and their reflection in the species and isotopic compositions of planktic organisms will be investigated.

During the third leg of METEOR cruise 34 the field activities of the Kiel Physical Oceanography group were completed. These are part of the Deep Basin Experiment (DBE) in

a core project of the World Ocean Circulation Experiment (WOCE), which is a major component of the World Climate Research Program. WOCE was established in 1979 by the World Meteorological Organization (WMO) and the International Council of Scientific Unions (ICSU) in cooperation with the UNESCO and the Scientific Committee on Oceanic Research (SCOR). WOCE encompasses planning, implementing and coordinating the global fieldwork and extensive modeling studies. The information gained will provide a better understanding of the ocean's role in climate and its changes resulting from both natural and antropogenic causes.

On the fourth leg of METEOR cruise no. 34 sediments were recovered on two transects perpendicular to the continental shelf and margin off northern Brazil, and east of the Amazon Fan. From these sediments the Late Quaternary surface and deep-water circulation in the western equatorial Atlantic shall be reconstructed.

An attempt was made to determine seasonal particle sedimentation in the important high-production region of the South Atlantic. Towards this goal time-released multiple sample collectors deployed during METEOR cruise 29 were retrieved and redeployed.

Several tracks were run across the North Brazil Current with the ship´s ACDP in order to trace its lateral extent. These tracks were complemented with CTD-profiles of the upper 1000 m.

Tab. 1: Legs and chief scientist of METEOR cruise no. 34

Leg M34/1
3 January 1996 - 26 January 1996
Cape Town/South Africa - Walvis Bay/Namibia
Chief Scientist: Prof. Dr. U. Bleil

Leg M34/2
29 January 1996 - 18 February 1996
Walvis Bay/Namibia - Walvis Bay/Namibia
Chief Scientist: Prof. Dr. H. Schulz

Leg M34/3
21 February 1996 - 17 March 1996
Walvis Bay/Namibia - Recife/Brazil
Chief Scientist: Prof. Dr. G. Wefer

Leg M34/4
19 March 1996 - 15 April 1996
Recife/Brazil - Bridgetown/Barbados
Chief Scientist: Dr. G. Fischer

Coordination:
Prof. Dr. G. Wefer

Master (F.S. METEOR):
Captain H. Bruns

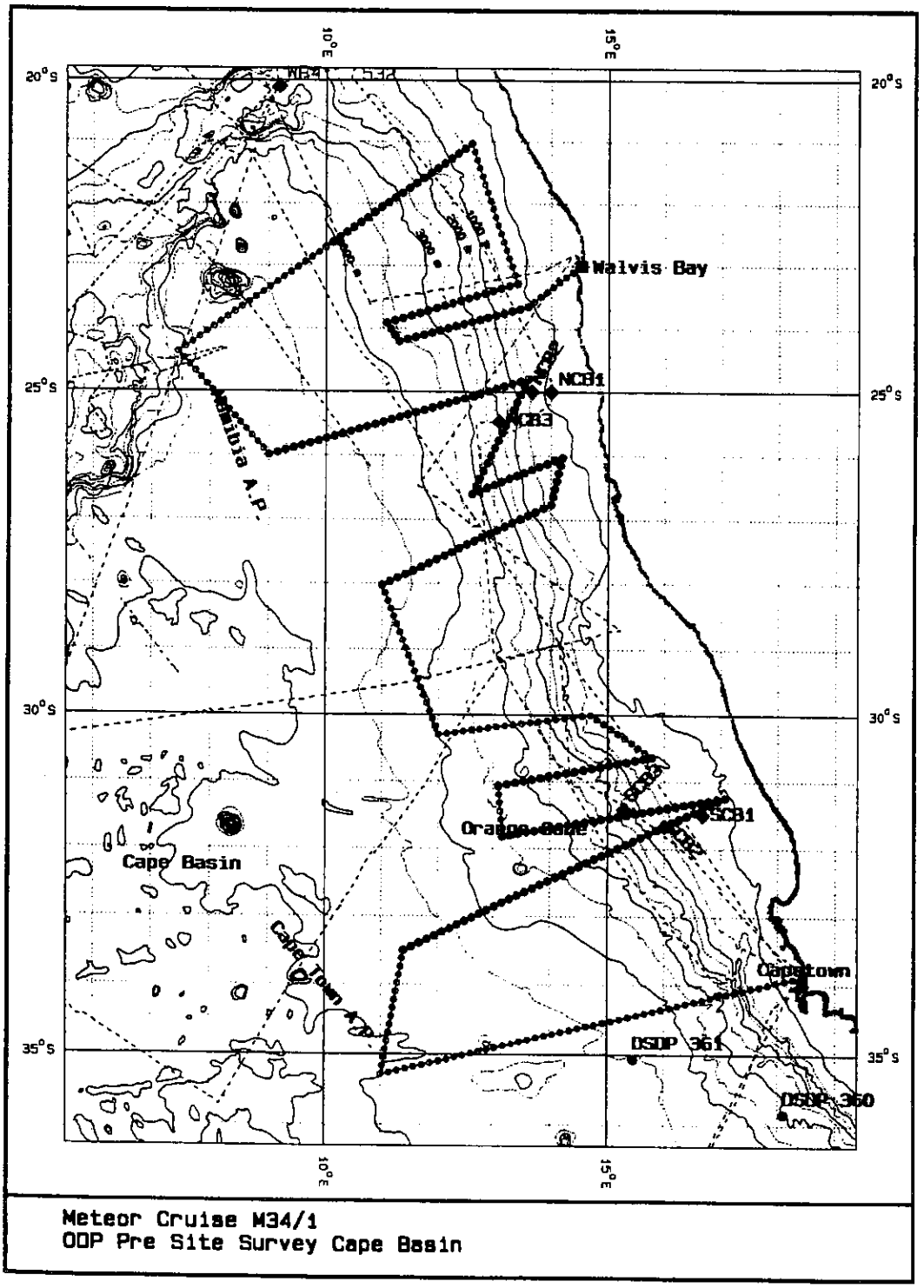

Fig. 1: Cruise track and working areas of Leg M34/1.

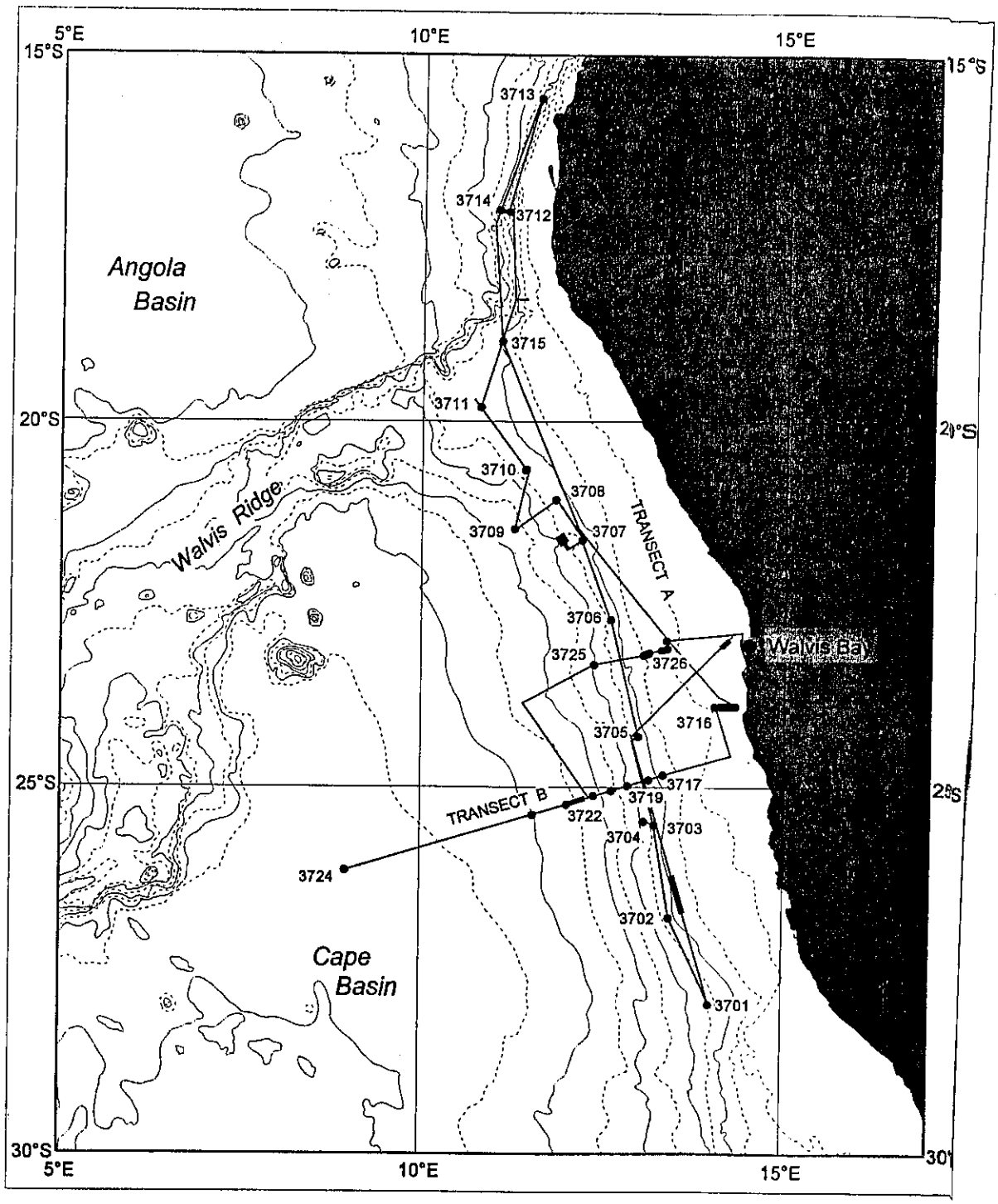

Fig. 2: Ship's track and sampling stations of METEOR cruise M34/2.

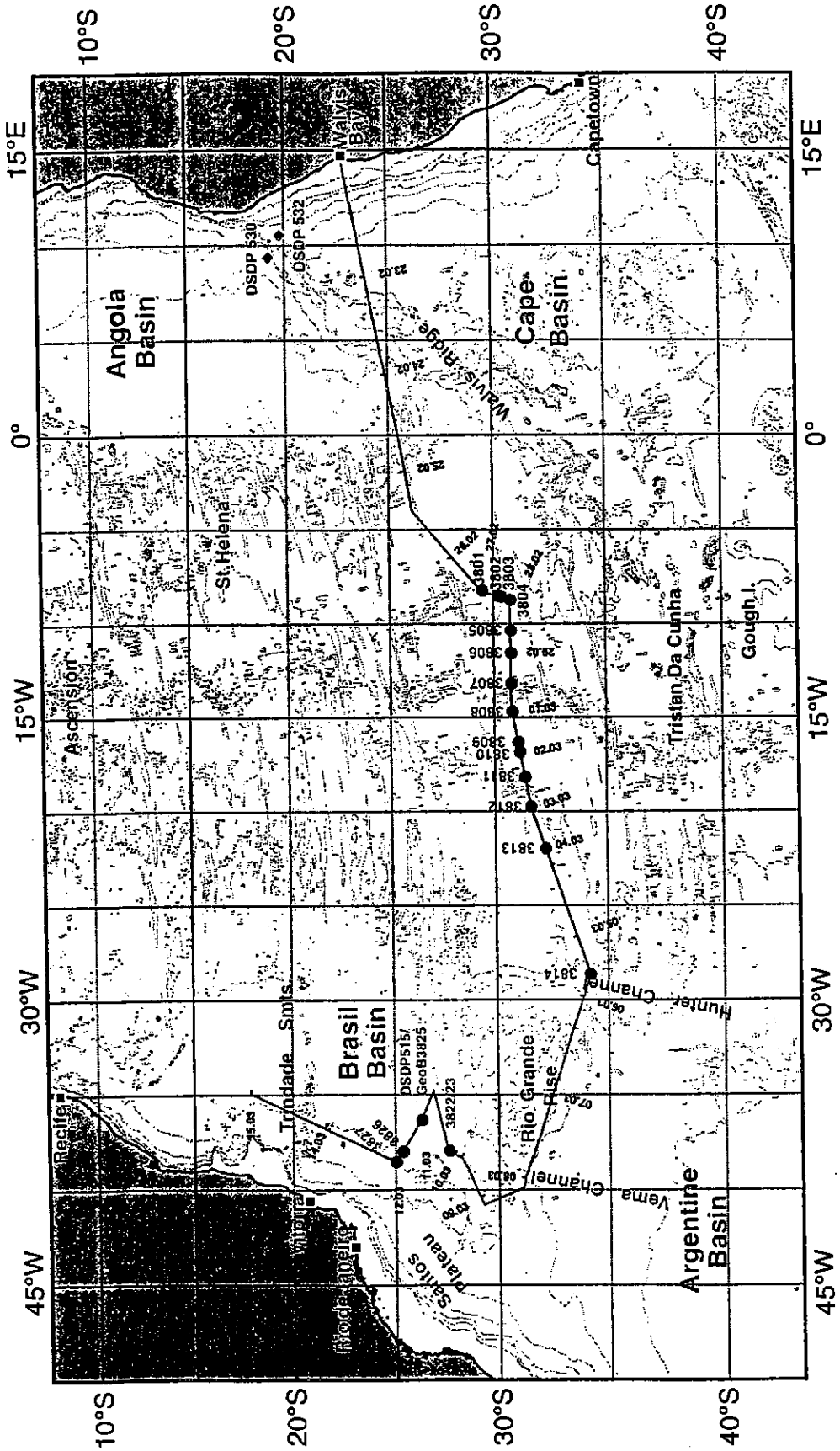

Fig. 3: Ship's track and sampling station of METEOR cruise M34/3.

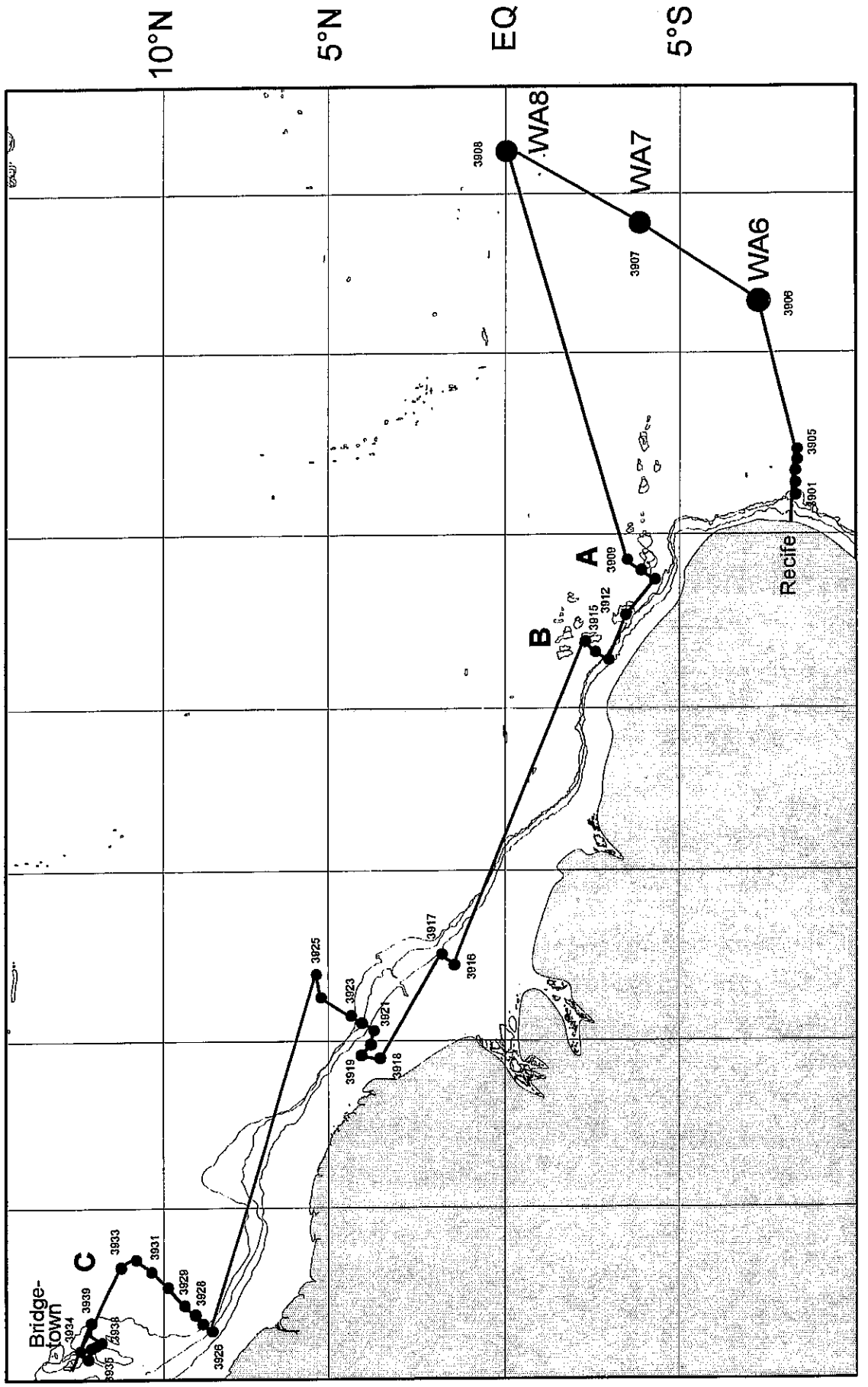

Fig. 4: Cruise track during M34/4. Mooring sites with sediment traps are indicated as black dots. A detailed map of the Amazon area is shown in chapter 5.4.11.4.

2 Participants

Tab. 2: Participants of METEOR cruise no. 34

Leg M 34/1

Name	Speciality	Institute
Bleil, Ulrich, Prof. Dr. (Chief Scientist)	Geophysics	GeoB
Brück, Liane, Technician	Geophysics	GeoB
Frederichs, Thomas, Dr.	Geophysics	GeoB
Haese, Ralph, Dipl.-Geol.	Geochemistry	GeoB
Hensen, Christian, Dipl.-Geol.	Geochemistry	GeoB
Hilgenfeldt, Christian, Dipl.-Ing.	Geophysics	GeoB
Hoek, Ramses, M.Sc.	Paleobiology	GeoB
Hübscher, Christian, Dr.	Geophysics	GeoB
von Lom-Keil, Hanno, Dipl.-Geophys.	Geophysics	GeoB
Janke, André, Dipl.-Geophys.	Geophysics	GeoB
Kreutz, Ralph, Technician	Geology	GeoB
Keenan, John, Consultant	Geophysics	SeisV
Little, Mark, B.Sc.	Geology	UofE
Martens, Hartmut, Dipl.-Ing.	Geophysics	AWI
Rosiak, Uwe, Technician	Geophysics	GeoB
Schmidt, Werner, Student	Geology	GeoB
Schneider, Ralph, Dr.	Geology	GeoB
Segl, Monika, Dr.	Geology	GeoB
Spieß, Volkhard, Prof. Dr.	Geophysics	GeoB
Uenzelmann-Neben, Gabriele, Dr.	Geophysics	AWI
Urbanek, Heike, Technician	Geophysics	GeoB
Zühlsdorff, Lars, Dipl.-Geophys.	Geophysics	GeoB

Leg M 34/2

Name	Speciality	Institute
Benz, Markus, Dipl. Biol.	Microbiology	UKB
Brinckmann, Markus, Technician	Marine Geology	GeoB
Dehning, Klaus, Technician	Marine Geology	GeoB
Dobeneck, Thilo von, Dr.	Geophysics	GeoB
Donner, Barbara, Dr.	Marine Geology	GeoB
Enneking, Karsten, Technician	Geochemistry	GeoB
Ferdelman, Tim, Dr.	Biogeochemistry	MPI
Fossing, Hendrik, Dr.	Biogeochemistry	MPI
Hensen, Christian, Dipl. Geol.	Geochemistry	GeoB
Hilgenfeld, Christian, Technician	Geophysics	GeoB
Hinrichs, Sigrid, Technician	Geochemistry	GeoB
Holby, Ola, Dr.	Biogeochemistry	MPI
Kirst, Georg, Dipl. Geol.	Marine Geology	GeoB
Kostka, Joel, Dr.	Biogeochemistry	MPI
Lom-Keil, Thomas von, Dipl. Geophys.	Geophysics	GeoB
Meyer-Schack, Birgit, Technician	Marine Geology	GeoB
Neumann, Kirsten, Technician	Biogeochemistry	MPI
Niewöhner, Christine, Dipl. Geol.	Geochemistry	GeoB
Ochsenhirt, Wolf-Thilo, Technician	Meteorology	DWD
Petermann, Harald, Dr.	Geophysics	GeoB
Rieß, Wolfgang, Dipl. Biol.	Biogeochemistry	MPI
Schink, Bernhard, Prof. Dr.	Microbiology	UKB
Schulz, Horst D., Prof. Dr. (Chief Scientist)	Geochemistry	GeoB
Siemer, Susanne, Technician	Geochemistry	GeoB
Slickers, Karsten, Technician	Marine Geology	GeoB
Steinmetz, Eckhart, Student	Geochemistry	GeoB
Wagner, Thomas, Dr.	Sedimentology	GeoB

Leg M 34/3

Name	Speciality	Institute
Wefer, Gerold, Prof. Dr. (Chief Scientist)	Marine Geology	GeoB
Buschhoff, Hella, Technician	Marine Geology	GeoB
Carlsen, Dieter, Technician	Marine Physics	IfMK
Dittert, Nicolas, Dipl.-Geol.	Sedimentology	GeoB
Eggerichs, Giesela	Marine Geology	GeoB
Flechsenhar, Kurt, Dr.	Meteorology	DWD
Giese, Martina, Dr.	Marine Geology	GeoB
Gingele, Franz, Dr.	Marine Geology	IOW
Grieger, Björn, Dr.	Modeling	GeoB
Henning, Renate, Technician	Sedimentology	GeoB
Klump, Jens, Dipl.-Geol.	Marine Geology	GeoB
Kuhnert, Henning, Dipl.-Geol.	Marine Geology	GeoB
Lamy, Frank, Dipl.-Geol.	Marine Geology	GeoB
Laser, Bernd, Dipl.-Geophys.	Geophysics	GeoB
Meyer, Anne, Technician	Hist. Geology	GeoB
Niewöhner, Christine, Dipl.-Geol.	Geochemistry	GeoB
Ochsenhirt, Wolf-Thilo, Technician	Meteorology	DWD
Pinck, Andreas, Dipl.-Ing.	Marine Physics	IfMK
Schmidt, Andrea, Dipl.-Geophys.	Geophysics	GeoB
Schmieder, Frank, Dipl.-Geophys.	Geophysics	GeoB
Scholz. Maike, Technician	Marine Geology	GeoB
Schweinsberg, Susanne, Technician	Marine Chemistry	IfMK
Steinmetz, Eckhard, Student	Geochemistry	GeoB
Vanicek, Michael, , Dipl.-Oceanogr.	Marine Physics	IfMK
Willems, Helmut, Prof. Dr.	Hist. Geology	GeoB
Wolff, Tobias, Dipl.-Geol.	Marine Geology	GeoB
Zenk, Walter, Dr.	Marine Physics	IfMK

Leg M34/4

Name	ciality	Institute
Arz, Helge, Dipl. Geol.	Marine Geology	GeoB
Baschek, Burkard, Student	Oceanography	IfM
Bassek, Dieter, Technician	Meteorology	DWD
Costa, Elen	Marine Geology	UFF
Dierssen, Holger	Marine Chemistry	UBBC
Deeken, Aloys	Marine Chemistry	UBBC
Diekamp, Volker	Marine Geology	GeoB
Eichner, Christiane, Dipl. Biol.	Biology	IOW
Engelbrecht, Imke, Student	Marine Geology	GeoB
Enneking, Karsten, Technician	Geochemistry	GeoB
Figueiredo, Alberto, Prof. Dr.	Marine Geology	UFF
Fischer, Gerhard, Dr. (Chief Scientist)	Marine Geology	GeoB
Flechsenhaar, Kurt, Dr.	Meteorology	DWD
Frederichs, Thomas, Dipl. Phys.	Geophysics	GeoB
Freesemann, Angelika, Dipl. Geol.	Micropaleontology	GeoB
Garternicht, Ulf	Oceanography	IfM
Herz, Matthias, von, Dr.	Sedimentology	GeoB
Hübscher, Christian, Dr.	Geophysics	GeoB
Karwath, Britta, Dipl. Geol.	Micropaleontology	GeoB
Kasten, Sabine, Dipl. Geogr.	Geochemistry	GeoB
Kinkel, Hanno, Dipl. Geol.	Sedimentology	GeoB
Kölling, Martin, Dr.	Geochemistry	GeoB
Miesner, Imke, Student	Microbiology	UBBC
Monfort, R. Carlos, von	Observation	Brazil
Ratmeyer, Volker, Dipl. Geol.	Marine Geology	GeoB
Schlünz, Birger, Dipl. Geol.	Marine Geology	GeoB
Schneider, Ralph, Dr.	Marine Geology	GeoB
Schmieder, Frank, Dipl. Geophys.	Geophysics	GeoB
Ruhland, Götz, Dipl. Geol.	Marine Geology	GeoB
Zabel, Matthias, Dr.	Geochemistry	GeoB

Tab. 3: Participating Institutions

AWI	Alfred-Wegener-Institut für Polar- und Meeresforschung Columbus Straße, D - 27568 Bremerhaven, Germany
DWD	Deutscher Wetterdienst - Seewetteramt - Bernhard-Nocht-Straße 76 D - 20359 Hamburg / Germany
GeoB	Fachbereich Geowissenschaften Universität Bremen Klagenfurterstarße D - 28359 Bremen / Germany
IfMK	Institut für Meereskunde an der Universität Kiel Düsternbrooker Weg 20 D - 24105 Kiel / Germany
IOW	Institut für Ostseeforschung Seestr. 15 D - 18119 Warnemünde / Germany
MPI	Max-Planck-Institut für Marine Mikrobiologie Celsiusstraße, D - 28359 Bremen, Germany
SeisV	Seisventures CC Geology & Geophysics Claremont 7735, Cape Town / South Africa
UBBC	Fachbereich 2 - Biologie/Chemie Abt. Marine Mikrobiologie Universität Bremen, Haferwende 12, 28357 Bremen, Germany
UBBC	Fachbereich 2 - Biologie/Chemie Abt. Meereschemie Universität Bremen, Leobenerstr., 28359 Bremen, Germany

UFF	Universidade Federal Fluminense Laboratorio de Geologia Marinha Niteroi, Rio de Janeiro, Brazil
UKB	Fakultät für Biologie der Universität Konstanz Universitätsstraße 10, D - 78464 Konstanz, Germany
UofE	University of Edinburgh Department of Geology and Geophysics West Mains Road, Edinburgh EH9 3JW / Scotland

3 Research Programme

Geophysics

The geophysical program during Leg M34/1 concentrates on seismic and echographic measurements along a number of profiles in the southern Cape Basin and in the northern and southern realm of the Namibian upwelling system as a site survey for the Ocean Drilling Program. A projected preliminary net of lines is supplemented by crossing profiles over potential drill sites which can only be defined according to the actual results during the cruise.

For the echographic profiling the two acoustic devices HYDROSWEEP and PARASOUND permanently installed on RV METEOR are employed. HYDROSWEEP provides detailed records of the surface morphology which, especially on the continental slope, should allow identification of areas where the sedimentation is least affected by episodic mass transport. Depending on the actual lithology, PARASOUND penetrates to between 20 and 150 m into the sediment column and achieves an acoustostratigraphic resolution of the near-surface deposits in the cm range, matching the typical intervals at which gravity core materials are sampled and measured.

High-frequency multichannel digital seismic reflection measurements overcome the inadequacies in depth penetration of the PARASOUND system. The profiles are shot with one or several GI Guns(s) as the seismic source and use a 600 m long streamer. With this instrumental configuration optimum results with regard to resolution and penetration have been obtained during a previous expedition with RV SONNE.

The composite acoustical records are designed to produce the highest possible structural resolution in the uppermost 200 to 500 m of the unconsolidated sediment column. The data sets should yield a complete record of those sedimentary sequences which can be penetrated

without major disturbances by the available ODP techniques (Advanced Hydraulic Piston Corer and Extended Core Barrel Corer).

For the entire gravity core material high resolution logs of the compressional wave velocity, magnetic susceptibility and, as a measure of density and porosity, the electrical conductivity are determined. Among others, these basic physical parameters characterizing the sediment structure and composition will be used for a quantitative interpretation of the ship's digital echographic records by means of synthetic seismograms. In order to retain the *in situ* conditions in optimal approximation, most of the measurements are carried out on board.

The various rock magnetic data sets contain significant variations allowing a determination of paleoclimatic and paleoceanographic fluctuations from the sedimentary sequences. In close cooperation with biostratigraphic and isotope-stratigraphic methods, shorebased paleomagnetic analyses are aimed at establishing a chronostratigraphic framework for the complete sediment material recovered.

Marine Geology

According to the seismoacoustic results, suitable sites for sampling the near-surface sediments are selected. These activities are fully integrated into the schedule of the echographic and seismic profiling program. Following successful experiences on various previous cruises, the combination of HYDROSWEEP and PARASOUND records can serve an excellent basis for the determination and positioning of sampling sites. Sediments are recovered with large box corers, gravity cores and multicorers. The large box corers are subsampled on board for biological / paleontological, sedimentological and geochemical analyses and for measurements of physical properties. The gravity cores and multicorer tubes are described, subsampled and prepared for conservation. Further studies of the sediment materials will be done within the scope of the Special Research Project (Sonderforschungsbereich 261) at Bremen University.

Underway, surface water samples are collected regularly during the cruise with the ship's sea water pump systems for the determination of chlorophyll-a concentrations and to obtain continuous plankton profiles. The biogenic detritus will be investigated for the regional distribution of species assemblages and for their bulk composition to quantify the ratios between opal, organic carbon and carbonate produced by surface water planktic communities. The organic material is analyzed in detail to study stable isotopes and individual organic compounds which can be related to specific phytoplankton organisms.

The regional distribution of the species assemblages of cyst forming dinoflagellates in the surface water, as well as the relation of living and empty cysts through the water column was determined. Sediment samples were taken to study variations of the past associations changing with glacial and interglacial periods.

There is little known about the recent distribution of coccolithophore communities, one of the most important groups of pelagic carbonate-producing organisms. During Leg M34/3 and M34/4, horizontal and vertical sampling profiles were collected to investigate the composition of the coccolithophorid communities in the water column. Surface water samples were collected regularly with the sea water pump while underway to receive a continuous plankton profile. To record the vertical composition of the coccolithophorid communities in the upper 200 m of the water column, samples were taken with Niskin bottles attached to the multinet.

Further samples were collected to study the shifts in carbonate production rates and preservation patterns during glacials and interglacials. Specific attention will be given to carbonate preservation as an indicator for changes in deep-water circulation. In particular, glacial/ interglacial shifts in the extension of NADW and AABW will be determined.

Geochemistry

The sediments were sampled for the studies of the long-term research project SFB 261. Various geochemical, microbiological and biogeochemical methods were used to analyze the sediment samples, which were taken with the multicorer and gravity corer. A group of various research facilities undertook the investigations of benthic remineralisation rates of organic substance and of the intensity of decomposition processes within the sediment. At selected locations different methods for determination of the remineralisation rates were compared. In a sediment region displaying very high benthic activity, a profile perpendicular to the Namibian coast line was laid out covering a range of water depths from the shelf off Namibia down to the deep Cape Basin. This profile should give quantitative information about the processes and about the rates of early diagenesis with respect to latitude (profile south/north) and to water depth (profile east/west).

Oceanography

During the third leg of METEOR cruise 34 the field activities of the Kiel Physical Oceanography group were completed. These are a part of the Deep Basin Experiment (DBE) in a core project of the World Ocean Circulation Experiment (WOCE), which is a major component of the World Climate Research Program. WOCE was established in 1979 by the World Meteorological Organization (WMO) and the International Council of Scientific Unions (ICSU) in cooperation with the UNESCO and the Scientific Committee on Oceanic Research (SCOR). WOCE encompasses planning, implementing and coordinating the global fieldwork and extensive modeling studies. The information gained will provide a better understanding of the ocean's role in climate and its changes resulting from both natural and antropogenic causes. The experimental contribution to WOCE of the Institute für Meereskunde at Kiel university covers the tropical and subtropical South Atlantic. As part of these studies the flow of Antarctic Intermediate Water at 800 m depth on its equatorward drift has been surveyed by RAFOS floats (Fig. 5) and other methods. Research groups from Brazil, France and the USA

are involved in these operations in the Brazil Basin as part of the Deep Basin Experiment. The DBE float contribution from Kiel was started in 1992 and has been successfully implemented since then. During the expedition three moored RAFOS signal generators, required for the navigation of floats, were recovered. In addition, supplementary hydrographic work to fill critical data gaps was performed on the western side of the Mid Atlantic Ridge.

A region of special interest in the global circulation is the western tropical Atlantic, where water exchange across the equator takes place. For the upper ocean, the major flow is from the South Atlantic to the North Atlantic by the North Brazil Current located just off the Brazilian shelf. Still unresolved is the question of how the water transfer towards the Caribbean occurs. Shipboard ADCP measurements are planned to investigate transports and water mass distributions as well as the continuation of the North Brazil Current toward the Caribbean. Several shipboard ADCP sections complemented by hydrographic CTD measurements are planned for sections crossing the North Brazil Current. On four earlier METEOR cruises, direct current observations of the North Brazil Current were carried out off the northeastern tip of Brazil and near the equator for different seasons. During M34/4, sections are planned near the northeastern tip of Brazil, but also further northwest to investigate the strength of the North Brazil Current and the flow toward the Caribbean.

Particle flux and stable isotopes

Seasonal particle sedimentation shall be monitored over several years in the western equatorial Atlantic. For this purpose, three moorings with multi-sample sediment traps were installed on a SW-NE-transect during Meteor cruise 29/3. These moorings were recovered and redeployed. Our objective is to receive information about productivity and export flux in the equatorial upwelling area as well as further south in the more oligotrophic gyre (northern Brazil Basin) on a longer-term basis.

The particles collected will be investigated for species composition of planktonic organisms and their stable isotope composition as well as for the composition of organic matter and terrigenous components. The aim is to identify seasonal variations which play an important role in the formation and interpretation of sediments. The results provide a basis for the reconstruction of paleocurrents and productivity conditions in the South Atlantic from sediment cores. To obtain more information about the amount, size and type of particles suspended in the water column or sinking through it, a high-resolution particle camera will be used preferentially at the sediment trap mooring sites.

The stable isotopes of particulate matter from the water column and from the surface sediments will also be studied in relation to organic matter degradation processes. Samples from the water column (casts/net plankton) and from the surface sediments (multicorer) were taken. The results of this study will be compared to data derived from the Baltic Sea to draw more general conclusions concerning the alteration of the nitrogen isotope signature.

Trace element cycling

The vertical transport of trace elements from the mixed layer until their burial in the sediments will be investigated in conjunction with the sediment-trap program. Several productivity regions typical of the western and the equatorial Atlantic will be studied. In addition to the predominantly rapid-sinking particles in the traps, suspended material will be sampled at the mooring stations during M34/4 by *in situ* pumps and GoFlo bottles. The comparison of the trace element composition in both kinds of particles from the water column with those of the sediments, and their relation to the vertical distribution of dissolved trace elements in the water column are expected to provide important clues to transport and sorption mechanisms as well as to the general geochemical behaviour of these elements in the ocean. Part of the particulate material collected by the *in situ* pumps will be provided for microbiological studies (AG U. Fischer, Microbiology). Particles will be studied with respect to microbiological colonization by bacteria.

4 Narrative of the Cruise

4.1 Leg M 34/1 (U. Bleil)

In the morning of January 3, 1996, the German research vessel METEOR left the port of Cape Town under bright skies to begin the first leg of its 34th cruise. All participants had arrived in South Africa and embarked safely and on time. This was also true for all of the scientific equipment, although 6 of the containers had unexpectedly been shipped from Bremen to Durban. Thanks to the competent support by the ship's agents both in Germany and on site, they finally reached Cape Town after several days of trucking on January 2, a very busy day for everybody unloading and installing the various laboratories.

High-resolution seismic and echographic measurements along a whole series of profiles over the continental margin off South Africa and Namibia were the chief objective of the scientific activities planned in the Cape Basin and on the Walvis Ridge during this cruise. Further processing and interpretation of the data sets will delimit a reliable basis to define appropriate localities for projected deep coring operations of the international Ocean Drilling Program (ODP). Above all, these are aimed at a comprehensive reconstruction of the Benguela Current paleoceanographic evolution from Cenozoic sedimentary deposits. Also on the agenda and integrated into the schedule of geophysical tasks was the sampling of surface sediments at a number of selected sites. Those materials will supplement the large sample collection of a long range special research project (Sonderforschungsbereich) at the University of Bremen. Their shipboard analysis is also intended to prepare for the subsequent cruise M34/2 in the same region. The team of scientists on board included 10 geophysicists, 4 geologists, 2 geochemists and a paleobiologist from the Geoscience Department of the University of Bremen and 2 geophysicists from the Alfred-Wegener-Institute for Polar and Marine

Research, Bremerhaven. As guests, a geologist from the University of Edinburgh and a South African geophysicist (Seisventures, Cape Town) also took part in the cruise.

The first multicorer was successfully secured on deck from about 1000 m water depth approximately 6 hours after departure. At this Station, GeoB 3601 on the upper continental slope southwest off the Cape Peninsula, two attempts with the gravity corer resulted in no recovery, presumably because of very sandy sediments in a depositional environment which is controlled by strong bottom currents. Farther downslope on this transect, at Stations GeoB 3602 and 3603, the gravity corer retrieved more than 10 m of sediments and the multicorer was also very successful on each cast. With completion of this first sequence of station work in the morning of January 4, the geological and geophysical laboratories were prepared for preliminary analysis and measurements of the sample materials.

The ensuing passage to the ODP site survey area in the southern Cape Basin (SCB) was used for an extended echographic profile with the PARASOUND and HYDROSWEEP systems through the abyssal plain crossing coring Site 362 of the former Deep Sea Drilling Project (DSDP). On the second half of this transit route detailed tests of the entire seismic equipment system were performed - without major problems although it was discovered that the streamer needed a new trimming. During the late evening of January 5, the initial about 200 nm long seismic line was begun at around 32.9° S / 13.0° E, and completed in the afternoon of Sunday, January 7. The research work of the first week at sea was favored by pleasant, calm weather conditions, temperatures slightly above 20°C, maximum winds of 5 Bft and a lot of sun.

By Wednesday of the second week, January 10, an additional 7 seismic reflection profiles over a total distance of some 260 nm had been recorded from the abyssal plain up to the South African shelf in the southern Cape Basin. All components of the seismic gear, and in particular the mobile air compressor units, proved to be very reliable throughout this period. Of central interest was the region around the projected ODP drill Site SCB-1, where a dense net of lines provided a perfect overview of an extremely complex sedimentary regime in water depths between 500 and 2000 m. The area is dominated to a large extent by numerous huge mass flow events on the continental slope. A preliminary inspection of selected survey segments on board showed that the recorded data are of almost continuous excellent quality. With their detailed processing it should be possible to prepare a sound proposal for coring strategies in this area allowing the reconstruction of the early paleoceanography of the southern Benguela Current branches.

At two particularly appropriate cross points of the seismic profiles late Quaternary sediment sequences were recovered with the gravity corer from water depths of around 1400 m on January 10 (Stations GeoB 3604 - identical with Site SCB-1 - and GeoB 3605). Despite quite heavy seas, and after several attempts, satisfactory results were also obtained with the multicorer retrieving undisturbed samples of the sediment / water interfaces. Together with the sediment series collected southwest off Cape Town during the first week of the cruise, these core materials document the oceanic component of the Benguela Current for about the

last about 200 000 years outside the present coastal upwelling cells. Preliminary examinations of planktic foraminiferal assemblages yielded 20 to 30 % tropical and subtropical species, while the remaining fraction was composed of groups typical of the South Atlantic surface water gyre and colder water masses from temperate latitudes. Intervals in the sediment columns with an extreme predominance of the polar form *Neogloboquadrina pachyderma* (sin.), as previously observed in the northern realms of the Benguela Upwelling System and on the Walvis Ridge, were not encountered at this point.

Further seismic profiling north of 30° S in the Orange Fan region was abandoned prematurely during the late evening of January 12, because of rapidly deteriorating sea condition. In contrast to the opening days of the cruise, rather adverse weather conditions characterized longer periods of the second week. While at first a high, long-wavelength swell originating from far southern storm systems brought the ship to unpleasant motions, the situation later became dominated by more local sources. This lack of expected southern summer did not affect the altogether very positive morale on board, however.

Seismic and echographic work was resumed in the northern Cape Basin (ODP target area NCB) northwest off Lüderitz on January 13 with much improved weather conditions which prevailed for most of the second half of the cruise. The continental margin was found to be considerably less influenced by massive downslope sediment transport here. After accomplishing the lines between 25 and 26° S in the early morning of January 15, Monday and Tuesday of the third week were devoted to sediment sampling. Both the multicorer and the gravity corer were very effictively employed at around 1800 m water depths at the crossing of the two seismic profiles (Station GeoB 3606 identical with the projected ODP drill Site NCB-2). The dark-greenish to almost black sediments retrieved, which released an intense cloud of H_2S upon opening of the core liners, clearly indicated that an extraordinary geochemical environment had been encountered. Preliminary analyses showed high contents of diatoms and organic matter with only very minor concentrations of carbonate. Such unusual deposits were previously unknown from below 1000 m water depth in the Cape Basin. They closely match the C_{org}-rich oozes recovered from less than 100 m water depth in a small topographic depression at the following Station GeoB 3607 on the inner Namibian shelf. Measurements on board yielded extreme sulfide concentrations in the pore waters of these materials which more or less dominated the laboratory atmospheres for an entire week.

After an overnight transit, the ship's meteorologist had to disembark on Tuesday morning at the port entrance of Walvis Bay for medical treatment ashore. According to information received during the following days his health condition rapidly ameliorated.

The sedimentary deposits sampled later during this same day at the last station (GeoB 3608) of this cruise from about 2000 m water depth parallel core materials previously seen in the northern Cape Basin (METEOR cruise M20/2), with typical greenish to white colors, suggesting carbonate-rich layers with variable amounts of organic matter. The total balance of sediment sampling on cruise M34/1 comprises 64 m of gravity cores (corresponding to 82 % of the core lengths applied) without suffering any losses or deformations. Also 82 % of the

multicorer tubes were filled with sediments up to a maximum height of 59 cm when recovered on deck.

Between Wednesday, January 17 and Wednesday, January 24, 176 hours of final seismic surveys were carried out in the Walvis Basin and on the southeastern Walvis Ridge without any interruptions. With a dense net of lines, apparently continuous and mostly undisturbed Neogene / Tertiary sedimentary sequences with relatively high sedimentation rates could be mapped in these regions. Altogether, measurements were performed along 16 profiles and very promising high-quality data sets were recorded. Crossing profiles were directed both over the proposed ODP drill Site WRY-1 in this area and DSDP Site 532 which was drilled in the early eighties. Coring results available from this latter location should help to integrate the regional seismostratigraphy into a well defined chronological framework.

The remarkably positive geophysical summary of this first leg of METEOR cruise M34 lists more than 123 000 shots on 30 reflection seismic profiles of almost 3000 km (1600 nm) total length. No substantial failures of the compressor systems, the GI-Guns or data acquisition units are to be reported. The only damage was to the streamer due to several leaks.

The scientific program was concluded with a small-scale PARASOUND and HYDROSWEEP survey of a sediment wave field in the neighborhood of DSDP drill Site 532 in the late evening of January, 25. The echographic registrations were also continued on defined courses heading towards Walvis Bay, where RV METEOR arrived in the morning of January 26, safely ending the first leg of its 34th cruise.

4.2 Leg M 34/2 (H. Schulz)

After a pleasant flight on schedule from Bremen and Konstanz via Frankfurt and Windhoek to Walvis Bay, the scientific group for cruise M34/2 arrived on board RV METEOR in the afternoon of January 28, 1996. The difference in temperature from minus 6°C in Bremen to plus 34°C in Windhoek was quite impressive but, exept for Axel Krack from the MPI lander group, everybody felt quite well. He had already had some problems with his left eye when we left Bremen. Now, after the flight, he suffered from a bad headache and was so seriously ill that he had to return to Bremen.

In the morning of the following day the three containers for the cruise were unloaded. The ship´s isotope-container arrived in the early afternoon of the 29th, so that we could leave Walvis Bay at 4 o´clock p.m. As the METEOR left the harbour of Walvis Bay, we received a first impression of the expected biogeochemical processes, since the seawater in the entire inner part of the bay had the whitish-yellow colour of freshly precipitated sulfur. The air was filled with the odor of biogeochemical H_2S.

On the 30th January we reached the most southern location of our south/north profile and started the sampling with the gravity corer and multicorer. Based on the Parasound results of the preceeding cruise M34/1, we were expecting soft and well stratified sediments, and thus good results with both coring devices at a water depth of 1300 meter. This assumption was verified throughout the cruise, as we obtained constantly wonderful results with the multicorer and cores up to a length of 14 meters with the gravity corer.

Also, the landers 'Elinor' and 'Profilur' of the Max-Planck-Institute for Marine Microbiology were successsfully employed and yielded interesting data. At location GeoB 3707 however the corrosion of the magnesium bolt was for 'Profilur' again the last hope for getting it back. In the meantime we carried out a sampling program in the vicinity and waited for a message from the lander via satellite, but eventually we had to continue the cruise with the sampling program along the south/north profile. Some days later we got the message that 'Profilur' had come back to the surface and so we were able to pick it up in good condition on the way back from the north to the beginning of the east/west profile. Since we were quite sure about the cause for the mistake and since it could be repaired, 'Profilur' could be used again together with 'Elinor' on the east/west profile.

The south/north profile at a water depth of 1300 meters from latitudes of 28° S to 17° S yielded very good core material at all 15 locations. The most interesting preliminary result is the fact that at all locations - exept the most southern one - the different productivity indicators always show very high values. At the end of the profile the cruise culminated with the sampling of the new location GeoB 3714, which was exactly the same as the old site GeoB 1023. Here all scientific groups worked intensively together and everybody wanted to have enough core material. So the multicorer had to go down 5 times and the gravity corer 4 times. The core lengths of the gravity corer were always between 12 and 13 meters.

The preliminary results from this location are very exiting. For the sulfate we still see a minor gradient from the bottom water into the sediment, which is even more interesting for the total diffusion/reaction pattern. The sulfide profile in porewater fits well with the sulfate profile, and both fit well with the methane profile, which gives us the reaction rates between sulfate and methane for the first time in deep-sea sediments. Also very exiting was the discover of bacteria slime with many needle-shaped bacteria with frequent (sulfur?)-enclusures close to the depth of sulfate reduction in the core. Many samples - together with many expectations - found their ways into the laboratories in Bremen and Konstanz.

The east/west profile was begun on February 11, 1996 at a latitude of 25° S from the shelf down to the deep-sea of the Cape Basin. After a few hours of searching for the megabacteria *Thioploca* on the shelf, we took samples at the core locations at water depths of 700, 1300, 2000, 2500, 3000, 3500, 4000 and 4800 meters. At all locations we again got very good cores from the multicorer and from the gravity corer, with core lengths between 12 and 13 meters.

At the two locations at 1300 m (GeoB 3718) and at 3000 m water depths (GeoB 3721) again all scientific groups worked together with their different methods at the same core material. At both locations both landers could again be used. Especially important was the use of 'Elinor' at GeoB 3721 (3000 m), where it had an extended stay of 60 hours of measurement on the sea floor, while in the meantime the other locations deeper in the Cape Basin were sampled. A PARASOUND/HYDROSWEEP profile and again a few hours of searching for *Thioploca* ended the scientific program.

On February 18, 1996, the METEOR returned to Walvis Bay, completing a cruise during which we found answers to many open questions concerning the processes of early diagenesis, and where we obtained new data for different biogeochemical reaction rates. Many scientific data and many valuable samples from the sediments of the Namibia upwelling were brought to Bremen and to Konstanz and will lead to many interesting results in the future.

4.3 Leg M 34/3 (G. Wefer)

METEOR departed Walvis Bay on Wednesday, February 21, 1996 at 20:00, beginning the 3rd leg of the 34th cruise. Departure was delayed by ca. 12 hours due to the late arrival of a participant because of bad weather conditions in Germany and the loading of a container with equipment. On board were 19 colleagues from the Geosciences Department of Bremen University, two members of the Sea Weather office in Hamburg, five colleagues from the Institute of Marine Sciences at the University of Kiel and one scientist from the Institute of Baltic Sea Research at Rostock-Warnemünde. On the way to the first station, PARASOUND and HYDROSWEEP were employed and a probe system for continual measurement of CO_2 pressure in the surface water and air was installed. Additionally, the sampling of plankton from the ship's membrane pump system was started. Furthermore, sediment cores from the Namibia/Angola upwelling area, taken during cruise M34/2 were opened, described, measured and subsampled for more sophisticated analysis at Bremen.

The first station on the east side (Angola Basin) of the Mid-Atlantic Ridge was reached on February 26 (Fig. 3). The objective of the transect perpendicular to the Mid-Atlantic Ridge was to reconstruct the current system and productivity of the water masses north of the subtropical convergence zone. Sediments were sampled at 13 stations with multicorer and gravity corer in water depths between 2500 m and 4500 m. Coring was supplemented by water sampling with CTD/Rosette for determination of species composition of dinoflagellates and coccolithophorids. Plankton was collected using a multiple closing net.

Initial results of the sediment analysis indicate that the 2 to 10 m long cores were collected with little disturbance of the recovered material. Core descriptions and initial stratigraphic analysis using color reflectance and magnetic susceptibility measurements show continuous sedimentation in most cores and normal sedimentation rates for a carbonate-dominated

subtropical oligotrophic area. After six days the sampling program on the transect perpendicular to the Mid-Atlantic Ridge extending from the Angola Basin into the Brazil Basin was completed and the first mooring station was reached on March 5.

On the morning of March 5 the K02 mooring with RAFOS signal generator was recovered. The mooring was about 3.5 km long and had been deployed more than two years earlier. At this station water was collected at various depths and plankton was sampled with a multiple closing net from different water depths. A sediment core was also retrieved here.

The next destination was a mooring which had been deployed south of the Vema Channel 3 years and 3 months before. On the way sampling activities at 3 CTD/Rosette stations were accomplished in the night of March 7 to 8. On the morning of March 8 the mooring with the signal generator was recovered within about 2 hours. The next stops were to collect sediment cores at the northern mouth of the Vema Channel. The objective was to obtain sediments with higher sedimentation rates, which were expected in drift sediments deposited due to a decrease in current speed of the Antarctic Bottom Water. After taking two cores the third mooring station was visited.

On morning of March 11 mooring K3 was recovered, consisting of a RAFOS signal generator and three current meters positioned in different water masses. During that night and the following day three cores were taken on the continental margin in water depths between 4200 and 3800 m. Additionally, water samples and plankton samples were taken. At approximately 22:00 on March 12 the journey to Recife got under way. On the way three water stations were sampled for studies of dinoflagellate and coccolithophorid distribution. On March 15 the 10th anniversary of the METEOR was celebrated with a deck party. The third leg of cruise 34 ended with the arrival at Recife on March 15 at 8:00.

4.4 Leg M 34/4 (G. Fischer)

RV METEOR departed from Recife, Brazil, on Tuesday, March 19, 1996 at 16:00 local time with a delay of about 8 hours due to the late arrival of some of the scientific and ship's equipment. In addition to two meteorolgists, 28 scientist were on board, most of whom were from the Geoscience Department of the University of Bremen. Other groups were from the Marine Chemistry and the Marine Microbiology Department of the University of Bremen, from the „Institut für Ostseeforschung" at Warnemünde and the „Institut für Meereskunde" at Kiel. Two marine geologists from the Universidade Federal Fluminense, Niteroi, Rio de Janeiro, were also on board, as was one observer from Brazil.

After leaving the 12 sm zone, we began with ADCP profiling and a first CTD profile (5 stations) to study water mass distribution and transport in the North Brazil Current. We also

started PARASOUND and HYDROSWEEP profiling to obtain information about ocean floor topography and the acoustic character of the sediment. Later, plankton material was taken from the ship's membrane pump to measure chlorophyll, study dinoflagellate and coccolithophore communities and to perform microbial studies. On March 21, we recovered the first sediment trap mooring (WA6, Fig. 4) deployed in August 1994 with two traps and one current meter; all instruments had worked perfectly. The two complete series of trap samples showed low seasonality and low fluxes in the oligotrophic gyre of the Brazil Basin. At this site, we further carried out water sampling with *in situ* pumps, GoFlo and Niskin water bottles and a mulitnet. After the deployment of a mooring with a similar configuration as WA6, we employed the multicorer to obtain surface sediments.

After completing work at this station, we continued our cruise track 260 sm to the northeast and reached the second sediment trap mooring site WA7 on March 23. We successfully recovered the entire array and obtained two more complete series of samples recording particle flux over the last 19 months. As expected, particle fluxes at this site located between the oligotrophic gyre and the equatorial upwelling region, were significantly higher than at the WA6 site. Later, we carried out an intensive water column sampling program using similar equipment as described for the first mooring site. In addition, we used a high-resolution particle camera in the profiling mode. In the early morning of March 24, we redeployed the mooring with a similar configuration and proceeded 270 sm to the third mooring site located close to the equator. We reached this location on March 25, and commenced with a sampling program of the water column. Early on March 26, we recovered the mooring WA8 completely and redeployed it shortly afterwards. After sampling the sediment surface with the multicorer, we continued our cruise to the southwest to begin with the first geological profile, A, located off the coast of northern Brazil between Fortaleza and Natal. We reached the starting point of transect A on Friday, March 29. Based on PARASOUND and HYDROSWEEP records, coring sites between 3100 m and about 830 m were chosen along the NE-SW transect A. Suitable sites were difficult to find due to extensive slumping structures and a rough bottom topography with channel systems at the continental margin. The shallowest site at 830 m corresponded to a coring site chosen by the JOPS expedition (core 3129) conducted with „RV VIKTOR HENSEN" in early 1995. We then proceeded to the beginning of the second NE-SW transect B located about 150 miles further to the west. Before commencing this profile, we cored another site in 770 m water depth (JOPS, core 3104). Along transect B, we sampled three sites with multicorer and gravity corer between 2200 and 3100 m water depth.

Early on Monday, April 1, we completed transect B and continued our track to the north, beginning an ADCP profile which followed the equator to the Amazon delta. Late Wednesday, April 3, we started geophysical profiling with PARASOUND and HYDROSWEEP and coring in the Amazon delta. The main objectives of this cooperative research with the Universidade Federal Fluminense, Niteroi, Rio de Janeiro, were to understand the sedimentation pattern in the delta foreset and its relationship to sea level fluctuations, as well as to study of the presence of Amazon ooliths. In the southern part of the delta, we observed sand waves crossed by erosion channels as well as fine-grained foreset sediments. We obtained one core with fine-grained, gas-containing foreset sediments from 35 m water depth; another core was retrieved from 70 m water depth. Surprisingly, the core catcher contained consolidated sandy beach rocks obviously covered by recent sediments. According to our geophysical profiling, it appears as if large areas of the delta are characterized by zero deposition. On April 5, we obtained two cores from 45 m water depth with clayey sediments containing high amounts of gas, presumably methane. The sediment surface was covered by abundant oysters, so we concluded that recent sedimentation must be very low. In the morning of April 6, we cored two sites in 100 and 130 m water depths in the northern part of the delta. Using a box corer, we recovered carbonate-bearing quartz sands, probably containing some ooids. At the deeper site, we retrieved clayey material containing carbonate particles. Some parts of the sediment were already consolidated by organisms and iron oxides/hydroxides (hard grounds).

We finished our coring and profiling program on the Amazon shelf and continued our track to the NE, continuing underway with ADCP and CTD measurements. Early on Sunday, April 7, we arrived at ODP site 940 which is located slightly east of the glacial Amazon channel. We retrieved sediments with the multicorer and gravity corer from the eastern overbanking sediments. Later, we routinely sampled the water column with pumps, Niskin and GoFlo bottles. Finally, we lowered the particle camera and the multinet. After about 24 hours, we concluded activities at this station and continued with detailed PARASOUND and HYDROSWEEP profiles crossing ODP sites 934, 935 and 936. On Monday, April 8, we started our transect 640 sm to the west to the next ADCP-CTD profile, located off Guyana, which we reached on Wednesday, April 10. There, we sampled 7 CTD stations from the continental rise to the deep sea. At two sites we used the particle camera in conjunction with the CTD. Late Thursday, April 11, the investigations off Guyana were finished and we commenced with geological profile C off Barbados, continuing our oceanographic studies. We used PARASOUND and HYDROSWEEP on a 200 sm SE-NW transect to investigate the

bathymetry and sediment structure on the continental margin off Barbados and searched for suitable core locations. Particularly between 1500 and about 2000 m water depths, core locations were rather easy to find and we obtained gravity cores and multicorer samples from four sites. Finally, we intended to find a deeper site on the continental rise off Barbados and obtained a core from 2467 m water depth. On Sunday morning, April 14, we finished our station work. We arrived in Bridgetown, Barbados, on early Monday April 15.

5 Preliminary Results

5.1 Marine Geoscience M 34/1

5.1.1 ODP Pre-Site Survey in the Cape Basin

(V. Spieß, U. Bleil, C. Hilgenfeldt, C. Hübscher, A. Janke, H. von Lom-Keil, H. Martens, R. Schneider, U. Rosiak, G. Uenzelmann-Neben, L. Zühlsdorff)

5.1.1.1 Introduction

The late Paleogene and Neogene geologic history documents major changes in the Earth's climate and ocean circulation systems. With the development of larger latitudinal temperature gradients, the Southern Ocean circumpolar currents and the glaciation of Antarctica, the conveyor belt system evolved which serves as the backbone and linkage for water and heat exchange between the oceans and hemispheres. Probably beginning in the Oligocene, the South Atlantic became a major pathway for both surface and deep water currents.

One of the key features of Atlantic surface water transport is the Benguela Current System. It develops at the Agulhas retroflection from cold circumpolar water masses and moves northwards along the southwest African coast. At the southern tip of Africa and north of 25°S, the current splits up in an oceanward directed limb (BOC = Benguela Ocean Current) and the coastal current (BCC). Associated features of great importance for the sedimentary input at the continental margin are coastal upwelling areas off Angola and Namibia with an extremely high biologic productivity.

To study the evolution of this system in the geologic past, in more detail since Miocene times, and its relationship and response to global climatic and oceanographic changes, coring operations of the Ocean Drilling Program (ODP) are scheduled for August - October 1997 to drill several depth transects on the southwest African continental margin. Based on proposal 354 by WEFER et al. (1995), six areas have been selected between the Congo Fan at 3° S and the southern Cape Basin at 31° S.

A major portion of the required site survey data has been collected during RV SONNE cruise SO 86 in April/May 1993 (BLEIL et al., 1995) for the northern Angola Basin (3° S off the River Congo), for the mid Angola Basin (12° S off Angola) and the southern Angola Basin (17° S in the northern part of the coastal upwelling zone). In addition, reference lines have been shot across DSDP Sites 530 in the Angola Basin and 532 on the Walvis Ridge. Cross profiles for two proposed drill sites in the northern Cape Basin have been also recorded, but the one over the deeper NCB site could not be finished due to technical problems.

Still missing were appropriate site survey data for the drill sites south of the Walvis Ridge in the Cape Basin. Two transects have been originally proposed at 25 and 31° S in particular to drill sediments which carry information about the early, pre-Miocene development of the Benguela Current System.

5.1.1.2 Methods

To survey the potential ODP drill sites in the Cape Basin during RV METEOR cruise M34/1, the high resolution multichannel seismic equipment of the Alfred-Wegener-Institute, Bremerhaven, and modern echosounder systems were used. The volume of the seismic source was optimized for structural resolution and the digital PARASOUND / PARADIGMA sediment echosounder system provides excellent data quality for the upper 20 to 100 m of the surface sediments. Additional information about the local bathymetry can be derived from the HYDROSWEEP swath sounder system which belongs together with the PARASOUND system to the permanent equipment of the research vessel.

5.1.1.2.1 Multichannel Seismics

The seismic acquisition equipment used during cruise M34/1 (Fig. 5) was based on a streamer of 600 m active length with 24 channels and a group length and spacing of 25 meters (Fig. 6). The lead-in length was constantly chosen as 200 meters which results in group offsets between 200 m and 800 m and an average towing depth between 10 and 30 meters.

As a seismic source a GI-Gun of 150 in^3 total volume with a generator volume of 45 in^3 was used. The seismic signal shows a broad spectral bandwidth with maximum frequencies, according to the towing depth of 1 - 2 m, of up to 250 Hz. The low frequency bubble pulse is suppressed by delayed injection of air from a second chamber. The resulting short wavelet was optimized for high resolution of the upper few hundred meters of the sedimentary column. Nevertheless, signal energy and penetration were not only sufficient to study the Neogene sediment cover in the working area, but also most of the sedimentary column down to Reflector AII of Cretaceous age could be imaged. The multichannel data were recorded with a GEOMETRICS ES-2420 instrument at a sampling rate of 0.5 ms, applying an anti-alias filter of 720 Hz (-3 dB). The recording parameters were chosen as:

- recording length 8 seconds,
- shot interval 10 seconds,
- ship's speed 4.9 knots,
- shot distance 25 meters,
- CMP distance 12.5 meters.

The data were stored with 2 conventional 9 track, 1/2" magnetic tapes drives with a data density of 6250 bpi, operated in a daisy chaining mode through the built-in SCSI interface. During the cruise altogether 850 magnetic tapes with 3600 ft length and a total volume of ~170 GigaByte of data were written.

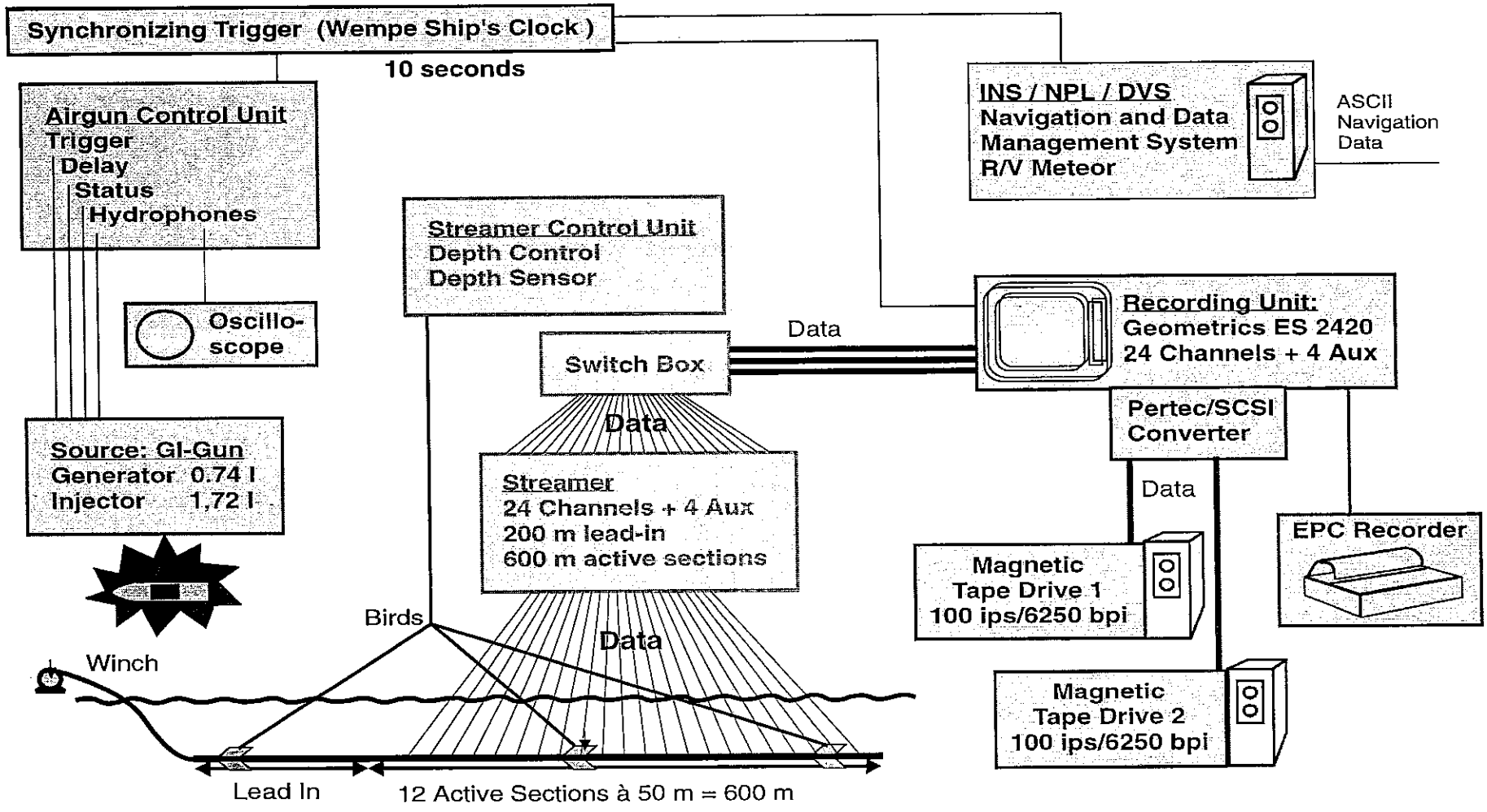

Fig. 5: Multichannel seismic instrumentation used during RV METEOR cruise M34/1. The ship's clock synchronizes the airgun and the recording unit. Four streamer groups of 6.25 m length were combined into one channel which leads to 24 channels for an active length of 600 m. At intervals of 10 s, which results in a shot distance of 25 m at 4.9 knots, the data were digitized with a sample rate of 0.5 s and stored on 1/2" magnetic tapes in daisy chain mode.

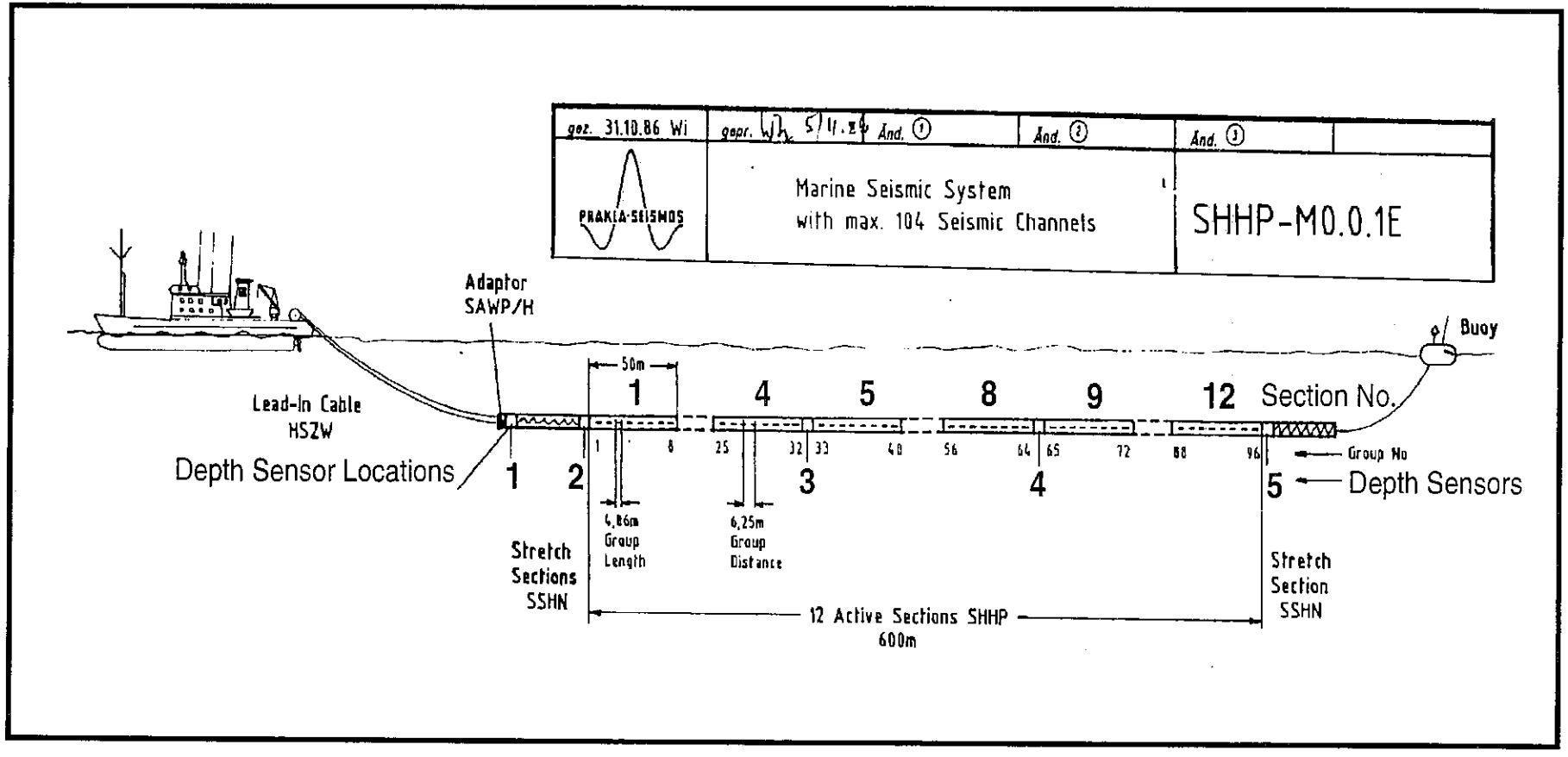

Fig. 6: PRAKLA-SEISMOS multichannel seismic streamer system used during RV METEOR cruise M34/1. Four groups (length 4.86 m, distance 6.25 m) are summed into one recording channel of ~25 m length. Locations of the 5 depth sensors are indicated by odd numbers. Their distances from the beginning of the active section are -150, 0, 200, 400 and 600 m.

Since RV METEOR is not equipped with high-pressure compressors for the airguns, a system of 4 Junkers compressors was provided by the University of Hamburg.

Although the seismic equipment in general was operating reliably during the whole cruise, individual streamer channels showed increasingly high noise levels due to leakage of sections. Apparently the aging of the streamer pipe caused fissures which widened during successive launches. Number of affected channels and noise level increased during the cruise, but a minimum of 16 channels were continuously available. The GI-Guns operated with a constant high signal quality for approximately 123'000 shots without repairs. The compressor system was maintained during the cruise with a continuous 6 hour watch schedule by two engineers to prevent system failures. Due to the redundancy of 2 (of 4) compressors, major breakdowns could be avoided.

Problems with the cable connection between the recording unit and tape drives could be partially circumvented, but occasionally a few shots were lost when changing between tape drives. Although the seismic coverage was reduced in these cases, temporal gaps were short and the streamer length was sufficient to assure a continuous spatial coverage.

5.1.1.2.2 PARASOUND / PARADIGMA Digital Echosounder System

The PARASOUND system works both as a low-frequency sediment echosounder and as high-frequency narrow beam sounder to determine the water depth. It makes use of the parametric effect which produces additional frequencies through nonlinear acoustic interaction of finite amplitude waves. If two sound waves of similar frequencies (here 18 kHz and e.g. 22 kHz) with sufficiently high primary amplitudes are emitted simultaneously, a signal of the difference frequency (e.g. 4 kHz) is generated. The new component is traveling within the emission cone of the original high frequency waves which are limited to an angle of only 4° for the equipment used. Therefore, the footprint size is much smaller than for conventional systems and both vertical and lateral resolution are significantly improved.

The PARASOUND system is permanently installed on the ship. The hull-mounted transducer array has 128 elements on an area of ~1 m^2. It requires up to 70 kW of electric power due to the low degree of efficiency of the parametric effect. In 2 electronic cabinets beamforming, signal generation and the separation of primary and secondary frequencies is carried out. With the third electronic cabinet in the echosounder control room the system is operated on a 24 hour watch schedule.

Since the two-way travel time in the deep sea becomes long compared to the length of the reception window of up to 266 ms, the PARASOUND system sends out a burst of pulses at 400 ms intervals, until the first echo returns. The coverage of this discontinuous mode depends on the water depth and produces non-equidistant shot distances between bursts. On average, one seismogram is recorded about every second providing a spatial resolution on the order of a few meters on seismic profiles at 4.9 knots.

The main tasks of the operators are system and quality control and the adjustment of the reception window. Because of the limited penetration of the echosounder signal into the sediment, only a short window close to the sea floor is recorded. The density of information is very high because of a resolution on the order of a few tens of centimeters.

In addition to the analog recording with the b/w DESO 25 device, the PARASOUND system was equipped with the digital data acquisition system PARADIGMA which was developed at the University of Bremen (SPIEß, 1993). The data are stored directly on 6250 bpi, 1/2" magnetic tapes using the standard, industry compatible SEGY format. A 486-processor based PC allows the buffering, transfer and storage of the digital seismograms at high repetition rates. From the emitted series of pulses usually every second pulse could be digitized and stored, resulting in recording intervals of 800 ms within a pulse sequence. The seismograms with a typical registration length of 266 ms for a depth window of ~200 m were sampled at a frequency of 40 kHz. The source signal was a bandlimited, 2 - 6 kHz sinusoidal wavelet of 4 kHz dominant frequency with a duration of 2 periods (~0.5 ms total length).

Already during the acquisition of the data an on-line processing was carried out. For all profiles echographic sections were plotted with a vertical scale of several hundred meters. Most of the changes in window depth could thereby be eliminated. These plots provide a first impression of variations in sea floor morphology, sediment coverage and sedimentation patterns along the ship's track. To improve the signal-to-noise ratio, the echogram sections were filtered with a wide bandpass filter. In addition, the data were normalized to a constant value well below the maximum average amplitude to enhance in particular deeper and often weaker reflections.

To study the influence of frequency and length of the source signal on the reflection pattern, these parameters were systematically varied at sites, where sediment cores were recovered ('source signal test'). The frequency of the source signal was increased in 0.5 kHz steps over the available frequency range from 2.5 to 5.5 kHz, while the length of the sinusoidal pulses was set to 1, 2, 4, and 8 periods. Each configuration was kept for a time span of 2 minutes to enable later signal stacking and an evaluation of the variability of seismograms from the same location. In order to quantify interference phenomena, seismograms recorded with different frequencies will be studied in detailed shorebased analyses.

5.1.1.2.3 HYDROSWEEP Swath Sounder System

The multibeam echosounder HYDROSWEEP on RV METEOR was routinely used during leg M34/1 and serviced by the system operator and the electronics engineers. During a 24 hour watch, the scientific crew operated continuously both the HYDROSWEEP and the PARASOUND echosounder systems in parallel. The HYDROSWEEP system worked without technical problems. It provided a complete coverage of the sea floor topography with

a swath width of twice the water depth. Since the weather conditions were good, the data quality was generally perfect with only a few data losses due to high sea states.

Just before the beginning of cruise M34/1 the HYDROSWEEP system was upgraded with the new real-time acquisition and control system HYDROMAP ONLINE as well as the postprocessing package HYDROMAP OFFLINE. Both components improved the shipboard work significantly and allowed immediate generation of maps in survey areas. Most of the data editing tasks could be performed by the system operator so that a complete data set was available at the end of the cruise. Several versions of maps were plotted according to the specific requirements of the scientific program.

5.1.1.2.4 On Board Data Processing

For immediate quality control of the seismic and echosounder data, a simple processing was applied. The digital echosounder records were read from magnetic tapes onto a hard disk and archived on DAT tapes. The transfer of the data into an internal image format with a compression factor of 10 allowed an immediate graphical output of selected profiles with the SE software package of the University of Bremen.

The seismic data, which were written in SEG-D format, were read from magnetic tapes by use of the SU software package (Seismic Unix) on a HP Apollo 715 workstation with a SCSI magnetic tape drive, a DAT tape drive and hard disks with 1 and 4 GigaByte capacity. Selected traces of each shot were demultiplexed, resampled, sorted and filtered.

Without velocity analyses and move-out correction, a brute stack section of the 4 nearest traces was generated for prioritized profiles across potential drill sites. About 2/3 of the complete data set were treated this way. The resulting seismic sections, which could be plotted on the new peripheral devices of the HYDROMAP Online processing system, served for an evaluation of the results, selection of additional crossing points and were also used to establish a preliminary seismostratigraphic concept.

5.1.1.3 Survey Strategy and Study Areas

From 3rd to 26th January, 1996, an ODP pre-site survey was carried out on the southwest African continental margin between 33 and 19° S during RV METEOR cruise M34/1. It was undertaken to study the Neogene evolution of the Benguela Current System in preparation of the upcoming ODP Leg 175. Figure 6 shows the cruise track, where seismic lines are indicated by thick lines. Table 4 summarizes the geographic locations and important parameters of the profiles.

Drill sites in the SCB (Southern Cape Basin, 31° S) and NCB (Northern Cape Basin, 25° S) regions were originally defined using seismic lines of AUSTIN and UCHUPI (1982). A detailed survey had to be carried out in the vicinity of the SCB sites, which lie in a slumped area, to identify individual blocks and locations with most complete sections. Based on a preliminary interpretation, the Paleogene section appears to be undisturbed down to 600 m below sea floor. This provides a good target for studies of the early development of the coastal current system. A small survey was run at 29° S in an area, where slumps had not been documented previously in the literature. The seismic lines reveal many local structures, indicating incisions and small slumps. A second profile was run across a mostly undisturbed section which will be proposed as an alternate site.

The northern Cape Basin sites lie in the range of the coastal upwelling cells and were targeted to image the temporal evolution of upwelling activities in the area. Two lines were shot across the proposed site which reveal an undisturbed section with a significantly different seismic signature than in the SCB regions. Increased penetration of the echosounder signal can be explained by a higher accumulation of fine grained clay and silt materials than further south.

A detailed seismic survey was carried out in the Walvis Basin between 19 and 22° S. This area is both affected by the oceanward migrating eddies originating from the upwelling cell and by redeposited sediment from the crest of the Walvis Ridge. The input from both these sources is controlled by the Benguela Coastal Current and upwelling. Because of the high sedimentation rates, detailed reconstructions of their variabilities will be possible.

Closely spaced seismic lines were shot to analyze the areal sedimentation pattern and to reconstruct the primary depositional processes in space and time. Several sites will be proposed for drilling which should provide very high resolution geological data of the Benguela upwelling activity off Namibia. Interpretation of seismic lines shot over DSDP Site 532 and the proposed Site WR-1 will be integrated to develop a stratigraphic framework and to further improve the regional understanding of the Walvis Basin.

Tab. 4: Summary of Multichannel Seismic Lines of RV METEOR cruise M34/1

GeoB / AWI	Date 1996	Start Time	Start Coordinates Latitude	Start Coordinates Longitude	Date 1996	End Time	End Coordinates Latitude	End Coordinates Longitude	Lead-In [m]	Source Volume [l] Generator	Source Volume [l] Injector	Shots	Length [km]
96-001	05.01.	21:34:00	32°56.67'S	13°01.95'E	07.01.	14:00:00	31°18.05'S	16°29.62'E	200	0.74	1.72	14556	363.90
96-002	07.01.	14:00:10	31°18.50'S	16°29.62'E	07.01.	15:35:00	31°11.68'S	16°26.90'E	200	0.74	1.72	569	14.20
96-003	07.01.	15:35:10	31°11.68'S	16°26.90'E	08.01.	08:40:00	31°29.91'S	14°51.44'E	200	0.74	1.72	5790	144.75
96-004	08.01.	08:55:00	31°30.49'S	14°51.02'E	08.01.	18:00:00	32°04.10'S	15°23.75'E	200	0.74	1.72	3270	81.75
96-005	08.01.	18:20:00	32°04.49'S	15°23.75'E	08.01.	22:21:00	31°55.19'S	15°45.91'E	200	0.74	1.72	1446	36.15
96-006	08.01.	22:28:00	31°54.71'S	15°45.87'E	09.01.	08:15:00	31°09.74'S	15°33.90'E	200	0.74	1.72	3286	82.50
96-007	09.01.	08:30:00	31°09.07'S	15°32.45'E	09.01.	12:35:00	31°12.99'S	15°10.69'E	200	0.74	1.72	1470	36.75
96-008	09.01.	12:44:00	31°13.70'S	15°10.00'E	09.01.	23:12:00	31°58.91'S	15°36.81'E	200	0.74	1.72	3768	94.20
96-009	11.01.	03:56:00	29°49.83'S	12°30.53'E	12.01.	04:30:00	29°10.41'S	14°38.73'E	200	0.74	1.72	8844	221.10
96-010	12.01.	05:06:00	29°10.46'S	14°39.79'E	12.01.	11:43:00	29°35.58'S	14°17.43'E	200	0.74	1.72	2382	59.55
96-011	12.01.	11:52:45	29°35.76'S	14°16.67'E	12.01.	19:37:08	29°10.42'S	13°43.63'E	200	0.74	1.72	2790	69.75
96-012	13.01.	15:21:00	25°49.75'S	13°49.74'E	14.01.	08:13:00	25°15.28'S	12°35.98'E	200	0.74	1.72	6072	151.80
96-013	14.01.	08:28:00	25°15.20'S	12°35.02'E	14.01.	15:38:00	25°49.49'S	12°39.94'E	200	0.74	1.72	2580	64.50
96-014	14.01.	15:43:40	25°49.74'S	12°40.12'E	15.01.	03:23:00	25°09.87'S	13°24.95'E	200	0.74	1.72	4200	105.00
96-015	17.01.	06:15:00	22°00.00'S	10°30.00'E	18.01.	14:03:00	20°27.00'S	12°45.00'E	200	0.74	1.72	11448	286.20
96-016	18.01.	14:20:00	20°27.00'S	12°45.00'E	18.01.	19:55:00	20°00.00'S	12°29.40'E	200	0.74	1.72	2370	59.25
96-017	18.01.	20:03:00	20°00.00'S	12°29.40'E	19.01.	20:12:00	21°12.00'S	10°48.00'E	200	0.74	1.72	8694	217.35
96-018	19.01.	20:22:00	21°12.00'S	10°48.00'E	20.01.	07:12:00	21°41.73'S	11°35.62'E	200	0.74	1.72	3900	97.50
96-019	20.01.	07:28:00	21°41.57'S	11°37.07'E	21.01.	00:03:20	21°15.18'S	12°59.62'E	200	0.74	1.72	5970	149.25
96-020	21.01.	00:12:00	21°14.83'S	12°59.67'E	21.01.	17:35:00	21°03.00'S	11°30.00'E	200	0.74	1.72	6258	156.45
96-021	21.01.	17:42:00	21°02.94'S	11°29.85'E	22.01.	03:50:00	20°36.89'S	10°43.56'E	200	0.74	1.72	3648	91.20
96-022	22.01.	03:53:00	20°36.73'S	10°42.95'E	22.01.	15:48:00	19°38.02'S	10°29.63'E	200	0.74	1.72	3930	98.25
96-023	22.01.	15:55:00	19°37.93'S	10°29.18'E	22.01.	17:55:00	19°45.56'S	10°23.72'E	200	0.74	1.72	720	18.00
96-024	22.01.	18:02:00	19°45.89'S	10°23.98'E	23.01.	06:27:00	19°35.58'S	11°28.35'E	200	0.74	1.72	4470	111.75
96-025	23.01.	06:36:00	19°36.13'S	11°28.49'E	23.01.	09:03:00	19°44.58'S	11°18.29'E	200	0.74	1.72	864	21.80
96-026	23.01.	09:16:00	19°43.89'S	11°17.84'E	23.01.	12:09:00	19°30.00'S	11°22.61'E	200	0.74	1.72	1038	25.95
96-027	23.01.	12:17:00	19°30.00'S	11°23.11'E	23.01.	18:36:00	19°52.03'S	11°41.89'E	200	0.74	1.72	2274	56.85
96-028	23.01.	18:46:00	19°52.75'S	11°42.08'E	24.01.	01:24:30	20°24.13'S	11°29.82'E	200	0.74	1.72	2088	52.20
96-029	24.01.	01:32:30	20°24.17'S	11°29.34'E	24.01.	06:38:00	20°12.72'S	11°04.14'E	200	0.74	1.72	1833	45.83
96-030	24.01.	06.49:40	20°12.72'S	11°04.14'E	24.01.	13:41:00	19°40.65'S	10°51.19'E	200	0.74	1.72	2472	61.80

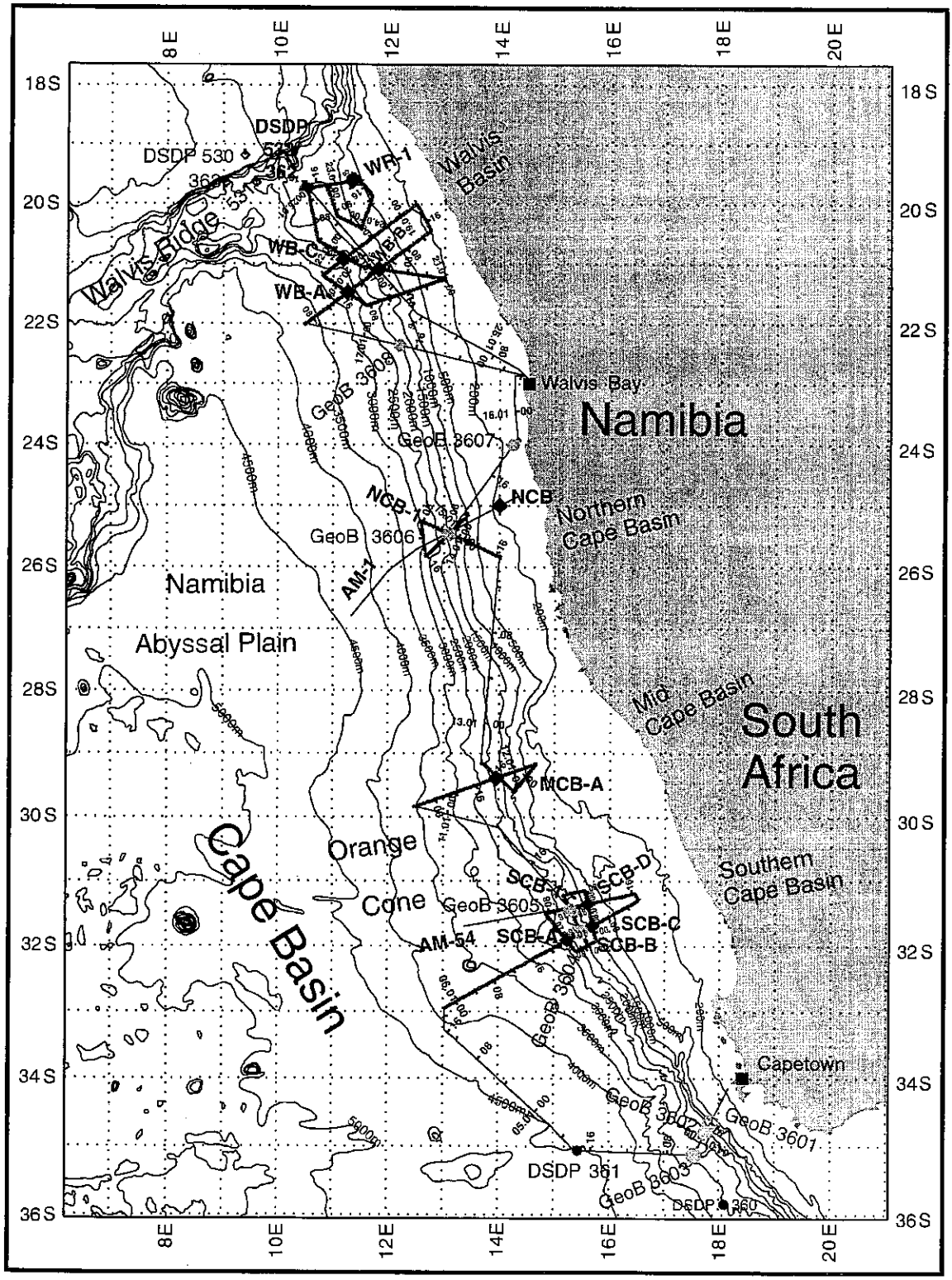

Fig. 7: Track chart of RV METEOR cruise M34/1. Seismic profiles are indicated by thick lines. Full diamonds denote crossings selected as potential ODP drill sites, light grey dots geologic sampling stations. Also shown are former DSDP sites and seismic profiles AM-1 and AM-54 of AUSTIN and UCHUPI (1982).

5.1.1.4 Cape Basin Stratigraphic Framework

The general structure of the Cape Basin continental margin developed during the Cretaceous after the breakup of Gondwanaland. It was summarized in several comprehensive papers, e.g. EMERY and UCHUPI (1984), DINGLE and ROBSON (1992), and therefore will not be repeated here in detail.

During the early opening of the South Atlantic in the Cretaceous, the sedimentation at the continental margin was characterized by intense terrigenous deposition. The sedimentation rate subsequently declined during the Paleogene. Aridification on the continent in Oligocene and Miocene led to a further decrease which in conjunction with intensified bottom water currents resulted in starved depositional conditions in the deeper parts of the Cape Basin.

As is widely documented in the literature (e.g. DINGLE, 1980; DINGLE and ROBSON, 1992), the Neogene sedimentation was accompanied by successive slope failures which occurred throughout the Tertiary due to the buoyant behavior of the sediment loaded margin. During the Pleistocene, a significant portion of the continental slope and rise was affected by further massive slumps, slides and debris flows, and in many places the Neogene sedimentary sequences was partially or completely removed. Consequently, high resolution seismic data were acquired over this area to investigate the sedimentary column at selected drill sites and to assure their structural integrity and stratigraphic completeness.

Only a few research cruises have collected marine seismic data in the Cape Basin. A reconnaissance study of single channel seismic surveys at the southwest African continental margin was published by EMERY et al. (1975). The main interest of their investigations was the structure of the continental margin. They identified two prominent reflectors in the Cape Basin which could be used for a basinwide seismostratigraphic identification.

The most prominent feature of seismic records in the South Atlantic is the seismic Reflector AII (Atlantis II; Reflector P of GERRARD and SMITH, 1984) which was first described by EMERY et al. (1975). It was assigned a late Aptian age by BOLLI et al. (1978) and indicates the 'earliest recognizable shelf-slope-rise relationship' (DINGLE and ROBSON, 1992) in the Cape Basin. Together with the second basinwide observable feature, Reflector D (Davie, EMERY et al., 1975, or L according to the nomenclature of GERRARD and SMITH, 1984) a seismostratigraphic framework is available which can be used as preliminary guideline for a chronostratigraphy.

For the sedimentary sequences between basement and Reflector AII, which can be subdivided into two separate units in the Cape Basin province, a Mesozoic, mostly Cretaceous age is assumed. The unit between Reflectors AII and D probably was deposited in the early Paleogene, whereas late Paleogene and Neogene sediments were found above Reflector D. For the sequence between AII and D, EMERY et al. (1975) mention a lack of reflectors, which was assigned to the absence of coarse sediments. Reflector D can be widely traced in the Cape Basin, but also tentatively correlated to a Miocene unconformity beneath the shelf.

Above Reflector D the authors observed mass movements which affected majors portions of these units in many seismic lines. Faults, sediment wedges, erosional planes, progradation and sediments overstepping from the rise onto the shelf were also described. The existence of a double shelf break further complicates the situation.

During Oligocene wide shelf areas were exposed, subject to erosion and deeply dissected. Subsequently, in Miocene, a sequence was deposited on the shelf which lies unconformably on older sediments. Within this sequence a further unconformity separates two units which were associated with a partial withdrawal of the ocean. Pliocene intensification of currents led to widespread erosion on the shelf, leaving only remnants of older deposits and phosphatic, glaukonitic sands. Due to eustatic sea level changes Pleistocene deposition was restricted to limited areas.

A drilling campaign of the Deep Sea Drilling Project was performed in 1975 to investigate the history of the southwest African continental margin (BOLLI et al., 1978; see Fig. 5). Two sites, 360 and 361 were drilled in the Cape Basin to study the sedimentary setting during the early opening of the South Atlantic and to date the prominent Reflectors AII and D of EMERY et al. (1975). Cenozoic deposition in the Cape Basin revealed major fluctuations and a relatively shallow position of the CCD. Pronounced dissolution phases were observed during the Eocene and earliest Oligocene, and less intense from middle to upper Miocene.

Site 360 off Cape Town is located in 2977 m water depth on a large slumped sediment block. The hole was washed down to 80 m before coring started. Mostly carbonaceous, nannofossil-rich sediments were encountered in the upper 3 lithologic units from 80 - 180, 181 - 388 and 388 - 568 m sub-bottom depth, ranging in age from lower Pliocene to upper Miocene, from upper to lower Miocene and from lower Miocene to upper Eocene, respectively. Marly nannofossil chalk was drilled from 568 - 840 m sub-bottom depth with a clay content well beyond 50 %.

Site 361 was drilled in 4547 m water depth in the Cape Basin on old oceanic crust. Coring started at 32 m sub-bottom depth, where upper Eocene to upper Paleocene sediments were identified. Below the uppermost unit (0 - 264 m) pelagic clay of Paleocene to Cretaceous age reveal drastic changes in the sedimentary setting.

According to the shipboard scientific party, the D horizon corresponds to an abrupt lithological break at Site 361 from up to 77 % carbonates to pure pelagic clays. Stratigraphically it was placed between the uppermost Paleocene and lowermost Eocene. Reflector AII represents a sudden transition from non-carbonate shales to a shale with interbedded thick, calcite cemented sandy mudstones and siltstones.

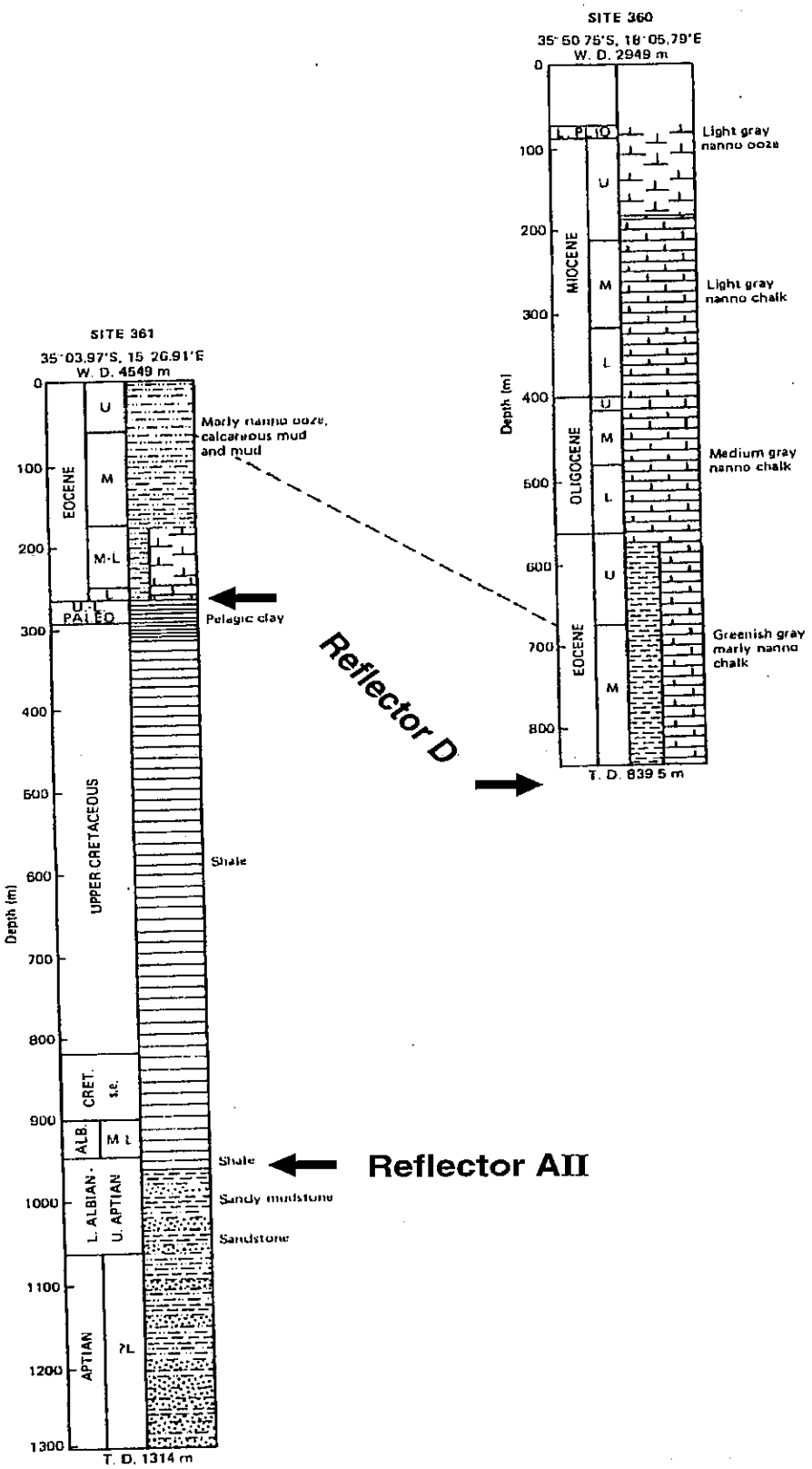

Fig. 8: Lithostratigraphy of DSDP Sites 360 and 361 in the Cape Basin which were also targeted to date the prominent seismic Reflectors D and AII (from BOLLI et al., 1978).

Compressional wave velocities nearly double from 2.25 to 4.5 km/s and bulk density increases from 2000 to 2400 kg/m^3. The age was upper Aptian (~110 Ma).

At DSDP Site 360 acoustic Unit I, which reaches down to Reflector D, could be further subdivided into 4 subunits of 230, 190, 95 and 390 ms thickness. The base of Unit Ia is marked by an increase of sand content in upper Miocene. Subunit Ib in the lowermost Miocene is characterized by an increase in p-wave velocity from 1.63 to 1.90 km/s together with a decrease in carbonate content. Within Unit Ic of middle Oligocene age velocity and carbonate content further increase. Extrapolation of drilling results of Subunit Id provides a middle Eocene age for Reflector D which corresponds to Reflector A identified in the northwest Atlantic Ocean.

At DSDP Site 361 Reflector D is found in the uppermost lithologic unit, representing an interface from nannofossil oozes to chalks and pelagic clay. Minor changes in carbonate content explain the relative lack of bedding and internal reflectors in Subunits Ia and Ib. The stratification in Subunit Ic results from sharp bedding contacts and variable carbonate contents. BOLLI et al. describe the nature of Subunit Id as stratified and undulating, possibly associated with enhanced terrigenous input of coarser silt and sand and variations in carbonate content. Lamination is caused by CCD fluctuations and dissolution.

The nature of Reflector D was described as 'crisp' by BOLLI et al. throughout the lower continental rise and attributed to the sharp change from carbonate sediments to pelagic clays which were thought to be the residue of Paleocene dissolution at this depth. Further upslope, its more diffuse appearance indicates the position of the lysocline, smoothing the carbonate gradient with depth.

AUSTIN and UCHUPI (1982) carried out a multichannel seismic survey in the southern and northern Cape Basin to study the deeper structure of the continental margin. They confirm the observation that Reflectors D and AII are rarely affected by slumping and that the D to AII sediments appear to be undeformed. Proposed drill sites NCB and SCB were based on these lines.

GERRARD and SMITH (1984) published results from borehole data, offshore geology and seismics related to exploration activities along the coast and focused on the Mesozoic successions. They introduced a new nomenclature for seismic reflectors, namely L for the Reflector D and P for Reflector AII. Isopach maps were compiled for the entire Cenozoic which reveal elongated depocenters along the margin seaward of the Mesozoic depocenters. In part their sediments may have been derived from uplifted Cretaceous basins under open ocean conditions. Sedimentation rates were lower than in the Cretaceous and had no impact on the general outline of the continental margin. Reflector L generally marks the base of the Eocene and results from a lowering of the relative sea level. Information about the Tertiary is mostly sparse due to the very thin units on the outer shelf and a lack of samples from boreholes.

5.1.1.5 Southern Cape Basin

The working area in the southern Cape Basin was chosen to investigate the early history of the Benguela Current and to detect possible influences of the Agulhas Current. The proximity to the continent allows the identification of local upwelling signals, sea level changes and a study of continental climate through component analysis of the terrigenous input.

In the original proposal three sites had been positioned on a depth transect, but in the course of the planning process and due to time constraints set by the panels, only one site was left for triple APC (Advanced Piston Corer) and XCB (Extended Core Barrel) coring down to 600 m sub-bottom depth at 31°25.0' S / 15°17.0' E.The site was selected on seismic Line AM-54 of AUSTIN and UCHUPI (1982) which was targeted to study the development of the continental margin during early opening stages of the South Atlantic. Their seismic characteristics were optimized to high signal penetration and low source frequency, and therefore resolution of the upper sediment layers is limited. With the small volume GI-Gun and a streamer group length of 25 m used during this cruise, the signal spectrum extends beyond 200 Hz and structural resolution is better than 10 m vertically and some 10 m laterally.

5.1.1.5.1 Survey Strategy and Bathymetry

It was well known from previous studies that the selected area had been affected by slumping during Neogene. It is also part of the Orange Sediment Fan which was intensely fed by the Orange River until Miocene and developed typical fan deposits in many parts.

Site SCB-1 had been positioned on the continental slope in a water depth, where hemipelagic sedimentation without fan deposits could be expected. The seismic survey was planned to understand the local depositional and tectonic framework and to identify locations, where slumping did not affect the structural integrity of complete sediment blocks.

Figure 9 shows the cruise track of altogether 8 seismic lines with a total length of 854 km recorded during RV METEOR cruise M34/1 in the vicinity of the proposed Site SCB-1. Crossing points of seismic lines are summarized in Table 5. The results of the HYDROSWEEP swath sounder survey are displayed in Figure 10. They reveal a high variability in morphology, already indicating the existence of major slump events. A ridge-type structure is observed between the two Lines GeoB/AWI 96-001 and -003. Slump scarps are identified e.g. on Line GeoB/AWI 96-001 in 2000 to 2500 m water depth.

Tab. 5: Crossings of seismic lines at proposed drill sites in the SCB working area

Site	Line GeoB/AWI	Shot Point	Date 1996	Time	Latitude	Longitude	Water Depth [m]
SCB-1	96-003	4375	08.01.	03:58	31°24.9'S	15°17.0'E	1382
	96-008	888	09.01.	15:17			
SCB-A	96-001	8992	06.01.	23:20	31°54.4'S	15°14.0'E	2234
	96-004	---	08.01.	15:27			
SCB-B	96-001	10124	07.01.	02:31	31°47.1'S	15°30.0'E	1507
	96-008	2641	09.01.	20:30			
SCB-C	96-001	10950	07.01.	04:51	31°41.4'S	15°41.9'E	887
	96-006	1026	09.01.	01:21			
SCB-D	96-003	3092	08.01.	00:22	31°21.3'S	15°36.5'E	778
	96-006	2576	09.01.	05:41			

5.1.1.5.2 Seismic Stratigraphy

The upper 1.5 seconds of Line AM-54 can be divided into 4 seismic units (Fig. 11). The uppermost Unit I has a thickness between 400 and 600 ms. Its distinct layering is interrupted by channel-like incisions, some of which can be traced ~200 ms into the sediment. Reflectivity remains relatively weak, some higher amplitude reflectors appear only in the upper part. The base of Unit I is a discordance with a rough to undulating surface of complex nature.

In Unit II below the unconformity amplitudes are comparably low as in Unit I, but the eastern and western sections of Line AM-54 show a different character, probably because of a different source signature. Within this unit of almost uniform thickness (~250 ms), the western portion has lower frequencies and a less consistent reflection pattern, while in the eastern part numerous weak reflectors are observed.

Unit III appears as a band of high amplitude reflections of 150 ms thickness thinning towards the shelf. Amplitudes successively increase at depth. In some intervals normal faulting can be identified which extends into Unit II. In mid Unit III a high amplitude reflector is associated with hyperbolic echoes. They may originate from a rough interface. A basal discordance can hardly be recognized due to the low frequency content of the seismic data. Reflectors beneath are parallel and of similar amplitudes.

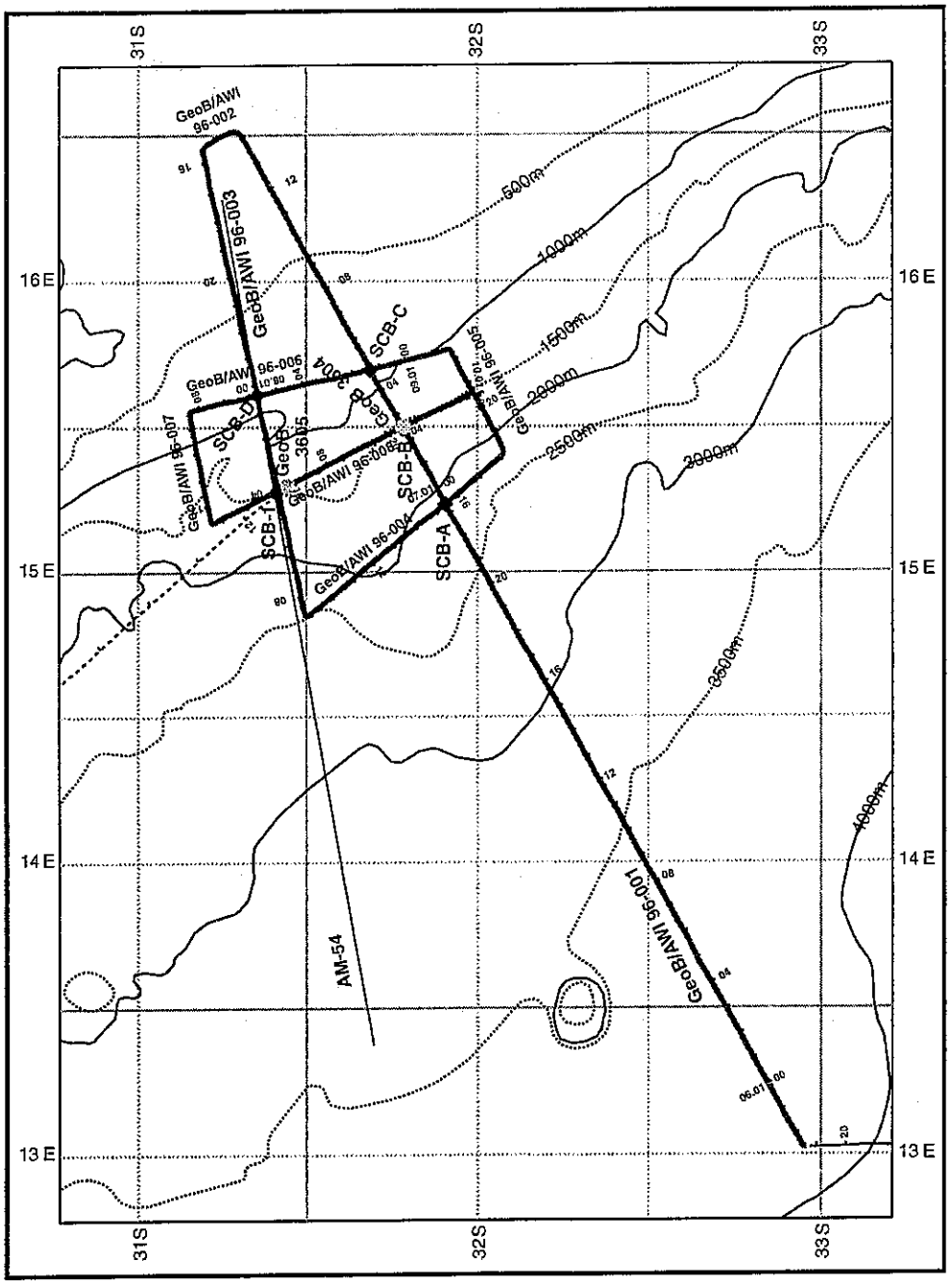

Fig. 9: RV METEOR M34/1 cruise track in the Southern Cape Basin study area, annotated with date (left side) and hours (right side) of the day. Seismic profiles are indicated by thick lines. Full diamonds denote crossings selected as potential ODP drill sites, light grey dots geologic sampling stations. Bathymetry was extracted from the Gebco Digital Atlas 1.01. Also shown is seismic profile AM-54 of AUSTIN and UCHUPI (1982). Thick lines are seismic profiles.

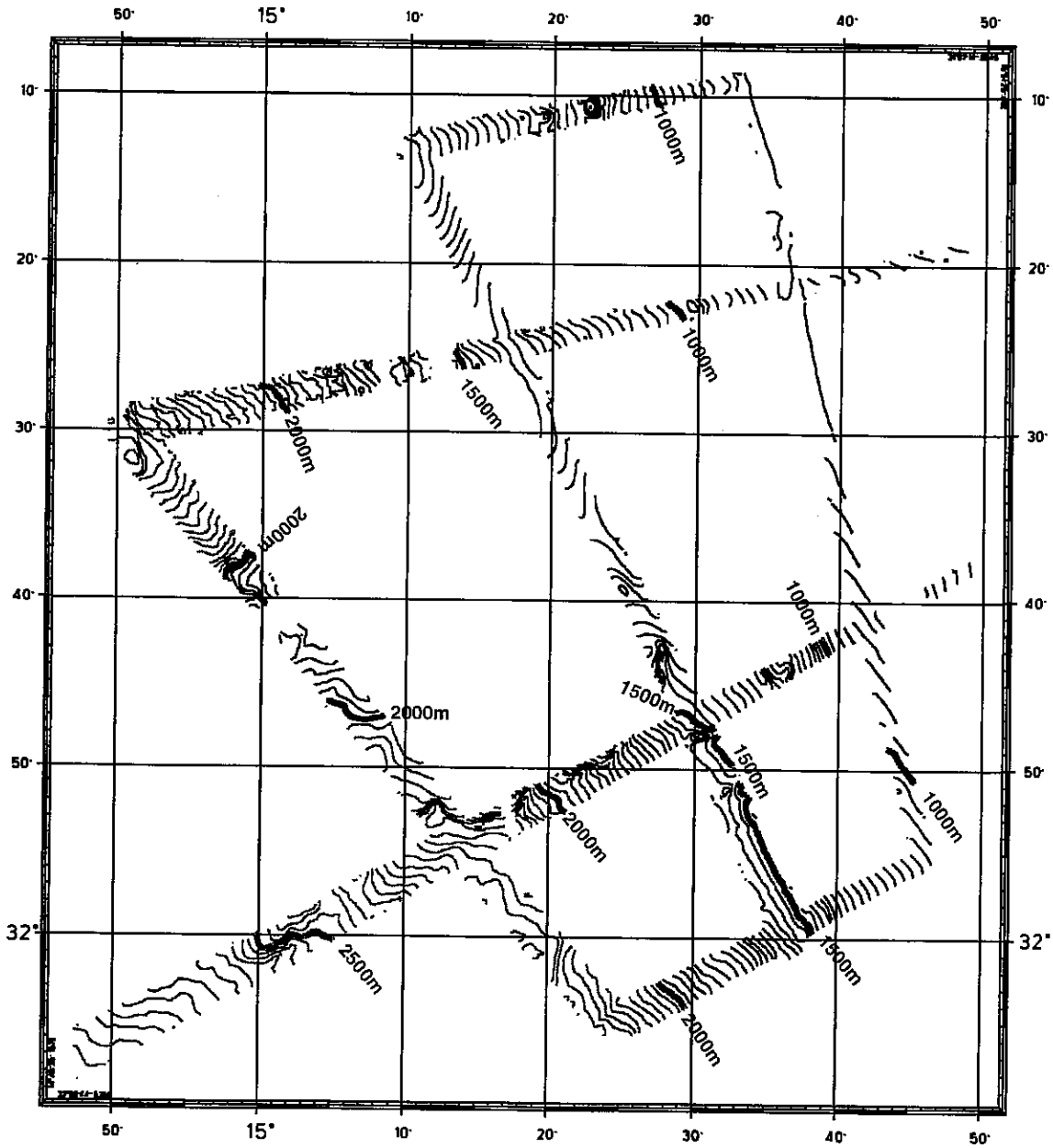

Fig. 10: Bathymetric survey with the HYDROSWEEP swath sounder system in the Southern Cape Basin study area (25 m contour intervals).

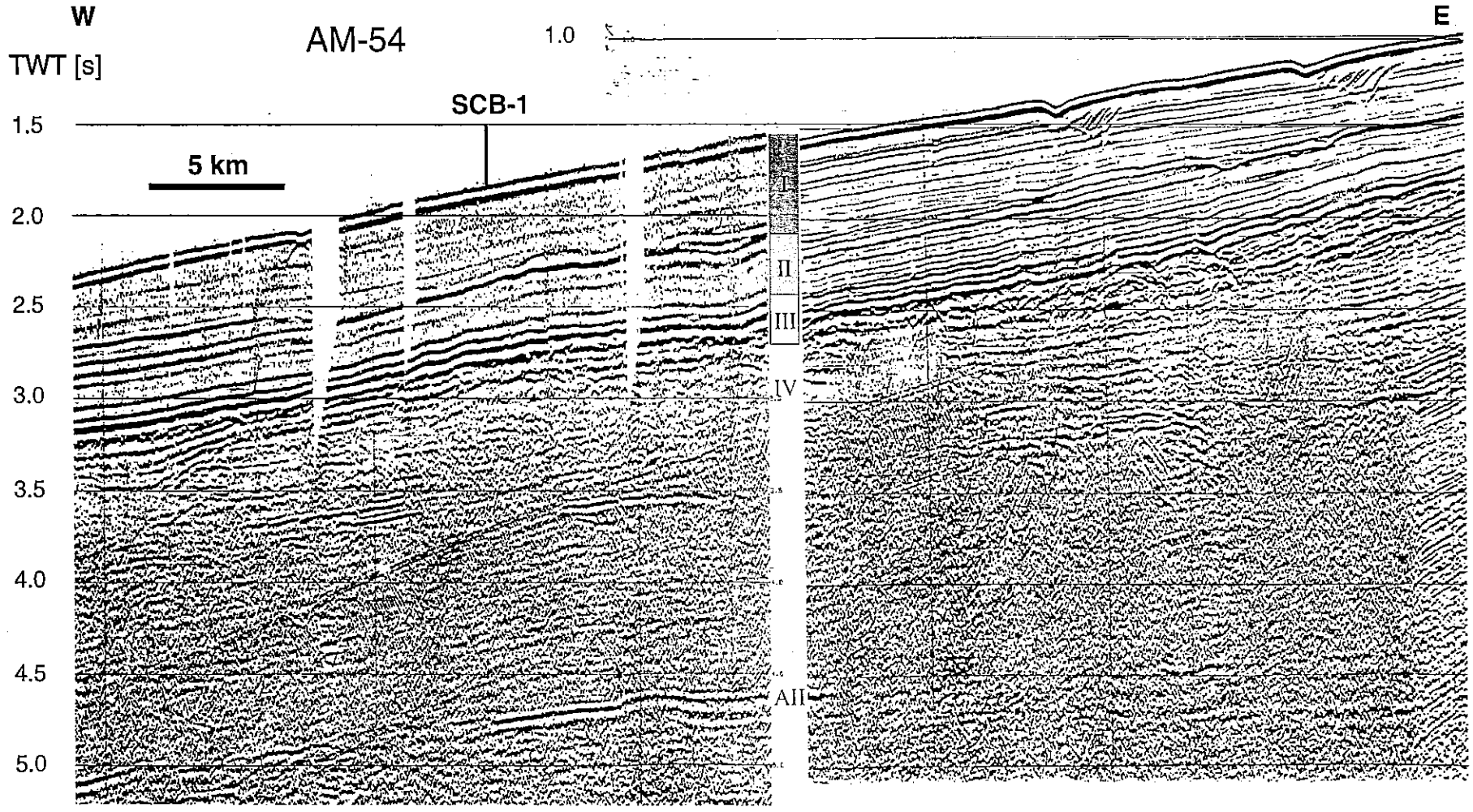

Fig. 11: Seismic Line AM-54 of AUSTIN and UCHUPI (1982) across the proposed drill Site SCB-1 in the Southern Cape Basin study area. Vertical axis is given in seconds of two-way-traveltime. Seismostratigraphic units are indicated in-between two parts of the profile with a different source signature. AII denotes the regional Cretaceous reflector identified by EMERY et al. (1975).

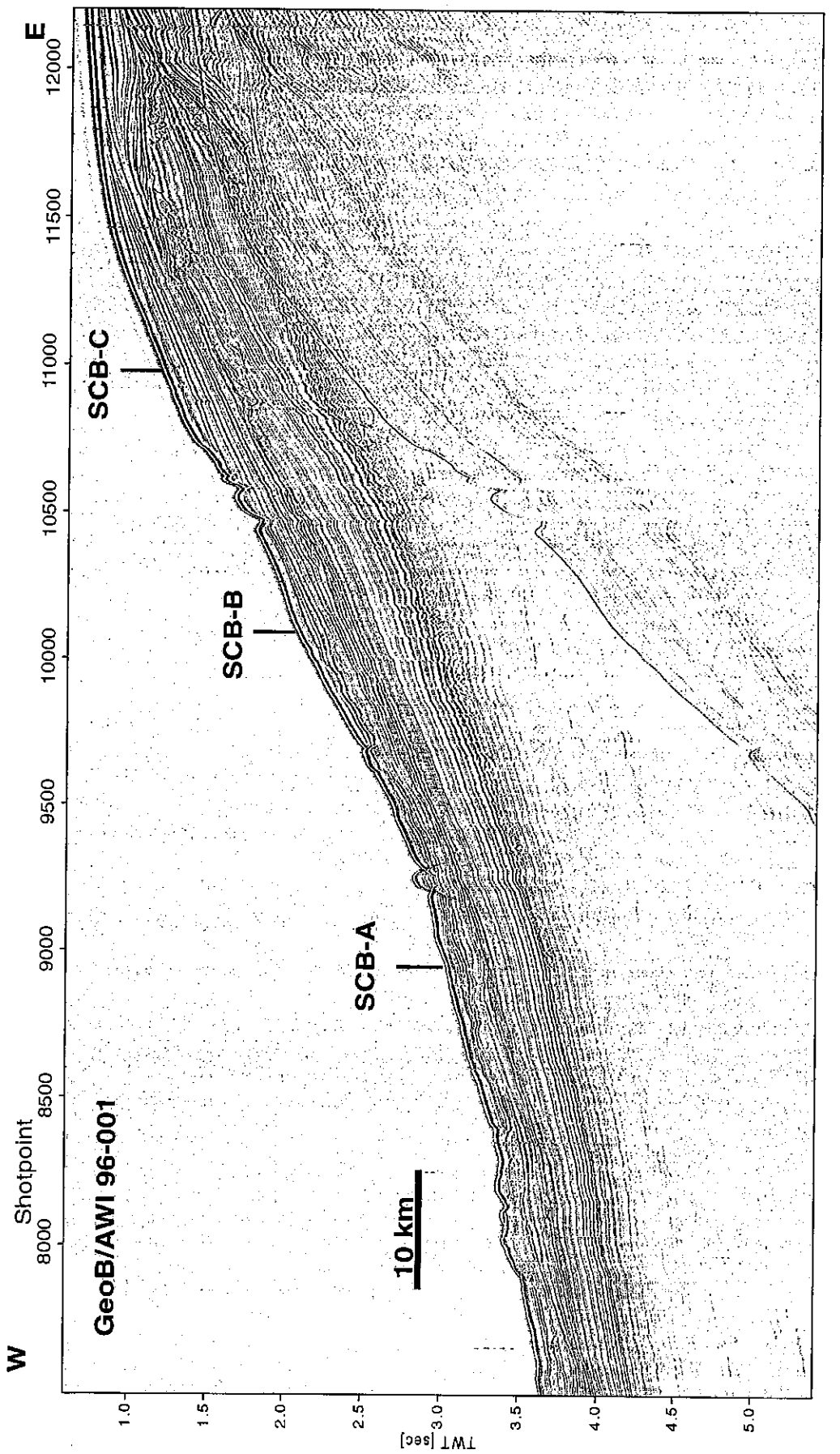

Fig. 12: Seismic Line GeoB/AWI 96-001 in the Southern Cape Basin study area between shotpoints 7500 and 12200 on the upper continental slope. The profile shows clear indications for slumping in the upper sedimentary unit, whereas the deeper sequences appear only slightly disturbed. Crossing with other seismic lines are indicated (see Fig. 9).

Unit IV shows distinct reflectors in the upper parts and a chaotic to disrupted pattern further downslope. Amplitudes gradually decrease at depth so that the base of this unit is difficult to determine.

Only seismic Units I to III are targeted for drilling. In the original proposal the base of Unit III was interpreted as Reflector L (GERRARD and SMITH, 1984) which denotes a Paleocene to Maastrichtian hiatus. The AII reflector (EMERY et al., 1975) or P reflector according to the nomenclature of GERRARD and SMITH (1984), traced between 4.5 and 5.0 seconds TWT, probably represents the drift-onset unconformity (DINGLE and ROBSON, 1992).

METEOR M34/1 Survey in the SCB Area

As was known from earlier studies by DINGLE (1980), DINGLE et al. (1987) and DINGLE and ROBSON (1992), major slump structures had been identified in the working area. Both seismic Lines GeoB/AWI 96-001 (Fig. 12) and GeoB/AWI 96-003 (Fig. 13), running perpendicular to the continental margin, show clear evidence for sediment tectonics, specifically in greater water depth. Therefore, the development of a seismostratigraphic concept and its application to all seismic profiles is not as straightforward as was expected from the older data.

Although in the vicinity of Site SCB-1 the sediment column appears to be only slightly disturbed, the seismic survey was carefully designed to allow for a detailed understanding of the continental margin evolution in the study area and its tectonic history.

Line GeoB/AWI 96-001 (Fig. 12) starts in a water depth of 5.1 s TWT with a relatively thin (400 ms) succession of parallel reflectors topped by increasingly thick debris flow units. In shallower waters well stratified sequences are disturbed by fault and slump features. Above 2.5 s TWT water depth the upper sedimentary series appear less affected by slumping, yet their surface is obviously eroded and incised in some intervals. The most complete upper sequence is found around SP 11000, where a wedge type reflection pattern has developed up to the outer shelf break in 0.8 s TWT water depth. Three locations for crossing profiles (SCB-A, SCB-B, SCB-C) have been defined from the on-line plot which was not suitable though to identify disturbances precisely enough for a final evaluation of drill sites.

Line GeoB/AWI 96-003 (Fig. 13) across Site SCB-1 is less influenced by sediment tectonism than Line GeoB/AWI 96-001. Although normal faulting of larger blocks is observed, and the shape of the base faults indicates horizontal displacement and a lack of structural integrity, the sedimentary units at Site SCB-1 seem to represent mostly undisturbed sections.

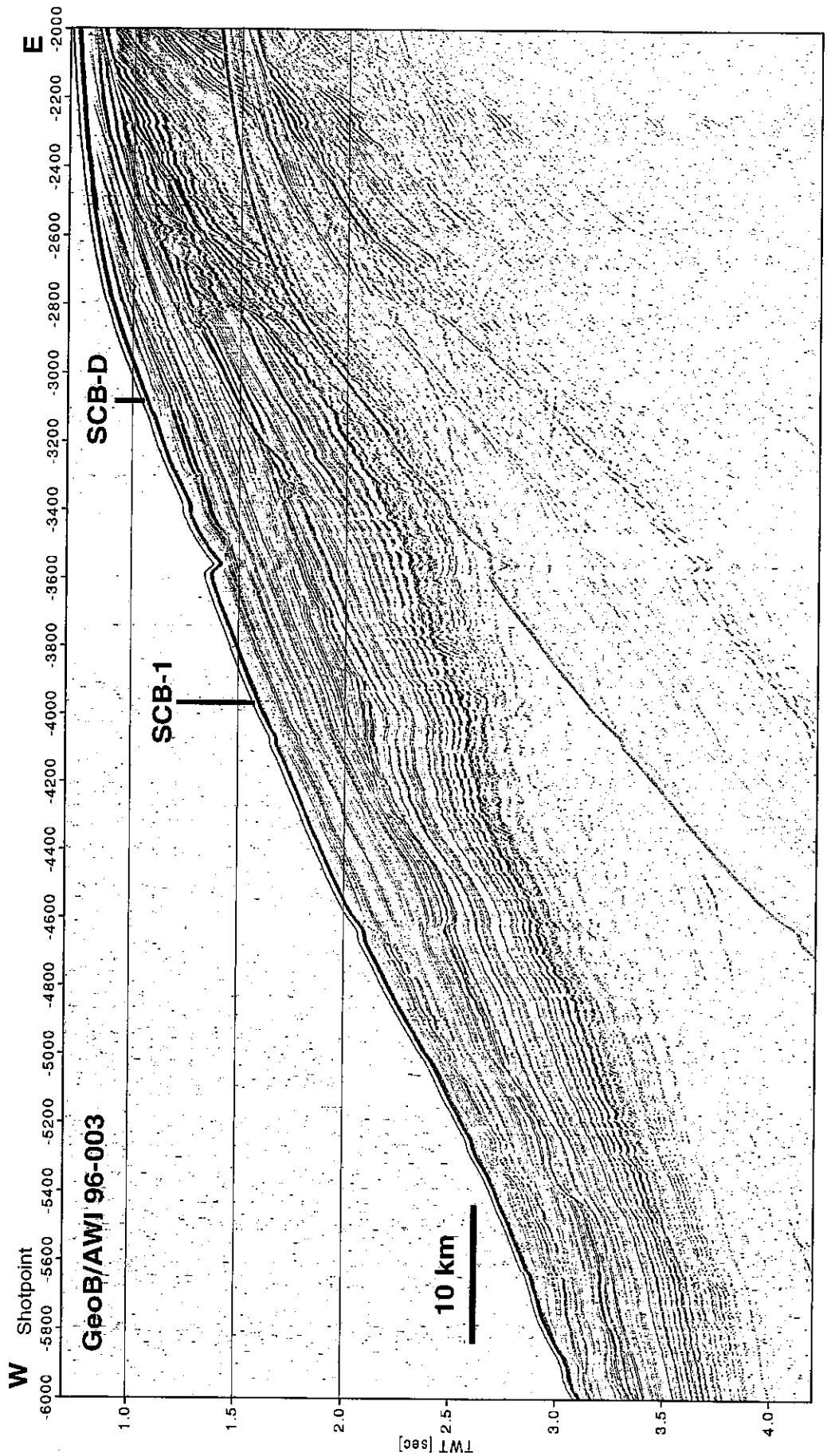

Fig. 13: Seismic Line GeoB/AWI 96-003 between shotpoints 2000 and 6000 across proposed Site SCB-1 in the Southern Cape Basin study area. The profile is less affected by slumping than Line GeoB/AWI 96-001. Crossing with other seismic lines are indicated (see Fig. 9).

Seismic Stratigraphy in the Vicinity of the SCB Sites

In comparison to Line AM-54 the seismic pattern is generally recognized and can be further refined with the two crossing Lines GeoB/AWI 96-003 and -008 in the vicinity of Site SCB-1 (Fig. 14). Seismic Unit I appears mostly well stratified with low amplitudes and contains 3 fine bands of higher amplitude reflectors. The reflector bands become thinner and increase in amplitude towards the prograding shelf break. Since the appearance of this reflection pattern depends on the plotting scale, the unit is not further subdivided. The thickness of Unit I at Site SCB-1 is ~450 ms TWT.

A ~100 ms thick curved decollement zone is clearly identified between Units I and II. The lower sedimentary unit is characterized by numerous reflectors of higher amplitude which become successively more disrupted by small normal faults at depth. An undulating to hummocky interface is found at the base, where the highest amplitudes are associated with hyperbolic echoes. This sequence can be correlated to Units II and III on Line AM-54. The contrasts between Units II and III are not very pronounced, but mainly consists of gradual changes in amplitude and a few low amplitude bands of 20 to 50 ms thickness. The transition between Unit II and III is placed at the base of two transparent intervals at ~2.7 - 2.8 s TWT. Its definition was also based on a comparison with the MCB working area (see chapter 5.1.1.6). A band of five equally spaced reflectors of 120 ms thickness, which increases to 180 ms further upslope, represents Unit III at the proposed drill site.

The base of Unit III is a hummocky zone of up to 100 ms thickness with numerous hyperbolae. In the vicinity of Site SCB-1 the reflection pattern of Unit IV appears discontinuous, amplitudes are subdued. Further up- and downslope, Unit IV is well developed with bands of variable reflection amplitudes. The seismic pattern of Units II to IV is also found on Line GeoB/AWI 96-001, but the appearance of the upper Unit I changes laterally for structural reasons. During the survey 4 additional crossing points SCB-A to SCB-D were selected as alternate drill sites (Fig. 9). The seismic sections in the vicinity of these sites are shown in Figures 15 to 18. Obviously the upper Unit I is heavily affected by downslope slumping with an irregular decollement interface. This probably inhibits drilling of continuous sections and requires careful seismostratigraphic analyses to define unconformities. Reflector AII, which was identified at Site SCB-1 at a depth of ~4.7 s on Line AM-54 (AUSTIN and UCHUPI, 1982), is not covered by Figures 13 and 14.

Since the major seismic units in the area are associated with fault planes, it is difficult at this stage to assign a chronostratigraphy. Seismic Unit III with high amplitudes differs significantly from the upper two units and we tentatively identify the reflector band in Unit III as Reflector D (or L). The nature of this reflector is different than observed at DSDP Site 361 which could be explained by the shallower water depth. A sharp transition from carbonate to pelagic clay cannot be expected here, but fluctuations in carbonate content and dissolution (CCD) are more likely.

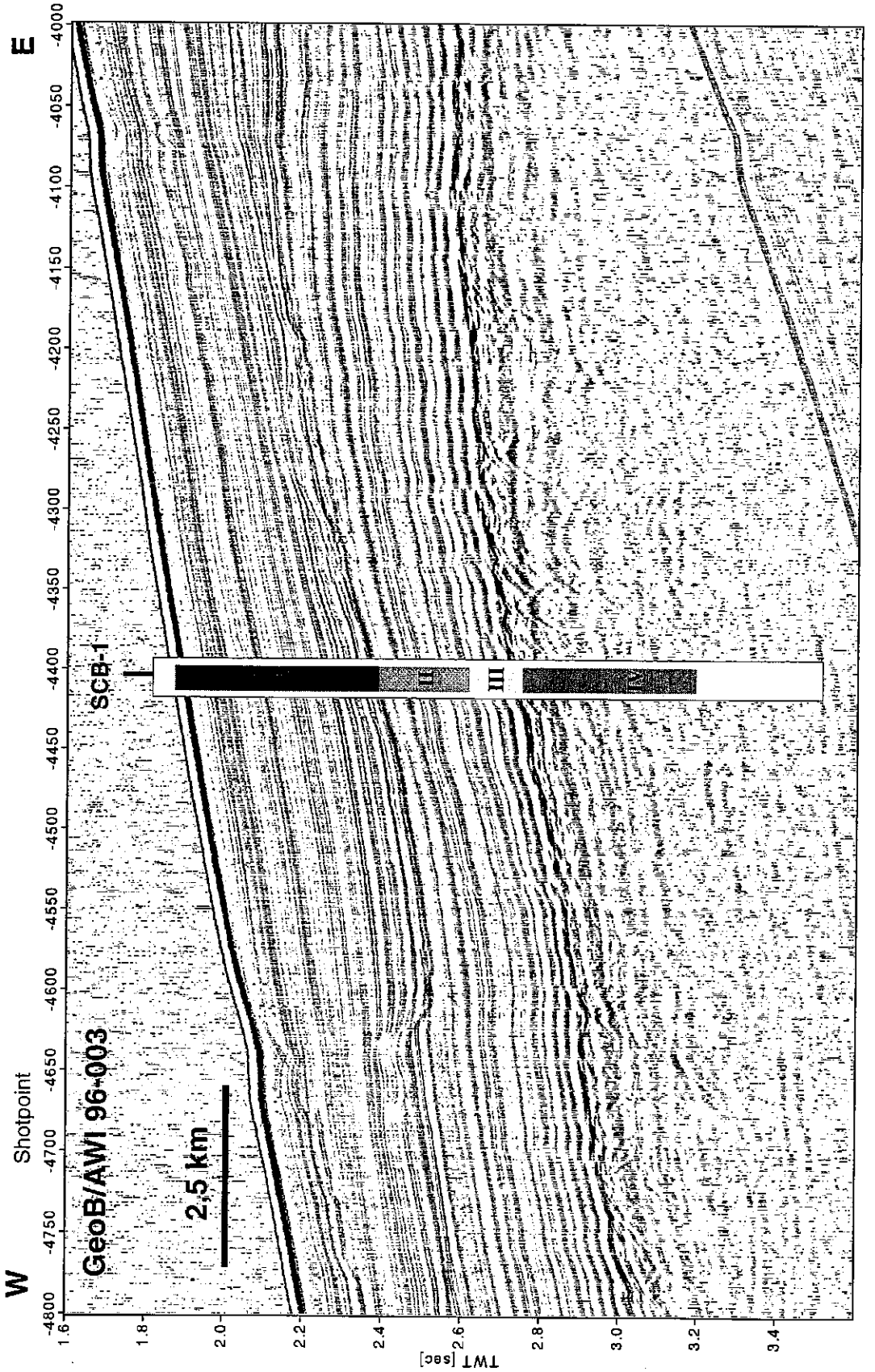

Fig. 14: Multichannel seismic Line GeoB/AWI 96-003 across the proposed drill Site SCB-1 in the Southern Cape Basin study area. Seismic units are indicated by numbers I to IV. See text for further explanations.

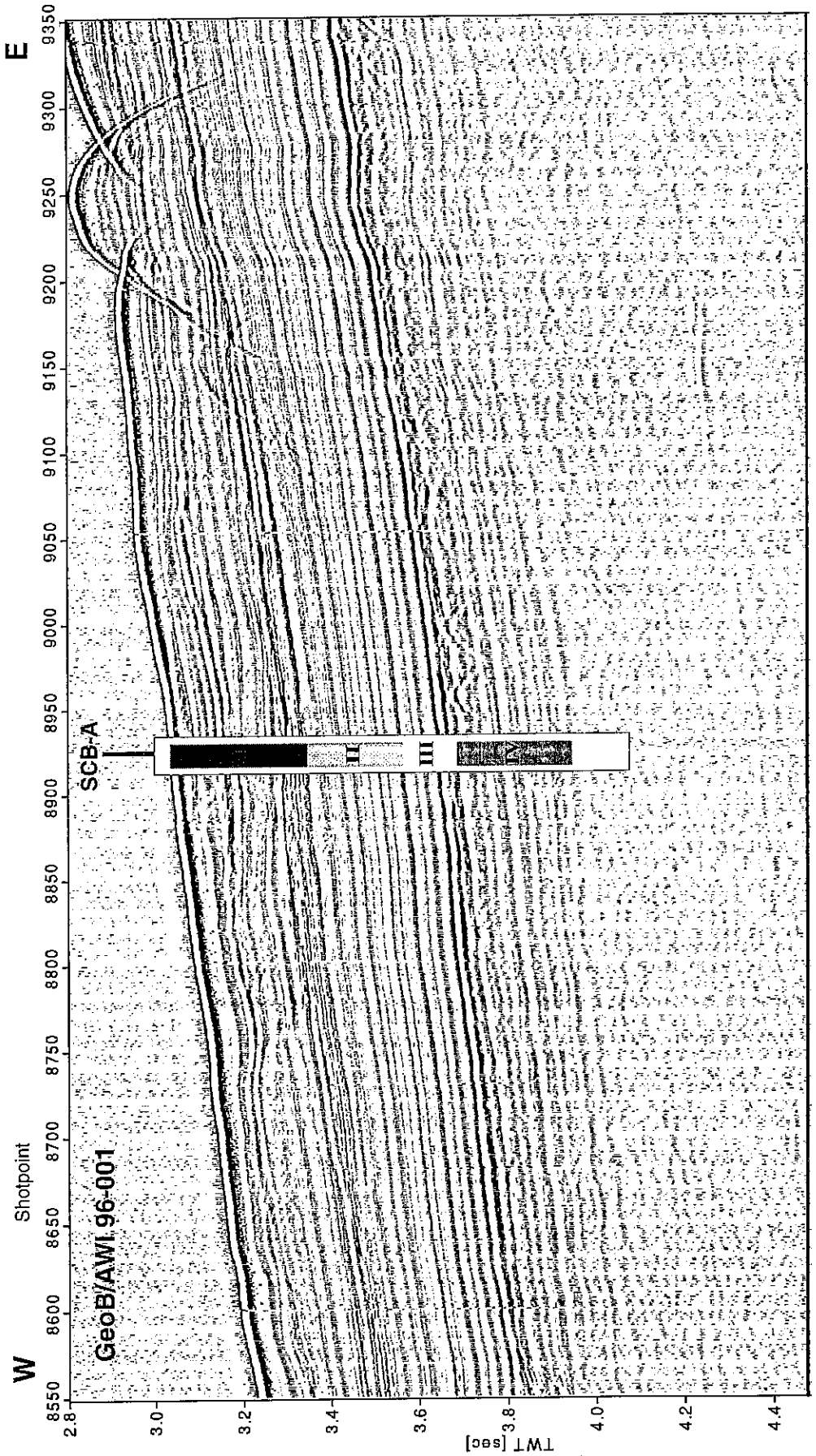

Fig. 15: Multichannel seismic Line GeoB/AWI 96-001 across Site SCB-A. See text for further explanations.

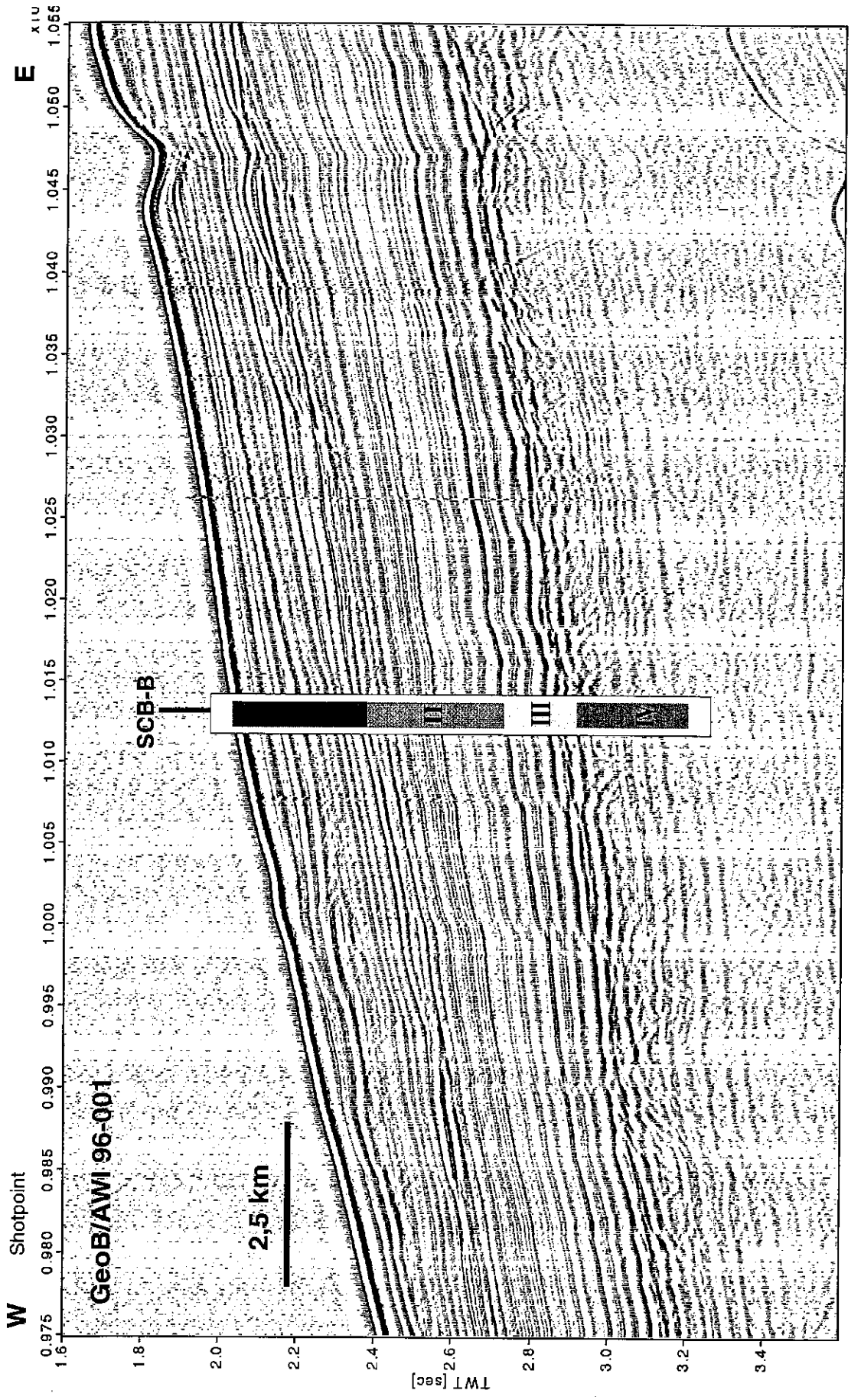

Fig. 16: Multichannel seismic Line GeoB/AWI 96-001 across Site SCB-B. See text for further explanations.

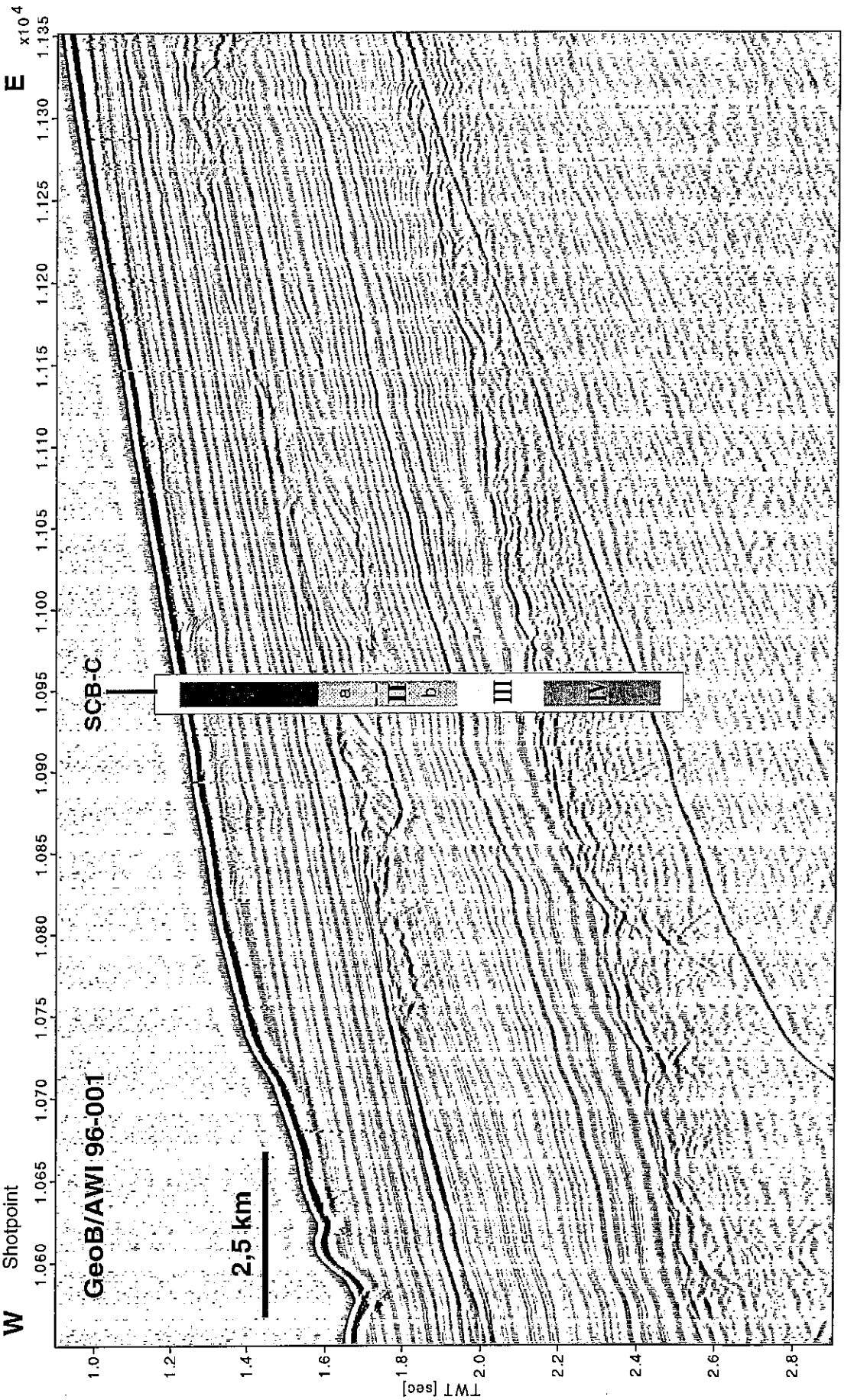

Fig. 17: Multichannel seismic Line GeoB/AWI 96-001 across Site SCB-C. See text for further explanations.

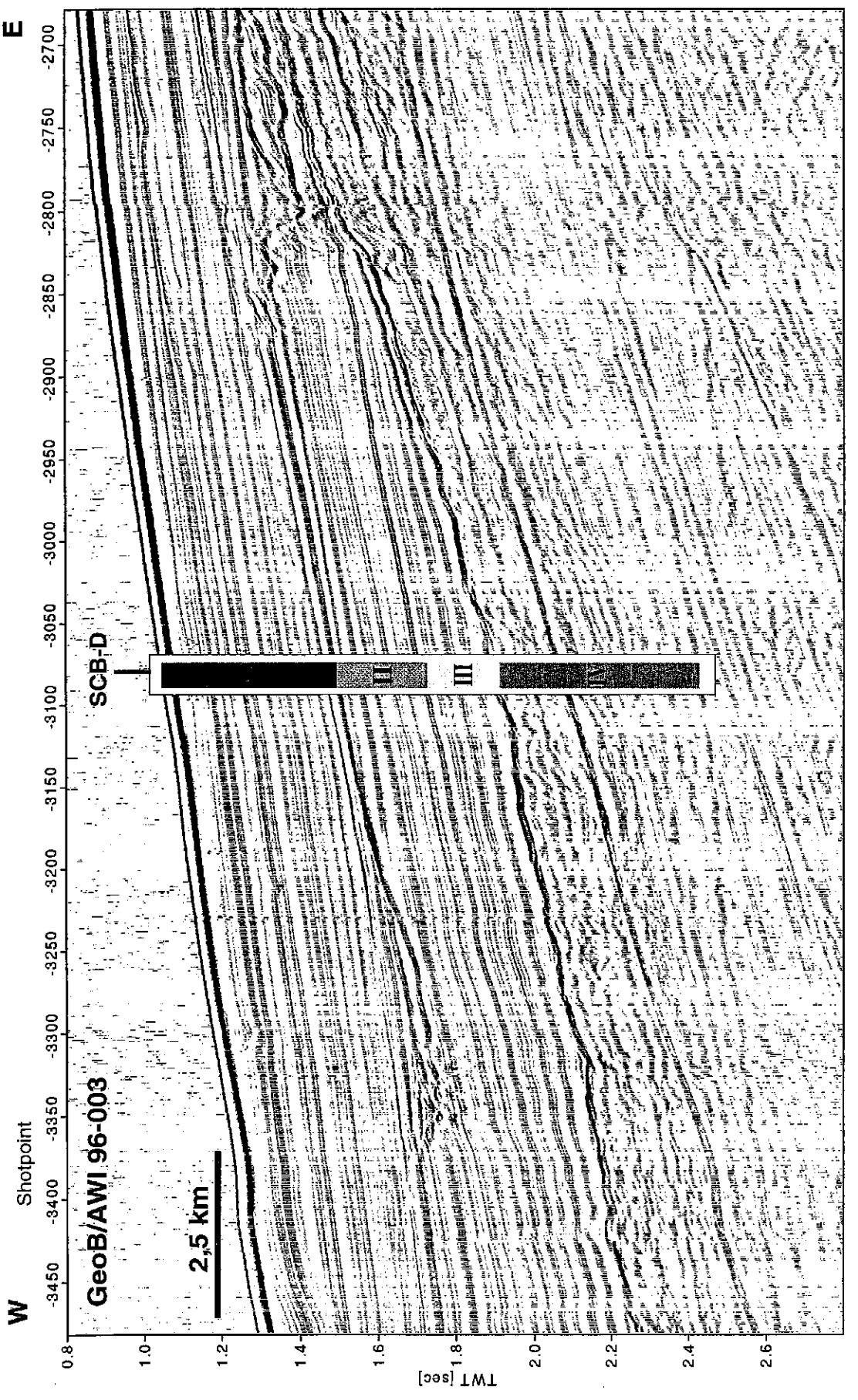

Fig. 18: Multichannel seismic Line GeoB/AWI 96-003 across Site SCB-D. See text for further explanations.

Although the interface between Units I and II may be a discontinuous gliding plane, it is also associated with a change in frequency content which might indicate a shift in sediment composition. A change from a depositional regime dominated by coarser terrigenous input, mainly from the Orange River, to a hemipelagic sedimentation could therefore be responsible for this transition in seismic character. It probably occurred in the Miocene as a response to the aridification of southern Africa and the increasing dominance of biogenic sediment components.

5.1.1.6 Mid Cape Basin

The Mid Cape Basin study area at 29° S was chosen in-between the main working areas at 31° S (SCB) and 25° S (NCB) on the northern side of the Orange Fan. In the structural map of DINGLE et al. (1987) it is situated at the southern rim of a slump region and might therefore be partially free of disturbances. A limited survey was carried out during this cruise to test the area for potential drill sites and also to collect data for a latitudinal correlation of seismostratigraphic interpretations. Since the drilling proposal was targeted to study the temporal and spatial evolution of the upwelling systems along the coast, seismic lines at intermediate latitudes should be essential to image these developments.

In fact, the vicinity of the crossing MCB-A of seismic Lines GeoB/AWI 96-009 and -011 provides an alternate drilling site which might be equally appropriate as the SCB sites to image the early onset of upwelling activities.

5.1.1.6.1 Survey Strategy and Bathymetry

The seismic lines were positioned according to the available data of DINGLE et al. (1987) and from previous PARASOUND surveys during METEOR cruises M20/2 and M23/1, POLARSTERN cruise ANT XI/5 and SONNE cruise SO 86. Surface sediments appeared to be mostly undisturbed in this area.

Figure 19 shows the location of the three seismic Lines GeoB/AWI 96-009 to -011 with a total length of 350 km. The crossing MCB-A (Tab. 6) had to be chosen during the survey from the single trace on-line plot which, mainly because of bad weather conditions, was of limited quality.

The HYDROSWEEP swath sounder survey (Fig. 20) revealed that several scarps exist. They are related to slump events, when major portions of the surface sediment (up to 100 m) were removed. Only on the upper slope, above 2000 m water depth the sedimentary sequences seem to be continuous.

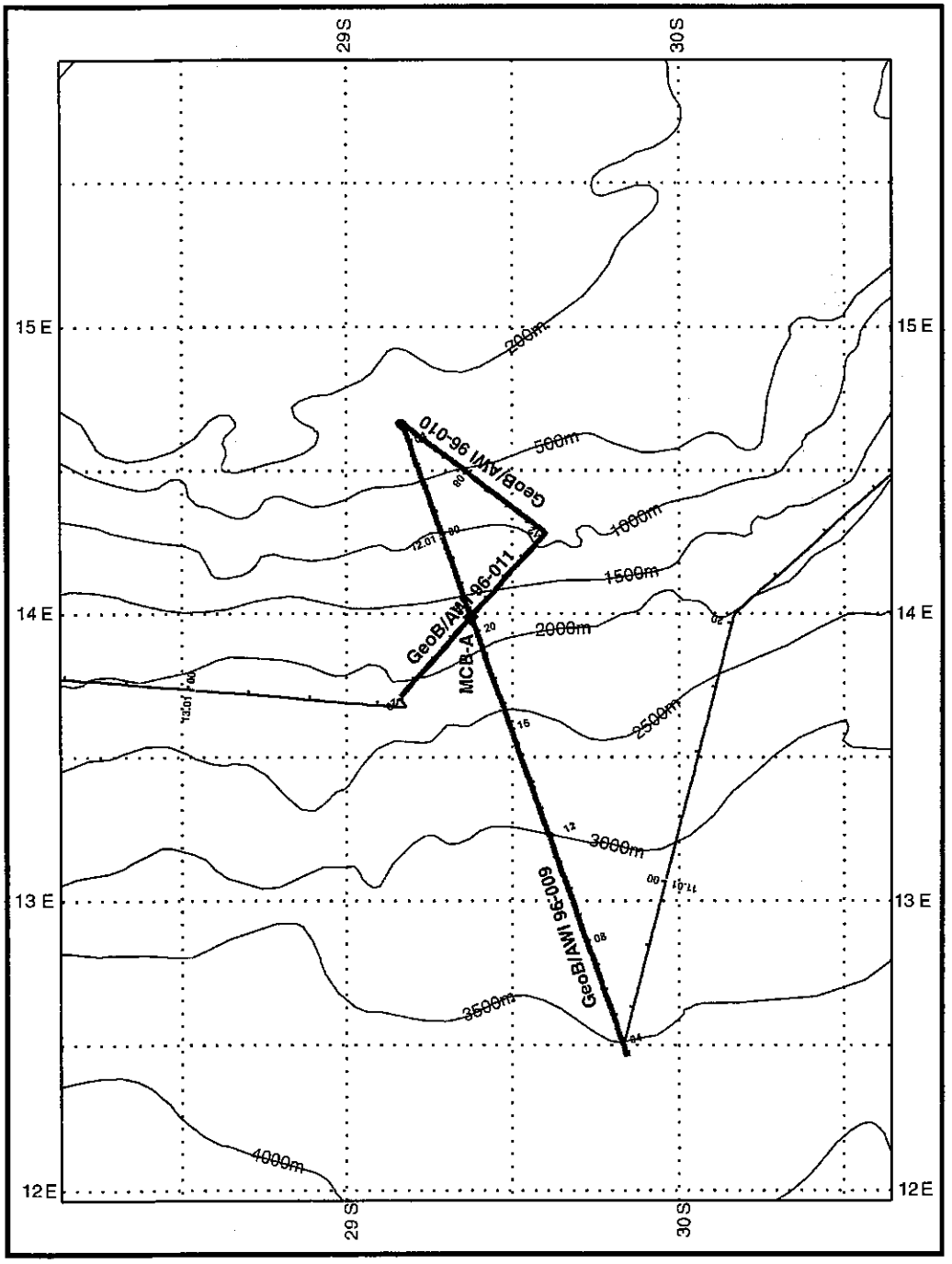

Fig. 19: RV METEOR M34/1 track chart in the Mid Cape Basin working area. Seismic profiles GeoB/AWI 96-009 to -011 (thick lines) and cruise track are annotated with date and time (every 4 hours), ticks are plotted at 1 hour intervals. Bathymetry was extracted from the Gebco Digital Atlas 1.01.

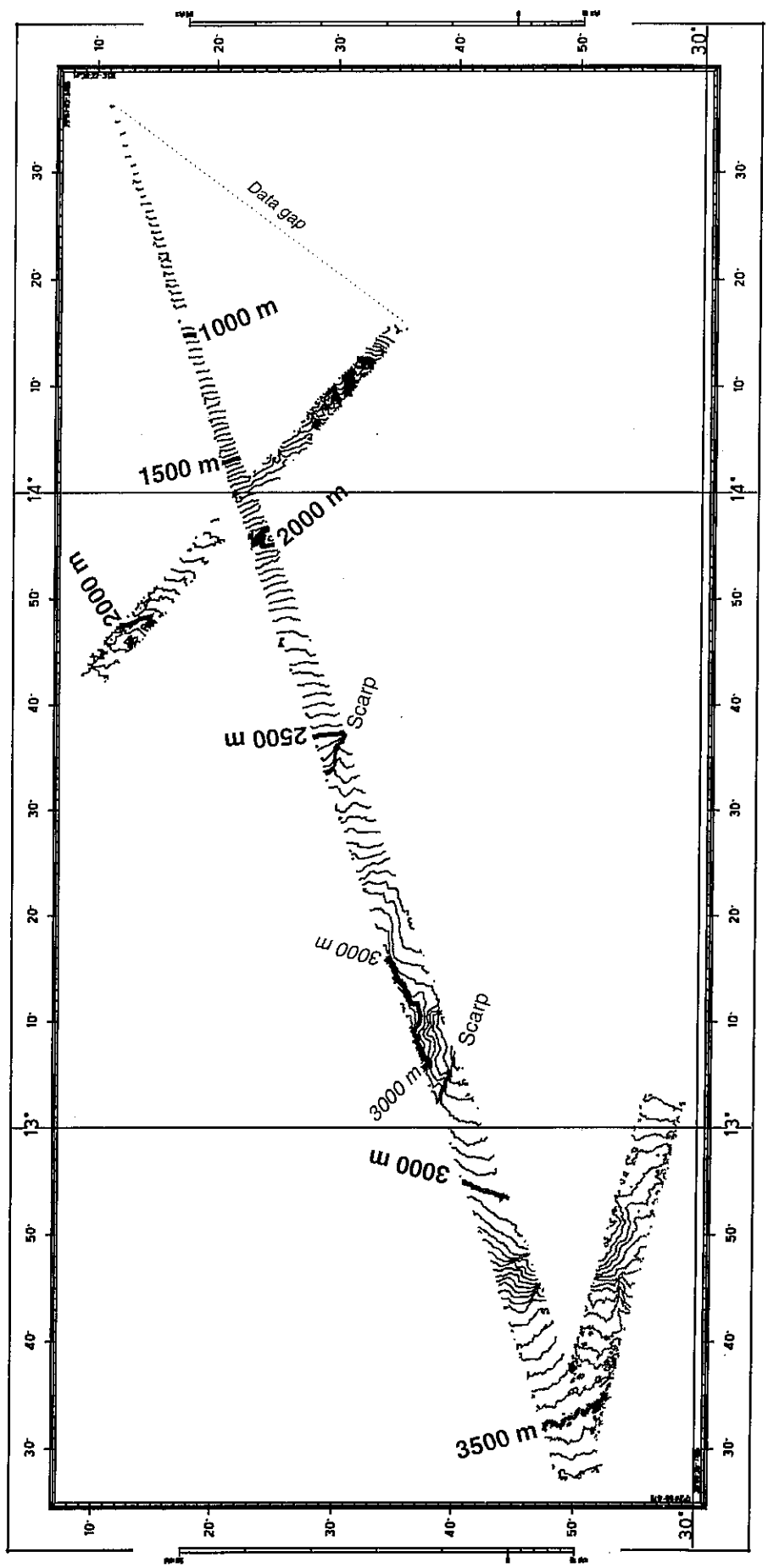

Fig. 20: HYDROSWEEP bathymetric survey in the Mid Cape Basin working area (25 m contour intervals).

Tab. 6: Crossings of seismic lines at proposed drill sites in the MCB working area

Site	Line GeoB/AWI	Shot Point	Date 1996	Time	Latitude	Longitude	Water Depth [m]
MCB-A	96-009	671	11.01.	20:38	29°22.5'S	13°59.4'E	1726
	96-011	684	12.01.	15.53			

5.1.1.6.2 Seismic Stratigraphy

Although the seismic character in the vicinity of the crossing MCB-A is different on profiles GeoB/AWI 96-009 (Fig. 21) and -011 (Fig. 22) compared to the SCB working area, several similarities were observed.

The most prominent feature is a band of high-amplitude reflectors between 800 and 1000 ms sub-bottom TWT. It appears to be identical with the base of seismic Unit II in the SCB area which was correlated to Reflector D (L) of Cretaceous to Paleocene age. The reflection pattern is smooth and no indication could be found for slumping or internal fracturing by small faults. The thickness of 1000 ms of the sediment package above Reflector D is slightly higher than the 850 ms in the SCB region.

This may indicate a higher sedimentation rate, but the sequence could also be more complete than in the slumping area further south. The listric fault planes of the slumps are responsible there that a significant portion of the sedimentary column close to the gliding interface is missing. The comparison of the two seismic patterns seems to confirm this assumption and yields a difference of ~150 ms.

It should be considered to include Site MCB-A into the drilling program as alternate site, since it will probably provide a more continuous section through critical periods of the Neogene than all sites in the SCB area.

The sediment package above Reflector D is less structured than at the SCB sites as the strongly reflecting gliding planes and an associated fracturing are missing. The upper 260 ms (seismic Unit I) are characterized by several reflectors of relatively high amplitude and low frequency, but there is indication from the geometry of these reflectors that they might be artifacts comparable to ghost signals or bubble pulses following the sea floor morphology and crossing internal reflectors of higher frequency.

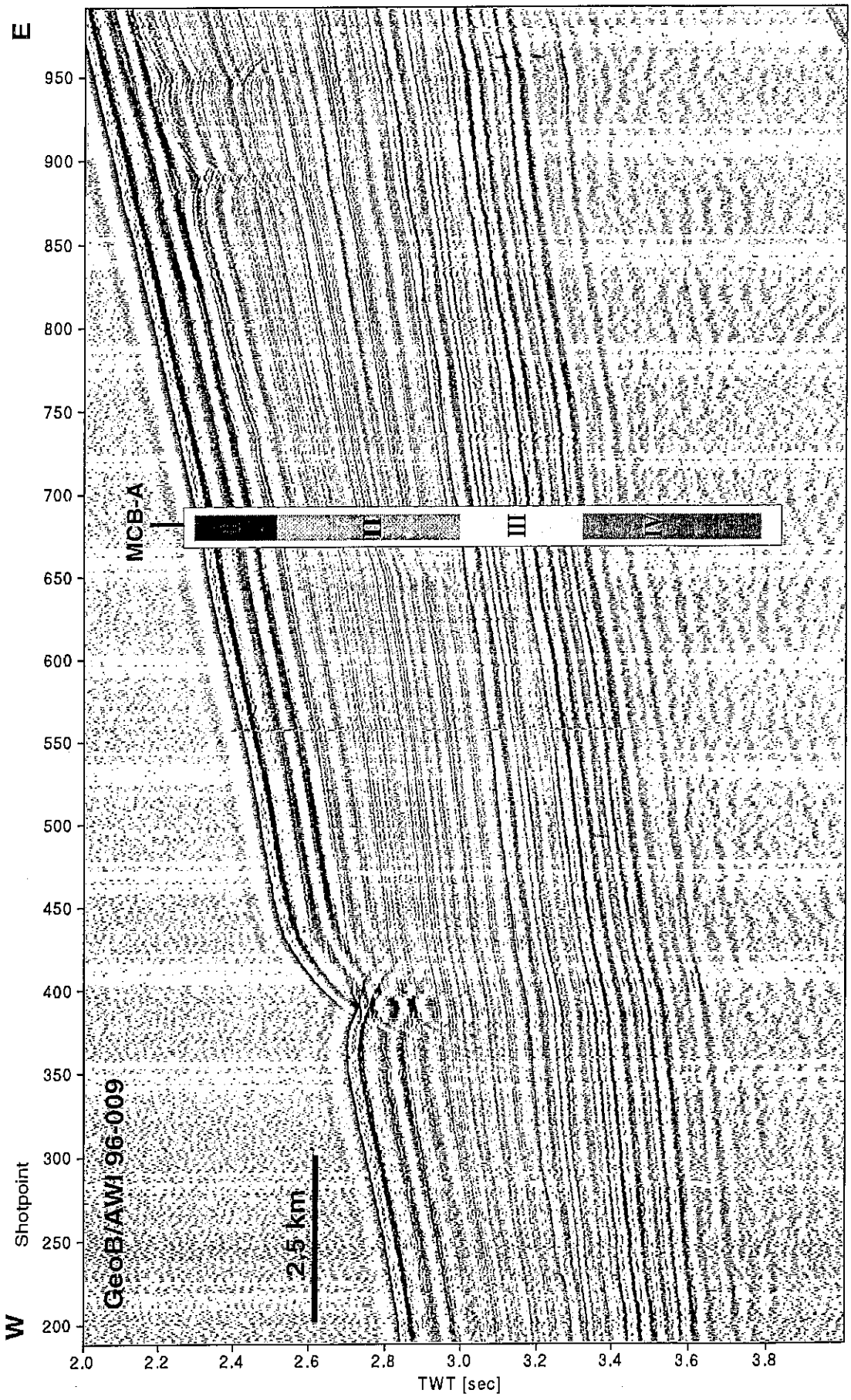

Fig. 21: Multichannel seismic Line GeoB/AWI 96-009 across Site MCB-A. See text for further explanations.

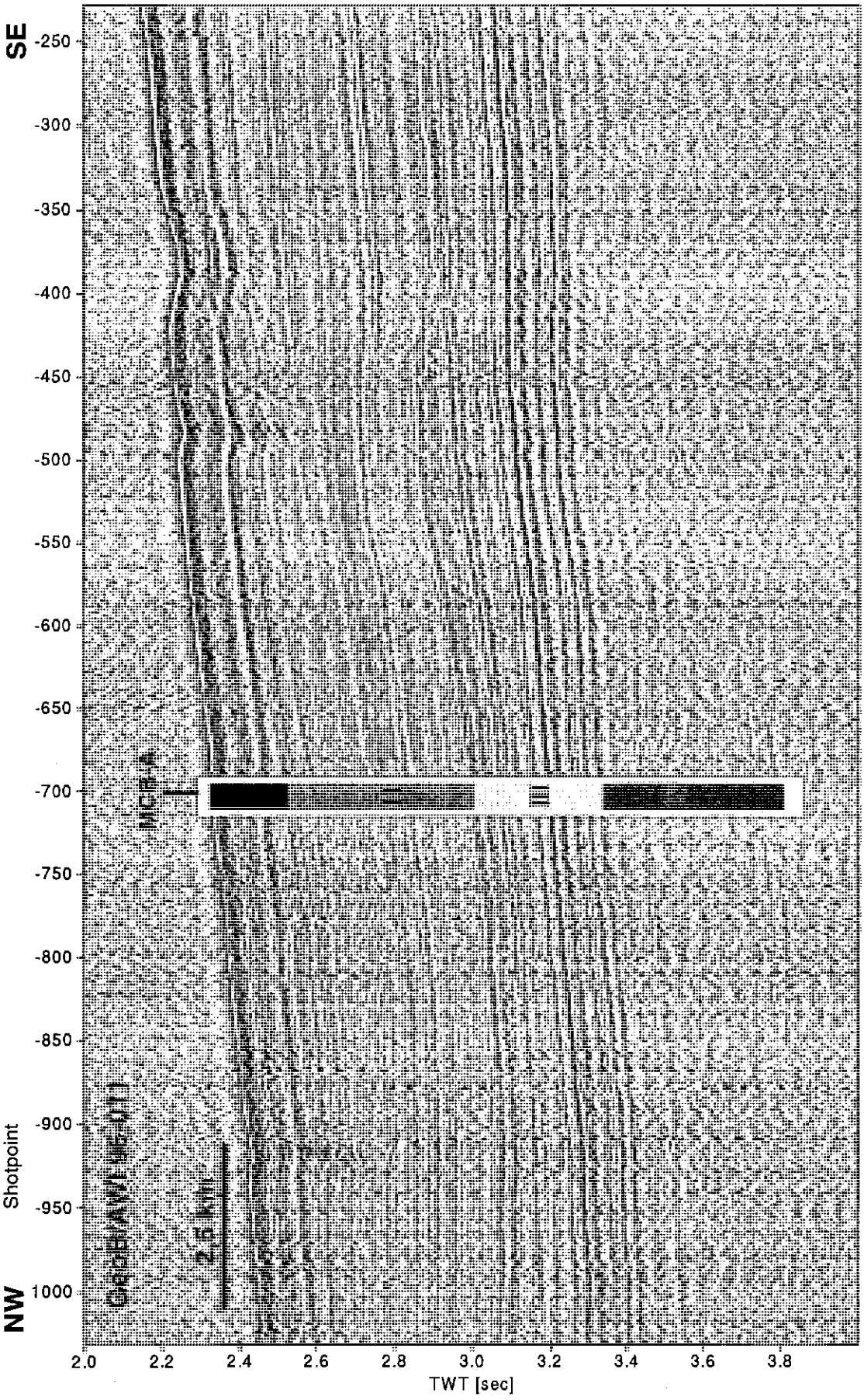

Fig. 22: Multichannel seismic Line GeoB/AWI 96-011 across Site MCB-A. See text for further explanations.

Seismic Unit II (260 to 700 ms) reveals numerous closely spaced low-amplitude reflectors. The variability in acoustic impedance and sediment physical properties seems to be low. The relative homogeneity of this unit indicates a stable hemipelagic sedimentation regime in this area, a high content of fine grained material and the absence of carbonate dissolution events.

Seismic Unit III between 700 and 1000 ms sub-bottom TWT contains a larger number of strong reflectors. Their reflection amplitudes increase to depth. Within the lower portion a reflector band is identified which can easily be correlated to the SCB sites. A preliminary interpretation would explain this feature with fluctuations in carbonate content due to successive events of carbonate dissolution or terrigenuous input. Most likely it can be identified as Reflector D (Cretaceous-Paleocene).

A more detailed chronology cannot be assigned at this stage of the analysis. It must await further data processing and comparative studies between the working areas.

5.1.1.7 Northern Cape Basin

The distribution of drill sites along the southwest African continental margin was chosen to image the latitudinal evolution of the Benguela Current System in space and time. The working area in the Northern Cape Basin (NCB) lies directly seaward of the currently most productive coastal upwelling cells. Therefore, the drill sites are targeted to study the variability of the upwelling system and mechanisms of 'leakage' of upwelling sediments into the hemipelagic realm and to analyze and date the onset and early stages of upwelling processes at this latitude.

Two drill Sites NCB-1 and -2 had been originally proposed on Line AM-1 of AUSTIN and UCHUPI (1982). The site in only 180 m water depth was not included in the final drilling plan due to time constraints and the general problems with drilling in shelf regions.

The area was visited during RV SONNE cruise SO 86, when multichannel seismic data were collected about perpendicular to Line AM-1. While the shallow water site could be sufficiently surveyed, the profile across the deeper site (NCB-1) had to be abandoned on the approach because of technical problems and, due to a lack of time, no further survey has been carried out.

During RV METEOR cruise M34/1 three additional seismic lines with a total length of 321 km were measured. Together with the previously collected data the vicinity of the proposed Site NCB-1 is now sufficiently studied to precisely locate a drill site.

5.1.1.7.1 Survey Strategy and Bathymetry

Since the shallow NCB site was well defined on seismic Line AM-1 of AUSTIN AND UCHUPI (1982) and Lines GeoB/AWI 93-042 to -044, only the vicinity of the deeper Site NCB-1 was surveyed to understand the local tectonic and depositional framework and its relationship to the continental shelf. Crossings of seismic lines and proposed drill sites are summarized in Table 7.

Tab. 7: Crossings of seismic lines at proposed drill sites in the NCB working area

Site	Line GeoB/AWI	Shot Point	Date 1996	Time	Latitude	Longitude	Water Depth [m]
NCB-1	96-012	3623	14.01.	02:10	25°27.6'S	13°05.3'E	1763
	96-014	2309	14.01.	22:11			
NCB-1A	96-012	3921	14.01.	03:00	25°25.8'S	13°01.3'E	1956
NCB-1B	96-014	1969	14.01.	21:13	25°30.8'S	13°01.7'E	2004

Figure 23 shows the track chart for the NCB working area which also includes the location of the previously collected multichannel seismic lines of RV SONNE cruise SO 86. The bathymetry as derived from the HYDROSWEEP swath sounder survey (Fig. 24) gives no indication for slumping or other disturbances. The continental slope is smooth with a moderate maximum slope angle of ~1.5° in the vicinity of the drill site.

5.1.1.7.2 Seismic Stratigraphy

Figures 25 and 26 show the seismic lines GeoB/AWI 96-012 and -014 which cross at Site NCB-1. In some intervals they reveal differences, but in general the area is characterized by an apparently continuous and mostly undisturbed sedimentation.

Line GeoB/AWI 96-012 leads from the shelf to a water depth of ~3000 m. The record on the shelf is severely affected by a bubble or ghost signal and multiple reflections. Processing of

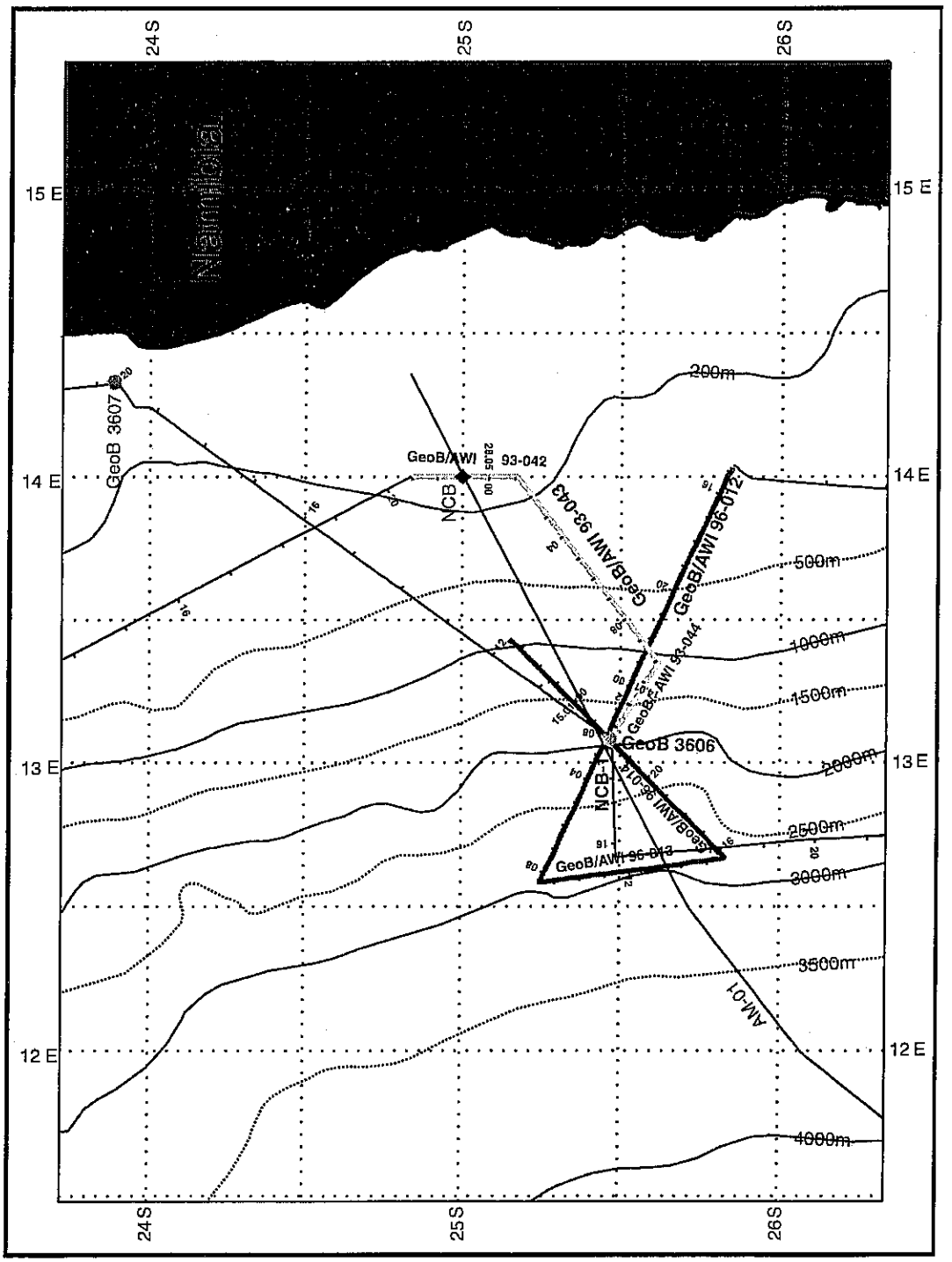

Fig. 23: RV METEOR M34/1 track chart in the Northern Cape Basin working area. Thick lines denote seismic profiles. Seismic lines of RV SONNE cruise SO 86 are plotted in light grey. Bathymetry was extracted from the Gebco Digital Atlas 1.01.

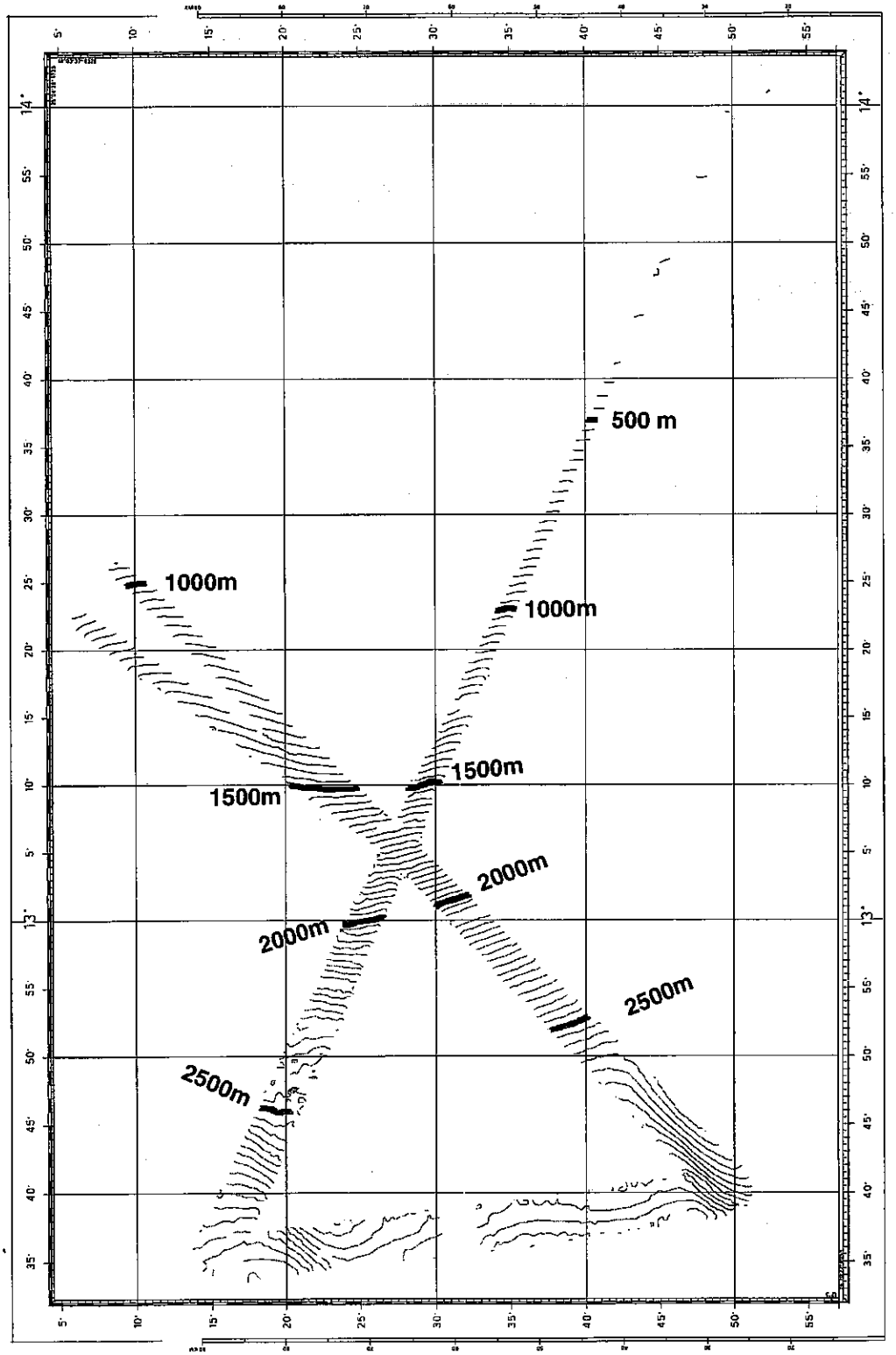

Fig. 24: HYDROSWEEP swath sounder survey in the Northern Cape Basin working area (25 m contour intervals).

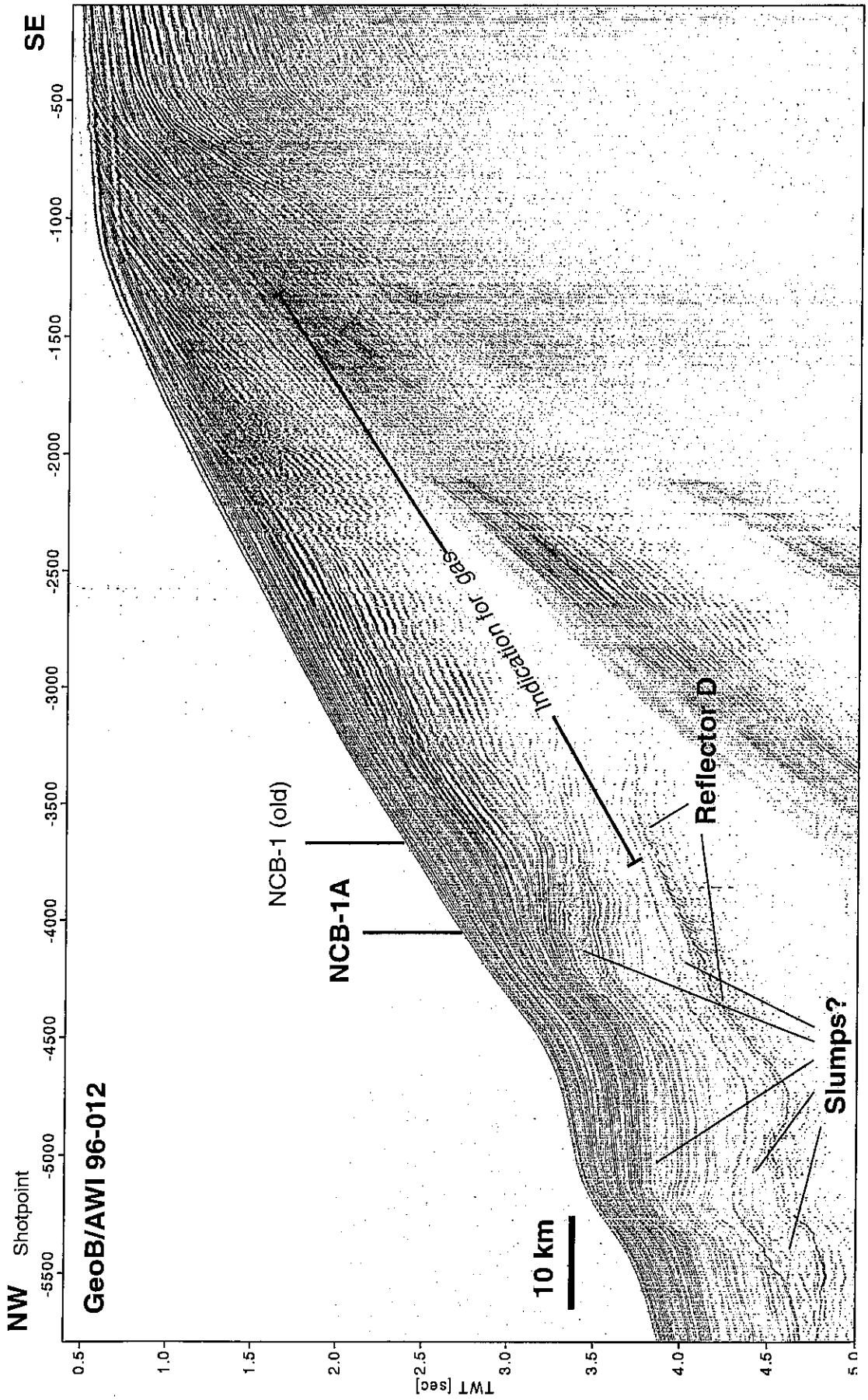

Fig. 25: Multichannel seismic Line GeoB/AWI 96-012 across Site NCB-1. See text for further explanations.

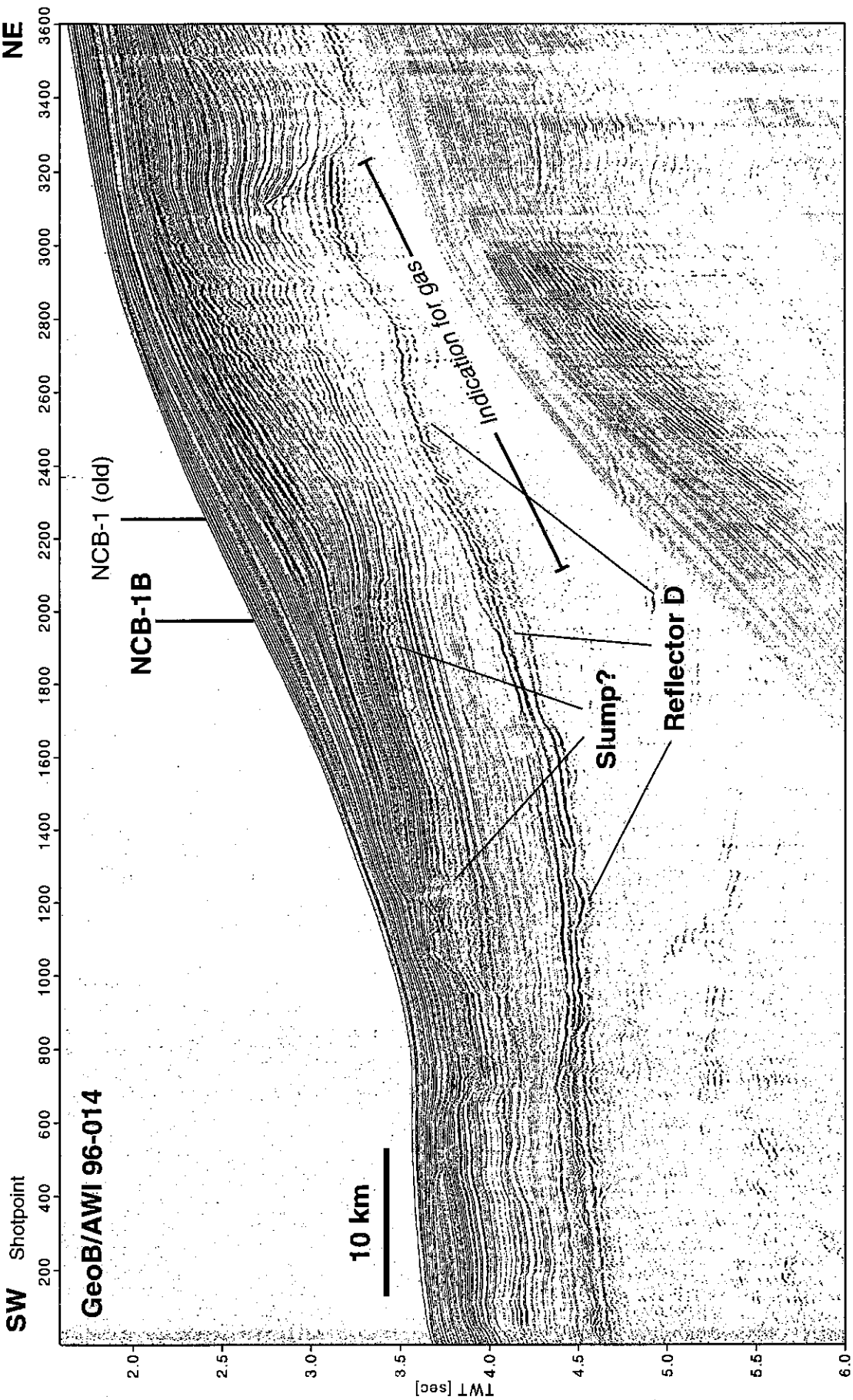

Fig. 26: Multichannel seismic Line GeoB/AWI 96-014 across Site NCB-1. See text for further explanations.

the multichannel data is required to disclose further details, the typical structure of a prograding shelf edge can already be recognized, however. The thickness of the uppermost sediment package increases towards Site NCB-1 and decreases slightly further downslope. The undulating morphology is related to deeper structures. Their nature cannot be determined from the present records.

Between SP 5800 and 3600 a band of strong reflectors can be identified at ~1 - 1.5 s sub-bottom TWT. The up to 200 ms thick, lens-shaped unit above probably originates from a slump event. The reflectors show a remarkable similarity to the working areas further south and are tentatively interpreted as Reflector D (L). Near Site NCB-1 the sediment thickness above Reflector D is 1.5 s TWT which is ~50 % higher than in the south. The additional sediment input is possibly derived from the coastal upwelling cells and increased surface water productivity.

From shotpoint 3800 to 2000 a band of reflectors with unusually low frequencies is observed ~200 - 300 ms below the sea floor masking all internal structures beneath. This gives strong evidence for gas accumulation which will affect the sediment properties and presumably inhibit the retrieval of undisturbed sediment cores.

The same observation can be made on the second seismic Line GeoB/AWI 96-014 across Site NCB-1 from shotpoint 2000 to 3200. Again several reflectors reveal unusually high amplitudes, but masking of lower sequences is less pronounced. In particular the reflector band at 1.3 - 1.5 s sub-bottom TWT can be traced along the profile and provides a suitable framework for the stratigraphic correlation of the base of Tertiary. Although major slump structures were not found, the lens-shaped unit is also seen on Line GeoB/AWI 96-014 between shotpoints 1000 and 2200.

It can be expected that the high organic input from the upwelling system will generate gas and affect the core quality. As areas of higher gas content must generally be avoided, the drill site should perhaps be moved further downslope, either to SP 4050 of Line GeoB/AWI 96-012 (Site NCB-1A) or SP 1950 of Line -014 (Site NCB-1B). The Neogene sequence is thinner at these locations and therefore also a high quality coring would be possible further back in time.

In Figures 27 and 28 two seismic units are defined above Reflector D which are mainly distinguished by their frequency content. The upper Unit I of 600 - 700 ms thickness reveals numerous closely spaced reflectors. Amplitudes are relatively low without a pronounced variability as observed in the working areas further south. The seismic patterns of this unit are very similar to those found in upwelling sediments off Angola north of Walvis Ridge at ~17°S during RV SONNE cruise SO 86.

Between seismic Units I and II an interval of hummocky to chaotic reflectors is observed which also lacks continuity in reflection energy. The variation in thickness of this interbedded layer hints to a slump mass: It was is not included as an individual seismostratigraphic unit.

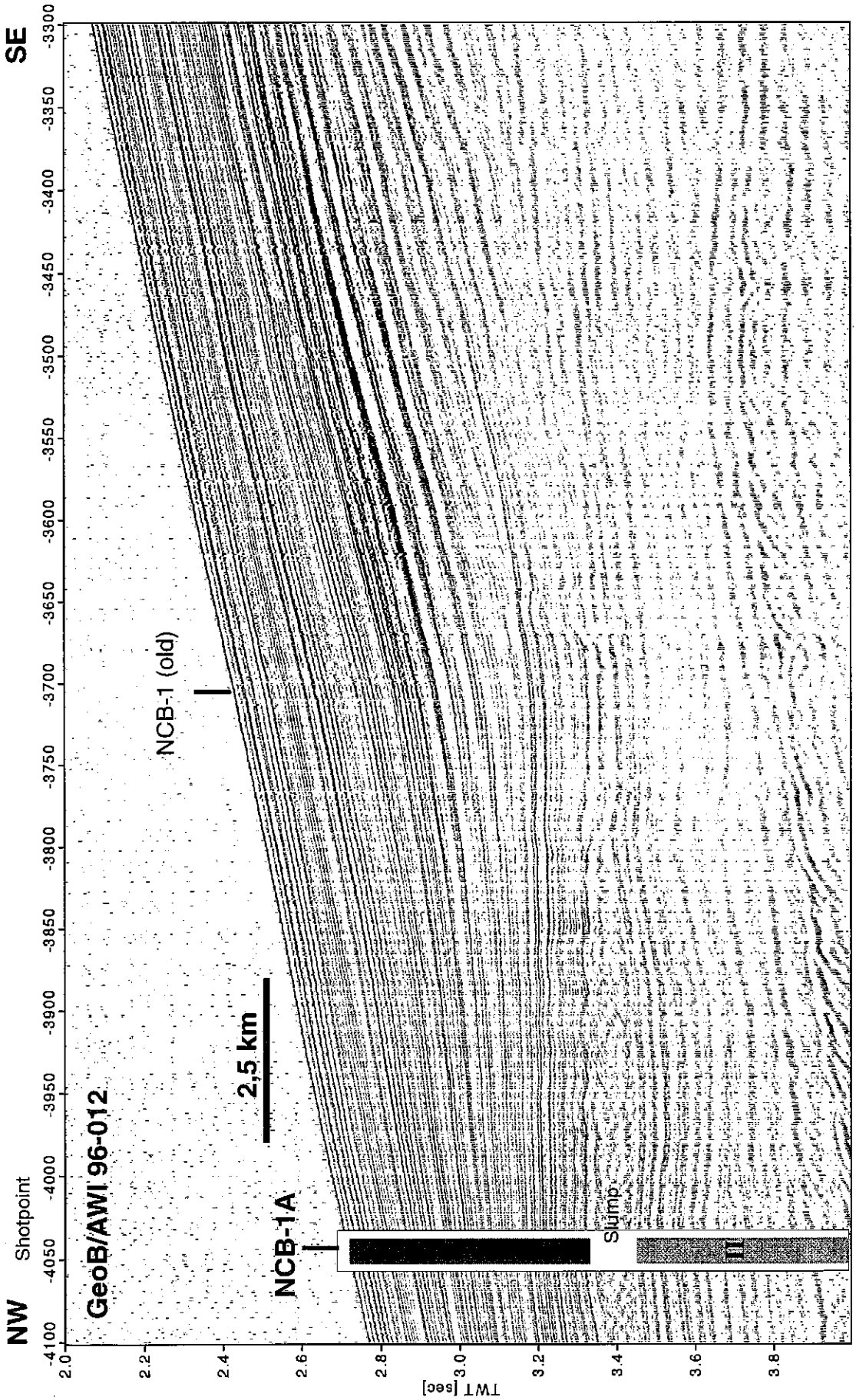

Fig. 27: Multichannel seismic Line GeoB/AWI 96-012 in the vicinity of Site NCB-1. See text for further explanations.

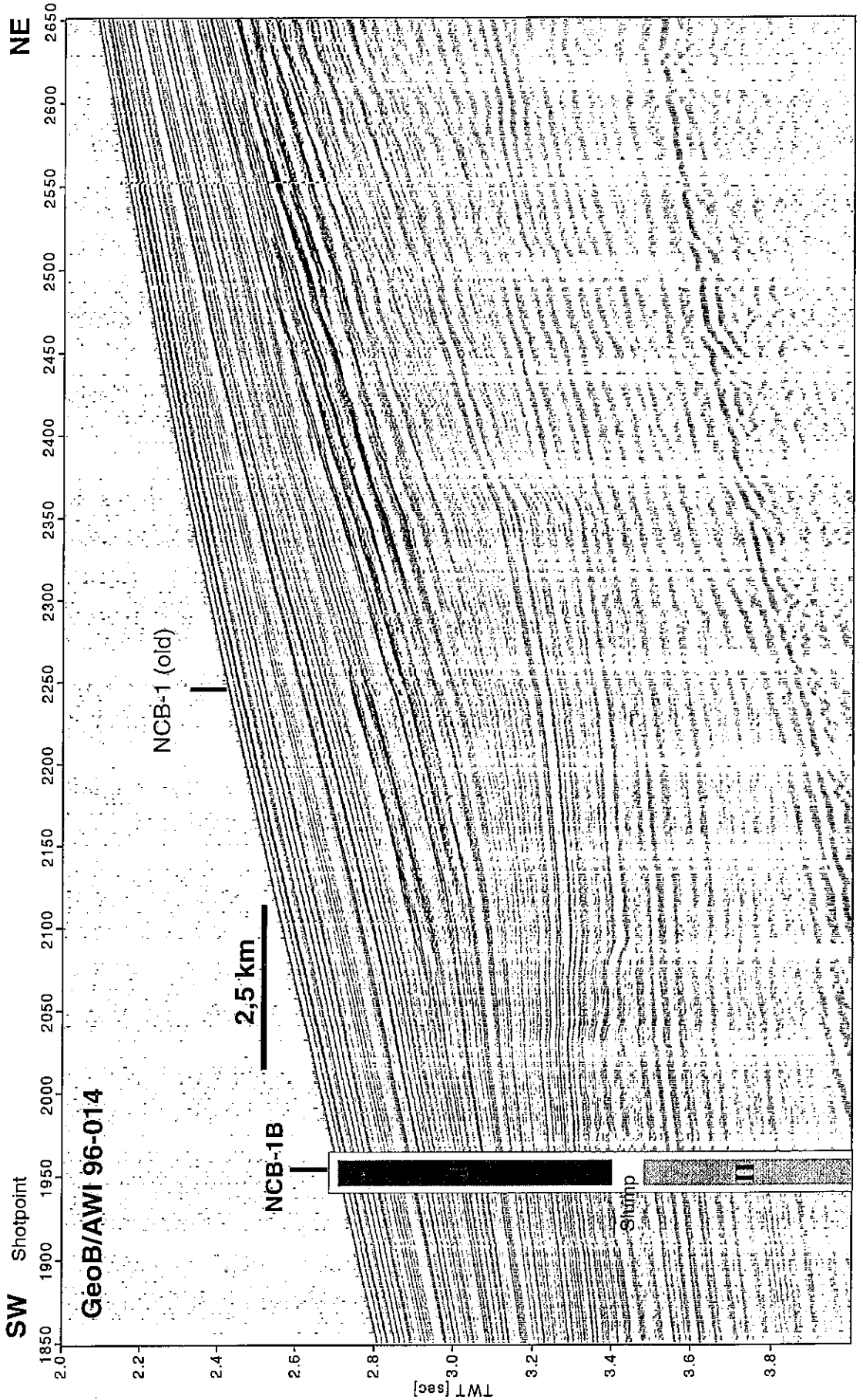

Fig. 28: Multichannel seismic Line GeoB/AWI 96-014 in the vicinity of Site NCB-1. See text for further explanations.

Below, the decreasing frequency content could be explained either by seismic attenuation or by a transition in lithologies from fine-grained, organic-rich materials to carbonaceous sediments. According to the current drilling plan, this Unit II will not be cored due to the great sub-bottom depth of ~700 ms. A further refinement of the seismostratigraphic units will again only be possible with a processing of the multichannel seismic data. In particular, the large variability in frequency content must be carefully evaluated to understand the nature of individual reflectors and reflector bands.

It can be speculated whether the slump interface between Units I and II also marks the onset of upwelling activity combined with a change in sea level and could be assigned an Oligocene/Early Miocene age.

5.1.1.8 Walvis Basin and Walvis Ridge

In the original drilling proposal one Walvis Ridge site was projected to study the upwelling signal transported from the coast to the location by the Benguela Current. The results were to be combined with DSDP Site 532/362 which was drilled in 1300 m water depth on the ridge crest. Subsequent studies of the Bremen geophysical group have shown that sedimentation in the vicinity of DSDP Site 532 is affected by small scale mud waves. The limits of direct comparisons where deposition is selective due to bottom currents should therefore be carefully evaluated.

Furthermore, the drilling results have revealed major unconformities of both long and short duration. Studies on GeoB gravity cores likewise showed numerous short hiatuses in the late Quaternary, presumably caused by the exposed location of the ridge crest in the center of the over wide areas erosive Antarctic Intermediate Water.

Therefore, not only the area around the proposed Site WR-1 was surveyed, but also connecting profiles to DSDP Site 532 and to a net of seismic lines in the Walvis Basin were measured.

Lines GeoB/AWI 96-022 and -021, running south-north from the Walvis Basin towards DSDP Site 532, exhibit pronounced erosive interfaces. Large portions of the sedimentary column are missing on Walvis Ridge which seem to be present in the Walvis Basin as continuous sections. Line GeoB/AWI 96-015 shows that seaward of the active coastal upwelling cells a depositional basin has developed. It documents stationary conditions over extended periods of time and appears neither be affected by slumping nor by bottom current erosion.

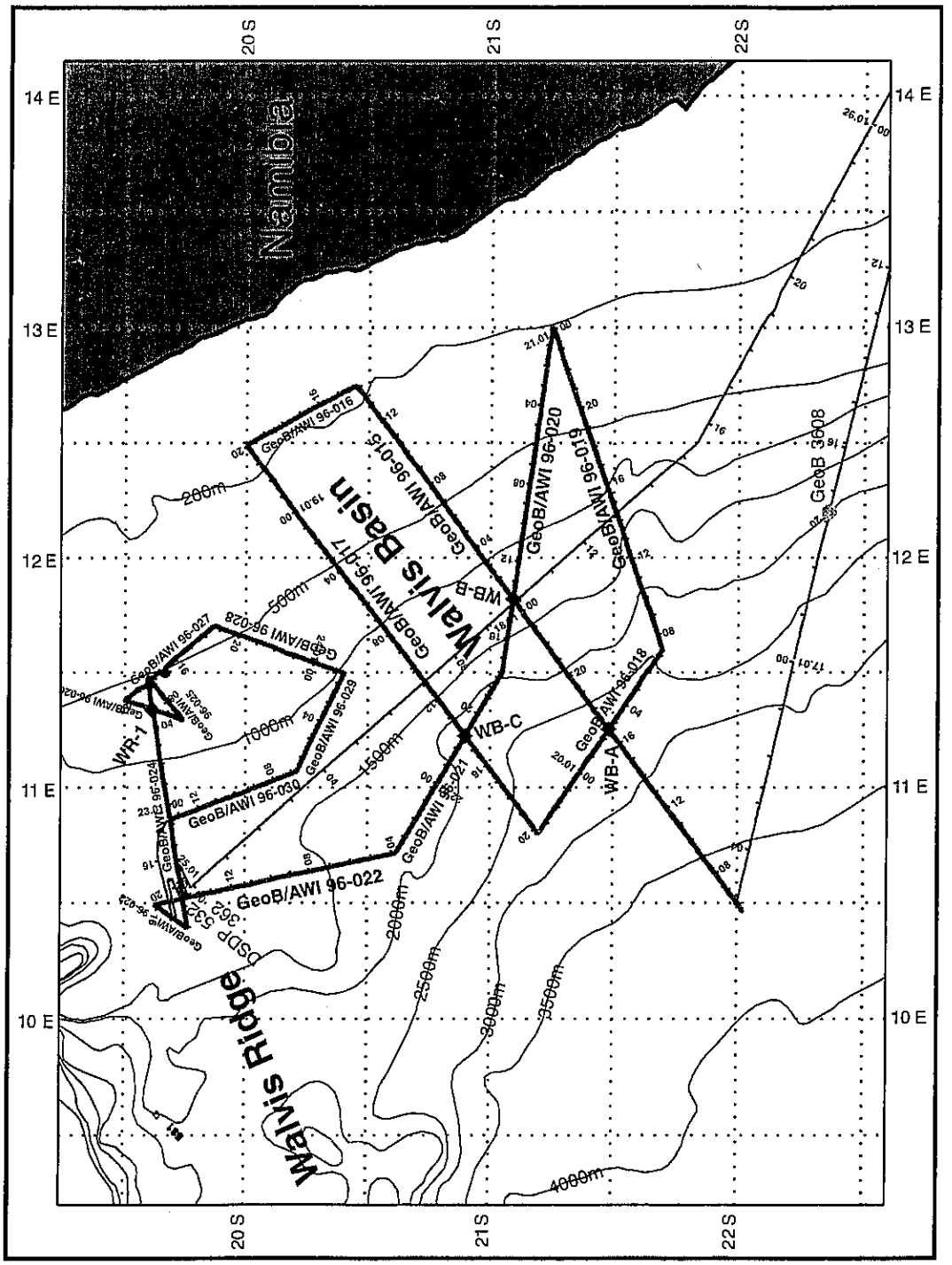

Fig. 29: RV METEOR M34/1 track chart in the Walvis Basin and on the Walvis Ridge. Thick lines denote seismic profiles. Bathymetry was extracted from the Gebco Digital Atlas 1.01.

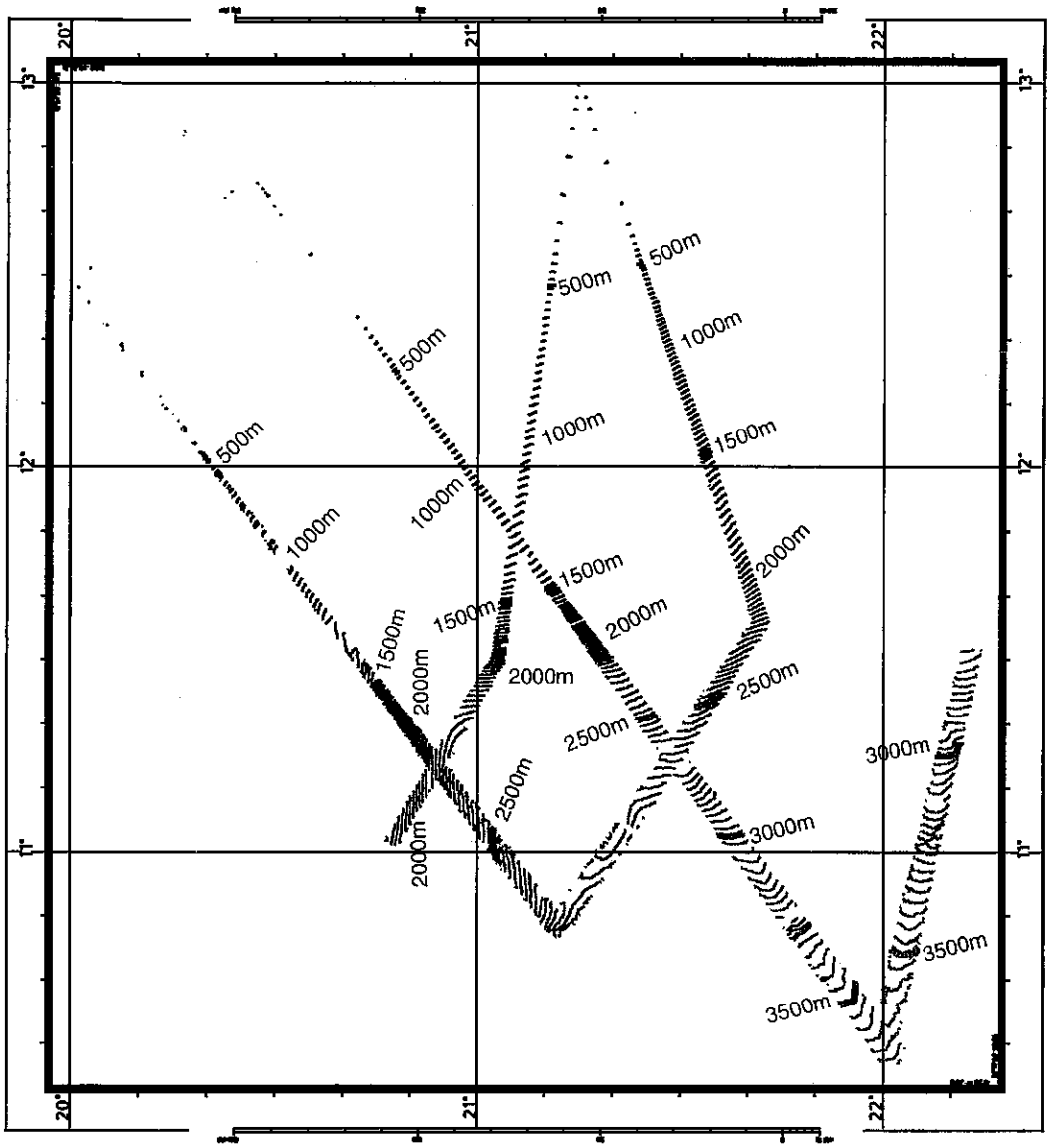

Fig. 30: HYDROSWEEP swath sounder survey in the Walvis Basin (25 m contour intervals).

5.1.1.8.1 Survey Strategy and Bathymetry

The track chart of RV METEOR cruise M34/1 in the Walvis Ridge / Walvis Basin area is shown in Figure 29. A net of 16 seismic lines with a total length of 1550 km was recorded. About 395 km are located on the crest and the southern flanks of the Walvis Ridge, 1155 km cover the Walvis Basin. The seismic survey was projected to image the regional deposition pattern influenced by different sources:

- upwelling sediment, transported by the Benguela Current and associated eddies traveling seaward,
- biogenic components derived from the locally higher productivity in nutrient loaded upwelling waters,
- eroded sediments from the Walvis Ridge crest. Their input depends on the intensity of the Benguela Counter Current.

The data will be integrated into a regional seismostratigraphic framework which should allow an analysis of sediment distribution patterns through time. Crossings of seismic lines and proposed drill sites are summarized in Table 8.

Tab. 8: Crossings of seismic lines and proposed drill sites in the Walvis Ridge / Walvis Basin working area

Site	Line GeoB/AWI	Shot Point	Date 1996	Time	Latitude	Longitude	Water Depth [m]
WR-1	96-024	3885	23.01.	04:54	19°37.0'S	11°20.4'E	763
	96-026	1411	23.01.	10:45			
WB-A	96-015	3758	17.01.	16:48	21°29.0'S	11°15.1'E	2707
	96-018	768	20.01.	02:28			
WB-B	96-015	6604	18.01.	00:46	21°05.6'S	11°49.2'E	1290
	96-020	4890	21.01.	13:52			
WB-C	96-017	---	19.01.	14:12	20°53.9'S	11°13.4'E	2201
	96-021	1189	21.01.	21:14			

5.1.1.8.2 Seismic Stratigraphy

From the large data set collected during the cruise 3 seismic profiles are shown. Lines GeoB/AWI 96-022 and -021 run south-north from the center of the Walvis Basin to DSDP Site 532 on the Walvis Ridge.

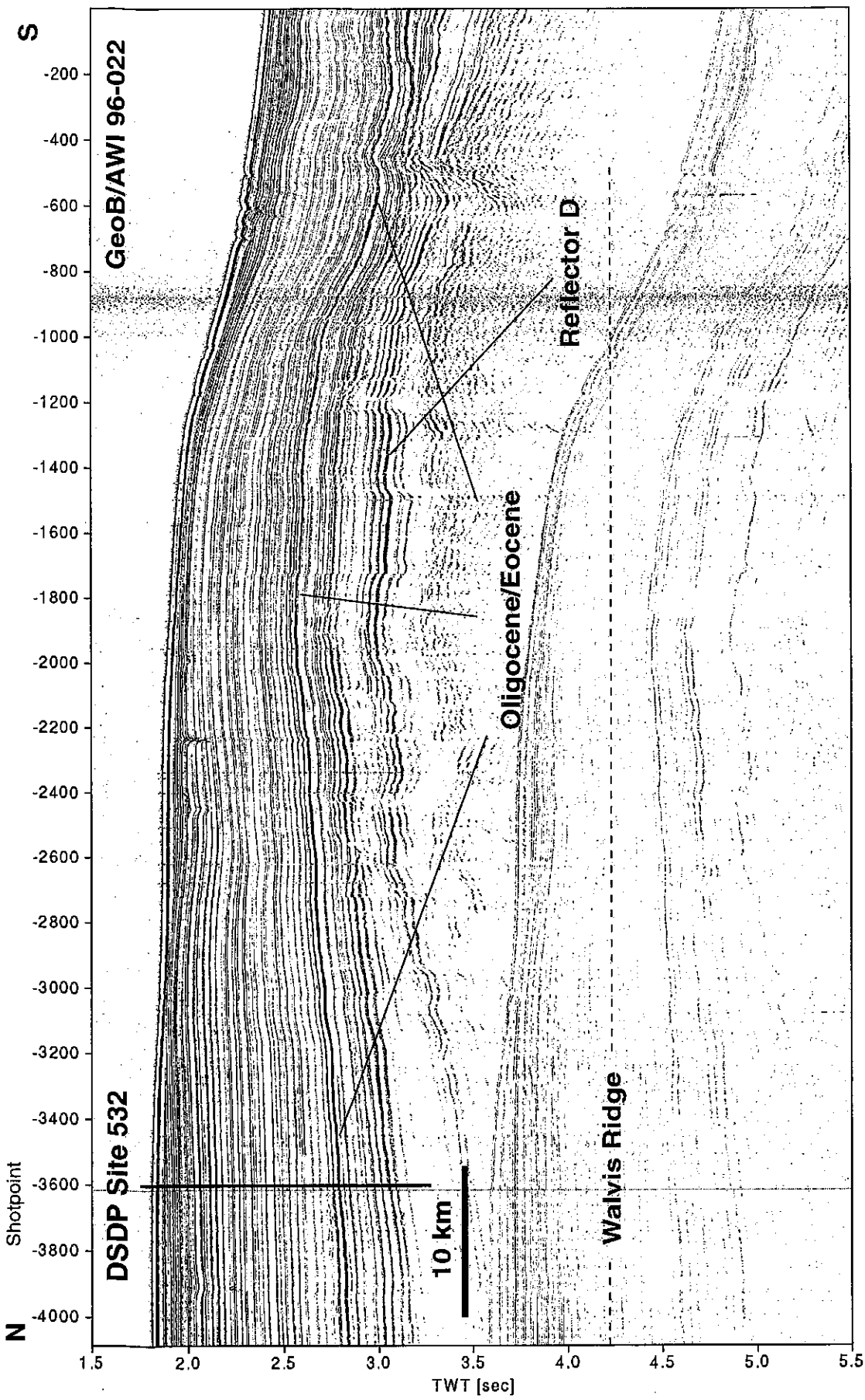

Fig. 31: Multichannel seismic Line GeoB/AWI 96-022 on the Walvis Ridge.

Line GeoB/AWI 96-022 (Fig. 31) crosses DSDP Site 532 thereby allowing to trace reflectors into the working area and to establish a seismostratigraphic framework. This will be subject to subsequent detailed analyses and is not discussed here extensively.

On the Walvis Ridge the surface sediments are affected by erosion. The thickness of the sediment column decreases slightly towards a basement high on the southern flank. The upper unit of closely spaced high frequency reflectors thickens significantly towards the basin, even more pronounced on Line GeoB/AWI 96-021 (Fig. 32). The second unit of lower amplitude and lower frequency reflectors remains almost constant in thickness throughout the area indicating a pelagic sediment source, probably of biogenic origin. The base of this second unit seems to be continuous on the Walvis Ridge, but is clearly an unconformity in the South. There, a giant slump event has apparently removed a major portion of the sediment package. The center of the slump scarp is crossed at SP 800 of Line GeoB/AWI 96-021. Other seismic lines further south show that the section becomes continuous again.

According to the drilling results at DSDP Site 532, an Oligocene to Eocene age can be assigned to the strong reflector at ~2.8 s TWT. This reflector is part of the undisturbed upper two units which extend down to 1 s sub-bottom TWT. The drilling of Neogene and late Paleogene sections in the Walvis Basin will therefore not be affected by the giant slump event. For younger sediments only minor local disturbances by vertical faulting (SP 1600, 1450, 1200 and 950) were observed on the southern ridge flank.

Line GeoB/AWI 96-015 (Fig. 33 and 34) is the longest profile of the Walvis Basin survey and runs in SW - NE direction perpendicular to the slope from a water depth of 3600 m onto the shelf. Although a major change in slope angle related to deeper structures occurs at SP 5000, the distribution of surface sediments is not severely affected.

In the deeper part of the basin irregular reflection patterns indicate a chaotic deposition below 600 ms sub-bottom TWT. These structures may well be relicts of the giant slope failure or alternatively could suggest a sediment fan or mass movements from the shelf. A wide sedimentary basin has developed landward of the 'escarpment', where the thickness of the upper sequences increases by a factor of 2 to 4. The signal penetration is generally higher than in the other working areas possibly related to higher sedimentation rates and finer materials.

The net of seismic lines will allow detailed correlations within the working area. The drilling results from DSDP Sites 532/362 can be used e.g. to identify a pronounced reflector close to the Eocene / Oligocene boundary which is clearly seen in most of the seismic profiles. A band of reflectors similar to all other areas is tentatively identified as Reflector D which has a Paleocene to Maastrichtian age at DSDP Site 360 off Cape Town.

A further refinement of these very preliminary results is possible only after completion of data processing which will also include three-dimensional analyses of depositional pattern, sedimentation rates and an identification of sediment sources.

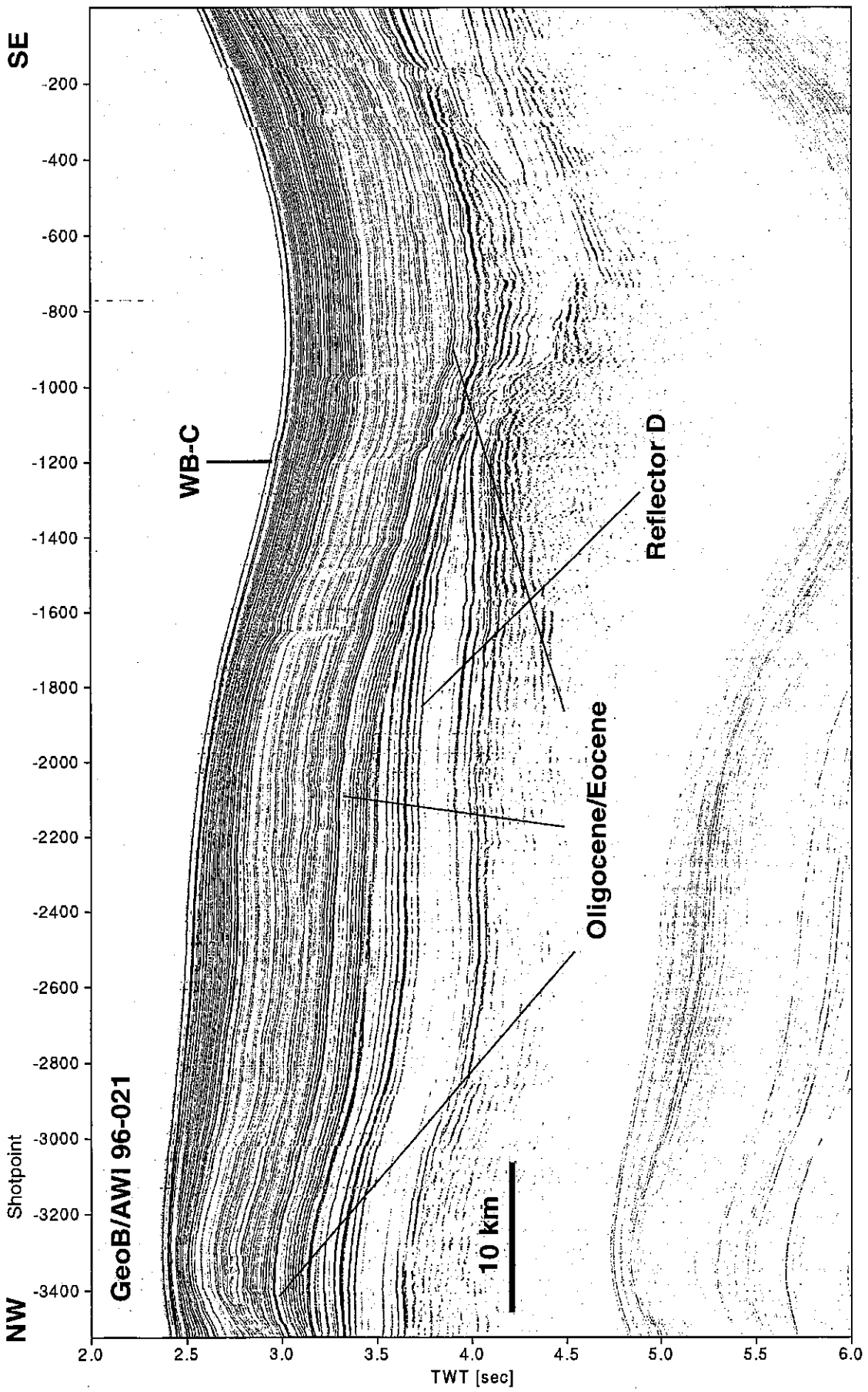

Fig. 32: Multichannel seismic Line GeoB/AWI 96-021 between Walvis Ridge and Walvis Basin.

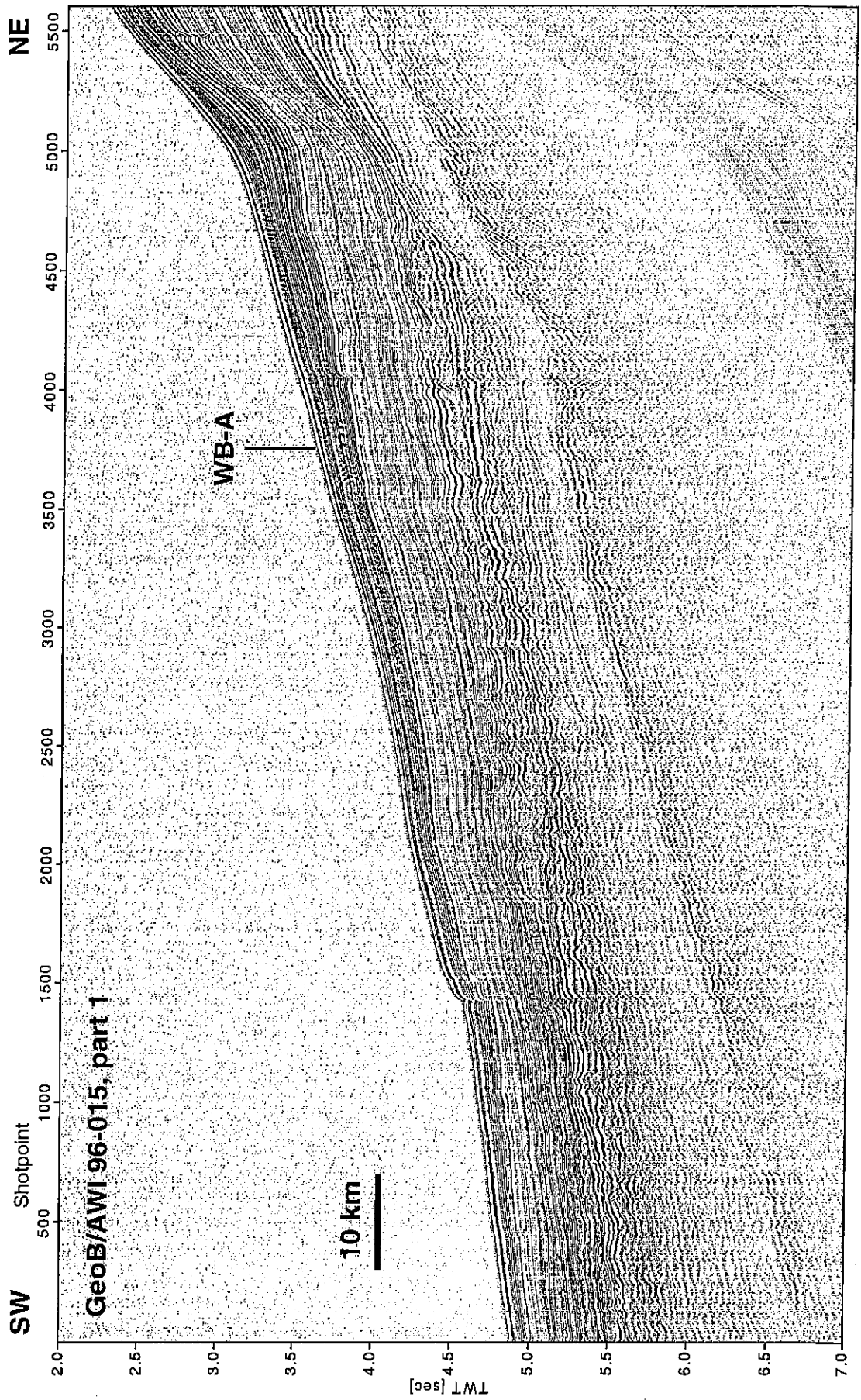

Fig. 33: Multichannel seismic Line GeoB/AWI 96-015 (part 1).

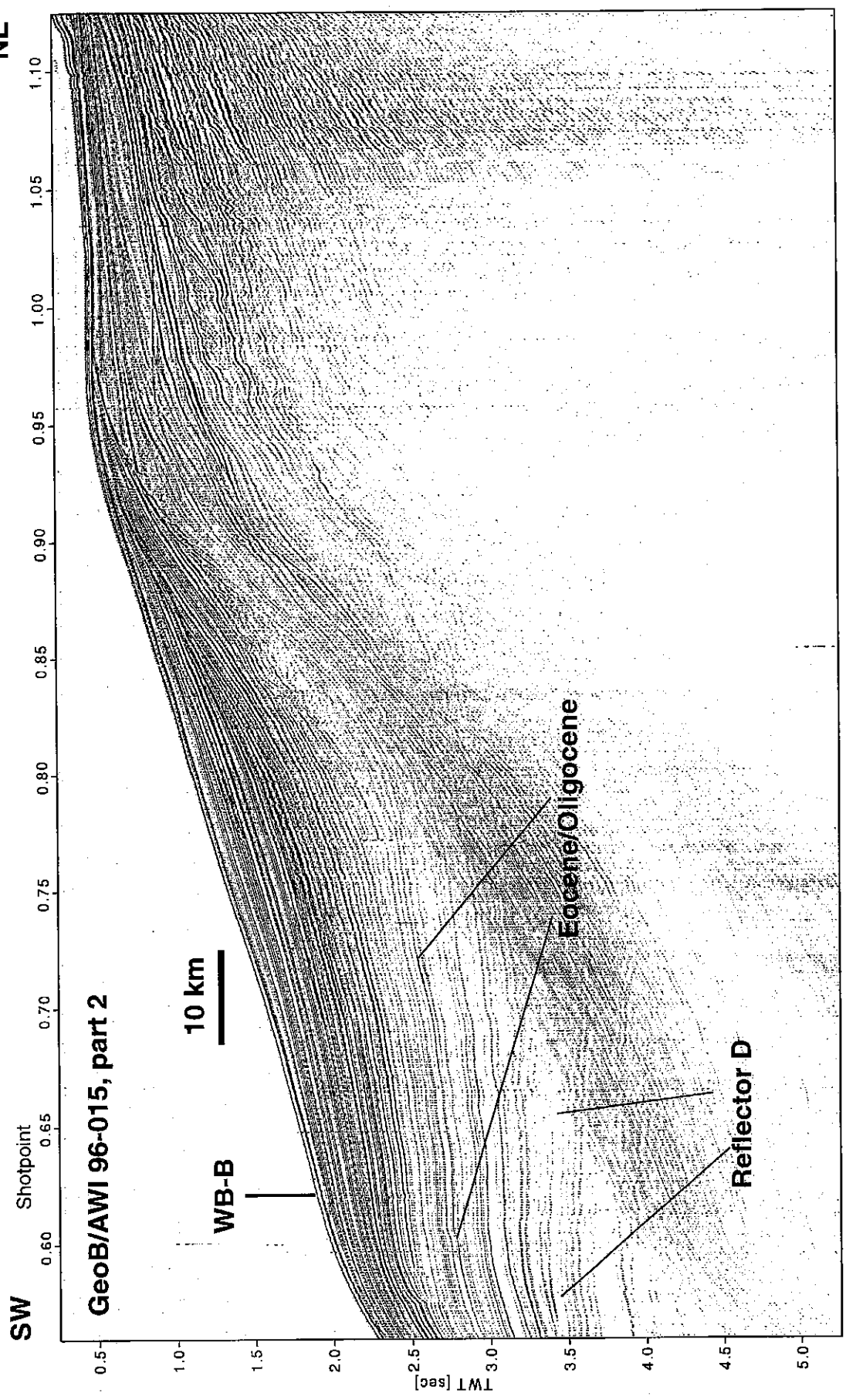

Fig. 34: Multichannel seismic Line GeoB/AWI 96-015 (part 2).

Seismic Line GeoB/AWI 96-024 across the proposed Site WR-1 in 780 m water depth is shown in Figure 34. A large number of strong reflectors in the upper seismic Unit I can either be explained by strong fluctuations in carbonate content or, as was observed in late Quaternary sediment cores from this area, by unconformities. The complete Line 96-024 (not shown here) contains even more evidence for strong bottom current activity and erosion. Therefore, a careful evaluation whether the selected site is suitable to study the variability of the Benguela Current system is suggest. Alternate sites could be selected in the Walvis Basin, where a greater continuity can be expected.

Although drilling will probably not even penetrate Unit I, a short discussion of the deeper units is given. The irregular reflection pattern between 1.6 and 2 s TWT (seismic Unit II) is likely to be caused by a slump structure. It becomes more regular in the western part of the profile and is characterized there by lower frequencies and weaker amplitudes. The appearance of Units II and III is similar. A discrimination based on amplitudes can only be carried out after processing of the complete data set and removal of the multiple energy which is observed below 2 s TWT. The base of Unit III (2.4 s TWT) is dated by correlation to DSDP Site 532 close to the Eocene / Oligocene boundary.

The crossings of seismic lines in the Walvis Basin will be proposed as alternate drill sites. They seem to be much more suitable to fulfill the objectives of the drilling proposal than Site WR-1.

Depending on the geologic time interval which shall be covered in the drill hole, sites with different sedimentation rates can be suggested. Site WB-A (Fig. 36) lies in the deeper part of the basin, where the upper seismic Unit I has a thickness of only 200 - 300 ms. It shows high reflection amplitudes and numerous high-frequency reflectors. At the base of Unit I the amplitude drops significantly, but reflectors are still closely spaced and of high frequency. Cross correlation with the other seismic lines allows the identification of the Eocene / Oligocene boundary in the middle of Unit II at ~4.25 s TWT. The thickness of Unit II is ~500 ms.

A clear change in frequency occurs at the base of Unit II. Unit III (thickness ~300 ms) is very similar to the other working areas, where Reflector D was interpreted as the base of the Tertiary. The seismic unit below shows reduced amplitudes, indicating relatively homogenous sediments.

Site WB-B (Fig. 37) is located at SP 6600 landward of the 'escarpment' at SP 5000 (Fig. 33). The seismic patterns generally reveal the same features. The high amplitude, high-frequency Unit I with about 600 ms is significantly thicker, Unit II with 500 ms is similar in thickness as at Site WB-A. This is a strong indication that the dominant sediment source has changed between the two units. Unit I should have received major proportions of sediments

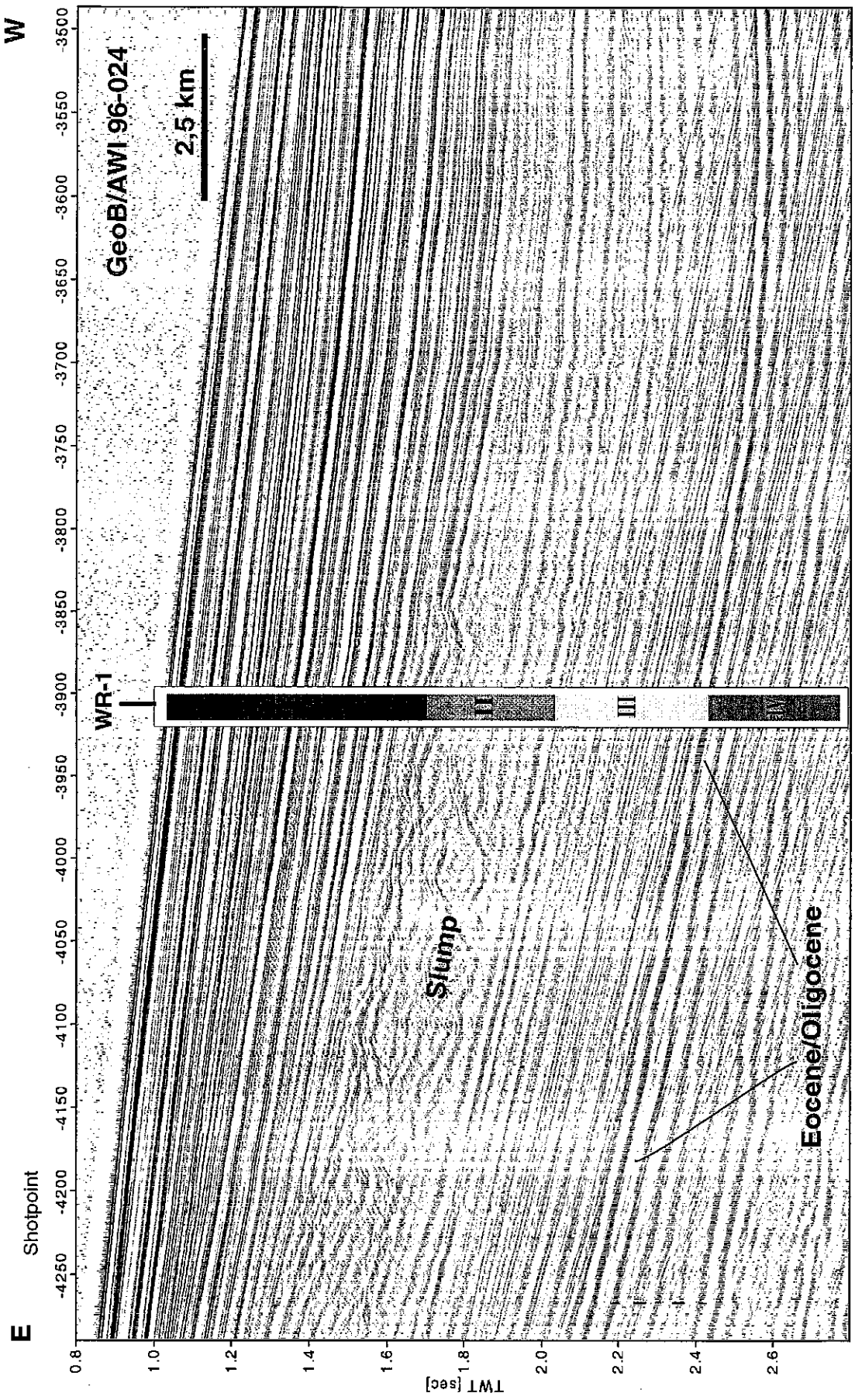

Fig. 35: Multichannel seismic Line GeoB/AWI 96-024 across proposed drill Site WR-1. See text for further explanations.

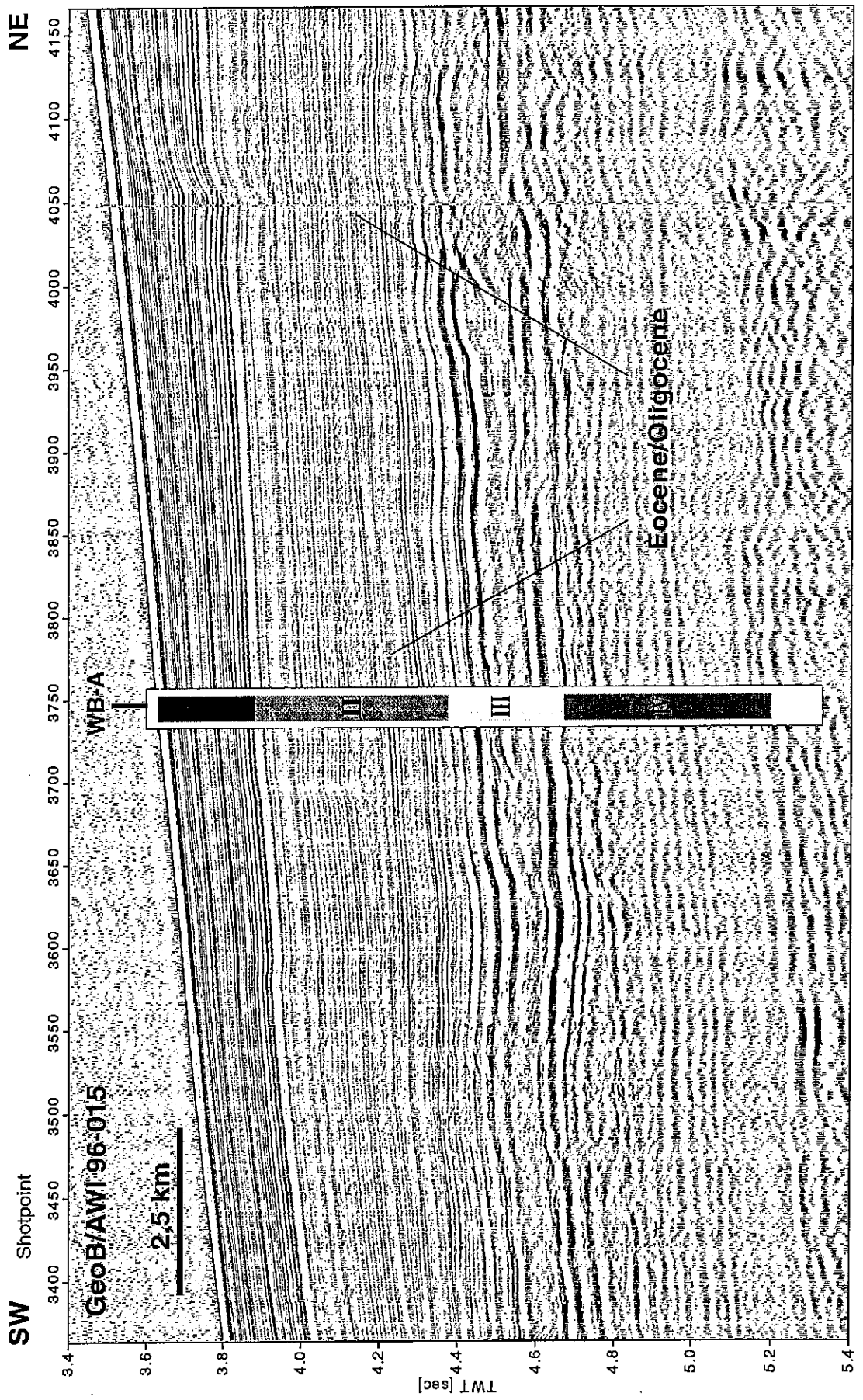

Fig. 36: Multichannel seismic Line GeoB/AWI 96-015 in the vicinity of proposed drill Site WB-A. See text for further explanations.

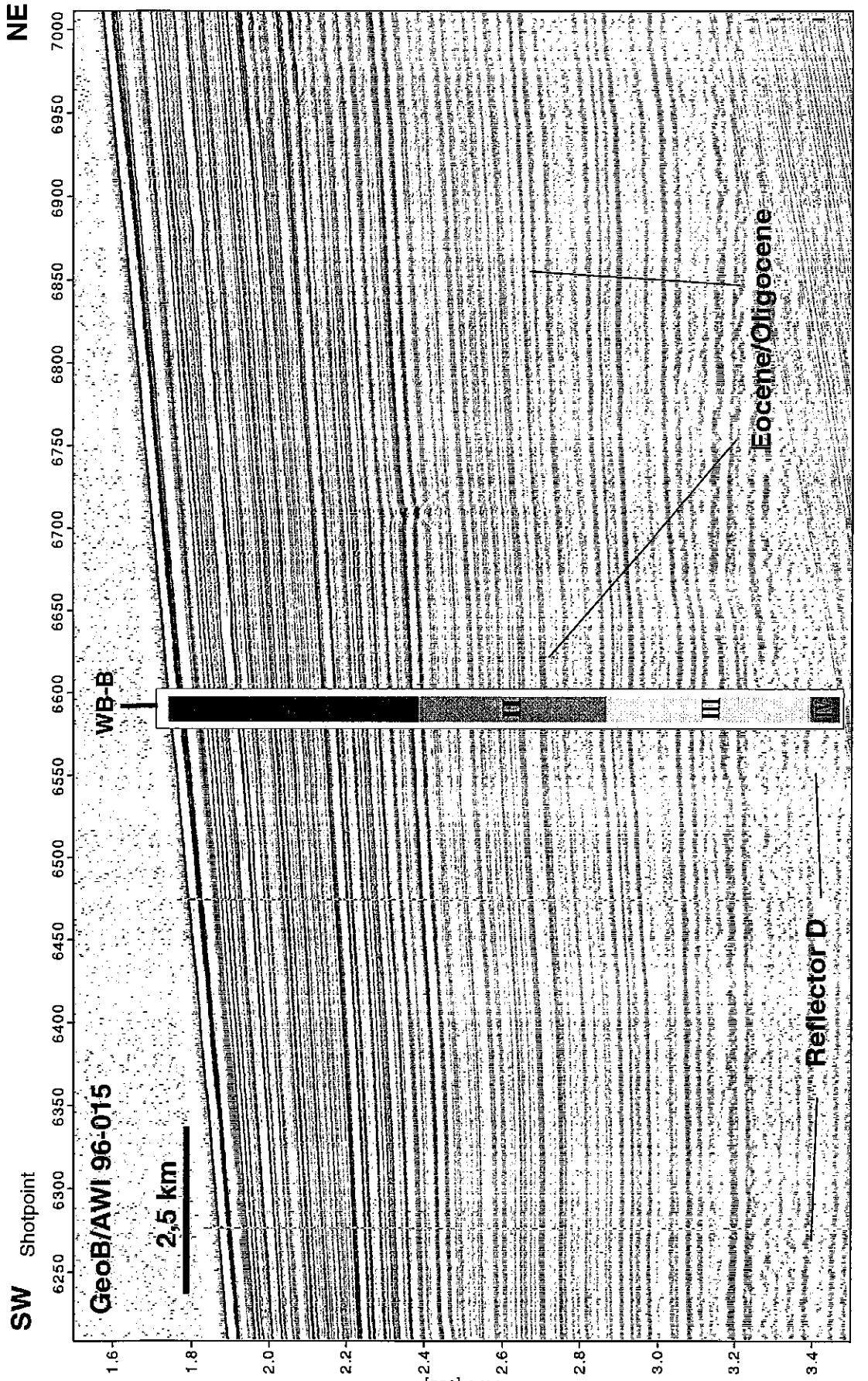

Fig. 37: Multichannel seismic Line GeoB/AWI 96-015 across proposed drill Site WB-B. See text for further explanations.

from upwelling and surface water productivity. This sediment input decreases with distance from the coast. The same situation was encountered in the upwelling cell off Angola at 17°S which was studied during RV SONNE cruise SO 86.

In contrast, Unit II probably received predominantly normal pelagic components which could be explained by a different sediment distribution pattern, a restriction of upwelling sediment to the shelf areas or a reduced activity of the upwelling system in its early stages of development.

Site WB-C (Fig. 38) is located further north in ~2000 m water depth. The seismic character is the same as at the other sites. The area is affected by a major slump event (see also Fig. 32) which has probably removed parts of Unit III. At this site the change in frequency content at the base of Unit II seems to be closer to the Eocene / Oligocene boundary which might reflect the influence of the Walvis Ridge as an additional sediment source.

5.1.1.9 Digital Echosounder Profiles

The PARASOUND sediment echosounder system was run continuously during the cruise and the data were collected in digital form with the PARADIGMA data acquisition system.

For the discussion of the drill sites these data, which usually do not penetrate deeper than 50 - 80 m, will not be interpreted at present with regard to seismic stratigraphy. They are suitable, however, to evaluate the structural framework and provide detailed insights to local depositional processes and possible disturbances.

For this purpose the high resolution echosounder records in the vicinity of the proposed drill sites (except for Site SCB-D) are shown in Figures 39 to 49.

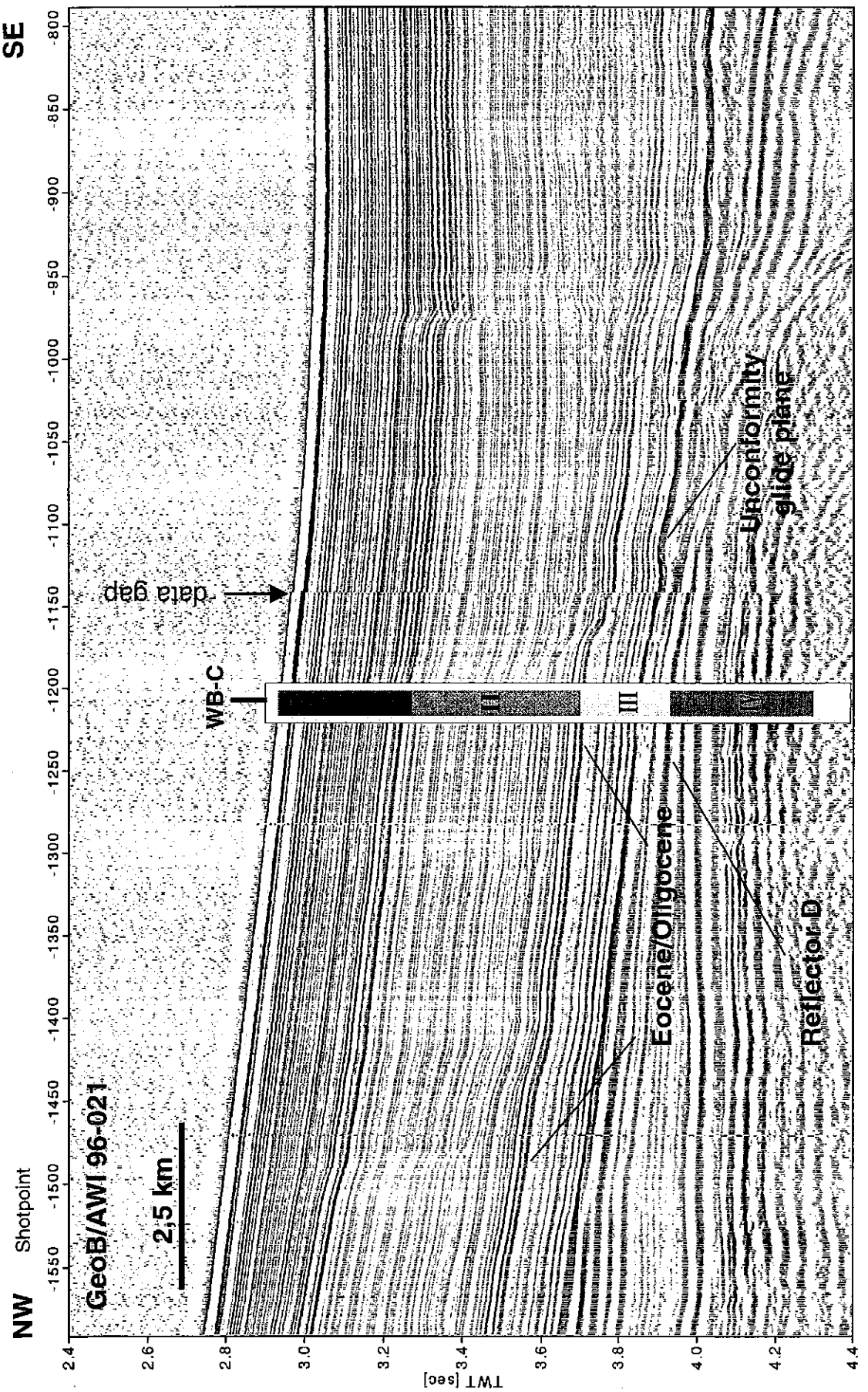

Fig. 38: Multichannel seismic Line GeoB/AWI 96-21 in the vicinity of proposed drill Site WB-C. See text for further explanations.

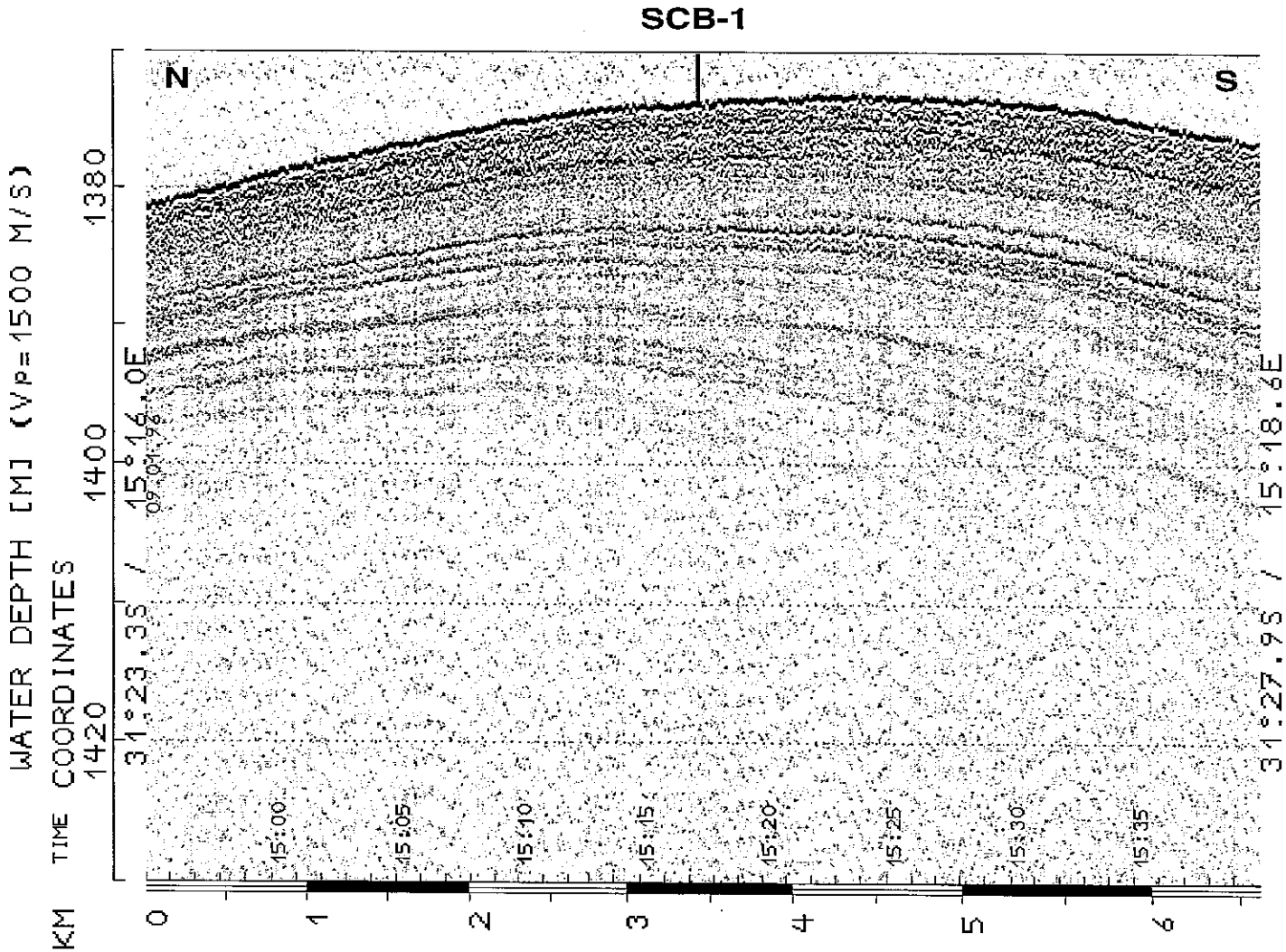

Fig. 39: Digital PARASOUND profile of Line GeoB/AWI 96-008 across Site SCB-1. The section is annotated with daytime, distance in km, water depth for a sound velocity of 1500 m/s and geographical coordinates at the begin and end of the section.

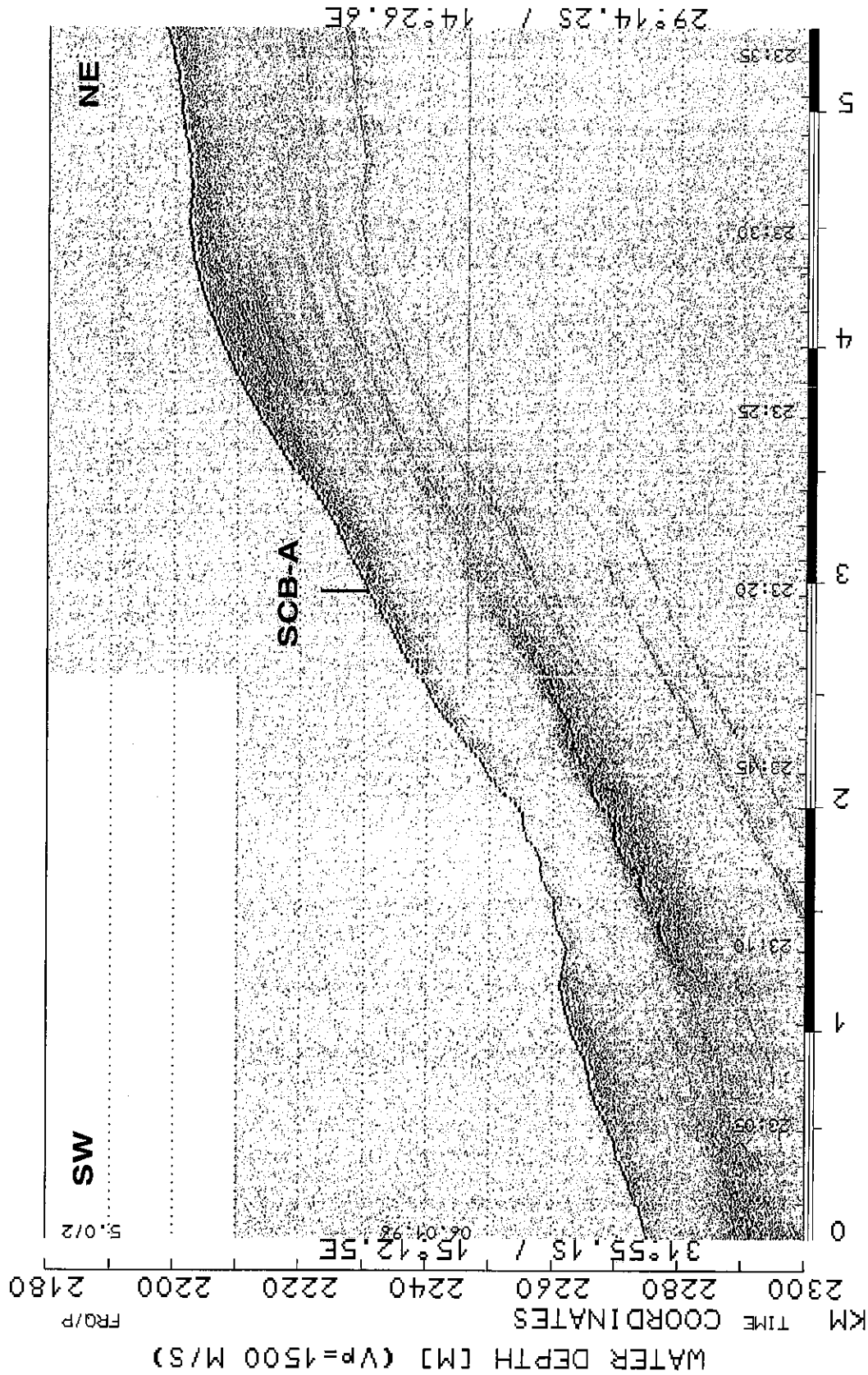

Fig. 40: Digital PARASOUND profile of Line GeoB/AWI 96-001 across Site SCB-A. For further explanations see Figure 39.

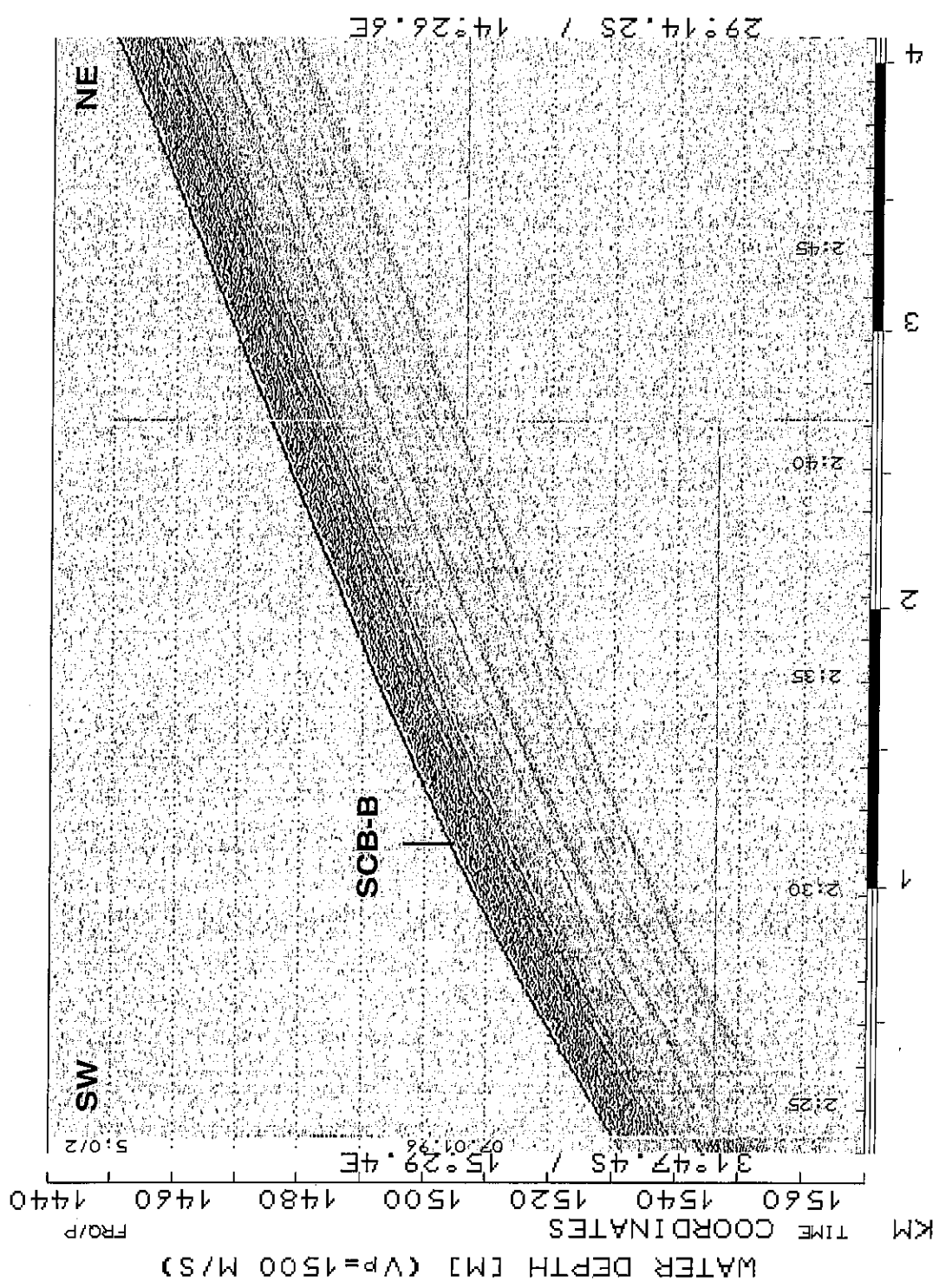

Fig. 41: Digital PARASOUND profile of Line GeoB/AWI 96-001 across Site SCB-B. For further explanations see Figure 39.

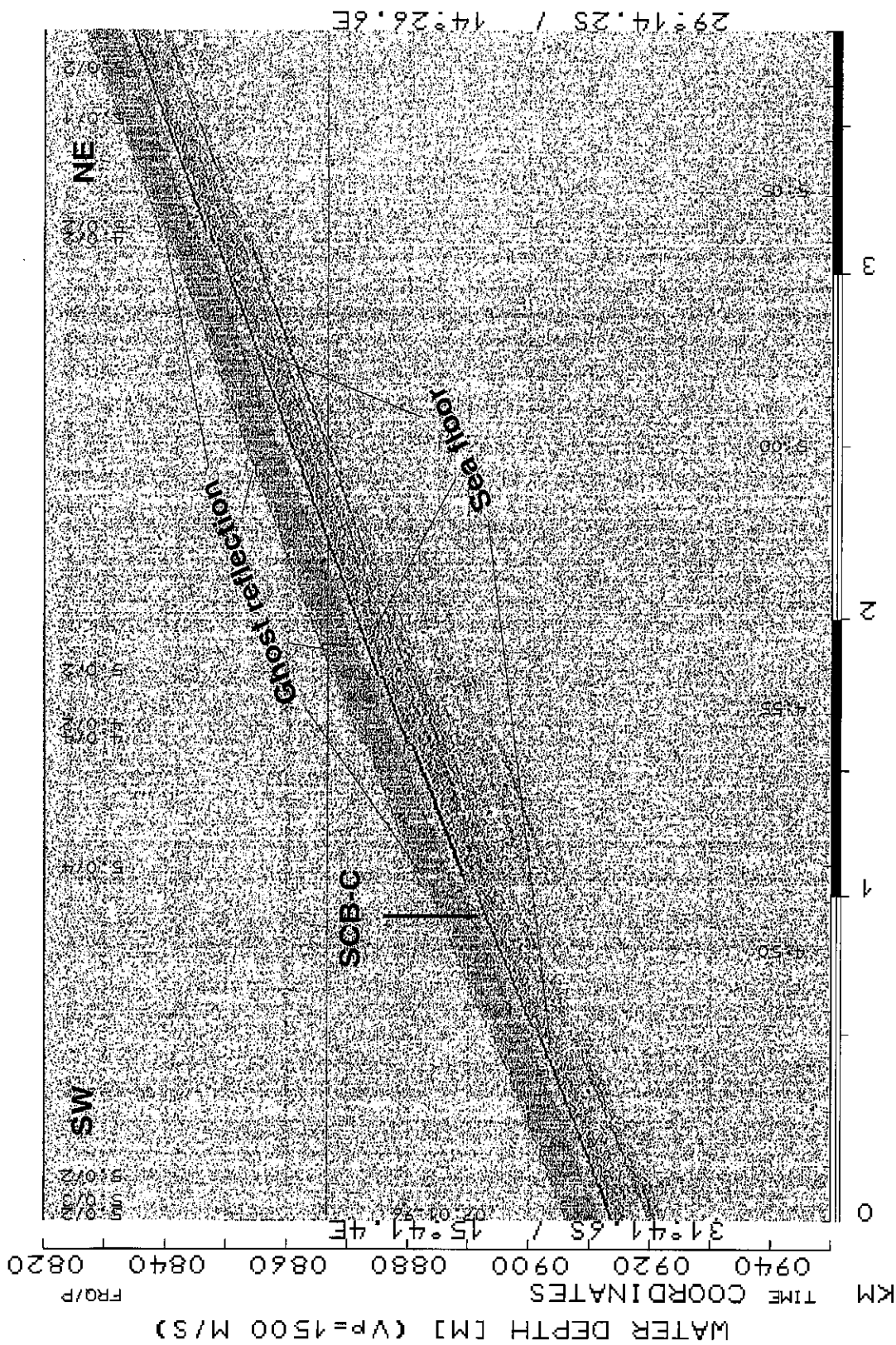

Fig. 42: Digital PARASOUND profile of Line GeoB/AWI 96-001 across Site SCB-C. For further explanations see Figure 39.

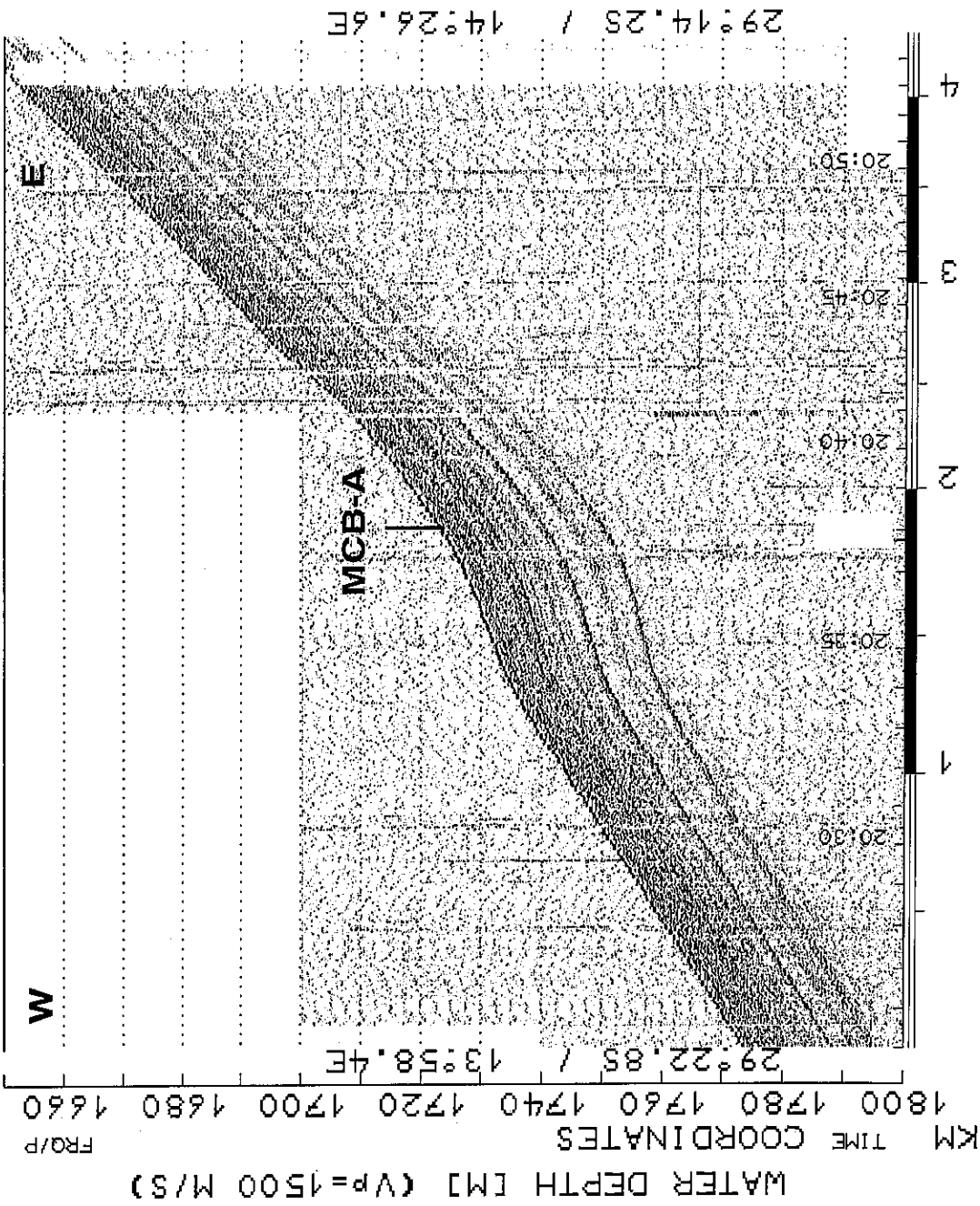

Fig. 43: Digital PARASOUND profile of Line GeoB/AWI 96-009 across Site MCB-A. For further explanations see Figure 39.

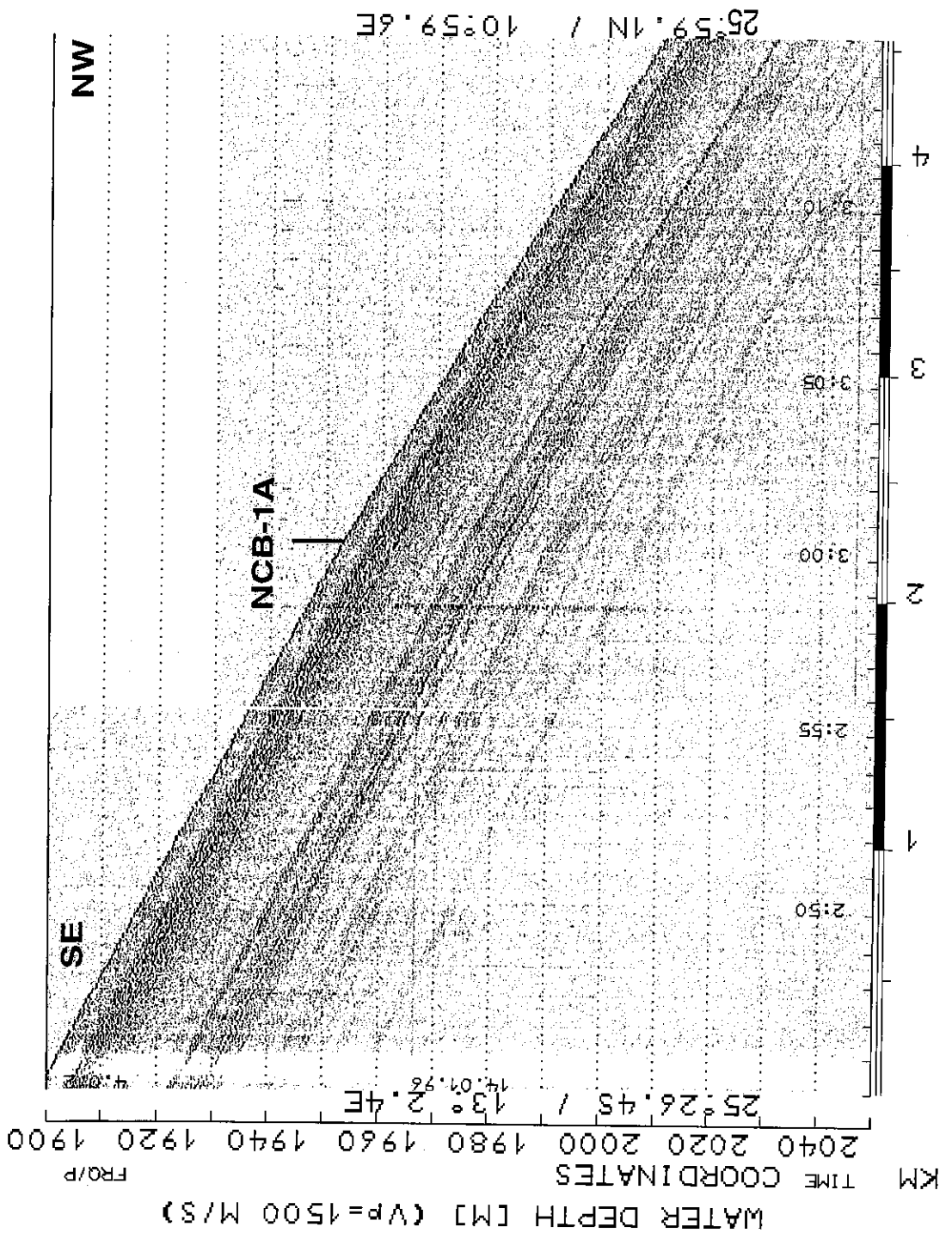

Fig. 44: Digital PARASOUND profile of Line GeoB/AWI 96-012 across Site NCB-1A. For further explanations see Figure 39.

Fig. 45: Digital PARASOUND profile of Line GeoB/AWI 96-014 across Site NCB-1B. For further explanations see Figure 39.

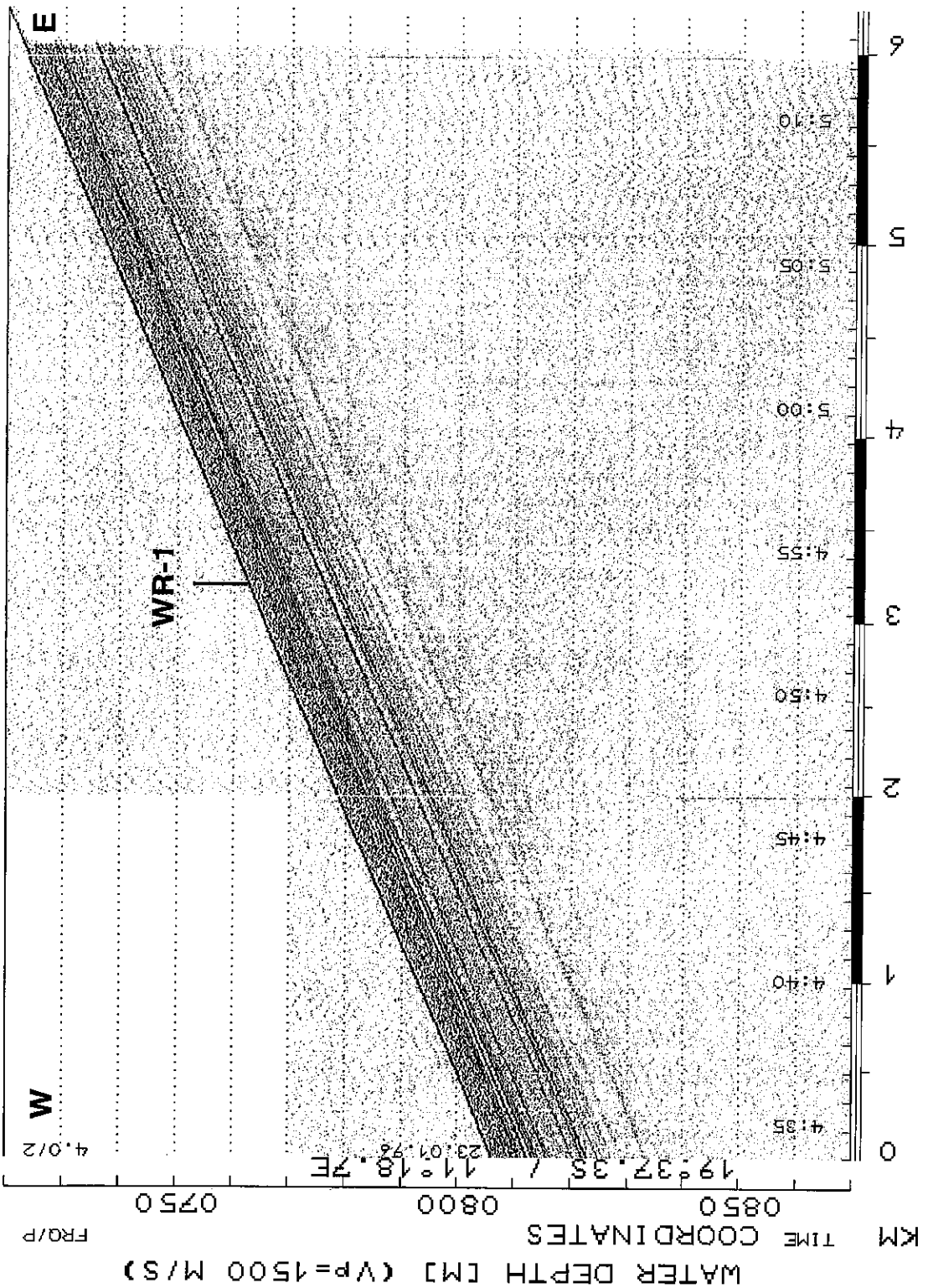

Fig. 46: Digital PARASOUND profile of Line GeoB/AWI 96-024 across Site WR-1. For further explanations see Figure 39.

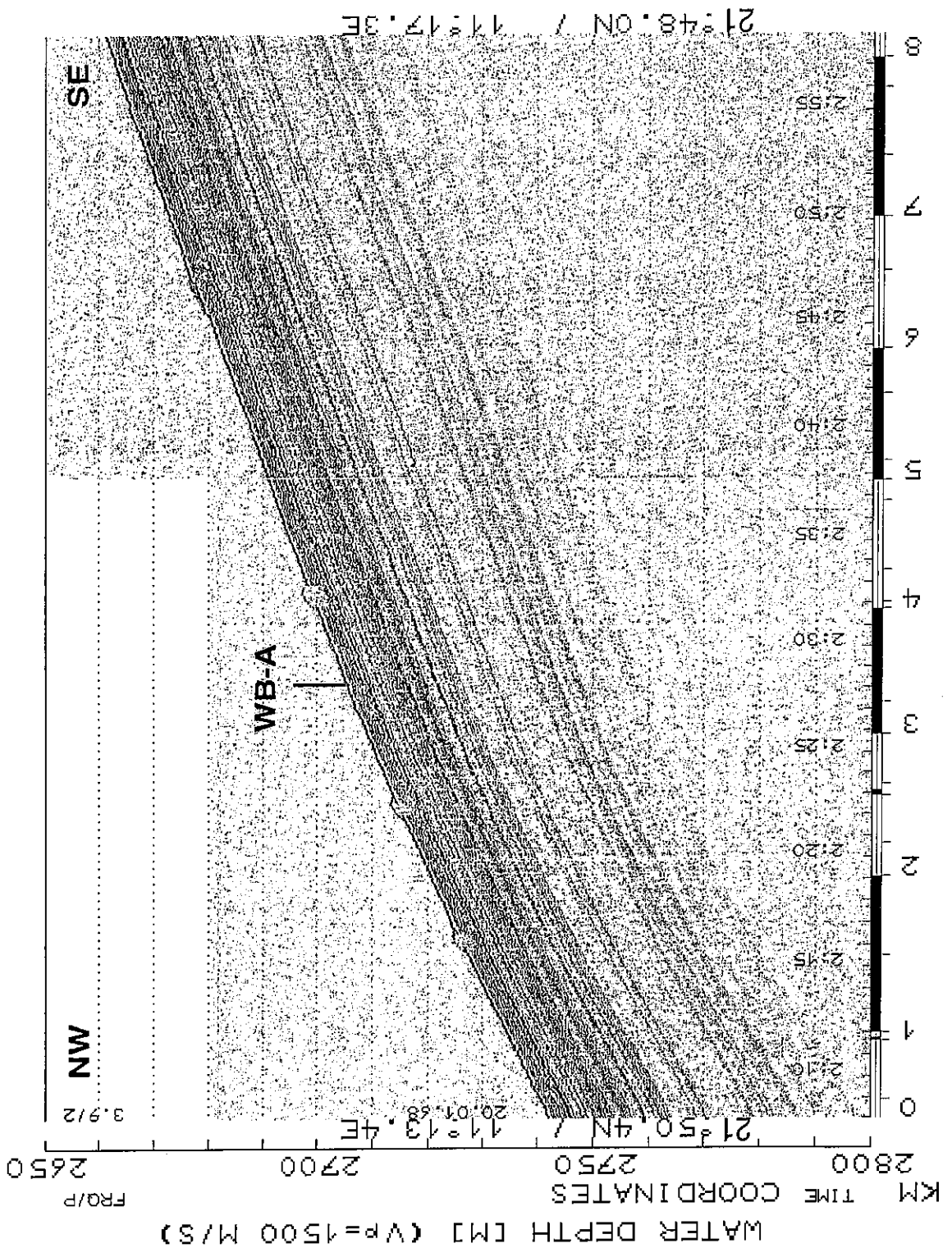

Fig. 47: Digital PARASOUND profile of Line GeoB/AWI 96-018 across Site WB-A. For further explanations see Figure 39.

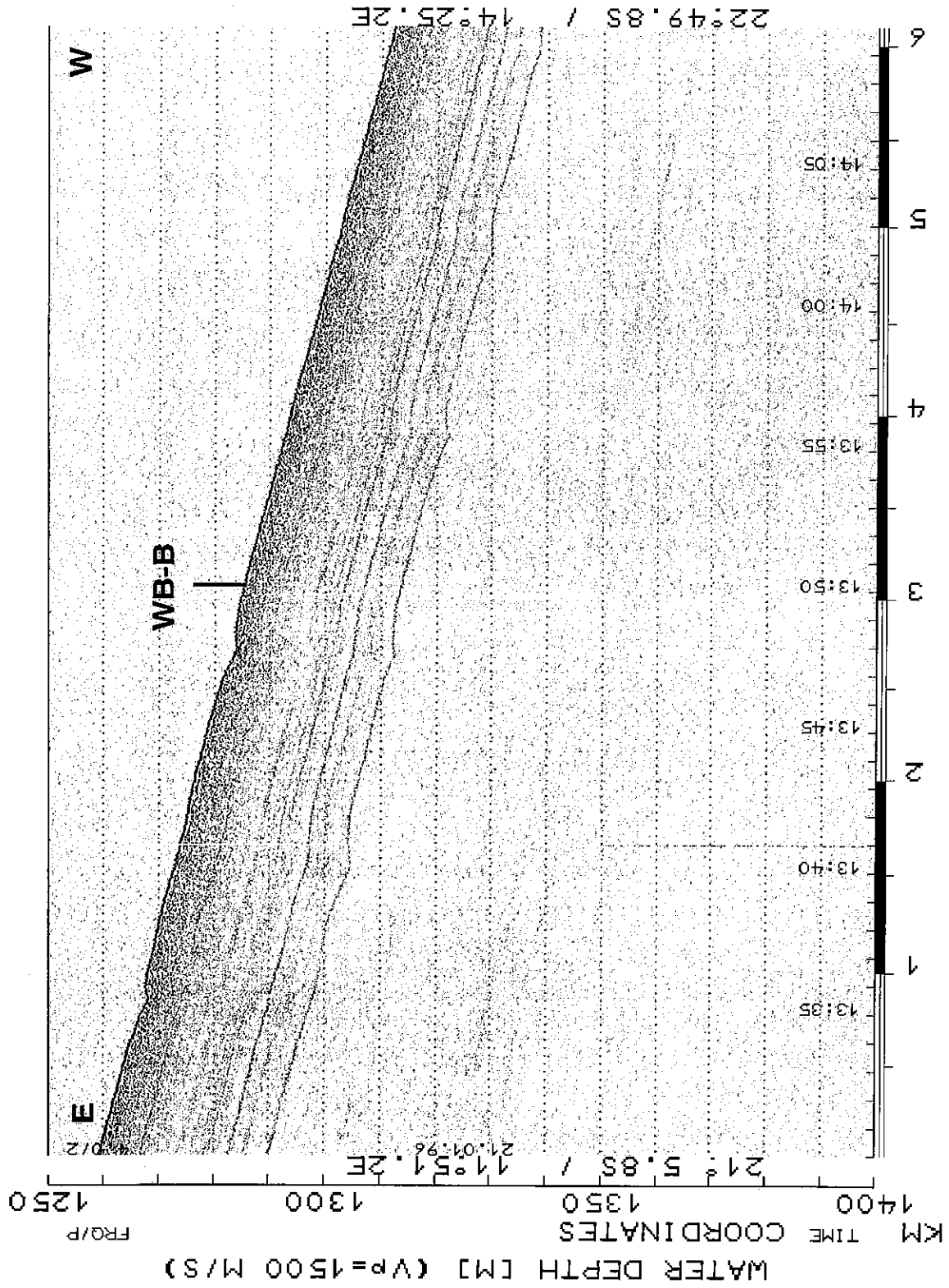

Fig. 48: Digital PARASOUND profile of Line GeoB/AWI 96-020 across Site WB-B. For further explanations see Figure 39.

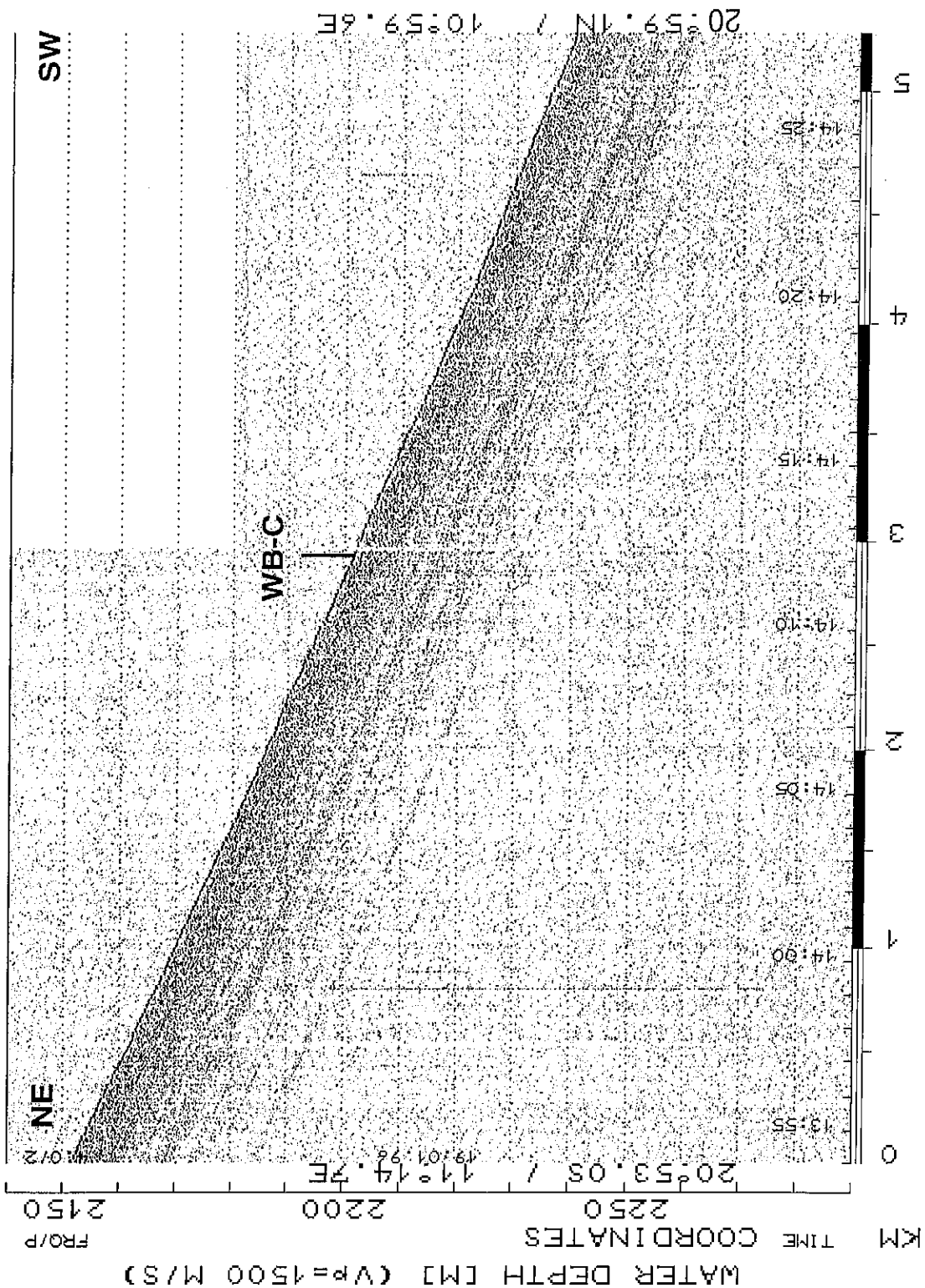

Fig. 49: Digital PARASOUND profile of Line GeoB/AWI 96-017 across Site WB-C. For further explanations see Figure 39.

5.1.2 Sediment Sampling

(R. Hoek, M. Little, R. Kreutz, W. Schmidt, R. Schneider, M. Segl)

A multicorer and a gravity corer were used to recover surface and late Quaternary sediments at 8 sampling stations on the continental slope off South Africa and Namibia from water depths between 400 and 3000 m. All relevant details of the sediment sampling operations are summarized in the station list (chapter 7.1.1).

5.1.2.1 Multicorer

The multicorer is designed to recover undisturbed surface sediment sections together with the overlying bottom water. The device used during cruise M34/1 was equipped with 4 small (6 cm diameter) and 10 large (8 cm diameter), 60 cm long plastic tubes. At most stations all tubes successfully retrieved the uppermost 22 to 45 cm of sediments covered with bottom water (chapter 7.1.2). In general, the following sampling scheme was practiced:

- 1 large tube was cut into 1 cm thick slices for the investigation of dinoflagellates;
- 1 large tube was cut into 1 cm slices and frozen for organic carbon geochemistry;
- 2 large tubes were cut into 1 cm slices for the investigation of foraminiferal assemblages;
- 1 small and 1 large tube were frozen as archive cores;
- surface sediments (0 - 2 cm) from 2 large tubes were sampled for the investigation of radiolarian assemblages and for organic carbon geochemistry, respectively;
- 1 small tube was cut in 1 cm slices for magnetic studies;
- bottom water samples for stable oxygen and carbon isotope analyses were stored in glass bottles;
- pore waters of 1 large tube were analyzed at two stations (GeoB 3607-1 and 3608-2).

5.1.2.2 Gravity Corer

With the gravity corer between 5.25 and 11.30 m long Late Quaternary sediment sequences have been retrieved at 7 stations. Altogether 63.99 m of sediments were recovered with this device during cruise M34/1. Before using the coring tools, the liners were marked with a straight line lengthwise, in order to be able to sample all core segments in the same orientation, in particular for paleomagnetic purposes.

Immediately after a core was recovered on deck, the liners were cut into 1 m segments, closed with caps at both ends, inscribed (Fig. 50) and stored in the laboratory to equilibrate to

ambient temperature. Subsequent to the shipboard whole-core geophysical measurements (Chapter 5.1.3), the segments were cut along-core in two halves, a work and an archive half.

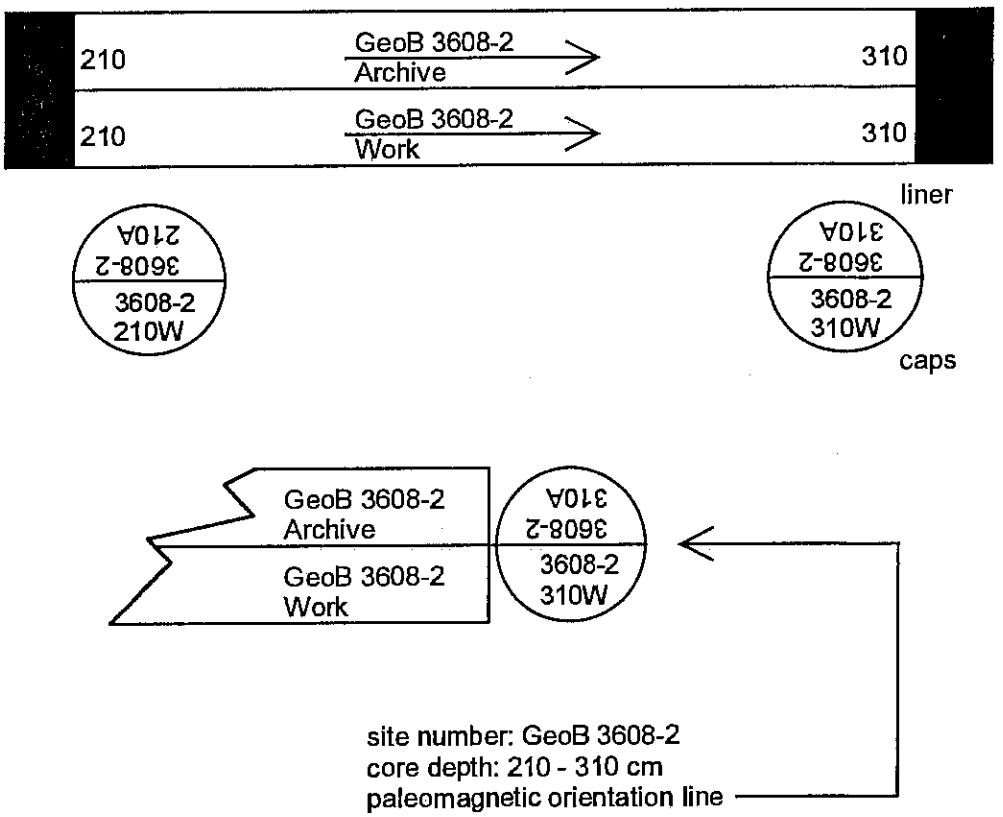

Fig. 50: Inscription scheme of gravity core segments.

The sediments were described, smear-slide samples were taken from distinctive layers and spectrophotometric measurements were carried out on the archive halves, which then were stored in a cool room at +4°C. From the work half two parallel series and a third series of syringe samples (10 ccm) were taken at a depth interval of 5 and 10 cm, respectively. These samples are intended for the determination of physical properties, stable isotopes, foraminiferal and dinoflagellate assemblages, as well as for mineralogy and organic geochemistry. An additional syringe sample series was taken in 20 cm intervals for a preliminary analysis of the planktic foraminiferal composition and variations of sand content in each core, whilst onboard.

A detailed list of samples taken on cruise M34/1 is available upon request from the Marine Geology Section, Geoscience Department, University of Bremen.

5.1.2.2.1 Analysis of Planktic Foraminiferal Abundances

(M. Little)

The aim of the study was to gain a preliminary record of the nature of variations in the planktic foraminiferal record, and to assimilate a tentative chronology for the gravity cores. For this stratigraphic analysis the cores were sampled every 20 cm usually with the addition of a 5 cm depth sample at the core top. Each 10 ml sample was washed using a 63 µm sieve to remove the sediment clay fraction, filtered, and the final residue dried at 60°C. Samples were then transferred into 10 ml vials and the sediment sand fraction measured. In cores GeoB 3607-2 and GeoB 3608-2, due to the lack of foraminifera, 20 or 30 ml samples were taken and the subsequent sand fraction data adjusted for consistency. Where possible at least 50 planktic foraminifera were counted for each sample and their relative abundances calculated. No sediment sieving or splitting was carried out, but the comparison of the GeoB 3608-2 data with previous records on both the shelf (GeoB 1711-4, 23° S / 14° E) and on the Walvis Ridge (GeoB 1706-2, 20° S / 12° E; LITTLE et al., 1996) suggests the sampling procedures were adequate for a preliminary analysis.

The recovered sediments differ considerably in compositions of planktic foraminifera. The cores retrieved from the southern Benguela region, SBR, (GeoB 3602-1, 3603-2, 3604-3 and 3605-2; Figs. 51 to 54) show a marked dominance in *Globorotalia inflata* and *Neogloboquadrina pachyderma* (dextral coiling). The two most southerly cores, GeoB 3602-1 and 3603-2, from 2000 and 3000 m water depth, respectively, reveal an average of 50 % abundance of *G. inflata* and additionally 20 % abundance of tropical species (*G. sacculifer*, *G. ruber* (white), *G. menardii*, *G. siphonifera*, and *Orbulina universa*). In the more northerly cores of the SBR, GeoB 3604-3 and 3605-2, a notable decrease in *G. inflata* abundance and a relative increase in *N. pachyderma* (dextral) and *Globigerina bulloides* is observed.

The cores from the Northern Benguela Region, NBR, (GeoB 3606-1, 3607-2 and 3608-2) are each very individual. Core GeoB 3606-1 (Fig. 55) was found to have enough foraminifera for analysis only in the top 350 cm (>50 specimens per sample), whereas in core GeoB 3607-2 almost no foraminifera were present, but a high abundance of diatom tests. The lack in foraminifera in both cases is assumed to be related to low foraminiferal dwelling in the coastal upwelling cell and to dilution by diatom tests, especially in core GeoB 3607-2; but also due to dissolution at depth, where foraminifera in both cores were always much less in number than the required 50 specimen per sample.

Core GeoB 3608-2 (Fig. 56) from the northern Cape Basin had the only complete foraminiferal record with a very different pattern to those of the southern cores. It showed a dominance of *Neogloboquadrina pachyderma* (sinistral coiling), and supplementary *N. pachyderma* (dextral) and *G. bulloides*. A sudden increase in the abundance of *G. inflata* occurs near the base of the core. This record identically matches those of cores GeoB 1706-2 and 1711-4 (LITTLE et al., 1996; SCHULZ et al., 1992) allowing for an initial stratigraphy and age model to be assigned.

Tab. 9: Preliminary age model for core GeoB 3608-2

Depth [cm]	Isotope Stage	Age [ka])
60	1 / 2 Boundary	12
180		20
240	2 / 3 Boundary	24
280		30
400		40
540		53
610	3 / 4 Boundary	59
700	4 / 5 Boundary	74
820	5.1	80

The other cores cannot be dated in this manner with correlation to earlier records. But a recurring spike of *G. bulloides* (seen best at 200 cm in GeoB 3605-2) in all cores allows for relative correlation. Also, in the southerly cores both tropical species and *G. inflata* are seen to vary cyclically which is assumed to a first degree to be approximating a 23 kyr periodicity. Using this, the following tentative maximum ages are ascribed to the other cores retrieved.

Tab. 10: Preliminary maximum ages of cruise M34/1 gravity cores

Core No.	Maximum Age (ka) / Isotope Stage	Method for dating
3602-1	~140 / 6	6 cycles of tropical foraminifera
3603-2	~210 / 7	8 / 9 cycles of *G. inflata*
3604-3	~140 / 6	*bulloides* maximum abundance
3605-2	~128 / 5.5	5 / 6 cycles of *G. inflata*
3606-1	---	no forams
3607-2	---	no forams
3608-2	~85 / 5.1	correlation with cores GeoB 1706-3 and 1711-4

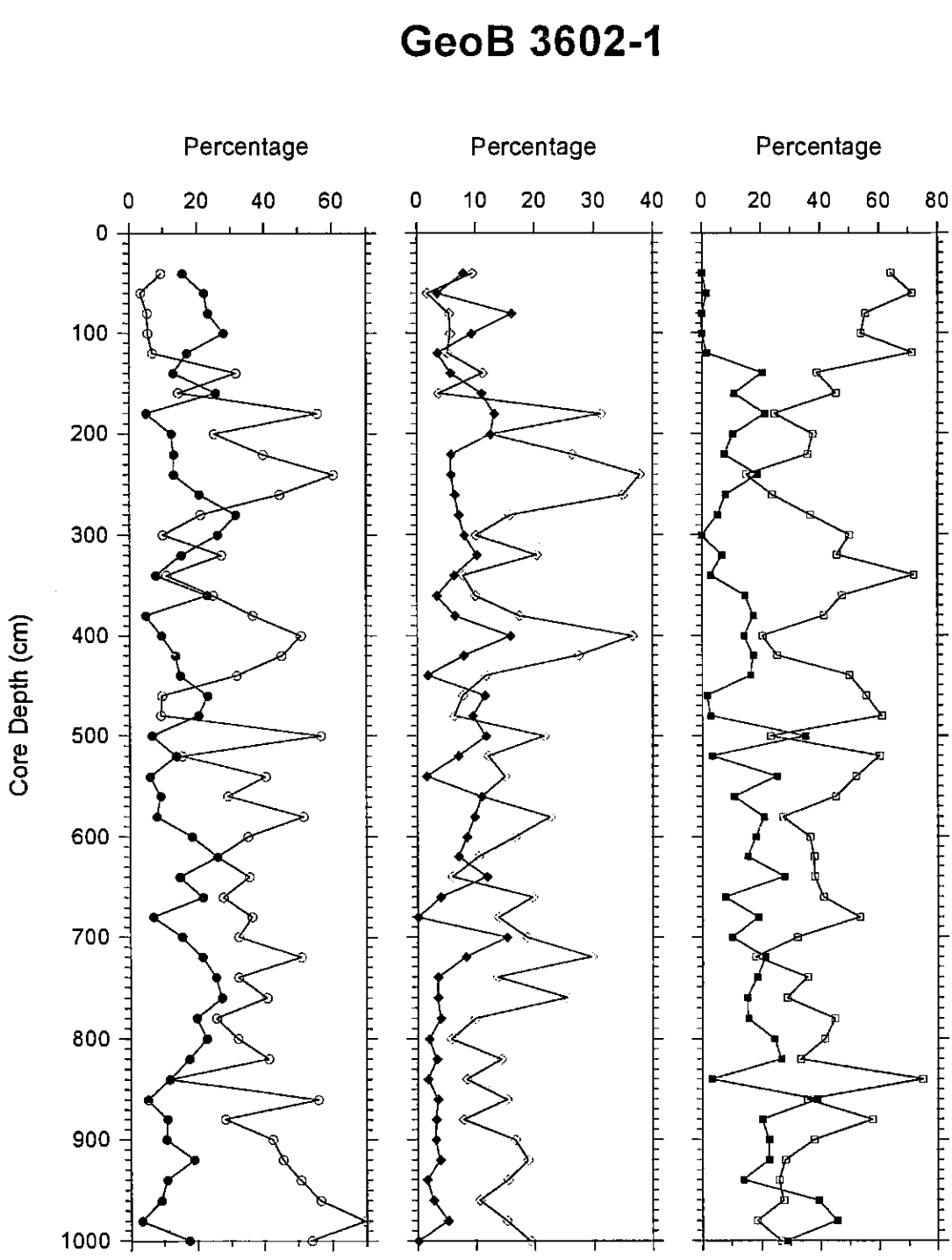

Fig. 51: Gravity core GeoB 3602-1 (southern Cape Basin) - preliminary results for planktic foraminifera assemblages. Left - tropical foraminifera [full circles]; cold water foraminifera (*N. pachyderma* (sin + dex) + *G. bulloi-des)* [open circles]. Center - *N. dutertrei* [full diamonds]; *G. bulloides* [open diamonds]. Right - *N. pachyderma* (dex) [full squares]; *G. inflata* [open squares].

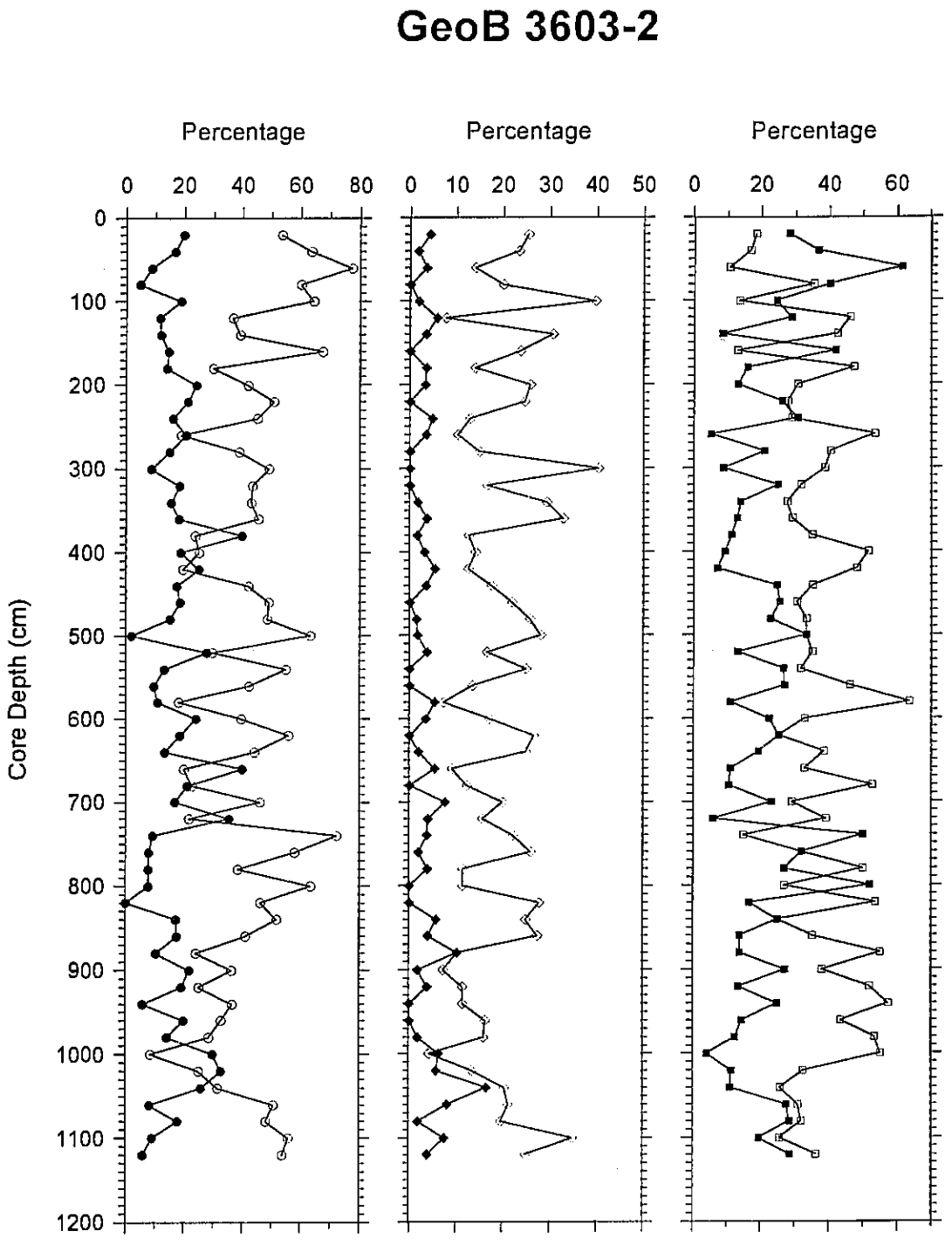

Fig. 52: Gravity core GeoB 3603-2 (southern Cape Basin) - preliminary results for planktic foraminifera assemblages. Left - tropical foraminifera [full circles]; cold water foraminifera (*N. pachyderma* (sin + dex) + *G. bulloi-des)* [open circles]. Center - *N. dutertrei* [full diamonds]; *G. bulloides* [open diamonds]. Right - *N. pachyderma* (dex) [full squares]; *G. inflata* [open squares].

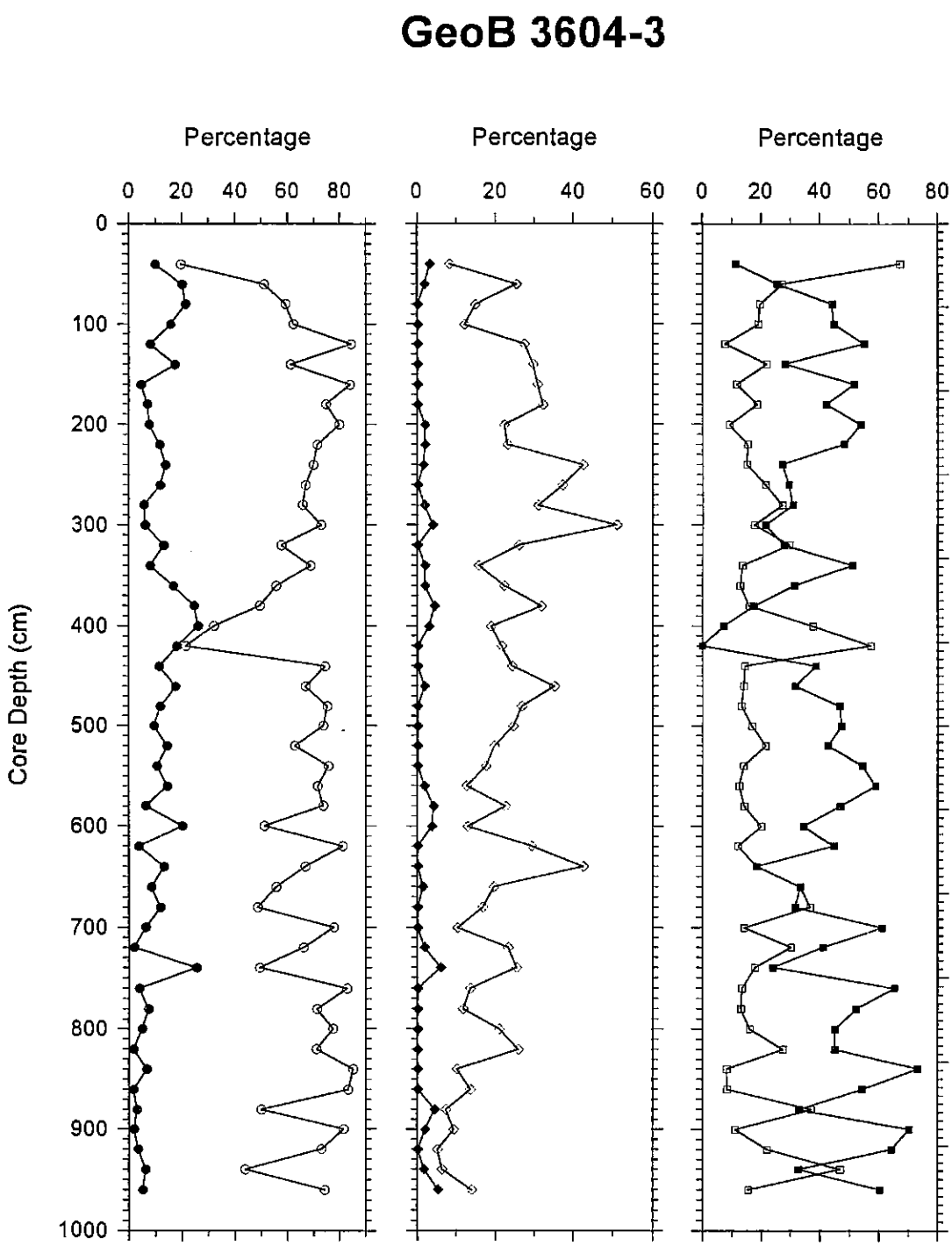

Fig. 53: Gravity core GeoB 3604-3 (southern Cape Basin) - preliminary results for planktic foraminifera assemblages. Left - tropical foraminifera [full circles]; cold water foraminifera (*N. pachyderma* (sin + dex) + *G. bulloi-des)* [open circles]. Center - *N. dutertrei* [full diamonds]; *G. bulloides* [open diamonds]. Right - *N. pachyderma* (dex) [full squares]; *G. inflata* [open squares].

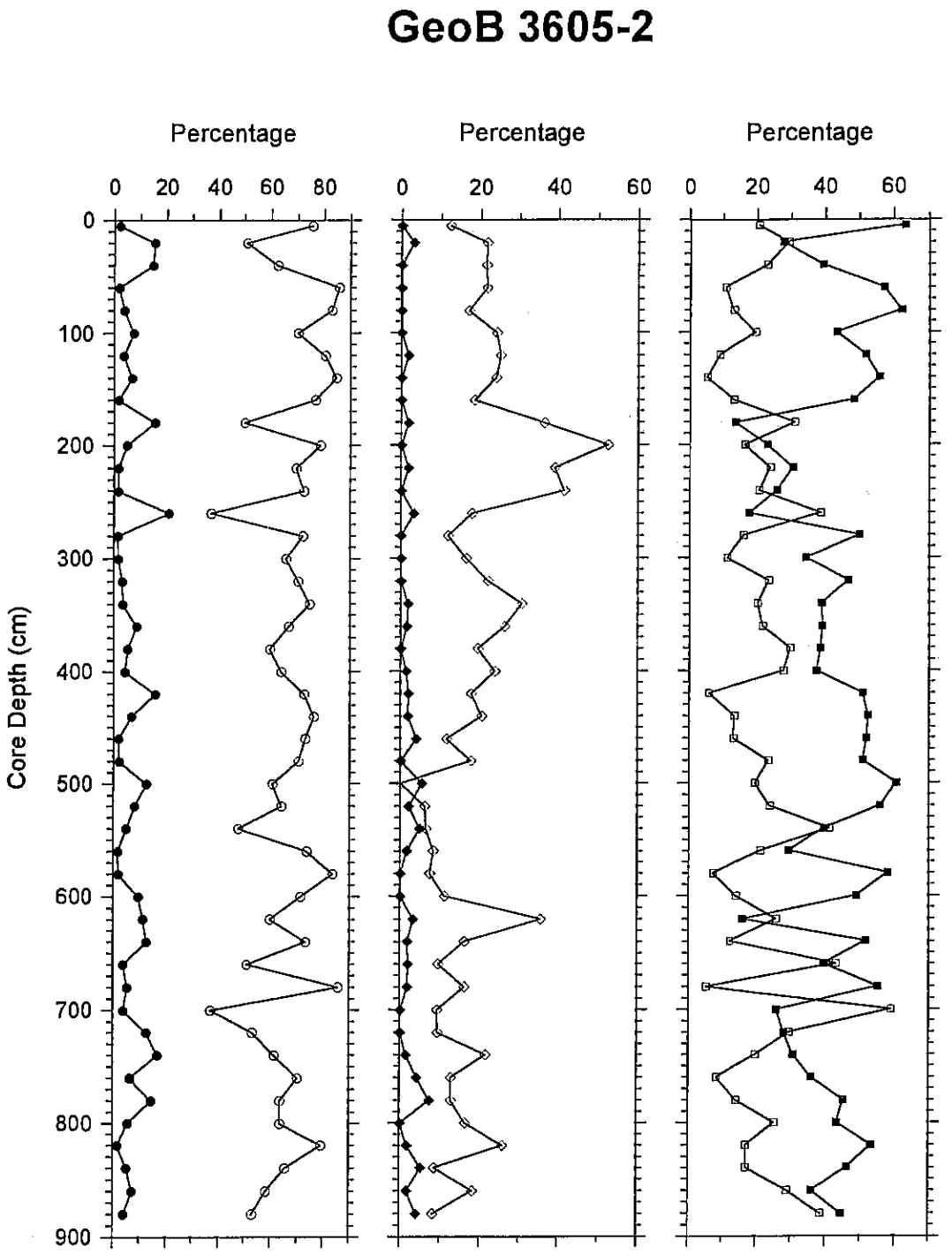

Fig. 54: Gravity core GeoB 3605-2 (southern Cape Basin) - preliminary results for planktic foraminifera assemblages. Left - tropical foraminifera [full circles]; cold water foraminifera (*N. pachyderma* (sin + dex) + *G. bulloi-des)* [open circles]. Center - *N. dutertrei* [full diamonds]; *G. bulloides* [open diamonds]. Right - *N. pachyderma* (dex) [full squares]; *G. inflata* [open squares].

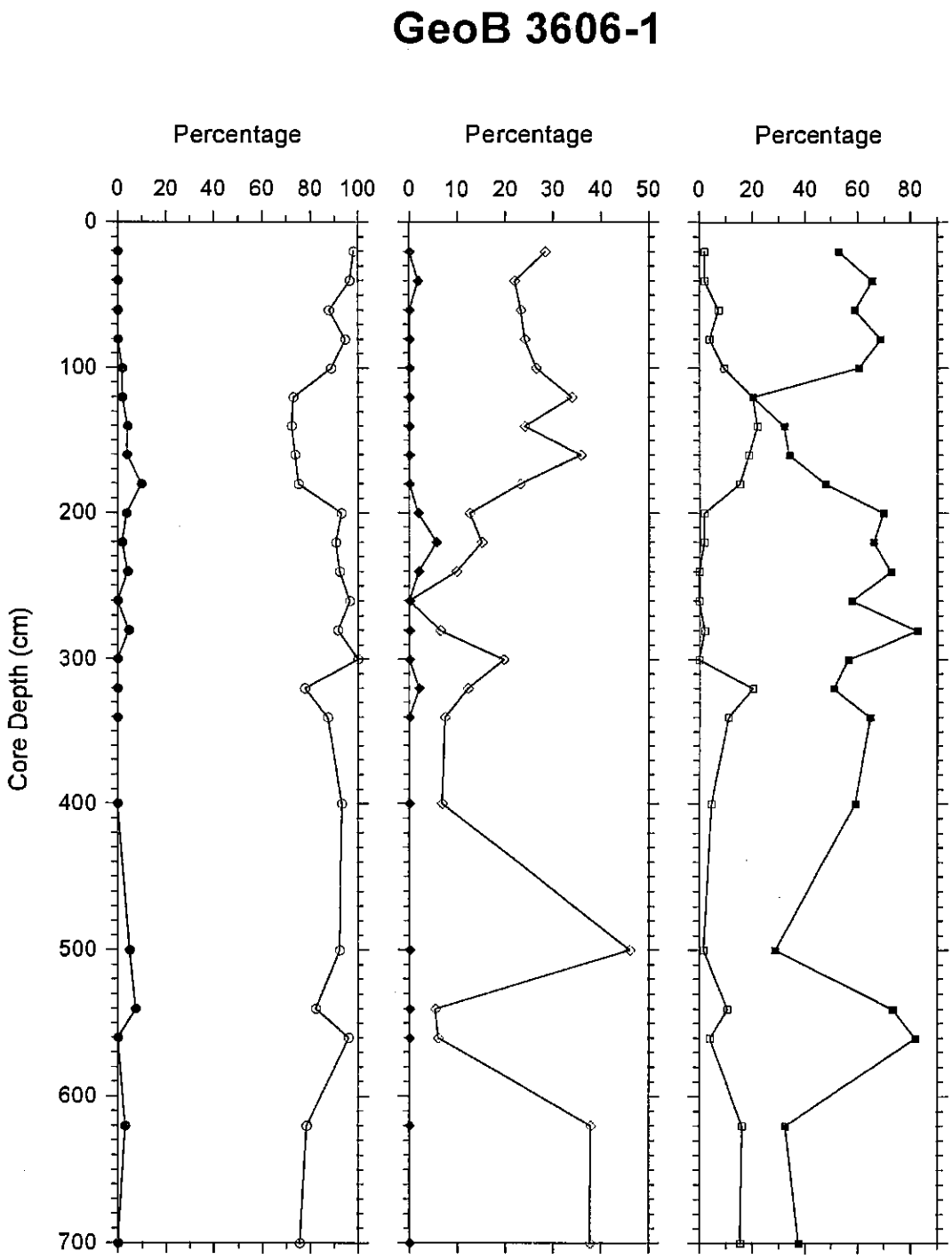

Fig. 55: Gravity core GeoB 3606-1 (Benguela upwelling center) - preliminary results for planktic foraminifera assemblages. Left - tropical foraminifera [full circles]; cold water foraminifera (*N. pachyderma* (sin + dex) + *G. bulloides)* [open circles]. Center - *N. dutertrei* [full diamonds]; *G. bulloides* [open diamonds]. Right - *N. pachyderma* (dex) [full squares]; *G. inflata* [open squares].

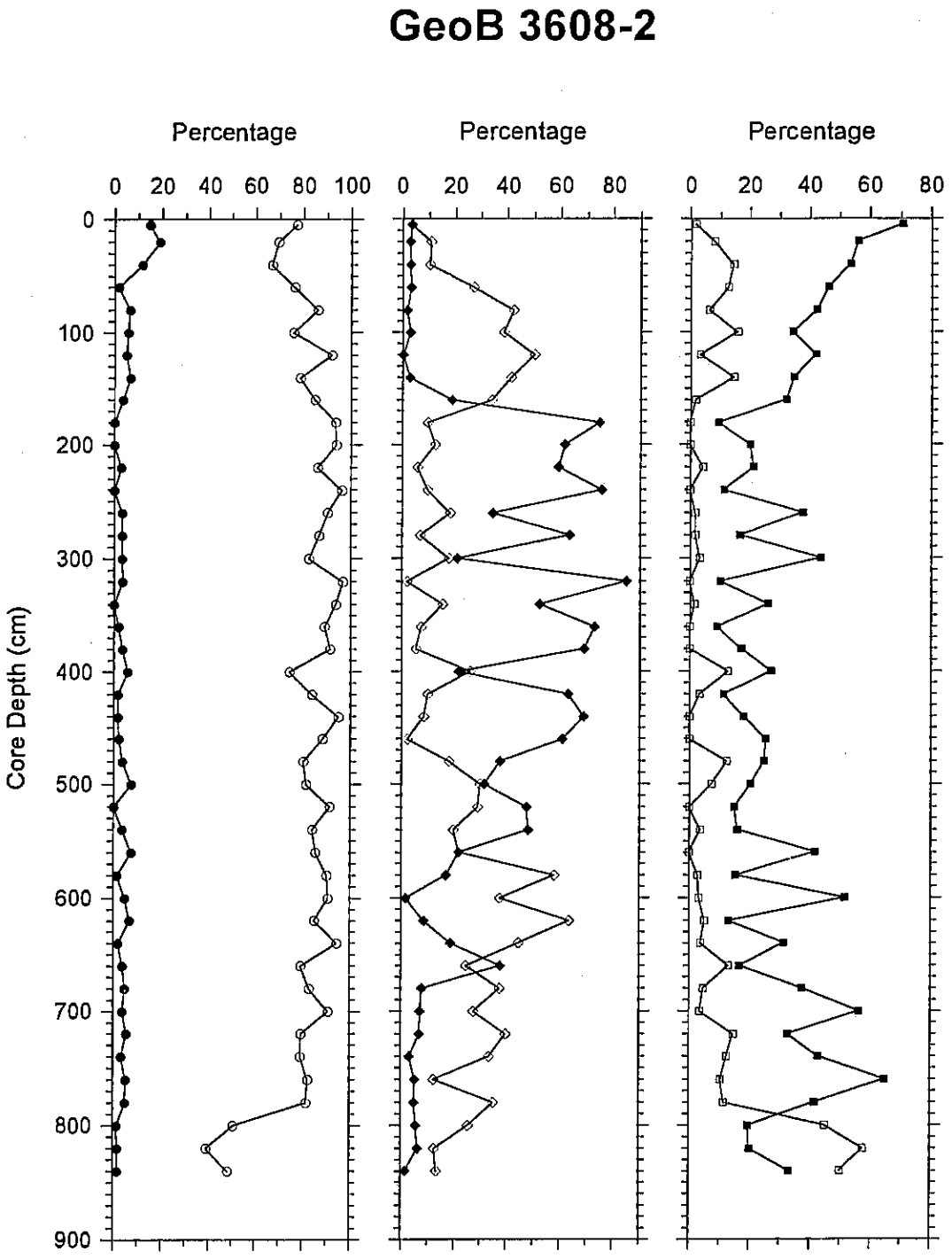

Fig. 56: Gravity core GeoB 3608-2 (northern Cape Basin) - preliminary results for planktic foraminifera assemblages. Left - tropical foraminifera [full circles]; cold water foraminifera (*N. pachyderma* (sin + dex) + *G. bulloi-des)* [open circles]. Center - *N. dutertrei* [full diamonds]; *G. bulloides* [open diamonds]. Right - *N. pachyderma* (dex) [full squares]; *G. inflata* [open squares].

5.1.2.2.2 Lithologic Core Summary

(R. Schneider)

This preliminary lithologic summary of the sediments retrieved with the gravity corer during cruise M34/1 is based on visual description, color scanner readings and microscopic inspection of smear slides taken from distinctive sediment horizons. Core descriptions are shown in Figures 57a to 63a, presenting main lithologies, their color according to the MUNSELL soil color chart, and sedimentary structures. A first measure of sediment grain size variations is provided by the sand content reported in Figure 64 for each core.

In order to obtain a more detailed picture of alternating intervals of grey to light green versus dark olive green sediment color, light reflection was determined quantitatively with a Minolta CM-2002 hand-held spectrophotometer. Digital reflectance data were routinely measured at 31 wavelengths in the visible light range (400-700 nm) on the split surface of the archive halves immediately after core opening. For this purpose the surfaces of the core segments were carefully scraped to expose a fresh, clean plane for the measurements at 2 cm intervals. To protect the photometer from being contaminated, a thin transparent plastic film (Hostaphan) was used to cover the wet surface of the sediment. Before measuring each core segment, the spectrophotometer was re-adjusted for white color reflectance by attaching a calibration cap. The data recorded were finally transferred to a PC. A graphic representation of the percent reflectance at three selected wavelengths (450 nm (blue), 550 nm (green), and 700 nm (red)) is shown in Figures 57a to 63a for each core. It is likely, that these color changes are due to changes in the sediment composition, particularly the ratio of carbonate or silicate (light and high reflection values) to organic residue and clay mineral (dark or low reflection values) content.

The sediments recovered can be grouped into three different types based on the shipboard sedimentological analysis. The sediments characteristic for the first group including cores GeoB 3602-1, 3603-2, 3604-3, and 3605-2 from the upper slope of the southern Cape Basin (31 to 35° S) consists mainly of nannofossil ooze (> 60 % from smear slide analysis) with varying amounts of foraminifera (Figs. 57a to 60a); the latter determine the degree of sand content (Fig. 64). Color reflectance is higher for all wave bands compared to the northern Cape Basin sediments which is attributed to high carbonate content and probably moderate organic carbon contents. The sandy, foraminifera rich intervals seem to represent either sediment sections where the fine fraction was partly winnowed by intensive bottom currents or small scale foraminiferal turbidites. No indication for downslope transport from the shelf was found in these coarser grained layers.

Cores GeoB 3606-1 and 3607-2 were retrieved from the upper continental slope and from a shallow inner shelf basin, respectively, located under the Benguela upwelling center

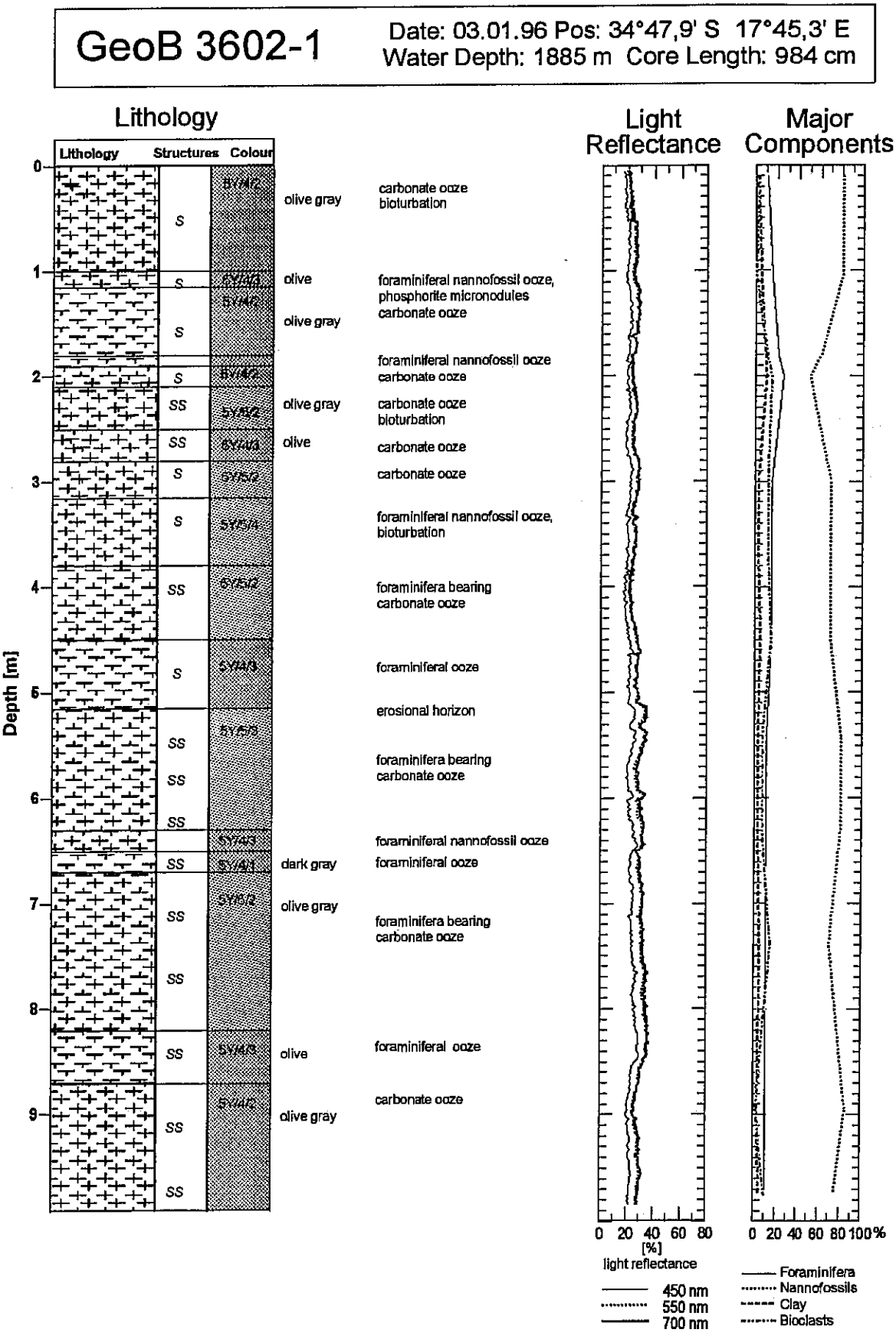

Fig. 57a: Gravity core GeoB 3602-1 (southern Cape Basin) - core description, smear slide and color scanner data, legend for stratigraphic columns see volume II page 74.

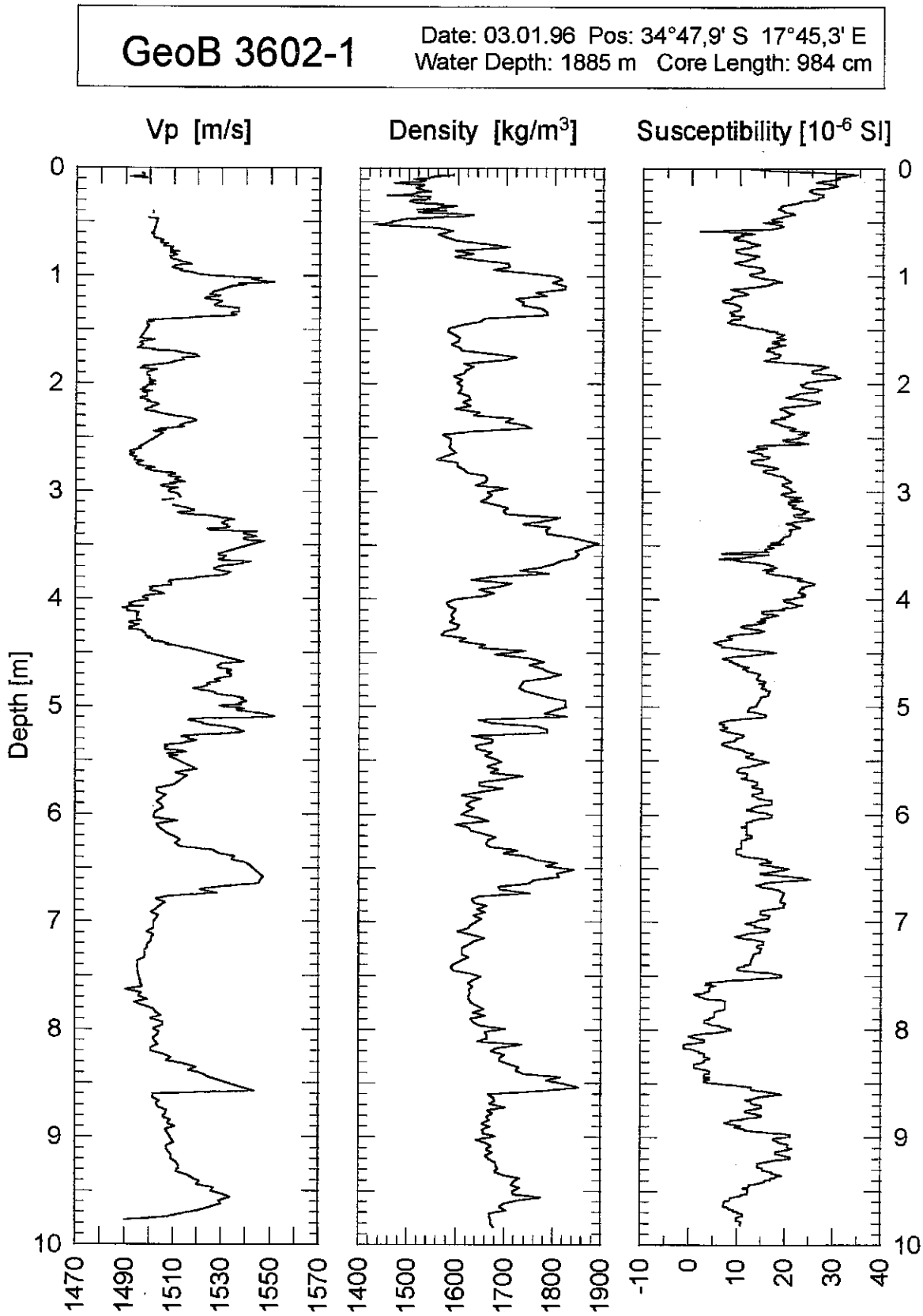

Fig. 57b: Gravity core GeoB 3602-1 (southern Cape Basin) - physical properties data.

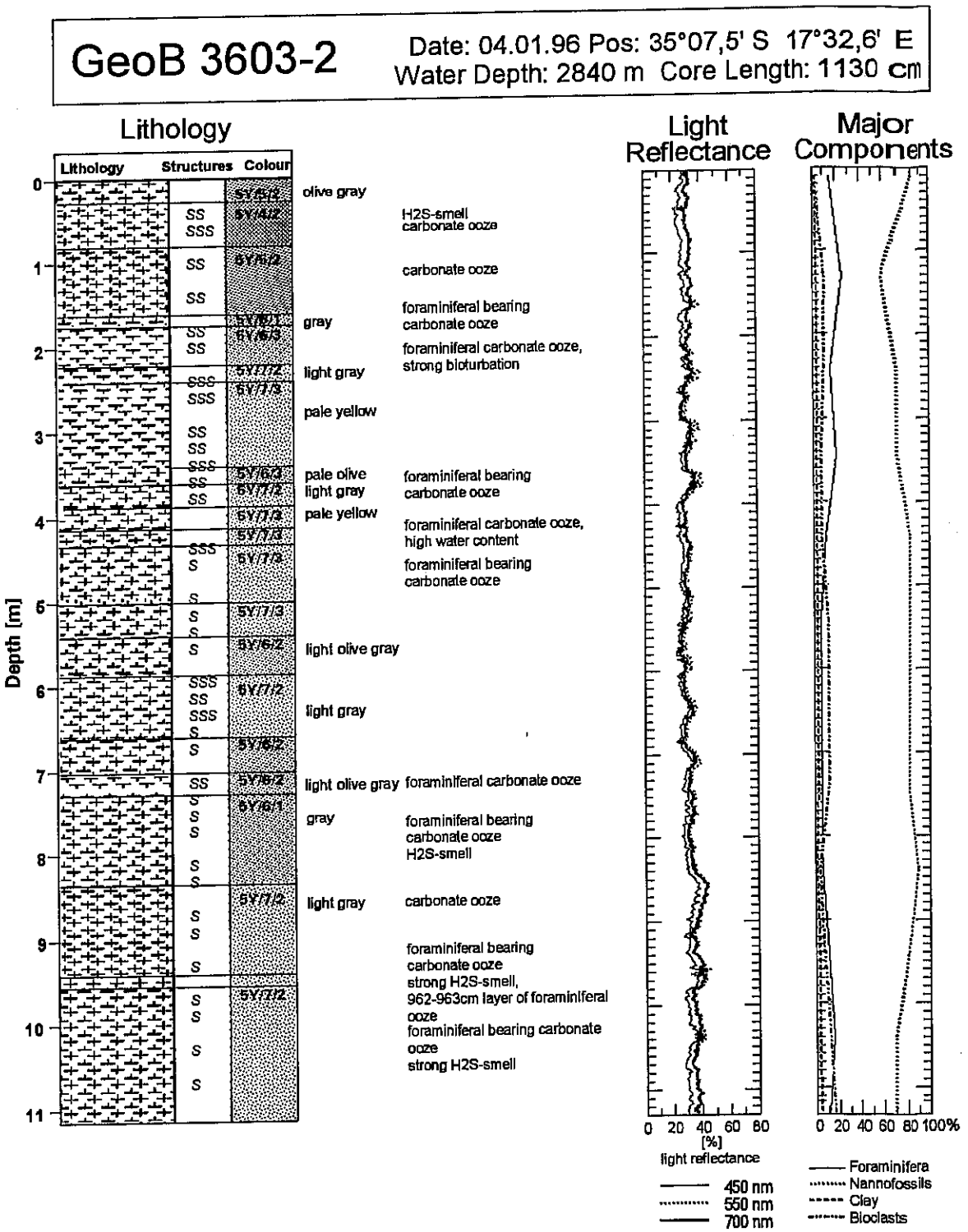

Fig. 58a: Gravity core GeoB 3603-2 (southern Cape Basin) - core description, smear slide and color scanner data.

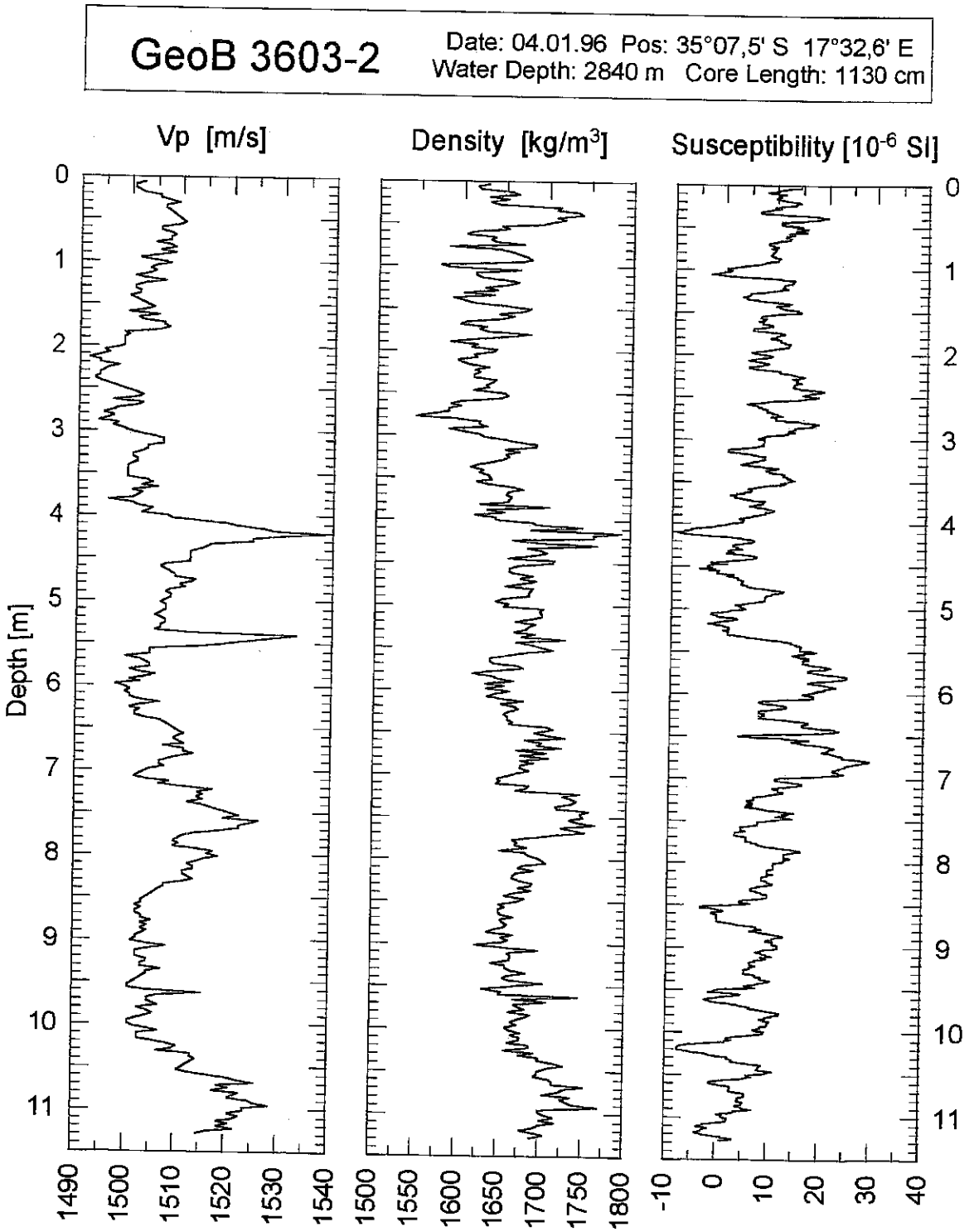

Fig. 58b: Gravity core GeoB 3603-2 (southern Cape Basin) - physical properties data.

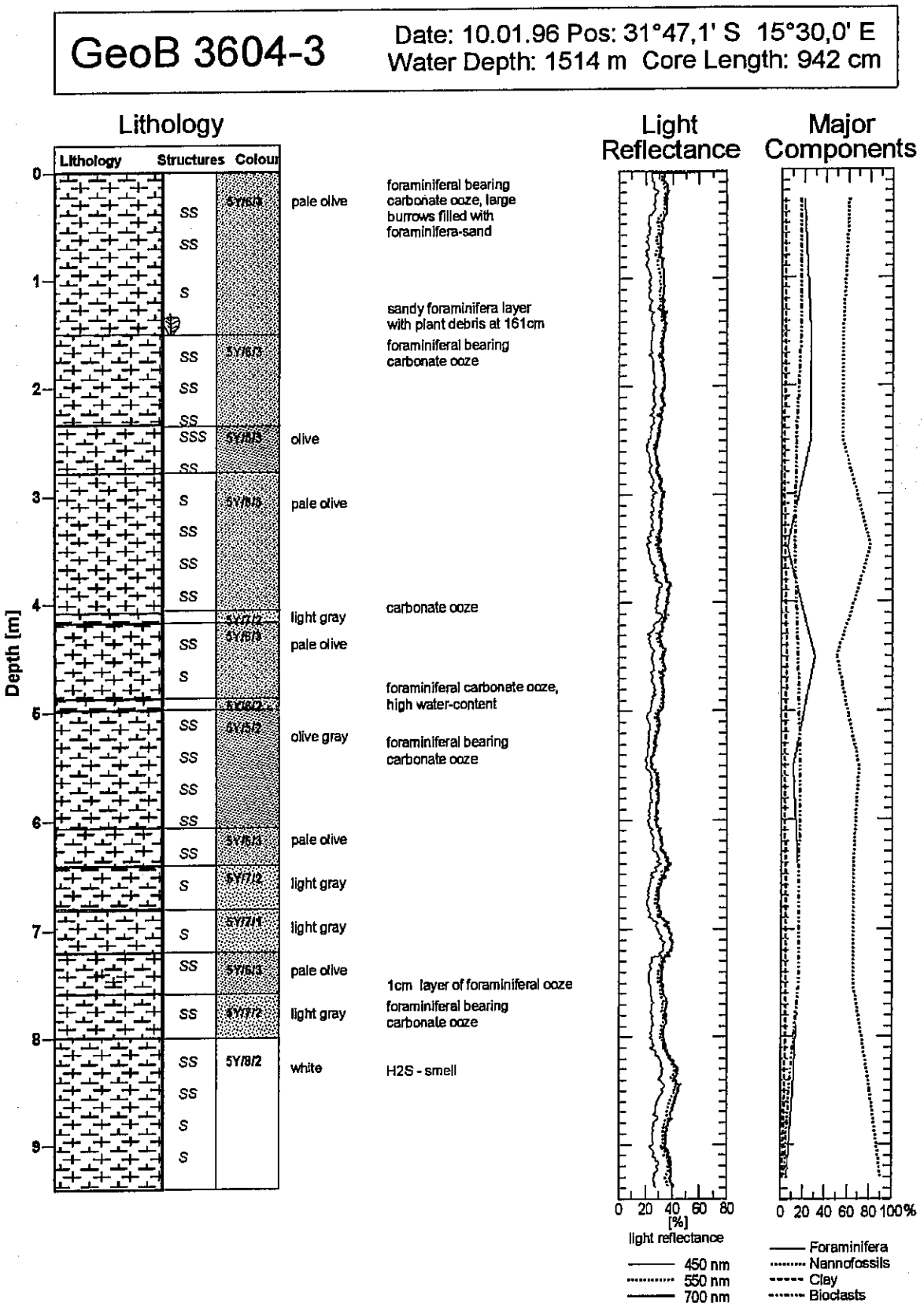

Fig. 59a: Gravity core GeoB 3604-3 (southern Cape Basin) - core description, smear slide and color scanner data.

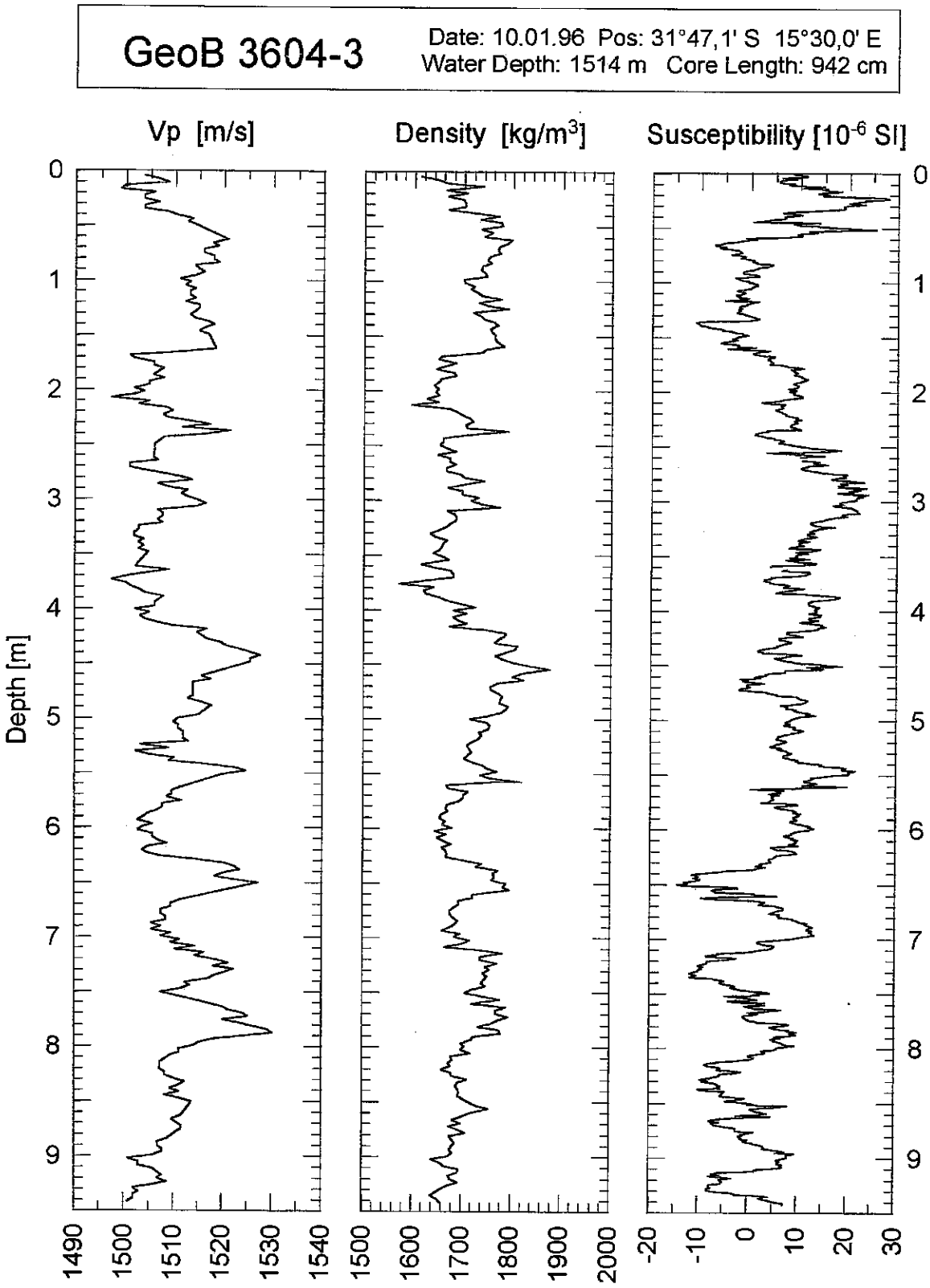

Fig. 59b: Gravity core GeoB 3604-3 (southern Cape Basin) - physical properties data.

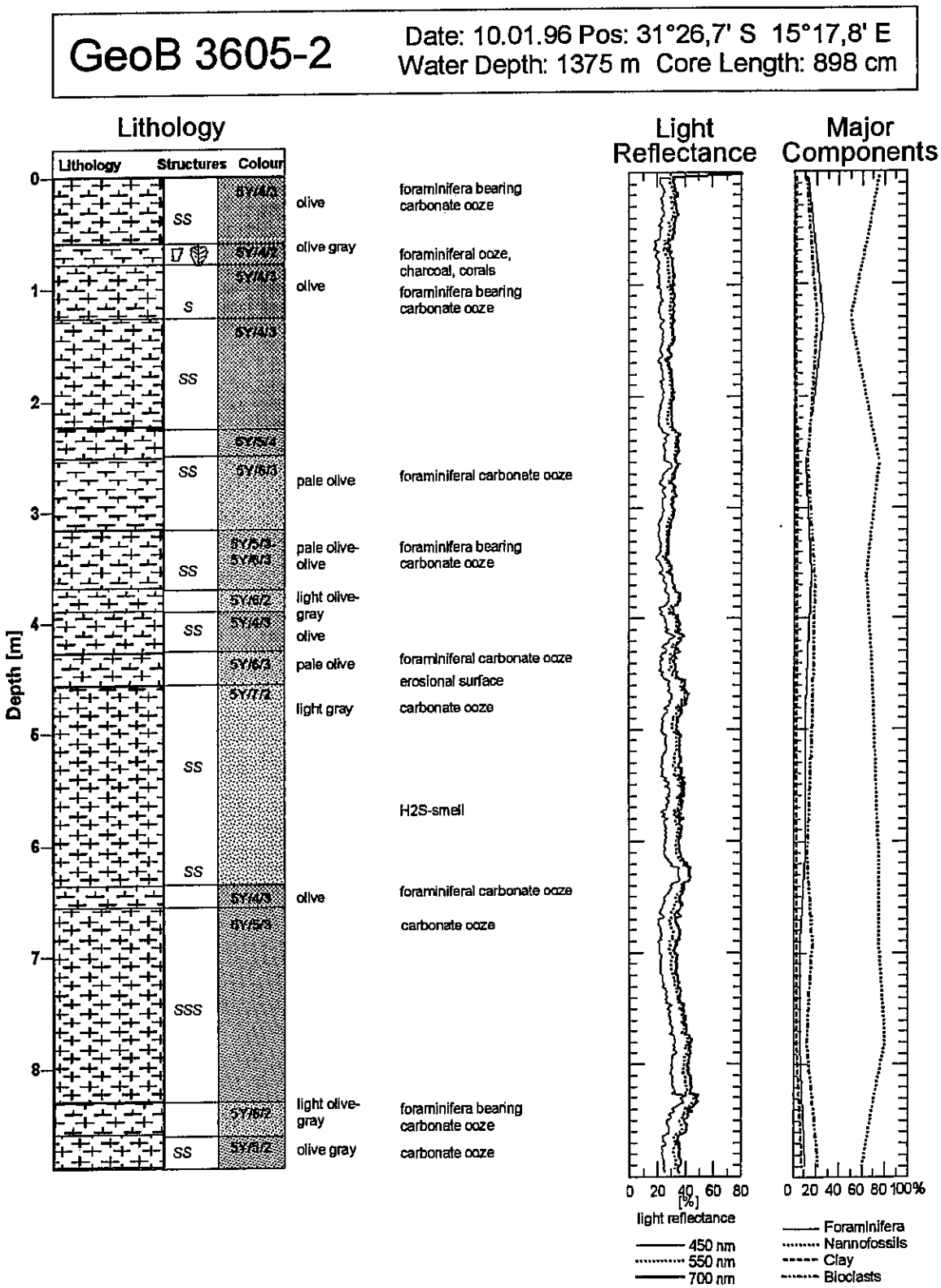

Fig. 60a: Gravity core GeoB 3605-2 (southern Cape Basin) - core description, smear slide and color scanner data.

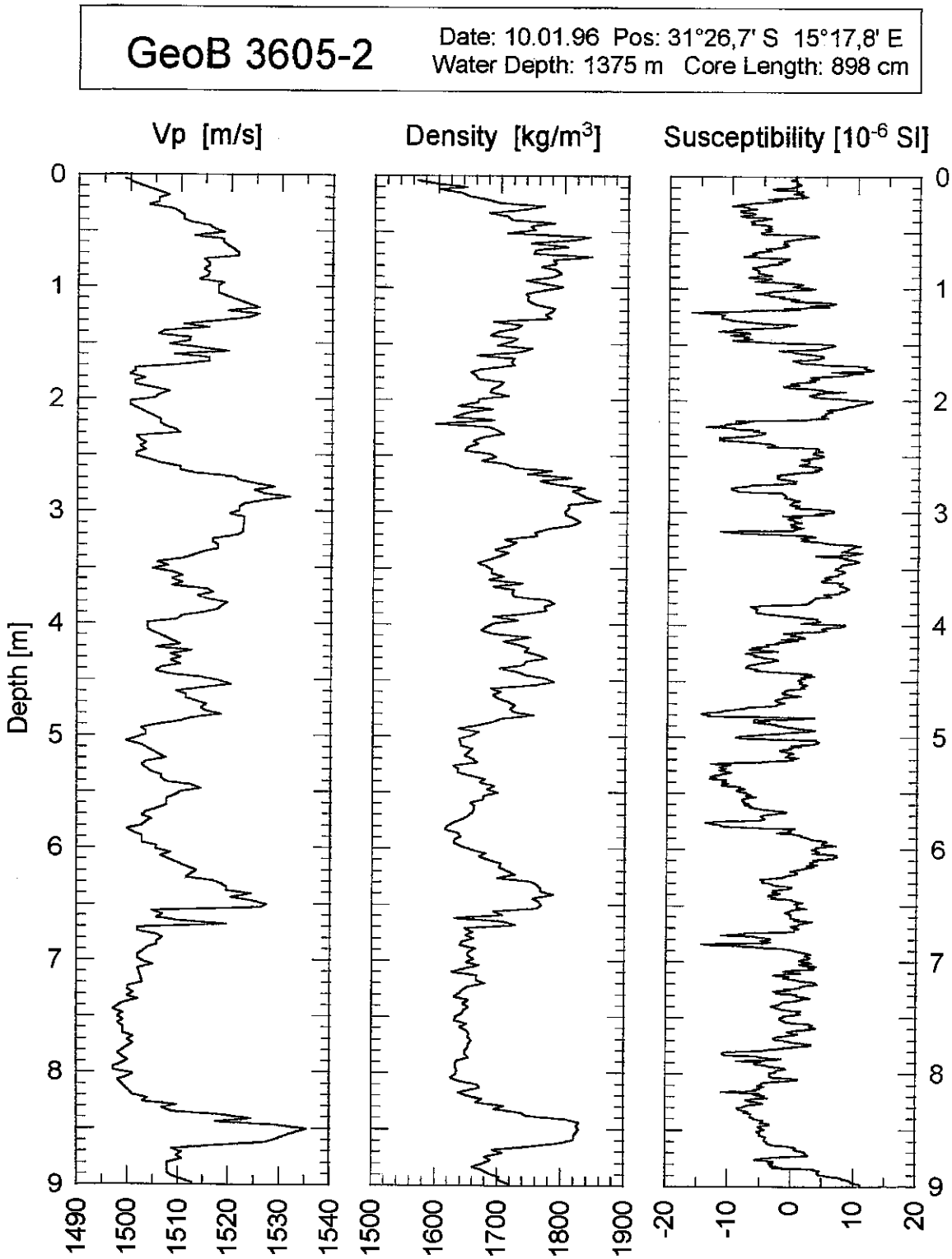

Fig. 60b: Gravity core GeoB 3605-2 (southern Cape Basin) - physical properties data.

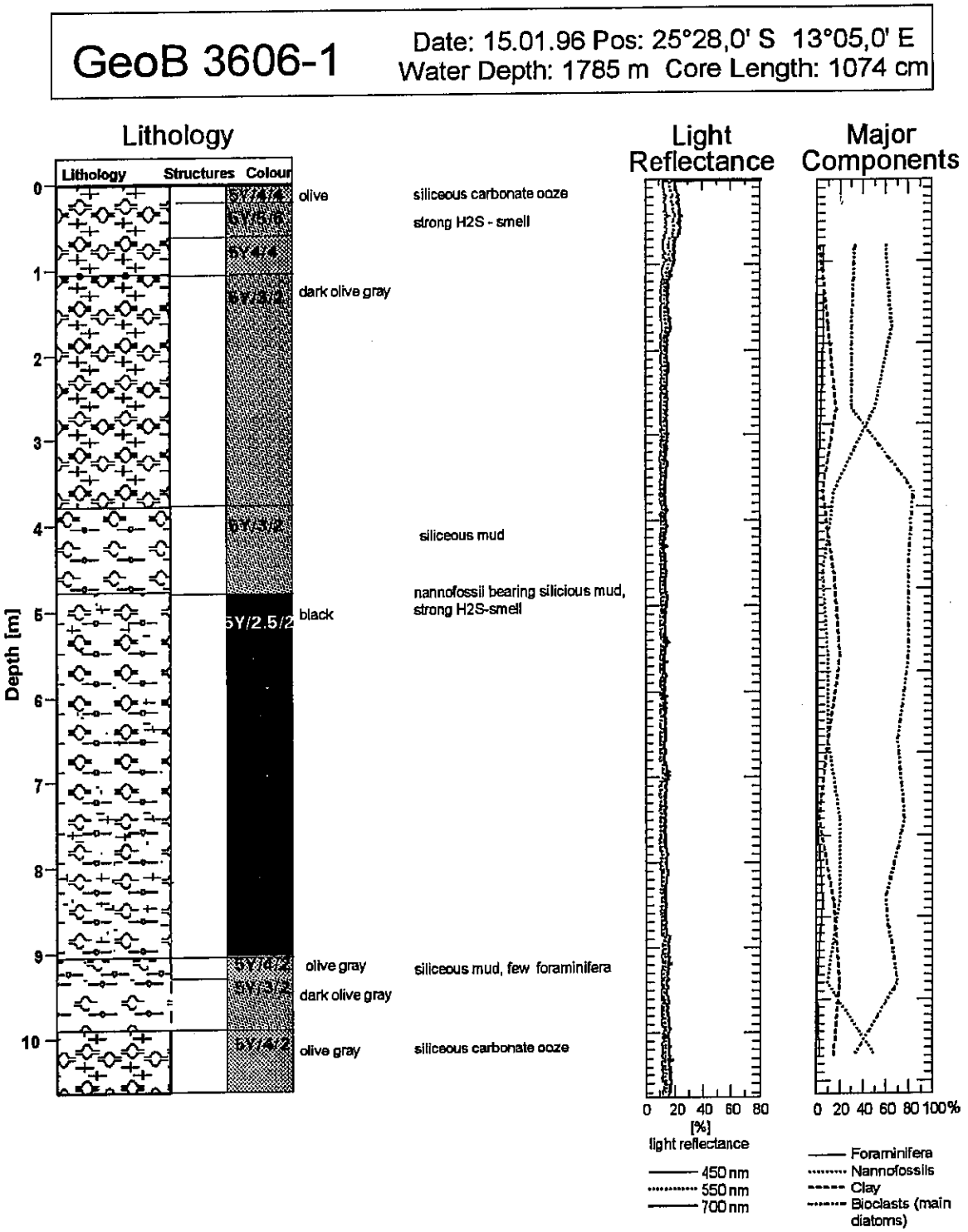

Fig. 61a: Gravity core GeoB 3606-1 (Benguela upwelling center) - core description, smear slide and color scanner data.

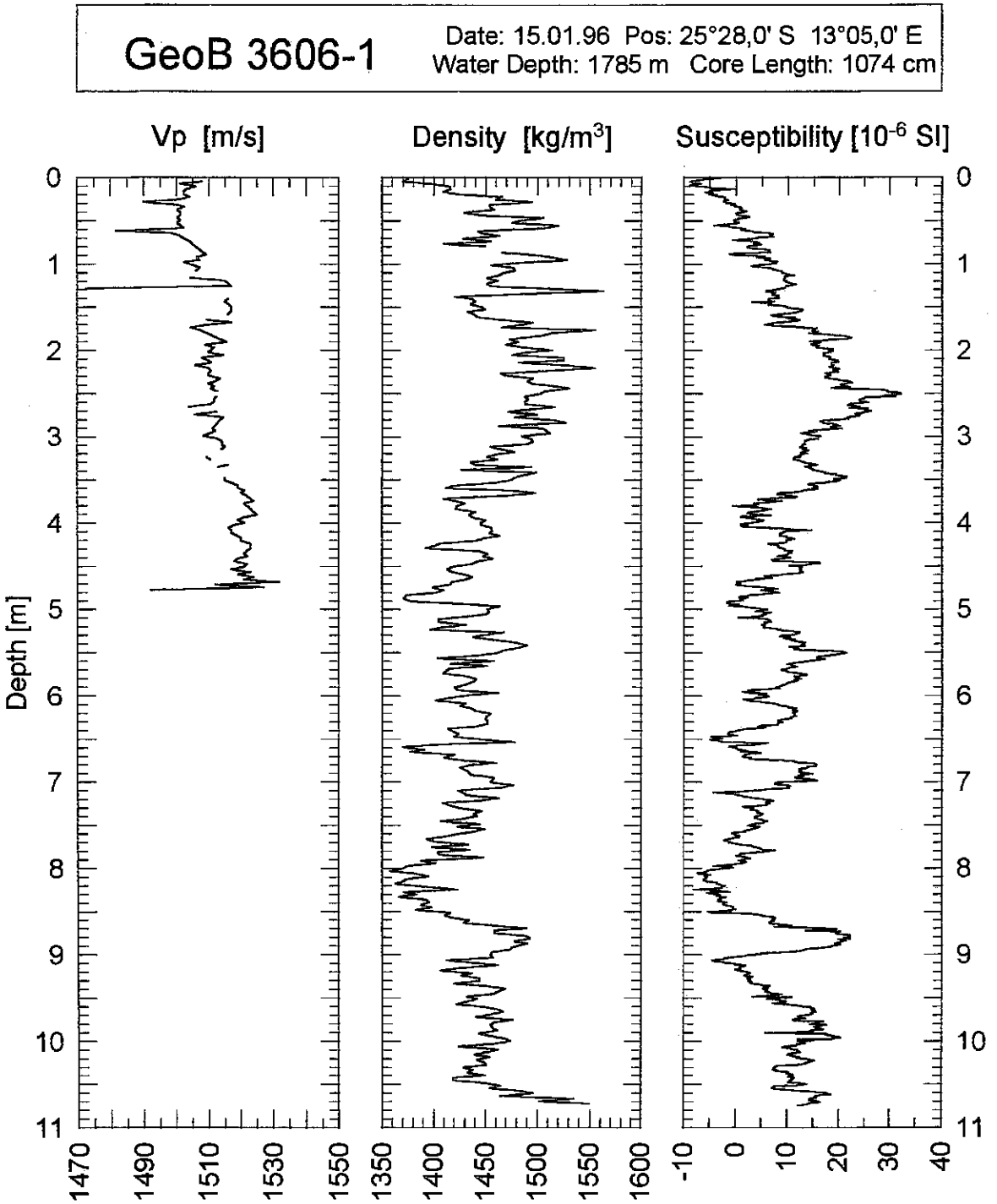

Fig. 61b: Gravity core GeoB 3606-1 (Benguela upwelling center) - physical properties data.

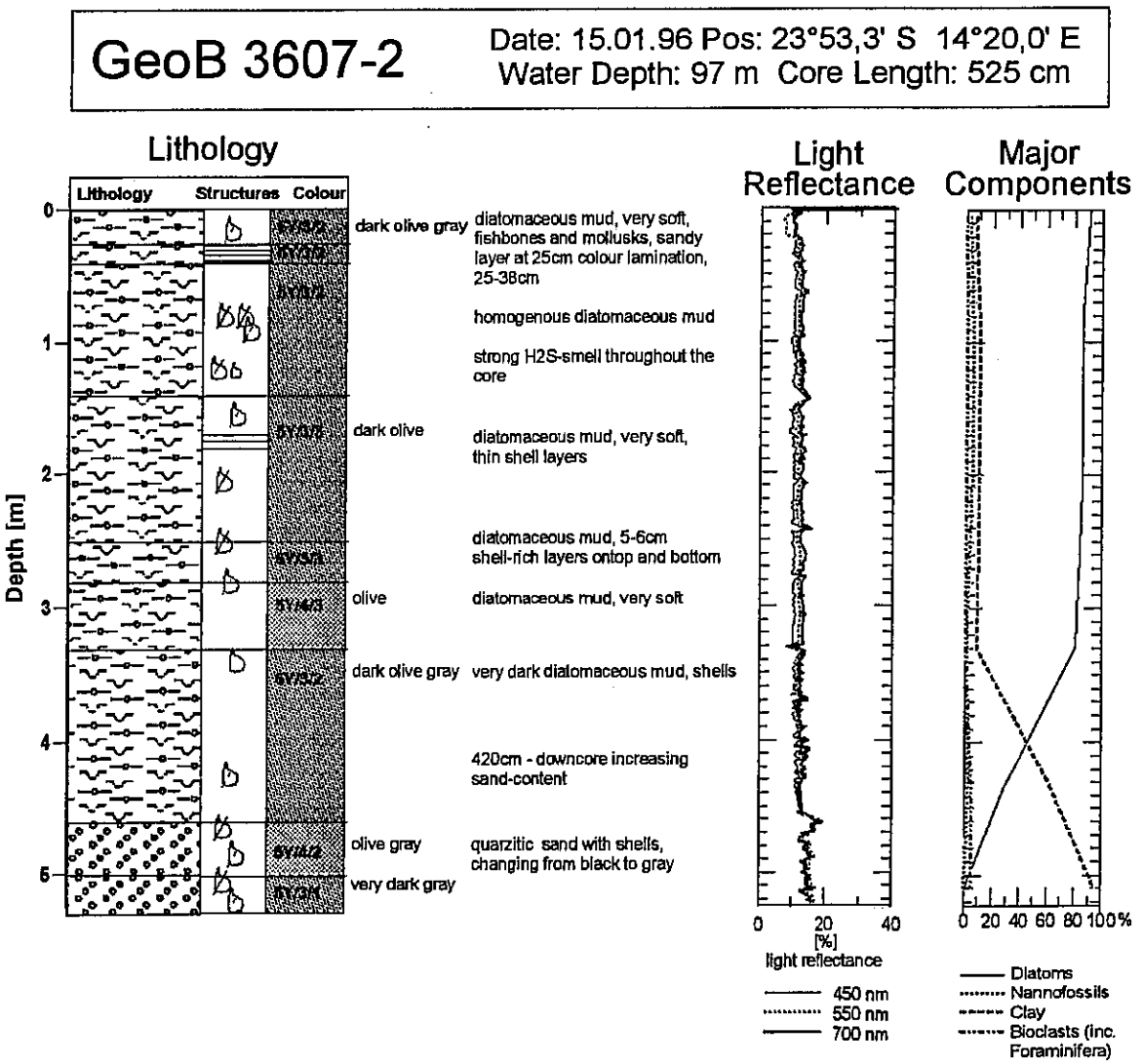

Fig. 62a: Gravity core GeoB 3607-2 (Benguela upwelling center) - core description, smear slide and color scanner data.

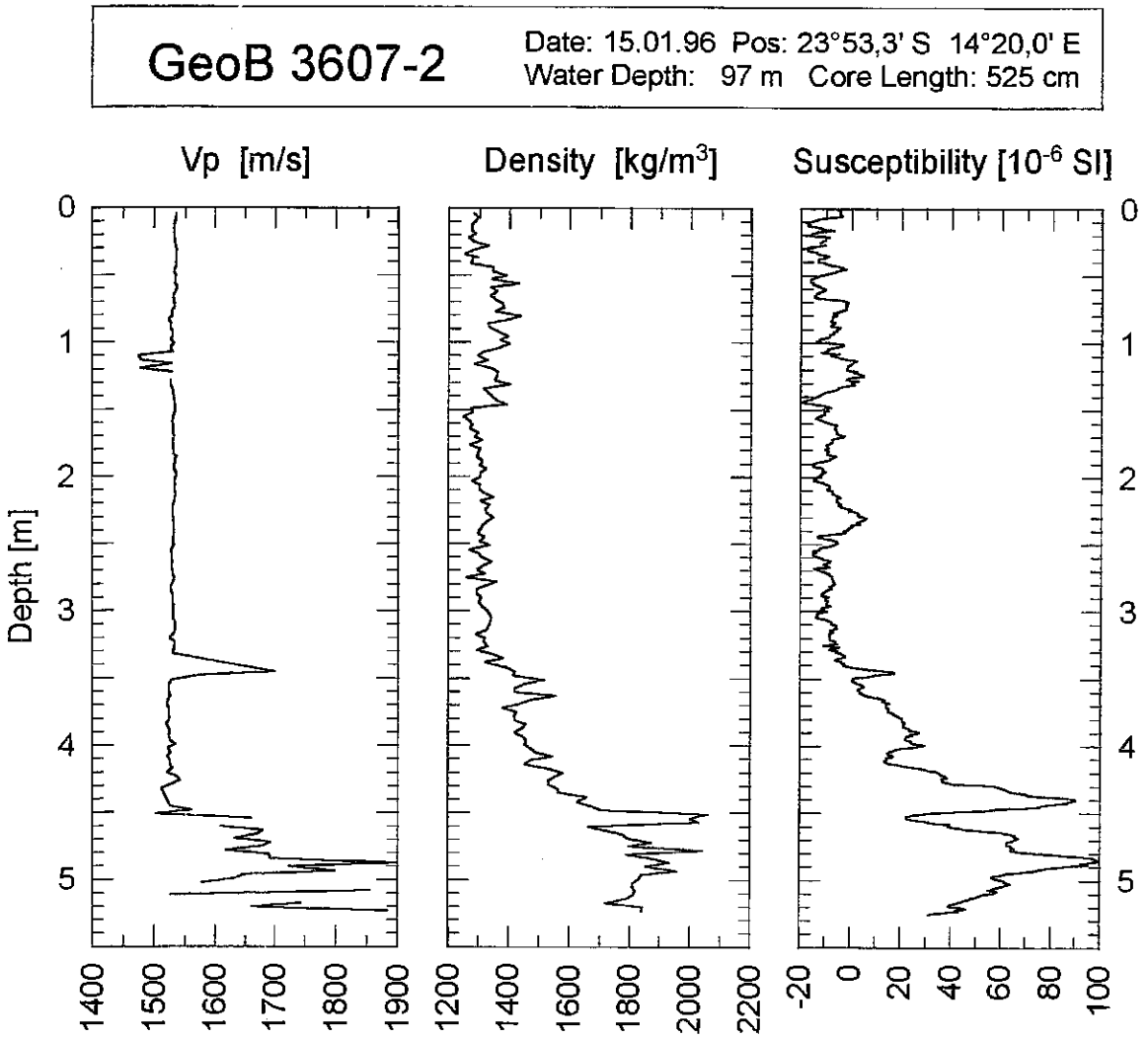

Fig. 62b: Gravity core GeoB 3607-2 (Benguela upwelling center) - physical properties data.

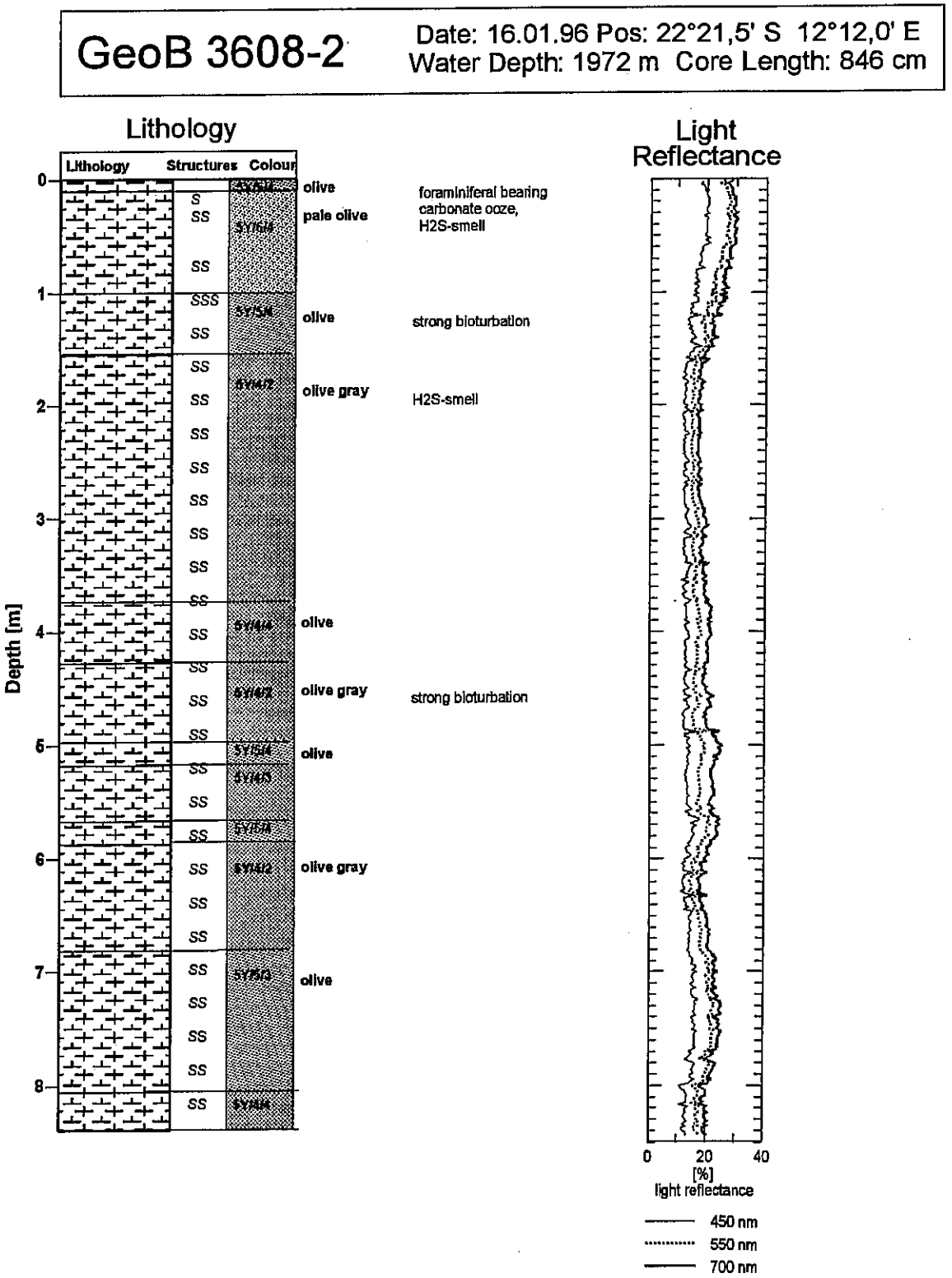

Fig. 63a: Gravity core GeoB 3608-2 (northern Cape Basin) - core description, smear slide and color scanner data.

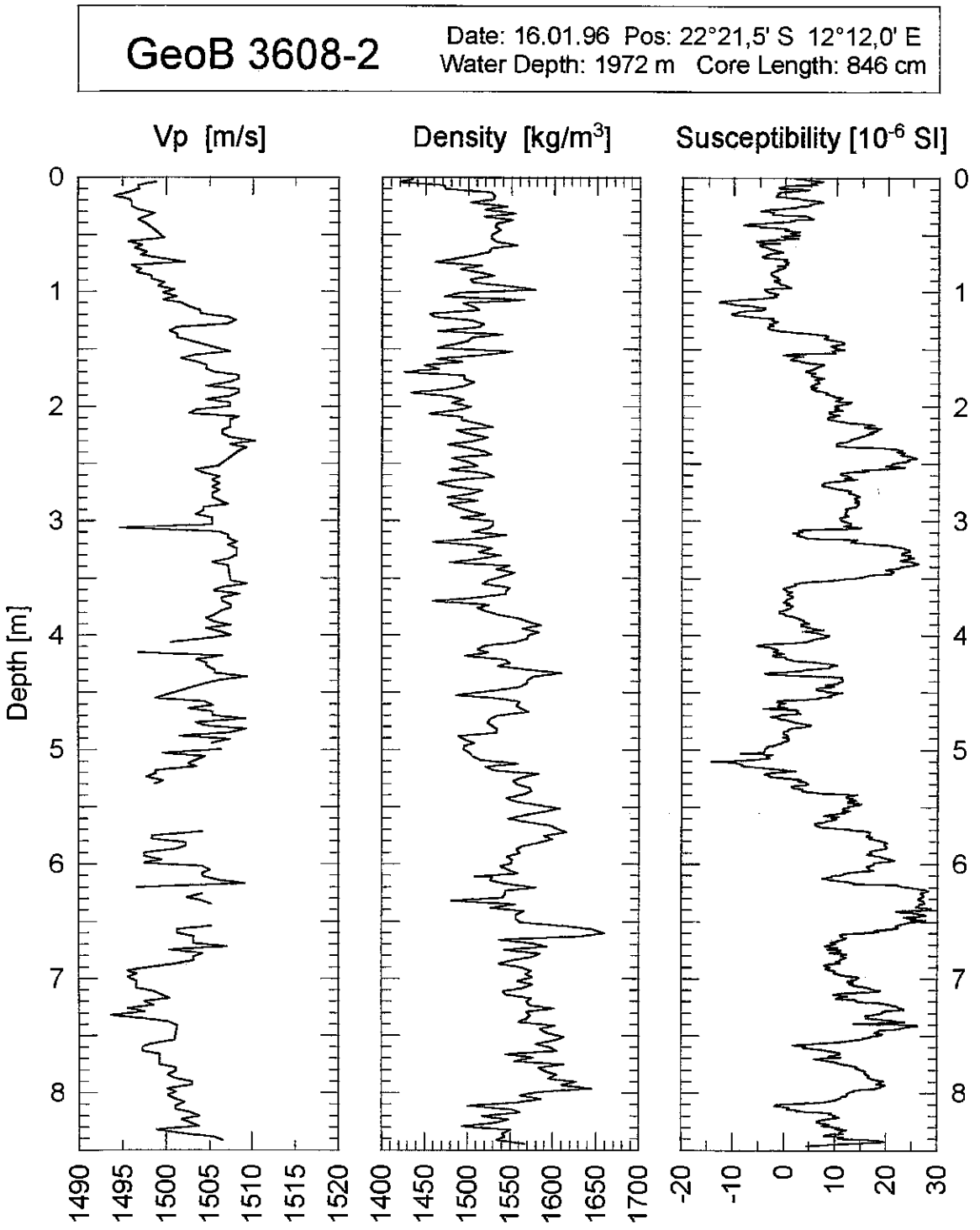

Fig. 63b: Gravity core GeoB 3608-2 (northern Cape Basin) - physical properties data.

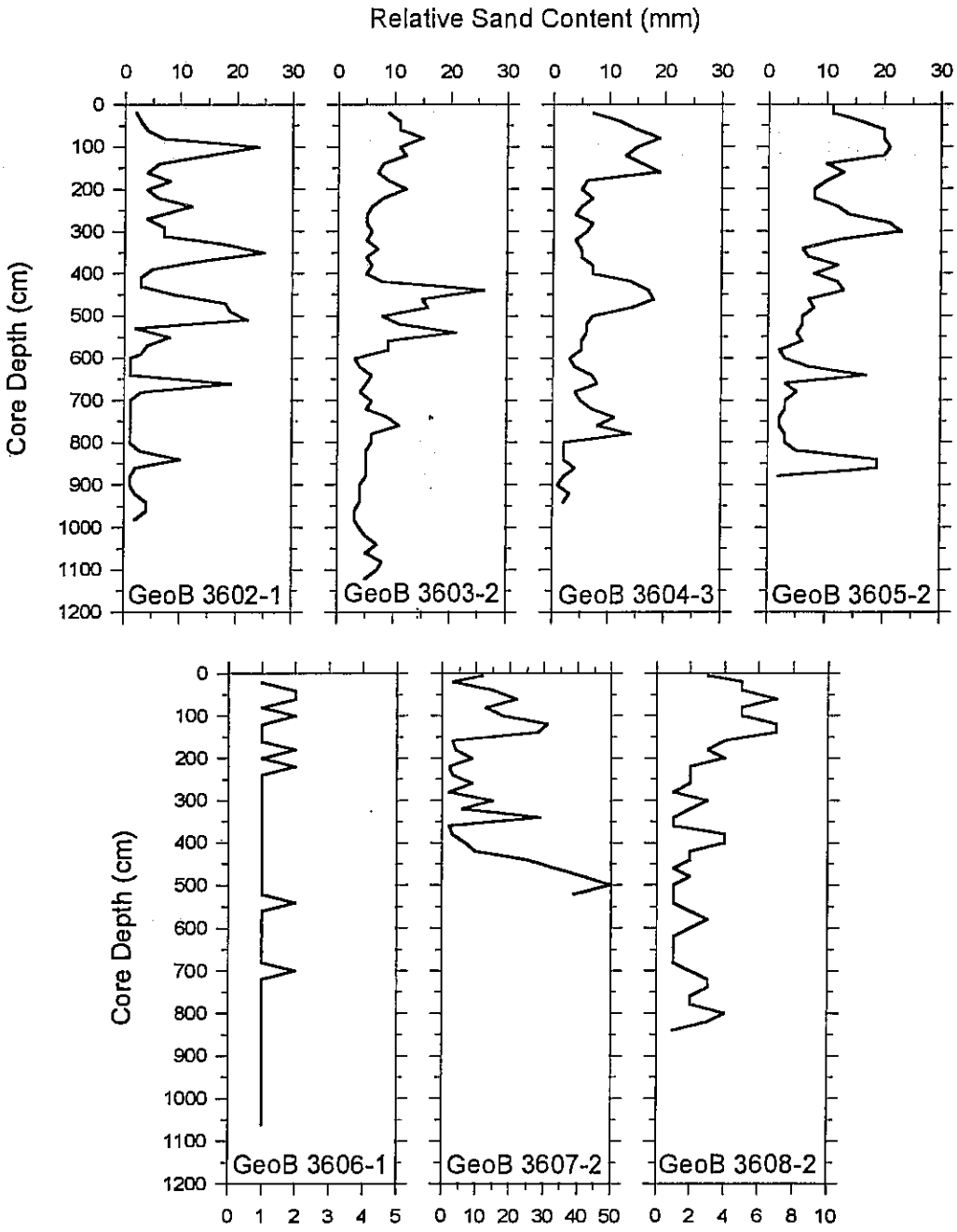

Fig. 64: Relative sand content (fraction >63 µm of 10 ml sediment, height in standard glass tube) versus depth in gravity core sediments.

off Namibia between 24 and 26° S. Their sediments built up the second type of late Quaternary deposits recovered during cruise M34/1. They are nannofossil bearing siliceous clays in the deeper core GeoB 3606-1 (1785 m water depth, Fig. 61a) and diatomaceous ooze intercalated with muddy shell layers in core GeoB 3607-2 from the shelf (97 m water depth, Fig. 62a), whereby the bottom end of the latter consists of a quarzitic sand. Foraminifera are generally absent in the shelf basin sediments and only rare in those from the upper continental slope. Light reflection is very low on the dark olive colored sediments, also indicating minimal carbonate content and probably high organic carbon concentration. Surprising is the high amount of biogenic opal in core GeoB 3606-1, mainly comprising detritus from diatoms, radiolaria and silicoflagellates, which has not been recognized in upper continental slope sediments north and south of the present study area when investigating gravity cores from similar water depths retrieved during METEOR cruise M20/2 (SCHULZ et al., 1992).

The third type of sediment was found in core GeoB 3608-2 from 1972 m water depth in the northern Cape Basin (23°20' S). This core is completely composed of foraminifera bearing nannofossil ooze and no sandy foraminifera layers were observed (Fig. 63a). Light reflectance values and sediment color, the latter varying between light and dark olive green, are on an intermediate level between those from the carbonate rich sediment type 1 group of the southern Cape Basin and those from carbonate poor but organic carbon and opal rich type 2 sediments from the Benguela upwelling center at about 25° S.

5.1.3 Physical Properties Studies

(T. Frederichs, L. Brück, C. Hilgenfeldt)

During METEOR cruise M34/1 all recovered gravity cores were subject to laboratory geophysical studies. A routine shipboard measurement of three physical parameters was carried out on the segmented sediment cores, comprising the determination of

- the compressional (P-) wave velocity v_p,
- the electric resistivity R_S, and
- the magnetic volume susceptibility κ.

These properties are closely related to the grain size, porosity and lithology of the sediments and provide high-resolution core logs (spacing 3, 3 and 1 cm, respectively) available prior to all other detailed investigations. In addition, oriented samples for later shore based paleo- and rockmagnetic studies were taken at intervals of 10 cm.

5.1.3.1 Physical Background and Experimental Techniques

The experimental set-up for the shipboard measurements was basically identical to that of previous cruises. Therefore, the descriptions given here are kept brief. For a more detailed

treatment of the experimental procedures see SCHULZ et al. (1991) for v_p and WEFER et al. (1991) for R_S.

P-wave velocity

The P-wave velocity v_p was derived from digitally processed ultrasonic transmission seismograms which were recorded perpendicular to the core axis with a fully automated logging system. First arrivals are picked using a cross-correlation algorithm based on the zero-offset signal of the piezoelectric wheel probes. In combination with a measure of the core diameter d the travel time of the first arrivals t lead to a P-wave velocity profile with an accuracy of 1 to 2 m/s.

$$v_p = (d - d_L) / (t - t_L)$$

where d_L is the thickness of the liner walls, t_L the travel time through the liner walls.

Following SCHULTHEISS and McPHAIL (1989), a temperature calibration of v_p is effected using the equation

$$v_{20} = v_T + 3 \cdot (20 - T)$$

where v_{20} denotes the P-wave velocity at 20 °C and T the temperature (in °C) of the core segment when logged. Simultaneously, the maximum peak-to-peak amplitudes of the transmission seismograms are evaluated to estimate attenuation variations along the sediment core. P-wave profiles can be used for locating strong as well as fine-scale lithological changes, e.g. turbidite layers or gradual changes in the sand, silt or clay content.

Electric resistivity, porosity and density

The electric sediment resistivity R_S was determined using a handheld sensor with a miniaturized four-electrodes-in-line ('Wenner') configuration (4 mm electrode spacing). A rectangular alternating current signal is fed to the sediment about 1 cm below the split core surface by the two outer electrodes. Assuming a homogeneously conducting medium, the potential difference at the inner two electrodes is directly proportional to the sediment resistivity R_S. A newly integrated fast resistance thermometer provides data for a temperature correction.

According to the empirical ARCHIE's equation, the ratio of sediment resistivity R_S and pore water resistivity R_W may be approximated by a power function of porosity ϕ

$$R_S / R_W = k \cdot \phi^{-m}$$

Following a recommendation by BOYCE (1968), suitable for seawater saturated clay rich sediments, values of 1.30 and 1.45 were used for the constants k and m, respectively. The

calculated porosity ϕ is subsequently converted to wet bulk density ρ_{wet} using the equation (BOYCE, 1976)

$$\rho_{wet} = \phi \cdot \rho_f + (1 - \phi) \cdot \rho_m$$

with a pore water density ρ_f of 1030 kg/m^3 and a matrix density ρ_m of 2670 kg/m^3. For the sake of an unbiased uniform treatment of all cores, these empirical coefficients were not adapted to individual sediment lithologies at this stage. Nevertheless, at least relative density changes should be well documented.

Magnetic volume susceptibility

The magnetic volume susceptibility κ is defined by the equations

$$B = \mu_0 \cdot \mu_r \cdot H = \mu_0 \cdot (1 + \kappa) \cdot H = \mu_0 \cdot H + \mu_0 \cdot \kappa \cdot H = B_0 + M$$

with the magnetic induction B, the absolute/relative permeability $\mu_{0/r}$, the magnetizing field H, the magnetic volume susceptibility κ and the volume magnetization M. As can be seen from the third term, κ is a dimensionless physical quantity. It describes the amount to which a material is magnetized by an external magnetic field.

For marine sediments the magnetic susceptibility may vary from an absolute minimum value of around $-15 \cdot 10^{-6}$ (diamagnetic minerals such as pure calcite or quartz) to a maximum of some $10'000 \cdot 10^{-6}$ for basaltic debris rich in (titano-) magnetite. In most cases κ is primarily determined by the concentration of ferrimagnetic minerals, while paramagnetic minerals such as clays are of minor importance. High magnetic susceptibilities indicate a high lithogenic input/high iron (bio-) mineralization or low carbonate/opal productivity and vice versa. This relation may serve for the mutual correlation of sedimentary sequences which were deposited under similar global or regional conditions.

The measuring equipment consists of a commercial Bartington M.S.2 susceptibility meter with a 125 mm loop sensor and a non-magnetic core conveyor system. Due to the sensor's size, its sensitive volume covers a core interval of about 8 cm. Consequently, sharp susceptibility changes in the sediment column will appear smoother in the κ core log and, e.g., thin layers such as ashes cannot appropriately be resolved by whole-core susceptibility measurement.

5.1.3.2 Shipboard Results

The coring program of cruise M34/1 was performed in the southern and the northern parts of the Cape Basin. The latitudinal extension of the studied area reached from 34° S just south of Cape Town to 22° S north of Walvis Bay. Coring stations were chosen at water depths from

around 100 to 3000 m. Cores GeoB 3604-3 and 3605-2 were recovered in the vicinity of the proposed ODP Site SCB-1 at the crossings of seismic profiles GeoB/AWI 96-008 / GeoB/AWI 96-001 and GeoB/AWI 96-008 / GeoB/AWI 96-003, respectively. Core GeoB 3606-1 represents the location of the proposed ODP Site NCB-1. It is situated at the crossing of seismic profiles GeoB/AWI 96-012 / GeoB/AWI 96-014. The very shallow station GeoB 3607 in a water depth of only 97 m was located at 24° S on the inner shelf off Namibia. The core recovery here was around 6 m, while the typical core lengths at the other sites were between 9 and 11 m. A total of seven sediment cores with a cumulative length of 64 m have been investigated applying physical properties measurements on board.

Physical property logs of the individual gravity cores are shown in Figures 53b to 63b. A compilation of the data is given in Figure 65. The cores consist mainly of carbonate (foraminiferal) ooze, except for Core GeoB 3607-2 which is composed of (sandy) diatomaceous mud. The very low magnetic susceptibilities in both areas of the Cape Basin reflect the low lithogenic input. Downcore variations are mainly controlled by the content of organic matter. The average suceptibilities in cores from the southern Cape Basin vary from $15 \cdot 10^{-6}$ SI (GeoB 3602-1) down to $-1.2 \cdot 10^{-6}$ SI (GeoB 3605-2). Mean values are around $9 \cdot 10^{-6}$ SI in all cores recovered in the northern Cape Basin (GeoB 3606-1 through GeoB 3608-2). The highest standard deviation is found in Core GeoB 3607-2 which is due to the heavy mineral content in the lower part of this core. These layers of fine sand cause distinct variations also in the other physical parameters, wet bulk density and compressional wave velocity. Average density values range from 1650 to 1750 kg/m^3 in the southern and from 1450 to 1550 kg/m^3 in the northern Cape Basin with a maximum density of 2600 kg/m^3 in Core GeoB 3607-2. The average P-wave velocities in the southern Cape Basin (1500 to 1510 m/s) differ only slightly from those of the northern Cape Basin (except for Core GeoB 3607-2 with 1554 m/s). They do not reflect the contrasts in wet bulk density of both areas. As observed in Core GeoB 3606-1, and to a lesser degree in Cores GeoB 3607-2 and 3608-2, frequently in the lower, sometimes also in the middle sections of the cores no acoustic measurements were possible, because of insufficient signal amplitudes. The explanation for this problem seems to be a degassing of H_2S due to pressure release. Gas bubbles in the sediment greatly attenuate sound transmission. Core to core correlation of the measured physical properties is only poor. Wet bulk density is the only parameter showing a distinct regional variance with significantly lower values in the northern than in the southern parts of the Cape Basin.

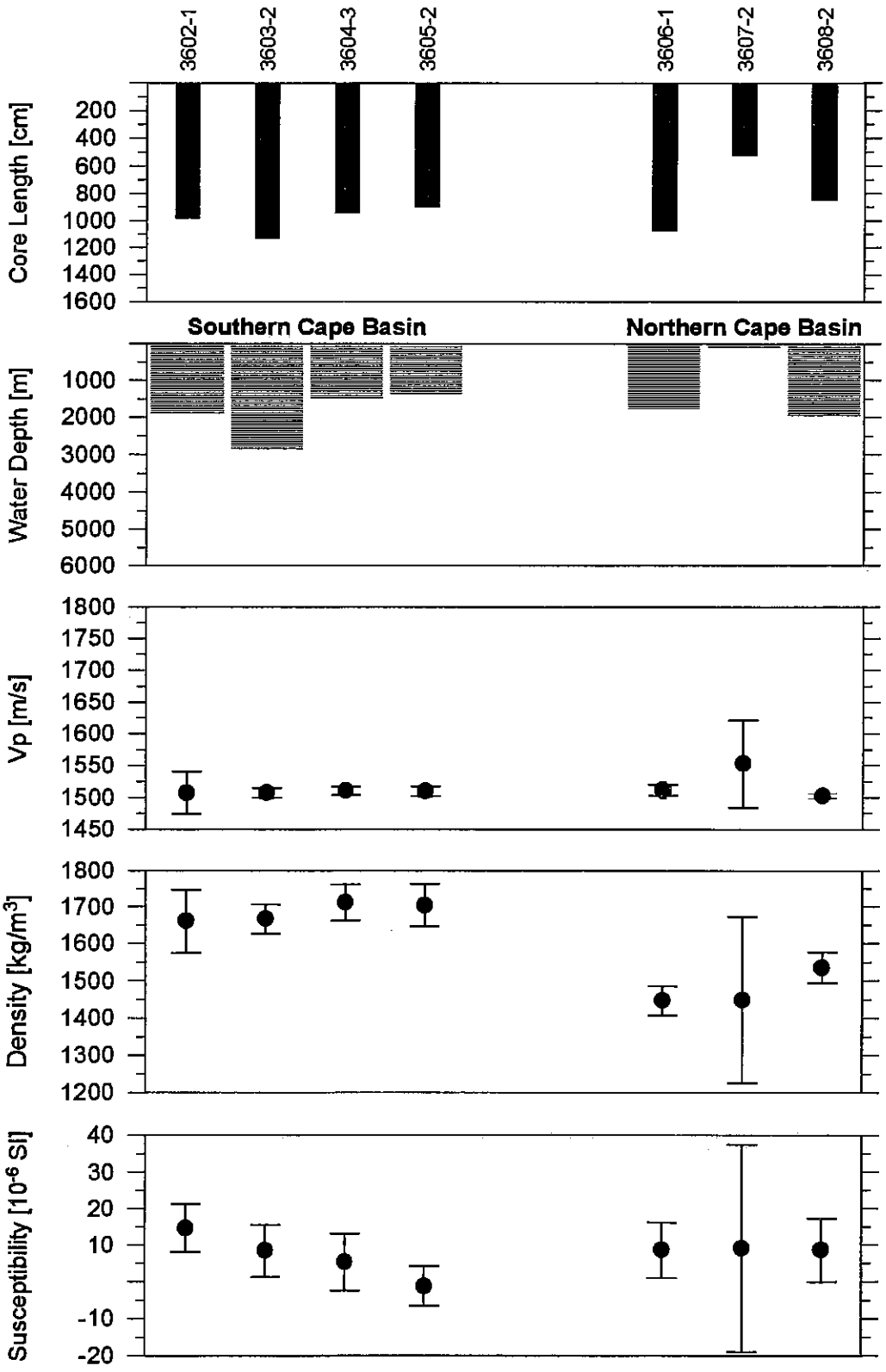

Fig. 65: Mean compressional wave velocity, density and magnetic susceptibility of gravity cores GeoB 3602-1 through 3608-2 as compared to variations in water depth at the sampling stations and core recovery. The vertical bars denote standard deviations.

5.1.4 Pore Water Chemistry

(R. Haese, C. Hensen)

The determination of diffusive pore water fluxes and geochemical processes reflecting early diagenetic mineralizations are main topics of the marine geochemistry studies. During cruise M34/1 in the first place numerous laboratory facilities had to be installed and new equipment prepared for the subsequent cruises M34/2-4. In particular on M34/2 geochemical and biogeochemical investigations are prime objectives. As new techniques needle electrodes for sulphide measurements and incubation experiments were tested. The latter should contribute to elucidate:

- effects of core recovery (temperature, decompression) and storing on geochemical and microbial processes,
- the advective pore water transport by bioirrigation, and
- the total fluxes across the sediment / water interface.

5.1.4.1 Experimental Methods

To prevent a warming of the sediments, the multicorer tubes were placed in a cooling room immediately after recovery and processed at a temperature of 4° - 6°C. All work on opened cores was carried out in a glove box under argon atmosphere. Two bottom water samples were taken for oxygen determination. The remaining water was then carefully removed by means of a siphon to avoid disturbance of the sediment surface. During the subsequent cutting of the core into slices for pressure filtration, pH and Eh measurements were performed at 0.5 cm intervals. Also electrical conductivity and temperature were determined to calculate density and porosity of the sediments. For pressure filtration Teflon- and PE-squeezers were operated with argon at a pressure gradually increasing to 5 bar. Depending on the porosity and compressibility of the sediments, up to 20 ml of pore water was retrieved through 0.2 µm cellulose acetate membrane filters.

The following parameters were measured on board: pH, Eh, conductivity, temperature, O_2, NO_3^-, NH_4^+, PO_4^{3-}, alkalinity, Fe^{2+}, S^{2-}, SO_4^{2-} and C^-. Bottom water O_2 was determined by Winkler titration, pH, Eh, S^{2-}, conductivity, and temperature with electrodes before pressure filtration and sulphide with an ion sensitive needle electrode calibrated for the pH range of the sediments. Measurements of nitrate, ammonium and phosphate were performed photometrically with an autoanalyser using standard methods. Alkalinity was calculated from titration of a 1 ml subsample with 0.01 - 0.05 m HCl. For the photometric analysis of iron concentrations 1 ml subsamples were taken within the glove box and immediately complexed with 10 µl of Ferrozin. Subsamples for sulphate and chlorine determinations by ion chromatography (HAPLY) have been diluted 1:20. The remaining pore water was acidified with HNO_3^- (suprapure) down to a pH value of 2 for storing and subsequent measurements of cations by ICP-AES and AAS. It will be maintained at 4°C until further treatment at the University of Bremen.

On sediments recovered with the multicorer at Station GeoB 3608 a 5 days incubation experiment was carried out in the cooling laboratory at a temperature of about 6.2°C. For this purpose a Plexiglas box (1.8 l volume) with a pump and tubing system was installed on top of the multicorer tube. The sediment was then pushed up until its surface reached the top of the multicorer tube, thereby moving the bottom water into the box and the tubing system. After air bubbles were expelled and 1.5 g KBr added (~ 7 mmol/l), the pump was switched on, simulating a laminated bottom water flow. During the following days bottom water samples were taken with a syringe through a small hole in the top of the box for the determination of pH, Eh, O_2, NO_3^-, NH_4^+, PO_4^{3-} and alkalinity. Each time the same amount of original bottom was added from a reservoir. Subsequent to the experiment, the sediments were processed as described above for pore water analysis.

5.1.4.2 Shipboard Results

Core GeoB 3607-1 recovered on the inner shelf southwest of Walvis Bay from a water depth of around 100 m was selected to test the new analytical method for sulphide. Beneath a 3 cm thick fluffy layer the sediments consist of fine grained diatomaceous mud with a very high organic matter content. The whole core as well as the bottom were strongly smelling of sulphide which was measured in 1 cm intervals, therefore. The complete results of pore water analyses are shown in Figure 66. Sulphate was the only oxidant present in bottom and pore waters, while oxygen, nitrate, and iron(II) were completely absent. The concentration profiles of alkalinity, ammonium and phosphate display highest mineralization rates of organic matter within the fluffy layer. Below 10 cm core depth phosphate is lacking in the pore water probably due to precipitation and/or adsorption to solid phases (phosphorites?). The principal gradients of ammonium, alkalinity, phosphate and sulphate exist between bottom water and the sediment surface. Sulphate reduction leading to organic matter mineralization products and sulphide must thus be strongest within the fluffy layer which was unfortunately not sampled for chemical analyses. Within the deeper layers of the sediment sulphate reveals an almost linear decrease to depth together with Eh and pH. The deepest sulphate reduction zone is not reached within the core. Between 20 and 25 cm depth, the concentration is still above 15 mmol/l. Sulphide concentrations constantly range between 400 - 450 µmol/l which is likely to reflect an artifact as the sensitivity of the needle electrode is limited to 400 µmol/l. For its application on higher sulphide concentrations, the pore water needs to be diluted by a reducing, alkaline solution (e.g. SAOB buffer).

The multicore GeoB 3608-1 was taken northwest of Walvis Bay at a water depth of about 2000 m. The sediments consist of light olive carbonate ooze. Results of pore water analyses of two cores are displayed in Figure 67. Changes in bottom water composition above the incubated core over time are shown in Figure 68. The data have not been corrected for dilution effects of the added reservoir bottom water. Bottom water oxygen content varied only insignificantly during incubation, concentrations of about 230 µmol/l indicated prevailing fully oxic conditions.

Nitrate build up by oxygen respiration and nitrate penetration depth are the most sensitive indicators for the intensity of near surface dissimilation processes available, since no oxygen concentration profiles were measured. The high amount of nitrate production is well documented by the distinct maximum within the uppermost 0.5 cm of the sediment columns of the incubated as well as the untreated core. Most of the nitrate is used up by denitrifying bacteria at a depth of about 2.5 cm. Both processes are also recorded in the pH and Eh profiles. Due to the release of protons (H^+) during oxidation of organic matter, nitrification produces a pH minimum at around the oxygen penetration depth (1 cm). Also a marked decrease in redox potential (Eh) is apparent in the uppermost sediments, correlating with the strongest decrease of nitrate concentration. At the end of the incubation period the nitrate peak is higher than immediately after recovery causing a steeper concentration gradient between bottom water and sediment. The nearly linear increase of nitrate in the bottom water towards the sediment surface suggests that most of the nitrate produced is released from the sediment.

In non-sulphidic seawater environments HCO_3^- is controlling the carbon dioxide system and therefore can be related to the amount of alkalinity. As organic matter mainly consists of C, N and P, products of early diagenesis are HCO_3^-, NH_4^+ and PO_4^{3-}. Compared to core GeoB 3607-1 the concentrations of organic matter mineralization products are 10 - 20 times lower at Site GeoB 3808. Concentration gradients of alkalinity and ammonium increase to 5 and 10 cm sediment depth, respectively, and remain about constant below this level indicating a reduced mineralization activity. Phosphate shows a distinct decrease between 2.5 - 7 cm which again could imply a fixation in the solid phase. Analogous to nitrate, a release into the bottom water led to an increase of phosphate concentrations during incubation. Ammonium could not be detected in bottom water at any time. Diffusing upwards it was oxidized before reaching the sediment surface. Small peaks of phosphate and ammonium in the uppermost sediment sample are ascribed to a thin fluffy layer on the sediment surface. As these high concentrations disappear during incubation, the fluffy layer was probably degraded. The downcore trends of all compounds are generally the same. Discrepancies exist in the deeper parts for alkalinity and Eh, however. Neither the strongly decreasing Eh, nor the sharp gradient change in alkalinity below 0.5 cm in the incubated core can be explained at present. Incubation also led to a steepening of the alkalinity gradient into the bottom water. This is attributed to a decrease of alkalinity in the bottom water rather than to an increased mineralization in the sediment.

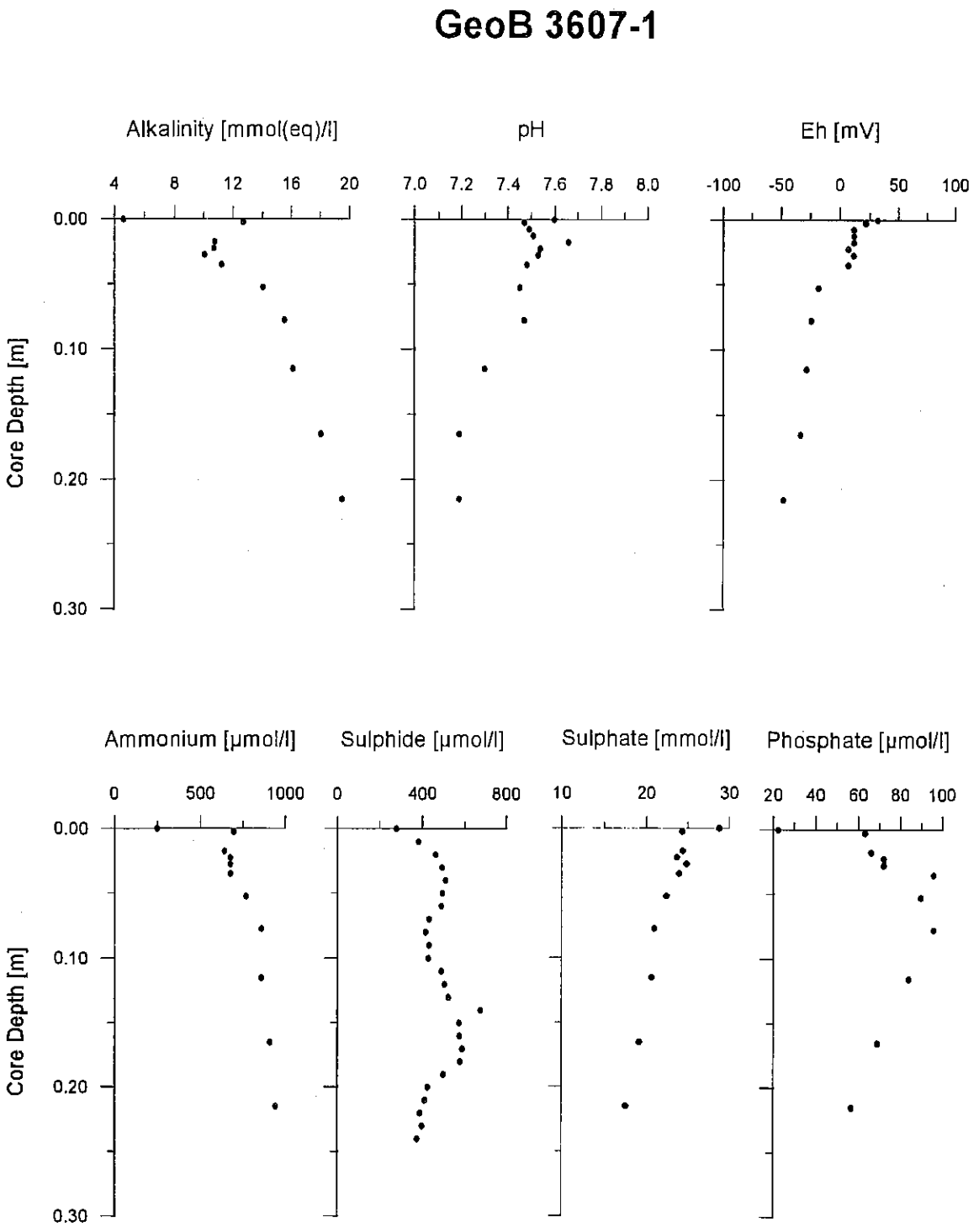

Fig. 66: Pore water concentration profiles in multicorer GeoB 3607-1.

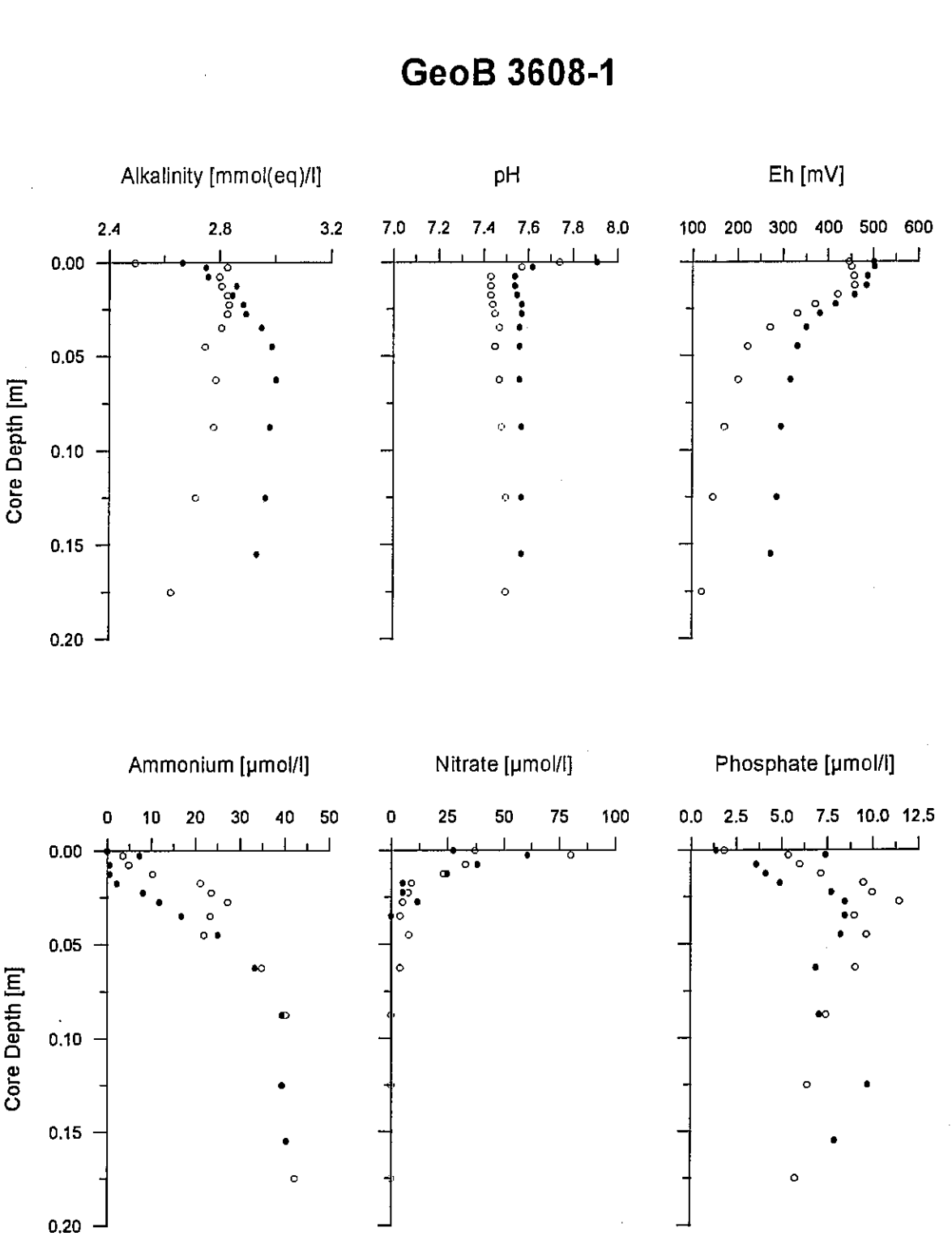

Fig. 67: Pore water concentration profiles in multicorer GeoB 3608-1. Open symbols - incubated, full symbols - untreated sediments.

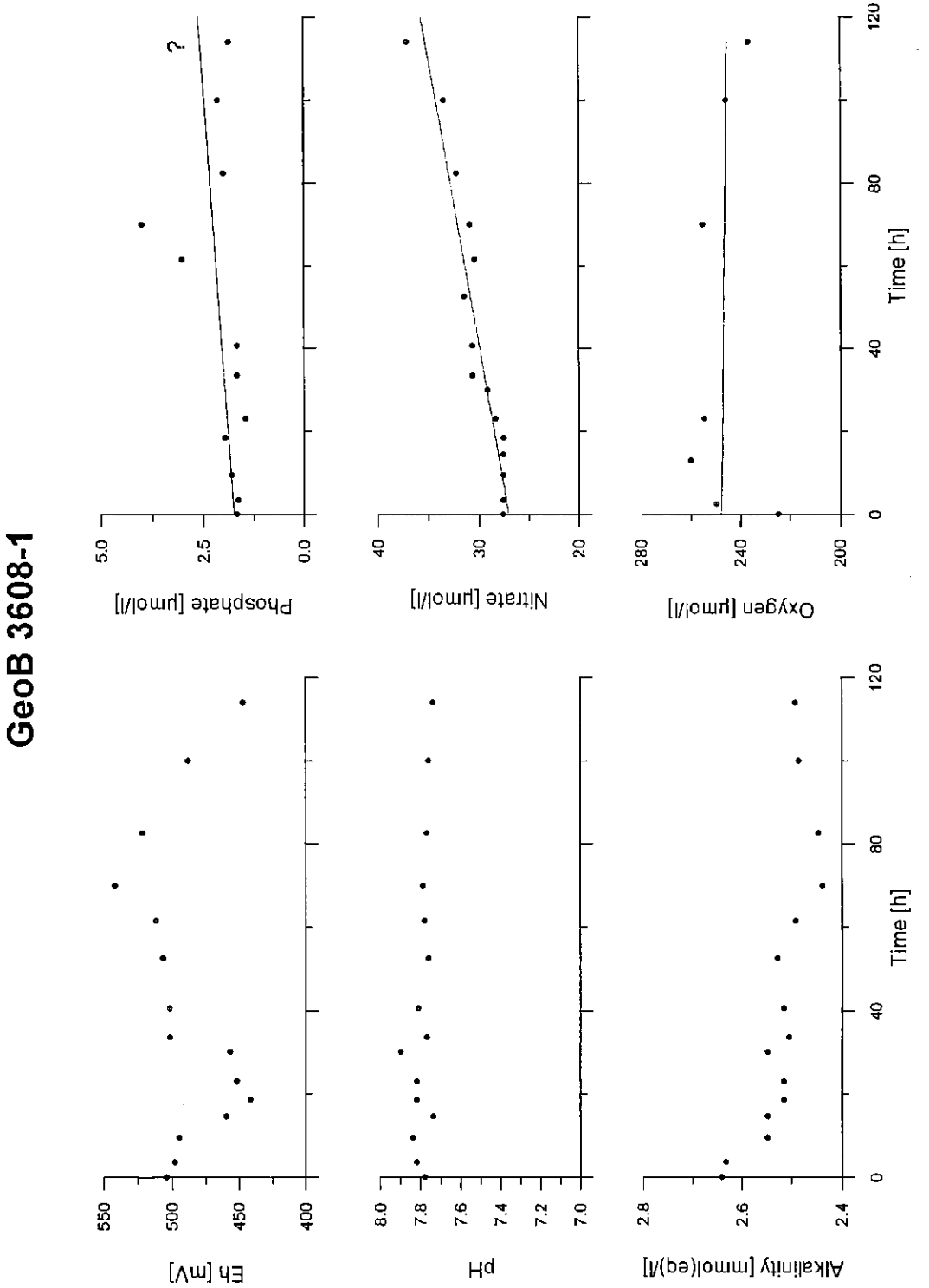

Fig. 68: Incubation experiment - bottom water data.

Alkalinity decreased within the first few hours of incubation and then remained relatively constant (Fig. 68). This effect can be explained by precipitation of calcium carbonate removing HCO_3^- from the bottom water. The short period to reach a constant HCO_3^- concentration is in good agreement with the time span needed for the calcite system to equilibrate. Precipitation can be caused by degassing of CO_2 due to decompression and warming during core retrieving. This is supported by a pH of 7.9 measured immediately after recovery. The constant pH on further incubation is probably due to the buffer capacity. The pH depth profiles reveal the same pattern and its decrease due to oxic respiration occurs at about 0.35 cm in both cores. The total shift must be related to a new equilibrium state established during incubation.

5.1.5 Plankton Sampling

5.1.5.1 Sampling for Chlorophyll-a Measurements

(M. Segl)

For the determination of chlorophyll-a concentrations in the surface waters, 0.5 l of seawater was collected 2 or 3 times a day from the ship´s clean seawater pump system (inlet at 3.5 m water depth). The water was filtered through glass fiber filters and frozen at -20°C. Chlorophyll-a measurements by means of photometry will be carried out in the University of Bremen laboratories.

The chlorophyll-a data should give information on the seasonal and regional variations in primary productivity thereby allowing a calibrating of satellite data for chlorophyll-a concentrations. Sampling locations are listed in Table 11.

Tab. 11: Sampling locations for chlorophyll-a measurements

Sample No.	Date 1996	Time [UTC]	Location	Water Depth [m]	Salinity [‰]	Temperature [°C]	Volume [l]
1	05.01.	09:40	33°34.1'S / 13°25.5'E	4341	33.38	21.2	0.5
2	05.01.	16:23	33°17.9'S / 13°04.1'E	4199	33.41	20.9	0.5
3	06.01.	06:13	33°35.6'S / 13°46.8'E	3691	33.45	21.2	0.5
4	06.01.	11:22	32°22.9'S / 14°13.7'E	3417	33.43	21.4	0.5
5	07.01.	06:08	31°38.0'S / 15°48.8'E	635	33.22	20.0	0.5
6	07.01.	11:05	31°25.9'S / 16°14.4'E	452	33.21	20.0	0.5
7	07.01.	16:08	31°12.1'S / 16°23.4'E	326	33.24	20.2	0.5
8	08.01.	06:12	31°27.2'S / 15°04.4'E	1884	33.21	19.4	0.5
9	08.01.	11:36	31°40.4'S / 15°00.7'E	1935	33.36	21.0	0.5
10	08.01.	16:07	31°57.0'S / 15°16.6'E	2293	33.38	21.2	0.5
11	09.01.	08:58	31°09.5'S / 15°29.8'E	889	33.27	19.9	0.5
12	09.01.	12:28	31°12.8'S / 15°11.2'E	1609	33.25	20.5	0.5
13	09.01.	16:08	31°28.5'S / 15°18.9'E	1385	33.28	20.7	0.5
14	10.01.	08:42	31°26.7'S / 15°17.9'E	1382	33.20	19.9	0.5
15	10.01.	16:00	30°44.4'S / 14°35.3'E	3455	33.42	21.0	0.5
16	11.01.	06:31	29°45.7'S / 12°44.3'E	3303	33.44	20.8	0.5
17	11.01.	11:33	20°37.3'S / 13°11.2'E	3029	33.38	21.1	0.5
18	11.01.	15:53	29°30.0'S / 13°35.2'E	2596	33.29	21.0	0.5
19	12.01.	08:50	29°24.8'S / 14°26.8'E	620	33.12	19.5	0.5
20	12.01.	11:12	29°33.7'S / 14°19.0'E	1014	33.07	19.5	0.5
21	12.01.	16:04	29°21.9'S / 13°58.6'E	1747	33.40	21.0	0.5
22	13.01.	06:21	27°21.6'S / 13°50.9'E	1328	33.20	20.5	0.5

Table 11 continued

23	13.01.	10:59	26°30.4'S / 13°56.0'E	408	32.92	17.9	0.5
24	13.01.	16:02	25°48.4'S / 13°55.9'E	324	32.66	17.1	0.5
25	14.01.	06:28	25°18.8'S / 12°44.4'E	2601	32.93	20.1	0.5
26	14.01.	12:48	25°35.8'S / 12°37.7'E	2909	32.89	19.1	0.5
27	14.01.	16:04	25°48.5'S / 12°41.6'E	2717	33.06	20.1	0.5
28	15.01.	06:04	25°25.6'S / 13°07.5'E	1623	32.83	18.3	0.5
29	15.01.	16:10	24°28.0'S / 13°52.4'E	277	32.56	17.3	0.5
30	16.01.	08:34	22°44.7'S / 13°56.4'E	131	32.60	18.3	0.5
31	16.01.	10:49	22°38.7'S / 13°29.3'E	215	32.71	18.8	0.5
32	16.01.	16:05	22°25.0'S / 12°27.6'E	1008	33.04	21.6	0.5
33	17.01.	06:05	22°00.1'S / 10°29.7'E	3669	33.34	22.0	0.5
34	17.01.	11:36	21°44.3'S / 10°52.8'E	3229	33.19	22.1	0.5
35	17.01.	17:19	21°27.3'S / 11°17.4'E	2660	33.08	22.0	0.5
36	18.01.	06:16	20°49.9'S / 12°11.8'E	624	32.95	20.9	0.5
37	18.01.	11:38	20°34.4'S / 12°34.4'E	---	32.95	20.4	0.5
38	18.01.	16:46	20°14.4'S / 12°37.7'E	149	32.84	19.4	0.5
39	19.01.	06:16	20°30.1'S / 11°47.0'E	360	33.10	21.3	0.5
40	19.01.	12:09	20°47.7'S / 11°22.2'E	1715	---	21.9	0.5
41	19.01.	16:25	21°00.4'S / 11°04.2'E	2462	---	21.9	0.5
42	20.01.	09:02	21°39.2'S / 11°45.1'E	1952	---	21.5	0.5
43	20.01.	11:06	21°35.8'S / 11°55.1'E	1716	---	21.6	0.5
44	20.01.	16:01	21°28.0'S / 12°19.4'E	971	---	21.2	0.5
45	21.01.	06:44	21°10.4'S / 12°26.6'E	584	32.93	20.3	0.5
46	21.01.	12:08	21°06.8'S / 11°58.3'E	1132	33.11	22.3	0.5
47	21.01.	16:52	21°03.5'S / 11°34.2'E	1688	32.96	22.8	0.5
48	22.01.	06:42	20°22.6'S / 10°39.7'E	1577	33.31	22.8	0.5
49	23.01.	06:23	19°35.7'S / 11°28.1'E	1011	33.12	21.7	0.5
50	23.01.	11:31	19°33.3'S / 11°21.7'E	704	33.19	22.5	0.5

5.1.5.2 Pumped Net Samples

(R. Schneider)

During the whole cruise plankton was sampled from surface waters (Tab. 12). For this purpose the shipboard clean seawater pump system was used to filter some 2000 to 5000 l through a net with a mesh size of 10 microns each day, mostly during daylight hours. The amount of seawater filtered depended on the plankton mass caught in the net. When the water flow was stopped by the material closing the net openings, the plankton was washed into plastic bottles and the sampling continued with the cleaned net. For each day the wet plankton samples were concentrated into one bottle and frozen at -20°C.

Tab. 12: Plankton Pump Samples

Sample No.	Date 1996	Start Filtration Local Time	Location	Salinity [‰]	Temperature [°C]	Water Clock	Stop Filtration Local Time	Location	Salinity [‰]	Temperature [°C]	Water Clock	Liters Pumped
1	05.01.	08:30	33°50.9'S / 13°47.9 E	35.61	20.9	336480	16:30	33°21.0'S / 17°07.0 E	35.65	20.9	339110	2630
2	06.01.	08:15	32°35.5'S / 13°46.9 E	35.74	21.2	339457	18:15	32°11.6'S / 14°37.8 E	35.73	21.4	343179	3722
3	07.01.	09:30	31°34.7'S / 15°55.9 E	35.49	19.6	343193	17:15	31°12.3'S / 16°28.1 E	35.33	20.1	346950	3757
4	08.01.	08:05	31°27.2'S / 15°05.2 E	35.58	19.5	346950	19:50	32°03.7'S / 15°23.2 E	35.73	20.7	351175	4225
5	09.01.	08:20	31°18.6'S / 15°35.8 E	35.53	20.0	351177	19:10	31°32.9'S / 15°21.6 E	35.57	20.6	354892	3715
6	10.01.	09:30	31°38.1'S / 15°24.6 E	35.56	20.0	355811	18:15	30°40.5'S / 14°31.2 E	35.72	20.9	358296	2485
7	11.01.	09:05	19°44.9'S / 12°47.1 E	35.71	20.6	358296	19:20	29°27.3'S / 13°49.8 E	35.58	21.2	361504	3208
8	12.01.	08:10	29°16.1'S / 14°34.5 E	35.30	19.8	361504	18:30	29°20.6'S / 13°56.9 E	35.69	21.1	364795	3291
9	13.01.	10:25	26°59.3'S / 13°53.2 E	35.24	19.5	365746	14:20	26°14.1'S / 13°57.8 E	34.94	16.1	366872	1126
10	13.01.	14:30	26°13.8'S / 13°57.8 E	35.86	15.9	366872	17:30	25°44.4'S / 13°58.6 E	34.98	17.1	367233	361
11	14.01.	08:15	25°19.3'S / 12°45.6 E	34.90	19.9	367234	17:25	25°49.0'S / 12°39.8 E	36.34	20.2	369090	1856
12	15.01.	07:25	25°20.4'S / 13°13.5 E	35.05	18.8	369090	14:05	25°05.3'S / 13°22.9 E	34.91	17.5	370071	981
13	15.01.	14:15	25°03.8'S / 13°24.2 E	34.90	17.6	370071	19:30	24°14.4'S / 14°03.1 E	34.77	16.5	370878	807
14	16.01.	08:05	22°51.3'S / 14°26.9 E	34.85	16.9	370878	10:30	22°44.7'S / 13°56.3 E	34.95	18.2	371053	175
15	16.01.	10:45	22°44.2'S / 13°55.0 E	34.95	18.0	371053	18:05	22°25.0'S / 12°27.5 E	35.31	21.6	372136	1083
16	17.01.	08:10	22°00.0'S / 10°29.9 E	35.63	22.0	372146	18:20	21°30.3'S / 11°13.2 E	35.36	21.9	374965	2819
17	18.01.	08:20	20°49.7'S / 10°12.1 E	35.25	20.9	374980	15:50	20°27.9'S / 12°43.7 E	35.26	20.6	376466	1486
18	18.01.	16:00	20°27.3'S / 12°44.4 E	35.20	20.5	376466	21:25	20°02.4'S / 12°30.9 E	35.19	19.6	378443	1977
19	19.01.	08:28	20°30.7'S / 11°46.3 E	35.43	21.3	378443	18:20	21°00.4'S / 11°04.4 E	---	21.9	381021	2578
20	20.01.	08:20	21°39.4'S / 11.31.7 E	---	21.2	381021	18:45	21°26.9'S / 12°23.1 E	35.28	21.1	385103	4082
21	21.01.	08:10	21°10.8'S / 12°28.4 E	35.24	20.4	385105	20:05	21°01.9'S / 11°28.2 E	35.40	22.7	387789	2684
22	22.01.	08:25	20°24.8'S / 10°40.0 E	35.57	22.8	387789	20:30	19°45.0'S / 10°27.5 E	35.50	23.2	392260	4471
23	23.01.	08:08	19°35.9'S / 11°26.9 E	35.47	22.0	392272	18:00	19°42.7'S / 11°33.8 E	35.40	22.8	395472	3200

Note: Ship's salinometer readings have been corrected by 2.3 ‰.

The plankton material will be investigated for the bulk composition of the biogenic detritus in order to quantify the ratios between opal, organic carbon and carbonate produced by near surface water plankton communities. The marine organic material will be analyzed in more detail. In particular, it is planned to determine the stable isotopes and individual organic compounds which can be related to specific phytoplankton organisms.

This type of data is needed to compare marine plankton production in the surface waters of different high productivity systems with fluxes of biogenic particles caught in sediment traps and found in the surface sediments beneath high productivity areas.

5.1.5.3 Net Sampling for Planktic Foraminifera

(M. Little)

The aim was to collect planktic foraminifera - specifically *Neogloboquadrina pachyderma* (dextral and sinistral coiling) for later DNA analysis (at Edinburgh University) from a variety of oceanographic settings in the Cape Basin. A large 63 μm plankton net was used for both the on route pumped and the on station planktic foraminiferal sampling. The pumped collection was obtained from about 5 m water depth underneath the ship, whilst the on station collection was achieved using a 50 m line with a coupled block and tackle. At station 1 all 50 m of the line were let out with sufficient weight attached for near vertical sampling. At station 2, the current was so strong that only 30 m of the line could be used for fear of entanglement with the ship. The final planktic residue, trapped in the 'cod-end', was diluted with fresh seawater and allowed to flocculate before 1.5 ml bulk samples were taken and immediately frozen for later DNA analysis. Site locations and further details of the sampling are listed in Table 13.

In the eutrophic/mesotrophic filaments (pumped collection sites 1, 2, 3 / on station sites 1, 2) the largest contributor to the plankton were dinoflagellates and various zooplankton. Foraminifera made up a minor component of the total plankton, possibly due to the depth of collection. Those that were present included *Neogloboquadrina pachyderma* (dextral) and *Globigerina bulloides*, with minor abundances of *Neogloboquadrina pachyderma* (sinistral), *Neogloboquadrina dutertrei*, *Globorotalia inflata* and sub-tropical/tropical species including *G. sacculifer*, *G. ruber* (white), *G. menardii*, *G. siphonifera*, and *Orbulina universa*. At the oligotrophic site (pumped collection site 4) by far the most common species were *G. inflata*, *N. pachyderma* (dextral) and sub-tropical/tropical species as listed above.

Tab. 13: Net Sampling for Planktic Foraminifera

	Local Time	Location Latitude	Location Longitude	Temperature Air [°C]	Temperature Water [°C]	Salinity [‰]	Water Depth [m]	Sample No.
Pumped Collection 1 - 13.01.96								
Start	13:10	26°32.8'S	13°55.9'E	19.6	18.3	32.92	411	1 - 10
Finish	13:40	26°20.3'S	13°57.2'E	19.0	16.0	32.61	378	
Pumped Collection 2 - 13.01.96								
Start	13:57	25°57.0'S	13°59.4'E	19.1	17.9	32.72	321	11 - 20
Finish	14:57	25°50.4'S	14°00.8'E	19.8	17.0	32.70	299	
Pumped Collection 3 - 15.01.96								
Start	13:10	25°13.2'S	13°16.9'E	18.7	19.0	32.77	1335	31 - 40
Finish	14:10	25°04.4'S	13°23.6'E	18.3	17.8	32.64	1025	
Pumped Collection 4 - 19.01.96								
Start	09:30	20°33.5'S	11°42.4'E	21.0	21.6		1055	51 - 55
Finish	10:55	20°37.9'S	11°36.1'E	21.3	21.8		1238	
Station Collection 1 - 15.01.06								
50 m Line	10:20	24°02.8'S	13°04.9'E	19.6	18.9	32.90	1788	21 - 30
Station Collection 2 - 15.01.96								
<30 m Line	10:30	23°53.4'S	14°20.0'E	16.3	16.0	32.74	97	41 - 50

5.1.5.4 Dinoflagellate Cyst Sampling

(R. Hoek)

Seawater plankton samples were collected from approximately 5 m water depth using the shipboard membrane seawater pump. Of special interest was the appearance of both calcareous and organic walled dinoflagellate resting cysts in the surface waters of the surveyed area.

Every morning a sample was collected over a three hours time interval using a 5.0 µm pore size polycarbonate sieve. The accumulated residue was sieved again through a 114 µm pore size polyethelene filter. Formaldehyde was added to the 5.0 - 114 µm fraction in order to preserve the sample for further analyses of biomineralization, ecology, life cycle and systematics of the dinoflagellate cysts at the University of Bremen.

Tab. 14: Sampling for Dinoflagellates

Sample No.	Date 1996		Location Latitude	Location Longitude	Time [UTC]	Temperature [°C]	Salinity [‰]	Water Depth
1	04.01.	Start	35°07'S	17°32'E	05:15	21.2	33.42	---
		Finish	35°06'S	17°09'E	07:37	21.2	33.42	---
2	05.01.	Start	33°54'S	13°52'E	05:55	20.9	33.37	---
		Finish	33°39'S	13°32'E	08:46	21.1	33.44	---
3	06.01.	Start	32°37'S	13°52'E	05:25	21.2	33.44	3706
		Finish	32°28'S	14°00'E	08:45	21.2	33.44	3601
4	07.01.	Start	31°38'S	15°48'E	06:00	20.0	33.22	641
		Finish	31°31'S	16°01'E	08:45	19.6	33.17	485
5	08.01.	Start	31°26'S	15°07'E	05:30	19.9	33.24	1735
		Finish	31°29'S	14°51'E	08:45	20.5	33.28	2381
6	09.01.	Start	31°21'S	15°36'E	05:35	19.7	33.22	776
		Finish	31°09'S	15°31'E	08:45	20.4	33.27	843
7	10.01.	Start	31°47'S	15°29'E	04:55	20.8	33.36	1520
		Finish [1)]	---	---	---	---	---	---
8	11.01.	Start	29°47'S	12°39'E	05:32	20.8	33.44	3427
		Finish [1)]	---	---	---	---	---	---
9	12.01.	Start [2)]	29°14'S	14°35'E	06:06	19.8	32.98	302
		Finish	29°24'S	14°26'E	08:45	19.5	33.11	618
10	13.01.	Start	27°29'S	13°50'E	05:32	20.6	33.23	1571
		Finish	26°56'S	13°53'E	08:40	19.1	32.94	488
11	13.01.	Start [3)]	26°13'S	13°57'E	12:32	15.5	32.64	355
		Finish	26°02'S	13°58'E	13:27	17.7	32.79	330
12	13.01.	Start [2)]	25°58'S	13°59'E	13:40	17.9	32.74	330
		Finish	25°58'S	13°59'E	13:45	17.9	32.74	323
13	14.01.	Start [2)]	25°19'S	12°46'E	06:00	19.6	32.85	2541
		Finish	25°16'S	12°35'E	08:45	20.3	33.01	2933
14	15.01.	Start	25°25'S	13°07'E	06:00	18.2	32.83	1615
		Finish	25°28'S	13°05'E	08:45	18.7	32.88	1765
15	17.01.	Start	22°00'S	10°29'E	05:55	22.0	33.34	3674
		Finish	21°51'S	10°42'E	09:03	21.9	33.24	3508
16	18.01.	Start	20°52'S	12°08'E	05:28	21.6	33.15	721
		Finish	20°42'S	12°22'E	08:42	20.8	33.00	345

Table 14 continued

Sample No.	Date 1996		Location Latitude	Location Longitude	Time [UTC]	Temperature [°C]	Salinity [‰]	Water Depth
17	19.01.	Start	20°29'S	11°47'E	06:10	21.2	33.07	908
		Finish [4]	20°37'S	11°36'E	08:49	21.8	---	1233
18	20.01.	Start [4,5]	21°40'S	11°33'E	06:45	21.2	---	2317
		Finish [4]	21°39'S	11°45'E	09:03	21.5	---	1949
19	21.01.	Start	21°11'S	12°31'E	05:39	20.4	32.87	468
		Finish	21°09'S	12°15'E	08:45	21.9	33.13	801
20	22.01.	Start	20°28'S	10°40'E	05:34	22.6	33.26	1704
		Finish	20°10'S	10°37'E	09:05	22.6	33.32	1428
21	23.01.	Start	19°36'S	11°25'E	05:55	22.1	33.10	632
		Finish	19°34'S	11°19'E	08:45	22.2	33.17	844
22	24.01.	Start	20°15'S	11°09'E	05:35	22.6	33.26	1265
		Finish	20°04'S	11°00'E	08:31	22.8	33.20	1318

1) pump not working
2) two 5 µm filters used
3) > 10 µm fraction
4) salinometer not working
5) passing red tide

5.2 Marine Geoscience M 34/2

5.2.1 Underway Geophysics

(H.v.Lom-Keil, T.v.Dobeneck, C.Hilgenfeldt, H.Petermann
and Shipboard Scientific Party)

5.2.1.1 Introduction

During METEOR cruise M34/2 the shipboard acoustical systems HYDROSWEEP and PARASOUND were used on a 24 hour schedule to record continuous high resolution bathymetric and sediment echosounding profiles. The PARASOUND seismograms were digitized and stored with the digital acquisition system PARADIGMA (SPIEß, 1993).

The underway geophysical program along several profiles on the Namibian continental margin serves the long term research objectives of the DFG Sonderforschungsbereich 261. The recorded digital data provide valuable information for surveying suitable coring stations in different sedimentation environments and for studies of sedimentary structures and processes.

5.2.1.2 Recording Parameters and Preliminary Data Processing

The shipboard sediment echosounder PARASOUND and the multibeam echosounder HYDROSWEEP were operated by the scientific crew during a 24 hour watch. Both systems worked without any technical problems. Due to the location of the HYDROSWEEP transducers in the ships hull, the data coverage of this system was not very good on some profiles, depending on the angle of incidence and the height of the seawaves.

A new control and recording system, HYDROMAP ONLINE (STN-Atlas-Elektronik GmbH), for the HYDROSWEEP System was installed on RV Meteor in December 1996. It allows an improved online monitoring and control of the system parameters and the swath-data quality by permitting the display of several different survey datasets at time in a windowed screen layout. Except for some minor problems, HYDROMAP ONLINE worked reliably without major breakdowns, and raw data recording was continously performed.

The multibeam sounder provides an image of the sea floor topography with a swath width of twice the water depth and, in combination with the sediment echosounder PARASOUND, serves as a a very efficient tool to select suitable coring sites based on the precise knowledge of the local topography and morphology, slope angles and sediment instabilities.

The sediment echosounder data were routinely registered as paper recordings with the DESO 25 device and in parallel digitally by means of the PARADIGMA 4.01 system (SPIEß, 1993). The data were directly stored on 6250 bpi, 1/2" magnetic tapes using the standard, industry-compatible SEGY-format.

The seismograms were sampled at 40 kHz with a typical recording length of 266 ms for a depth window of ~200 m. The source signal was a non bandlimited sinusoidal wavelet of 4 kHz dominant frequency with a duration of 2 periods.

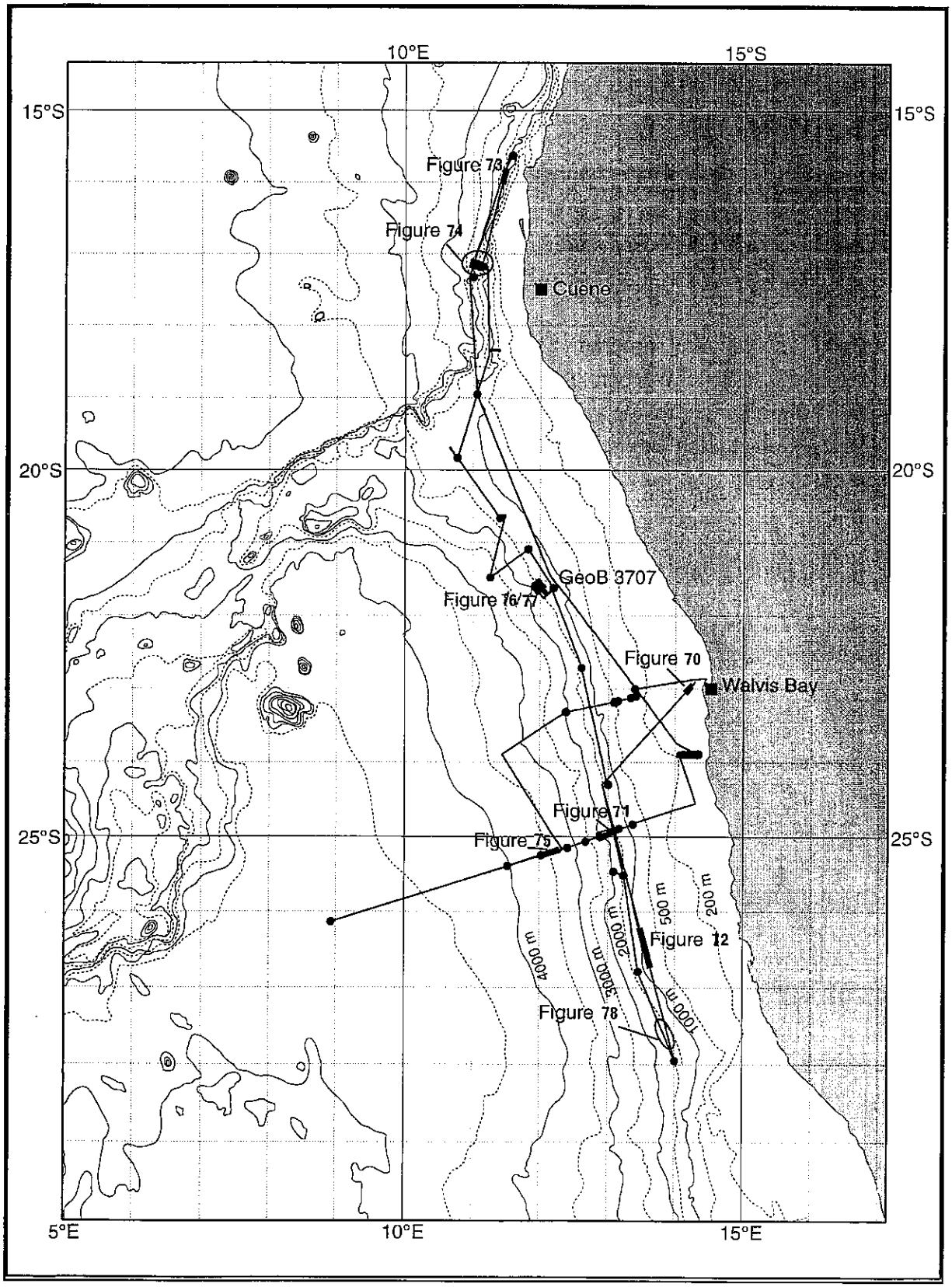

Fig. 69: Cruise track of RV METEOR on the Journey M34/2 off the Namibian coast. The presented examples are denoted by thick lines and named accordingly.

A preprocessed coloured seismic section was produced online with an HP PaintJet printer, using a vertical depth scale of several hundred meters to eliminate most of the jumps in the reception window depth. To supress low frequency acoustic and high frequency electronic noise the seismograms were filtered with a wide bandpass filter from 1.5 to 10.0 kHz. In addition the data were normalized to a constant value much smaller than the maximum amplitude. In particular deeper and weaker reflections were amplified thereby. These plots give a first impression of variations in sea floor morphology, depositional patterns and sedimentary structures along the ship's track.

To study the influence of frequency and length of source signal, these parameters were varied systematically at core sampling stations ('Source signal test'). The signal frequency was repeatedly increased in 0.5 kHz steps from 2.5-5.5 kHz while the pulse length was set to 1, 2 and 4. Each combination was recorded for 2 minutes to enable seismogram stacking. To analyze interference phenomena and to enhance resolution for direct comparison with core measurements of sediment physical properties (p-wave velocity and wet bulk density), seismograms with different frequencies will later be studied more in detail.

5.2.1.3 Shipboard Results

During cruise METEOR M34/2 mainly two narrow corridors were studied by core sampling and echosounder surveys. The first area extends in South-North direction from 28° S / 14° E to 15°30' S / 11°30' E, following the 1300 m isobath of the upper continental slope. The second area in East-West direction leads from 24°30' S / 14°20' E on the Namibian shelf to 26°10' S / 9° E in the central Cape Basin, ranging in water depth from 100 to 4800 m.

In addition to echosounder lines on transit between the coring sites, three detailed echographic surveys were carried out. They were performed at a lower travel speed of 7 kn to improve the lateral resolution of small scale sediment structures. The distances between the survey profiles were adjusted to the water depth, the HYDROSWEEP swath width and the specific scientific targets and sediment structure dimensions.

The following figures show typical examples of digital PARASOUND sections for different sedimentary environments visited during the cruise. In order to image adequately the observed features, the digital seismogram sections were prepared for printing by translating the amplitudes of individual traces into grey scales on a 600 dpi laser printer. The depth axis is given in meters, based on a constant water sound velocity of 1500 m/s. The distance scale is represented by black and white bars at the bottom of each figure, each bar standing for 1 km. Two bathymetric charts resulting from HYDROSWEEP data are also presented. They were provided by the ship's system operator and produced with the new HYDROMAP postprocessing system.

Figure 69 shows a map of the ship's track of Meteor cruise M34/2 including core sampling stations. The locations of the figures discussed are emphasized by thicker lines and annotations.

The first example was recorded on the Namibian shelf from 22°56' S / 14° 13' E to 23°04' S / 14°07' E in a water depth of 100-120 m (Fig. 70). The signal penetration varies significantly between 3 - 5 m and 25 - 30 m. The abrupt lateral changes in signal penetration are probably caused by a high content of free gas in the sediment, which causes a high reflection coefficient on top and attenuates sound waves further down.

In intervals with a higher signal penetration a layer of high reflection amplitudes can be recognized at ~10 m sub bottom depth, which may be interpreted as an older, eroded beach surface, consisting of larger grain size particles.

The upper continental slope in intermediate water depths off the Namibian coast and south of the Wavis Ridge is characterized by a smooth topography and parallel, well stratified sediment layers, indicating undisturbed sedimentation. Figure 71 shows an example of this sedimentation pattern from 24°56' S / 12°57' E to 24°52' S / 13°11' E. The water depth ranges from 1625 m to 1250 m with a signal penetration up to 100 m. Some thin layers of weak reflections or total transparency might be interpreted as indicators for deposition of homogenous upwelling related sediment packages.

The search for suitable sediment sampling sites on the continental slope south of the Walvis Ridge was greatly eased because of the predominance of this sedimentation pattern in the preferred water depth of 1300 m.

On the southern end of the South-North corridor indications for bottom currents were found. The digital PARASOUND section shown in Figure 72 was recorded from 26°14' S / 13°28' E to 26°42' S / 13°37' E in a water depth of 725 - 950 m. In the northern part of the section a significant lateral variation in sediment thickness can be recognized, with layers thinning southward, and erosional features are observed in both recent and buried sediments. Further to the south several high amplitude reflectors crop out at the sea floor, where they are completely eroded.

North of Walvis Ridge the upper continental slope is characterized by a rough topography with steep slopes and deep incisions. The penetration of PARASOUND signals is very low, not exceeding 10-20 m. The situation is further complicated by the occurrence of side-echoes, which are often difficult to distinguish from true structures. The example in Figure 73 was recorded from 16°1' S / 11°25' E to 15°49' S / 11°28' E. Obviously the complexity of the sediment structures in this area hampers the finding of suitable coring sites.

In greater water depths the slope angle is decreasing and places for coring were easier to find. In the vicinity of sites GeoB 3714 and GeoB 3712, a detailed echographic survey could be carried out. Due to the calm weather conditions a HYDROSWEEP dataset of very high

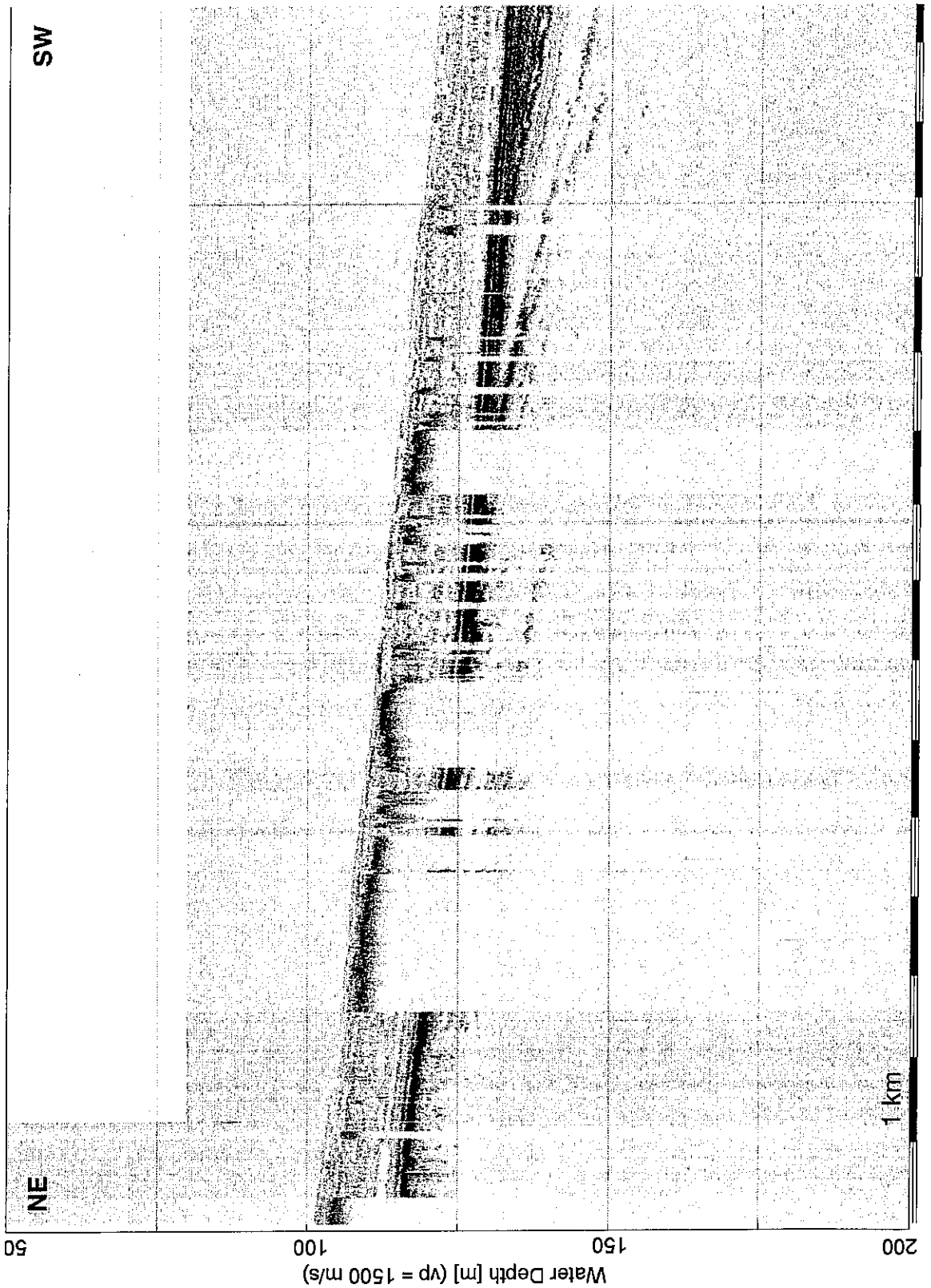

Fig. 70: PARASOUND-Record on the Namibian shelf off Walvis Bay.

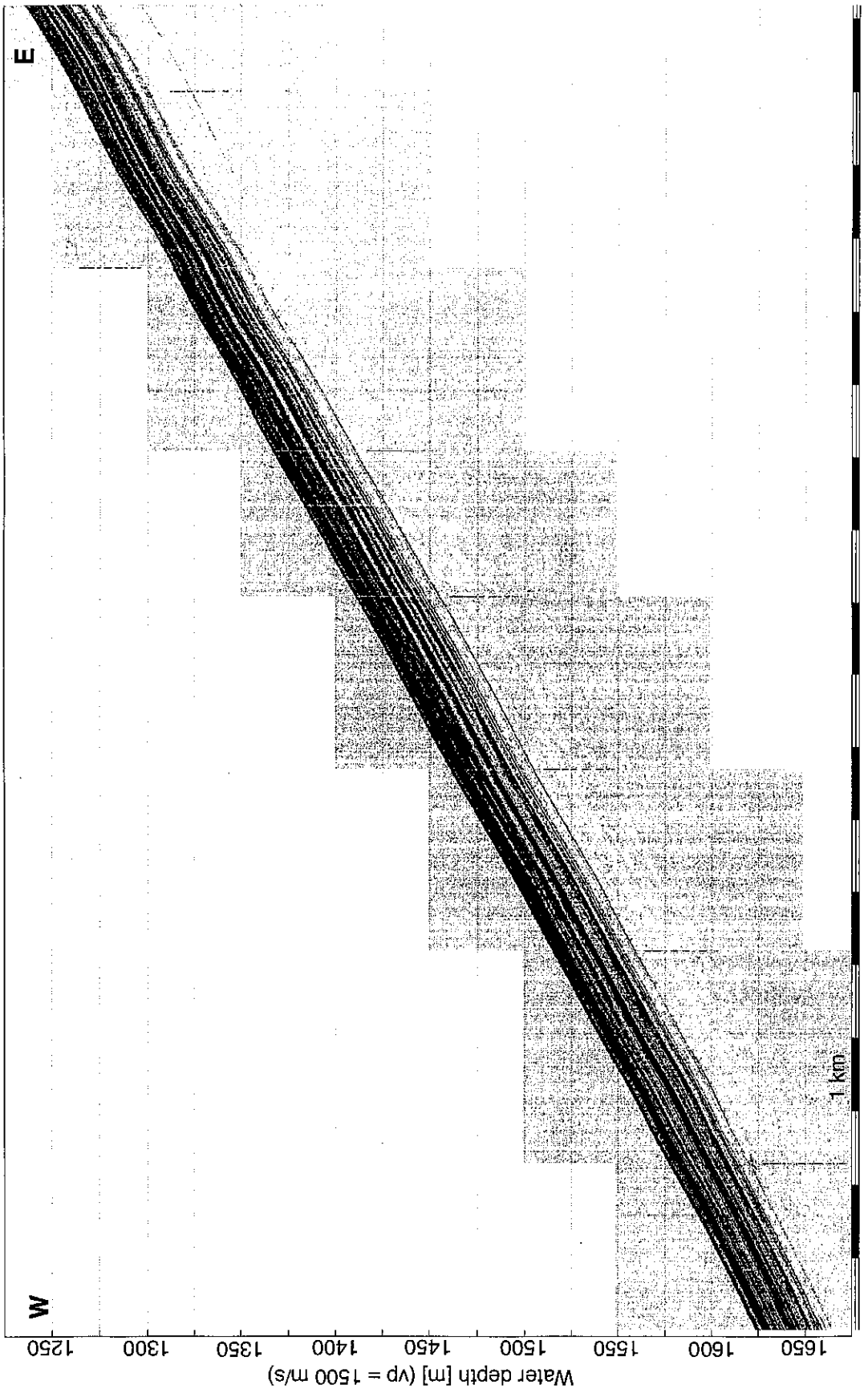

Fig. 71: PARASOUND-Echogram of the upper continental slope in the northern Cape Basin.

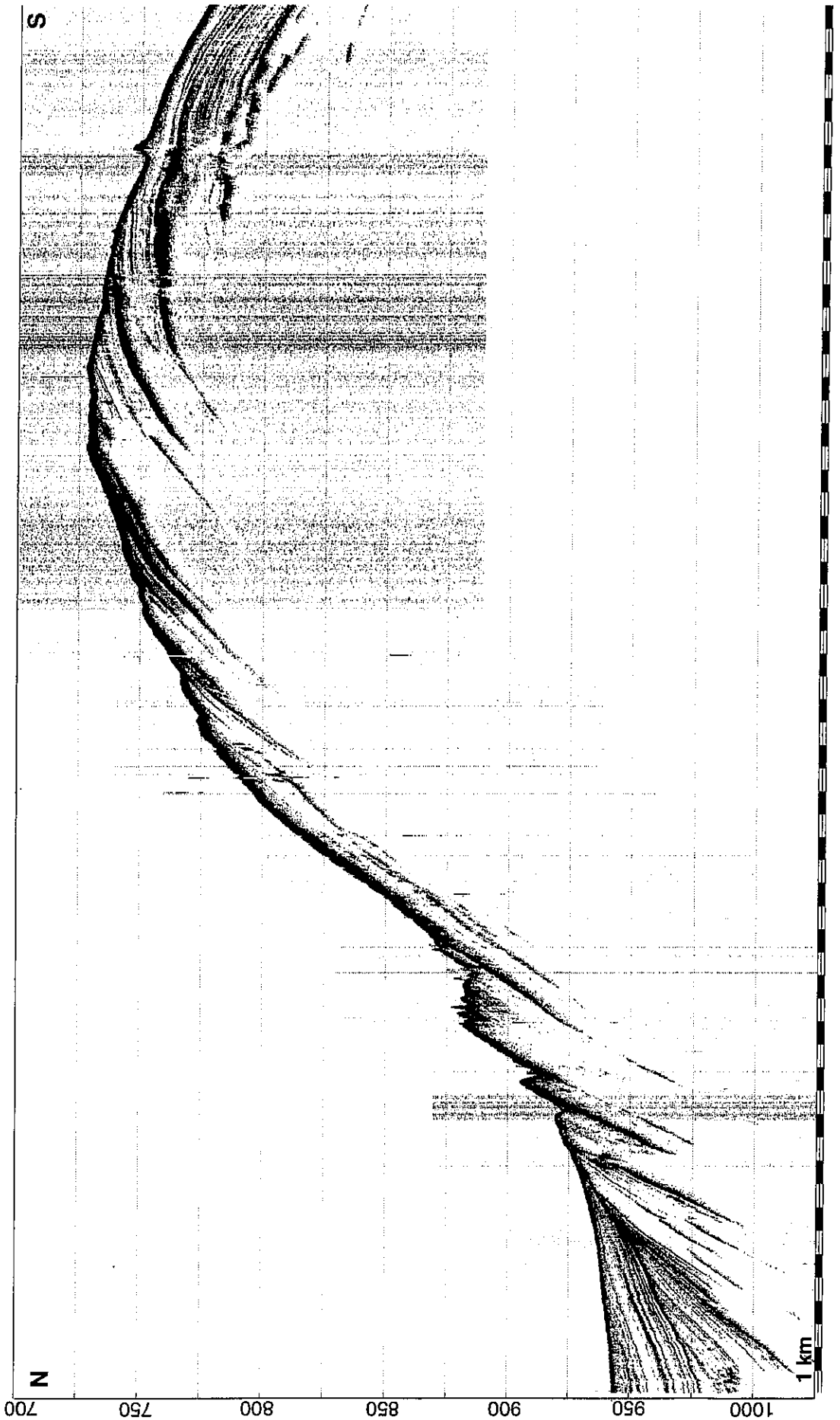

Fig. 72: PARASOUND-Section of erosional structures on the upper continental slope off the Namibian coast.

quality could be acquired. The lateral distance between survey profiles was chosen to ensure a complete coverage of the seafloor by the multibeam echosounder in an area of approximately 15 x 25 km. The bathymetric data is presented in Figure 73.

In the second working area in East-West direction the reflection pattern shown in Figure 71 could be traced down to a water depth of 3000 m. In greater depths (3200 - 3600 m) the stratified sediment layers are interrupted by several small updoming structures with reduced internal reflection amplitudes. An example for these features is given in Figure 75, recorded from 25°16' S / 11°55' E to 25°11' S / 12°15' E. The lateral extent of the updoming structures ranges from 200 to 900 m. A second short profile running parallel to the slope in the same water depth confirms the small size of these structures both perpendicular and parallel to the slope. The origin of these features is not yet understood.

In addition to the core sampling program at site GeoB 3707 a 12 hour echographic survey of a microscale mudwave field could be performed nearby. The surveyed area extends from 21°34' S / 11°52' E in the north-western corner to 21°42' S / 12°7' E in the south-eastern corner (see Figure 76). The water depth in this area ranges from 1740 m to 1570 m. The survey data can be supplemented by a profile recorded in this region in 1993 during the cruise SONNE SO 86 (BLEIL et al., 1993). Figure 77 shows the digital sediment echographic data. The echosounder profiles cross the mudwave field approximately perpendicular to the strike direction. The high horizontal and vertical resolution of the PARASOUND system allows detailed studies of the internal structure of these small scale mudwaves. The elevation is only ~2 - 3 m with wave lengths from 100 to 500 m.

The signal penetration of 30 - 40 m allows a reconstruction of the evolution of the waves. The former wave crests are easily recognisable and the static character of the waves can be derived from the symmetric shape. A slight increase in wave height is observed from southwest to northeast, i.e. from 1700 m to 1570 m water depth.

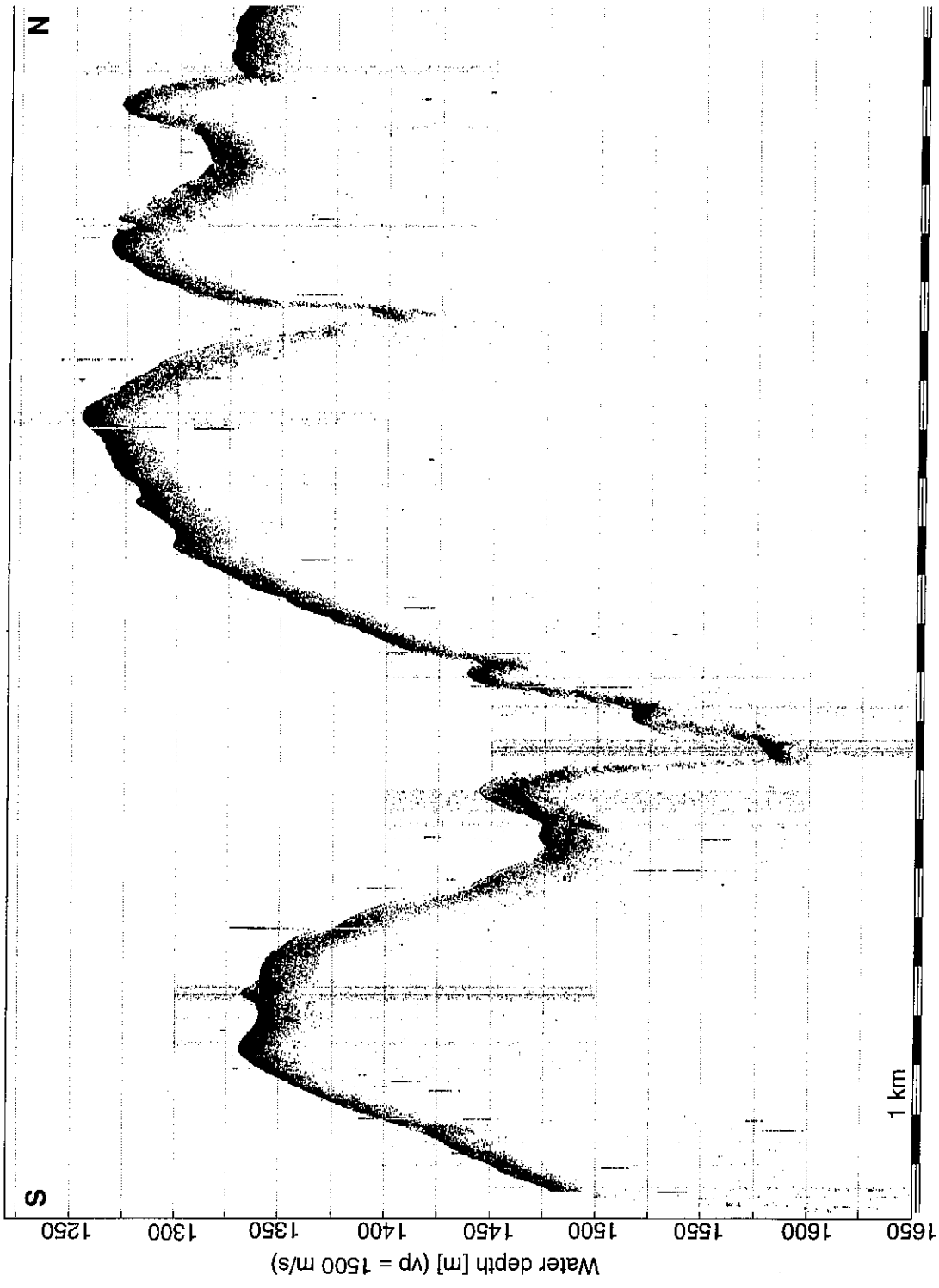

Fig. 73: PARASOUND-Section on the continental slope north of the Walvis Ridge.

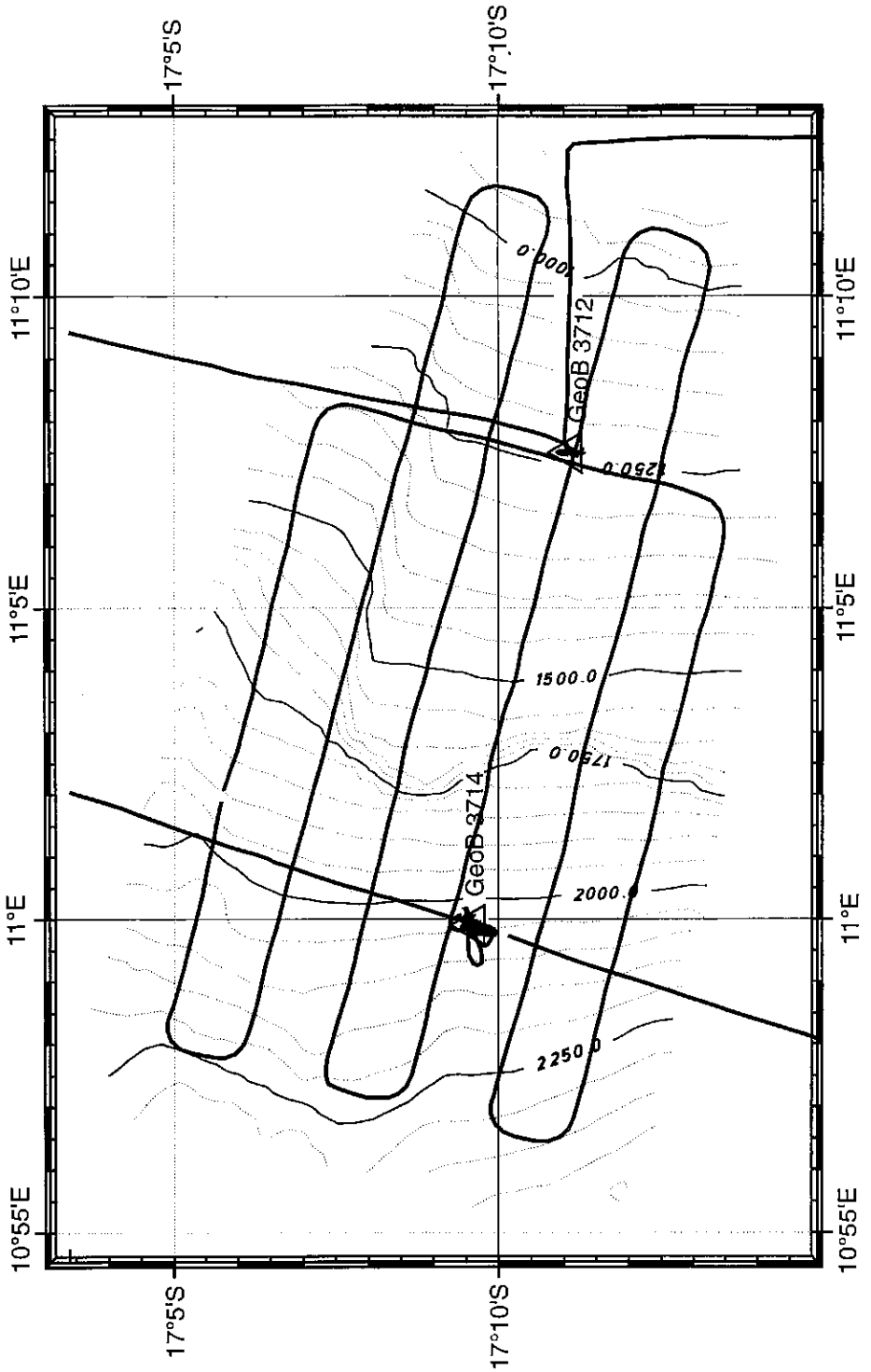

Fig. 74: HYDROSWEEP-Map of the vicinity of sites GeoB 3712 and GeoB 3714. The isobaths are 50 m apart. The ship track in this area is marked by thick lines.

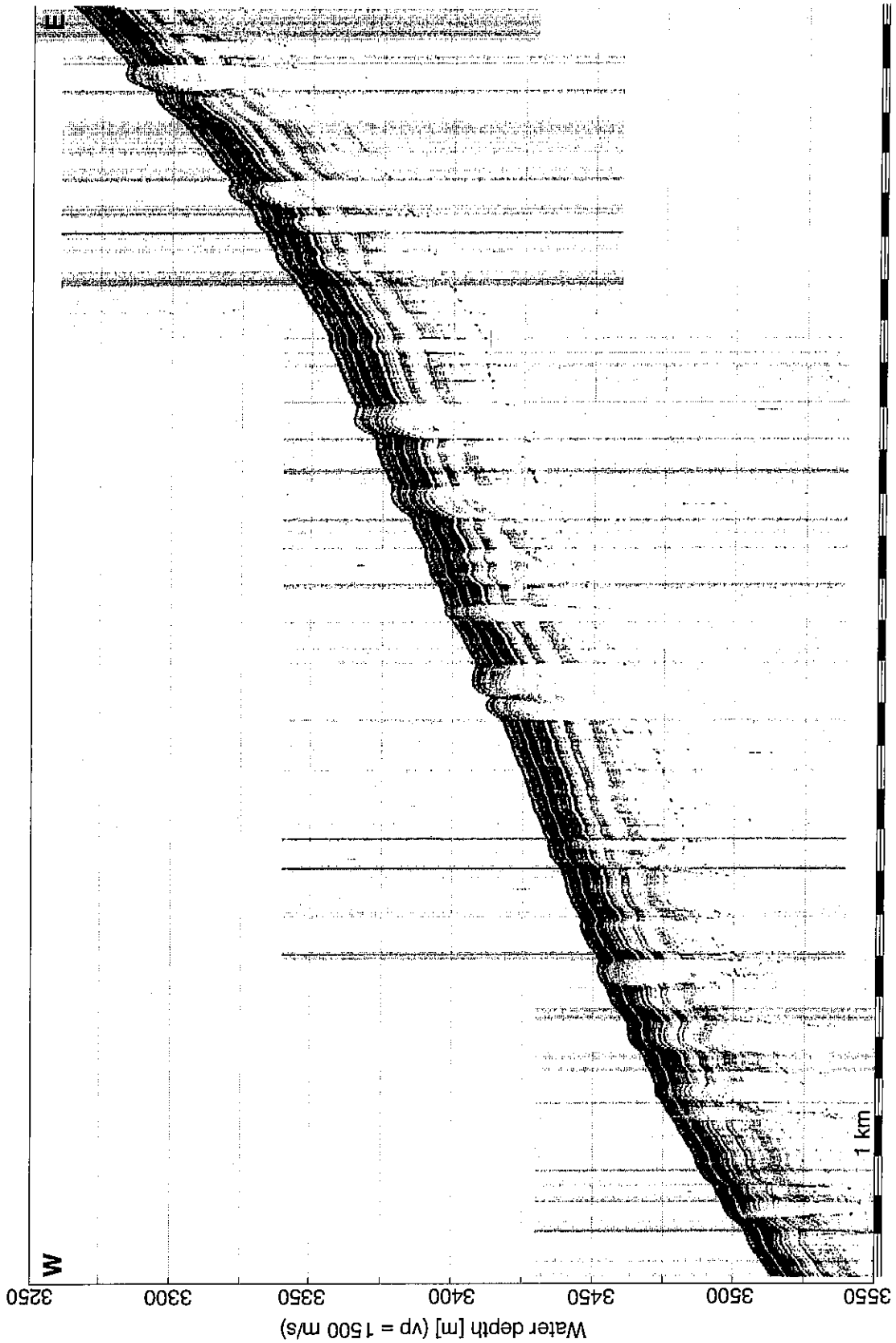

Fig. 75: PARASOUND-Section on the lower continental slope off the Namibian coast showing stratified sediment layers intermitted by small scale updoming structures.

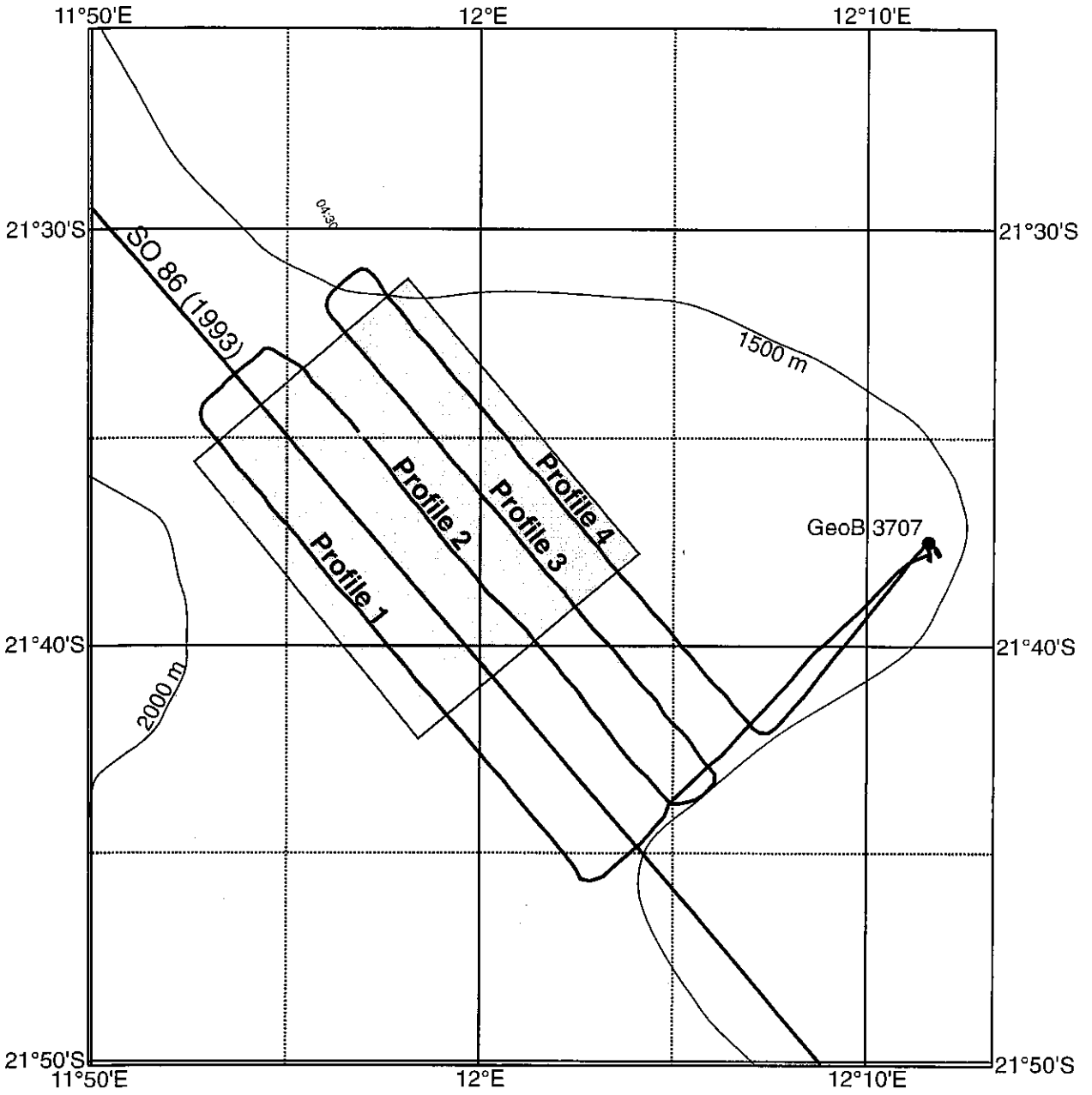

Fig. 76: Ship track of RV Meteor during mudwave survey. The area presented in Figure 77 is emphasized by the shaded rectangle.

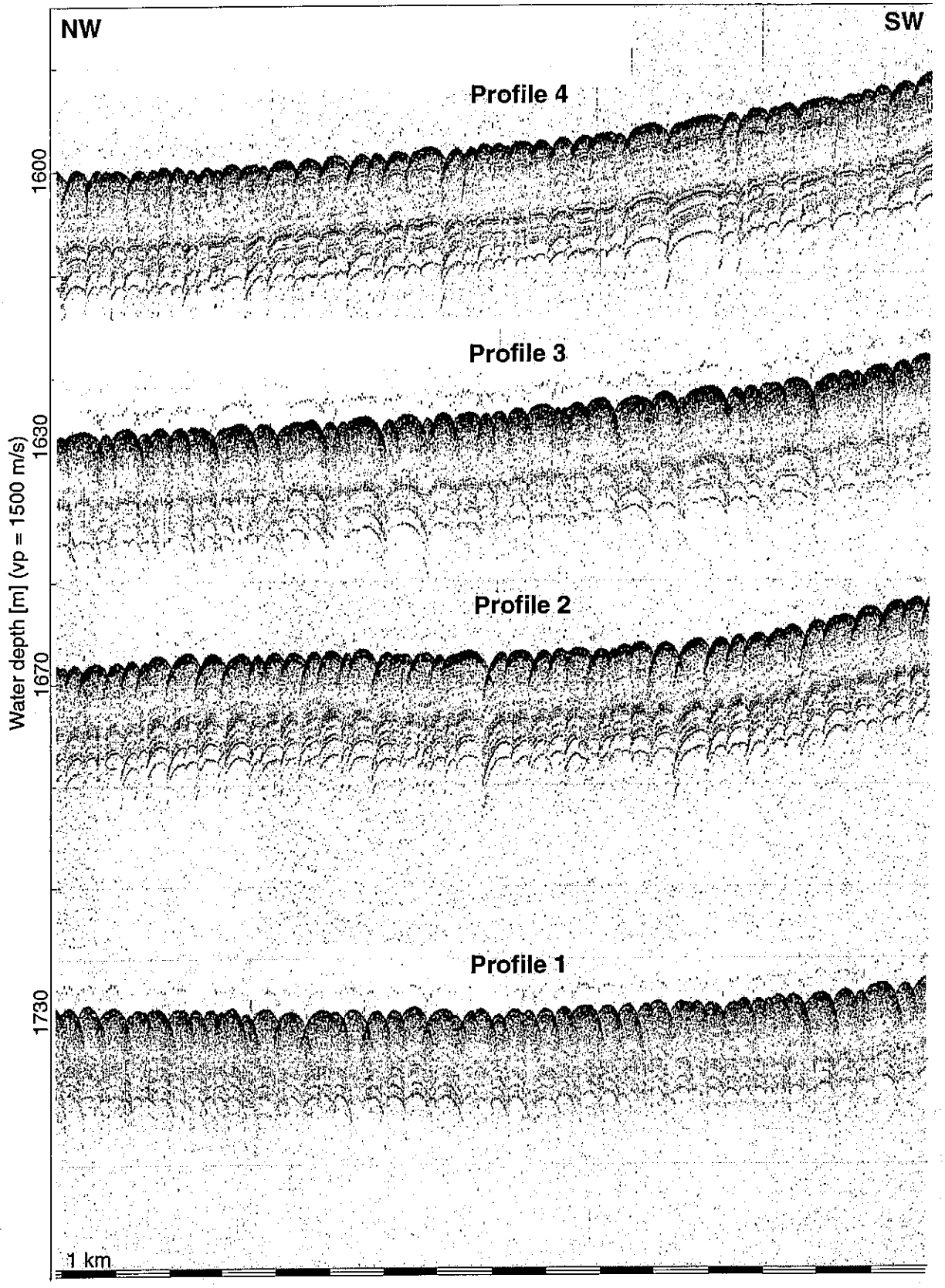

Fig. 77: PARASOUND-Profiles recorded during the mudwave survey near station GeoB 3707. The four profiles are plotted in the same order and relative distance as shown in Figure 76.

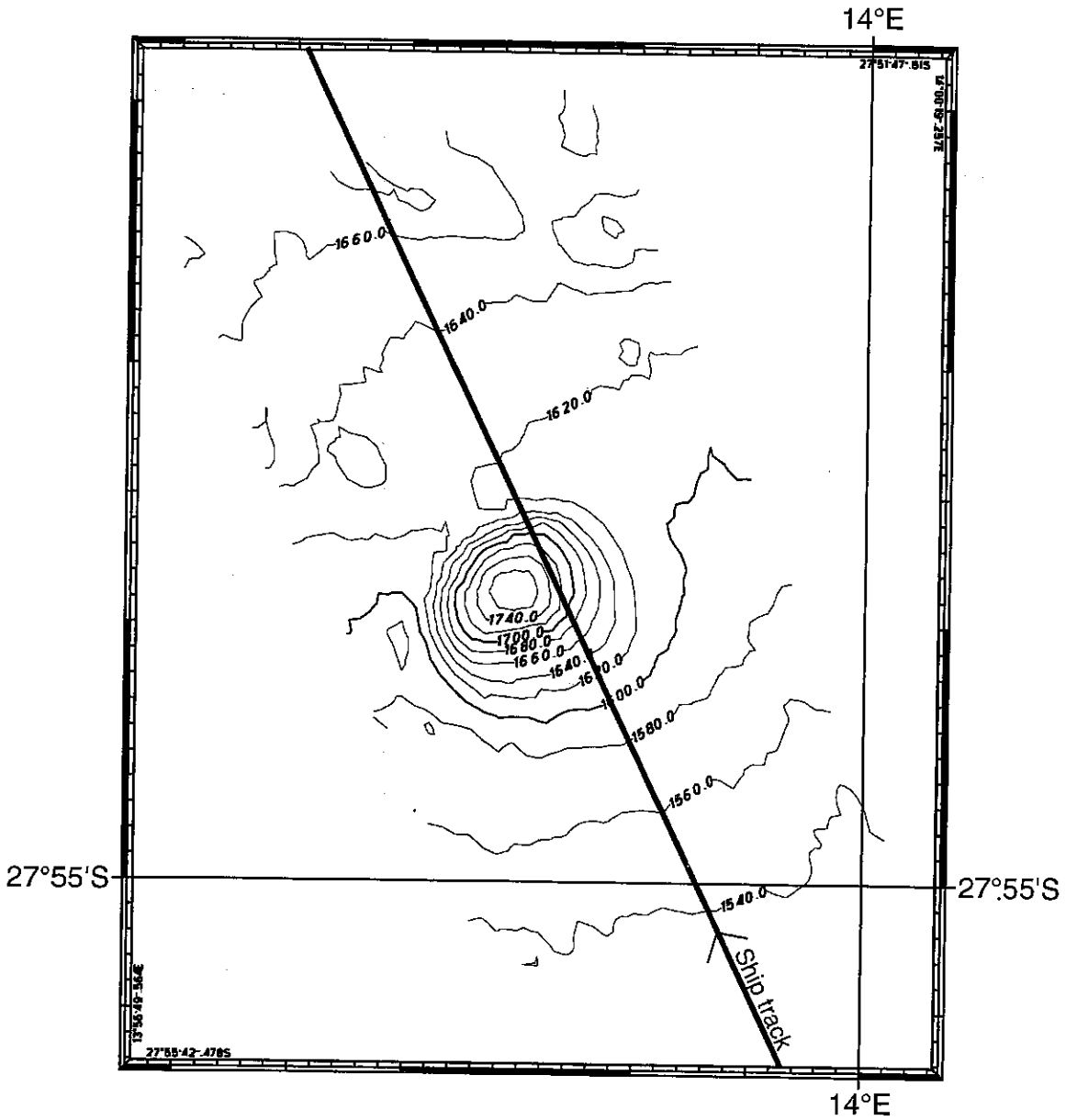

Fig. 78: HYDROSWEEP swath data recorded near GeoB 3701. The depth intervall between the isobaths is 20 m.

The micro scale mudwave field has been recognized already on SONNE cruise So 86 (BLEIL et al., 1993) and METEOR cruise M34/1 (BLEIL et al., 1996) on the upper continental slope of the Cape Basin in water depths of 1200 - 1700 m between 19° S and 22° S and were partially surveyed at 19°45'S / 10°30' E on METEOR cruise M34/1.

Figure 78 shows a special feature which was recorded on a line from 27°55' S / 13°59' E to 27°52' S / 13°58' E on transit from site GeoB 3701 to site GeoB 3702 with the multibeam echosounder HYDROSWEEP. In this region several circular topographical troughs were encountered with diameters of 1000 - 2000 m and in some places as deep as 160 m. The steep walls unfortunately inhibit a suitable image of sediment structures with the PARASOUND

system. These troughs were also already encountered during cruise M34/1. Their genesis is still unclear.

5.2.2 Sediment Sampling

5.2.2.1 Multicorer

(M. Brinkmann, K. Dehning, B. Donner, G. Kirst, B. Meyer-Schack, K. Slickers and T. Wagner)

With the multicorer sediment cores between 20-42 cm were taken at 26 stations (chapt. 7.2.1 and 7.2.2). It was the main tool for sampling undisturbed sediment surfaces together with the overlying bottom water. The multicorer used, was equipped with eight large tubes (diameter 10 cm) and four small tubes (diameter 6 cm).

At every small station two large tubes were taken for the study of foraminiferal assemblages. They were sliced in 1 cm pieces, and stored in ethanol with bengal rose at 4°C. The sediment surface of one small tube was taken for diatom and radiolarian studies and stored in methanol (diatoms) and ethanol/bengal rose (radiolarians) at 4°C. One large and three small tubes were used as archive cores and frosted at -20°C. Three large cores were kept for the studies of Corg, sliced into 1 cm pieces and deep frozen at -20°C. Two large tubes were for geochemical investigations (oxygen-analysis, conductivity) five to six for biogeochemical investigations (porewater, sulfate reduction rate, density) and one more for magnetobacterial studies.

Bottom water samples for stable isotope analysis (^{18}O, ^{13}C) were taken from one large tube, the one containing the clearest water.

At every great station ten large tubes more were taken for the analysis of the porewater and Fe-reduction. For Fe/nitrate investigations one to two large tubes were used. The great station GeoB 3714 - the former GeoB1023 - was sampled with five multicorer deployments to satisfy each research group with enough sampling material.

Two special station, GeoB 3716 and GeoB 3726, both in very low water depths (ca. 100m) were sampled various times with the multicorer (13 times, 3 times) in order to find bacterial fields of Thioploca. The recovery of sediment was pretty good, the recovery of bacteria very small.

5.2.2.2 Gravity corer

(M. Brinkmann, K. Dehning, B. Donner, G. Kirst, B. Meyer-Schack, K. Slickers and T. Wagner)

In order to obtain sediment cores from the late Quaternary, a gravity corer with a 12, 14, 15 or 18 m pipe was used. In total 32 cores were retrieved with recoveries between 591 and 1409 cm. During transect A along the shelf most cores were from water depths of 1200-1300 m. Here we had 24 coring stations. Transect B going from shelf to deep sea basin brought cores from water depths from 800 to 4800m. On this transect 9 coring stations were maintained. The exact coring locations and equipment used are given in the station list (chapt. 7.2.3).

With the gravity corer in total 360,2 m of sediments were recovered. Geologists, sedimentologists, geochemists and biogeochemists sampled the material. Before using the coring tool, the liners had been marked lengthwise with a straight line, in order to retain the same orientation for all core segments. After deployment, the core liners were cut into 1m-segments, closed with caps on both ends and inscribed according to a standard scheme.

A temperature equilibration (minimum 24 hours) was needed before the physical properties could be measured. For sampling the core segments were cut into two halves. One half (archive) was used for core description, core photography, smear-slide analysis and for measurements of backscattered light using a colour-scanner. The electrical conductivity was measured at 2 cm intervals on the work half. Also the sampling for paleomagnetic investigations in 10 cm intervals was carried out at the work half. And at last three series of syringes for organic geochemical and faunal studies were taken at 5 cm intervals. The sampling holes were plugged with pieces of polystyrol and each core half was stored separately in a core tube. Finally a sponge soaked in a fungicide solution was put into each tube before closing in order to avoid fungal growth. The storing of the tubes was in 4°C.

On METEOR cruise 34/2 a Minolta CM-2002 hand-held spectrophotometer was used to measure percent reflectance values of sediment colour at 31 wavelength channels over the visible light range (400-700 nm). Digital reflectance data of spectrophotometer readings were routinely obtained at 3 cm spacing from the surface of the archive half immediately after core opening. The surface of the cores were scraped with a knife to expose a fresh, unsmeared surface for measurements. A thin transparent plastic film (Hostaphan) was used to cover the wet surface of the sediment and to procect the photometer lense. Before measuring the spectrophotometer was calibrated for white colour reflectance. Photometric readings were transferred to a personal computer and selected wave band reflection profils (450, 550, and 700 nm) were graphically presented.

5.2.3 Visual core Descriptions
(G. Kirst and T. Wagner)

5.2.3.1 Methods

During Meteor cruise 34/2 twenty-one gravity cores were recovered with total lengths between 5.9 and 13.8 m. The coring locations and related water depths are given in the station list (chapt. 7.2.1). Due to the short duration of Meteor cruise 34/2, only seven cores were subjected to shipboard geological analysis. The preliminary lithologic summary of these cores is based on visual core descriptions, color scanner readings and microscopic inspections of smear slides taken from representative lithologies and special or unique layers of special interest. Core descriptions are shown in Figures 79a to 99a and present dominant lithologies, their color acording to the MUNSELL soil color chart, and sedimentary structures. The sediment classification scheme used on Meteor cruise 34/2 is based on ODP conventions (GRAHAM and MAZULLO, 1988). In order to obtain more detailed information on changes in lithologic colors, which alternate from light gray to light olive gray versus olive gray and dark olive gray, light reflection was measured quantitatively by spectrophotometry in the wave length band of visible light (400-700 nm). The reflectance of three selected wave lengths 450 nm (blue), 550 nm (green), and 700 nm (red) is shown in Figures 79a to 99a for the respective cores. Variations in the lithologic color probably reflect changes in the sediment composition, particulary of relative proportions of biogenous carbonate and silicate (light and high reflection values) to organic matter and clay minerals (dark and low reflectance values).

5.2.3.2 Shipboard Results, Part 1

Sediments recovered along the S-N core transect from the northern Cape Basin to the Walvis Ridge and the southern Angola Basin are closely related to the late Quaternary history of continental upwelling off Namibia. Fourteen cores along this transect were taken from similar water depths of about 1300 m with exception of cores 3709-2 and 3714-8, which were recovered from water depths of 2700 m and 2100 m, respectively. Lateral variations in dominant lithologies along this transect display variable, light colored, and carbonate rich sediment sections in the south (core GeoB 3701-3, Fig. 79a) changing to rather monotonous, dark colored, and probably organic rich deposits in the north (for example see cores GeoB 3707-10 and 3014-8, Figs. 84a and 90a). These lithologic variations depict a longitudinal profile from the southern transition of the modern upwelling area off NW-Namibia through its central sector off Walvis Bay and transits into its northern area above the southern Angola Basin.

Core GeoB 3701-3 from the northern Cape Basin at 28° S consists of carbonaceous oozes with variable amounts of foraminifera (Fig. 79a). Bioturbation is weak to moderate throughout the core. Color reflectance profils are much higher and more variable for all wave

lengths shown (Fig. 79a) compared to upwelling dominated sediments further north. This pattern is attributed to generally high carbonate contents and probably moderate to low organic carbon contents. Four coarse grained intervals are observed below 3 mbsf. These foraminiferal sand layers likely record periods of enhanced bottom current intensities (contour currents) which caused winnowing of the fine grained sediment fraction. A preliminary stratigraphic subdivision of the sedimentary column seems possible by combination of reflectance profils of core GeoB 3701-3 with shipboard biostratigraphic data published for core GeoB 1716-3 (SCHULZ et al., 1992), a core which is located at the same position as GeoB 3701-3. According to these results, the base of core GeoB 3701-3 reaches into oxygen isotopic stage 6. Interglacial oxygen isotope stages 5 and 1 are documented in the sediment sections between 825 cmbsf to 460 cmbsf and 50 cmbsf to the sediment surface, respectively. Corresponding estimates of average linear sedimentation rates indicate intermediate levels for interglacial sections, about 7 and 4 cm/ky for isotopic stages 5 and 1, respectively, and drastically increased levels during glacial sections, approximately up to 16 cm/ky for oxygen isotope stage 2 (2/3 stage boundary set at 240 cmbfs).

Cores GeoB 3702-1, 3705-4, 3707-10, 3708-2, 3710-3, and 3714-8 were taken in the central and northern sectors of the Namibian upwelling area between 1300 m and 2100 m water depth. CALVERT and PRICE (1979) report from surface sediments of this area some of the highest organic carbon contents of the modern ocean. Very high flux rates of carbonaceous and especially of siliceous plankton result in the establishment of oxygen depleted to anoxic depositional conditions at the sea floor which strongly enhances the preservation potential of marine organic matter. The corresponding type of sediment is a dark olive siliceous ooze with variable but intermediate to low contents in calcium carbonate and very high levels in organic carbon. This type of lithology dominates throughout all cores investigated between 27° S and 15° S. Variations in the composition of these upwelling deposits are low as it is indicated by continuous relative proportions of carbonaceous and siliceous components versus organic matter and clay and persistent low light reflectance values. Intensive H_2S smell was recognized below 90 to 250 cmbsf. Bioturbation features were rarely observed due to the homogenous structure of the sediments. Remarkably are open, organic (?)-coated tube structures of about 1 cm in diameter and 20 to 30 cm in length, which preferentially are subvertically oriented and are located between five to seven meters core depth (for example see core GeoB 3714-8, Fig. 90a). These open tubes are interpreted to represent either residual worm burrows or degasing channels, which seems reasonably considering very high gas contents in this sedimentary type.

5.2.3.3 Shipboard Results, Part 2

(J.Klump, H. Kuhnert, F. Lamy and T. Wolff)

The following cores were retrieved on cruise M34/2 but - because of lack of time - opened and sampled during the third leg (cruise M34/3):

GeoB 3703-9, GeoB 3706-2, GeoB 3709-2, GeoB 3711-3, GeoB 3712-3, GeoB 3715-3, GeoB 3717-3, GeoB 3718-10, GeoB 3719-1, GeoB 3720-3, GeoB 3721-3, GeoB 3722-2, GeoB 3723-1 and GeoB 3724-4.

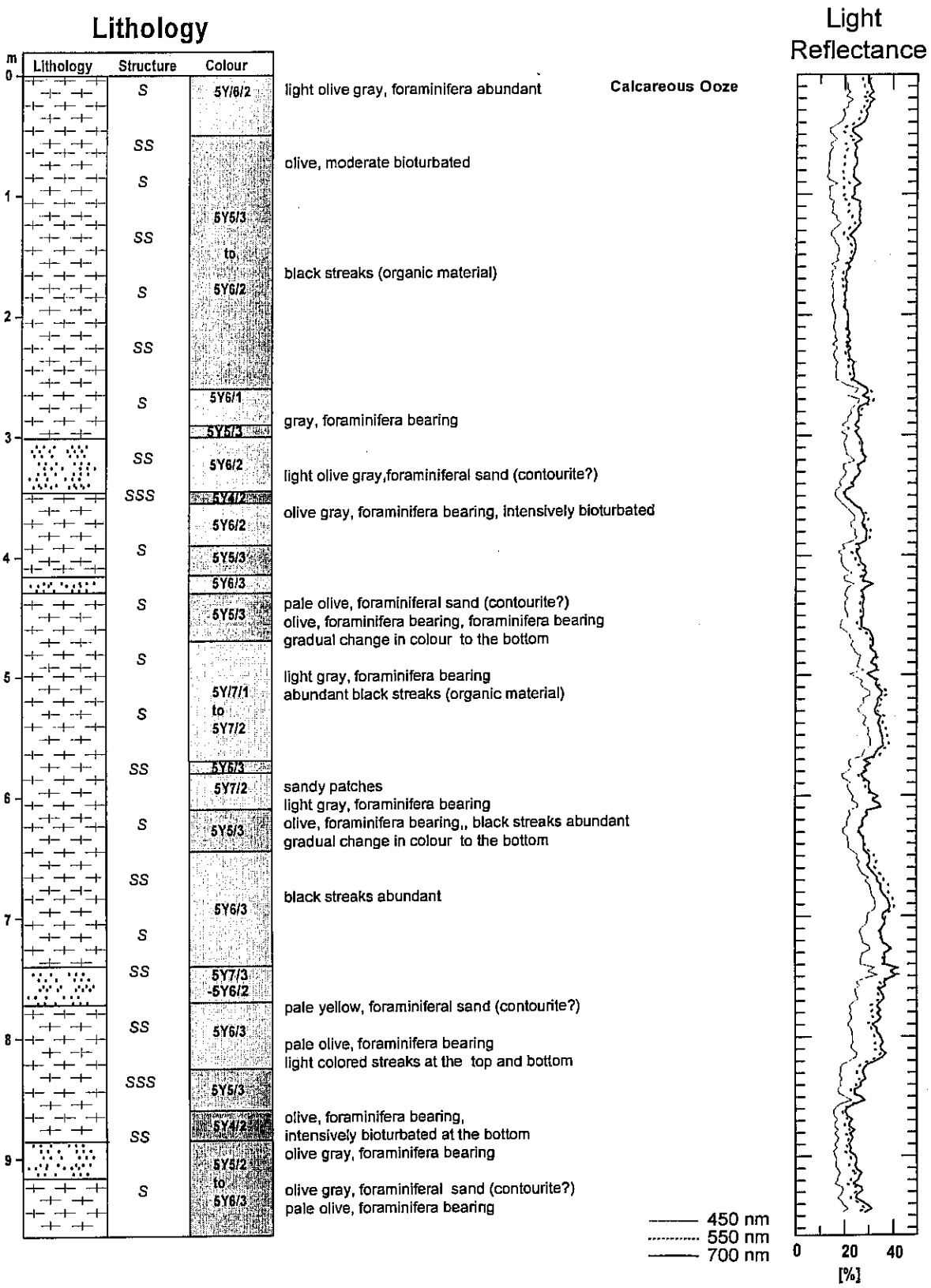

Fig. 79a: Core 3701-03: Core description, legend for stratigraphic columns see volume II page 74.

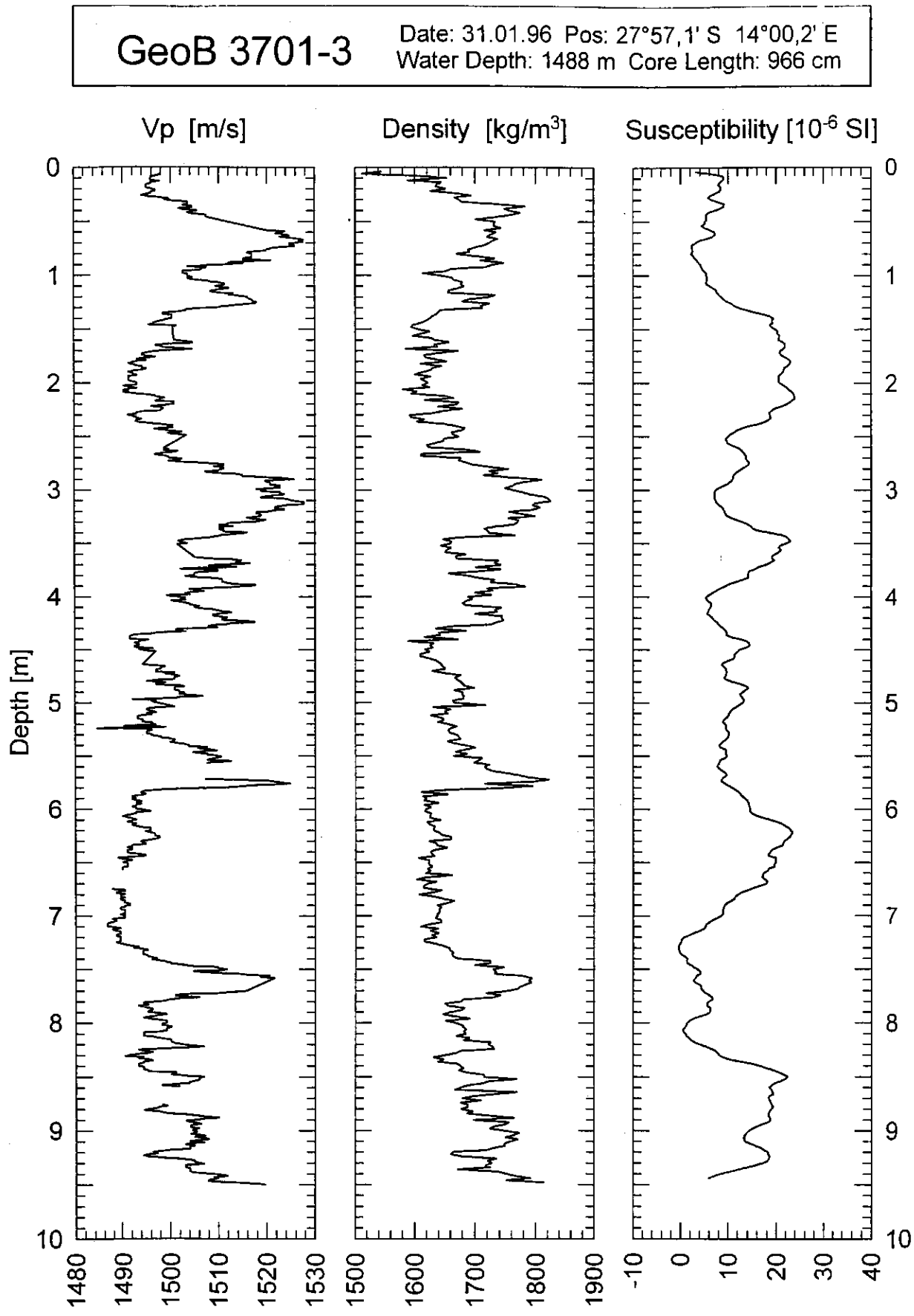

Fig. 79b: Core 3701-03: Physical properties data.

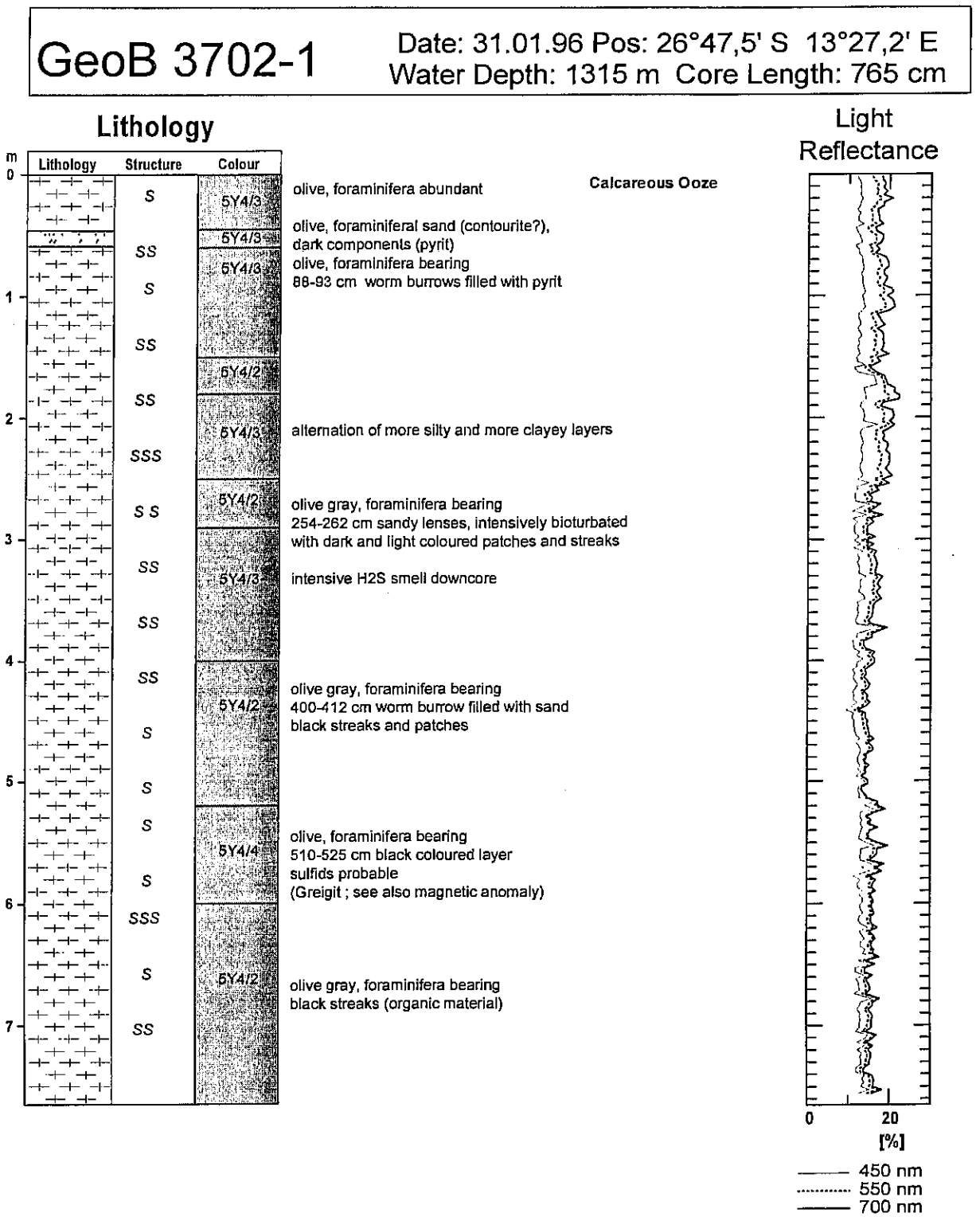

Fig. 80a: Core 3702-1: Core description.

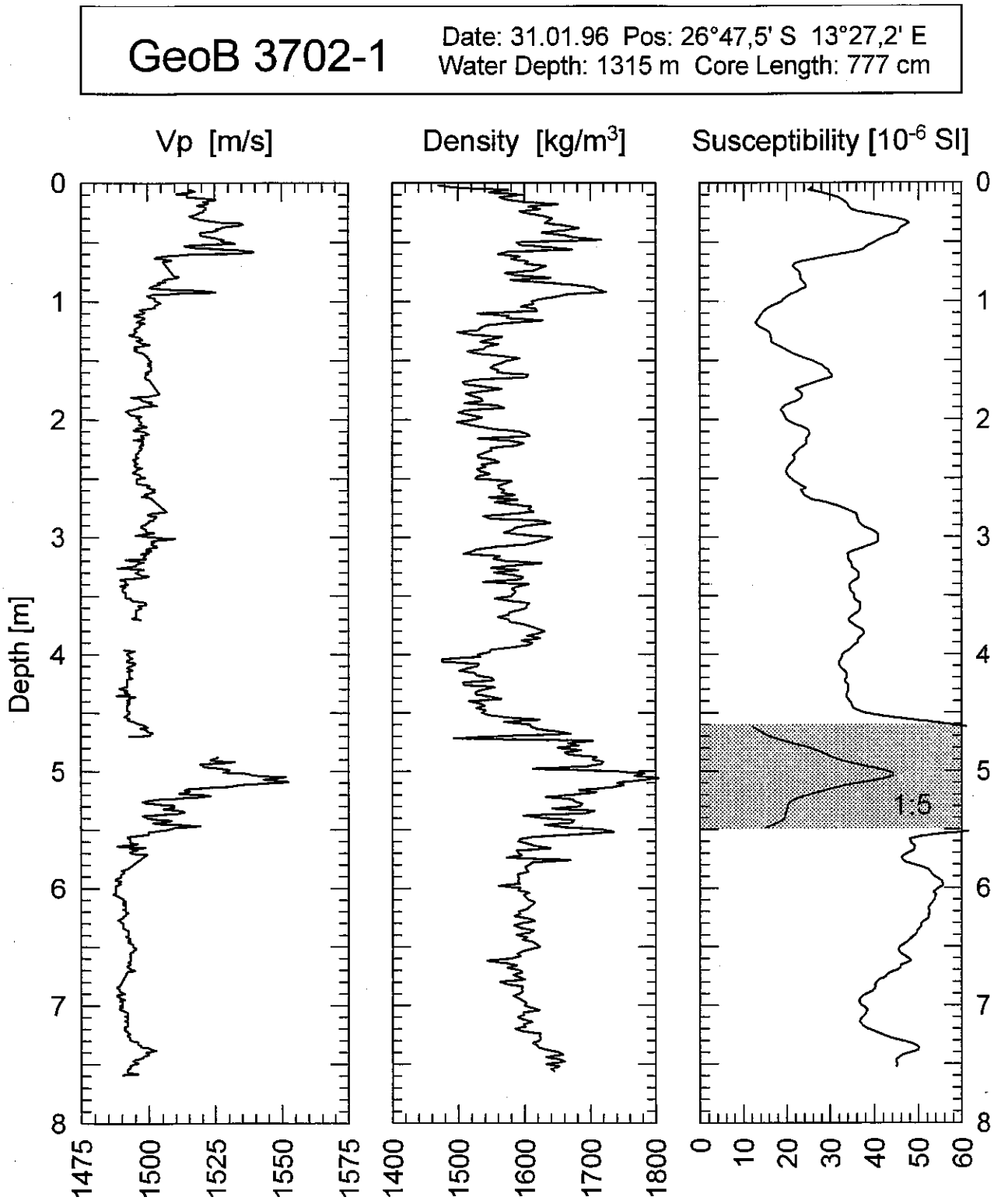

Fig. 80b: Core 3702-1: Physical properties data.

GeoB 3703-9

Date: 01.02.96 Pos: 25°30,9' S 13°14,0' E
Water Depth: 1373 m Core Length: 933 cm

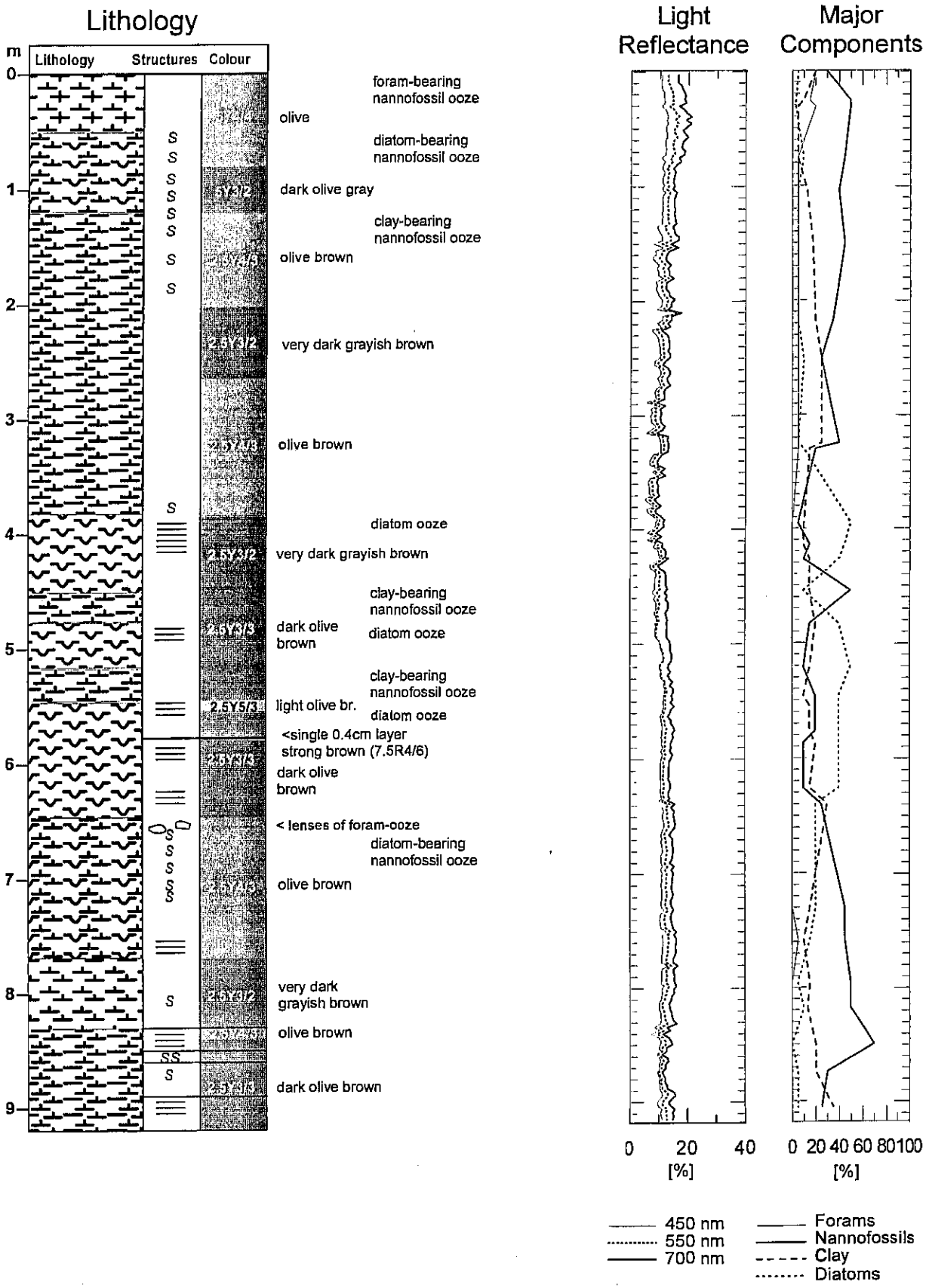

Fig. 81a: Core 3703-9: Core description.

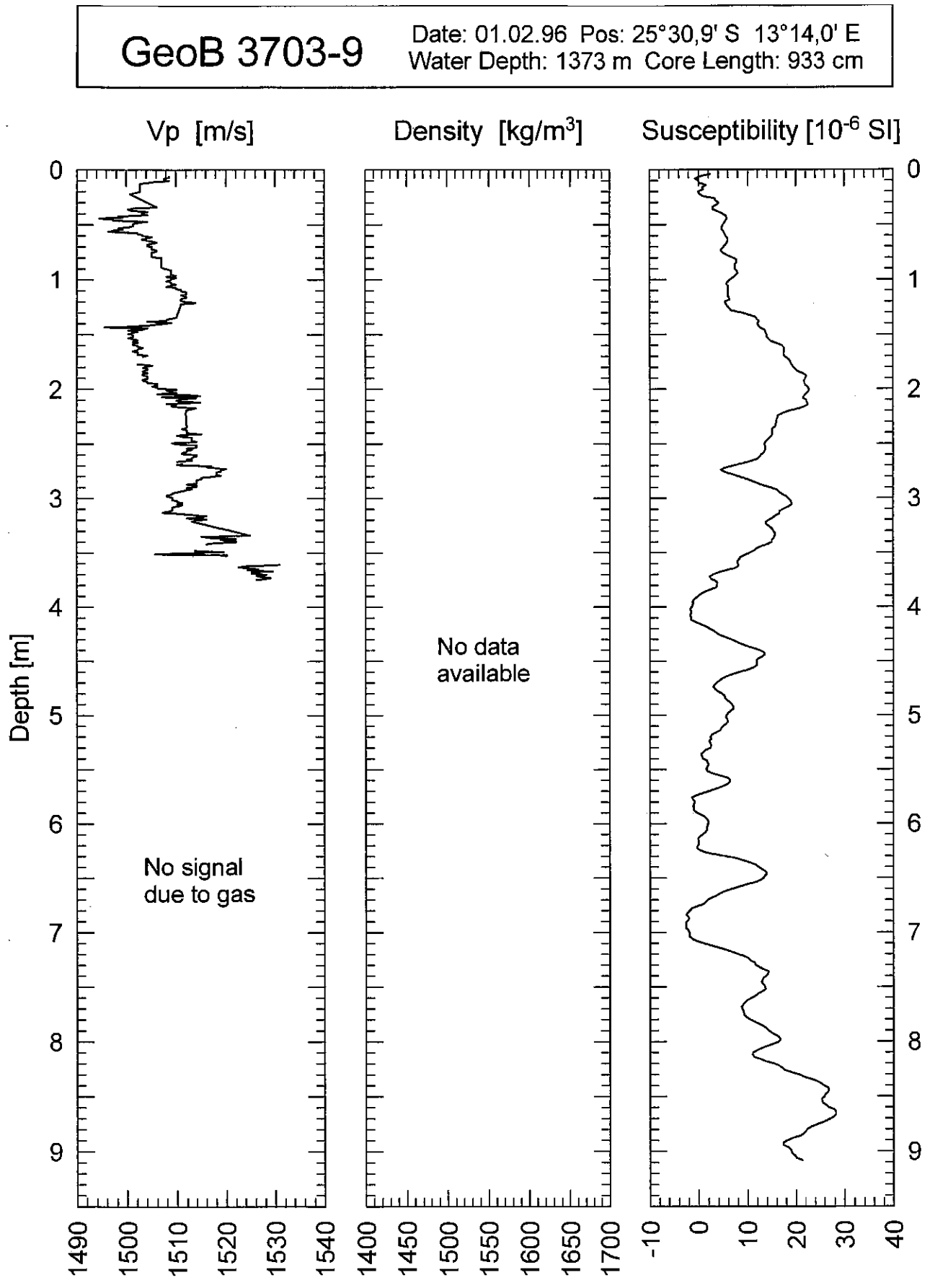

Fig. 81b: Core 3703-9: Physical properties data.

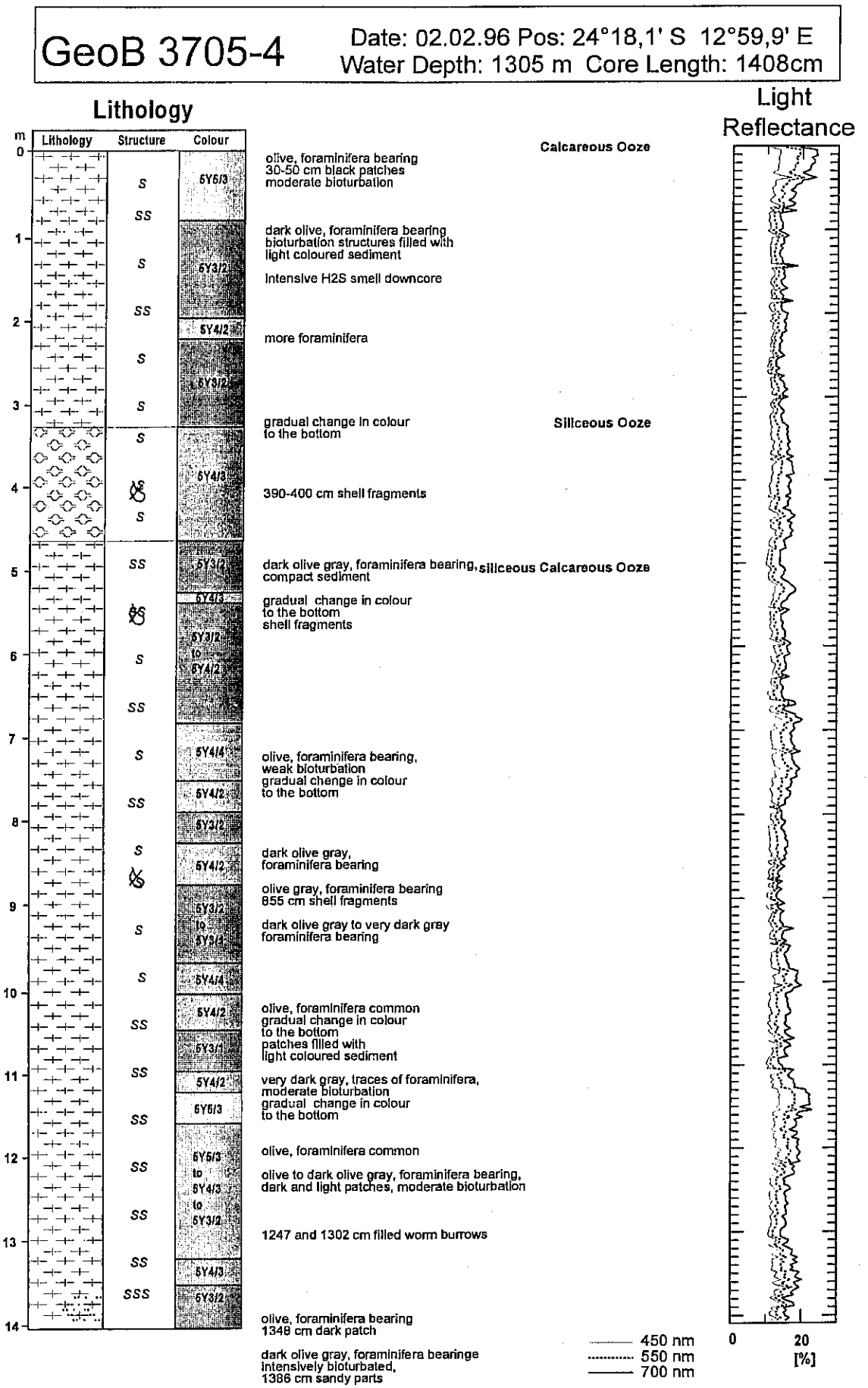

Fig. 82a: Core 3705-4: Core description.

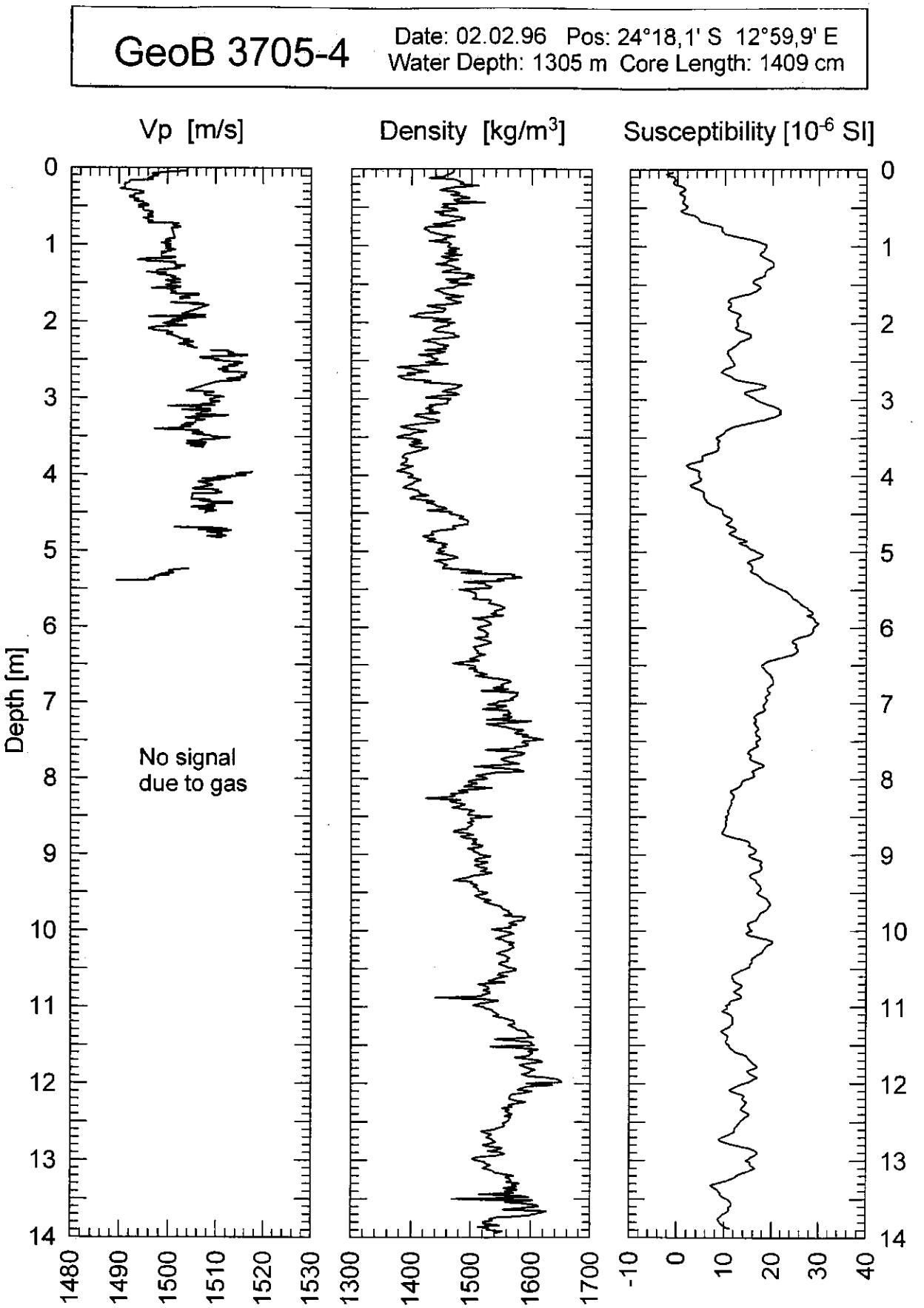

Fig. 82b: Core 3705-4: Physical properties data.

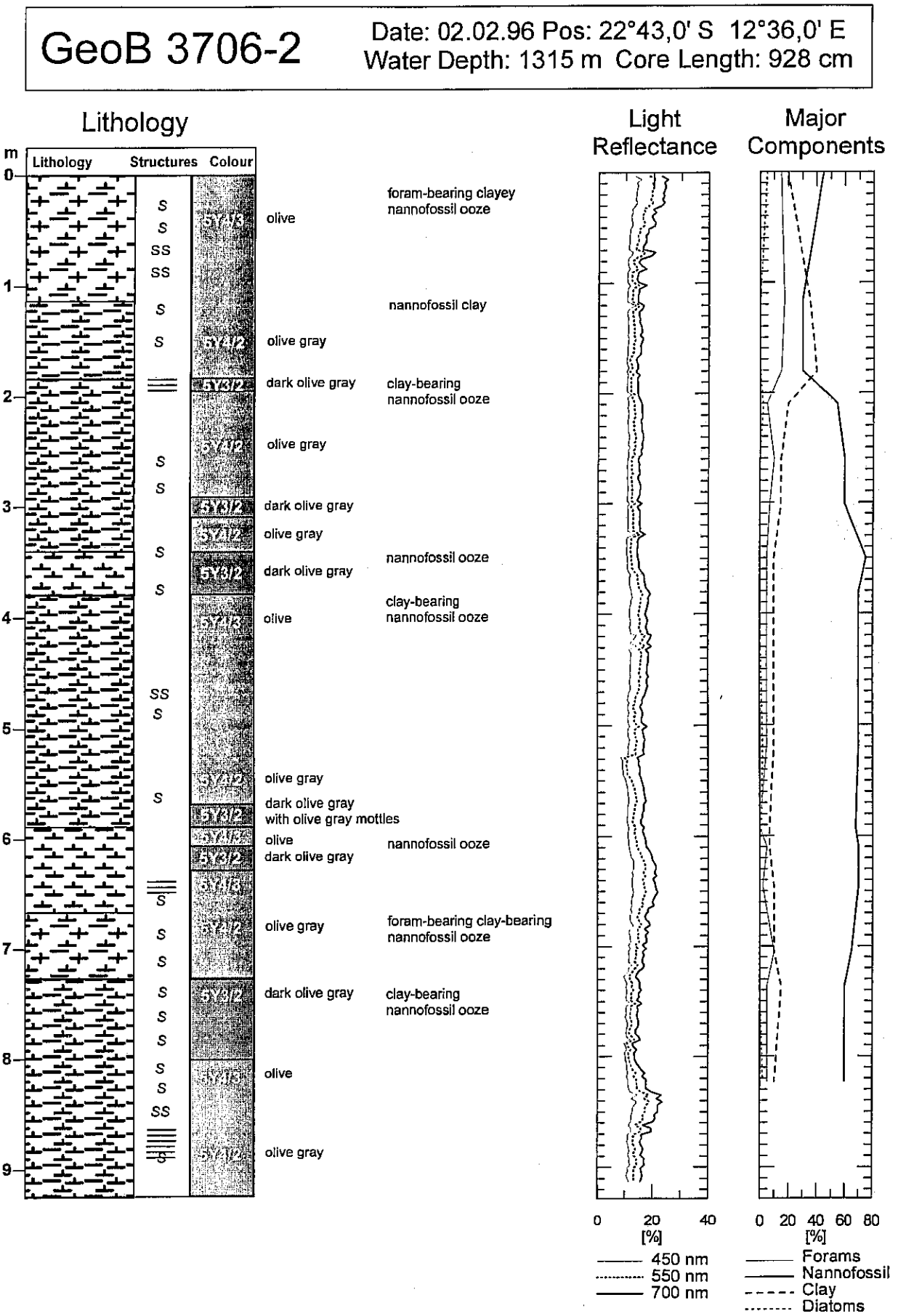

Fig. 83a: Core 3706-2: Core description.

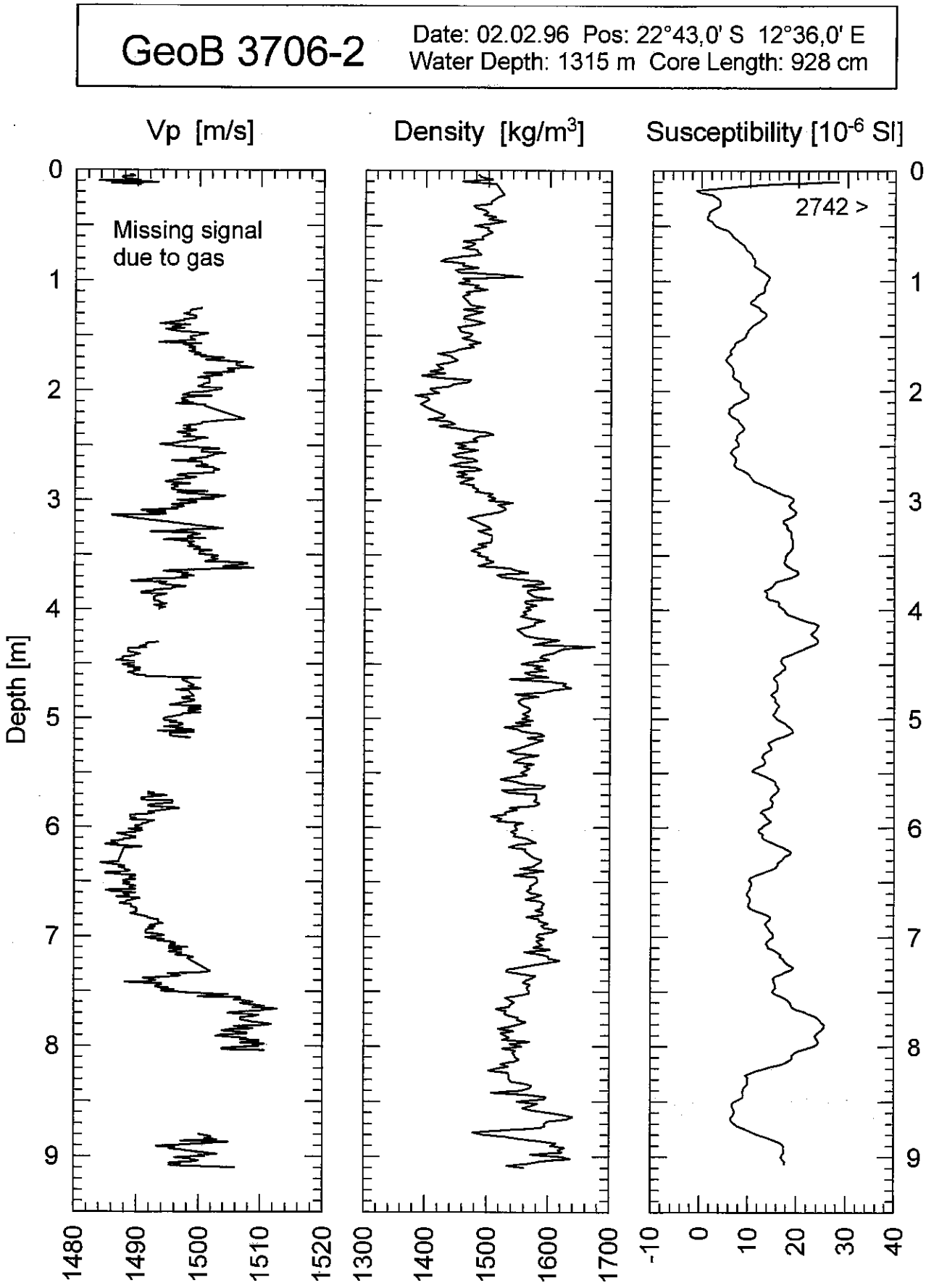

Fig. 83b: Core 3706-2: Physical properties data.

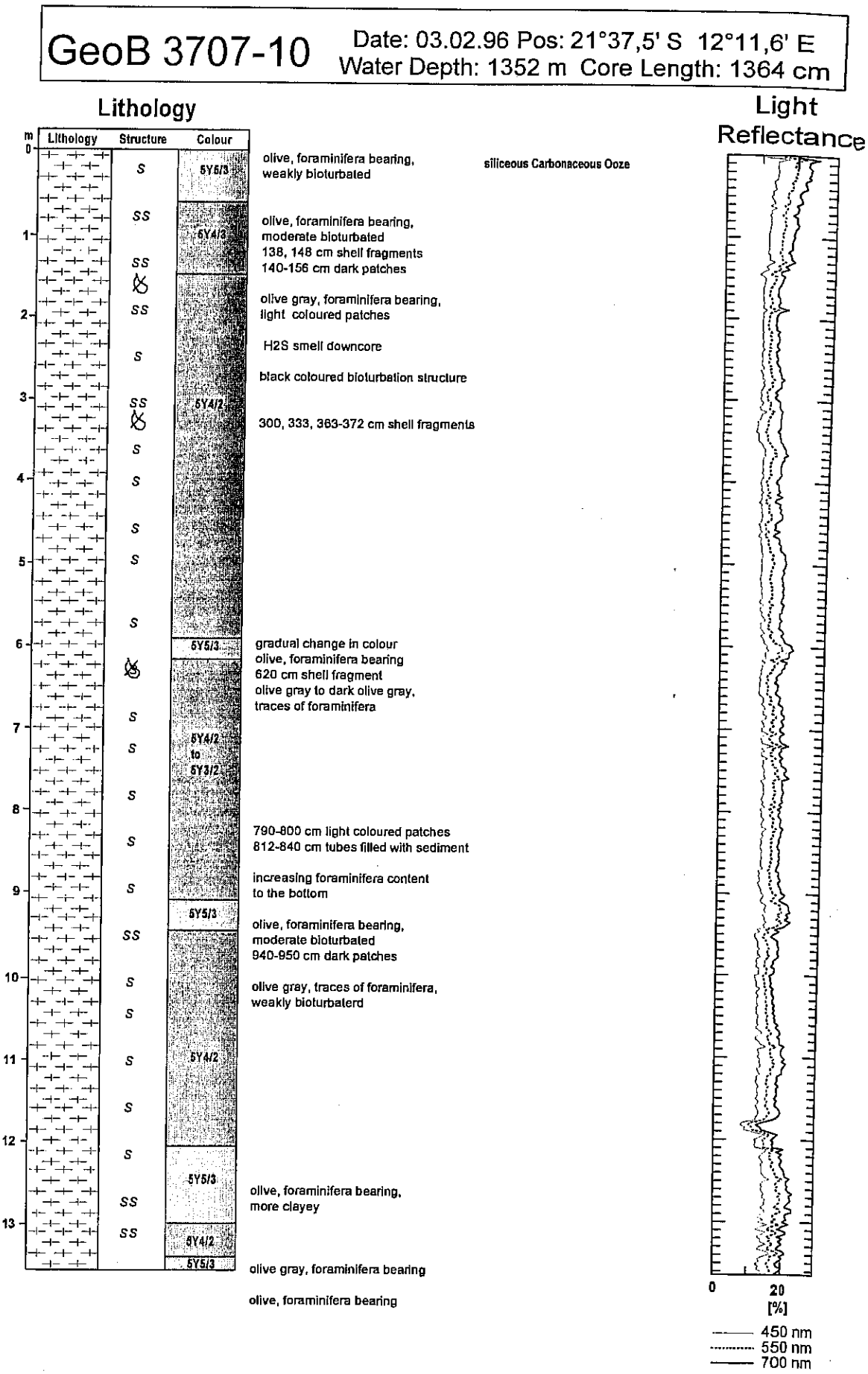

Fig. 84a: Core 3707-10: Core description.

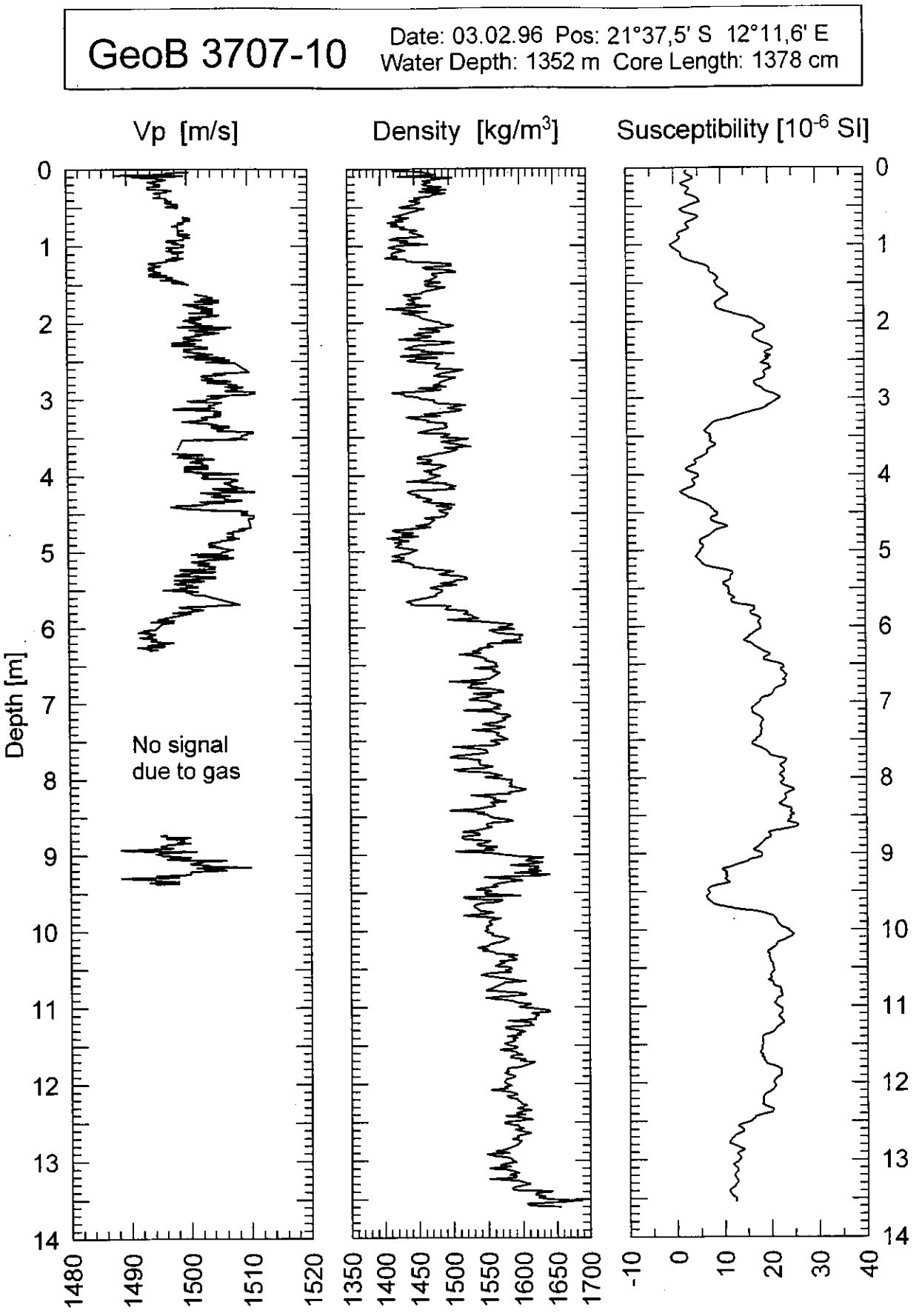

Fig. 84b: Core 3707-10: Physical properties data.

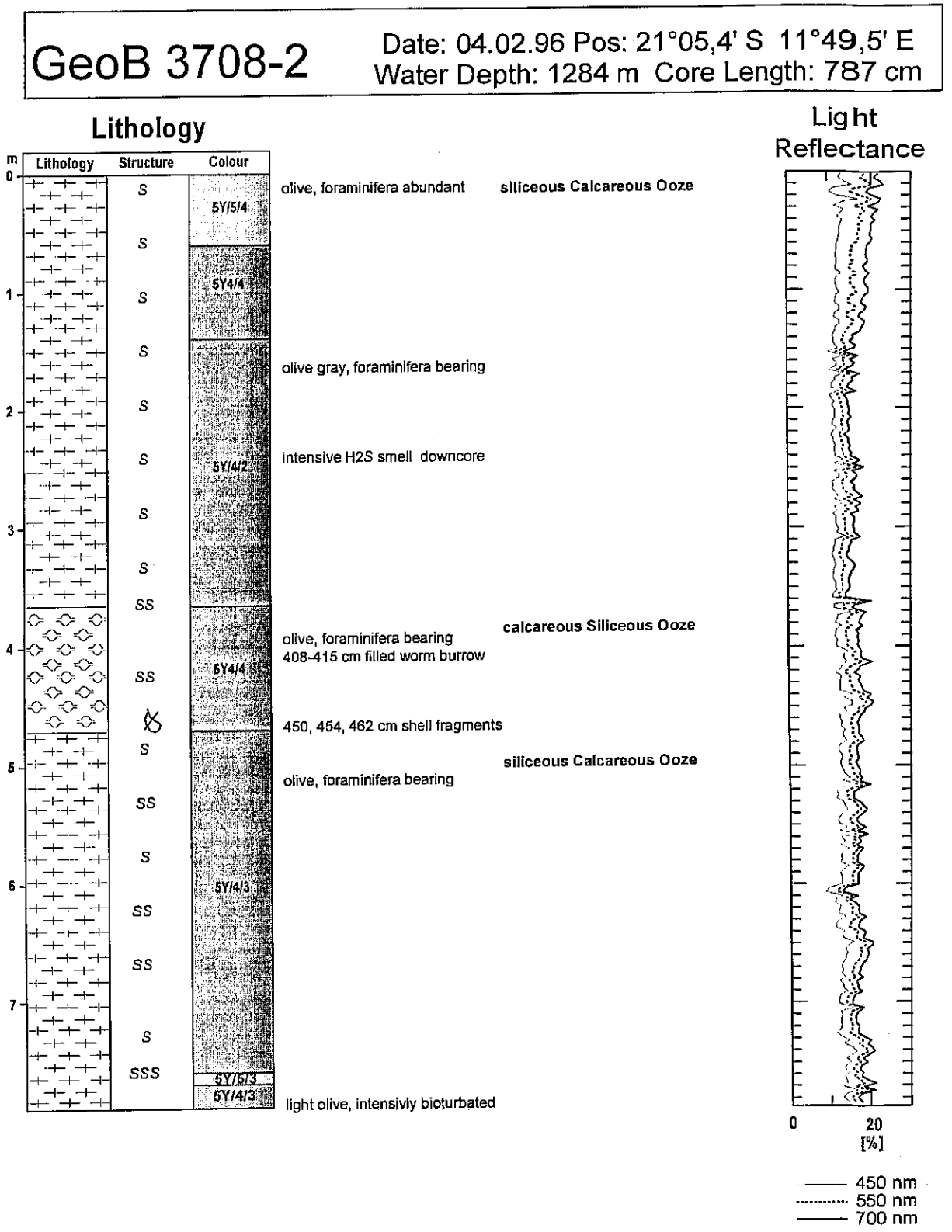

Fig. 85a: Core 3708-2: Core description.

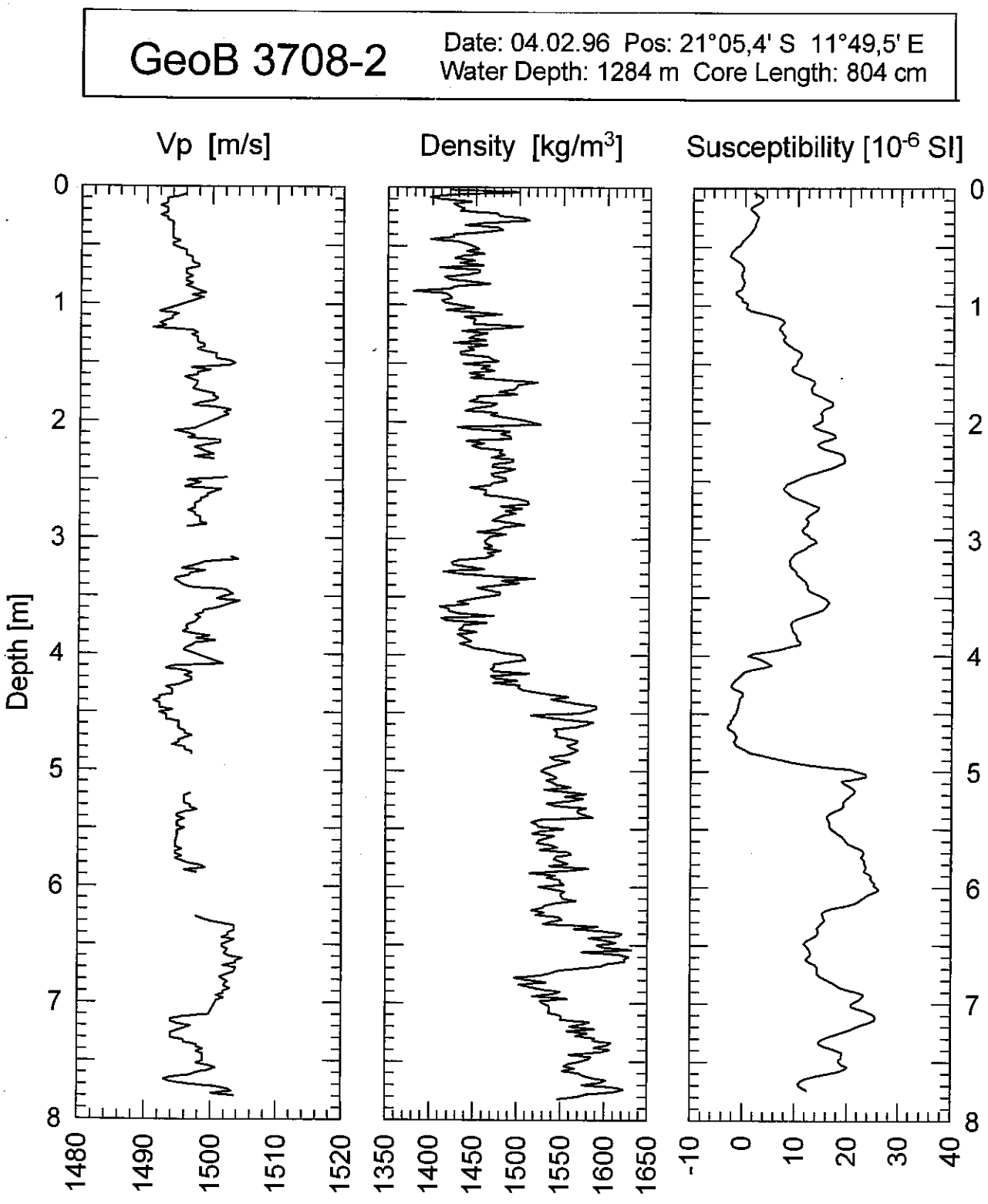

Fig. 85b: Core 3708-2: Physical properties data.

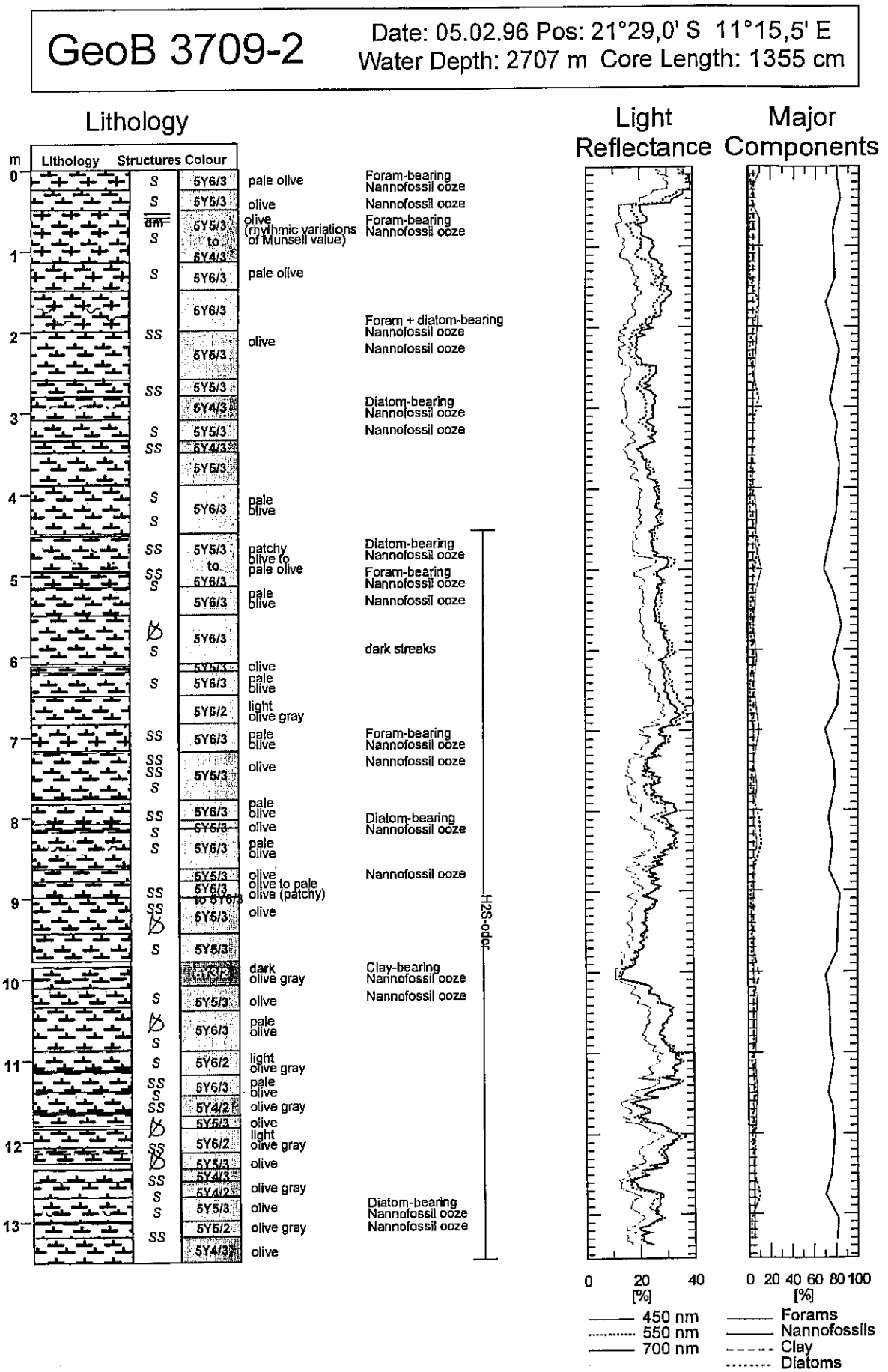

Fig. 86a: Core 3709-2: Core description.

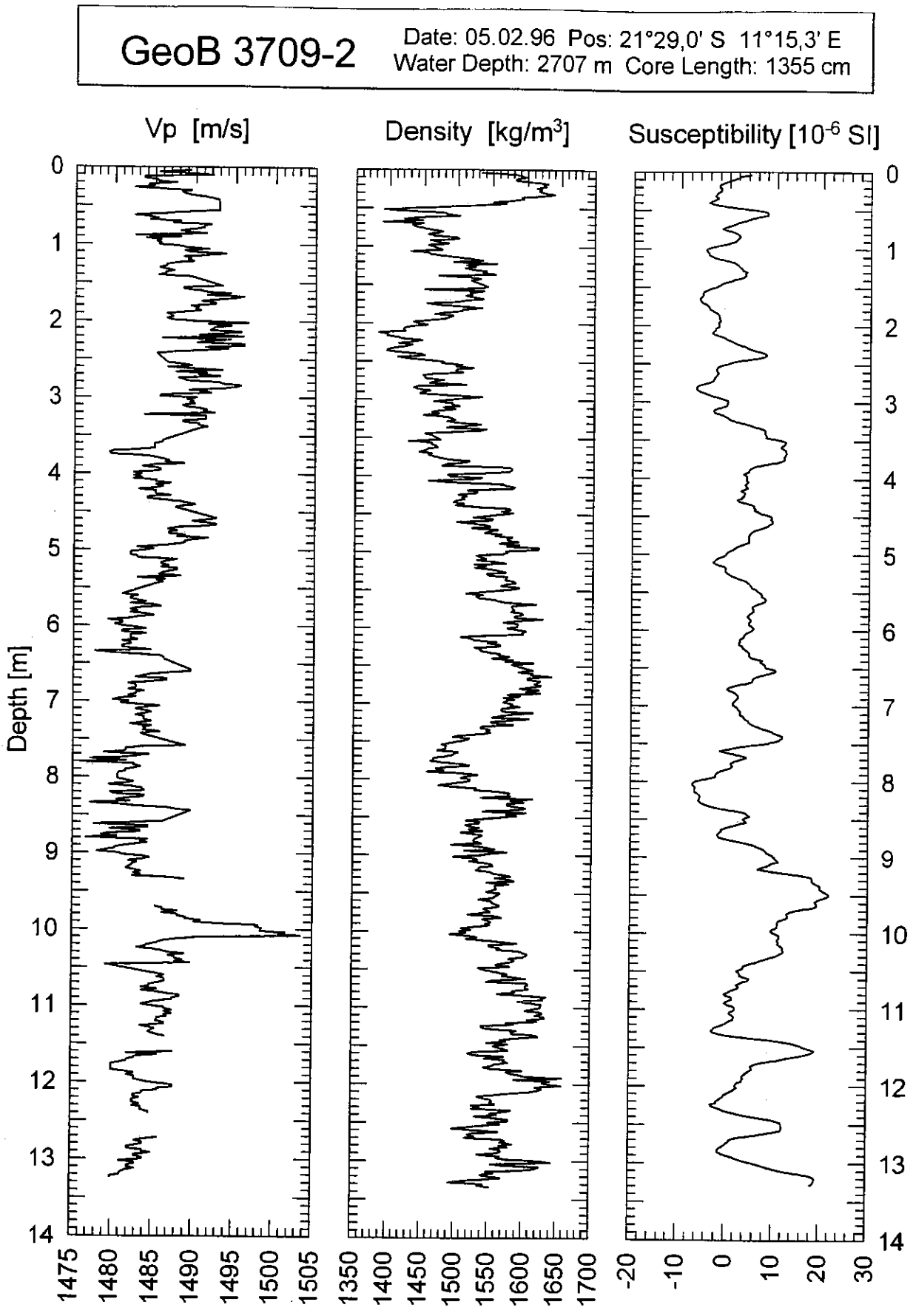

Fig. 86b: Core 3709-2: Physical properties data.

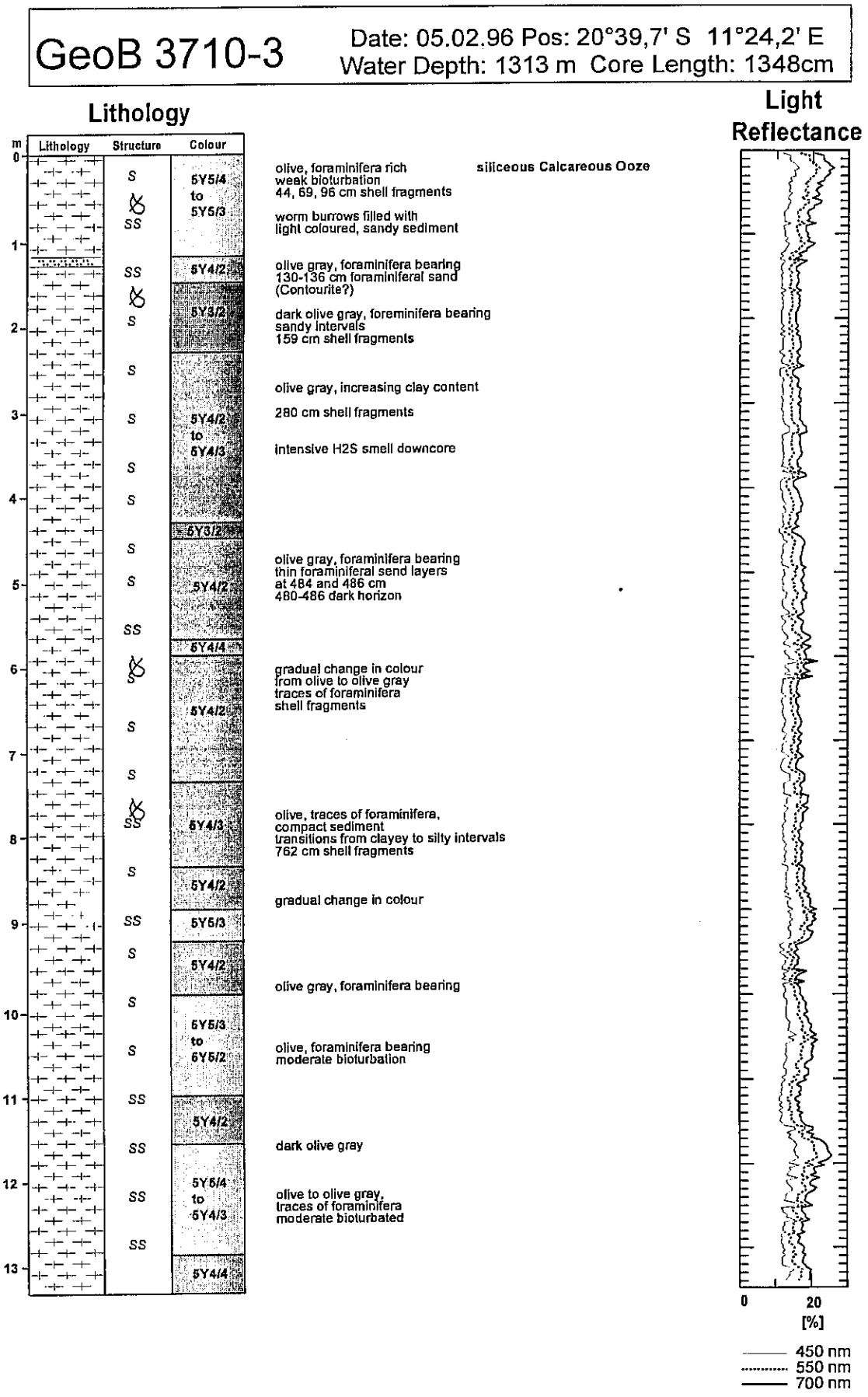

Fig. 87a: Core 3710-3: Core description.

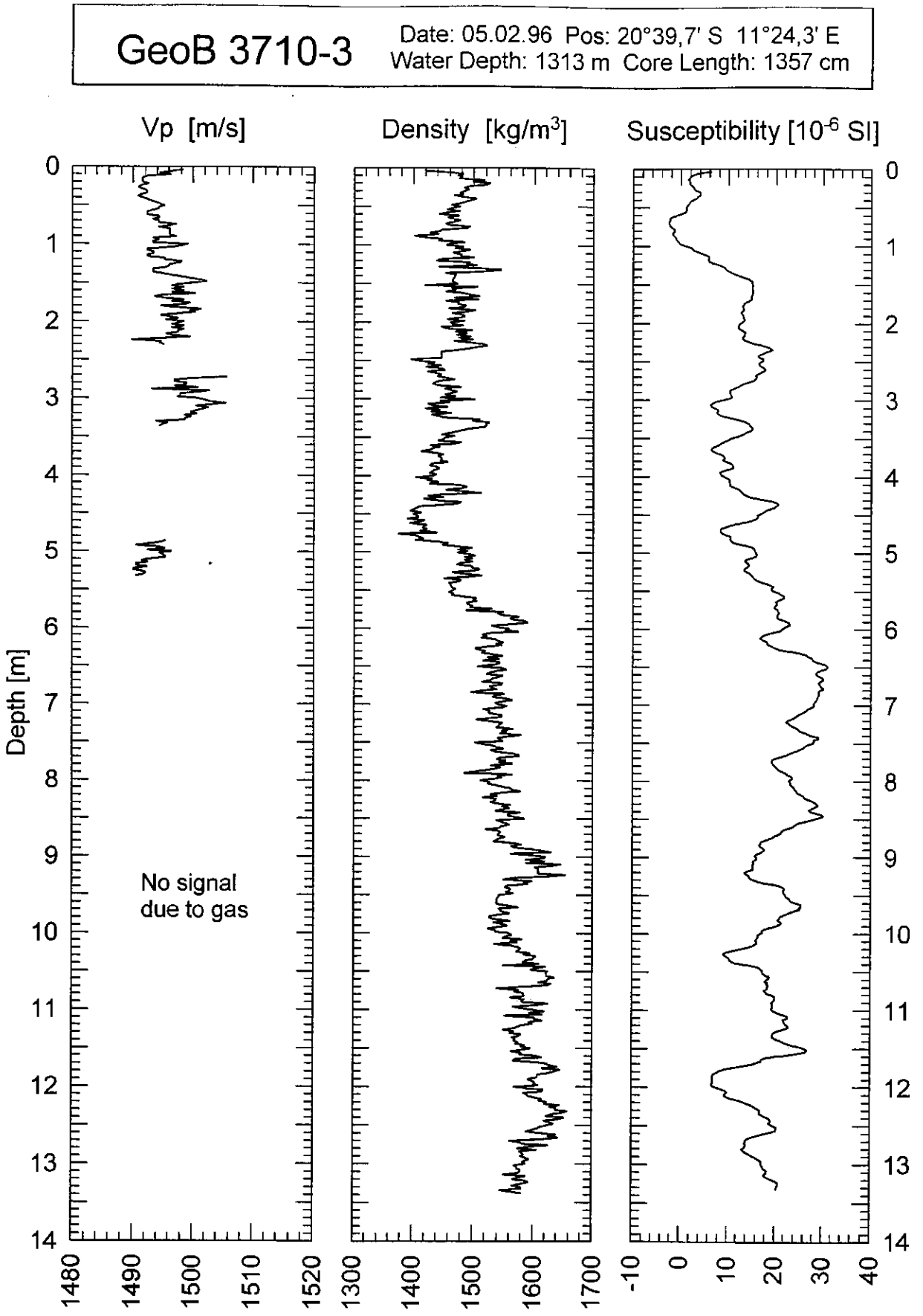

Fig. 87b: Core 3710-3: Physical properties data.

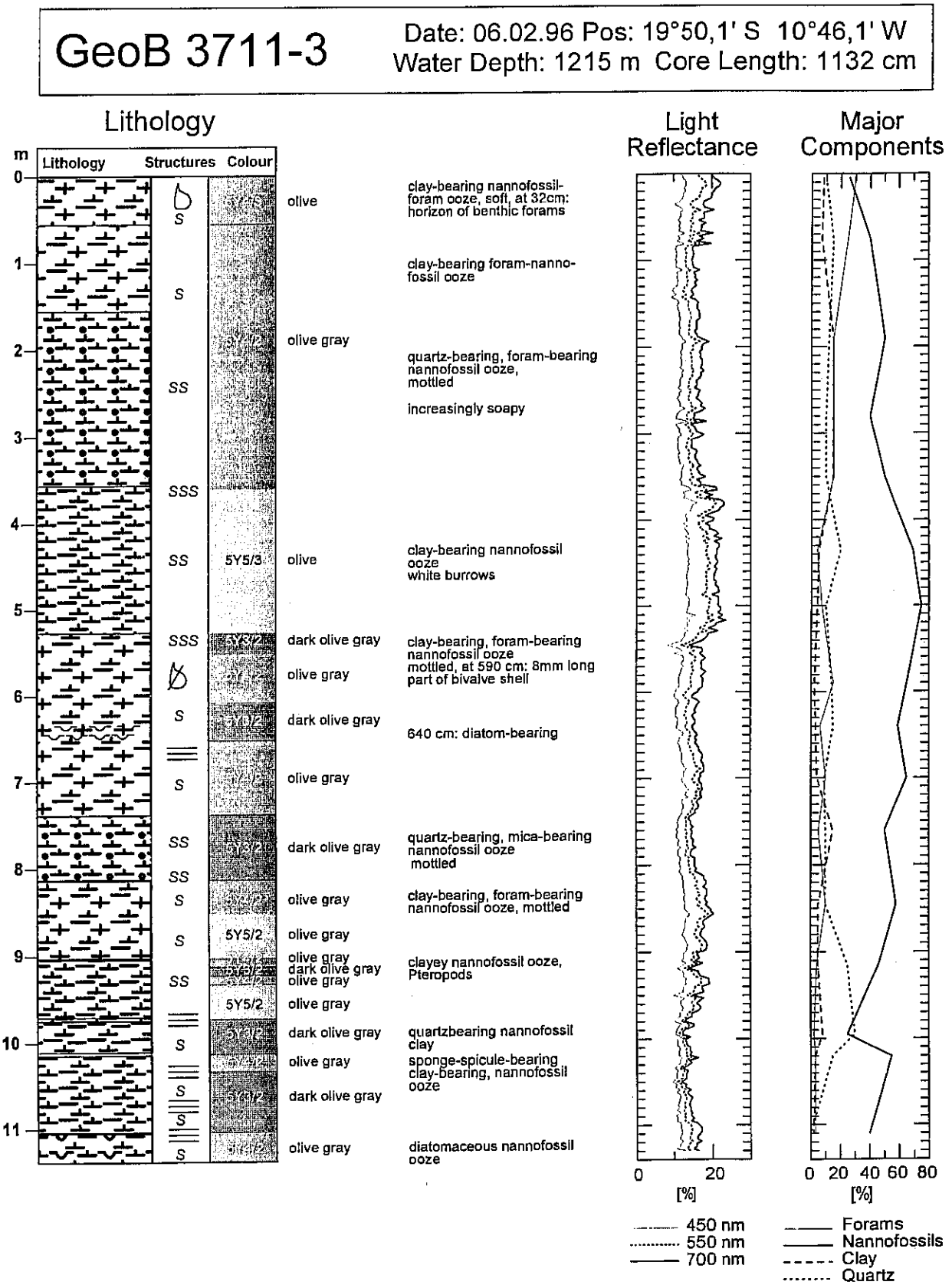

Fig. 88a: Core 3711-3: Core description.

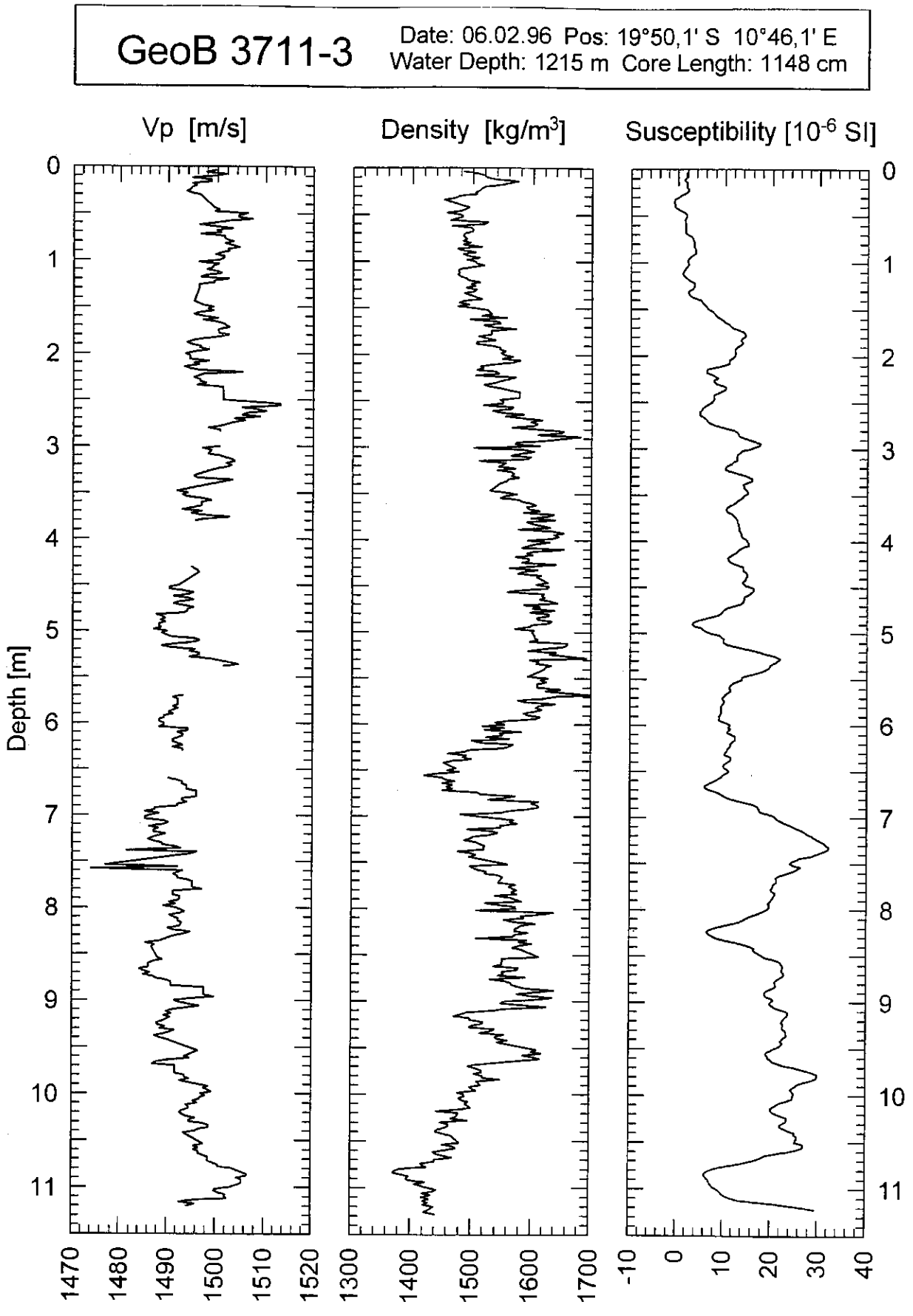

Fig. 88b: Core 3711-3: Physical properties data.

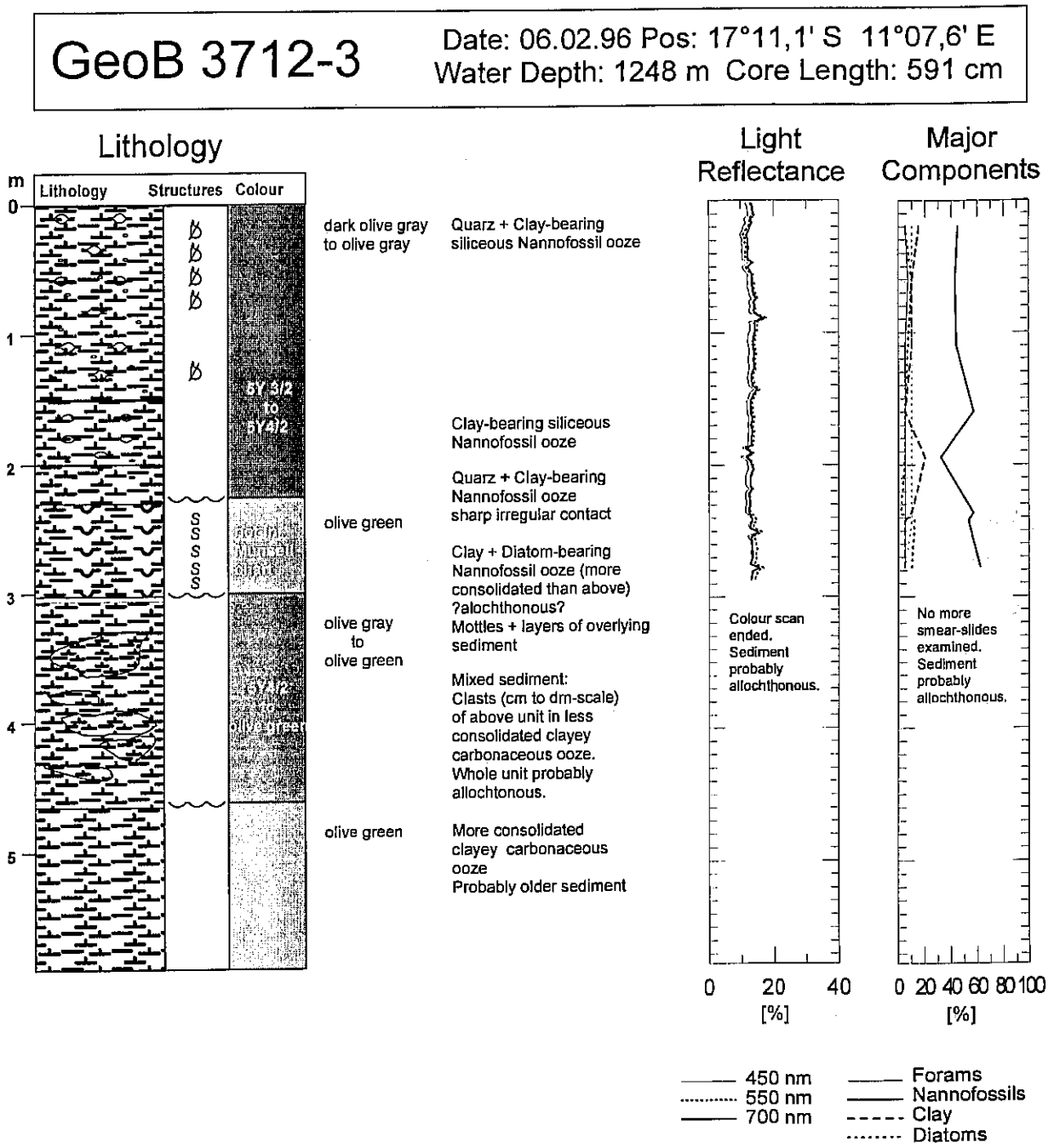

Fig. 89a: Core 3712-3: Core description.

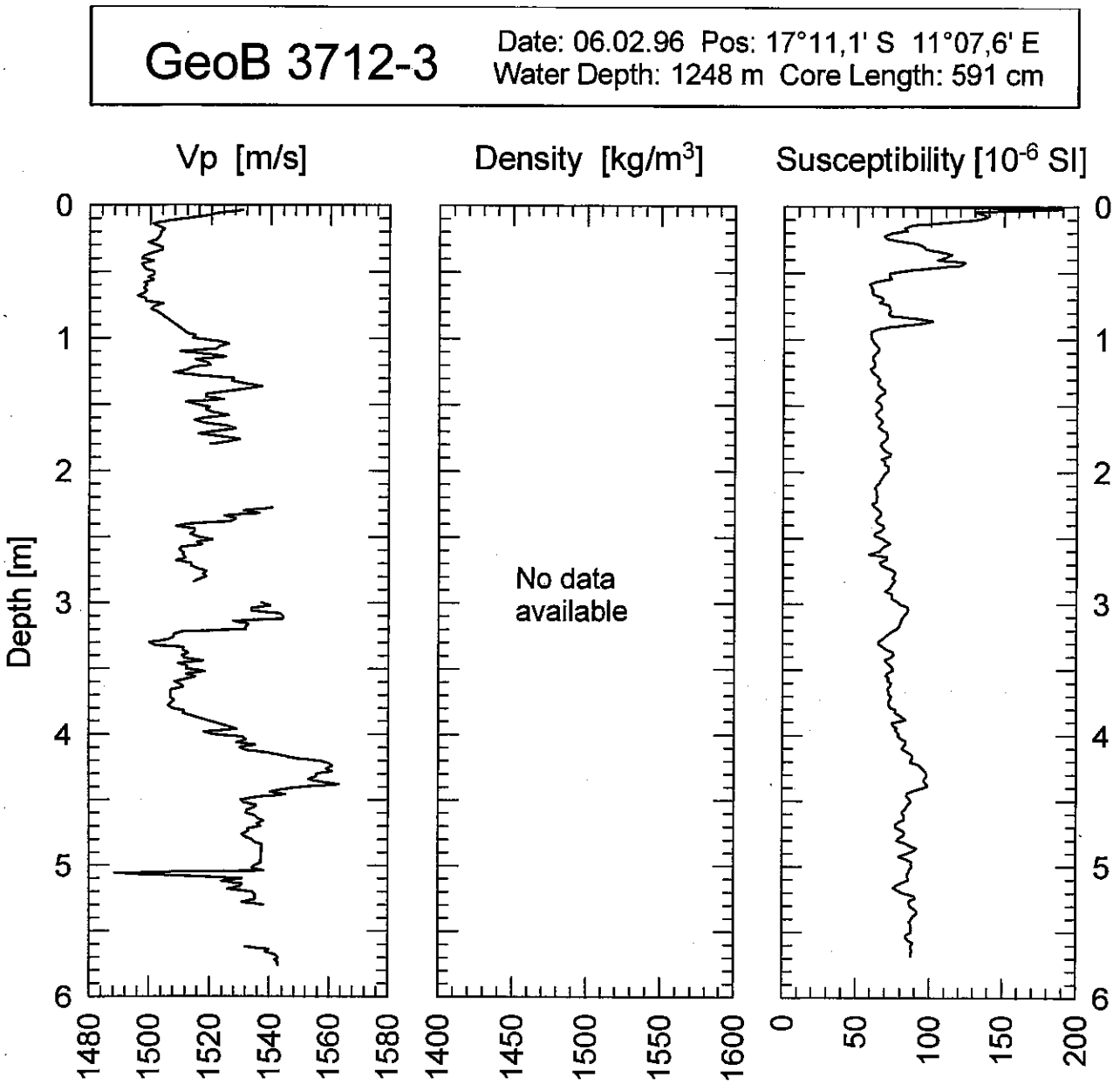

Fig. 89b: Core 3712-3: Physical properties data.

GeoB 3714-8

Date: 08.02.96 Pos: 17°09,5' S 10°59,9' E
Water Depth: 2062 m Core Length: 1195cm

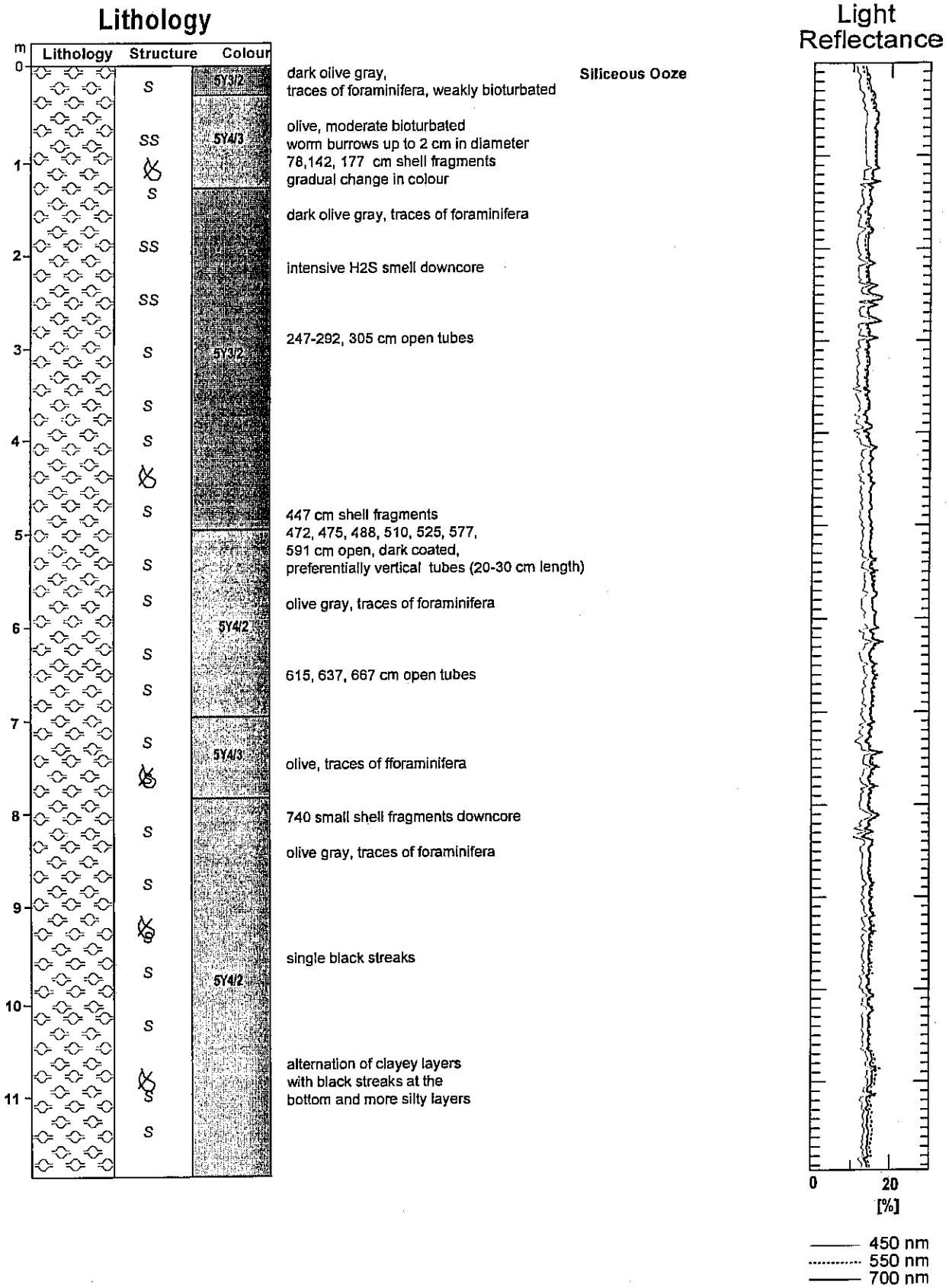

Fig. 90a: Core 3714-8: Core description.

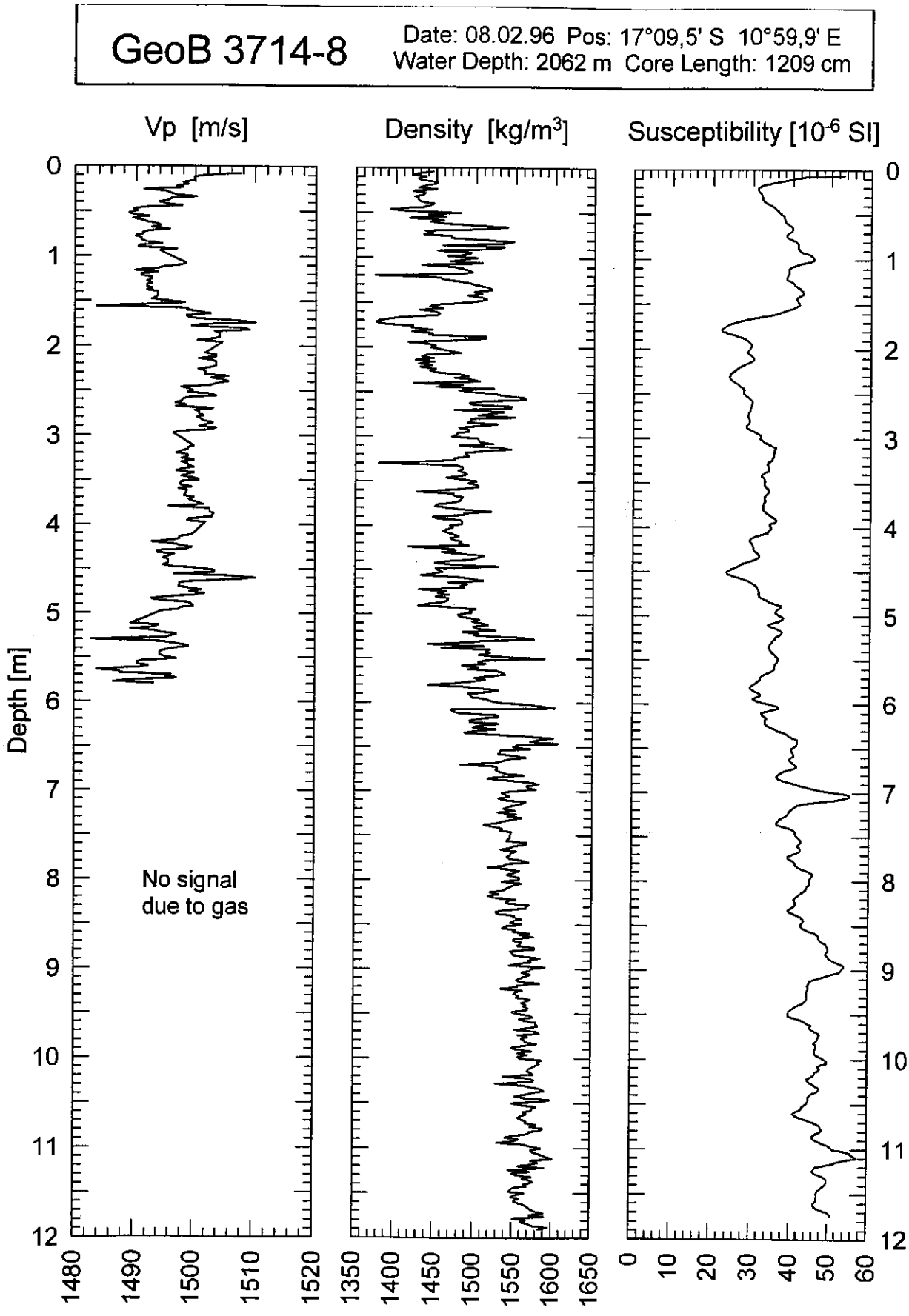

Fig. 90b: Core 3714-8: Physical properties data.

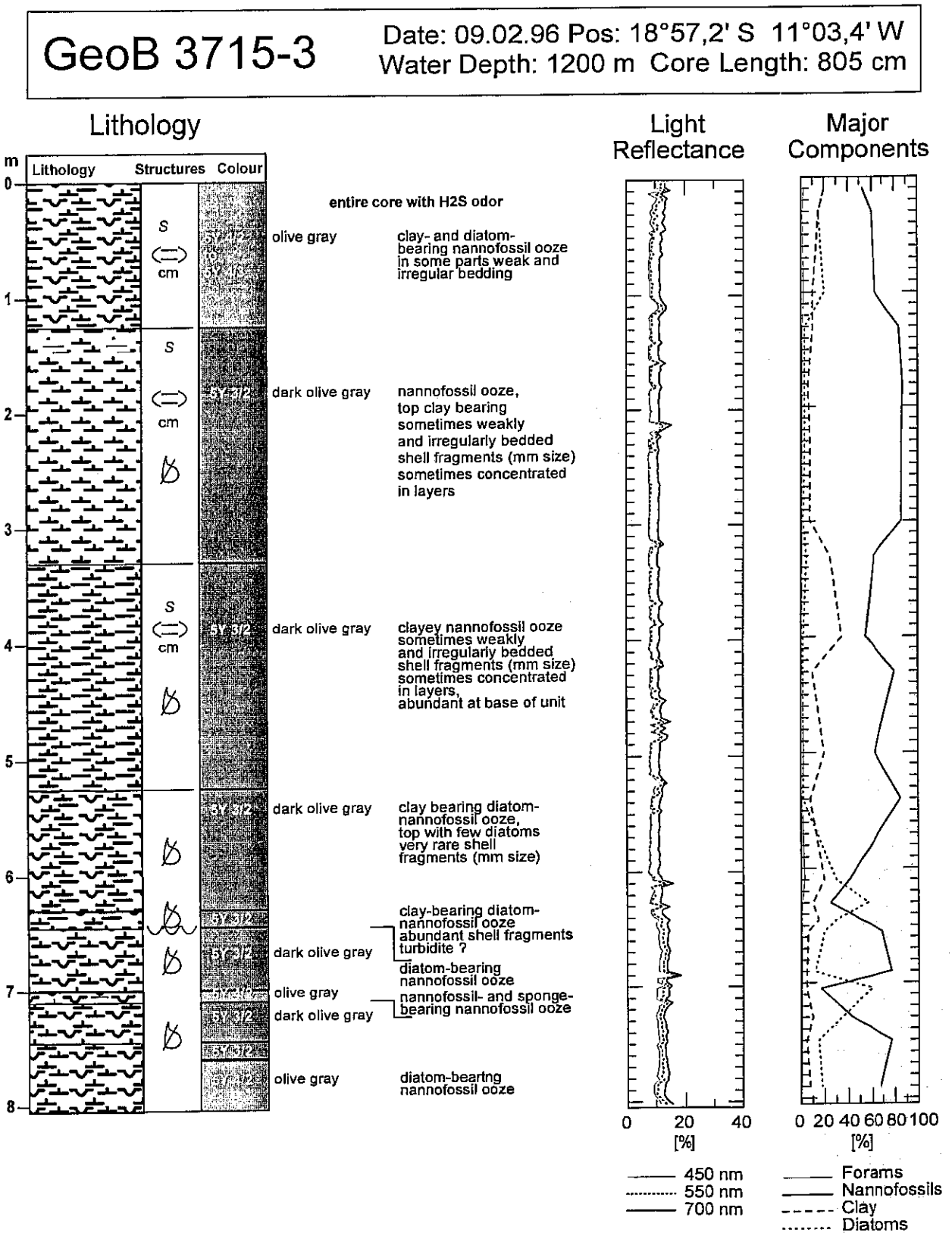

Fig. 91a: Core 3715-3: Core description.

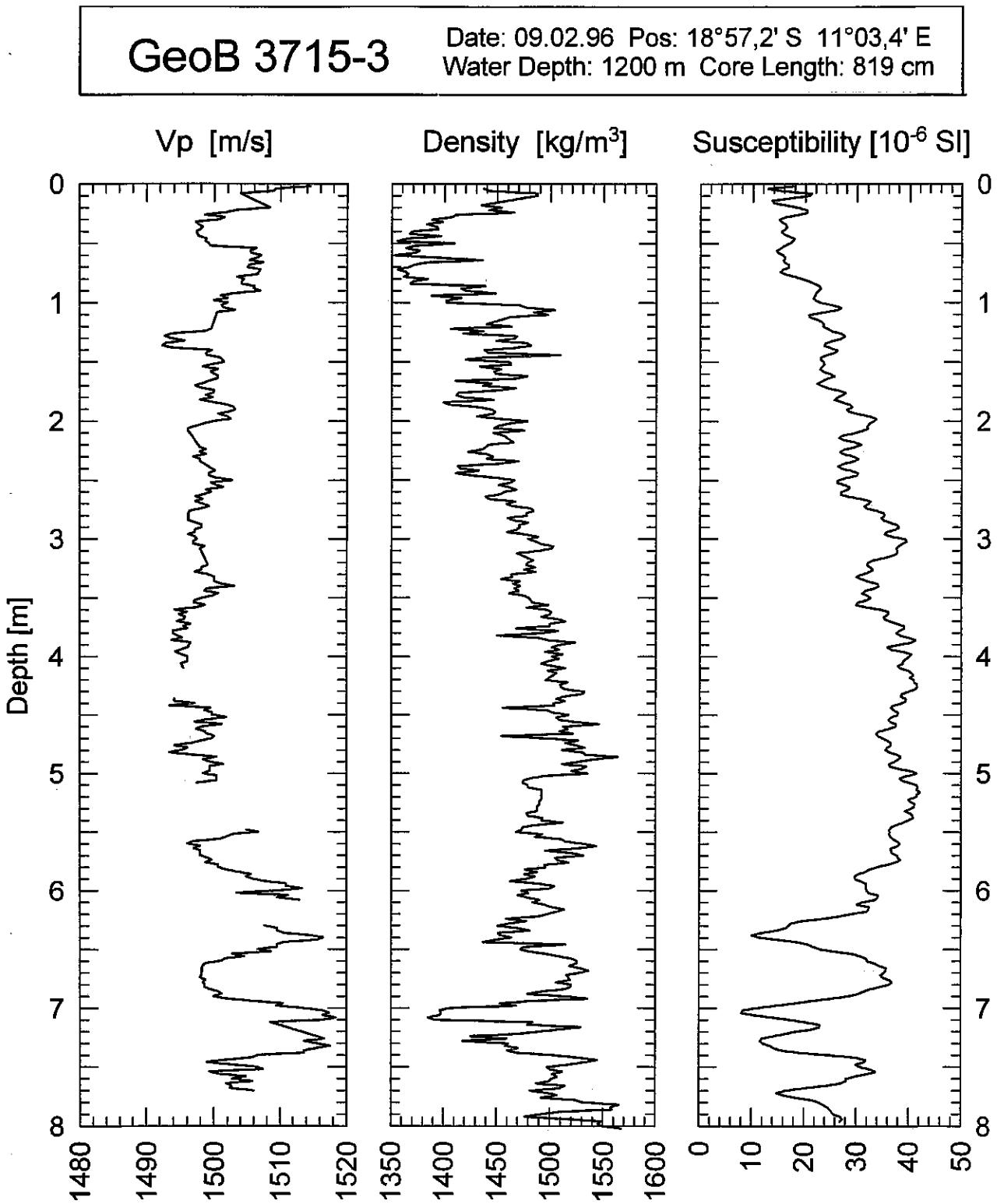

Fig. 91b: Core 3715-3: Physical properties data.

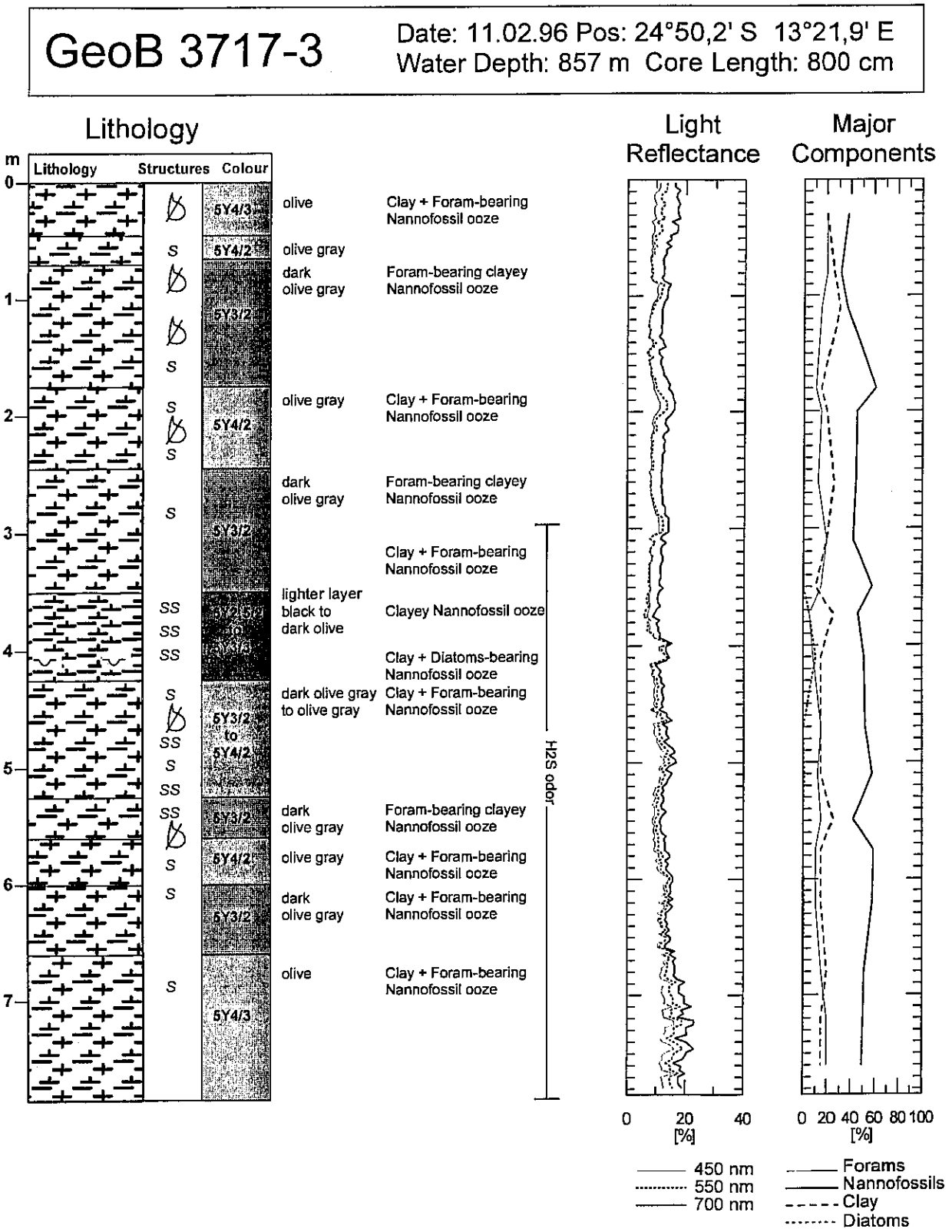

Fig. 92a: Core 3717-3: Core description.

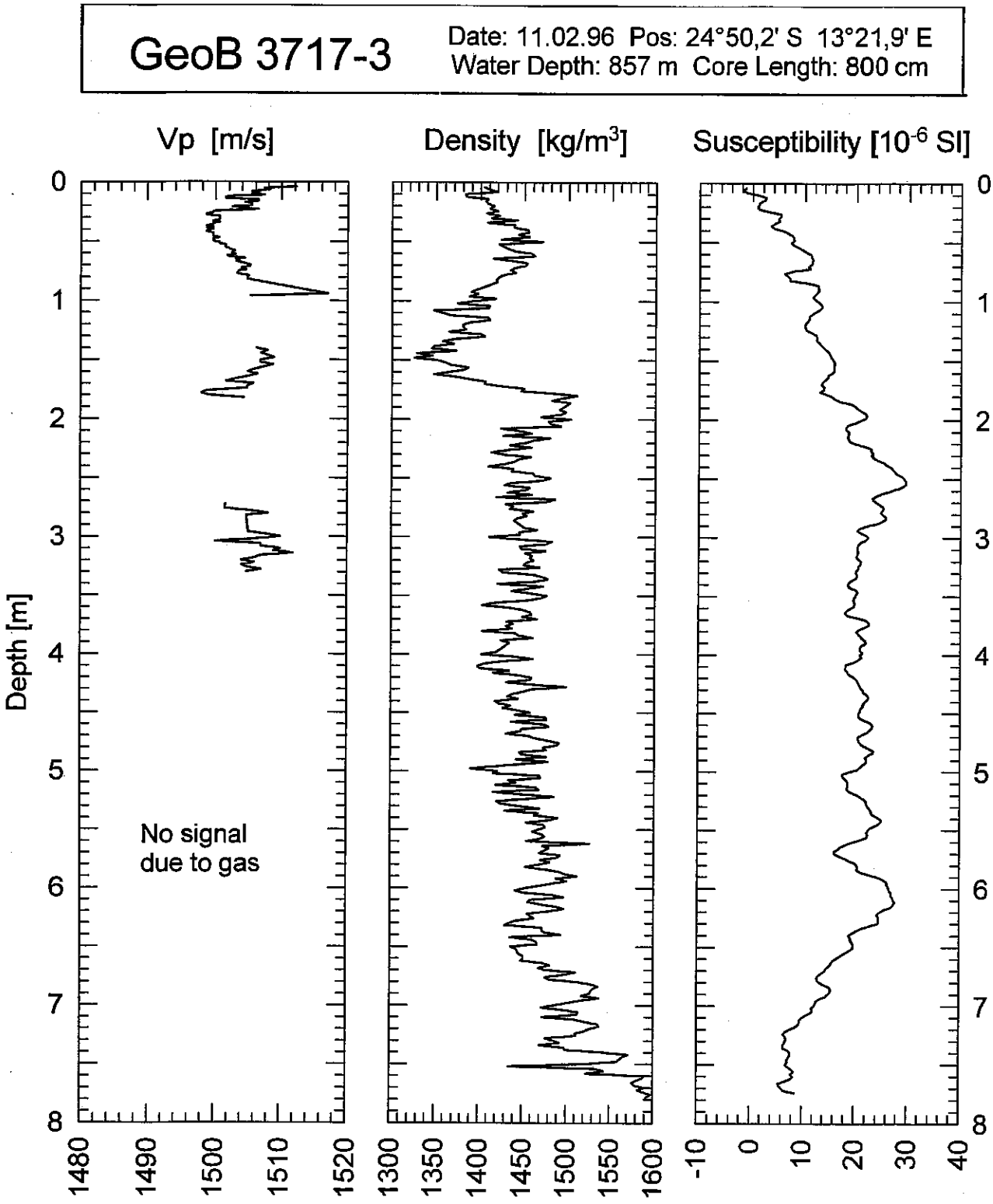

Fig. 92b: Core 3717-3: Physical properties data.

GeoB 3718-10

Date: 12.02.96 Pos: 24°53,7' S 13°09,7' E
Water Depth: 1350 m Core Length: 1374 cm

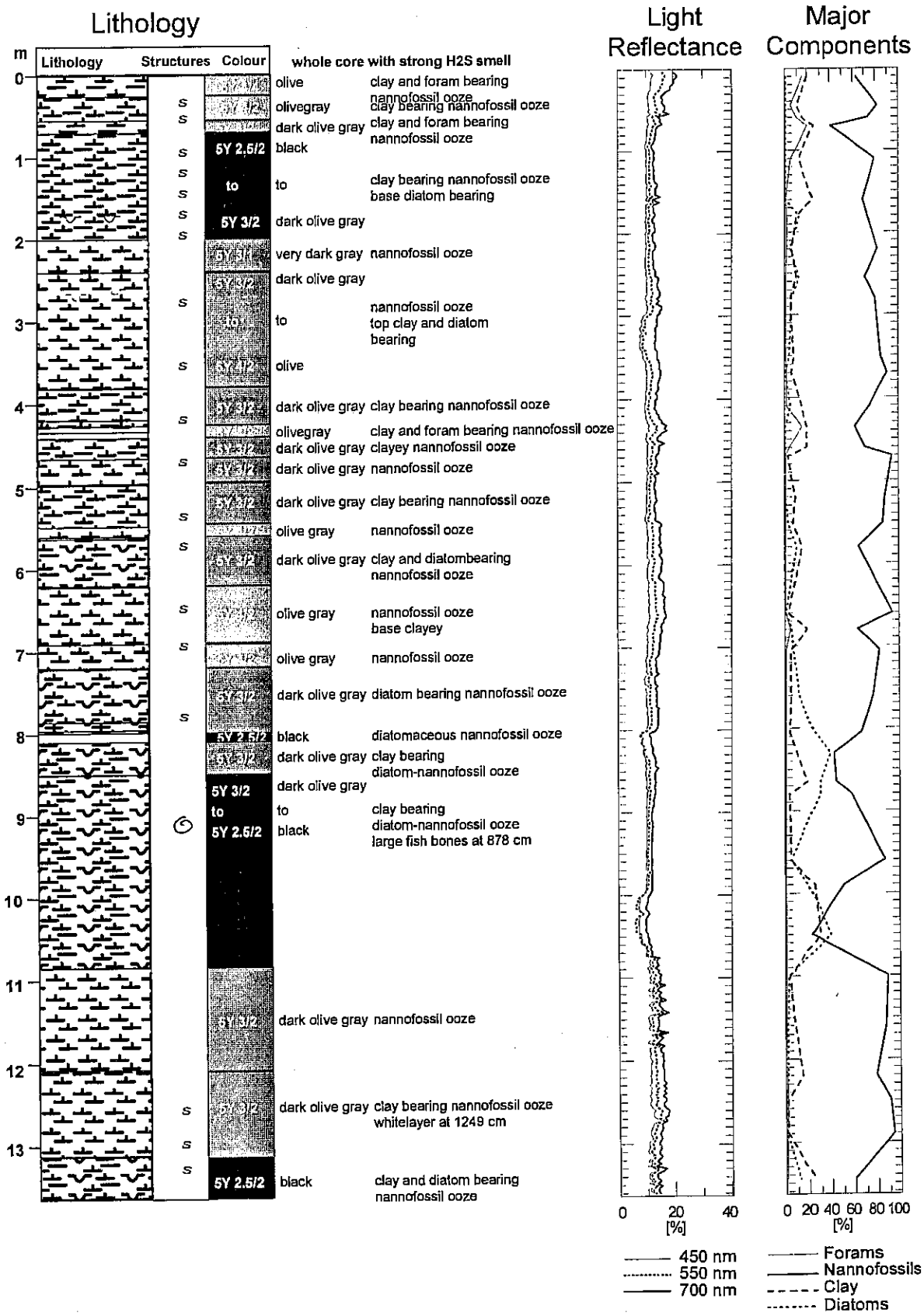

Fig. 93a: Core 3718-10: Core description.

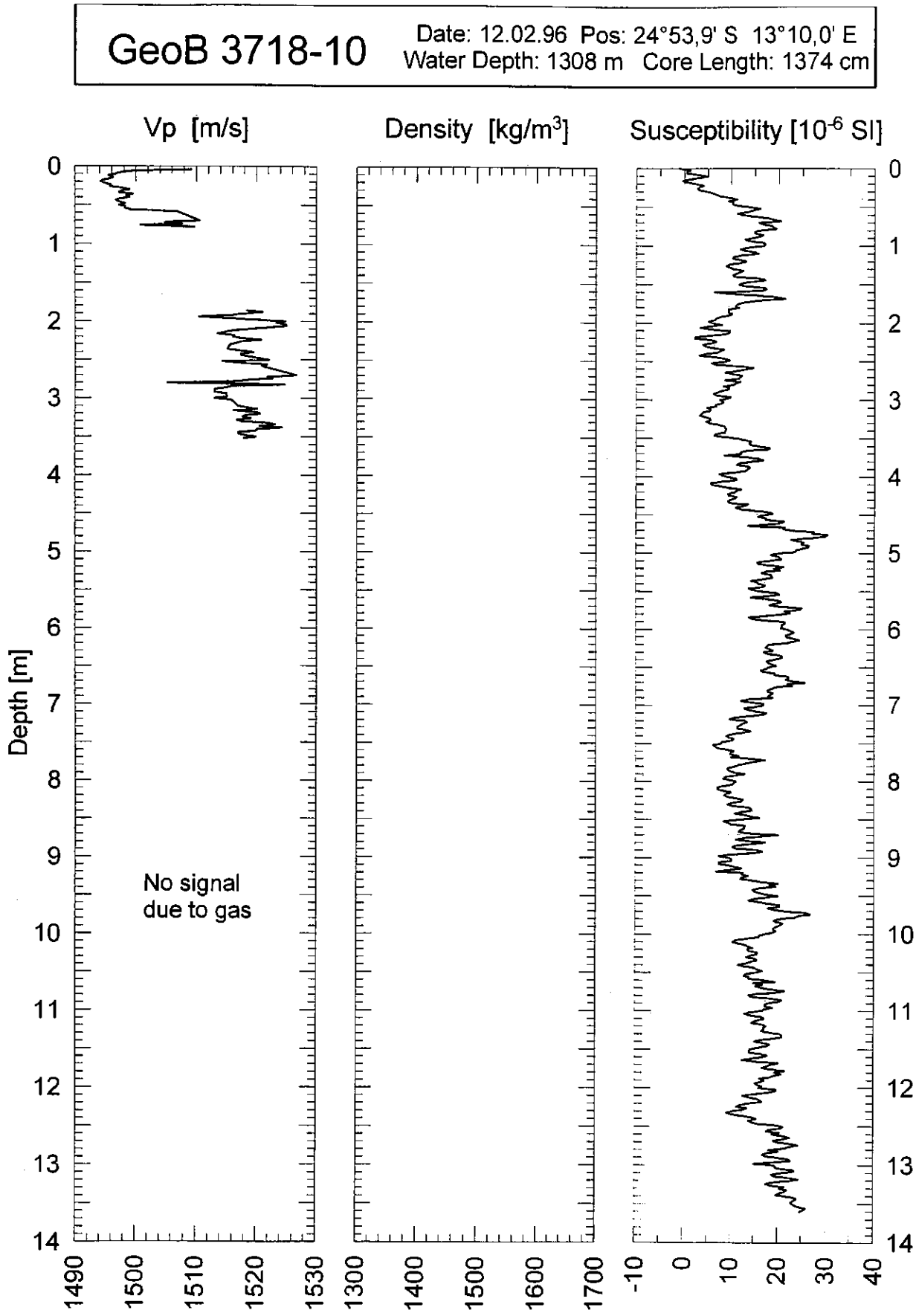

Fig. 93b: Core 3718-10: Physical properties data.

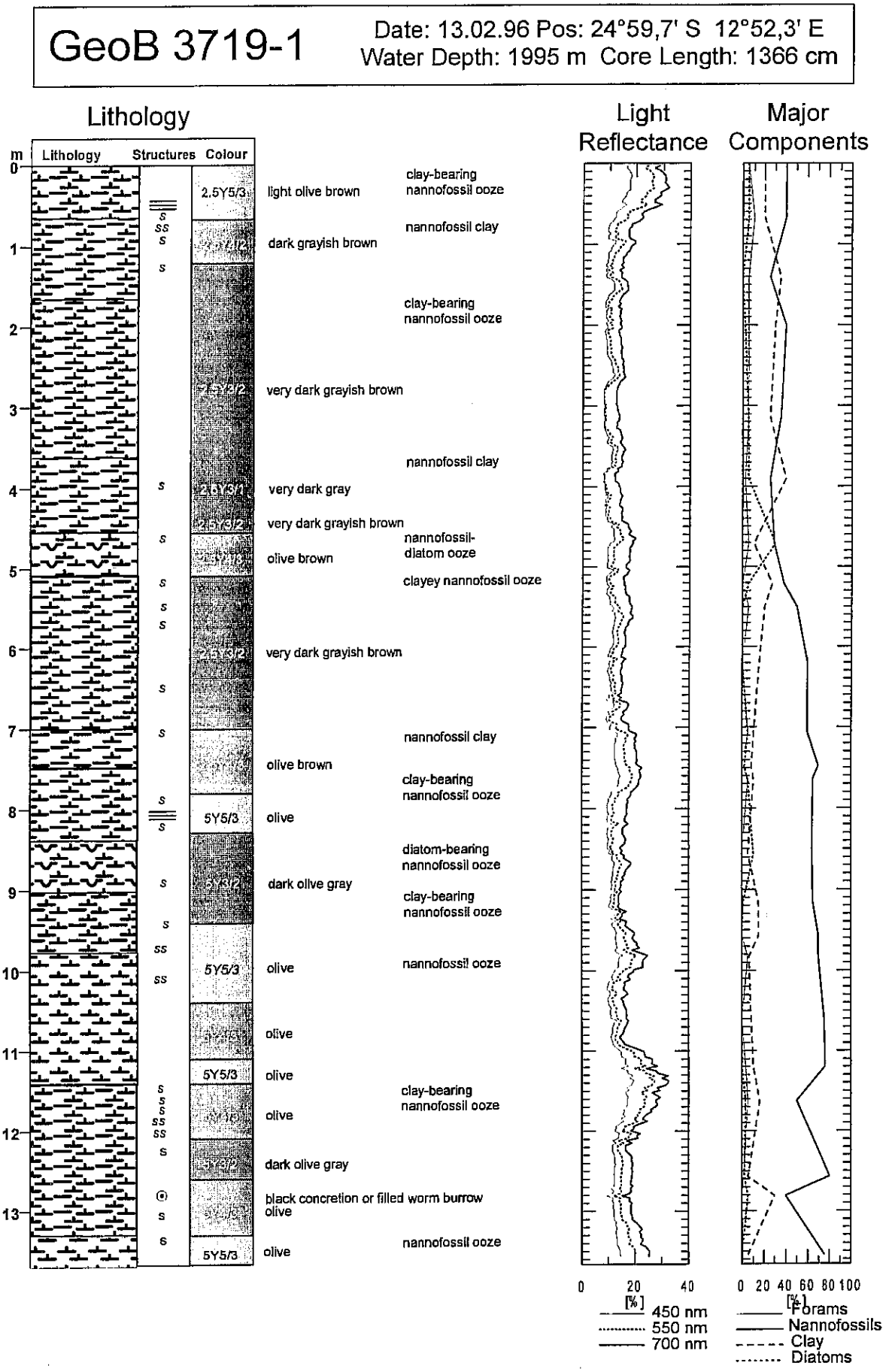

Fig. 94a: Core 3719-1: Core description.

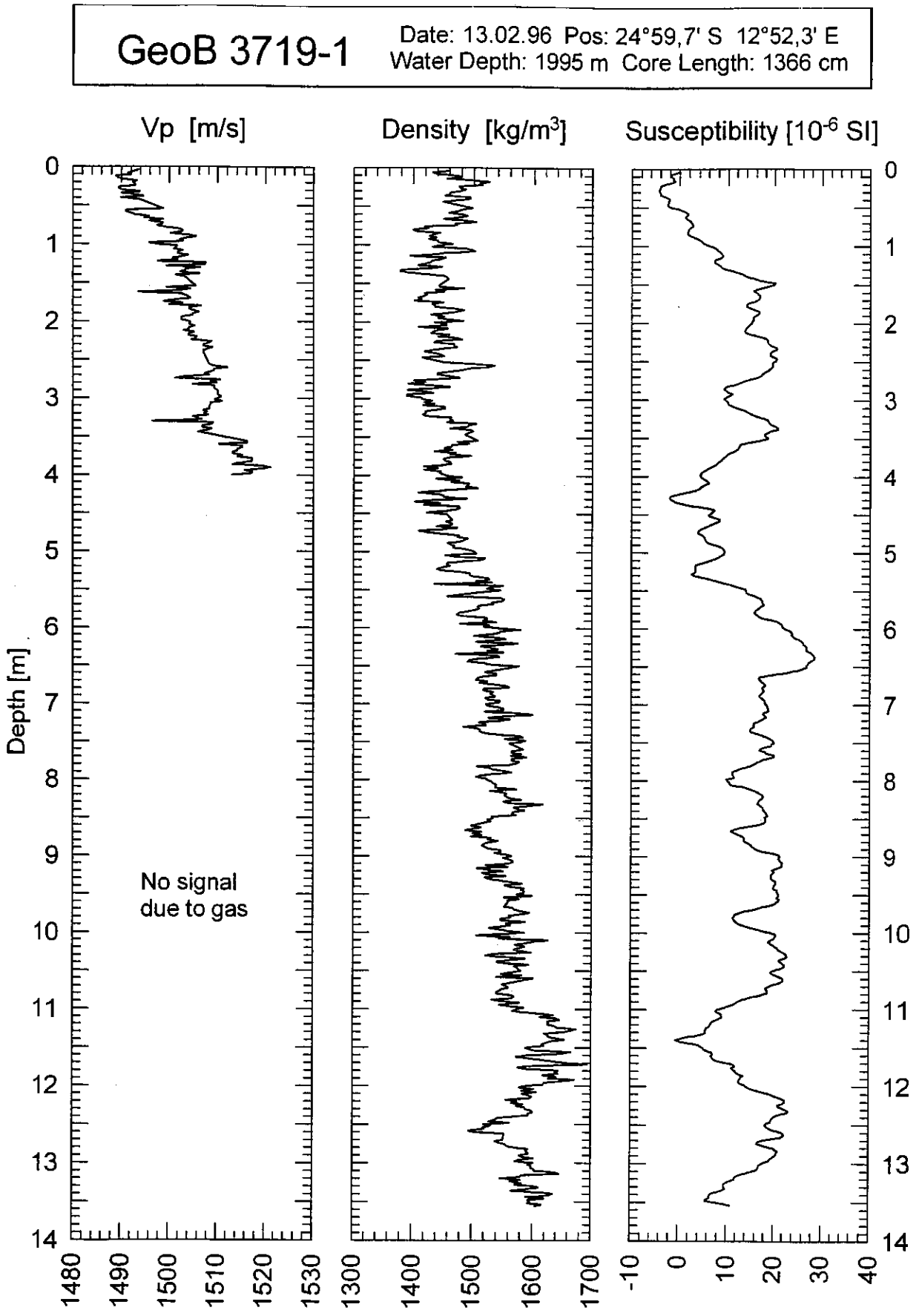

Fig. 94b: Core 3719-1: Physical properties data.

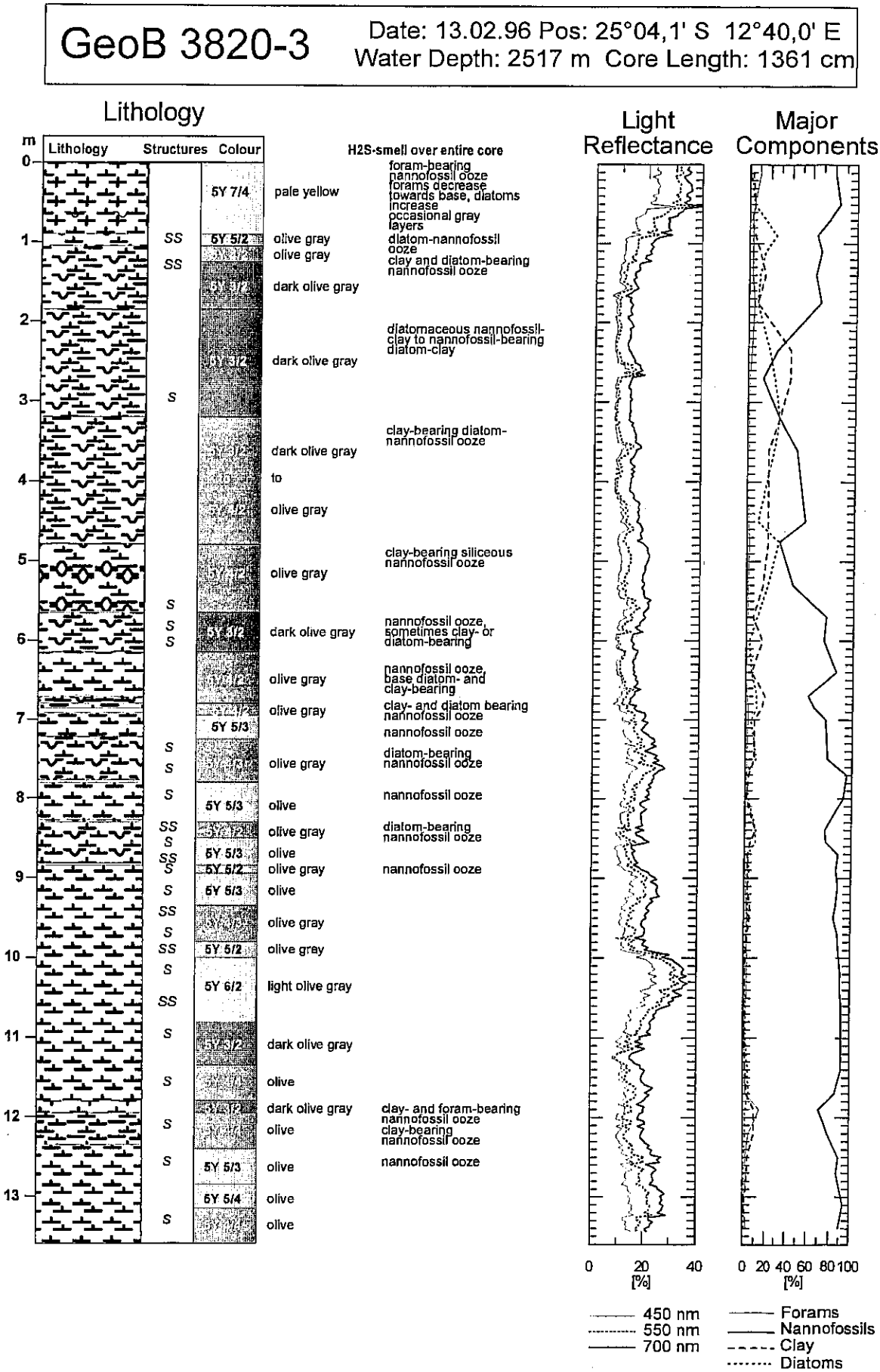

Fig. 95a: Core 3720-3: Core description.

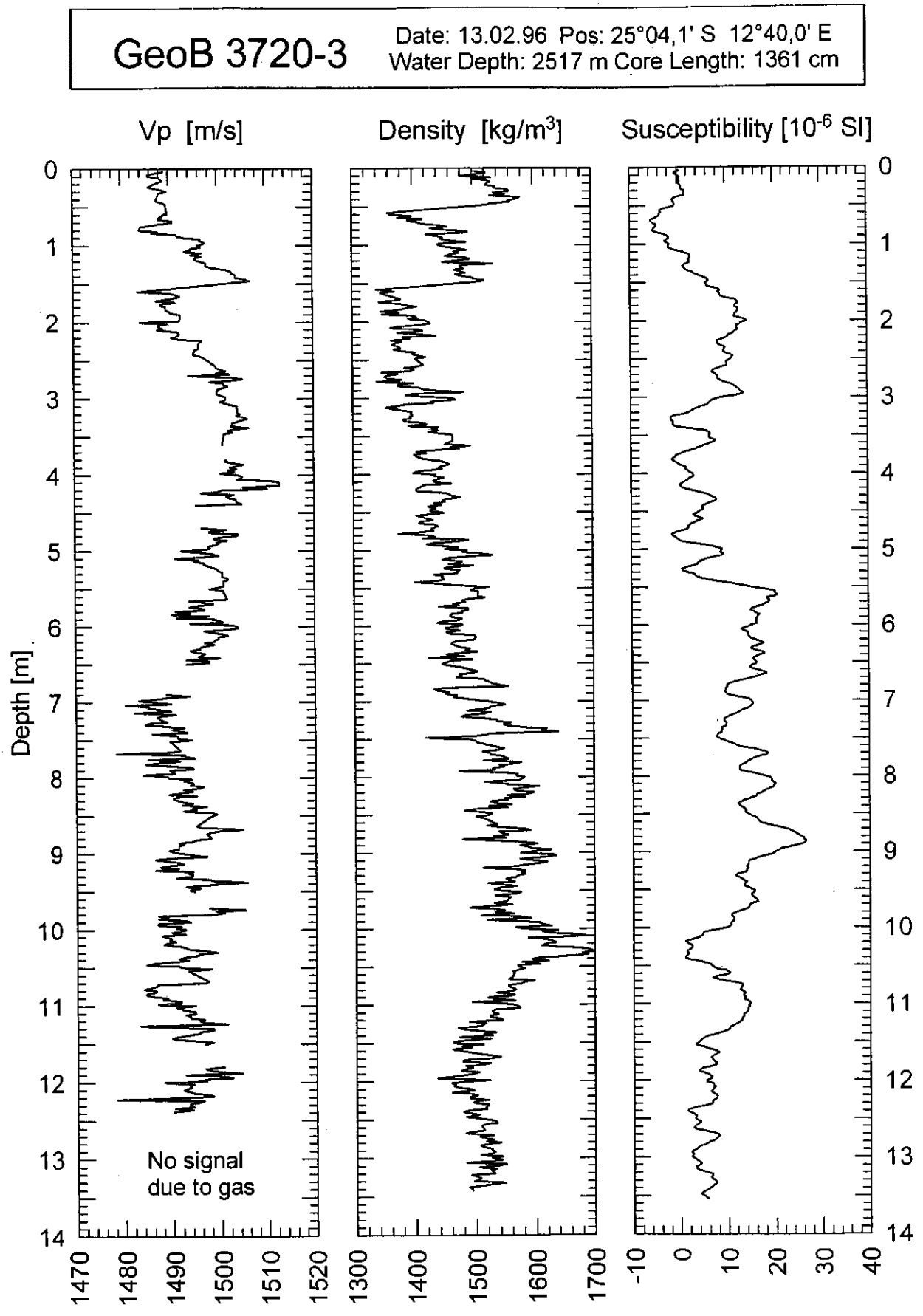

Fig. 95b: Core 3720-3: Physical properties data.

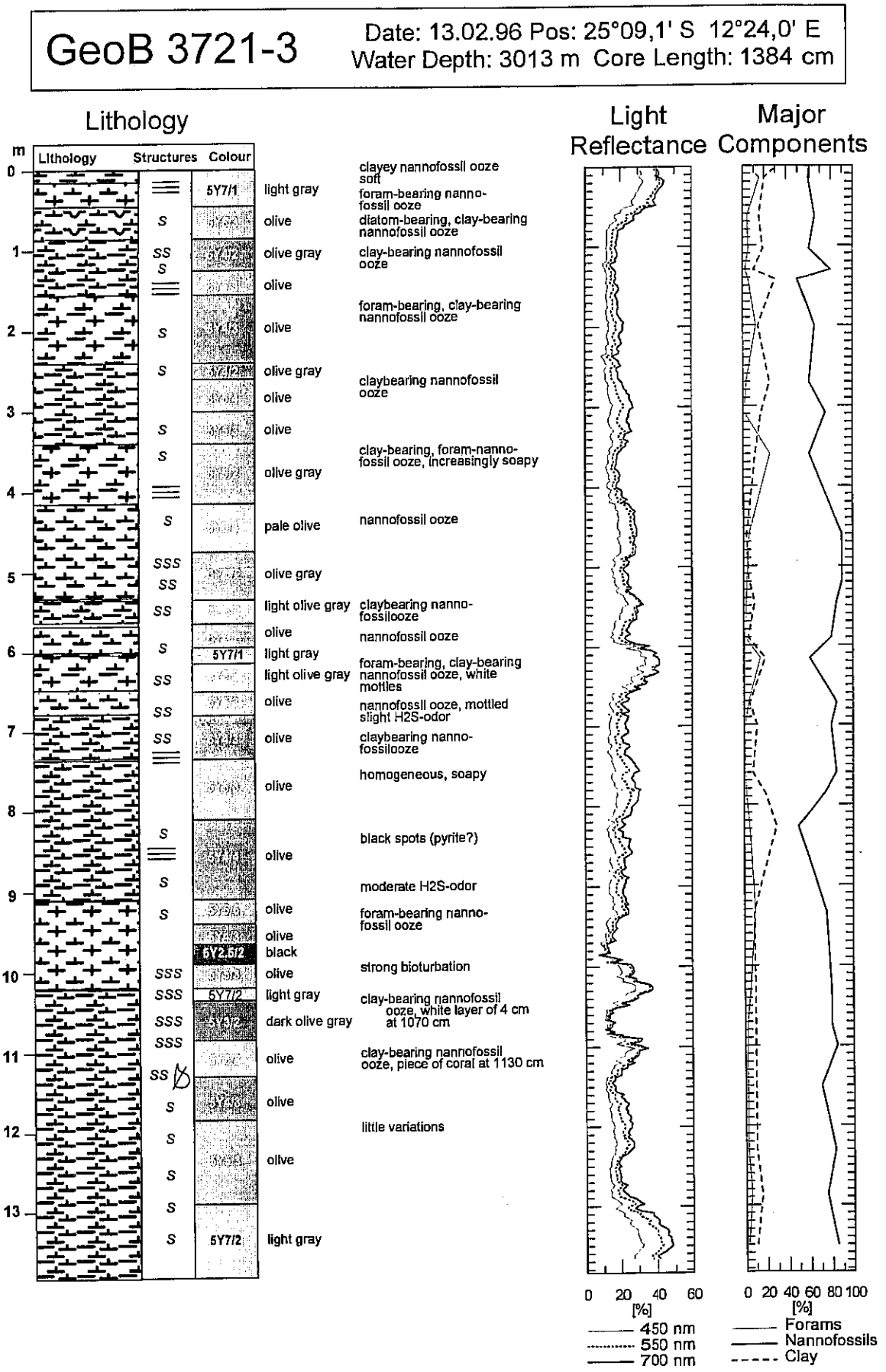

Fig. 96a: Core 3721-3: Core description.

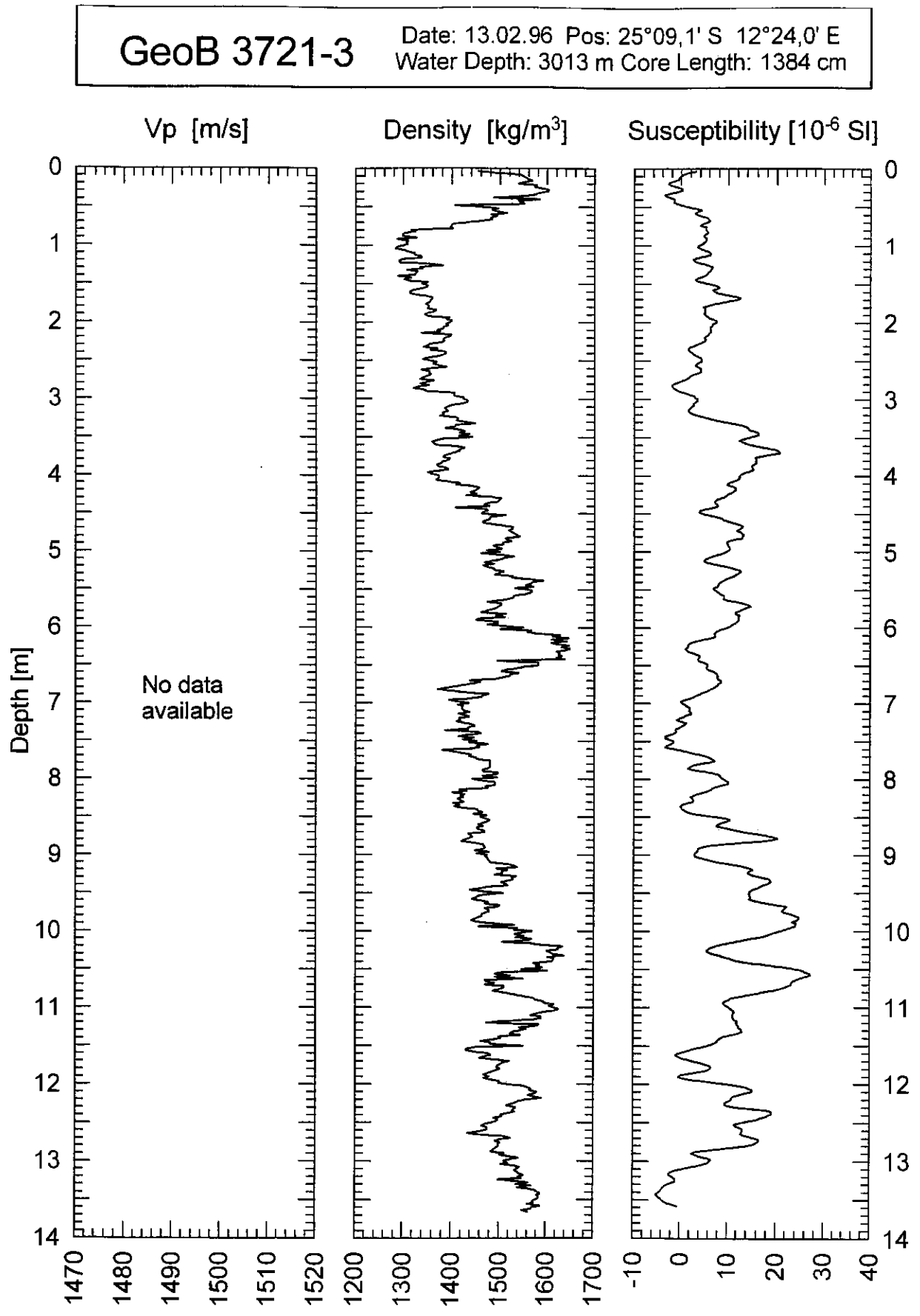

Fig. 96b: Core 3721-3: Physical properties data.

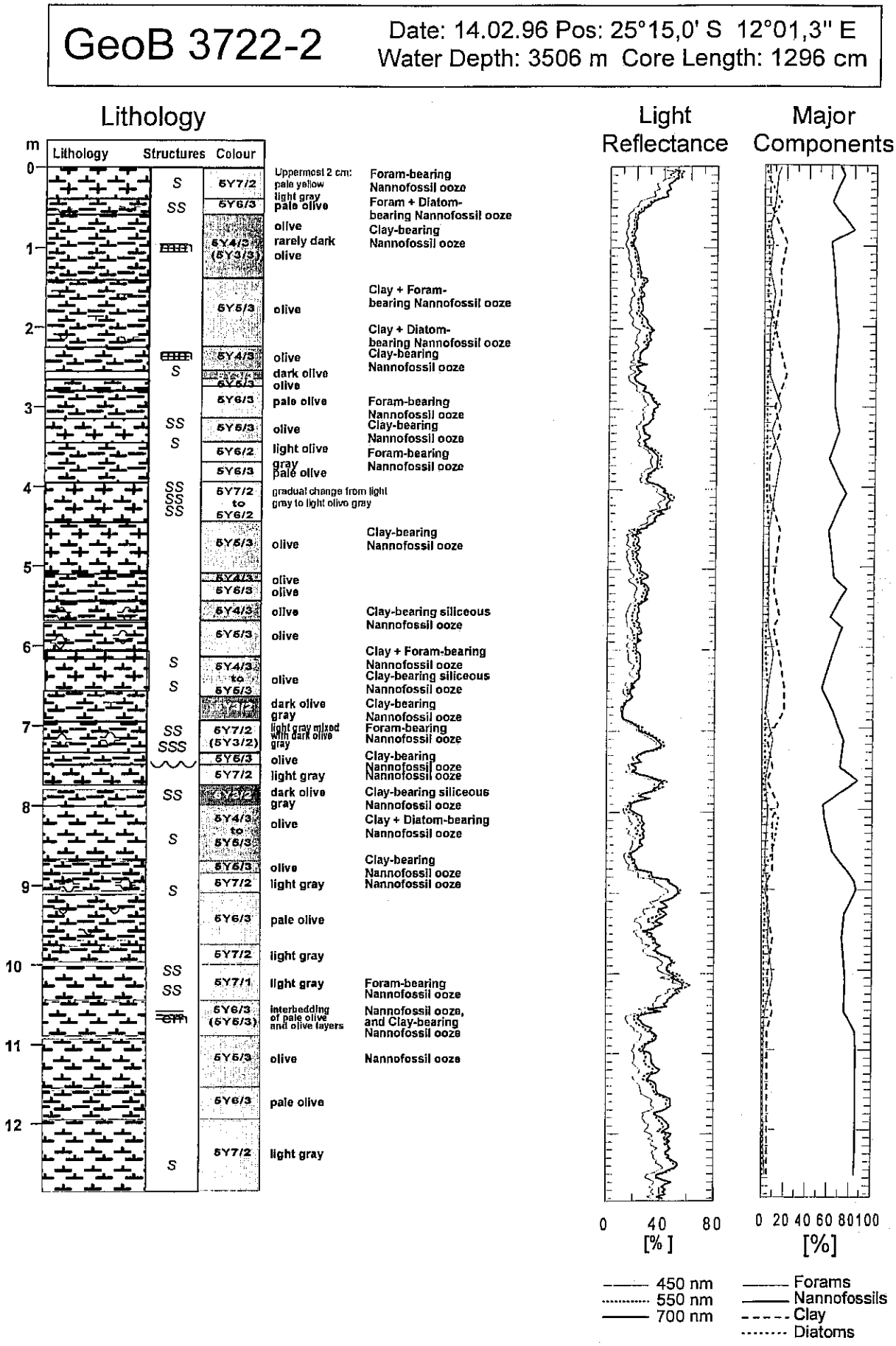

Fig. 97a: Core 3722-2: Core description.

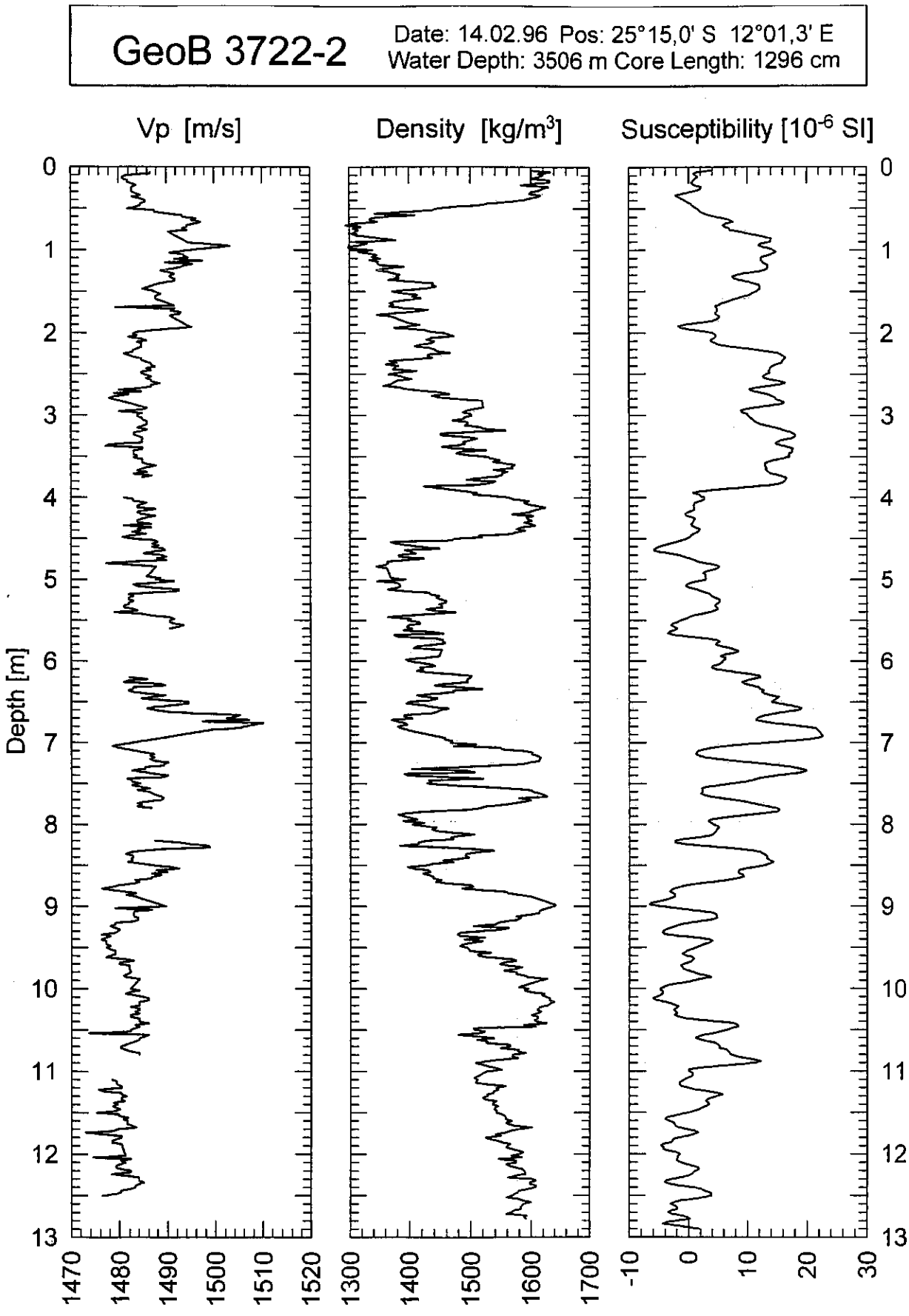

Fig. 97b: Core 3722-2: Physical properties data.

GeoB 3723-1

Date: 14.02.96 Pos: 25°23,6' S 11°31,6' E
Water Depth: 4003 m Core Length: 1253 cm

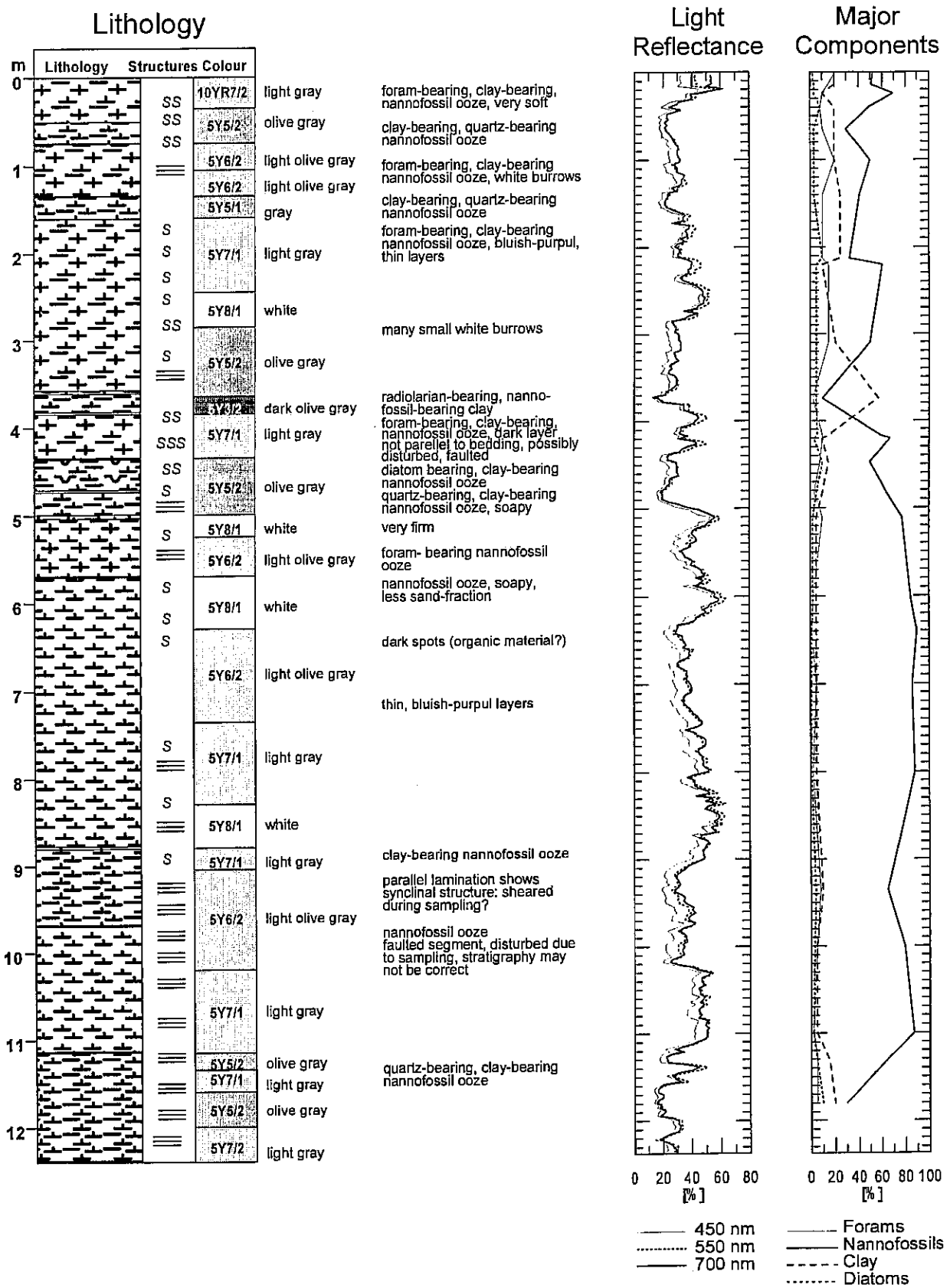

Fig. 98a: Core 3723-1: Core description.

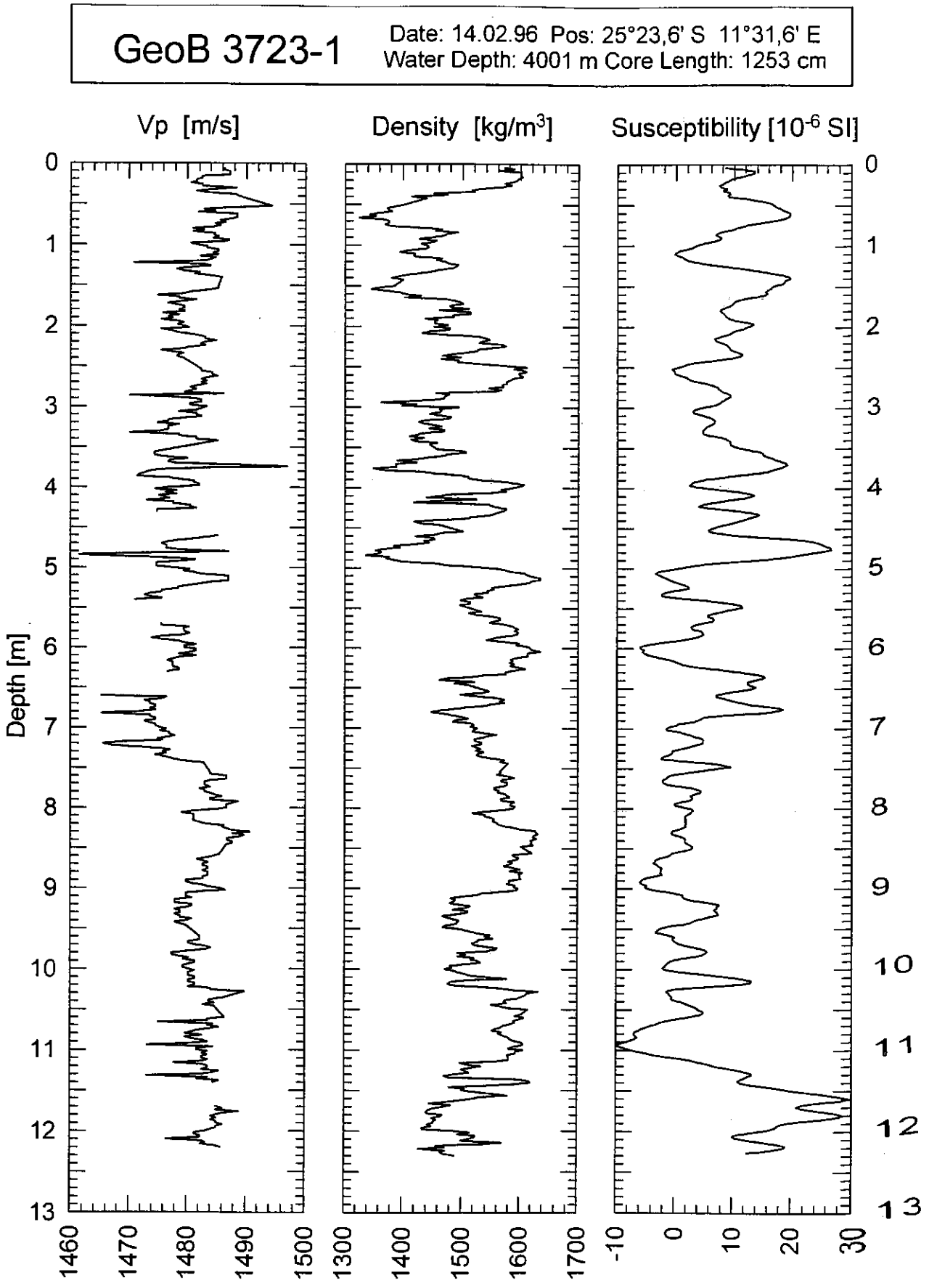

Fig. 98b: Core 3723-1: Physical properties data.

GeoB 3724-4

Date: 15.02.96 Pos: 26°08,2' S 8°55,6' E
Water Depth: 4763 m Core Length: 1123 cm

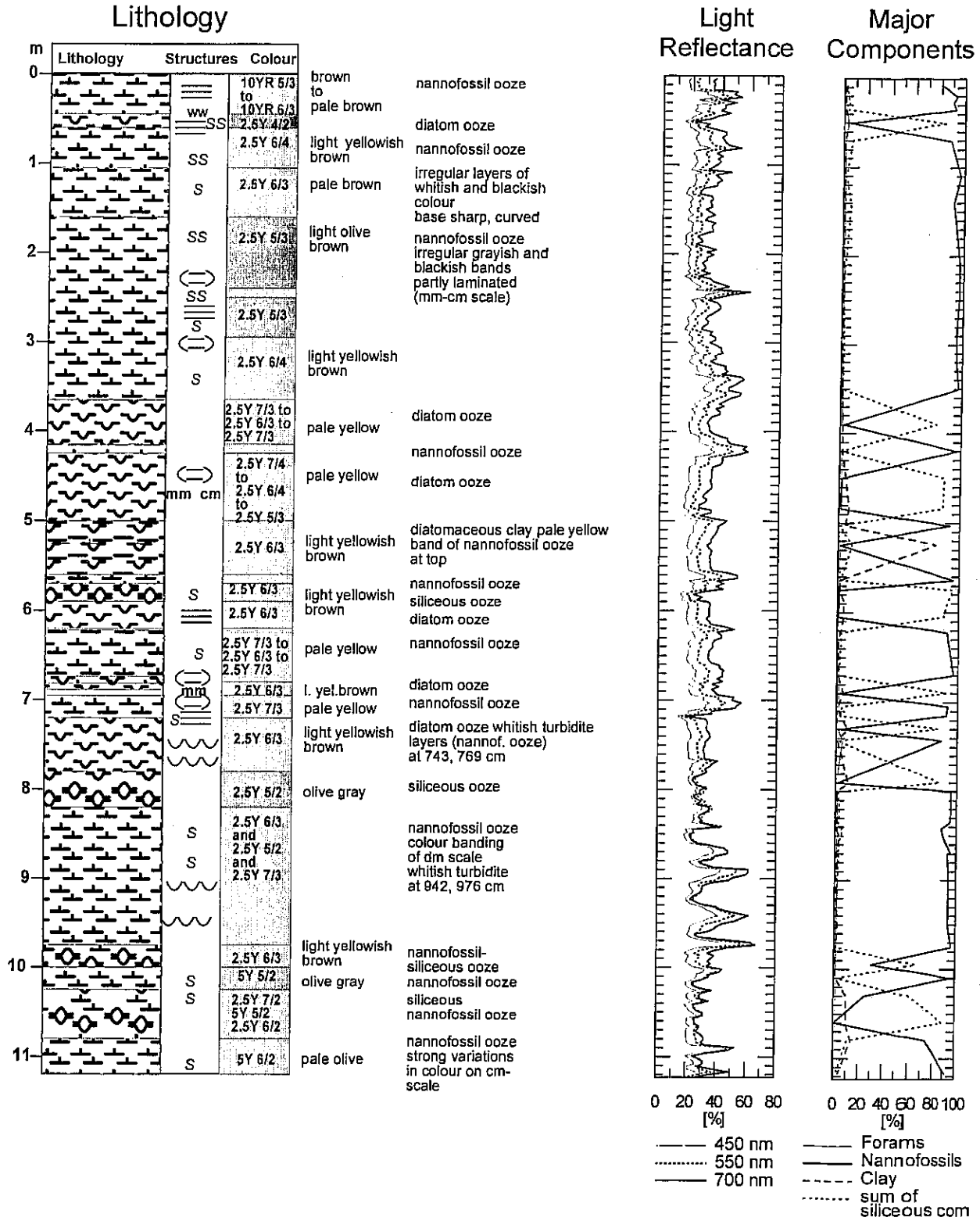

Fig. 99a: Core 3724-4: Core description.

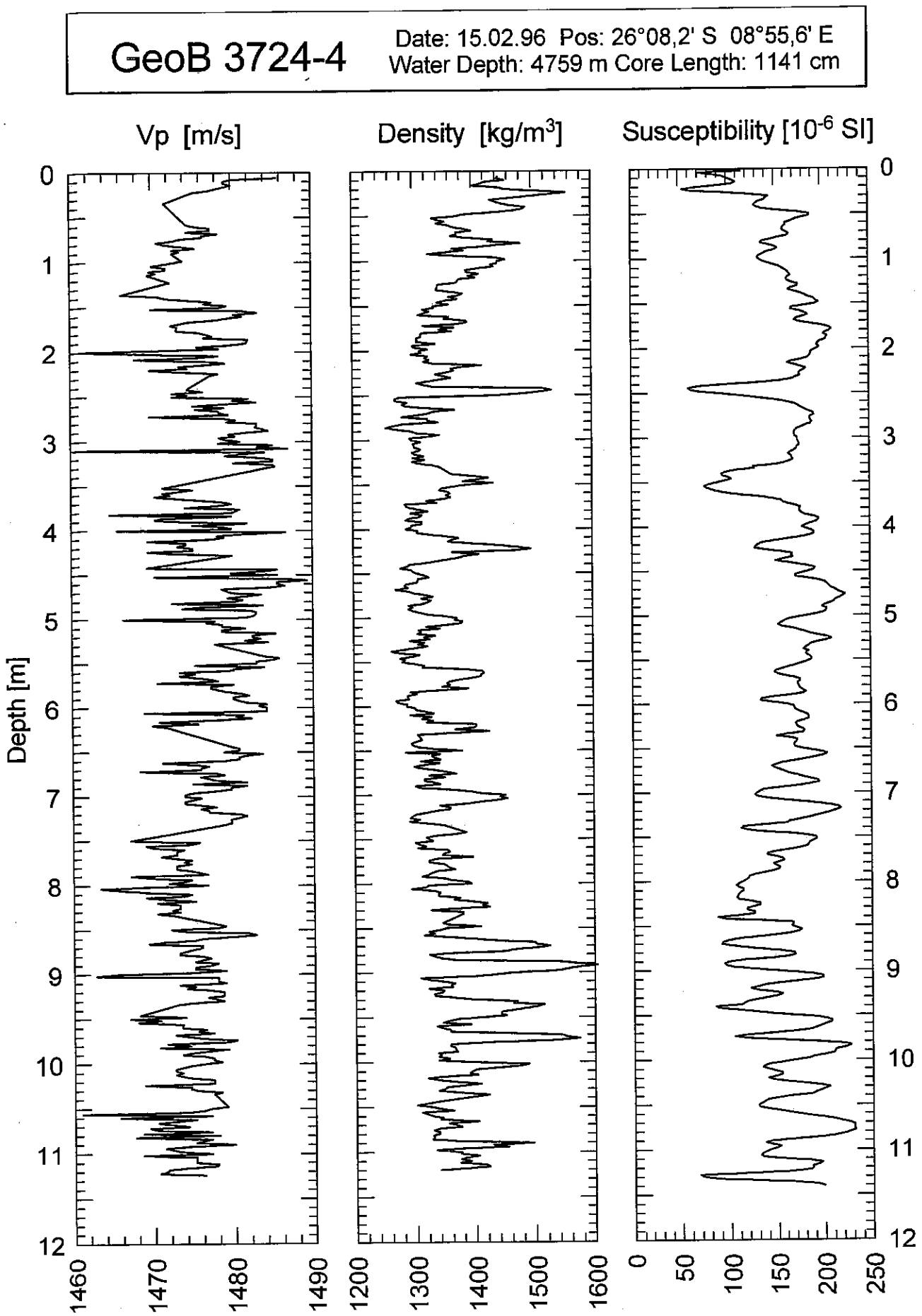

Fig. 99b: Core 3724-4: Physical properties data.

Core Descriptions

Core GeoB 3703-9 (position: 25°30,9'S/ 13°14,0'E, water depth: 1373 m, length 918 cm, Fig. 81a):

The top 330 cm of this core are composed of nannofossil ooze with abundant foraminifera in the top 50 cm. Further down core the clay content increases to become the dominant component towards the bottom end of the core. There are several incursions of diatoms at 75 to 104 cm and around 250 cm depth down core. From 330 cm to 395 cm the diatom content increases to form the dominant component of the sediment down to a depth of 430 cm and again around 483.5 cm, and from 546 to 720 cm. Below 330 cm diatoms are generally abundant. The colour of the core is various shades of olive and the strong odor of H_2S indicates a reducing environment.

Core GeoB 3706-2 (position: 22°43,0'S/12°36,0'E, water depth: 1315, length: 915 cm, Fig. 83a):

The dominant sedimentary component in this core is clay-bearing nannofossil ooze. Foram-bearing nannofossil ooze with high clay content can be found in two sections of this core: from top to 110 cm and from 680 cm to 720 cm. The clay content is low from 110 cm to 185 cm, from 345 to 380 cm and around 610 cm. The colour of the core is different shades of olive to dark olive gray. Bioturbation is visible in most parts of the core and mostly low to moderate. The sediment has a high content of H_2S, which indicates a reducing environment.

Core GeoB 3709-2 (position 21°29,0S/11°15,5'E, water depth: 2707 m, length 1355 cm, Fig. 86a):

This core is composed almost uniformly of nannofossil ooze. Forams are present as minor components in the top two metres, arond 500 cm and around 700 cm, diatoms are present as minor component around 280 cm, 460 cm, 800 to 840 cm, and around 1280 cm. Clay as a minor components can be found around 990 cm. The top half is pale to olive in colour, the bottom half olive to olive gray. The clay-bearing layer around 990 cm is dark olive in colour. Bioturbation is common throughout the core and is of light to moderate degree. Shell fragments are found at 570 cm and below 900 cm. H_2S is present from 450 cm down core.

Core GeoB 3711-3 (position: 19°50,1'S/10°46,1'E, water depth:1215, length: 1132 cm, Fig. 88a):

The dominant sedimentary component of this core is nannofossil ooze. Forams are the dominant component at the core top down to a depth of 55 cm. The now following section of the core is characterized by alternating layers of quartz-bearing, clay-bearing and foram-bearing nannofossil ooze. The clay content increases from 800 cm to 1010 cm until clay becomes the dominant component. Towards the end of the core sponge-spicule-bearing clay-bearing nannofossil ooze can be found, which is followed by diatomaceous nannofossil ooze. The colour of the core varies between olive, olive gray and dark olive gray. Bioturbation is moderate to strong, decreasing towards the bottom of the core. The last two metres of the core show some parallel bedding.

Core GeoB 3712-3 (position 17°11,1'S/11°07,6'E, water depth: 1248 m, length 577 cm, Fig. 89a):

The top 230 cm of the core are composed of quartz-bearing clay-bearing nannofossil ooze. Siliceous tests are present in minor amounts in the top 150 cm and shell fragments in the top 120 cm. The colour of this unit is dark olive gray to olive gray. The base of the top units rests on a scour surface. A more consolidated clay-bearing diatom-bearing nannofossil ooze is found from 230 to 285 cm. It contains mottles, indicating bioturbation, and layers of the overlying sediment. Its colour is olive green. The base of this unit again rests on a scour surface below which cobble to small-boulder-sized clasts of semi-consolidated clayey carbonaceous ooze are found in a carbonaceous ooze matrix. The colour of the clasts is olive green, the colour of the matrix olive gray. This unit again rests on a scour surface. The bottom of the core is composed of semi-consolidated clayey carbonaceous ooze. Its colour is olive green.

Core GeoB 3715-3 (position: 18°57,2'S/11°03,4'E, water depth: 1200 m, length 805 cm, Fig. 91a):

Most of the core consits of nannofossil ooze with accessory to minor amounts of clay. Diatoms increase in abundance below 520 cm and form a major proportion of the sediment around 620 cm and 720 cm. Millimetre-size shell fragments can befound throughout the core and sometimes are concentrated in single layers. A scour surface can be found below the first diatom-rich layer at 647 cm. All other contacts are gradational on a scale of centimetres to decimetres. The entire core is of dark olive gray and olive gray colour. Bioturbation is low, but might not be apparent due to the small variation in colour of the sediment. The material exudes an odor of H_2S.

Core GeoB 3717-3 (position 24°50.1'S 013°21.9'O, water depth: 861 m, length 800 cm, Fig. 92a):

The sediments of this core are composed of nannofossil ooze with minor to major amounts of clay. Minor amounts of forams can be found in most parts of the core except around 360 cm and 400 cm. The latter bears diatoms instead. The colour of the sediments is olive to dark olive gray. Shell fragments can be found in the top 200 cm and from 400 to 600 cm. Bioturbation is moderate from 350 to 550 cm and low in all other parts. H2S is present from 280 downward.

Core GeoB 3718-10 (position: 24°53,7'S/13°09,7'E, water depth: 1350 m, length 1363 cm, Fig. 93a):

Nannofossil ooze with minor to major amounts of clay comprises most of this core. Foraminifera can be found in the top five metres. Diatoms are present in most sections of the core and are most abundant between 700 and 1100, where they sometimes exceed nannofossiles in abundance. The colour of the core is mostly dark shades of olive to black. There is no apparent connection between colour and lithology. Bioturbation, where visible, is

low. Megafossile fish-remains were found at 878 cm. The high content of H_2S indicates a reducing environment.

Core GeoB 3719-1 (position: 24°59,7'S/12°52,3'E , water depth: 1995 m, length 1366 cm, Fig. 94a):

Most of core 3719-1 is composed of nannofossil ooze with a high clay content. Clay becomes the dominant component around 140 cm and 390 to 420 cm. Clay is only an accessory component below 945 cm. Diatoms are the dominant component from 470 to 510 cm. From 150 cm down to the bottom of the core the presence of H_2S indicates a reducing environment. The colour of the core is brown in the top 3 metres and changes through shades of brown and grey until it is of uniform olive colour from 700 cm to the bottom of the core. Bioturbation is most intense from 1110 cm to 1210 cm. At 1163 cm a brown concretion of 1.5 cm diameter was found and identified under the microscope as ikaite.

Core GeoB 3720-3 (position: 25°04,1'S/12°40,0'E, water depth: 2517 m, length 1361 cm, Fig. 95a):

The core consists of nannofossil ooze with minor to major amounts of clay and diatoms. The proportions of clay and diatoms are highest in the upper part of the core (above 580 cm) where they may become the dominant components. Forams are present in accessory amounts only with the exception of an unusual peak between 1180 and 190 cm, probably representing a bioturbated turbidite layer. The entire core is of olive to dark olive gray colour and exudes a strong odor of H_2S.

Core GeoB 3721-3 (position: 25°09,1'S/12°24,0'E , water depth: 3013 m, length: 1368 cm, Fig. 96a):

The entire core is composed of nannofossil ooze, mostly with clay or forams as minor components. Diatoms are present as a minor component between 45 and 85 cm. At 1130 cm a piece of a coral was found. A slight odor of H_2S can be noticed from the beginning of the bottom half, increasing down core. The colour of the core shows a distinct cyclic variation from light gray to various shades of olive. Bioturbation is moderate to strong and found throughout the core, obliterating most of the parallel lamination of the sediment.

Core GeoB 3722-2 (position 25°15.0'S/12°01.3'E, water depth: 3506 m, length 1283 cm, Fig. 97a):

Nannofossil ooze is the dominant sedimentary component of this core. Clay, diatoms and forams can be found in some sections in minor amounts but generally decreasing below 900 cm. The colour of the sediment is olive to pale olive with a few lighter sections, especially towards the bottom of the core. Millimetre-scale laminations can be seen around 100 cm and 230 cm, centimetre-scale laminations are present between 1050 and 1090 cm. A scour surface might be found at 751 cm. Bioturbation is apparent only in the lighter coloured sections. It is of moderate to strong degree.

Core GeoB 3723-1 (position: 25°23,6'S/11°31,6'E , water depth: 4003 m, length: 1237 cm, Fig. 98a).

Nannofossil ooze constitutes the dominant sedimentary component of this core. The top 3.5 metres of the core a characterized by a cyclic succession of foram-bearing clay-bearing nannofossil ooze and clay-bearing quartz-bearing nannofossil ooze. A layer of radiolaria-bearing nannofossil ooze can be found around 370 cm. Diatoms as a minor component can be found between 435 and 465 cm. Below 465 cm the core is again dominated by nannofossil ooze with clay, forams, and quartz as minor components. The colour of the core is characterized by a cyclic succession of lighter and darker shades of gray ranging from white to dark olive gray. The white layers are highly viscous. The upper part of the core is moderately bioturbated, decreasing down core. Parallel laminations becore more distinct towards the bottom of the core. Below 900 cm deformations due to sampling by the gravity corer can be seen. As a result parts of the stratigraphy might be missing.

Core GeoB 3724-4 (position: 26°08,2'S/08°55,6'E , water depth: 4763 m, length 1123 cm, Fig. 99a):

This core consists of nannofossil ooze and diatom or siliceous ooze with varying amounts of clay. In smear slides some samples look the same as nannofossil ooze under single-polarized light, but differ markedly when viewed under crossed polarizers. No or dull gray extinction colours occur. These sections are referred to as siliceous ooze.

Bioturbation is weak to medium and is present throughout the core. Colours range from light yellowish brown to olive gray. Weak bedding of mm- to cm-scale is visible by grayish bands, dominantly above 2.5 m. At 743, 769, 942 and 976 cm turbidites of a few cm thickness are intercalated. They consist of light gray nannofossil ooze.

Spectrophotometry

The light reflectance of all gravity cores was measured at 31 wavelength channels in the range of visible light (400 - 700 nm). This method is used to quantify the colour of the sediment.

A Minolta CM-2002™ hand-held spectrophotometer was used. The readings were taken immediately after splitting the core. The archive halves of the cores were scraped with a knife to expose a fresh, unsmeared surface for the measurements. The core was then covered with a transparent plastic film to protect the camera. Measurements were taken every 3 cm to resolve small scale color changes. Before measurements were taken, a white calibration of the spectrophotometer was perfomed using a white calibration cap. The calibration surface was covered with the same plastic film as the core to avoid any bias in the readings. The data were stored in the instrument and later transferred to a personal computer using the program "PROCOMM PLUS" ™. They were then further processed using the program COLREAD to be able to import them into a spreadsheet program.

The reflectance profiles at the three wavelengths (450 nm, 550 nm, 700 nm) are shown next to the core diagrams. These three wavelengths give a good overview of sediment colour spectrum, since they cover most of the spectrum measured. In addition they represent the colours blue, green and red, respectively.

In most cores a significant negative correlation with magnetic susceptibility can be seen, which can be explained by the dependence of both, high reflectance and low susceptibility on calcite concentration on the one hand and low reflectance and high susceptibility of ferro-manganese minerals on the other.

In addition, the calcite content is dependent on paleoceanographic conditions at the time of deposition so that colour reflectivity can often be used as a first stratigraphic proxy.

5.2.4 Physical Properties Studies

(T. von Dobeneck, C. Hilgenfeldt, H. Keil, B. Laser, A. Schmidt and F. Schmieder)

During METEOR cruise 34/2 the recovered gravity cores were subject to laboratory geophysical studies. A routine shipboard measurement of three physical parameters was carried out on the segmented sediment cores, comprising the determination of

- the compressional (P-) wave velocity v_p,
- the electric resistivity R_S, and
- the magnetic volume susceptibility κ.

These properties are closely related to the grain size, porosity and lithology of the sediments and provide high-resolution core logs (spacing 2 cm) available prior to all other detailed investigations. In addition, oriented samples for later shore based paleo- and rock magnetic studies were taken at intervals of 10 cm.

5.2.4.1 Physical Background and Experimental Techniques

The experimental set-up for the shipboard measurements was basically identical to that of previous cruises. Therefore, the descriptions given here are kept brief. For a more detailed treatment of the experimental procedures we refer to WEFER et al. (1991) for R_s and to SCHULZ et al. (1992) for v_p.

P-wave velocity

The P-wave velocity v_p was derived from digitally processed ultrasonic transmission seismograms, which were recorded perpendicular to the core axis with a fully automated logging system. First arrivals are picked using a cross-correlation algorithm based on the

'zero-offset' signal of the piezoelectric wheel probes. In combination with a measure of the core diameter d the travel time of the first arrivals t lead to a P-wave velocity profile with an accuracy of 1 to 2 m/s.

$$v_p = (d - d_L) / (t - t_L)$$

where d_L is the thickness of the liner walls and t_L the travel time through the liner walls.

Following SCHULTHEISS and MCPHAIL (1989), a temperature calibration of v_p is effected using the equation

$$v_{20} = v_T + 3 \cdot (20 - T)$$

where v_{20} is the P-wave velocity at 20°C and T the temperature (in °C) of the core segment when logged. Simultaneously, the maximum peak-to-peak amplitudes of the transmission seismograms are evaluated to estimate attenuation variations along the sediment core. P-wave profiles can be used for locating strong as well as fine-scale lithological changes, e.g. turbidite layers or gradual changes in the sand, silt or clay content.

Electric resistivity, porosity and density

The electric sediment resistivity R_s was determined using a handheld sensor with a miniaturized four-electrodes-in-line ('Wenner') configuration (electrode spacing: 4 mm). A rectangular alternating current signal is fed to the sediment about 1 cm below the split core surface by the two outer electrodes. Assuming a homogeneously conducting medium, the potential difference at the inner two electrodes is directly proportional to the sediment resistivity R_s. A newly integrated fast resistance thermometer simultaneously provides data for a temperature correction.

According to the empirical ARCHIE's equation, the ratio of sediment resistivity R_s and pore water resistivity R_w may be approximated by a power function of porosity ϕ

$$R_S/R_W = k \cdot \phi^{-m}$$

Following a recommendation by BOYCE (1968), suitable for seawater saturated, clay rich sediments, values of 1.30 and 1.45 were used for the constants k and m. The calculated porosity ϕ is subsequently converted to wet bulk density ρ_{wet} using the equation (BOYCE, 1976)

$$\rho_{wet} = d \cdot \rho_f + (1 - \phi) \cdot \rho_m$$

with a pore water density ρ_f of 1030 kg/m^3 and a matrix density ρ_m of 2670 kg/m^3. For the sake of an unbiased uniform treatment of all cores, these empirical coefficients were not adapted to individual sediment lithologies at this stage. Nevertheless, at least relative density changes should be well documented.

Magnetic volume susceptibility

The magnetic volume susceptibility κ is defined by the equations

$$B = \mu_0 \cdot \mu_r \cdot H = \mu_0 \cdot (1 + \kappa) \cdot H = \mu_0 \cdot H + \mu_0 \cdot \kappa \cdot H = B_0 + M$$

with the magnetic induction B, the absolute/relative permeability $\mu_{0/r}$, the magnetising field H, the magnetic volume susceptibility κ and the volume magnetisation M. As can be seen from the third term, κ is a dimensionless physical quantity. It describes the amount to which a material is magnetised by an external magnetic field.

For marine sediments the magnetic susceptibility may vary from an absolute minimum value of around $-15 \cdot 10^{-6}$ (diamagnetic minerals such as pure calcite or quartz) to a maximum of some $10.000 \cdot 10^{-6}$ for basaltic debris rich in (titano-) magnetite. In most cases κ is primarily determined by the concentration of ferrimagnetic minerals while paramagnetic minerals such as clays are of minor importance. High magnetic susceptibilities indicate a high lithogenic input/high iron (bio-) mineralisation or low carbonate/opal productivity and vice versa. This relation may serve for the mutual correlation of sedimentary sequences which were deposited under similar global or regional conditions.

The measuring equipment consists of a commercial Bartington M.S.2 susceptibility meter with a 125 mm loop sensor and a non-magnetic core conveyor system. Due to the sensor's size, its sensitive volume covers a core interval of about 8 cm. Consequently, sharp susceptibility changes in the sediment column will appear smoother in the κ core log and, e.g., thin layers such as ashes cannot appropriately be resolved by whole-core susceptibility measurement.

5.2.4.2 Shipboard Results

Sampling Sites and Recovery

The coring program of cruise 34/2 consisted of two perpendicular cross transects A and B. Profile A (GeoB 3701-3715) followed the 1300 m isobath of the Namibian continental margin from the Northern Cape Basin to the very Southern Angola Basin. With a latitudinal extension from 28° S to 15° S this line covered the biologically most productive areas of the Benguela Current coastal upwelling system. Coring stations were chosen approximately every 100 km at depths between 1200 m and 1500 m avoiding stretches marked by bottom current erosion. Deeper stations at 2000 m (GeoB 3714) and 2700 m (GeoB 3709) were cored for ODP presite survey. The cross profile B (GeoB 3717-3725) with stations at 850 m, 1300 m, 2000 m, 2500 m, 3000 m, 3500 m, 4000 m and 4700 m was started at 25° S at the shelf edge and terminated in the deepest part of the Northern Cape Basin.

Due to the generally very soft, clay-rich sediments the core recovery was exceptionally good with typical yields of 8 m to 14 m. A total of 21 sediment cores with a cumulative length of 238 m was investigated applying physical properties measurements (upper part of Fig. 99).

Initial Results

A compilation of the average physical properties of all cores is given in the lower part of Figure 100. The dots mark the median values of compressional wave velocity, density and magnetic susceptibility for each core, the vertical bars denote their standard deviations. Detailed core logs are shown in combination with core descriptions.

The measurement of p-wave velocity was frequently inhibited in lower core sections by heavy H_2S and CH_4 degassing linked to pressure release. Gas deposits between core and liner and small gas bubbles in the sediment matrix totally attenuate the high frequencies (100-400 kHz) of the ultrasonic wavelet. In the most affected cores meandering degassing vents of finger size, which lead from the gas-rich lower core parts all the way to the top led to many outliers and important data gaps even in the uppermost segments. This phenomenon is known, but not with such severity, from other anoxic environments. Due to these degassing vents it is doubtful that the attenuation measure can be used for core zonation. The generally very low average values of v_p between 1476 and 1512 m/s (except 1522 m/s for GeoB 3712-3) reflect high porosity (up to 80% mean) and clay content. A trend of lower velocities with greater depths is obvious (transect B). The variability of v_p along the isobath of transect A indicates, however, that additional factors apply.

The conductivity measurement was much less disturbed by degassing and provided complete density logs showing small, but significant lithological variations mainly in clay content. The rather high apparent data noise level is linked to intense bioturbation, which often gives the split cores a mottled appearance and allows for considerable lateral and vertical porosity variance at short scale. Some density logs show distinct paleoclimatic features, which may

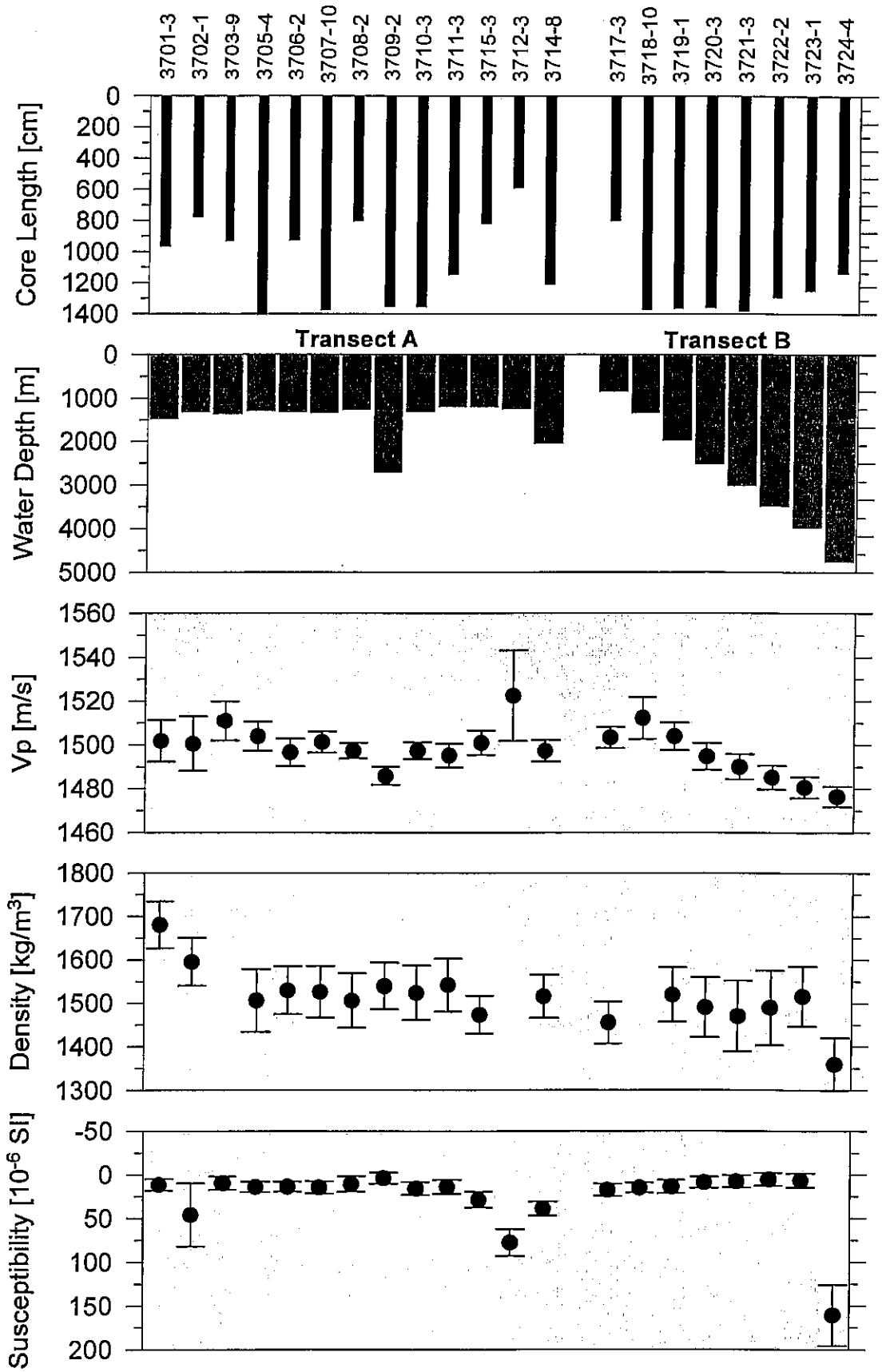

Fig. 100: Mean compressional wave velocity, density and magnetic susceptibility of gravity cores GeoB 3701-3 through 3724-4 as compared to variations in water depth at the sampling stations and core recovery. The vertical bars denote the standard deviations.

allow mutual core correlation. The average density values, which were calculated on the basis of porosity, vary little around 1500 kg/m^3 except for three cores (GeoB 3701-3, 3702-1 and 3724-4). This finding is in accordance with the observed extreme uniformity of sediment color and structure in most of the cores.

Magnetic measurements of anoxic sediment are generally involved with the problem of reduction and dissolution of common Fe^{3+}-bearing minerals (magnetite, maghemite, hematite). A low terrigenous input in this region and magnetic mineral diagenesis explain for the very low susceptibility values encountered at most stations. It is quite likely, that the total susceptibility ranging from slightly negative ($-10*10^{-6}$ SI) to low positive values ($40*10^{-6}$ SI) simply reflects the ratio of diamagnetic minerals (calcareous and siliceous fraction) to paramagnetic iron-rich clay and iron sulphides. If this assumption should be verified by shore-based hysteresis measurement, the paleomagnetic polarity information has probably not been preserved. But systematic variations of the susceptibility signal are apparent for most cores, which seem suitable to establish a relative core stratigraphy of both transects using several dated cores from this region, standard paleoclimate curves and dated susceptibility logs from adjoining regions (THIEßEN, 1993). It should be possible to define also a chrono stratigraphic setting for all cores of M34/2. A trend of decreasing susceptibility with depth is noticeable for transect B. Only the outermost core (3724-4) displays a much higher average susceptibility of $160*10^{-6}$ SI, which accounts for a differing sedimentation environment. The higher average value of GeoB 3702-1 is due to a sharp susceptibility peak, which corresponds to a broad dark layer at 500 cm depths - possibly a greigite (Fe_3S_4) precipitation horizon. The extremely high values at the core top of 3706-2 are due to coring contamination (barrel flexure). Core GeoB 3712-3 displays three (unexplained) susceptibility peaks in the top segment and an untypically high plateau value of $60\text{-}90*10^{-6}$ SI in the lower part. In order to suppress an experimentally induced high-frequency noise component a 5 point running average has been applied to all shown susceptibility logs.

5.2.5 Biogeochemical Studies

5.2.5.1 *In Situ* Oxygen Dynamics and pH-Profiles

(O. Holby and W. Rieß)

On this cruise we have deployed a free falling *in situ* chamber lander system (Elinor) and a free falling *in situ* oxygen and pH profiler (Profilur) at the stations listed below. Also indicated are laboratory studies that include incubations of, and oxygen profiles in sediment collected by a multicorer (Tab. 15).

Tab. 15:

Station	Elinor	Profilur	Laboratory
GeoB 3703	X	X	
GeoB 3705		X	
GeoB 3706		X	
GeoB 3707	X	X	
GeoB 3714	X		X
GeoB 3718	X	X	X
GeoB 3719		X	
GeoB 3721	X	X	X

Elinor

This pre-programmed free falling lander system is designed to incubate *in situ* a sediment surface of 900 cm^2 with preferably 10 to 15 cm overlying water. The water inside the chamber was stirred with eight revolutions per minute, which create a diffusive boundary layer of about 0.7 millimetre. Mineralisation processes were studied by measuring the total flux of oxygen from overlying water into the sediment, and fluxes of mineralisation products between the sediment and the overlying water. The flux of total oxygen was measured by two clarkstyle electrodes connected to the lid and through Winkler titration of withdrawn water samples. Samples for CO_2, Mn and nutrients were collected by a watersampling system, to be analysed back in Bremen, with the purpose to study the importance of different electron acceptors and the rate of mineralisation processes. Elinor also transport the incubated sediment up to the surface for further studies of biomass and different chemical parameters.

Profilur

This pre-programmed free falling lander system is designed to sample oxygen and pH profiles *in situ* with a depth resolution of 25 to 200 µm. The lander carries seven oxygen electrodes and three pH electrodes. The electrodes can penetrate the surface sediment upto about 10 to 15 centimetres depth. Through this system the oxygen penetration and the diffusive flux of oxygen can be determined. Different processes in the sediment might be followed through the pH profile. The system takes a watersample of five litres 50 cm above the sediment surface for calibration of the electrodes and chemical analysis of bottom water. A camera system is mounted for documentation and analysis of the sediment.

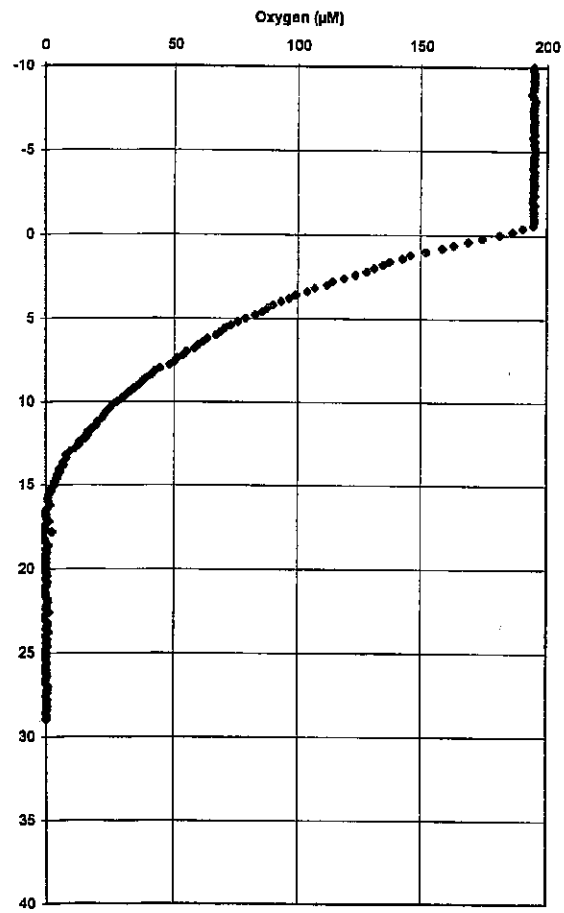

Both landers can be used to measure profiles of temperature, pressure, oxygen and pH (Profilur) in the water column, as they descend or/and ascend (Profilur). Uptake processes of oxygen can be studied by combining the results from the two landers. The landers give a good opportunity to study exchange rates in "undisturbed" sediments.

Fig. 101: Oxygen profile in the sediment at station GeoB 3706, measured by Profilur; depth scale in mm.

Laboratory

The *in situ* measurements were supported by measurement on sediment cores recovered by a multicorer, and incubated under near *in situ* conditions. Comparison between the data obtained by the landers and laboratory data gives information on the disturbance of sediment processes caused by bringing the sediment to the surface.

Preliminary Results

A typical oxygen profile in the sediment from station GeoB 3706, measured *in situ* by Profilur, is presented in Figure 100. According to this profile the diffusive transport of oxygen into the sediment is 2.7 mmol m^{-2} d^{-1} at station GeoB 3706. Preliminary values of diffusive transport of oxygen into the sediment obtained by Profilur during this cruise range from 1.5 to 4.1 mmol m^{-2} d^{-1}.

The oxygen concentration in the water column, measured during the ascent of Profilur, at station GeoB 3706 is presented in Figure 102. In this profile the surface water is

oversaturated with oxygen down to apprximately 30 m. There is an oxygen minimum around 400 m. To be mention is that our electrodes are sensitive to temperature changes, during this deployment they are calibrated for 3°C. This means, in the upper part of the water column, where the temperature is considereble higher the absolut value should be considered, thought the pattern/trend may be correct.

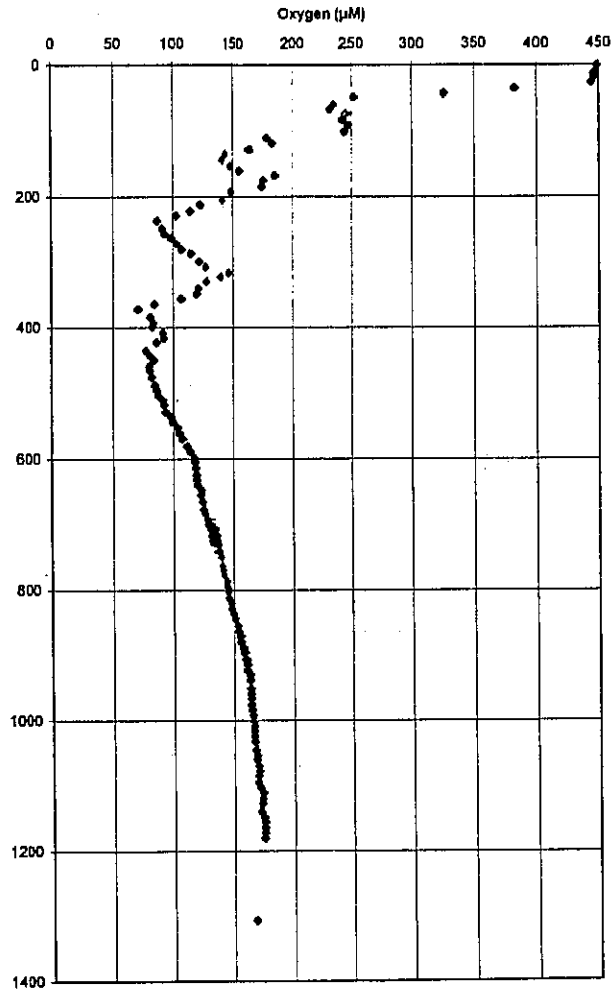

Fig. 102: Oxygen profile in the water column at station GeoB 3706, measured by Profilur; depth scale in m.

5.2.5.2 Pore Water Chemistry

(K. Enneking, C. Hensen, S. Hinrichs, C. Niewöhner, S. Siemer, E. Steinmetz)

Main research interests of the marine geochemistry group are the investigation of early diagenetic mineralization processes through determination and quantitification of diffusive pore water fluxes. On this cruise we focused on near surface as well as on anoxic mineralization processes: Near surface oxic processes were mainly characterized by measuring diffusive oxygen uptake and release of nutrients into the bottom water. These investigations were supplemented by other working groups with in situ measurements of oxygen and pH (O. Holby and W. Rieß, chapter 5.2.5.1) and incubation experiments for the quantification of single redox reactions within the upper 10 centimeters of the sediment (J. Kostka, chapter 5.2.5.3). Investigations of deeper anoxic processes were mainly based on determinations of methane, hydrogen sulfide, and sulphate in gravity cores. Additionally, detailed studies of sulphate reduction rates were carried out by T. Ferdelman and H. Fossing (chapter 5.2.5.4). To get more information about the organisms responsible for the redox

reactions and their metabolism the same gravity cores were sampled after pore water analyses by M. Benz and B.Schink (chapter 5.2.5.6).

Experimental Methods

To prevent a warming of the sediments on board all cores were immediately placed in a cooling room after recovery and maintained at a temperature of 4°-6° C.

Multicorer tubes taken for oxygen microelectrode measurements were kept in a cooling box at in situ temperatures. Overstanding bottom water was sampled and filtered for subsequent analyses. Additionally, two Winkler bottles were filled to determine bottom water oxygen concentrations. Oxygen depth profiles were recorded within an hour after recovery. A second multicorer-core was processed immediately after recovery. Therefore, the remaining bottom water was carefully removed with help of a siphon to avoid destruction of the sediment surface. During the subsequent cutting of the core into slices for pressure filtration, pH and Eh measurements were performed with a minimum depth resolution of 0.5 cm. Conductivity and temperature were measured subsequently on the parallel core to calculate sediment density and porosity.

The gravity cores were first cut into segments of 1 m length. Immediately after storing in the cooling laboratory 2·4 cm rectangles were sawed into the PVC liner for taking syringe samples for methane and H_2S analysis in order to prevent too much loss of both gases. Samples were taken every 20 to 25 cm according to sampling intervals for pore water gaining. 5 ml sediment samples were injected into 50 ml septum vials containing 20 ml of a concentrated (1.2M) NaCl-solution for methane determination. $HgCl_2$ was added to the solution to prevent any subsequent organic activity producing further amounts of methane. After closing the vial tightly and shaking methane in the sample becomes enriched in the headspace of the bottle. For H_2S determination 2.5 ml sediment samples were added to 5 ml SAOB buffer solution in small cintillation-bottles and shaked well. SAOB prevents degassing of H_2S, precipitation of metal sulfides and oxidation of S^{2-} ions in solution.

Within a few days after recovery the gravity cores were cut lengthwise and processed. On the working halves pH and Eh were determined and sediment samples were taken for pressure filtration. Conductivity and temperature were measured in the archive halves. Samples for sequential extractions of the solid phase were kept in gas-tight glas bottles under anoxic atmosphere. The storage temperature for all sediments was -20° C to avoid dissimilatory oxidation.

All work done on opened cores was carried out in a glove box under argon atmosphere. For pressure filtration Teflon- and PE-squeezers were used. The squeezers were operated with argon at a pressure gradually increasing up to 5 bar. Depending on the porosity and compressibility of the sediments, up to 20 ml of pore water were received from each sample. The pore water was retrieved through 0.2 µm cellulose acetate membrane filters.

Pore water analysis of the following parameters were carried out during this cruise:

O_2, NO_3^-, NH_4^+, PO_4^{3-}, alkalinity, Fe^{2+}, H_2S, SO_4^{2-}, Cl^-, CH_4, F^-, Eh, pH, and conductivity (porosity).

Bottom water oxygen concentration was determined by Winkler titration. Oxygen, pH, Eh, conductivity, and temperature of the sediment was determined with electrodes before the sediment structure was disturbed by sampling for pressure filtration. Nitrate, ammonium and phosphate were measured photometrically with help of an autoanalyser using standard methods. Alkalinity was calculated from a volumetric analysis by tritration of 1-1.5 ml sample with 0.01-0.1 m HCl. For the analysis of iron concentrations subsamples of 1 ml were taken within the glove box and immediately complexed with 10 µl of Ferrozin and determined photometrically afterwards. Subsamples for sulphate and chloride determinations were diluted (1:20) and analysed by ion chromatography (HPLC). Fluoride was determined by an ion-sensitive electrode. The sediment-SAOB mixture was diluted with 5ml of dest. water and the sulfide(=H_2S) concentration was determined potentiometrically. For detection of methane 25µl of the headspace gas was injected into a gas-chromatograph. For both, H_2S and methane determination methods the concentrations have to be related to the sediment porosity. Since corrected porosity data were presently not available we assumed a uniform porosity of 0.6 in all gravity cores for calculation of the concentrations. These concentrations will be recalculated subsequently at Bremen University.

The remaining pore water samples were acidified with HNO_3^-(suprapure) down to a pH value of 2 for storing and subsequent determination of cations by ICP-AES and AAS. All pore water samples will be maintained at 4°C until further treatment in Bremen.

Shipboard Results

Geochemical analyses were carried out along two transects at altogether 21 locations off Namibia and Angola. At all locations bottom water oxygen concentrations and oxygen-microprofiles in the sediment were measured. At 14 locations pore water of surface sediments recovered by multicorer was analysed. Additionally, 4 gravity cores were recovered and sampled for pore water and subsequent sediment analysis.

Surface Mineralization Processes

All locations on Transect A were chosen between 1200-1300 m water depth (except GeoB 3704, 3709, 3714) to be able to compare differences in mineralization activities along the continental slope from south to north. Since mineralization processes depend on the supply of degradable organic matter from the water column conclusions to variations in surface productivity could be drawn from those results. Oxygen penetration depths revealed from microprofiles (Fig. 103) and oxygen bottom water concentrations along Transect A (GeoB 3701-3715) are shown in Figure 103a/b. Bottom water oxygen concentrations are stable around 200 µmol/l between GeoB 3701-3709 and decrease to values around 150 µmol/l at the northern locations. Deepest oxygen penetration into the sediment was measured at GeoB

3701, which is probably situatedout of the central upwelling area, and at GeoB 3704, 3709 at water depths of about 2000 m. Highest microbial activity in the Northern Cape and Southern Angola Basin with oxygen penetration depths of 10 mm and below could be detected between

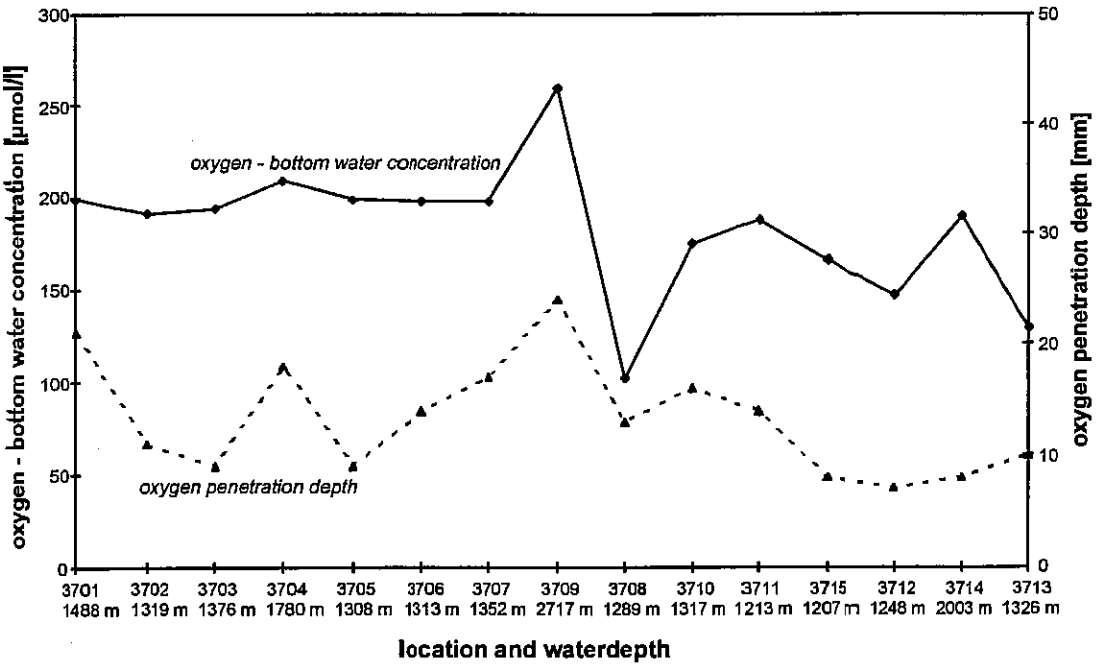

Fig. 103: Oxygen bottom water concentrations and oxygen penetration depth on Transect A.

GeoB 3703-3705 and GeoB 3712-3715. Inbetween oxygen penetration is around 15 mm, which probably reflects inhomogeneities in primary production of the upwelling area as mentioned above.

Transect B started at a water depth of 850m (GeoB 3717) and lead down the continental slope into the basin to a water depth of 4800m (GeoB 3724). Oxygen penetration depths increased with increasing water depth (Fig. 104) At GeoB 3723 and 3724 the penetration depth is more than 4 cm (data not shown), but the depth of zero concentration could not be determined.

Nitrate production by oxygen respiration and nitrate penetration depth are the next sensitive indicators for the intensity of near surface dissimilation processes. Nitrate concentration profiles of all multicorers sampled are displayed in Figure 105a/b. The amount of nitrate production is well recorded by the high peaks within the uppermost 0.5cm of the sediment at nearly all locations. Most of the nitrate is released into bottom water or used up by denitrifying bacteria at depths of 2.5-5 cm with exception of GeoB 3724, where nitrate is not consumed within the sampled sediment depth. However, the pattern of mineralization activity as gained by oxygen profiles is not clearly reflected by the depth of maximum nitrate

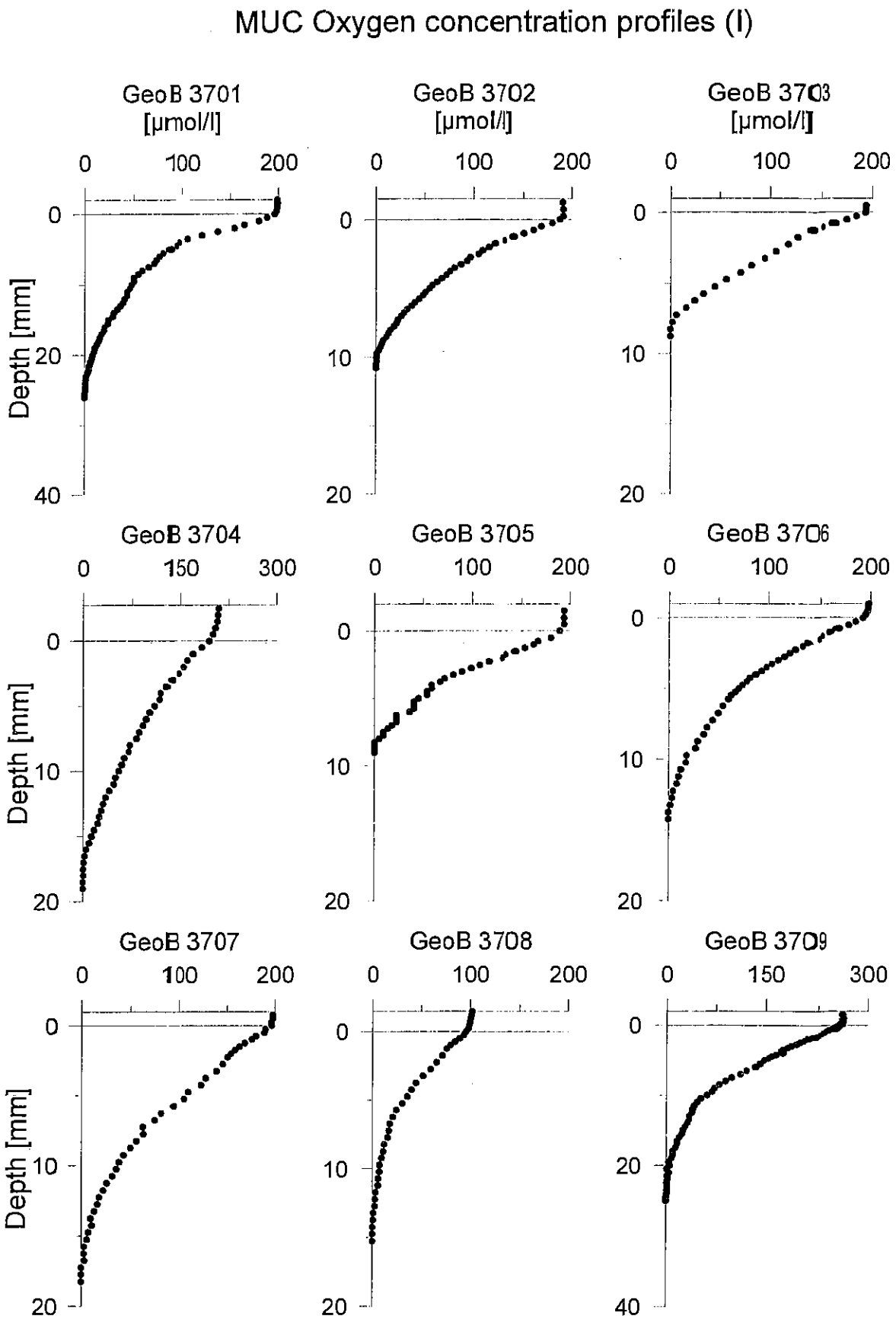

Fig. 104a: Oxygen concentration profiles (Tansect A and B).

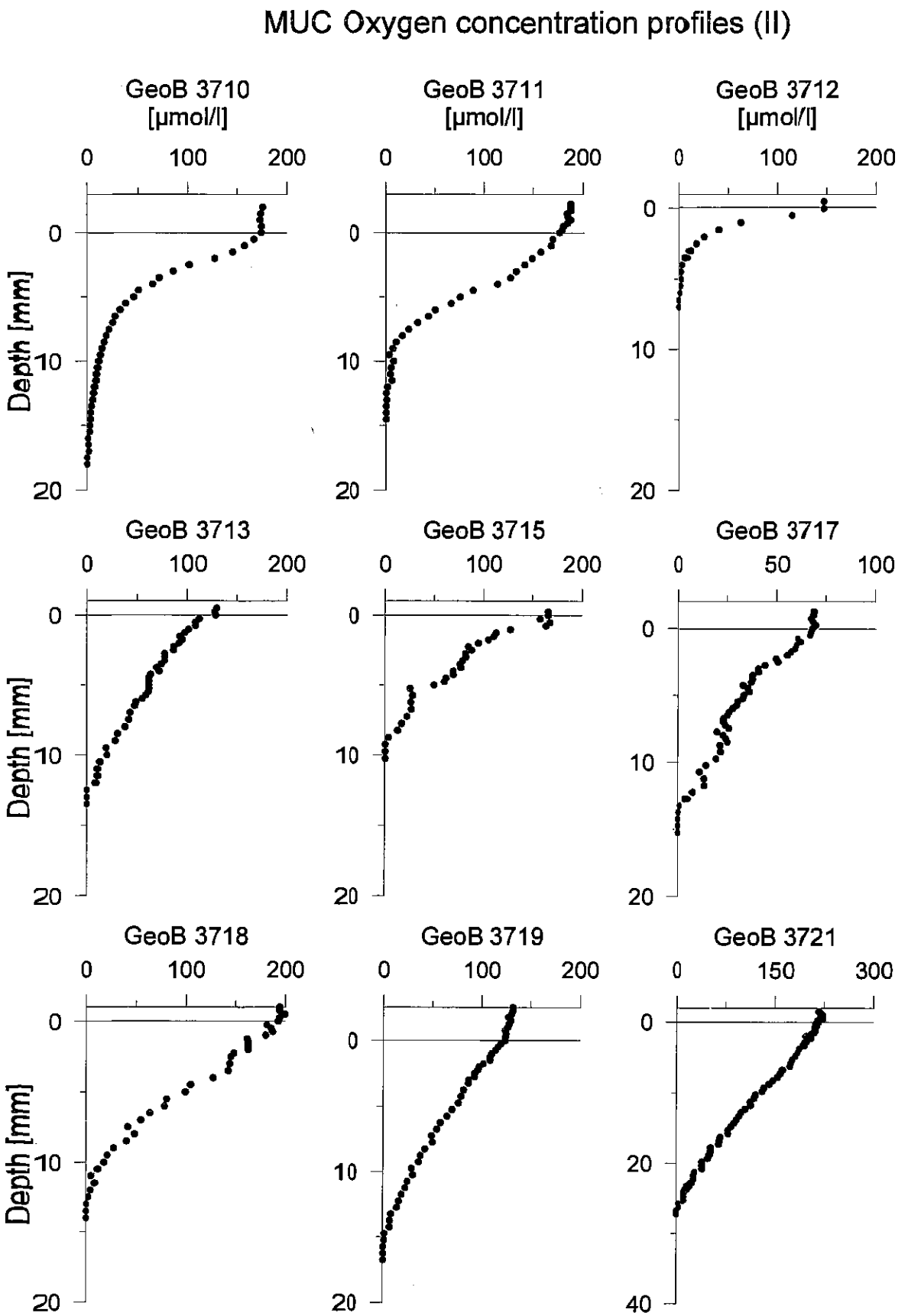

Fig. 104b: Oxygen concentration profiles (Tansect A and B).

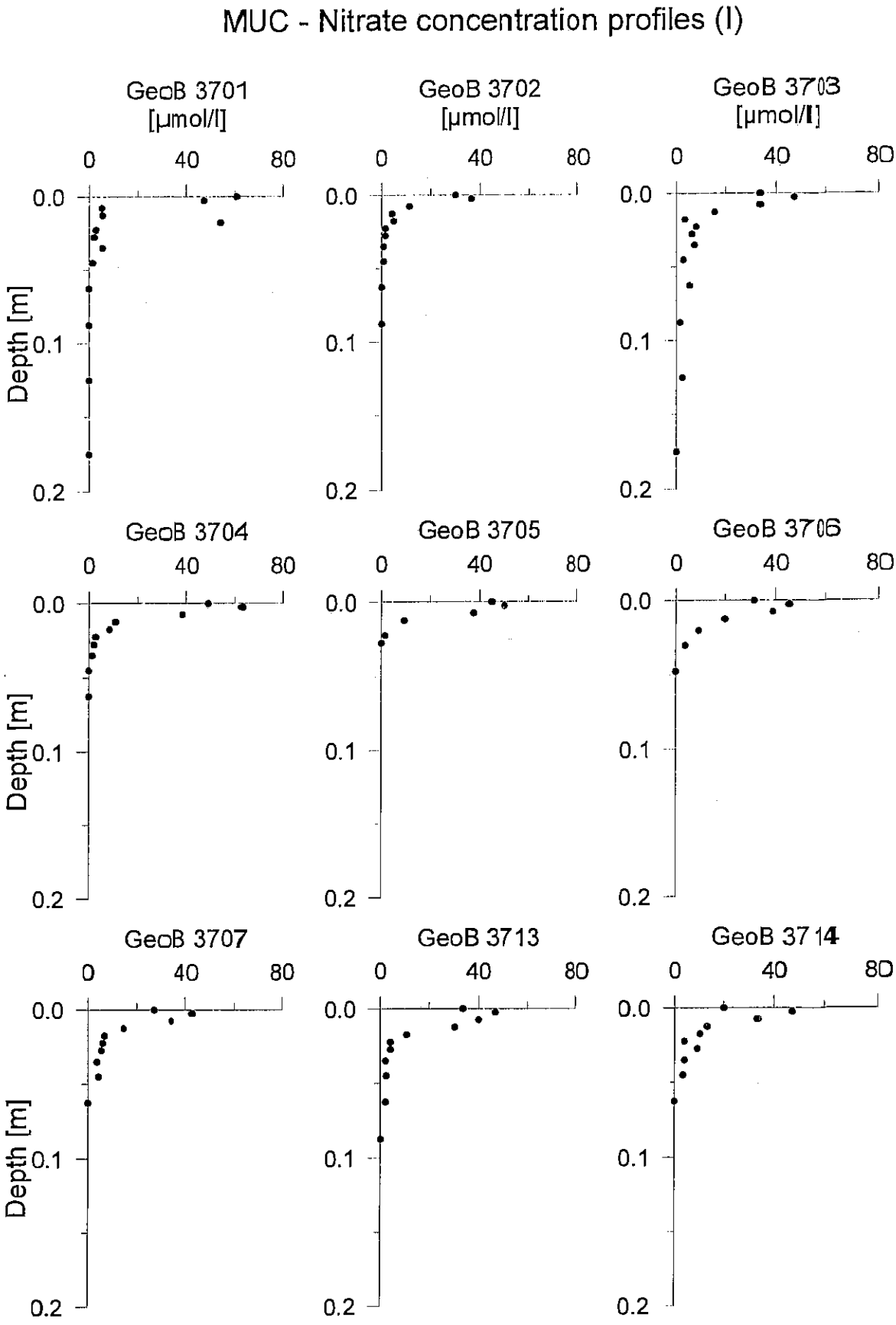

Fig. 105a: Nitrate concentration profiles (Transect A and B):

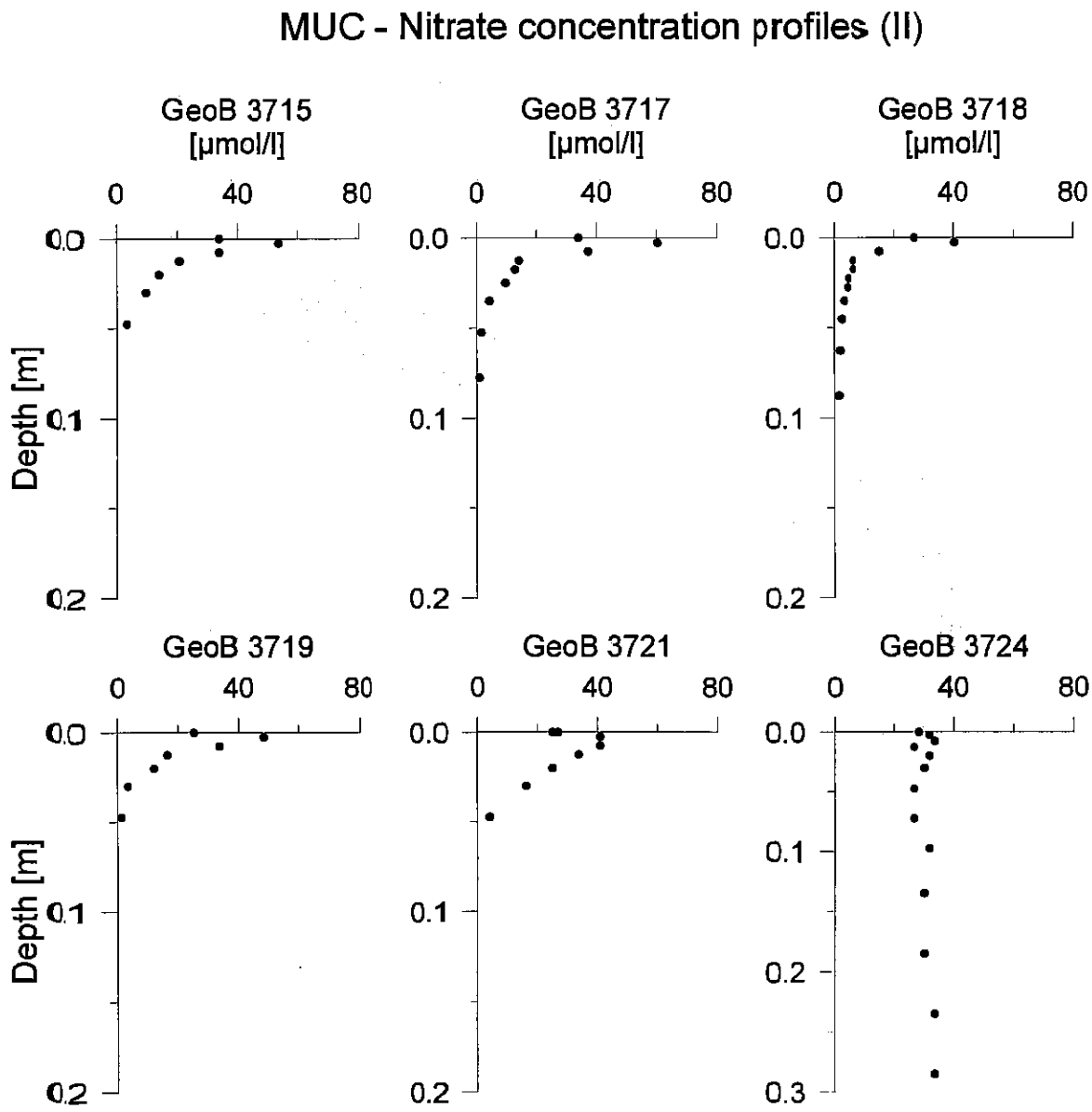

Fig. 105b: Nitrate concentration profiles (Transect A and B).

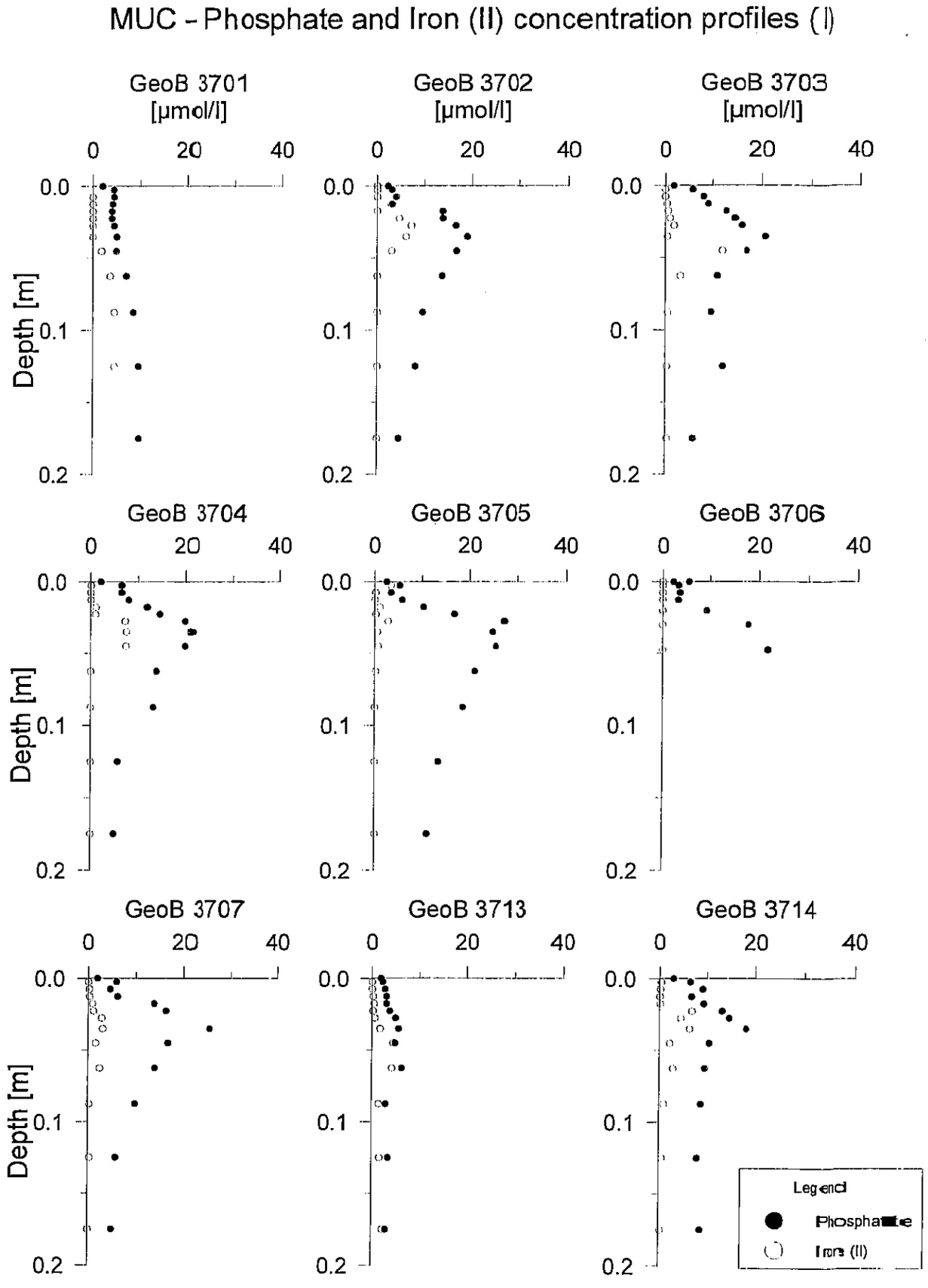

Fig. 106a: Phosphate and iron concentration profiles (Transect A and B).

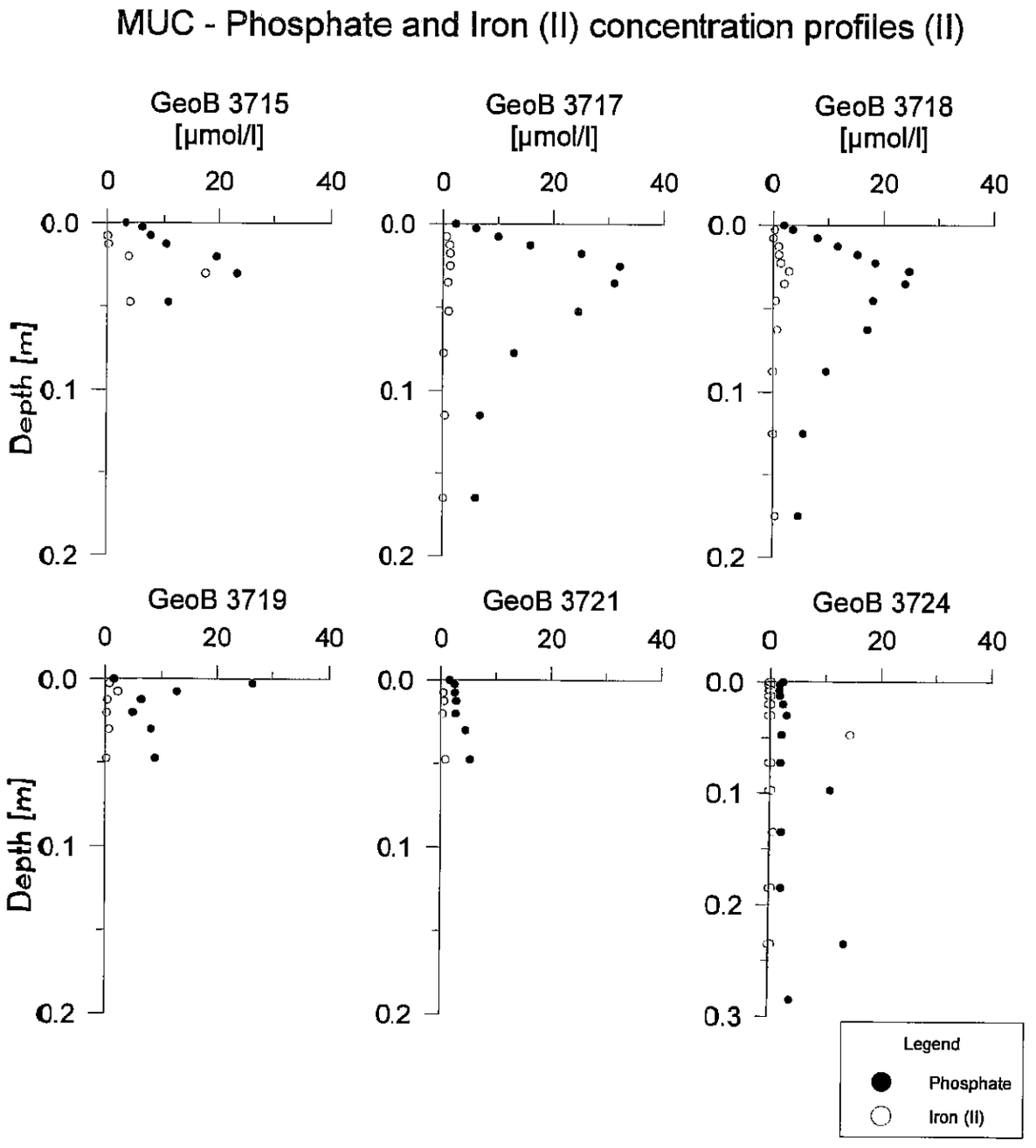

Fig. 106b: Phosphate and iron concentration profiles (Transect A and B).

concentrations or the nitrate penetration depth. Both processes are also recorded on pH and Eh profiles which are not presented here. Nitrification due to oxygen consumption creates a pH minimum at about oxygen penetration depth. This is due to the release of protons (H^+) during oxidation of organic matter. A distinctive decrease of the redox potential (Eh) is apparent within the uppermost sediment, correlating with the strongest decrease of nitrate concentration or nitrate penetration depth.

A striking pattern is also revealed by comparing phosphate and iron (II) concentration profiles in the surface sediments. Phosphate concentrations generally increase from bottom water into the sediment due to organic matter decay. The maximum concentrations are between 3-5 cm. Below this depth phosphate is fixed to the solid phase as can be deduced from decreasing pore water concentrations. Peaks of dissolved iron in pore water occur at the same depth as phosphate peaks. Below this depth also iron is fixed. Both phosphate and iron release are probably controlled by the same process which has still to be identified. Iron reduction due to organic matter oxidation might be one process, but higher iron concentrations would be necessary for the amount of phosphate released.

Anoxic mineralization processes

Anoxic mineralization processes were investigated on 4 gravity cores. GeoB 3703, 3718 are locations from the same area southwest off Walvis Bay at the same water depth. As can be deduced from oxygen penetration depths the mineralization activity at both locations is very high and the same pattern of mineralization processes becomes obvious. Pore water results are shown in Figure 106 and 107 (NIEWÖHNER et al., sub.).

At GeoB 3703 sulphate reduction occured at a sediment depth of 3.5 m. The pore water gradient shows a linear decrease from the bottom water down to this depth and there coincides with the steepest decrease in methane concentration diffusing upwards from greater sediment depths. The coincidence of both gradients clearly reveals that methane is oxidized by sulphate producing H_2S and CO_2. An increase of H_2S is recognizable in this zone, but highest concentrations were measured at depths between 6-9 m. Since there is no source for H_2S deeper in the sediment this concentration profile is not reliable. The alkalinity profile shows the steepest gradient between the sediment surface and the sulphate reduction zone representing CO_2 production by methane oxidation. Below this depth the concentration increases with a lower gradient caused by methane fermentation processes at greater sediment depths. In opposite to the gradient change within the alkalinity profile ammonium and phosphate concentration profiles show a nearly linear concentration gradient from the surface to the bottom of the core. Because both are products of organic matter degradation they cannot display the same gradient change at the sulphate reduction zone, since methane is oxidized quantitatively by sulphate and not organic matter.

The same pattern of concentration profiles is recognizable at GeoB 3718. The sulphate reduction zone is placed in nearly 6m sediment depth. At the same depth maximum concentrations of more than 20 mmol/l H_2S were detected, suggesting that sulphate is

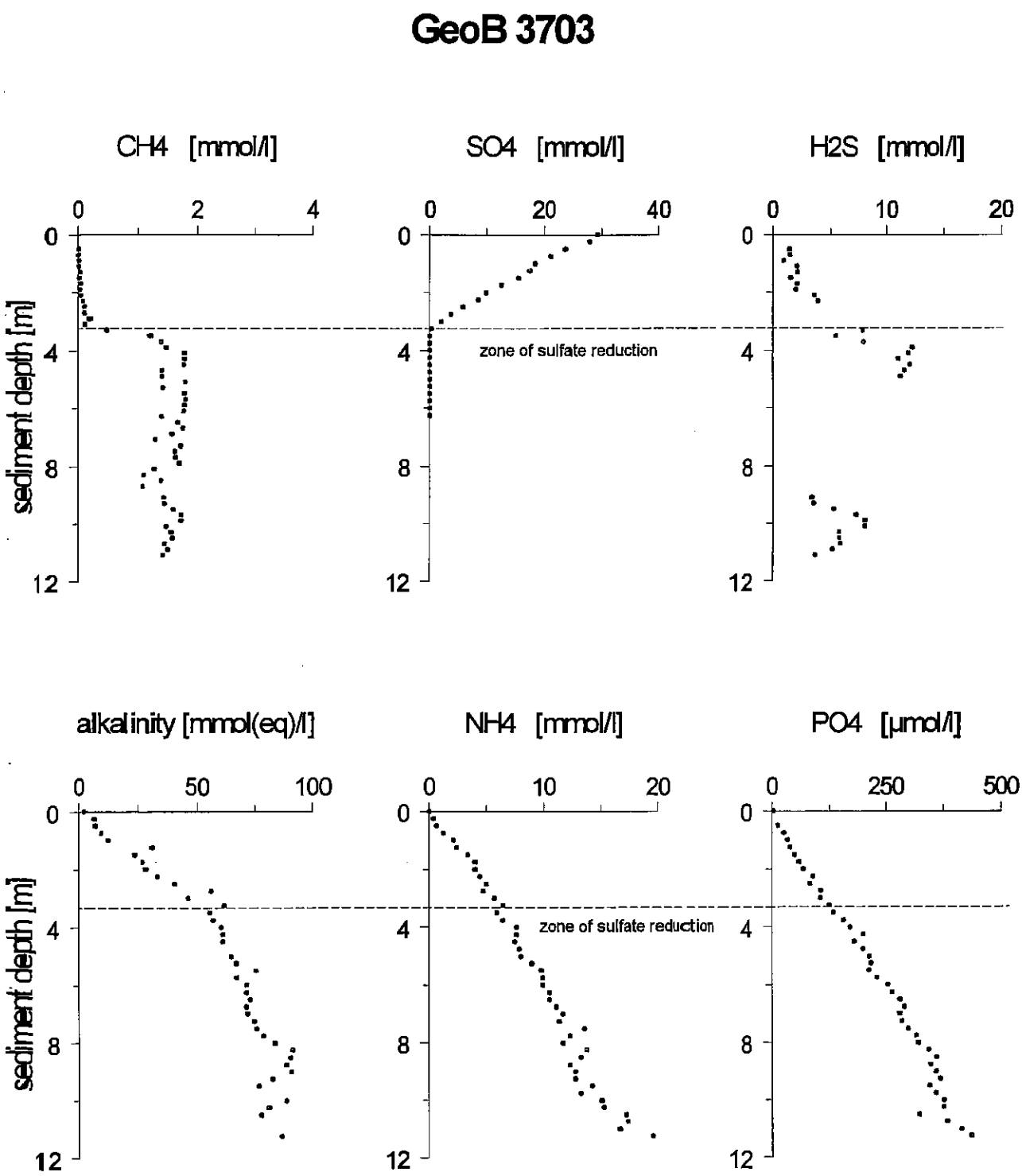

Fig. 107: Pore water concentration profiles of GC 3703-8.

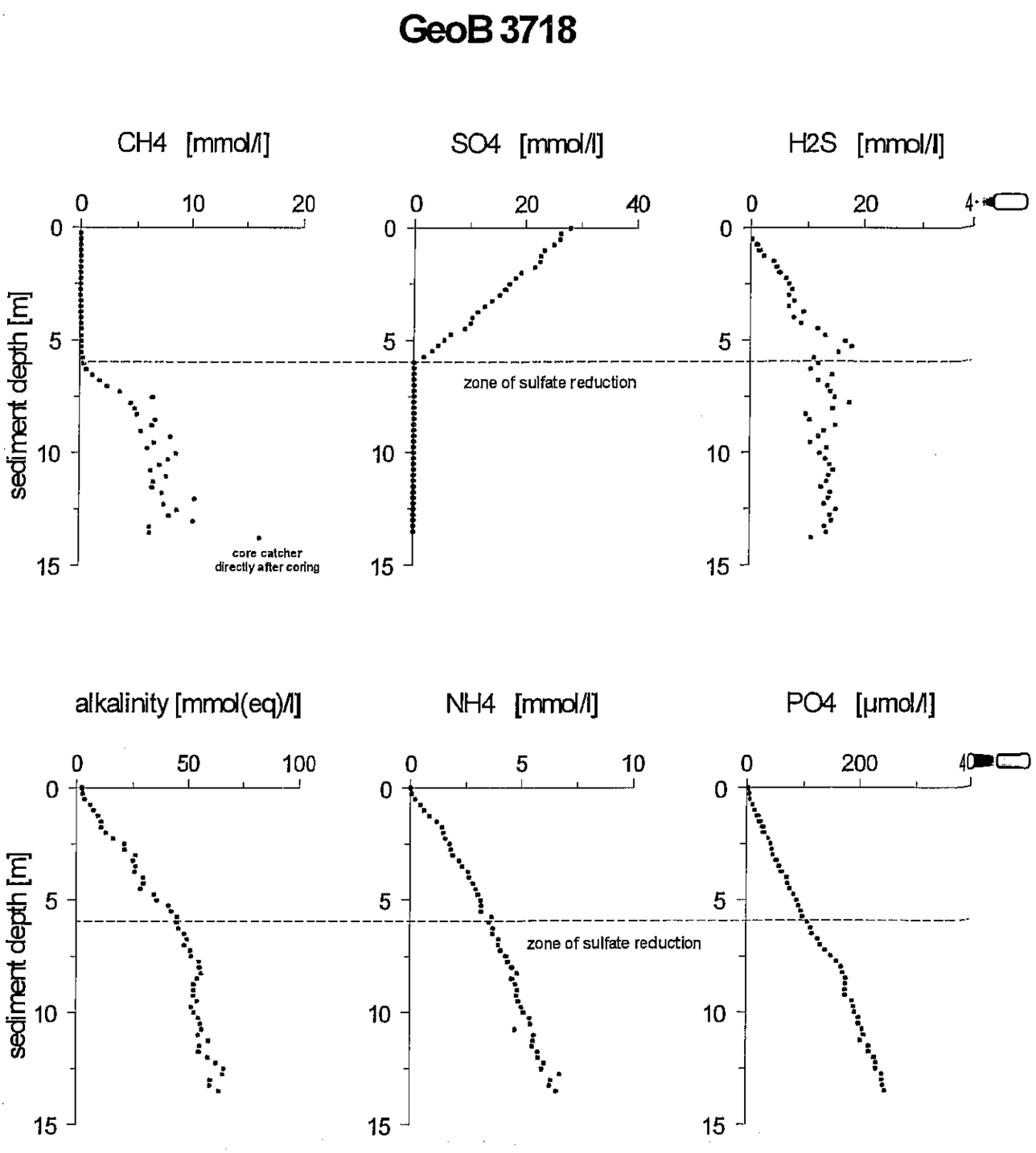

Fig. 108: Pore water concentration profiles of GC 3718-9.

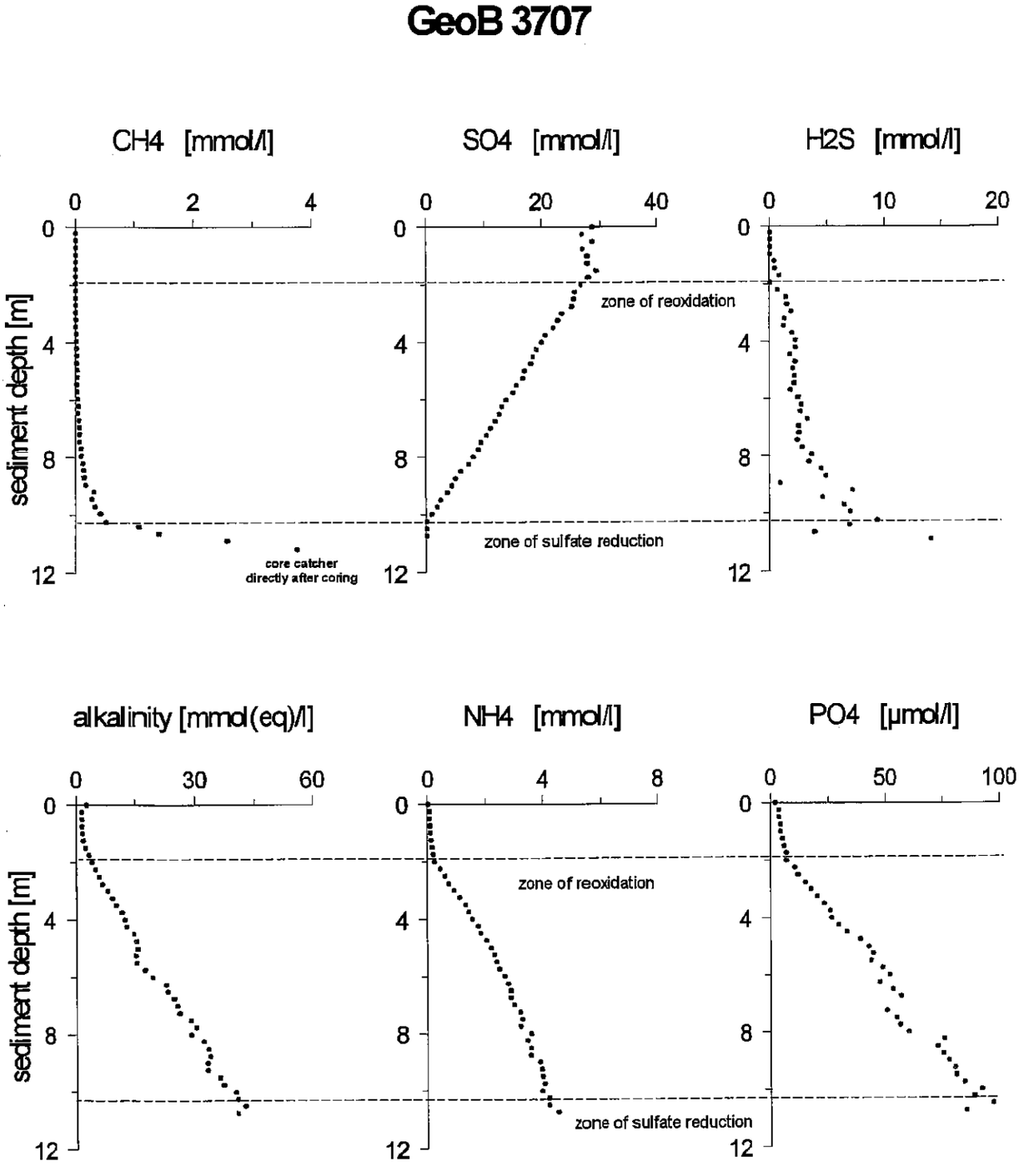

Fig. 109: Pore water concentration profiles of GC 3707-9.

GeoB 3714

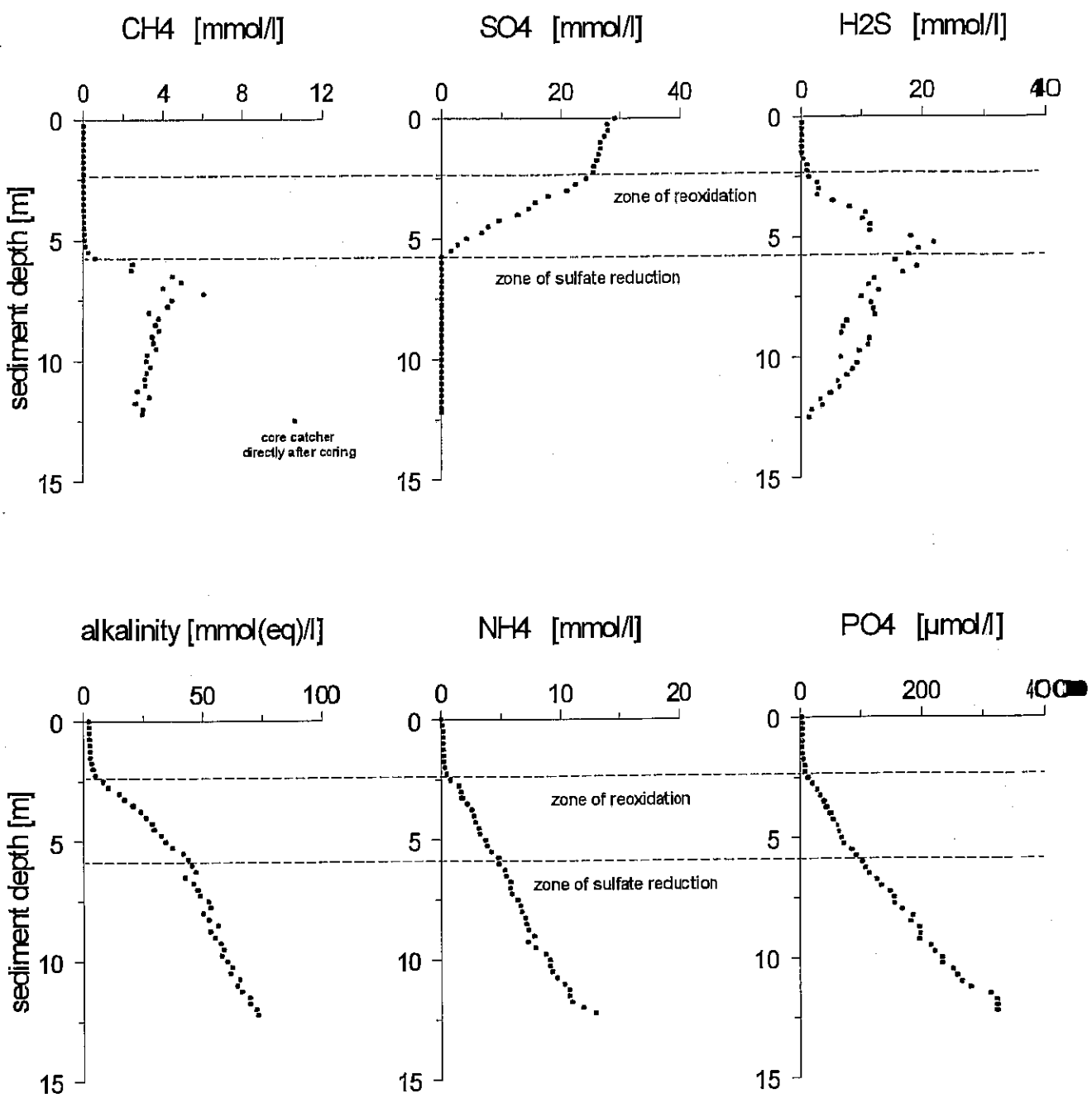

Fig. 110: Pore water concentration profiles of GC 3714-9.

quantitatively reduced to sulfide during methan oxidation. Maximum concentrations of methane scatter around 10 mmol/l which is 5 times more than detected in GeoB 3703. A core catcher sample taken immediately after coring contained nearly 20 mmol/l, suggesting that a high amount of methane is already degassed before sampling. Concentrations of ammonium and phosphate at the bottom of the core are a factor 2-3 lower suggesting lower fermentation activities than at GeoB 3703.

Gravity cores GeoB 3707 and 3714 show a different pattern of pore water concentration profiles. GeoB 3707 is located in the northern Cape Basin northwest off Walvis Bay and GeoB 3714 in the southern Angola basin. The results from pore water analyses are displayed in Figure 108 and 109 (NIEWÖHNER et al., sub.). At GeoB 3707 the sulphate reduction zone is located at a depth of 10 m again coinciding with the steepest methane concentration gradient and maximum H_2S concentrations in pore water. The sulphate concentration gradient shows a linear decrease between 1.8 m and 10 m what means only diffusive transport to the sulphate reduction zone. Between bottom water and 1.8 m sediment depth there is no difference in sulphate concentration. This means that there has to be a source of sulphate at this depth, otherwise the diffusion gradient must be linear over the whole sediment depth. We ascribe this to a reoxidation of sulfide to sulphate. Further investigations have to be done on this problem, to find out which redox partner is able to oxidize H_2S in these quantities. At GeoB 3714 this process is recognizable nearly at the same sediment depth, whereas the sulphate reduction zone occurs already in 5.5 m. The main difference between both locations is that there exists a low gradient between sulphate concentrations in bottom water and the reoxidation zone. Furtermore H_2S could be detected above the reoxidation zone, diffusing upwards with a low gradient. Therefore the reoxidation of sulfide to sulphate is not complete, possibly due to insufficient supply of the oxidizing redox partner. At a depth of about 10 m sulfide concentrations nearly go down to zero suggesting a fixation as metal (Fe) sulfides. Below the reoxidation zone concentration profiles of ammonium, alkalinity and phosphate show the same behaviour as described for the first two cores. The gradient change of these parameters within the reoxidation zone is another point which needs further investigation to elucidate the prime processes.

5.2.5.3 Rates and Pathways of Carbon Oxidation

(J. Kostka)

Introduction

The purpose of this project was to study mineralization rates and the partitioning of respiration processes in sediments of the upwelling region off southern Africa (17 to 25° S). The focus was to sample sediments from the continental slope (water depth of 1000 to 2000 m) at deeper water depths than have been studied previously. Though evidence is available for the diversity of carbon oxidation pathways in marine sediments, a general understanding of their relative importance and regulation has not been reached. Previous work has shown that the importance of aerobic respiration to carbon oxidation may have been overestimated

and that pathways other than sulfate reduction, such as metal respiration, contribute substantially to anaerobic carbon oxidation.

This study therefore applied a multilateral approach involving direct measurements of the accumulation of minerlization products (dissolved inorganic carbon, ammonium), sulfate reduction rates, and the depth distribution of potential oxidants. The range of oxygen penetration depths (0.8 to 1.8 cm) measured at the stations sampled indicates that these sediments may well display a diversity of mineralization pathways from 0 to 10 cm sediment depth.

Methods

Measurements were conducted at four stations including: 3703-6, 3707-5, 3714-4, and 3718 (water depths of 1000 to 2000 m). All sample processing was carried out in a nitrogen-filled glove bag at 4°C in the cold room of the F/S Meteor and was initiated within a few hours of core sampling. The top 10 cm of sediment was sectioned and pooled from 8 to 12 multicores per station. The sediment was placed into oxygen-impermeable bags with no headspace and incubated for 5 to 10 days at bottom water temperature (4°C). Samples were taken from the bags at regular intervals for the determination of mineralization products. Sediment for porewater analysis was centrifuged at 5000 rpm for 15 min. and the resulting porewater filtered through a 0.2 µm syringe filter. Sediment samples were frozen immediately for solid phase analysis. Shipboard measurements focused on the determination of production rates of dissolved inorganic carbon and ammonium. These were measured with a rapid flow-through injection analysis technique. Determinations of sediment pH, porewater pH, and reduced Fe in porewater were also carried out on board. Samples were retrieved and archived for the following analyses upon return to the Max Planck Institute:

Porewater:	Fe, Mn, nitrate, phosphate, sulfide, Ca, pH
Solid phase:	Fe(III), Fe(II), Mn(IV), Mn(II), FeS, pyrite

For sulfate reduction rates, radiolabelled sulfate was employed in 2 hour incubations on board and the samples stored in zinc acetate for later analysis. Ammonium adsorption coefficients will also be determined from sediment samples treated with potassium chloride and frozen.

Results

Ammonium gradients at the four stations ranged from 50-100 µM in the top 10 cm of sediments (Fig. 111). Porewater ammonium concentrations at 1 cm depth in the sediment averaged 5-20 uM (Fig. 111). No ammonium was detected in bottom water samples using the methods employed on ship.

Dissolved inorganic carbon (DIC) was measured in bottom water to be 2.108 mM and small gradients were detected with depth in the sediment to 10 cm from 2.2-2.3 mM in the surface to 2.4-2.8 mM at depth at the four stations sampled (Fig. 112). In general, depth profiles of mineralization products showed larger gradients in surface sediments at the most active

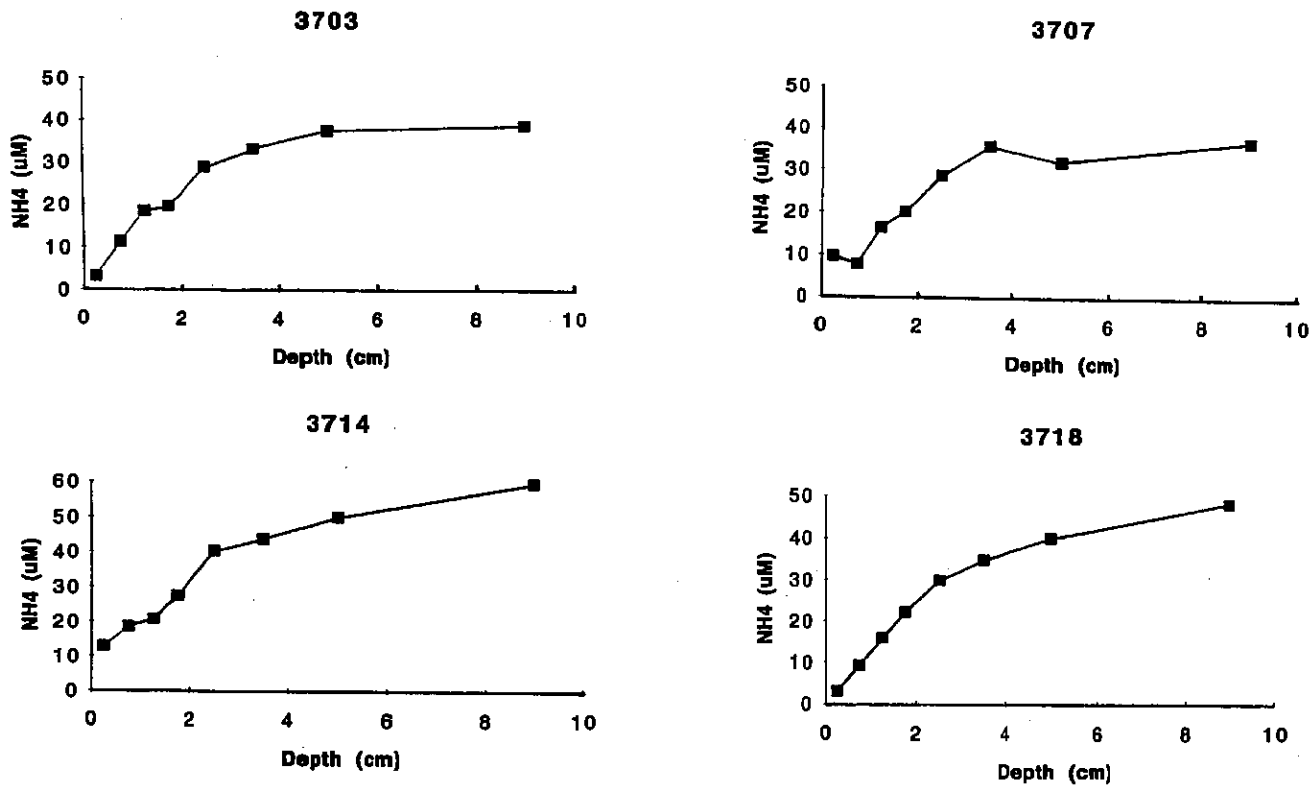

Fig. 111: Porewater ammonium measured on board ship using a flow injection analysis technique.

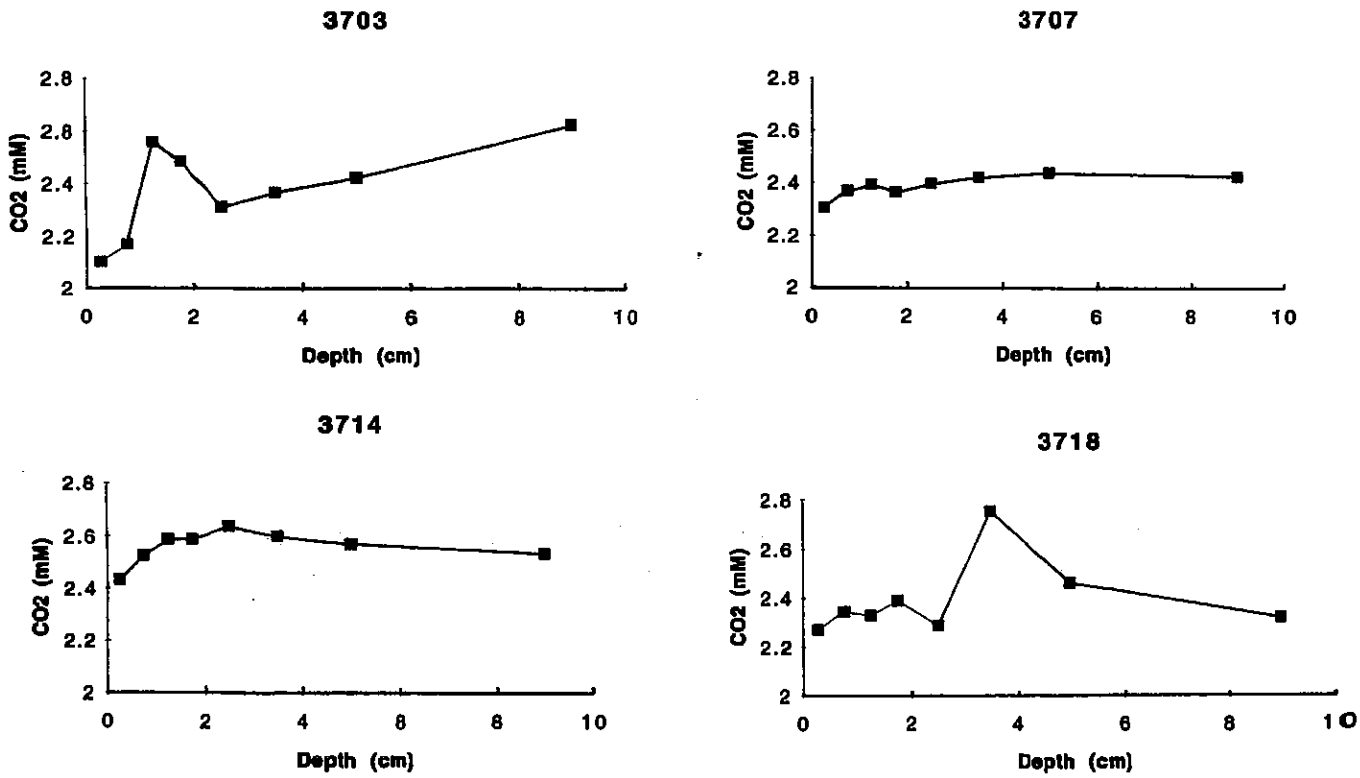

Fig. 112: Dissolved inorganic carbon measured in porewaters on board ship using a flow injection analysis technique.

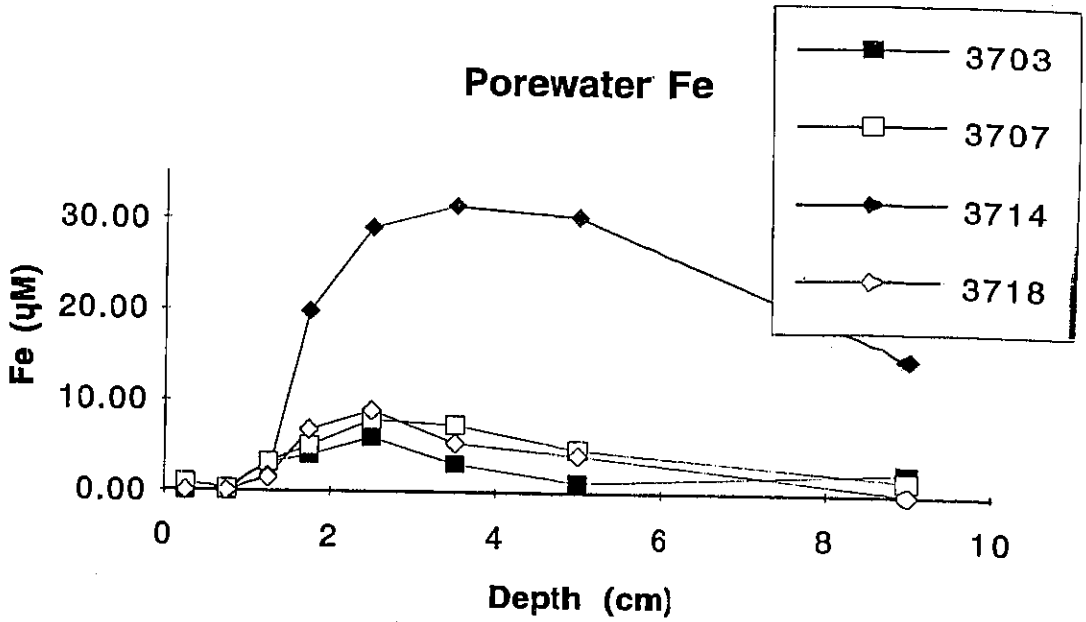

Fig. 113: Reduced iron in porewater.

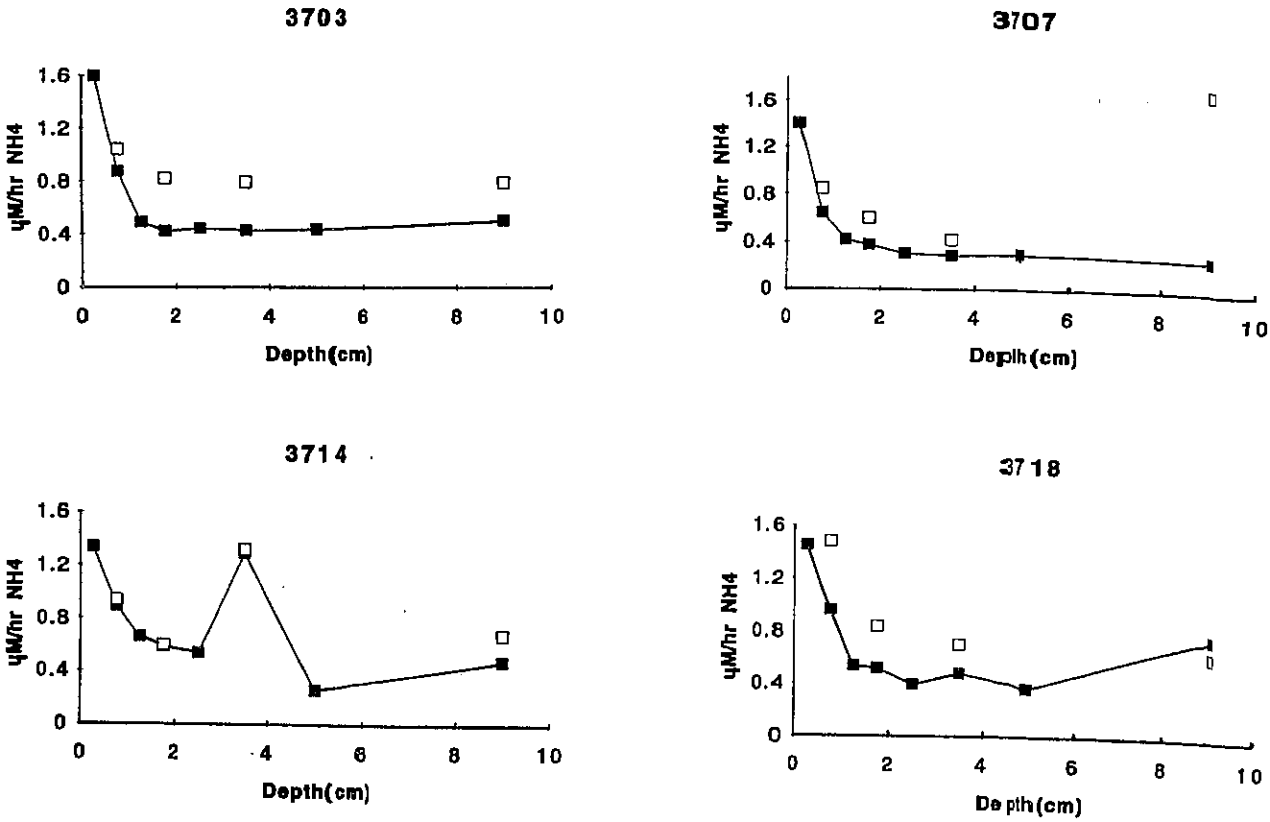

Fig. 114: Ammonium production rates measured in sediment incubations. Open symbols represent unamended sediment treatments and filled symbols represent treatments to which 20 µM molybdate was added.

station (3714) and smaller gradients at the least active station (3707). Rates of activity are discussed below.

Maxima in reduced Fe were detected in porewaters at 2 to 4 cm sediment depth and concentations ranged from 2 to 30 μM at the four stations sampled (Fig. 113). Increases in Fe(II) were detected in sediment incubations from all stations, indicative of Fe reduction. Station 3714 showed the highest porewater Fe concentrations (15 to 30 uM) and the largest increase (2–20 times the original concentration) in the bag incubations.

A minimum in porewater pH was measured at 2-4 cm sediment depth and a small but measurable decrease in pH was measured upon incubation of sediment in the bags.

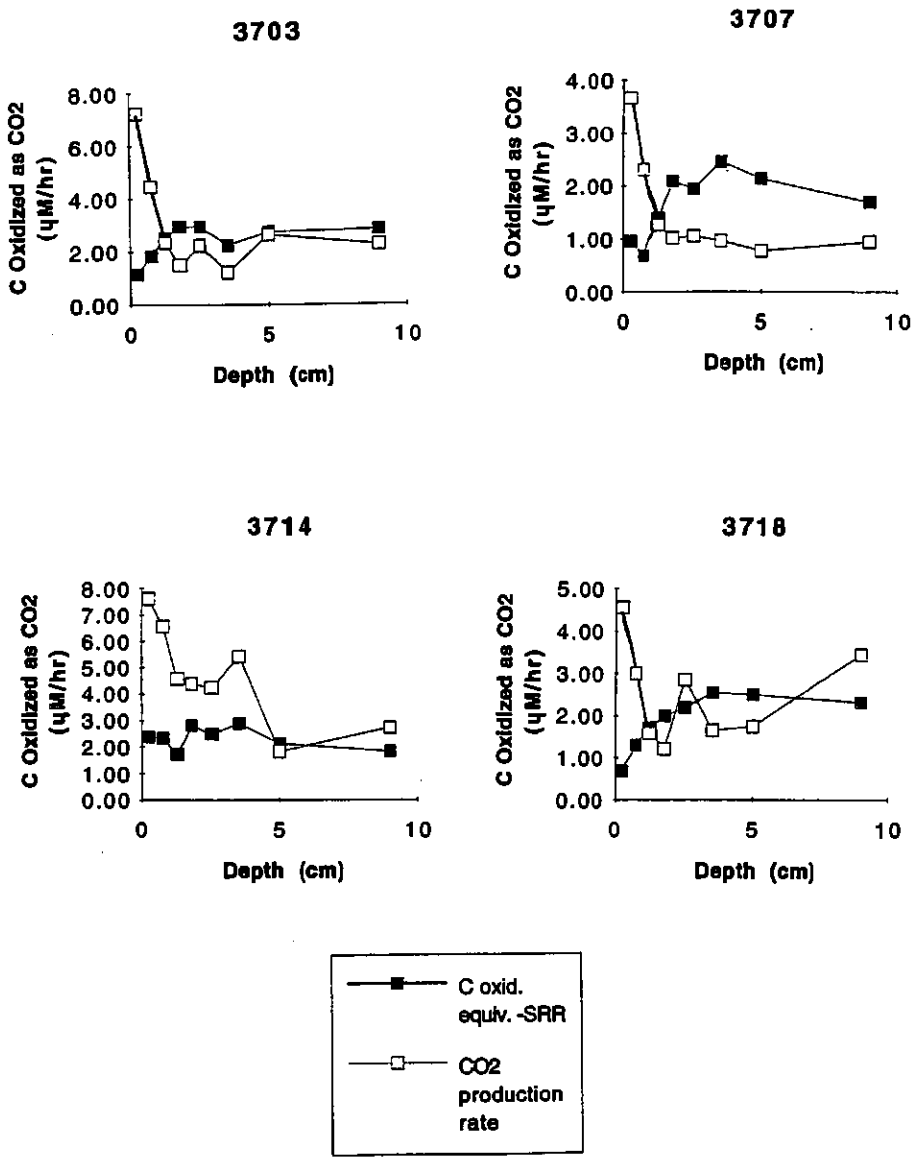

Fig. 115: Production rates of total dissolved inorganic carbon (open symbols) measured in sediment incubations, and the equivalent amount of carbon oxidized as CO_2 (filled symbols) estimated from independently measured sulfate reduction rates.

Production rates of DIC and ammonium determined from the regression of concentration with time were highly linear (usually r^2=0.95 and above). Figures 114 and 115 show that rates of ammonium and DIC production decreased rapidly with depth in the top 10 cm of sediment. Depth profiles of ammonium production were in general similar at the four stations (Fig. 114). However, DIC production profiles differed between stations (Fig. 115) and this may be due to the effects of carbonate precipitation. The open symbols in Figure 114 represent production rates in sediments treated with molybdate to inhibit sulfate reduction. Apparently, ammonium production was stimulated in molybdate treatments at three out of the four stations. This could either be caused by a microbial response or by a change in ammonium adsorption in the bags. Further interpretation will depend on the determination of ammonium adsorption coefficients.

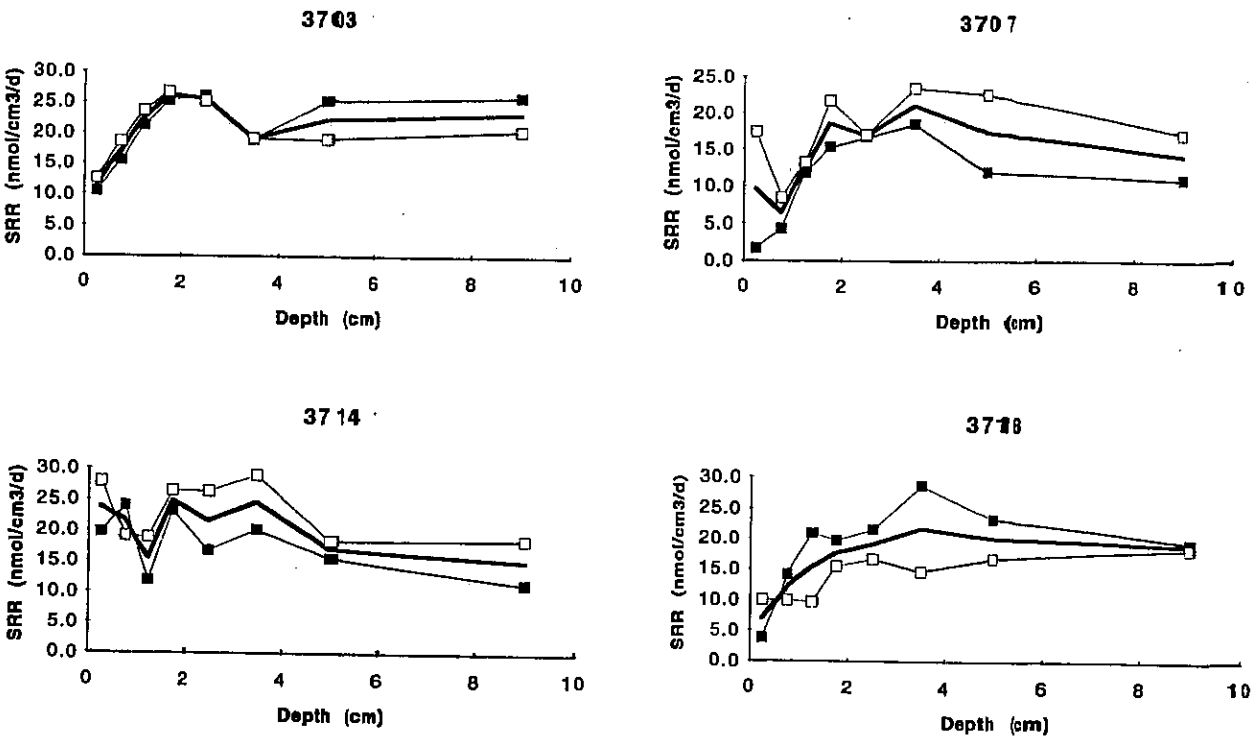

Fig. 116: Sulfate reduction rates measured via radiolabelled sulfate in syringe microcores sampled from sediment incubations during first few days of incubation. Dark line represents the average of duplicate measurements.

Rates of production, when integrated by area over the top 10 cm of sediment, ranged from 2 to 6 mmol/m2/d for DIC and 0.6 to 1.0 mmol/m2/d for ammonium. The four stations gave the following order of production activity: 3707< 3703=3718< 3714 (Fig. 114 and 115). These rates generally showed a negative correlation with oxygen penetration depth. Treatment of the sediment from station 3714 with sodium molybdate resulted in a decrease in mineralization rate below 3 cm sediment depth indicating that sulfate reduction may be a dominant pathway for anaerobic carbon oxidation. An intriguing but as yet unexplained

maximum in DIC and ammonium production was measured at 3.0-4.0 cm sediment depth at station 3714 as well.

These mineralization rates are lower than those of any other sediment studied using the bag incubation technique to date. In continental margin sediments associated with an upwelling zone off central Chile, THAMDRUP and CANFIELD (in press) found integrated rates of 9 to 12 mmol/m2/d for DIC and 0.8 to 1.1 mmol/m^2/d for ammonium production. These measurements were made in sediments of comparable water depth (1000 - 2000 m).

Sulfate reduction rates are presented in Figure 116. These rates were comparable at the four stations with a maximum observed at 20 to 30 nmol/cm3/d. An increase was observed with sediment depth at all stations with the exception of the most active station, 3714. At 3714, larger rates were observed closer to the sediment surface and these decreased or remained stable with depth. These rates may be adjusted after further analysis of sediment density and porosity. Assuming a stoichiometry of 2:1 for DIC production to sulfate consumption, equivalents of carbon oxidation as total CO_2 produced are calculated from the sulfate reduction rates and presented in Figure 115. A comparison of equivalents of carbon oxidized during sulfate reduction to the total DIC produced indicates that sulfate reduction is the dominant pathway for carbon oxidation in these sediments.

Tab. 16: Integrated rates of DIC production, ammonium production, and sulfate reduction at four stations sampled for bag incubations off the coast of Namibia. Rates are integrated areally to 10 cm depth. Units are in mmol/m^2/d

	DIC Production	NH4 Production	Sulfate Reduction
Sta. GeoB3703	4,46	0,928	2,19
Sta. GeoB3707	1,98	0,648	1,55
Sta. GeoB3714	6,05	0,991	1,85
Sta. GeoB3718	4,28	1,02	1,83

Summary

Mineralization rates were low in comparison to previous studies in agreement with preliminary observations of a lack of enhanced productivity that could be attributed to upwelling nutrients at the time of our cruise (GeoB 34/2). Though low, rates were comparable (within a factor of two) to those measured using the same incubation technique in sediments from another upwelling zone (off central Chile) at similar sediment and water depths. After preliminary analysis, rates appeared to show a negative correlation with oxygen

penetration depth as would be expected. Independently measured sulfate reduction rates were also low in comparison to previous studies in corroboration with rates derived from mineralization products. A comparison of equivalents of carbon oxidized via sulfate reduction to total DIC production revealed that sulfate reduction appears to be the dominant respiration pathway at the four stations sampled off the Namibian coast. These preliminary conclusions will be expanded and may change pending further analysis of porewater constituents, sulfate reduction rates, and solid phase species.

5.2.5.4 Sulfate Reduction Rates through the Sulfate-Methane Transition Zone in South-West African Continental Margin Sediments

(T. Ferdelman, H. Fossing and K. Neumann)

Goal

A unique feature of the pore waters profiles from south-west African continental margin sediments is the striking change in sulfate, hydrogen sulfide, and alkalinity gradients that occur at sediment depths of more than 4 meters (SCHULZ et al., 1994). Whereas, there appears to be little or no sulfate reduction in the uppermost three to six meters of sediment (as deduced from the lack of gradients in sulfate concentration over depth), sulfate reduction appears to commence at greater depths. It has been hypothesized by SCHULZ et al. (1994) that this deep sulfate reduction is linked to the oxidation of methane. The principal goal of this project is to test this hypothesis by directly measuring sulfate reduction rates using the ^{35}S tracer method. Further constraints on rates of sulfate reduction can be obtained from the measurements of stable sulfur isotopes. Evidence for methane oxidation is sought through the analysis of the isotopic composition of methane.

Methods

We processed two gravity cores, one each from Station GeoB 3703 and from Station GeoB 3714 (site of former GeoB 1023) with lengths of 9.5 and 12.8 meters respectively. The cores were cut into one meter sections and immediately sampled from the top of each section for methane and sulfate in order to establish the location of the sulfate-methane transition zone. Core sections were stored vertically at 4°C and processed in a cold room at temperatures between 4 and 6°C. A series of samples were taken over 20 cm sections over most of the cores, except in the methane-sulfate transition zone, where the frequency of sampling was increased to every 10 cm.

Core sections were sampled for the following parameters from the tops of individual core sections and working downwards.

(1) Sulfate Reduction Rates

Three sub-cores (1.3 x 5 cm) were taken for labelling and incubation for the measurement of sulfate reduction rates. Incubation times for each set of samples were 24, 48, and 72 hours. The sub-cores were incubated in the dark at 4-5°C before termination and preservation of the samples.

(2) Methane Concentration

One sub-core was taken for the determination of methane concentration and immediately preserved for later onboard measurement.

(3) Methane Isotope Composition

Duplicate sub-cores were taken and immediately preserved for the later determination of $^{13}CH_4/^{14}CH_4$ ratio measurements (to be shipped to B. Popp, University of Hawaii).

(4) Molecular Probes of Bacterial Diversity and Abundance

Samples were obtained for Dr. Gerard Muyzer (MPI, Bremen) for bacterial population studies using molecular gene probes. Approximately 200 µl sample was taken and preserved in paraformaldehyde for the possible quantification of specific bacterial populations, e.g., sulfate reducers, using Fluorescent In Situ Hybridization techniques. Another sub-core was aseptically taken and frozen for later extraction and screening of DNA and RNA sequences.

(5) Pore Water

Pore waters were expressed through 0.4 µ filters from 2 x 3.6 cm sub-slices of sediment into glass syringes using an Ar purged pneumatic pore water press. Pore waters were preserved with a 2 % $ZnCl_2$ solution for later analysis of sulfate and hydrogen sulfide. In addition to providing ancillary data for the evaluation of results from this core, the sulfate values are required for the accurate calculation of sulfate reduction rates. At Station GeoB 3703, aliquots of pore water were also derivatized with bromobimane for the later determination of sulfur intermediates (i.e., thiosulfate).

(6) Stable Sulfur Isotopic Composition

Two 2 x 3.6 cm sub-slices of sediment were preserved in zinc acetate and frozen for the later determination of del-^{34}S values of pyrite and sulfate (in cooperation with D. Canfield, MPI-Bremen).

(7) Porosity

One sub-core was taken for the later determination of sediment porosity and as archival material.

Preliminary Results

The majority of samples await further processing and analysis in our laboratory in Bremen. We can only report at this time on methane distributions and sporadic sulfate concentrations.

The methane profiles are consistent with those measured by the Uni-Bremen Geochemistry group (as reported in chapter 5.2.5.2). At Station GeoB 3703 the steep gradient leading to saturation values lies just below 3 meters. At Station GeoB 3714 the gradient begins at approximately 6 meters as shown in Figure 117. It is interesting to note the large difference between values measured immediately after the core was retrieved from over 2000 meters water depth and the equilibrium values measured at depth after a few days standing in the cold room.

The few sulfate concentrations measured from the tops of the core sections of GeoB 3714 show decreasing values from 2 meters down to 6 meters, thus, the sulfate-methane transition zone lies a bit deeper in this core than in GeoB 3703.

One notable observation was made on GeoB 3714. At 6.3 meters, just a bit deeper than the sulfate-methane transition zone, a pocket of slime was observed in one of the numerable channels or tubes located through the core.

Samples of this slime were immediately given to Prof. Bernhard Schink and Dr. Harald Petermann for microscopic observation, who observed large densities of a single type of spindle shaped bacteria. Further description of these bacteria may be found in M. Benz and B. Schink's report (chapter 5.2.5.6). Further sub-samples were given to B. Schink, as well as frozen, for transport and examination in Bremen at MPI.

5.2.5.5 Spatial Variability of Sulfate Reduction Rates in Surface Sediments along the South-West African Continental Margin

(T. Ferdelman, H. Fossing and K. Neumann)

In continental shelf and slope sediments, sulfate reduction is a major, if not the most important, bacterial process in remineralizing organic carbon. Therefore, a wide areal coverage of sulfate reduction rate determinations were made using the whole-core ^{35}S injection method on triplicate samples from the following stations.

Alongshore Transect (A):	3701, 3702, 3703, 3705, 3706, 3707, 3710, 3711, 3712, 3712,3713, 3714 (2000 m), 3715
Cross-slope Transect (B):	3717 (864 m), 3718 (1321 m), 3719 (1991 m), 3721 (3031 m),3724 (5000 m)

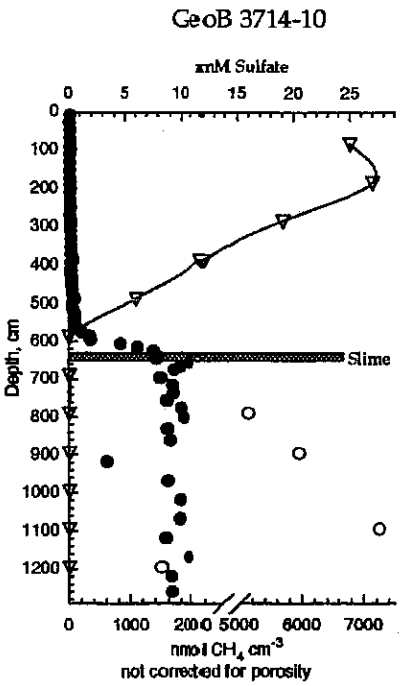

Fig. 117: Distribution of pore water sulfate (triangles) and methane (circles) in core GeoB 3714. The open circles are values of methane sampled immediately after the core was brought on to the deck.

Sub-cores of up to 30 cm length were obtained from each station from a multi-core sampler. In addition to sub-cores for sulfate reduction, a sub-core for the measurement of porosity and sulfate was also obtained. The samples await further processing and analysis in Bremen.

At Stations GeoB 3716 (shelf sediments south of Walvis Bay) and GeoB 3726 (continental slope between 300 and 500 m) we looked for the presence of *Thioploca*, which are large, filamentous sulfur bacteria, visible to the naked eye and who form dense mats in some upwelling areas (e.g., Chile, Peru). We were without success in our search, except for the possible existence of very small singular filaments in the sulfidic sediments of GeoB 3716. Our search was limited by lack of information concerning hydrographic structure and sediment types of potential search areas; this null result should not be interpreted as representing the outcome of a systematic survey.

5.2.5.6 Anaerobic Microbial Activity in the Sediment Column

(M. Benz and B. Schink)

Introduction

Participation of our group in this trip was initiated on the basis of earlier measurements by the geochemistry research group, Bremen, (Prof. Schulz) on the distribution of dissolved compounds in porewaters from sediment cores obtained in the upwelling zone at the coast of Namibia and Angola. Our work concentrated on new, so far unknown or ill-documented microbial metabolic activities present in these unusually rich anoxic sediments. The studies by the group of Prof. Schulz provided indications of the following activities which challenged a thorough microbiological examination:

1. In numerous sediment profiles, ammonia disappeared in depth layers to which molecular oxygen had no access. Depending on the respective core, either nitrate, manganese (IV), iron(III), or sulfate had to be assumed to serve as oxidant for ammonia which would probably be converted to dinitrogen gas. According to the present-day microbiological literature, ammonia is oxidized only by oxygen-dependent bacteria which attack the ammonium molecule by a mono-oxygenase reaction (SCHLEGEL, 1992). First indications of a nitrate-dependent ammonia oxidation by bacteria in sewage digestor contents or by nitrifying bacteria were published only very recently by two research groups (VAN DE GRAAF et al., 1995; BOCK et al., 1995); involvement of an oxygen-independent nitrogen cycle in electron transfer from reduced to oxidized water layers was suggested on the basis of studies in the Black Sea (JØRGENSEN et al., 1991).

2. After reduction in deeper sediment layers, sulfide was reoxidized nearly quantitatively in higher layers where only iron (III) or manganese (IV) could serve as oxidants. The process had not been documented yet in detail. It was open whether this reoxidation was only a chemical or a biologically catalyzed activity; complete oxidation of sulfide to sulfate indicated a microbial activity.

3. Nitrate was reduced in zones where manganese (II) or iron (II) could serve as electron donor. Nitrate-dependent oxidation of ferrous iron was recently described for the first time by our research group, in cooperation with the group of Prof. Widdel, Bremen (STRAUB et al., 1996). The present study should find out whether this activity is of importance also in a marine anoxic habitat.

4. Methane was discussed as a major electron source for sulfate reduction in deeper sediment layers although existence of methane had so far not been documented in these sediments. If a major contribution of methane oxidation to sulfate reduction could be verified the microbiological basis of sulfate-dependent methane oxidation would be a further challenge to explore. There are numerous documentations of anaerobic methane oxidation by other research groups (HOEHLER et al., 1994, and further references quoted therein), mostly for shallow marine sediments. Nonetheless, nobody has so far a microbial culture at hand that is able to catalyze a net oxygen-independent oxidation of methane *in vitro*, and the biochemistry of methane oxidation under such conditions is entirely enigmatic.

5. The energetics of sulfate reduction and methane formation from hydrogen in deeper sediment layers should be reevaluated on the basis of measurements of hydrogen partial pressures in these sediment layers by a trace gas detector of very high sensitivity. Data on hydrogen partial pressures could also provide hints whether sulfate-dependent methane oxidation (see point 4) is catalyzed by a single organism or by a "syntrophic" association of, e. g., methanogenic and sulfate-reducing bacteria.

It is obvious from this survey that our interest was mainly oriented towards a basic understanding of new microbial activities rather than providing exact figures on transformation rates or fluxes. However, our findings, if successful, could help to interprete such data supplied by other groups, especially those by the geochemistry group.

Experiments

Sediment material from core sampling sites GeoB 3701, 3703, 3707, 3714, and 3718 was used for the following experiments.

Microbial activities were assessed in slurries that were incubated both at *in situ* temperature (4°C) and at room temperature (21°C). Unfortunately, we could not provide suitable facilities for incubations at 10-15°C. Original sediment samples from depth layers exhibiting maximum activities were diluted with equal volumes of anoxic bicarbonate-buffered marine mineral salts medium in serum bottles sealed with latex rubber septa, and supplemented with the respective reactants under an oxygen-free atmosphere of helium/carbon dioxide (80/20). Oxidation of ammonia was followed with N-15 ammonia as sole source of reduced nitrogen, together with either nitrate, ferric iron hydroxide, or manganese dioxide; the latter two were prepared fresh by alkaline precipitation to ensure maximum reactivity, followed by subsequent washing to remove excess chloride ions. Disappearance of nitrate and ammonia, and formation of nitrite, ferrous iron and manganese(II) were followed in subsamples taken at regular intervals. Gas samples were removed and stored in small glass vials sealed with butyl rubber stoppers and lined with a saturated ammonium sulfate solution, for later mass spectrometric analysis of formed N-15 dinitrogen gas.

Nitrate-dependent oxidation of ferrous iron was assayed with nitrate and ferrous iron sulfate prepared in oxygen-free solution under helium/carbon dioxide gas mixture. The stock solution was colourless to slightly green before use indicating that ferric iron was not formed to substantial amounts. Oxidation of ferrous iron was followed in subsamples taken at regular intervals, and contents of ferrous and total iron were assayed separately (ferrozin method before and after chemical reduction with hydroxylamine).

Controls for non-biological oxidation processes were run in parallel assay bottles killed with 5 % formaldehyde, and treated like the regular assay bottles.

Microbial population sizes were estimated in Most-Probable-Number (MPN) dilution series in anoxic bicarbonate-buffered mineral media containing trace elements and vitamins, under an atmosphere of helium/carbon dioxide. Media contained N-15 ammonia and the respective specific reactants analogous to the incubation experiments described above. All growth media contained a low (1 mM) amount of acetate to cover possible assimilatory requirements of the microorganisms to be enriched. Supply of an organic cosubstrate should allow to check also for possible mixotrophic or cometabolic transformations of the respective substrate combinations.

Cultivation of sulfide-dependent iron(III) or manganese(IV) reducers and sulfate-dependent methane oxidizers could not be initiated on the ship because these cultivations require more sophisticated cultivation approaches, e. g. gradient culture techniques. Sediment samples exhibiting the respective activities were taken and sealed under anoxic atmosphere for further examination in our home laboratory.

Distributions of ferric and ferrous iron as well as of manganese(II) and (IV) in the sediment columns were assayed by the above-mentioned methods in discrete layers of interest for our activity assays after extraction with 1 M HCl for 24 hours.

Gas samples were extracted from the gravity cores as soon as possible after coring, in cooperation with the geochemistry group. Parts of these extracted gas samples were transferred with syringes into small glass vials sealed with butyl rubber stoppers and lined with a layer of saturated ammonium sulfate solution, for later analysis of hydrogen contents by a high-sensitivity mercury reduction hydrogen detector.

First results

Unfortunately, microbial activities in deep sediments are low. The activity assays supplemented with high nitrate concentrations (10 mM) exhibited after 5-7 days strong formation of nitrite (50 µM to 2 mM) which could chemically oxidize ferrous iron to the ferric state. Later experiments were started with repeated additions of nitrate at lower concentrations (0.5 mM) to prevent such non-biological side reactions. Also in these assays, ferrous iron was oxidized, nitrate was reduced and no ammonia was formed.

The Most-Probable-Number (MPN) assays showed slow growth and nitrite formation from nitrate in the very first tubes, indicating at least that they were not contaminated with fast-growing allochthonous bacteria. It is too early to evaluate these experiments now because just the last positive dilution tubes have to be counted in MPN population estimates, just those ones that develop last.

Assays of the various forms of particulate iron in sediment columns confirmed the expected prevalence of ferric iron in the surface sediments and of ferrous iron in layers below the nitrate reduction zone. About 10 to 15 mM total iron was found in the solid phase of cores 3703, 3707, 3718 within the upper 5 cm, and about 40 mM in core 3714. The dominant redox state of iron in these layers was ferrous iron. Nonetheless, significant amounts of acid-soluble ferric iron could be detected down to at least 50 cm depth.

Oxidation products of N-15 ammonia in slurry assays and MPN tubes have to be identified by gas chromatography/mass spectrometry in our home lab upon return.

An unusually long, thin, rod-shaped bacteria-like organism was found at high numbers in slimy channels (worm holes?) in core 3714-9 at a depth of about 620 cm, right in the region where maximum sulfate-dependent methane oxidation was observed. Samples of this material were diluted in a medium containing sulfate and methane, and also in a similar medium containing peptone, glutamate, acetate, and ethanol as substrates. If we get anything growing we will check for its possible involvement in the geochemical transformation processes observed.

We also tried to take samples of the magnetic bacteria studied by H. Petermann in culture, with ferrous iron and nitrate as substrates, but we cannot judge yet whether this approach was successful.

These and all further experiments have to be continued in our labs in Konstanz before any conclusions can be drawn. The same applies to the hydrogen analyses in the extracted gas samples.

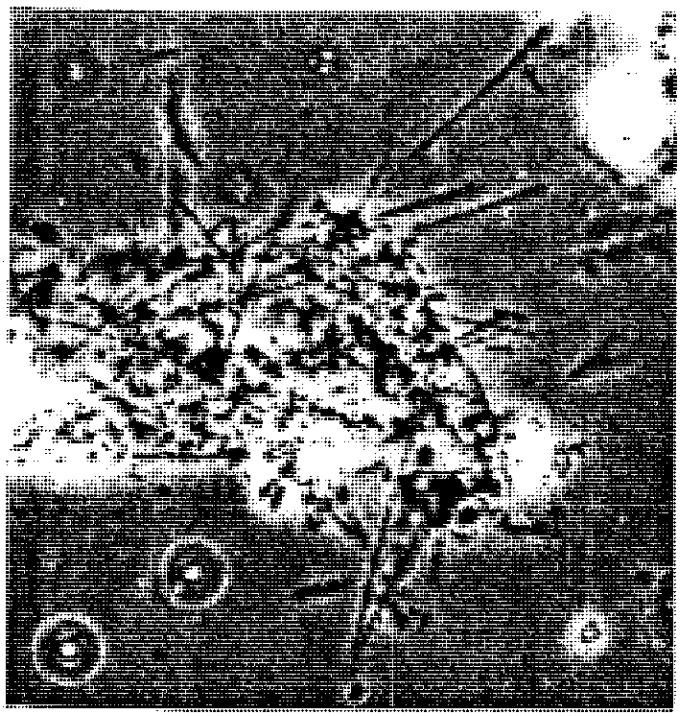

Fig. 118: Bacteria-like organisms, found in core 3714-9 at a depth of about 620 cm. 1100-fold-magnification.

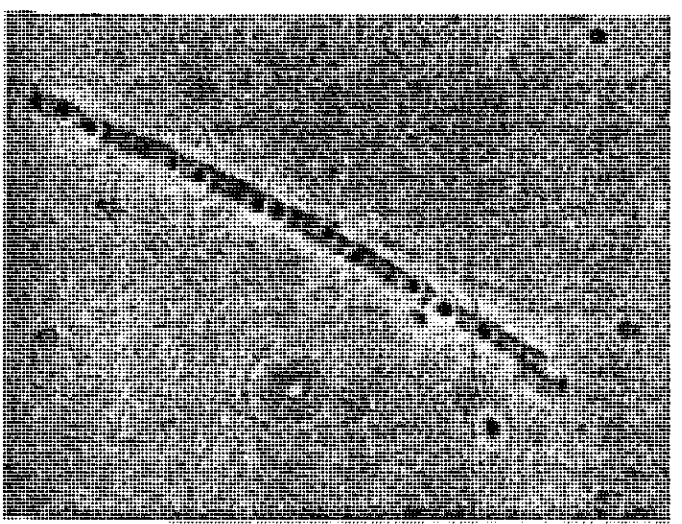

Fig. 119: 2760-fold-magnification.

Acknowledgement

We want to express our gratitude to the chief scientist, Prof. Dr. H.D. Schulz, and his crew for his invitation to participate in this unique research experience, for a perfect organization of the total trip and all the logistic help before and during the cruise. We are grateful as well to the crew of the research vessel METEOR for their perfect cooperation in all technical problems arising on board, as well as to the DFG and the BMBF, Bonn, for financial support and for supply and maintenance of this excellent research vessel. Part of this research program is supported by SFB 248 "Stoffhaushalt des Bodensees", Universität Konstanz.

5.2.6 Magnetotactic Bacteria

(H. Petermann)

5.2.6.1 Introduction

Magnetotactic bacteria synthesize intracellularly magnetite particles of distinct morphologies and in a narrow size distribution. These particles are called magnetosomes. Their formation is controlled by a membrane that surrounds the magnetosomes. Magnetotactic bacteria live in the sediment within a well defined near surface layer.

The biological advantage of intracellular magnetite formation is not yet satisfactorily understood. A possible explanation is that magnetotactic bacteria use their magnetosomes for orientation in the Earth's magnetic field. When displaced from their adequate environment in the sediment, they can swim back along a straight line parallel to the Earth's magnetic field. Magnetotactic bacteria from the northern hemisphere preferably swim towards the north, magnetotactic bacteria from the southern hemisphere swim to the south. In both cases they swim down to the sediment.

After lysis of the organic parts of the bacteria, magnetosomes are preserved in many sediments and contribute to a variable degree to the remanent magnetization. Due to their specific magnetic properties, they should be excellent recorders of the palaeomagnetic signal.

5.2.6.2 Sampling

During the cruise surface sediment samples recovered with the of multiple corer at 23 sites were investigated for living magnetotactic bacteria (Tab. 17). For each core depth profiles were taken with a piston pipette, that allows to sample individual layers. When the pipette is sticked through the sediment surface to a chosen depth, the piston prevents collecting particles from higher layers.

5.2.6.3 Investigation Technique

During earlier expeditions it turned out, that magnetic bacteria from deep-sea sediments are rather sensitive to warming in the laboratory. In order to attain quantitative estimates of the number of magnetotactic bacteria, the samples were therefore kept cool during each step of the investigation:

After retrieval on board the cores were immediately stored in a refrigerator. Measurements indicated that temperature in the core never was higher than 8°C.

Microscopic observations were done at room temperature of about 20°C. During observation the specimen slide was cooled by pumping iced water through the microscope table. To prevent advection of warmer air from the laboratory, an insulated metal lid with a glass cover was installed over the microscope slide. Measurements indicate that the temperature rises to about 14°C when the sample is carried from the core stored in the refrigerator to the microscope. After three minutes under the metal lid the temperature of the speciman decreased to less than 10°C, the equilibrium temperature does not exceed 7°C.

During the cruise living magnetotactic bacteria were investigated using a specially equipped inverse microscope. Three pairs of orthogonal coils cancel the Earth's magnetic field and provide a homogeneous magnetic field $< 3 \cdot 10^{-4}$ T of adjustable direction. Magnetotactic bacteria can be identified by their swimming behaviour parallel to the magnetic field. Bacteria that follow repeated changes of the field direction can definitely be distinguished from nonmagnetic bacteria.

50 µl of sediment suspension (from a defined depth) are placed to the microscope slide. Depending on the water content, a fringe of water of variable extent forms around the sediment. Magnetotactic bacteria swim parallel to the direction of the applied magnetic field until they reach the edge of the drop where they are counted. Important observations are recorded on videotape.

It was not possible to detect magnetotactic bacteria in the central part of the drop, because an observation is complicated there by the dense suspension of opaque minerals which move due to the vibration of the ship.

5.2.6.4 Results

Magnetotactic bacteria were detected at 22 of 23 sampling sites. A summary of the results including geographical position, water depth, maximum number of magnetotactic bacteria in 50 µl and the depth of their highest concentration is given in Table 17.

At almost all sites from water depths of less than 2600 m extremely high concentrations of magnetotactic bacteria were found. The only exception was the first station GeoB 3701 at a water depth of 1488 m. The colour of the sediment pale olive (5Y6/3), as well as the

porewater profiles (see Enneking et al., chapter 5.2.5.2) indicate, that the first site lies south if the Benguela upwelling area. On transect B leading from shallow sites on the upper continental slope to the center of the Cape Basin the abundance of magnetotactic bacteria drastically decreased with increasing distance from the coast especially for water depths of more than 2600 m. In the core GeoB 3724 from a water depth of 4759 m actively swimming magnetotactic bacteria could not be unambiguously identified. In 0.5 cm depth one living bacterium could be observed, that three times followed the changing field direction, but other times did not. Therefore it could not be safely identified as a magnetotactic bacterium. The geographic distribution of the samples with a classification of the respective numbers of magnetotactic bacteria is shown in Figure 120.

Table 17: Sampling sites, maximum number of magnetotactic bacteria in 50 µl of sediment and depth of maximum abundance of magnetotactic bacteria. At four stations the numbers of magnetotactic bacteria are bracketed, because not enough observations could be done to get reliable results

Station	Latitude	Longitude	Water depth [m]	Maximum number of magnetotactic bacteria	Depth of maximum abundance [cm]
Transect A					
GeoB 3701	27°57.1'S	14°00.2'E	1488	25	3
GeoB 3702	26°47.5'S	13°27.3'E	1311	30000	2
GeoB 3703	25°31.0'S	13°13.9'E	1376	10000	2
GeoB 3704	25°28.0'S	13°05.0'E	1780	(12000)	2
GeoB 3705	24°18.2'S	12°59.8'E	1308	15000	2
GeoB 3706	22°43.2'S	12°36.1'E	1313	10000	2.5
GeoB 3707	21°37.5'S	12°11.6'E	1347	20000	1.6
GeoB 3709	21°29.0'S	11°15.3'E	2709	60	3
GeoB 3710	20°39.7'S	11°24.2'E	1312	20000	1
GeoB 3711	19°50.1'S	10°46.1'E	1214	10000	2
GeoB 3712	17°11.2'S	11°07.5'E	1243	5000	1.5
GeoB 3713	15°37.6'S	11°34.9'E	1322	10000	1.5
GeoB 3714	17°19.6'S	10°59.9'E	2062	12000	1
GeoB 3715	18°57.3'S	11°03.4'E	1203	(2000)	2
Transect B					
GeoB 3717	24°50.0'S	13°21.8'E	858	80000	0.6
GeoB 3718	24°53.7'S	13°09.8'E	1310	18000	1.5
GeoB 3719	24°59.8'S	12°52.4'E	1995	9000	2
GeoB 3720	25°04.1'S	12°40.0'E	2518	4500	3
GeoB 3721	25°09.1'S	12°15.0'E	3017	15	2
GeoB 3722	25°15.0'S	12°01.4'E	3505	(1)	1
GeoB 3723	25°23.6'S	11°31.5'E	4024	7	0.5
GeoB 3724	26°08.2'S	08°55.6'E	4759	0	-
GeoB 3725	23°19.0'S	12°22.2'E	1984	(10000)	3

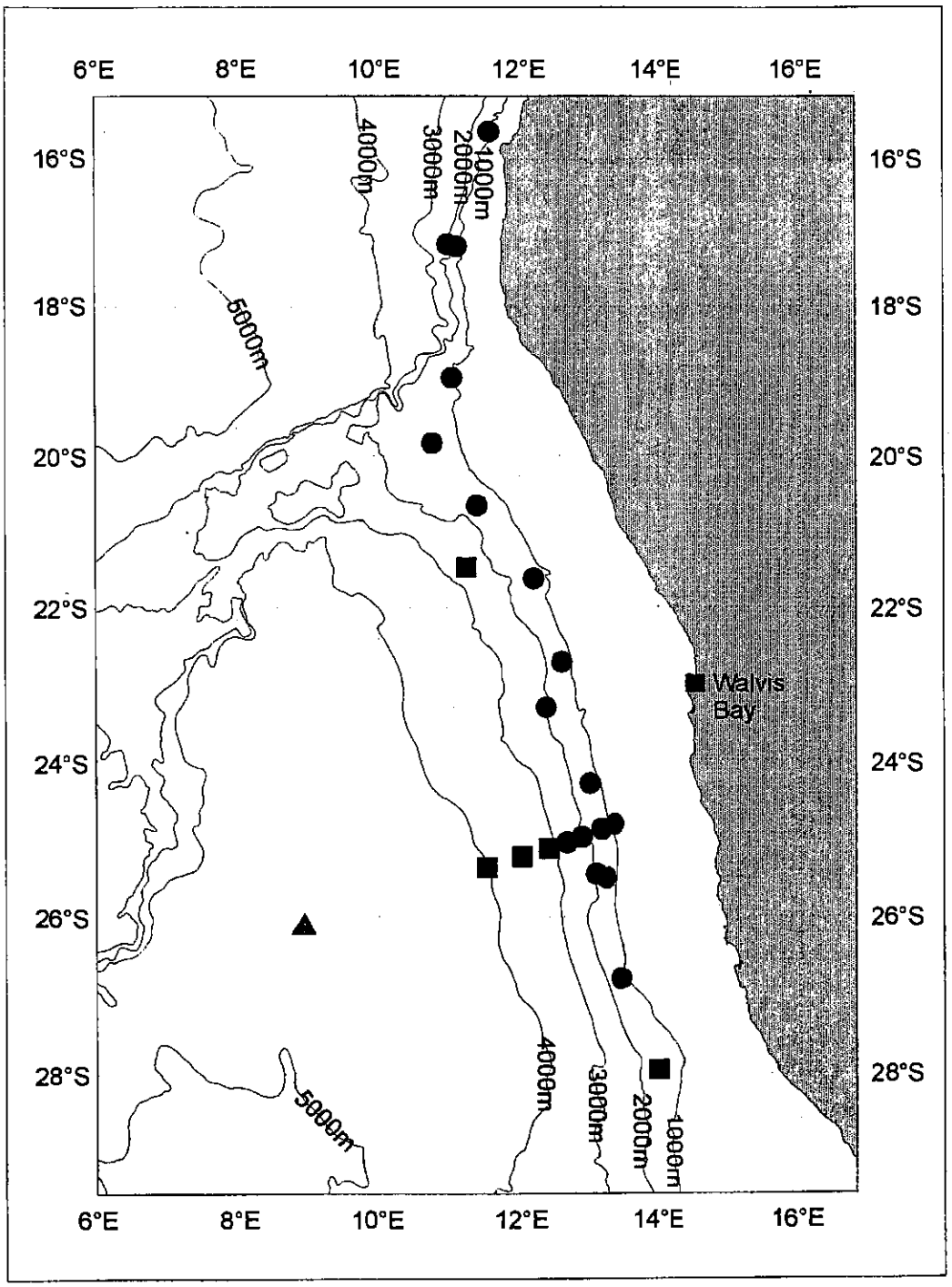

Fig. 120: Map of the sampling sites for magnetotactic bacteria. Dots denote sites with maximum concentrations of more than 100 magnetotactic bacteria, filled squares sites with maximum concentrations between 1 and 100 in a sample of 50 µl. The filled triangle marks the site, where no actively swimming magnetotactic bacteria could be detected.

The numbers of magnetotactic bacteria were generally very high at the stations of transect A, except the first station. The actual maximum numbers are plotted versus the geographical latitude in Figure 121.

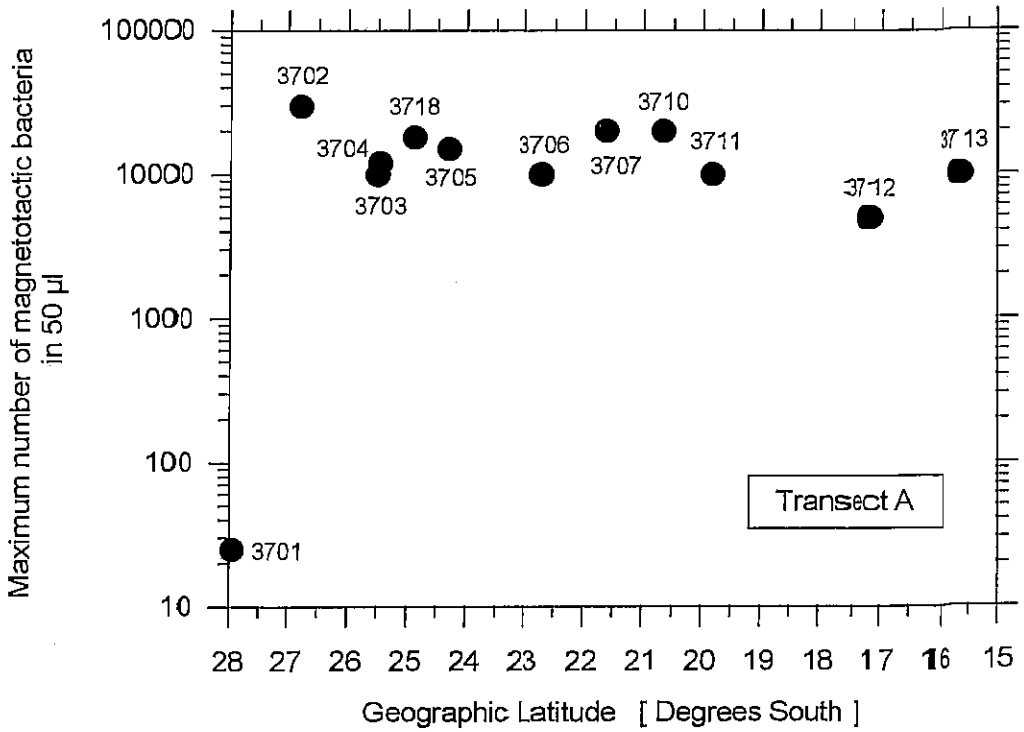

Fig. 121: Maximum concentrations of magnetotactic bacteria in 50 µl for the stations on transect A of water depths between 1200 m and 1800 m. The data point labels denote the GeoB number.

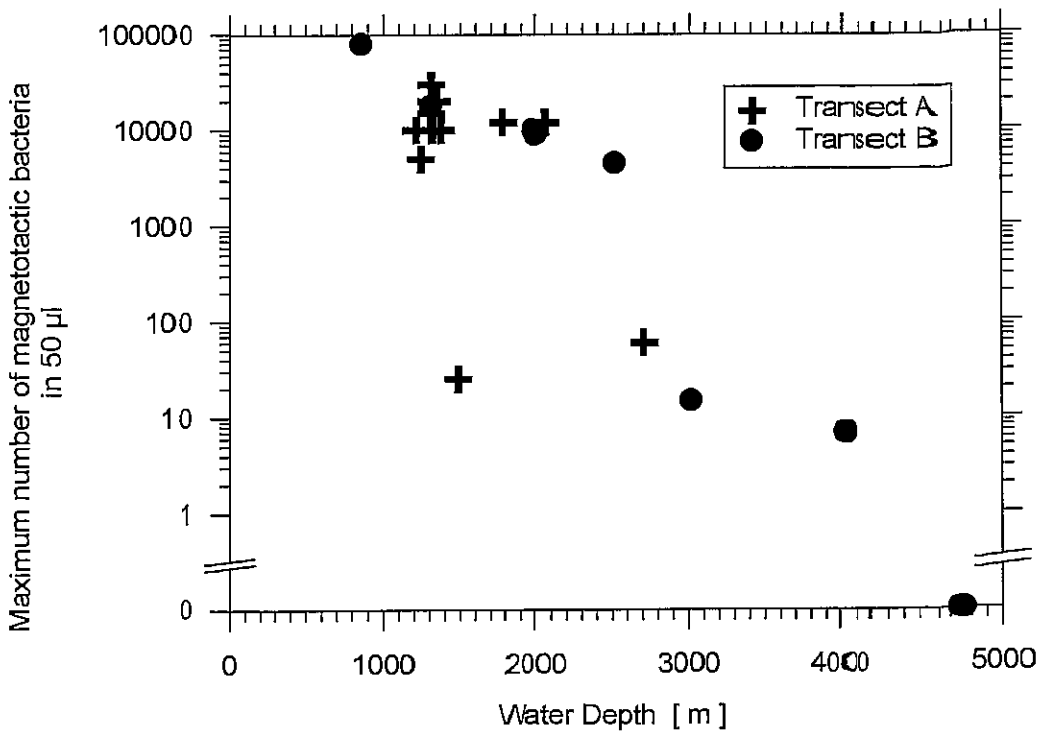

Fig. 122: Maximum concentrations of magnetotactic bacteria as a function of water depth at the sampling sites. Different symbols denote stations of Transect A, Transect B and the other stations.

From Figure 120 and Table 17 it is obvious, that the number of counted magnetic bacteria decreases with increasing water depth at the sampling site. In Figure 121 the maximum concentrations of magnetotactic bacteria at each site is plotted as a function of water depth. A drastic decrease occurs at water depths of more than 2600 m.

Depth profiles of magnetotactic bacteria

At every site the depth distribution of the magnetotactic bacteria in the sediment was determined. They live in close to the sediment-surface, the depth of the highest concentration varying between 0.5 and 3 cm (see Tab. 17). No actively swimming magnetotactic bacteria were found in layers deeper than 20 cm. Figure 122 depicts the depth profiles of magnetotactic bacteria for six stations combined with depth profiles of nitrate and iron in the pore-water (data from Enneking et al., chapter 5.2.5.2). Maximum numbers of magnetotactic bacteria were found in the denitrification zone below the maximum concentration of nitrate. Oxygen penetrates into the sediment to about the depth of maximum nitrate concentration. Thus most of the magnetotactic bacteria live in anaerobic sediments, indicating that the majority of magnetic bacteria permanently dwells in the anoxic zone.

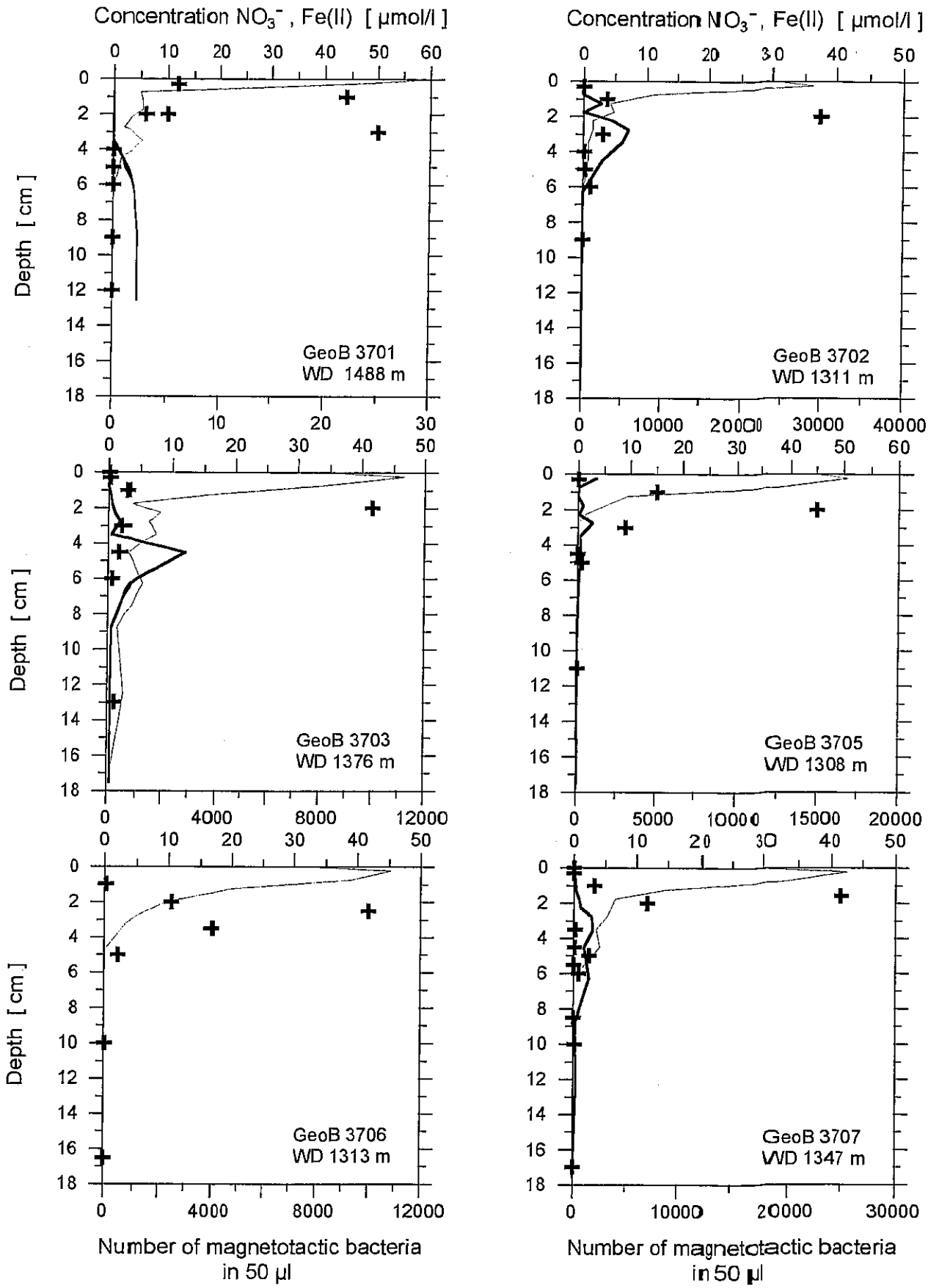

Fig. 123: Depth profiles of magnetotactic bacteria (symbols), of nitrate (thin solid line) and of iron measured in the pore-water (data from Enneking et al., chapter 5.2.5.2) for six stations. The names of the stations and the respective water depths are noted in each plot.

5.2.7 CTD-Profiling

(B. Donner and G. Kirst)

The hydrographic conditions were recorded by a Seabird SBE 19 CTD profiler which was used at 24 stations. Equipped with a data storing unit, the profiler can be deployed without being connected to shipboard instruments. It was attached to the cable 20 to 50 m (depending on the water depth of the stations) above the multicorer. The SBE 19 has sensors for pressure, conductivity, temperature and oxygen. Additionally, it is supplemented with a Sea Tech 25 cm light beam transmissiometer. The parameters' measuring is done in 0,5 sec intervals during the down-diving and also during up-diving. After each deployment the raw data were read out immediately and (according to the diving) split into downcast and upcast values. The downcast data were averaged and used for a standard plot.

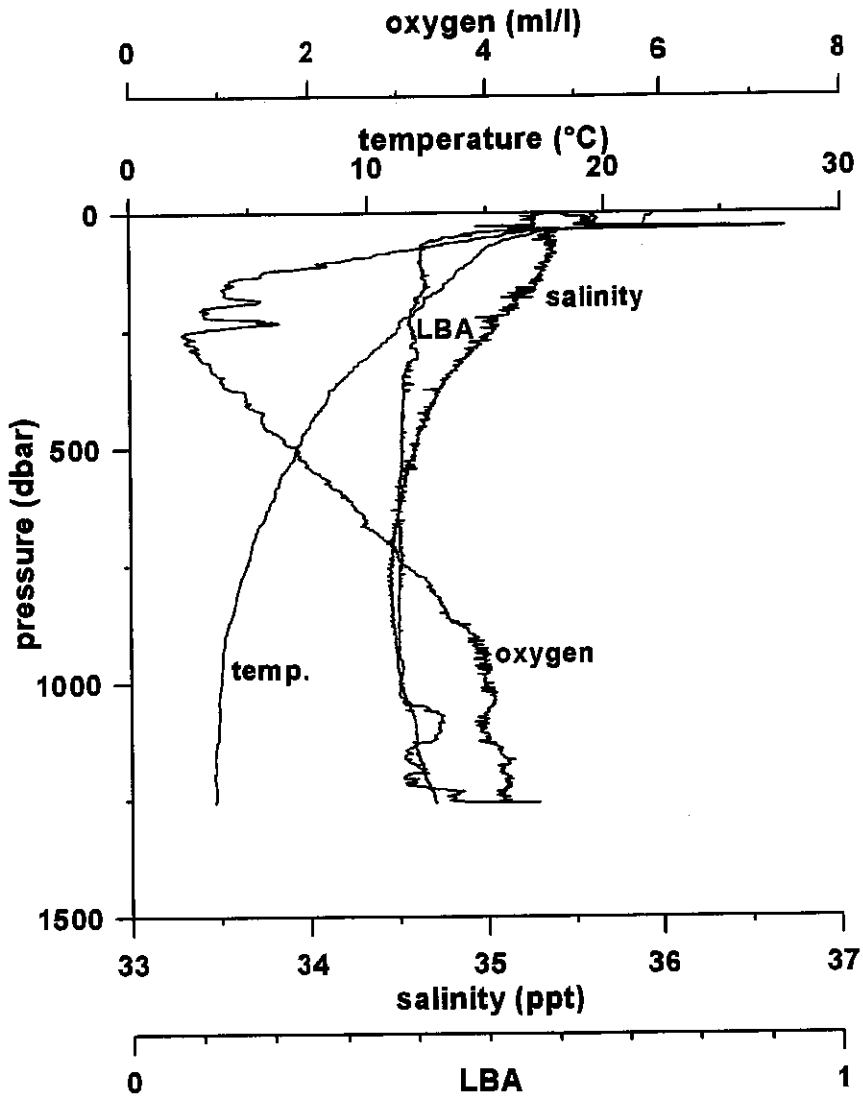

Fig. 124: CTD-data from station GeoB 3708-1 in the northern Cape Basin (wd 1286 m).

During the deployment of the SBE 19 on transect A (northern Cape Basin to southern Angola Basin) the O_2 recording became worse from cast to cast. We rinsed the sensor with fresh water, cleaned it with detergent (Triton X 100), but, probably due to high nutrient concentrations in this upwelling area, the sensor was blocked and from then on recorded only periodically. During transect B (from shelf to deep sea basin) we reached greater water depths with clearer, nutrient poor waters and expected a better recording. But, here also, the sensor only worked during the upper few 100 meters and then clogged. The O_2 membrane is very fragile, once defect or clogged, it is not possible to regenerate it. For METEOR cruise M34/4 a new sensor was ordered.

Figure 124, as an example, shows the data from a station in the northern Cape Basin, wd 1286 m. All sensors worked during the downcast. The O_2 minimum is in ca. 100-300 m water depth. Temperature is 3°C at the sea floor. The light beam attenuation is nearly constant from 50 m downwards, becoming greater near the sea floor. In the upper 50 m it is also greater due to the higher nutrient concentrations (photic zone).

5.2.8 Pumped Net Samples

(B. Donner, G. Kirst, B. Meyer-Schack and K. Slickers)

Marine plankton from surface waters was sampled during the whole cruise (Tab. 18). Each day we filtered 100 to 2000 l with the help of the shipboard-installed pump. The exact amount of water depended of its plankton concentration. The quicker the 10 µm net openings closed, the sooner the water flow was stopped and registered. The concentrated plankton in the net was washed into Kautex bottles and frozen at -20°C. The net was washed and used again.

The material will be used to investigate the composition of biogenic detritus. We are interested in a comparison with the fluxes of biogenic particles caught in sediment traps.

5.2.9 Sampling for Chlorophyll-a Measurements

(B. Donner, G. Kirst, B. Meyer-Schack and K. Slickers)

For the determination of chlorophyll-a concentrations in surface waters, 0.5 l of seawater was collected 3 times a day from the ship's seawater pump (inlet in 3.5m water depth). The water was filtered onto glass fibre filters, kept dark and frozen to -20°C. The measurements of chlorophyll-a will be carried out in Bremen.

The chlorophyll-a data should give information on the seasonal and regional variations in primary productivity and, therefore make it possible to calibrate satellite data for chlorophyll-a concentrations.

For sampling locations see Table 19.

Tab. 18: Plankton Pump Samples M34/2

		Start Filtration:						Stop Filtration:						
Nr.	Date	Time (Local)	Position Latitude	Longitude	Sal. [°/oo]	Temp. [°C]	Water-clock	Time (Local)	Position Latitude	Longitude	Sal. (°/oo)	Temp. (°C)	Water-clock	liters pumped
1	30.01.96	08:30	25°00,3 S	13°07,0 E	32,80	19,6	395472	16:00	26°31,1 S	13°34,2 E	32,98	19,8	395661	189
2	31.01.96	12:15	26°50,5 S	13°28,4 E	33,02	20,9	396404	21:20	25°31,4 S	13°11,4 E	32,09	19,3	398075	1671
3	01.02.96	08:15	25°31,0 S	13°13,9 E	32,75	18,1	398075	09:15	25°31,0 S	13°13,9 E	32,75	18,1	398269	194
4	02.02.96	10:00	24°18,2 S	12°59,8 E	32,97	21,0	398269	13:45	24°07,9 S	12°56.4 E	32,96	20,9	399350	1081
5	03.02.96	09:45	21°37,5 S	12°11,6 E	33,11	22,2	399350	20:00	21°37,5 S	12°11,6 E	33,10	22,1	400661	1311
6	04.02.96	08:15	21°39,9 S	12°05,1 E	33,26	22,5	400661	20:00	21°05,4 S	11°49,5 E	33,10	22,2	402685	2024
7	05.02.96	08:20	21°24,5 S	11°16,4 E	33,10	22,2	402685	20:00	20°09,2 S	11°00,7 E	33,20	22,0	404552	2133
8	06.02.96	07:45	18°57,3 S	11°03,3 E	33,55	23,0	404552	14:40	18°09,6 S	11°13,7 E	33,29	19,9	405562	1010
9	07.02.96	08:00	15°40,7 S	11°31,0 E	33,95	23,7	405569	18:00	16°48,5 S	11°07,2 E	33,58	21,5	405989	420
10	08.02.96	08:00	17°10,9 S	11°06,3 E	33,20	19,3	405992	18:30	17°09,6 S	10°59,9 E	33,49	21,2	406300	311
11	09.02.96	08:30	18°26,7 S	11°01,2 E	33,39	22,1	406300	17:40	19°30,2 S	11°17,6 E	33,26	22,0	407245	1945
12	11.02.96	14:30	24°43,8 S	13°40,9 E	32,58	17,6	407355	16:00	24°48,9 S	13°24,0 E	32,54	17,7	407835	480
13	12.02.96	08:00	25°00,5 S	12°53,4 E	32,91	20,6	407836	14:15	24°53,7 S	13°09,6 E	32,72	19,0	408452	617
14	13.02.96	08:40	25°04,1 S	12°40,2 E	33,13	21,7	408459	20:00	25°9,1 S	12°24,0 E	33,23	22,1	412262	3803
15	14.02.96	08:50	25°14,9 S	12°01,4 E	33,18	22,1	412268	20:20	25°27,1 S	11°19,1 E	33,02	21,4	416136	3868
16	15.02.96	08:45	26°07,9 S	08°56,0 E	33,47	22,4	416140	17:30	26°08,2 S	08°55,6 E	33,49	22,6	420446	4306
17	16.02.96	09:15	25°31,6 S	11°03,9 E	33,27	22,0	420453							

Salinitätswerte von Schiffssalinometer korrigiert um 2,3 %o (keine Eichung nach Werftaufenthalt !!!)

Tab. 19: Sampling locations for chlorophyll-a measurements

No.	date	time UTC	location	water-depth [m]	salinity [‰]	water-temperature [C]	sample-volume [l]
51	30.1.96	11:25	25°52.6S; 13°22.6E	1099	32,91	20,3	0.5
52	30.1.96	16:10	26°41.4S; 13°37.2E	755	33,05	20,7	0.5
53	31.1.96	5:55	27°38.4S; 13°51.2E	1665	33,08	20,9	0.5
54	31.1.96	10:20	26°50.5S; 13°28.4E	1325	33,02	20,6	0.5
55	31.1.96	17:30	26°00,4S; 13°15,1E	1200	32,09	19,3	0.5
56	1.2.96	5:15	25°31.0S; 13°13.7E	1384	32,75	18,1	0.5
57	1.2.96	16:30	25°31.0S; 13°13.0E	1412	32,77	19,0	0.5
58	2.2.96	6:00	24°18.5S; 12°59.9E	1306	32,92	20,9	0.5
59	2.2.96	13:45	24°07,9S; 12°56.4E	1359	32,96	20,9	0.5
60	2.2.96	18:10	23°14.6S; 12°43.6E	1183	33,05	21,5	0.5
61	3.2.96	12:15	11°37.5S, 12°11.6E	1352	33,12	22,3	0.5
62	3.2.96	19:00	21°37.4S, 12°11.8E	1347	33,09	22,2	0.5
63	4.2.96	07:40	21°36.8S, 12°02.3E	1587	33,25	22,4	0.5
64	4.2.96	13:00	21°38.0S, 12°11.9E	1350	33,16	22,3	0.5
65	4.2.96	18:00	21°14.1S, 11°55.5E	1291	33,22	22,5	0.5
66	5.2.96	07:30	21°29.0S, 11°15.4E	2709	33,08	22,1	0.5
67	5.2.96	13:45	20°39.7S, 11°24.0E	1314	33,12	21,8	0.5
68	5.2.96	18:50	20°18.5S, 11°07.9E	1313	33,32	22,3	0.5
69	6.2.96	07:30	18°58,6S, 11°02,9E	1212	33,50	23,0	0.5
70	6.2.96	13:30	18°20.9S, 11°15.6E	1283	33,33	21,7	0.5
71	6.2.96	19:00	17°16.6S, 11°12.6E	753	33,25	19,4	0.5
72	7.2.96	08:00	15°41.4S, 11°30.9E	1675	33,97	23,7	0.5
73	7.2.96	13:30	15°58,5S, 11°24.6E	1420	33,81	22,4	0.5
74	7.2.96	20:00	17°07.1S, 11°00.7E	1988	33,13	20,2	0.5
75	8.2.96	07:30	17°11.6S, 11°09.5E	1097	33,25	19,2	0.5
76	8.2.96	12:30	17°09,5S, 11°00.1E	2044	33,47	20,8	0.5
77	9.2.96	07:30	18°14,8S; 11°00.3E	2947	33,38	22,1	0.5
78	9.2.96	13:20	18°57,3S; 11°03.5E	1197	33,54	23,7	0.5
79	9.2.96	19:30	17°51,3S: 11°26,7E	754	33,40	22,4	0,5
80	10.2.96	08:00	21°51,5S; 12°28,4E	909	32,90	21,4	0,5
81	10.2.96	13:30	22°41,5S; 13°09,3E	314	32,90	20,8	0,5
82	11.2.96	08:00	24°02,3S; 14°06,7E	160	32,60	17,0	0,5
83	11.2.96	13:30	24°40,0S; 13°53,8E	230	32,53	16,5	0,5
84	11.2.96	18:20	24°50,0S; 13°21,8E	858	32,58	17,7	0,5
85	12.2.96	07:50	25°20,1S; 12°51,6E	2060	32,90	20,9	0,5
86	12.2.96	14:00	24°53,7S; 13°09,6E	1316	32,78	19,0	0,5
87	13.2.96	07:30	25°00,5S; 12°49,9E	2087	32,98	21,4	0,5

No.	date	time UTC	location	water-depth [m]	salinity [‰]	water-temperature [C]	sample-volume [l]
88	13.2.96	18:15	25°08,9S; 12°23,8E	3029	33,26	22,4	0,5
89	14.2.96	08:00	25°15,0S; 12°01,3E	3508	33,20	22,1	0,5
90	14.2.96	13:10	25°23,6S; 11°31,7E	4000	33,10	21,9	0,5
91	14.2.96	19:30	25°24,2S; 11°29,5E	4038	33,11	21,8	0,5
92	15.2.96	07:30	26°03,9S; 09°10,0E	4735	33,50	22,4	0,5
93	15.2.96	13:15	26°08,2S; 08°55,6E	4764	33,50	22,5	0,5
94	16.2.96	08:00	25°34,9S; 10°52,3E	4340	33,34	22,1	0,5
95	16.2.96	13:45	25°17,8S; 11°52,4E	3650	33,22	22,3	0,5
96	17.2.96	07:30	23°43,7S; 11°42,3E	3070	33,26	22,4	0,5
97	17.2.96	13:30	23°19,2S; 12°22,1E	1984	33,04	21,9	0,5

Publications from METEOR expeditions in other reports

Gerlach, S.A., J. Thiede, G. Graf und F. Werner (1986): Forschungsschiff Meteor, Reise 2 vom 19. Juni bis 16. Juli 1986. Forschungsschiff Poseidon, Reise 128 vom 7. Mai bis 8. Juni 1986. Ber. Sonderforschungsbereich 313, Univ. Kiel, 4, 140 S.

Siedler, G., H. Schmickler, T.J. Müller, H.-W. Schenke und W. Zenk (1987): Forschungsschiff Meteor, Reise Nr. 4, Kapverden - Expedition, Oktober - Dezember 1986. Ber. Inst. f. Meeresk., 173, Kiel, 123 S.

Wefer, G., G.F. Lutze, T.J. Müller, O. Pfannkuche, W. Schenke, G. Siedler und W. Zenk (1988): Kurzbericht über die Meteor - Expedition Nr. 6, Hamburg - Hamburg, 28. Oktober 1987 - 19. Mai 1988. Berichte, Fachbereich Geowissenschaften, Universität Bremen, 4, 29 S.

Müller T.J., G. Siedler und W. Zenk (1988): Forschungsschiff Meteor, Reise Nr. 6, Atlantik 87/88, Fahrtabschnitte Nr. 1 - 3, Oktober - Dezember 1987. Ber. Inst. f. Meeresk., 184, Kiel, 77 S.

Lutze, G.F., C.O.C. Agwu, A. Altenbach, U. Henken-Mellies, C. Kothe, N. Mühlhan, U. Pflaumann, C. Samtleben, M. Sarnthein, M. Segl, Th. Soltwedel, U. Stute, R. Tiedemann und P. Weinholz (1988): Bericht über die "Meteor" -Fahrt 6-5, Dakar - Libreville, 15.1.-16.2.1988.Berichte - Reports, Geol. Paläont. Inst., Univ. Kiel, 22, 60 S.

Wefer, G., U. Bleil, P.J. Müller, H.D. Schulz, W.H.Berger, U. Brathauer, L. Brück, A. Dahmke, K. Dehning, M.L. Durate-Morais, F. Fürsich, S. Hinrichs, K. Klockgeter, A. Kölling, C. Kothe, J.F. Makaya, H. Oberhänsli, W. Oschmann, J. Posny, F. Rostek, H. Schmidt, R. Schneider, M. Segl, M. Sobiesiak, T. Soltwedel und V. Spieß (1988): Bericht über die Meteor - Fahrt M 6-6, Libreville - Las Palmas, 18.2.1988 - 23.2.1988. Berichte, Fachbereich Geowissenschaften, Universität Bremen, 3, 97 S.

Hirschleber, H., F. Theilen, W. Balzer, B. v. Bodungen und J. Thiede (1988): Forschungsschiff Meteor, Reise 7, vom 1. Juni bis 28. September 1988, Ber. Sonderforschungsbereich 313, Univ. Kiel, 10, 358 S.

METEOR-Berichte
List of publications

89-1	(1989) Meincke, J., Quadfasel, D.	GRÖNLANDSEE 1988-Expedition, Reise Nr. 8, 27. Oktober 1988 - 18. Dezember 1988. Universität Hamburg, 40 S.
89-2	(1989) Zenk, W., Müller, T.J., Wefer, G.	BARLAVENTO-Expedition, Reise Nr. 9, 29. Dezember 1988 - 17. März 1989. Universität Hamburg, 238 S.
90-1	(1990) Zeitschel, B., Lenz, J., Thiel, H., Boje, R., Stuhr, A., Passow, U.	PLANKTON'89 - BENTHOS'89, Reise Nr. 10, 19. März - 31. August 1989. Universität Hamburg, 216 S.
90-2	(1990) Roether, W., Sarnthein, M., Müller, T.J., Nellen, W., Sahrhage, D.	SÜDATLANTIK-ZIRKUMPOLARSTROM, Reise Nr. 11, 3. Oktober 1989 - 11. März 1990. Universität Hamburg, 169 S.
91-1	(1991) Wefer, G., Weigel, W., Pfannkuche	OSTATLANTIK 90 - EXPEDITION, Reise Nr. 12, 13. März - 30. Juni 1990. Universität Hamburg, 166 S.
91-2	(1991) Gerlach, S.A., Graf, G.	EUROPÄISCHES NORDMEER, Reise Nr. 13, 6. Juli - 24. August 1990. Universität Hamburg, 217 S.
91-3	(1991) Hinz, K., Hasse, L., Schott, F.	SUBTROPISCHER & TROPISCHER ATLANTIK, Reise Nr. 14/1-3, Maritime Meteorologie und Physikalische Ozeanographie, 17. September - 30. Dezember 1990. Universität Hamburg, 58 S.
91-4	(1991) Hinz, K.	SUBTROPISCHER & TROPISCHER ATLANTIK, Reise Nr. 14/3, Geophysik, 31. Oktober - 30. Dezember 1990. Universität Hamburg, 94 S.
92-1	(1992) Siedler, G., Zenk, W.	WOCE Südatlantik 1991, Reise Nr. 15, 30. Dezember 1990 - 23. März 1991. Universität Hamburg, 126 S.
92-2	(1992) Wefer, G., Schulz, H.D., Schott, F., Hirschleber, H. B.	ATLANTIK 91 - EXPEDITION, Reise Nr. 16, 27. März - 8. Juli 1991. Universität Hamburg, 288 S.

92-3	(1992) Suess, E., Altenbach, A.V.	EUROPÄISCHES NORDMEER, Reise Nr. 17, 15. Juli - 29. August 1991. Universität Hamburg, 164 S.
93-1	(1993) Meincke, J., Becker, G.	WOCE-NORD, Cruise No. 18, 2. September - 26. September 1991. NORDSEE, Cruise No. 19, 30 September - 12 October 1991. Universität Hamburg, 105 pp.
93-2	(1993) Wefer, G., Schulz, H.D.	OSTATLANTIK 91/92 - EXPEDITION, Reise Nr. 20, M 20/1 und M 20/2, 18. November 1991 - 3. Februar 1992. Universität Hamburg, 248 S.
93-3	(1993) Wefer, G., Hinz, K., Roeser, H.A.	OSTATLANTIK 91/92 - EXPEDITION, Reise Nr. 20, M 20/3, 4. Februar - 13. März 1992. Universität Hamburg, 145 S.
93-4	(1993) Pfannkuche, O., Duinker, J.C., Graf, G., Henrich, R., Thiel, H., Zeitschel, B.	NORDATLANTIK 92, Reise Nr. 21, 16. März - 31. August 1992. Universität Hamburg, 281 S.
93-5	(1993) Siedler, G., Balzer, W., Müller, T.J., Rhein, M., Onken, R., Zenk, W.	WOCE South Atlantic 1992, Cruise No. 22, 22 September 1992 - 31 January 1993. Universität Hamburg, 131 pp.
94-1	(1994) Bleil, U., Spieß, V., Wefer, G.	Geo Bremen SOUTH ATLANTIC 1993, Cruise No. 23, 4 February - 12 April 1993. Universität Hamburg, 261 pp.
94-2	(1994) Schmincke, H.-U., Rihm, O.	OZEANVULKAN 1993, Cruise No. 24, 15 April - 9 May 1993. Universität Hamburg, 88 pp.
94-3	(1994) Hieke, W., Halbach, P., Türkay, M., Weikert, H.	MITTELMEER 1993, Cruise No. 25, 12 May - 20 August 1993. Universität Hamburg, 243 pp.
94-4	(1994) Suess, E., Kremling, K., Mienert, J.	NORDATLANTIK 1993, Cruise No. 26, 24 August - 26 November 1993. Universität Hamburg, 256 pp.

94-5	(1994) Bröckel, K. von, Thiel, H., Krause, G.	ÜBERFÜHRUNGSFAHRT, Reise Nr. 0, 15. März - 15. Mai 1986. ERPROBUNGSFAHRT, Reise Nr. 1, 16. Mai - 14. Juni 1986. BIOTRANS IV, Skagerrak 86, Reise Nr. 3, 21. Juli - 28. August 1986. Universität Hamburg, 126 S.
94-6	(1994) Pfannkuche, O., Balzer, W., Schott, F.	CARBON CYCLE AND TRANSPORT OF WATER MASSES IN THE NORTH ATLANTIC - THE WINTER SITUATION, Cruise No. 27, 29 December - 26 March 1994. Universität Hamburg, 134 pp.
95-1	(1995) Zenk, W., Müller, T.J.	WOCE Studies in the South Atlantic, Cruise No. 28, 29 March - 14 June 1994. Universität Hamburg, 193 pp.
95-2	(1995) Schulz, H., Bleil, U., Henrich, R., Segl, M.	Geo Bremen SOUTH ATLANTIC 1994, Cruise No. 29, 17 June - 5 September 1994. Universität Hamburg, 323 pp.
96-1	(1996) Nellen, W., Bettac, W., Roether, W., Schnack, D., Thiel, H., Weikert, H., Zeitschel, B.	MINDIK (Band I), Reise Nr. 5, 2. Januar - 24. September 1987. Universität Hamburg, 275 S.
96-2	(1996) Nellen, W., Bettac, W., Roether, W., Schnack, D., Thiel, H., Weikert, H., Zeitschel, B.	MINDIK (Band II), Reise Nr. 5, 2. Januar - 24. September 1987. Universität Hamburg, 179 S.
96-3	(1996) Koltermann, K.P., Pfannkuche, O., Meincke, J.	JGOFS, OMEX and WOCE in the North Atlantic 1994, Cruise No. 30, 7 September - 22 December 1994. Universität Hamburg, 148 pp.
96-4	(1996) Hemleben, Ch., Roether, W., Stoffers, P.	Östliches Mittelmeer, Rotes Meer, Arabisches Meer, Cruise No. 31, 30 December 1994 - 22 March 1995. Universität Hamburg, 282 pp.

96-5 (1996) Lochte, K., Halbach, P., Flemming, B.W.
Biogeochemical Fluxes in the Deep-Sea and Investigations of Geological Structures in the Indian Ocean, Cruise No. 33, 22 September - 30 December 1995.
Universität Hamburg, 160 pp.

96-6 (1996) Schott, F., Pollehne, F., Quadfasel, D., Stramma, L., Wiesner, M., Zeitzschel, B.
ARABIAN SEA 1995, Cruise No. 32, 23 March - 19 September 1995.
Universität Hamburg, 163 pp

97-1 (1997) Wefer, G. Bleil, U. Schulz, H. Fischer, G.
Geo Bremen SOUTH ATLANTIC 1996 (Volume I), Cruise No. 34, 3 January - 18 February 1996.
Universität Hamburg, 254 pp.

97-2 (1997) Wefer, G. Bleil, U. Schulz, H. Fischer, G.
Geo Bremen SOUTH ATLANTIC 1996 (Volume II), Cruise No. 34, 21 February - 15 April 1996.
Universität Hamburg, 268 pp.

METEOR-BERICHTE

97-2

Geo Bremen South Atlantic 1996
Cruise No. 34
21 February - 15 April 1996
Volume II

Edited by:
Gerold Wefer, Ulrich Bleil, Horst Schulz, Gerhard Fischer

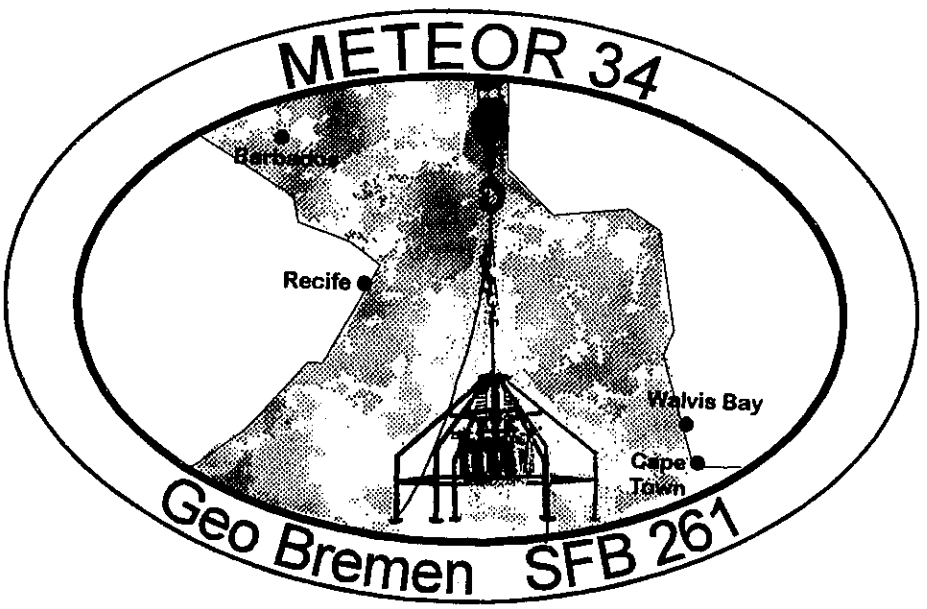

Editorial Assistance:
Sylvia Kemle-von Mücke

Universität Bremen Fachbereich Geowissenschaften

Leitstelle METEOR
Institut für Meereskunde der Universität Hamburg

1997

Table of Contents
Volume I

Table of Contents
Volume II

5.3 Marine Geoscience M 34/3

5.3.1 Hydrographic Observations and Recovery of the Moorings

(W. Zenk, M. Vanicek, D. Carlsen, A. Pinck)

Cruise M34/3 represented the last in a row of hydrographic expeditions from Kiel to the Brazil Basin. The Marine Physics Department of the Institut für Meereskunde (IfM) in Kiel is steadily involved in these studies of the western South Atlantic since 6 years. Surveys began in December 1990 during METEOR cruise Nr. 15 (M15). They were continued in December 1992 (M22) and June 1994 (M28), enhanced by POLARSTERN cruise ANT XII in November 1994 (SIEDLER and ZENK, 1992; SIEDLER et al., 1993; ZENK and MÜLLER, 1995; BOEBEL and SCHMID, 1995).

The scientific objectives of all these expeditions were in accordance with the requirements of the World Ocean Circulation Experiment (WOCE), a major component of the international World Climate Research Program. WOCE encompasses planning, implementation and coordinating of a global network of hydrographic observations and extensive modeling studies. The hydrographic work during M34/3 was part of the Deep Basin Experiment, a subprogram in Core Project 3 of WOCE.

WOCE contributions of IfM Kiel include the flows of Antarctic Intermediate Water and Antarctic Bottom Water in the tropical and subtropical South Atlantic. Research groups from Brazil, France, Germany, and the United States are incorporated in these scientific operations. During M34/3 supplementary hydrographic work was conducted to fill critical data gaps. We further recovered three RAFOS sound sources. They were moored on the southern margin of the Brazil Basin to provide insonification required for RAFOS float missions. RAFOS floats are neutral buoyant Lagrangian current meters. For the direct determination of prevailing circulation features of Antarctic Intermediate Water they were ballasted for the 900 m depth level (BOEBEL et al., 1996). Our float work in the western South Atlantic began in 1992. The majority of 72 deployed RAFOS floats from Kiel finished already their missions. The few remaining instruments from IfM Kiel are expected to terminate their underwater missions by mid of 1996. Three Aanderaa current meters were included in one of the sound source moorings (K3). It was their task to record current vectors in intermediate and near-bottom waters.

A summary of oceanographic stations is presented in Figure 125, Table 20 (in the next paragraph) contains the inventory of CTD stations taken during M34/3, while mooring activies are compiled in Table 21.

Methods

For the observation of continuous temperature and salinity profiles a conductivity-temperature-density recorder (CTD) by Neil Brown Instruments, Inc. (NB3) was used. In parallel, the geo-

logical group on board operated a Sea Bird CTD profiler in combination with their bottom samplers and corers. For intercomparison purposes a few CTD stations were occupied with simultaneous recordings of both devices.

The NB3 probe operated on the cable in combination with a rosette sampler holding 12 bottles (10 liter each), a pinger and a newly installed altimeter for bottom distance detection. The Sea Bird probe (SBE 19) is a self-contained instrument including an internal memory for data storage. Therefore this instrument could be easily attached to the NB3 unit for intercomparisons. Data were retrieved right after finishing of up-profiles via a serial memory dump.

In the beginning of the cruise a number of software adaptation were performed. A crucial role in CTD data analysis plays the proper match of sensor response time constants for temperature and conductivity. In case of inadequate adjustment, CTD profiles of inferred salinity show a great number of artificial spikes. Typical for an over/ undercompensated time constant match is a systematic shift towards higher/lower salinity values. An optimal adjustment of the time constant is essential for all fine- and microstructure studies in the water column. 'Best' performance characteristics for the used CTD probe NB3 was found by applying a time constant of 90 ms.

As an example Figure 126 demonstrates the impact of the time constant choice (no correction, 90, 140 ms) on the calculated salinity profiles. Data are taken from the initial test station No. 35 still on the eastern side of the Mid Atlantic Ridge (for position see Fig. 125). The profile contains a subset of salinity (S) data between the surface and a pressure (p) level of 300 dbar (Fig. 126a). One recognizes two high gradient zones (Fig. 126b) at ~50 and at ~240 dbar. Gradient profiles (dS/dp) were obtained by a simple first differencing scheme. In context with a sampling rate of approximately 0.1 $dbar^{-1}$ this method implies a high wave number filter. The same information presented as histograms (Fig. 126c) illuminates the influence of the time constant choice even more clearly.

The strictly simultaneous use of both CTD systems at nearly the same observation level in the same rosette mount stand offers us the opportunity for an intercomparison of both devices. Figure 127 shows the assembly of the two CTD instruments. The NB3 unit is situated in the center of the rosette sampler. In the foreground to the left we recognize the SBE 19 probe. When comparing hydrographic parameters sampled by both instruments, the problem of absolute pressure readings occurred to be a major one. The absolute member of the pressure calibration polynominum of the NB3 probe was tuned to a best fit with the Sea Bird probe. The still remaining differences between both instrument readings are shown in Figure 128. Apart from the mixed layer and the main thermocline of the water column temperature, electrical conductivity, and salinity agree well within reasonable limits. The intercomparison was performed with preliminary calibrations of the NB3 instrument, prior to the availability of check values from the rosette sampler. Future analyses need to consider better synchronisation of sampling intervals of the tested CTD systems.

Although both CTD systems were equipped with Beckman oxygen sensors neither of them delivered any useful results. The known necessity for oxygen titration of discrete samples in order to evaluate oxygen raw data profiles was once more confirmed. Due to shortage of qualified personnel no such analyses could be planned prior to the cruise.

We were disappointed about the malfunction of the altimeter by Tritech Inc., Ltd. which had been newly integrated into our NB3 system. A comparison of independent information was planned about the CTD's bottom clearance from the attached pinger, the standard bottom finder switch and the brand-new altimeter with its remote digital readout.

The rosette water sampler that was operated jointly with the NB3 CTD probe, delivered samples necessary for CTD salinity calibrations. 141 samples from the gradient poor depth levels (20 m, > 2200 m) were analyzed by an Autosal salinometer (No. 4) operated on board. Further water samples from the rosette were provided to interested members of other working groups on the METEOR. All CTD data were freely exchanged with the restraint of the preliminary character of the salinity data.

On the Stratification of the Subtropical South Atlantic

All CTD data collected by the NB3 system during the cruise are shown in Figure 129 - 142. Besides header information each figure contains full profiles of in-situ temperature and salinity (S). Beneath these two profiles we display potential temperature (θ) below 3000 dbar (deep stations only) and a θ/S diagram. Although the diagrams were drawn from preliminary data we expect postcruise corrections to be small, i.e. graphic alteration will not be recognizable.

The shown sets of figures can be separated into five categories:

(a) In accordance with the geological objectives of the cruise we took three CTD stations (Fig. 129 - 131) along the transect across the Mid Atlantic Ridge. Sta. 35 (see Fig. 129) displays the hydrographic stratification in the southern Angola Basin. Under a shallow mixed layer we find the upper most characteristic water mass, the South Atlantic Central Water with its tight θ/S relation (~ 6°C < θ <12°C) and an enclosure of Mode Water with reduced stratification at about 150 dbar. The most prominent feature in the salinity profile has its well expressed minimum at ~ 900 dbar. It is the manifestation of the Antarctic Intermediate Water laying above the North Atlantic Deep Water. The latter water mass reaches down to the bottom of the Angola Basin. No traces of Antarctic Bottom Water (θ < 2.0°C) could be identified, neither in the column of the eastern station (Sta. 35, Fig. 129) nor above the Mid Atlantic Ridge (Sta. 42, Fig. 130). We encountered this water mass on Sta. 47 (Fig. 131), not before reaching the southeastern end of the Brazil Basin (> 3300 dbar).

(b) After an intermediate station (Sta. 48, Fig. 132) at Hunter Channel primarily for biological purposes, a series of three full depth CTD stations (W to E: Sta. 51 - 49, Fig. 133 - 135) was occupied at Vema Sill (ZENK et al., 1993). With these new observations we continued a series

of deep stations in the region of the Vema Channel where a significant trend towards higher temperatures had been recorded by a number of methods and institutions since early 1991 (ZENK and HOGG, 1996).

(c) A second CTD series with three stations (W to E: Sta. 55, 53, 54, Fig. 136 - 138) was taken approximately 350 km north of the Vema Sill. Because of the narrowness of the Vema Channel a modest Hydromap survey was necessary to find its deepest trough at 28°S10' pointing towards the Northeast. Weddell Sea Deep Water, a subtype of Antarctic Bottom Water with $\theta <$ 0.2°C, is advected by the flow through the Vema Channel.

(d) A single CTD station No. 58 (Fig. 139) was taken in connection with mooring work (K3) in the region of the Vema Extension, ~ 840 km downstream from the Vema Sill. As expected a rich pool of Antarctic Bottom Water and Weddell Sea Deep Water was found. Detailed information on the advection of these water masses is contained in the over two year long current meter records that were recovered in connection with sound source K3.

(e) The four remaining CTD soundings collecting rosette samples for biological and geological purposes were performed on the return leg between the Vema Extension and Northeast Brazil (Sta. 61 - 64, Fig. 140 - 143). Since these CTD stations cover the upper 1500 dbar of the water column (Antarctic Intermediate Water), they will enhance the hydrographic data inventory of the Deep Basin Experiment in WOCE.

For any details on the well known large scale stratification of the South Atlantic the reader may refer to the literature (i.e. REID, 1989; HOGG et al., 1996). Cruise M34/3 contributes to the WOCE data record in a limited but rather distinct way. For our supplementary investigations we had chosen choke points for the exchange of watermasses in the Vema Channel and its northward extension.

Tracks of Continuous Environmental Parameters (DVS data)

The METEOR is equipped with an automatic logger for various under-way data (Datenverteilsystem, DVS). To provide an overview of the accessible hydrographic DVS data we display in Figures 144 and 145 the large-scale distribution of selected parameters. The full data set will be available at the Deutsches Ozeanographisches Datenzentrum (DOD) in Hamburg.

The graphs present hourly subsamples of recorded sea surface temperatures (SST), uncalibrated salinity, difference between air temperature and the SST, wind speed and depth. In case of the last three series we show records from two different sensors / systems: starboard and port side of the ship and depths by PARASOUND and HYDROSWEEP echosounders. According to the preferred cruising direction of the ship during the first and the second half of leg M34/3, the abscissa represents a projection of DVS longitude (Fig. 144) or latitude (Fig. 145). Please note that both figures contain preliminary data that need to be validated prior to any further utilization.

We took at least two daily samples from the ship-borne thermosalinograph, preferably on stations. With a total of 37 salinity probes we calculated a necessary salinity correction which is

displayed in Figure 146. On the y-axis of this figure we show the salinity value displayed by the thermosalinograph ($S_{Thermosalinograph}$). The associated corrected value ($S_{Autosal}$) is given on the x-axis. A linear correction curve is given by

$$S_{Autosal} = S_{Thermosalinograph} \cdot 0.8411 + 7.515$$

No difference between check values taken on stations (in Fig. 146) and underway (in Fig. 146) could be recognized. We informed the ship's management about the inferior calibration of their thermosalinograph. The case is under investigation.

Moorings and Performance of Recovered Instruments

The technical purpose of our work on the METEOR was the recovery of three sound sources. Table 21 summarizes logistical details of mooring activities.

Moorings and sound sources

In agreement with our international partners in WOCE all sound sources were moored at a nominal depth of 1000 m (Fig. 147). This depth roughly coincides with the intermediate minimum in the vertical distribution of sound velocity in the Brazil Basin guarantying optimal performance of the RAFOS technology (KÖNIG and ZENK, 1992).

The first sound source (K02) recovered on 5th March was moored for barely two years (Fig. 148). Slight corrosion traces were visible. The attached zinc anodes had the end plates well protected. The anodes were reduced by 95 % of their original volume. The control electronics was in excellent shape. It responded properly. A time drift of O(5) s advance was documented by comparison with the GPS reference time. This time base had to be transferred manually onto the personal computer communicating with the sound source. All sound sources are manufactured by WRC, Inc. of Falmouth, MA.

Three days later sound source mooring K2 was totally recovered. This success relied critically on the proper performance of the lithium batteries that were used in the acoustic release. Three years and three month sets a new record in mooring deployment periods of the Institut für Meereskunde. As expected corrosion marks were not to overlook (Fig. 149). However, not a single mooring component seemed to have reached its ultimately expected life time. Best results in terms of corrosion protections were obtained by the glass housings of the watch dog transmitter and the MAFOS monitor. Also the over ten years old acoustic release by Oceano Instruments showed no visible sign of corrosion. The sound source electronics had work properly as an intern clock check and a following power test transmission indicated right after recovery. The time base of the sound source clock showed an advance of O(6) s.

Finally on 11th March the remaining mooring K3 that was planned to be recovered during M34/3 was reach in the Vema Extension (Fig. 150). Without any difficulties the release re-

sponded from > 4800 m depth. The following recovery occurred in less then three hours. We were delighted to see the rotors of all three current meters spinning when they reached the surface. With surprise we noted that corrosion had worked less then what we had experienced in the previous cases. Again, an interrogation of the sound source clock showed the accuracy of the internal clock to be of O(6) s advance within the deployment duration of over three years.

MAFOS monitors

Mooring K02 contained a sound recorder monitoring the performance of the southern sound array of the Deep Basin Experiment. This instrument group was introduced as 'MAFOS' by ZENK et al. in 1992. Basically MAFOS monitors are RAFOS floats without release and transmitter. They are moored. Besides their ability to listen to RAFOS signals they represent self-contained temperature and pressure recorders for hydrographic applications. MAFOS 5 worked properly for 528 days until its battery capacity came to an end. Figure 151 shows preliminary time series from the instrument in mooring K02 below the Antarctic Intermediate Water core (1100 m).

Identical instrumentation as in mooring K02 was used in mooring K2. As before all instruments performed excellently. In fact, a second time series of temperature and pressure fluctuations in the Antarctic Intermediate Water, this time from the Vema Channel, could be extracted from the data memory of MAFOS 12 in K2 (Fig. 152). Data capacity (534 days) expired before the recovery of the device.

Means and standard deviations of pressure and temperature time series from K02 and K2 are summarized in Table 25 together with the moored data from K3. Table 26 contains all deployment intervals and recording duration.

Currents in the Vema Extension

For brevity we called the region to the North of Vema Sill 'Vema Extension', i.e. the northeastward continuation of the Vema Channel. From the hydrographic standpoint this trough deserves special interest because bottom waters that have passed the Vema Sill once again are channeled by the topography before they can plunge into the greater depths of the southern Brazil Basin (> 5000 m).

Two Aanderaa current meters (type RCM8) were moored in the Weddell Sea Deep Water (q < 0.2°C) and in the Antarctic Bottom Water (q < 2.0°C), 15 and 512 m above the ground at K3. A third instrument was mounted above the sound source itself at 997 m in the Antarctic Intermediate Water. The current meters recorded at a sampling interval of 2 h for 27.5 months before they reached their end of storage capacity (Tab. 26). Data processing began on board the METEOR and was continued in the laboratory in Kiel (Tab. 27). Methods of data treatment are similar to those described in TARBELL et al. (1994) and ZENK and MÜLLER (1995).

Figure 153 - 158 present the current meter records in various forms as time series and histograms. A series of vector plots with North positive upward is given in Figure 159. In this case data were ensemble averaged over 12 hours with 50 % overlapping. We chose a preliminary mode because a number of technical details are still under investigation. Among them are post-cruise temperature calibration checks and discussions with the manufacturer about unexplained solitary jumps in two of the instruments reference channels and other details. According to Aanderaa Instruments, Nestun, Norway, these faults are caused by a defect read relay in the reference-temperature range resistor. They may have also effected the pressure reading of the top instrument (S/N 10074). Technical and logistical details are summarized in Table 24. Means and standard deviations of all unfiltered time series are summarized in Table 25. Table 26 gives a complete overview of the time frame of all IfM moorings and their performance in the Deep Basin Experiment (beyond the scope of the M34 mooring activities).

Topographic surveys

Two smaller HYDROSWEEP surveys were conducted during M34/3 for more clarity of topographic effects on bottom currents. The first survey partially repeated an earlier effort to map the Vema Sill (SIEDLER and ZENK, 1992, ZENK et al., 1993). The repeatability of the 1990 and 1996 surveys showed the expected results. Minor details may be a consequence of the two different post processing software packages used for both products.

The second survey (Fig. 160) shows the local topography at the Vema Exit where CTD stations 53 - 55 were occupied (cf. Tab. 20). The available time on board allowed no further surveys of this choke point region where the flow of Antarctic Bottom Water seems to lose its topographic guidance before it is channeled again by the Vema Extension (Mooring K3 in Fig. 125).

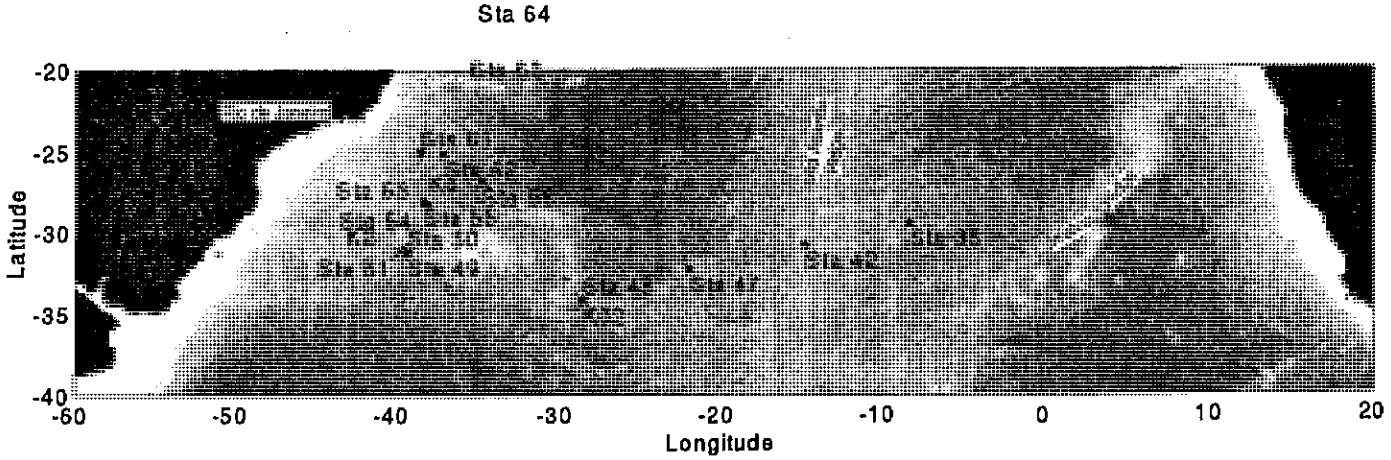

Fig. 125: Geographical map of the hydrographic stations of METEOR cruise M34/3. The majority of the stations is concentrated on the western side of the subtropical South Atlantic. K02, K2 and K3 denote mooring positions where RAFOS sound sources were recovered more than three years after deployement. K02 and K2 contained MAFOS monitors. K3 served also as platform for recovering current meters in the depth range of the Antarctic Intermediate Water and the Antarctic Bottom Water.

Tab. 20: Inventory of CTD stations

Stat/ Prof.	GeoB Nr.	Date 1996	Time UTC	Latitude	Longitude	Depth (m)	Remarks	Fig.
35/1	3801	26Feb	12:46	29° 30.12' S	008° 17.38' W	4534	East MAR, SeaBird	129
42/2	3808	29Feb	22:59	30° 48.70' S	014° 42.68' W	3212	MAR	130
47/3	3813	3Mar	12:40	32° 16.21'S	021° 58.18' W	4346	West MAR, SeaBird	131
48/4	3814	5Mar	14:50	34° 10.02' S	028° 37.62' W	4390	Hunter Ch, upper1500 near mooring K02	132
49/5	3815	7Mar	20:47	31° 11.99' S	039° 18.76' W	4477	Vema Sill, east ~ M15/49, Prof. 47	135
50/6	3816	7/8Mar	23:32	31° 11.96' S	039° 21.06' W	4578	Vema Sill, centre ~ M15/43, Prof. 42	134
51/7	3817	8Mar	02:30	31° 11.87' S	039° 25.98' W	4595	Vema Sill, west, SeaB ~ M15/41, Prof. 40	133
53/8	3819	9Mar	11:55	28° 11.79' S	038° 17.91' W	4756	Vema Ch, exit, centre	137
54/9	3820	9Mar	16:02	28° 17.60' S	038° 06.34' W	4686	Vema Ch, exit, east	138
55/10	3821	9Mar	20:06	28° 07.34' S	038° 17.96' W	4584	Vema Ch, exit, west	136
58/11	3824	11Mar	06:02	26° 52.19' S	034° 48.23' W	4780	Vema Extension 1 nm west of moor.K3	139
61/12	3827	12Mar	22:12	25° 01.85'S	038° 32.48'W	3861	upper 1500 m only	140
62/13	3828	13Mar	19:01	22° 09.76' S	037° 04.63' W	3907	upper 1500 m only	141
63/14	3829	14Mar	16:01	19° 00.71' S	035° 29.94' W	4213	upper 1500 m only	142
64/15	3830	15Mar	12:59	15° 33.89' S	34 59.70' W	4442	upper 1500 m only	143

⇑ Last station ☺ ☺ Jubilee Station: 10 years FS METEOR

Tab. 21: Mooring activities. For location of moorings see Figure 125

Sta No.	Ext No.	Int No.	Date ⇓ deployed ⇑ recovered	Latitude	Longitude	Depth m	Instr Type	Rem
M28/322	K02	3522	⇓ 2Jun1994	34°13.36'S	28°38.37W	4335	SoSo86	window 01:35UTC
							MAFOS5	
							WD9243	
M34/48			**⇑ 5Mar1996**				**100% recovered**	
							GeoB No 3814	
M22/583	K2	350	⇓ 6Dec1992	31°07.5' S	39°54.1 W	3807	SoSo49	window 00:30UTC
							MAFOS12	
							WD5514	
M34/52			**⇑ 8Mar1996**				**100% recovered**	
							GeoB No 3818	
M22/616	K3	349	⇓ 18Dec1992	26°52.0' S	34°47.2' W	4864	SoSo68	window 01:00UTC
							3 ACM	
							WD5508	CB, Fl
M34/58			**⇑ 11Mar1996**				**100% recovered**	
							GeoB No 3824	

Abbreviations

ACM	Aanderaa current meter
CB	HF bouy transmitter (citizen band)
Fl	Flash light
MAFOS	Sound recorder
SoSo	Sound source
WD	'Watch Dog' ARGOS transmitter

Tab. 22: K2-mooring logistics and technical details of MAFOS monitor # 12 and sound source #49 (Fig. 149). For abbrevations see Table 24

Mooring at location K2
IfM mooring number V350

Deployed at 31°07.5'S, 39°54.1'W on 6 DEC 1992 (M22)
Recoverd on 8 MAR 1996 (M34)
Depth 3807 m
First record (instr. on position): 7 DEC 1992 01:55 UTC

Instrument ID	S/N	Nominal depth (m)	Sampling (h)	Transmission UTC	Sensors	Cycles (day intervals)	Remarks
V350101	MAFOS 12	900	24		TEMP PRESS	534 534	Instrument built by IfM Kiel RAFOS-electronic
V350102	SoSo 49	1000		00:30			Sound source by WRC, Inc.

Tab. 23: K02-mooring logistics and technical details of MAFOS monitoring #5 and sound source #86 (Fig. 149). For abbrevations see Table 24. Mooring K02 replaced mooring K0 which was lost in early 1994 (see also Fig. 151c). Time series are shown in Figure 151a-c

Mooring at location K02
IfM mooring number V352 2

Deployed at 34°13.4'S, 28°38.4'W on 2 JUN 1994 (M28)
Recoverd on 5 MAR 1995 (M34)
Depth 4335 m
First record (instr. on position): 3 JUN 1994 01:55 UTC

Instrument ID	S/N	Nominal depth (m)	Sampling (h)	Transmission UTC	Sensors	Cycles (day intervals)	Remarks
V352202	MAFOS 5	ca. 1100	24		TEMP PRESS	528 528	Instrument built by IfM Kiel RAFOS-electronic
V352201	SoSo 86	ca. 1000		01:35			Sound source by WRC, Inc.

Tab. 24: K3-mooring logistics and technical details on recording current meters and sound sources #68 (Fig. 149). Time series of indicate parameters (*) are shown in Figure 153, 155, 157

Mooring at location K3
IfM mooring number V349

Deployed at 26°52.0'S, 34°47.2'W on 18 DEC 1992 (M22)
Recoverd on 11 MAR 1996 (M34)
Magnetic deviation: 24°W
Depth 4864 m
First record (instr. on position): 19 DEC 1992 00:00 UTC

Instrument ID	S/N	Aanderaa type	DSU Nr.	DSU S/N	First calibration	Depth (m)	Sampling (h)	Trans-mission UTC	Sensors (Channel Nr.)	Cycles	Remarks
V349101	10074	RCM8		4878	25 JUN 1990	997	2		LTEMP(2)*, CON(3), PRESS(4), DIR(5)*, SPD(6)*	10042	jumps in ref. and pressure channels, short temp record (660 cycles)
V349103	10078	RCM8		3642	25 JUN 1990	4352	2		LTEMP(2), CON(3), ATEMP(4)*, DIR(5)*, SOD(6)*	10043	jumps in ref. channel, pressurized by expired lithium battery
V349104	9819	RCM8		2731	2 NOV 1990	4849	2		LTEMP(2), CON(3), ATEMP(4)*, DIR(5)*, SPD(6)*	10043	at different noise levels in channels 2 and 4
V349102	SoSo 68					1097		01:00			Sound source by WRC, Inc.

Abbreviations:

M22, M34	METEOR cruises 22, 34
LTEMP	low temperature range
ATEMP	arctic temperature range
PRESS	pressure
CON	electrical conductivity
DIR	direction } vector averaged
SPD	speed } vector averaged

Tab. 25: Means and standard deviations (Std) of records from moored instruments according to Tables 21 and 26. No filter procedures were applied prior to the calculations. For general abbreviations see Table 24, UC = zonal, VC = meridional current component

Instrument	ID	Nominal depth (m)	Parameter	Mean	±	Std	Units	Cycles
V349101	(K3)	997	LTEMP	4.015	±	0.069	°C	660
			SPD	5.49	±	4.14	cm s^{-1}	10042
			UC	-1.05	±	4.46	cm s^{-1}	10042
			VC	-0.38	±	5.12	cm s^{-1}	10042
V349103	(K3)	4352	ATEMP	0.838	±	0.178	°C	10043
			SPD	7.83	±	5.51	cm s^{-1}	10043
			UC	5.13	±	6.56	cm s^{-1}	10043
			VC	1.67	±	4.43	cm s^{-1}	10043
V439104	(K3)	4849	LTEMP	0.567	±	0.073	°C	10043
			ATEMP	0.852	±	0.129	°C	10043
			SPD	13.68	±	9.31	cm s^{-1}	10043
			UC	12.10	±	9.45	cm s^{-1}	10043
			VC	4.59	±	4.14	cm s^{-1}	10043
V350101	(K2)	900	TEMP	4.859	±	0.234	°C	534
			PRESS	905.9	±	79.3	dbar	534
V352202	(K02)	1100	TEMP	3.686	±	0.168	°C	528
			PRESS	986.5	±	8.2	dbar	528

Tab. 26: Deployment intervals of all IfM sound sources (K) in the Deep Basin Experiment (heavy lines). Recording durations of associated current meters and MAFOS monitors are included (dashed lines). For details see Table 22-25. For further information on the deployment strategy see SIEDLER et al. (1993) and BOEBBEL and Schmid (1995). Position of sound sources are displayed in Figure 149

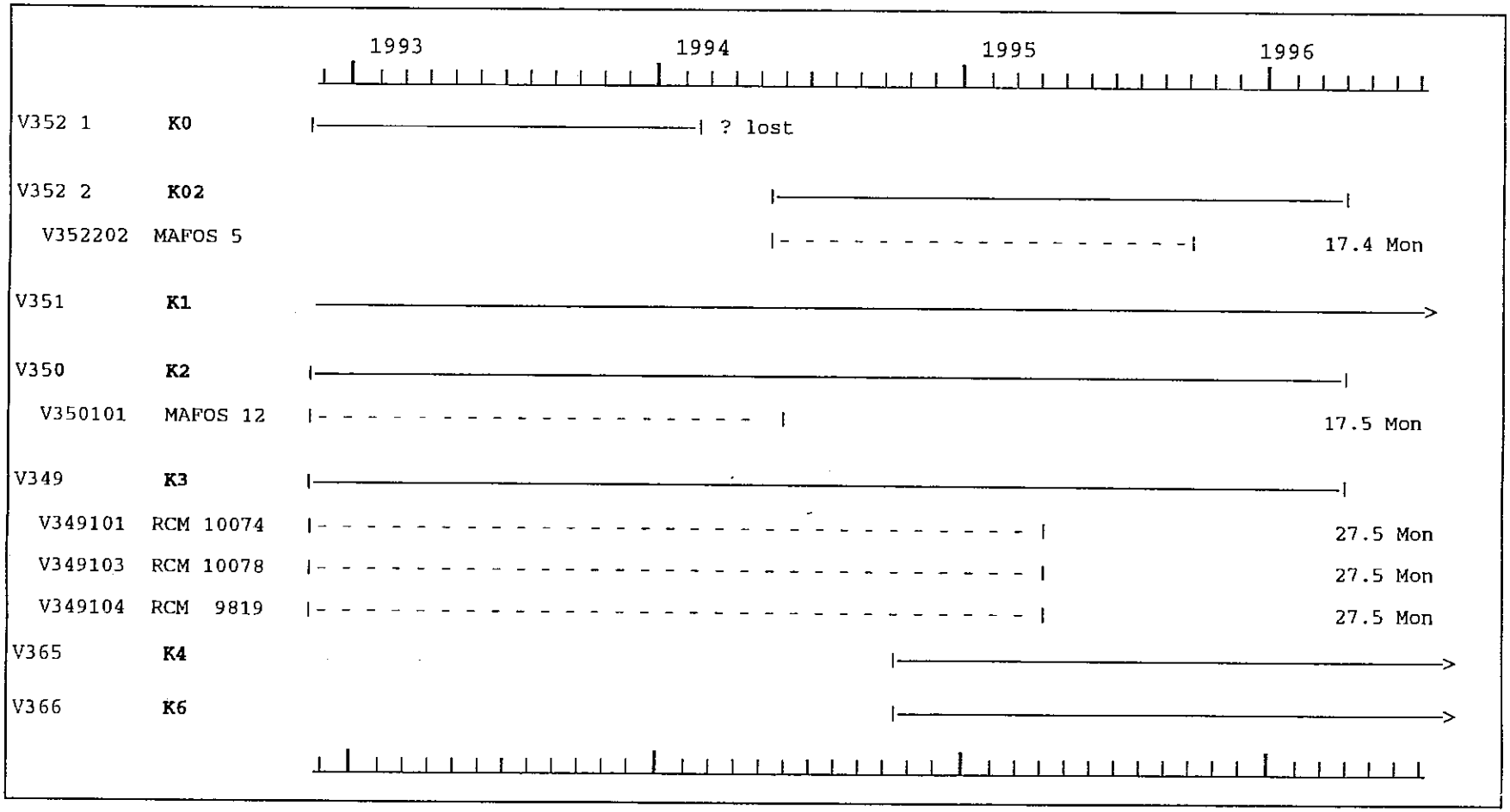

Tab. 27: Coefficients applied for the preliminary calibration of Aanderaa current meter records of moorings K3. Directions were additionally corrected by the magnetic deviation of 24° W. Final calibrations of temperatures will be arranged after postcruise calibration coefficients become available. For abbreviations see Table 24

Instr. ID (S/N)	Depth (m)	Channel Nr.	Sensor	A	a	B	b	c	d	Units
V349101	997	2	LTEMP	-2.400	1.83e-1	2.295e-2	-5.1e-4	-1.344e-6	1.937e-9	°C
(10074)		4	PRESS	-34.63		6.954e-1				kp cm^{-2}
		5	DIR	1.0		3.500e-1				°TC
		6	SPD	1.1		2.906e-1				cm s^{-1}
V349103	4352	2	LTEMP	-2.422	1.83e-1	2.294e-2	-5.1e-4	-1.344e-6	1.937e-9	°C
(10078)		4	ATEMP	-2.635		8.154e-3		-1.601e-7	7.99e-11	°C
		5	DIR	1.0		3.500e-1				°TC
		6	SPD	1.1		2.906e-1				cm s^{-1}
V349104	4849	2	LTEMP	-2.761	1.83e-1	2.329e-2	-5.1e-4	1.344 -6	1.937e-9	°C
(9819)		4	ATEMP	-2.635		8.154e-3		-1.601e-7	7.99e-11	°C
		5	DIR	1.0		3.500e-1				°TC
		6	SPD	1.1		2.906e-1				cm s^{-1}

Calibrated value = (A + a) + (B + b)N + C N^2 + dN^3; N = recorded raw data

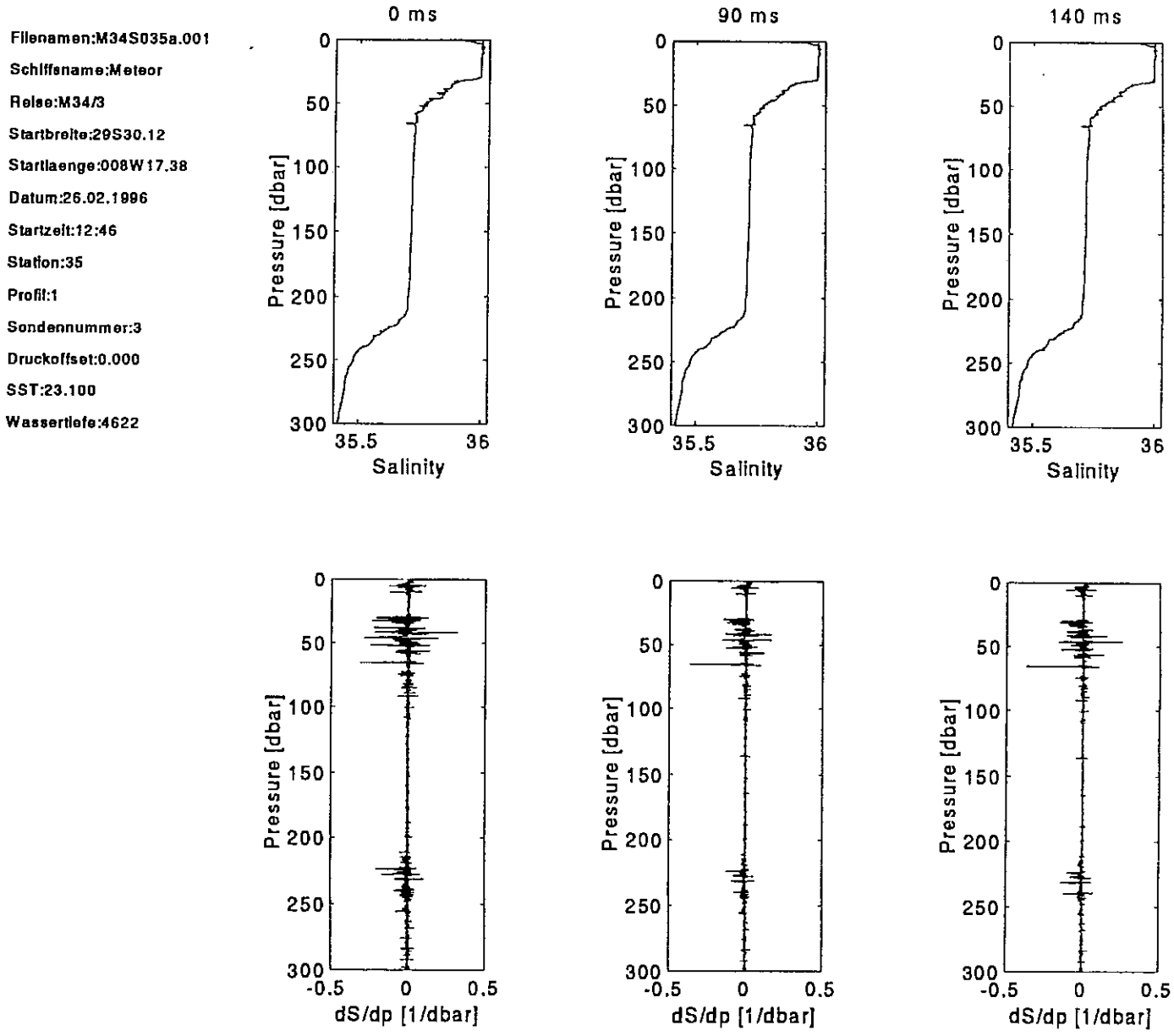

Fig. 126a: Determination of the optimal time constant of the NB3 probe. Selected cases for 0, 90 and 140 ms are shown from left to right. Salinity and salinity gradient profiles in the top 300 m of the water column.

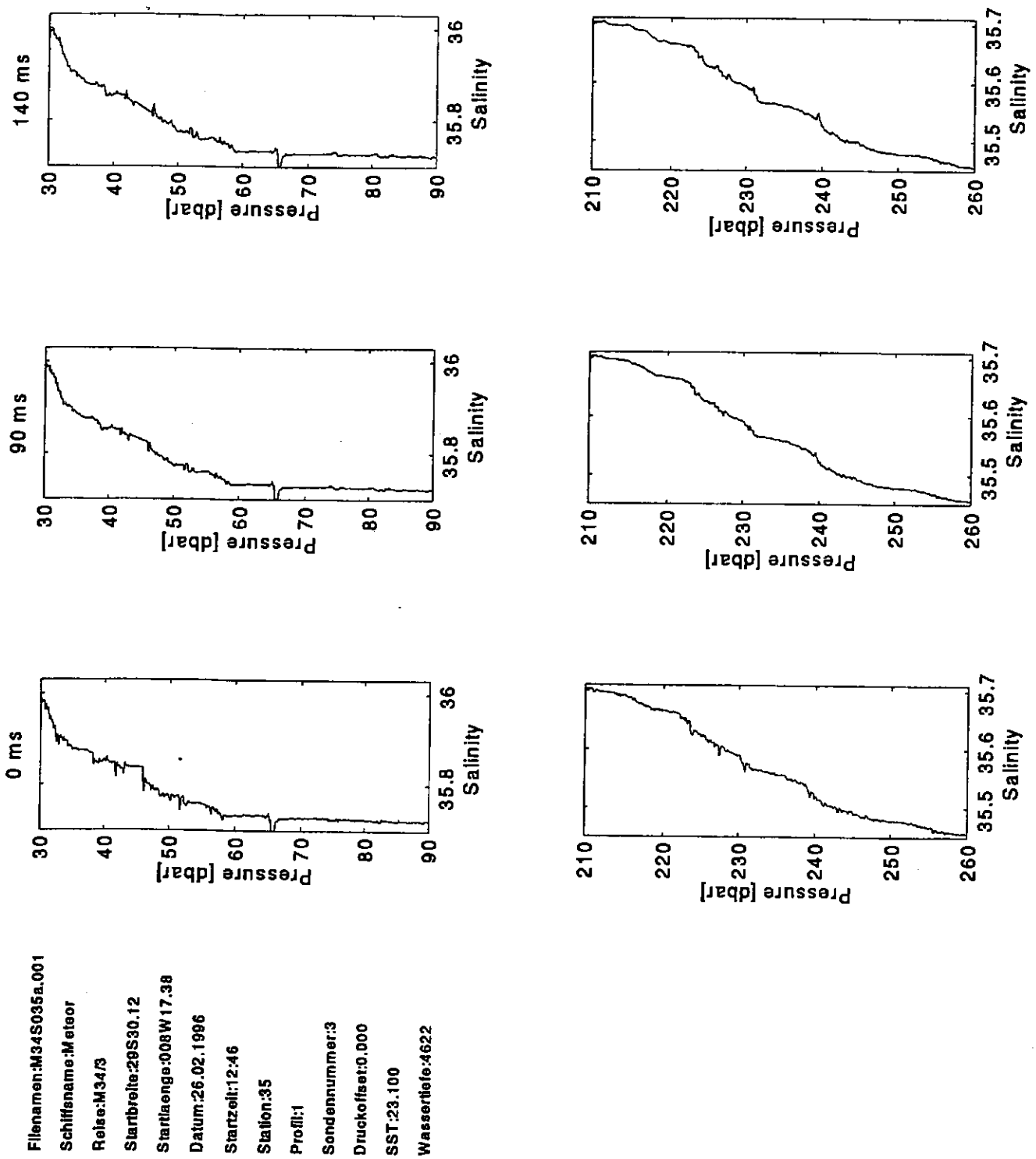

Fig. 126b: Determination of the optimal time constant of the NB3 probe. Selected cases for 0, 90, and 140 ms are shown from left to right. Zoomed salinity profiles in two high-gradient zones.

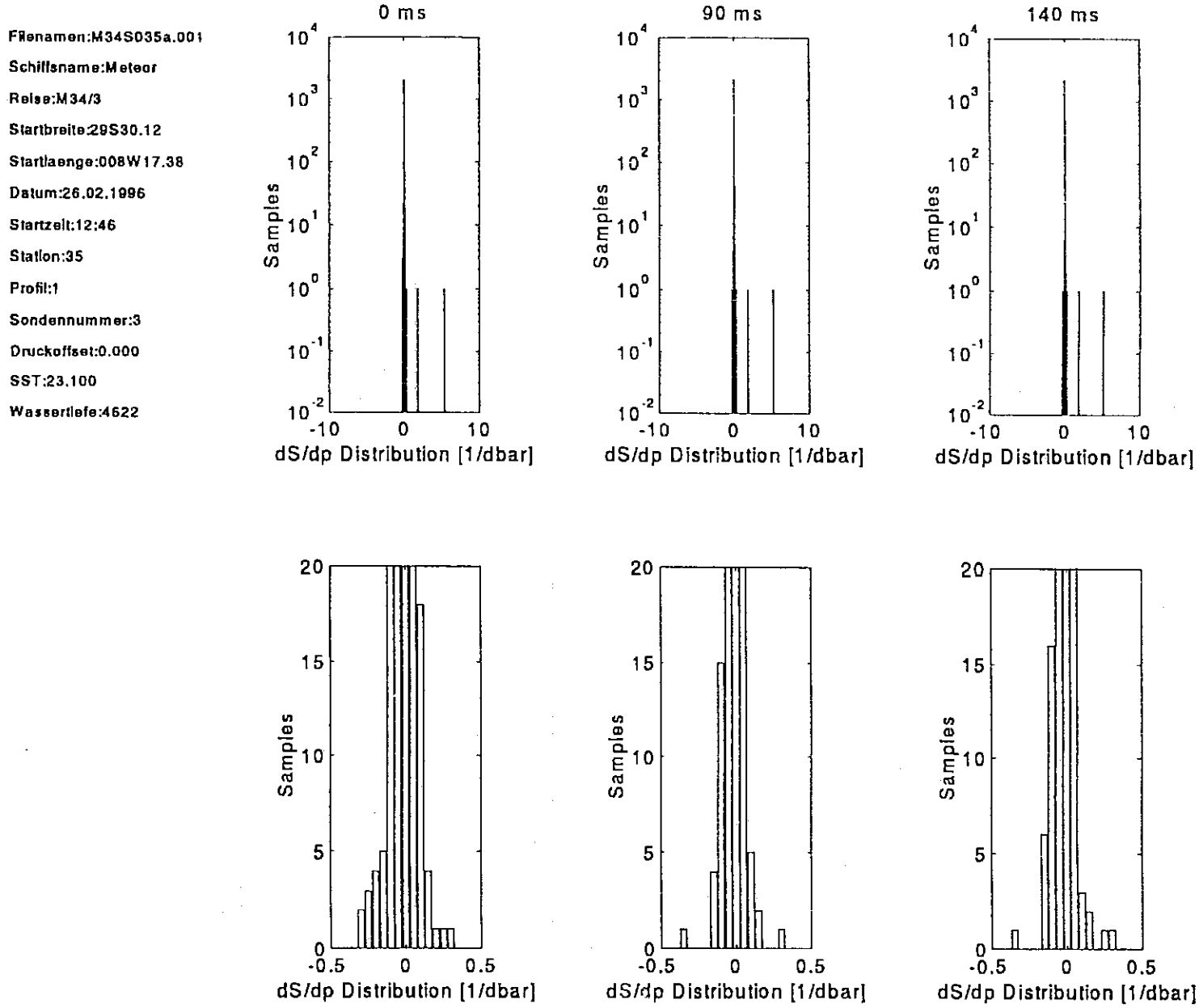

Fig. 126c: Determination of the optimal time constant of the NB3 probe. Selected cases for 0, 90, and 140 ms are shown from left to right. Histograms of salinity gradients in two different classes, -1-+10 (top) and -0.1-+0.5.

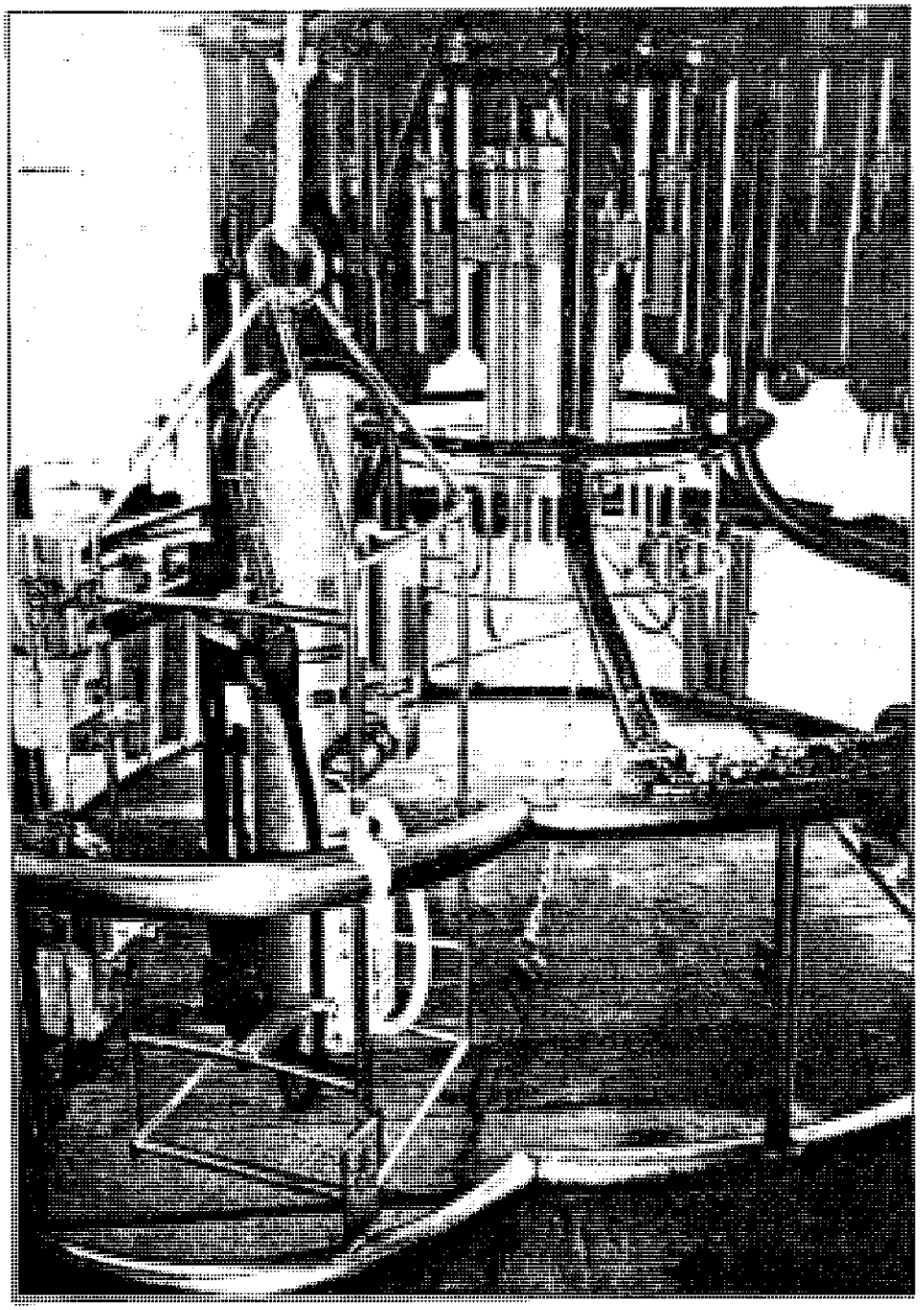

Fig. 127: Rosette mount stand with two CTD probes and water samplers. The Neil Brown unit (NB3) is centred in the inner rosette. The selfrecording Sea Bird instrument (BE-19) is attached to the frame (foreground left).

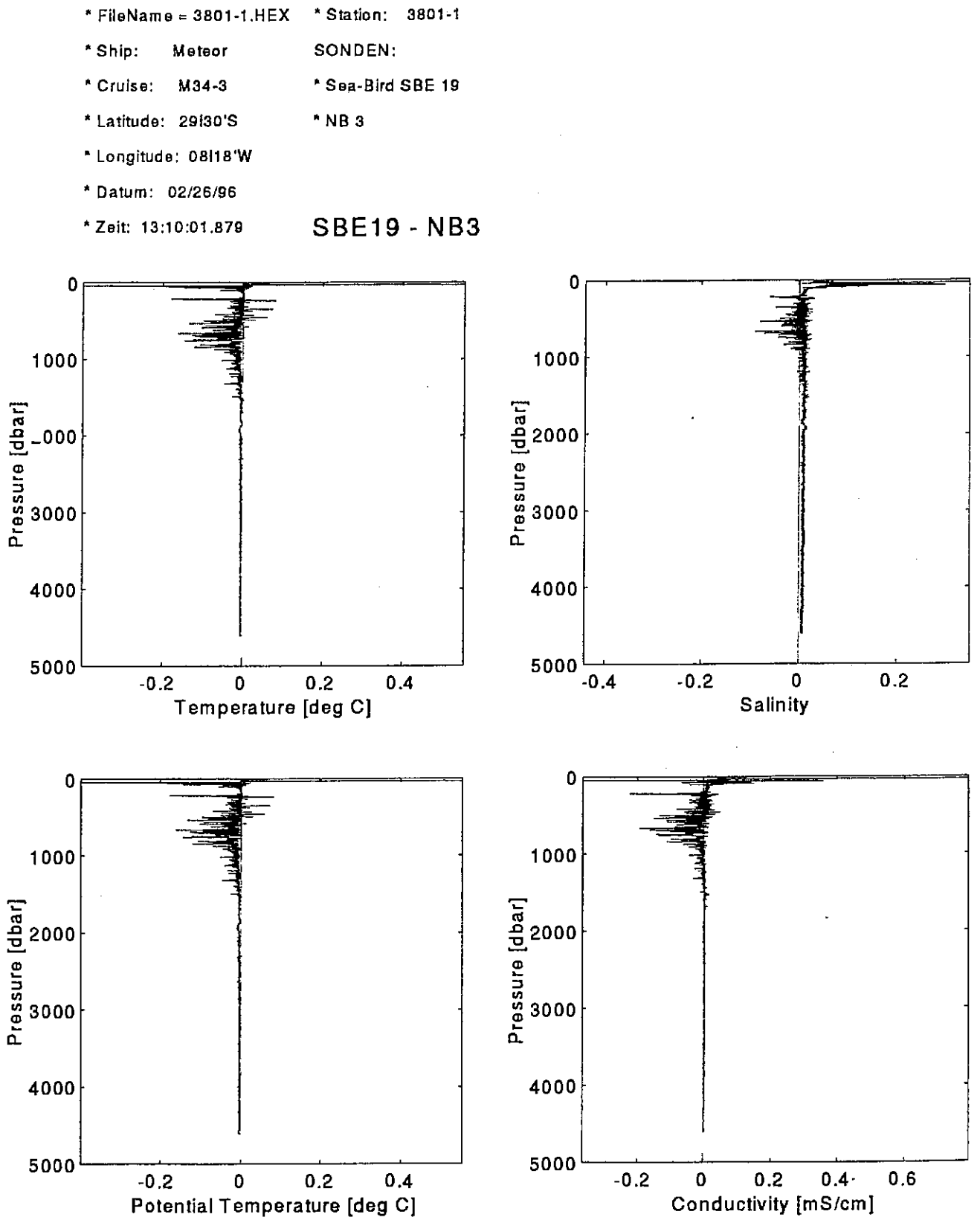

Fig. 128: Intercomparison of Neil Brown and Sea Bird CTD probes on Sta. 35 (see Fig. 125). Note that the shown differential curves were obtained prior to the final CTD calibrations by salinometer data from water samples.

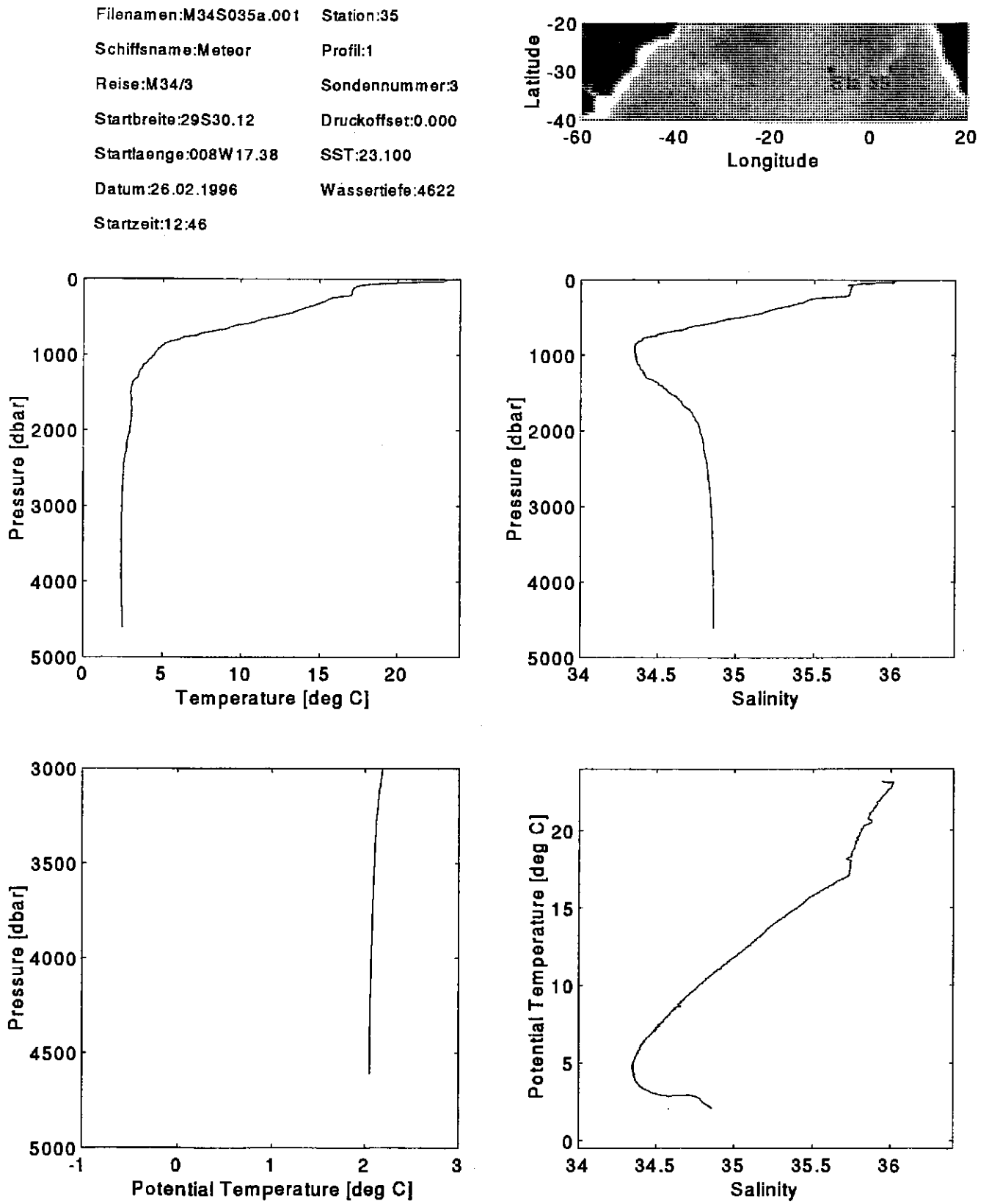

Fig. 129: CTD Station 35, Angola Basin.

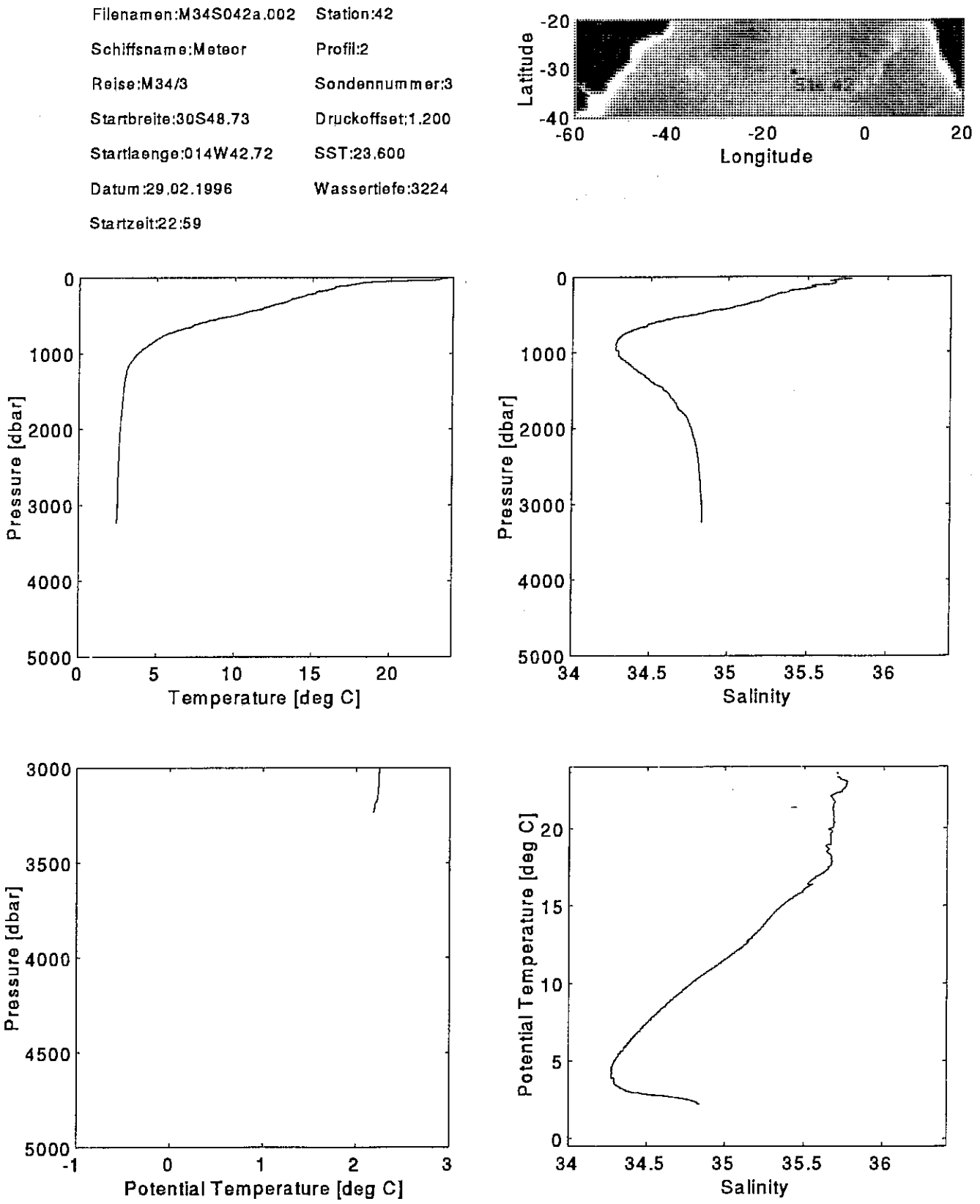

Fig. 130: CTD Station 42, Middle Atlantic Ridge.

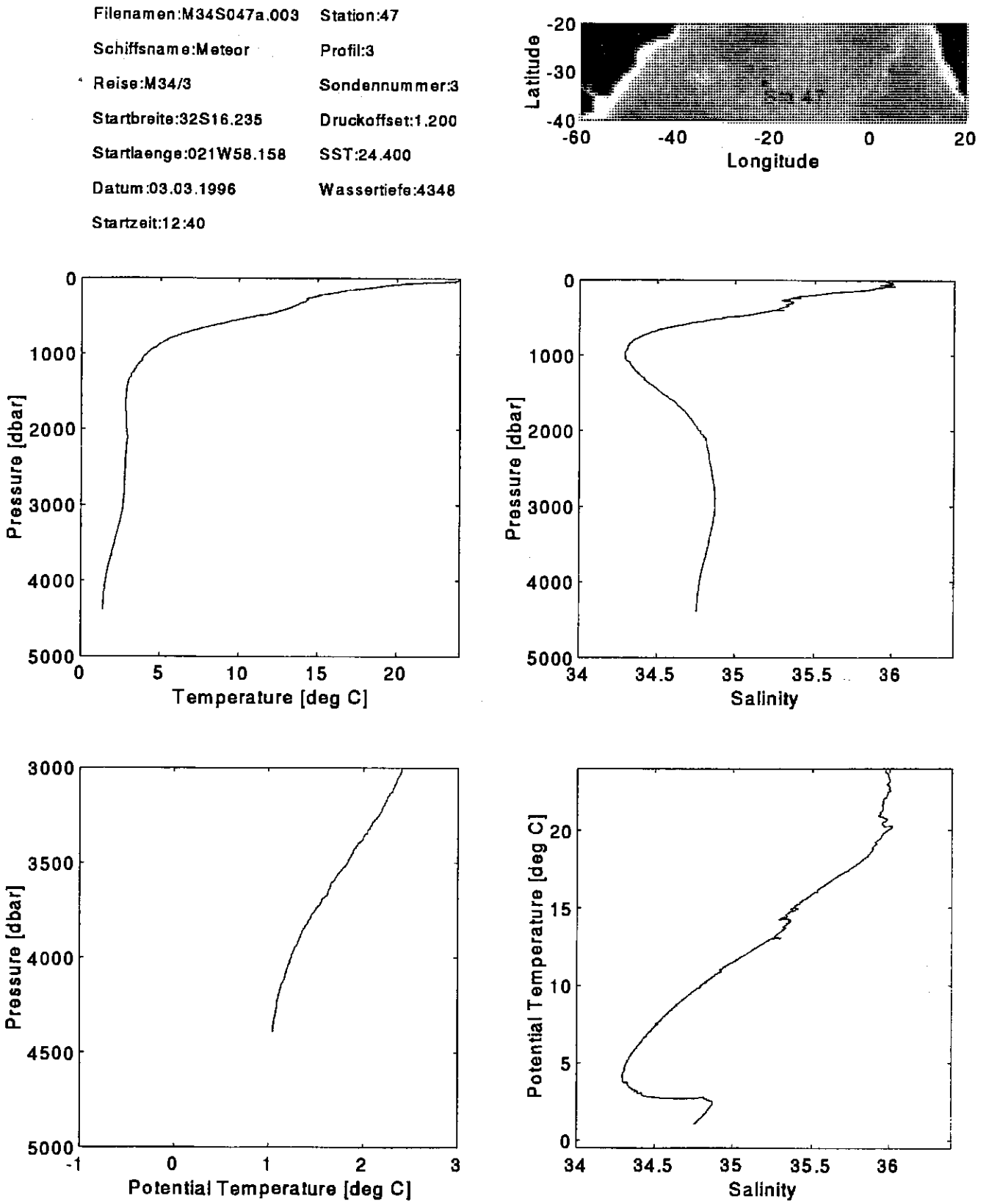

Fig. 131: CTD Station 47, west of Middle Atlantic Ridge.

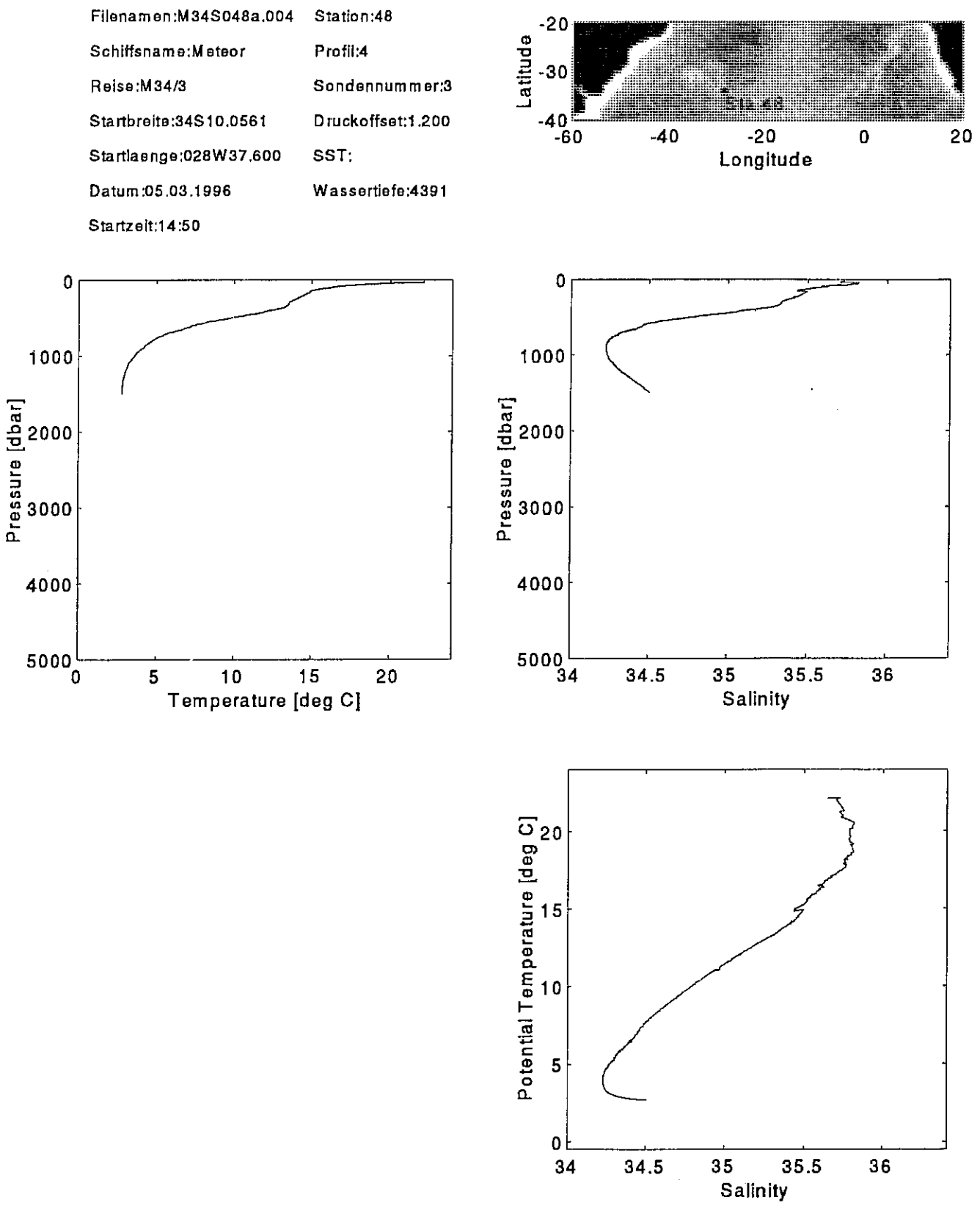

Fig. 132: CTD Station 48, Hunter Channel.

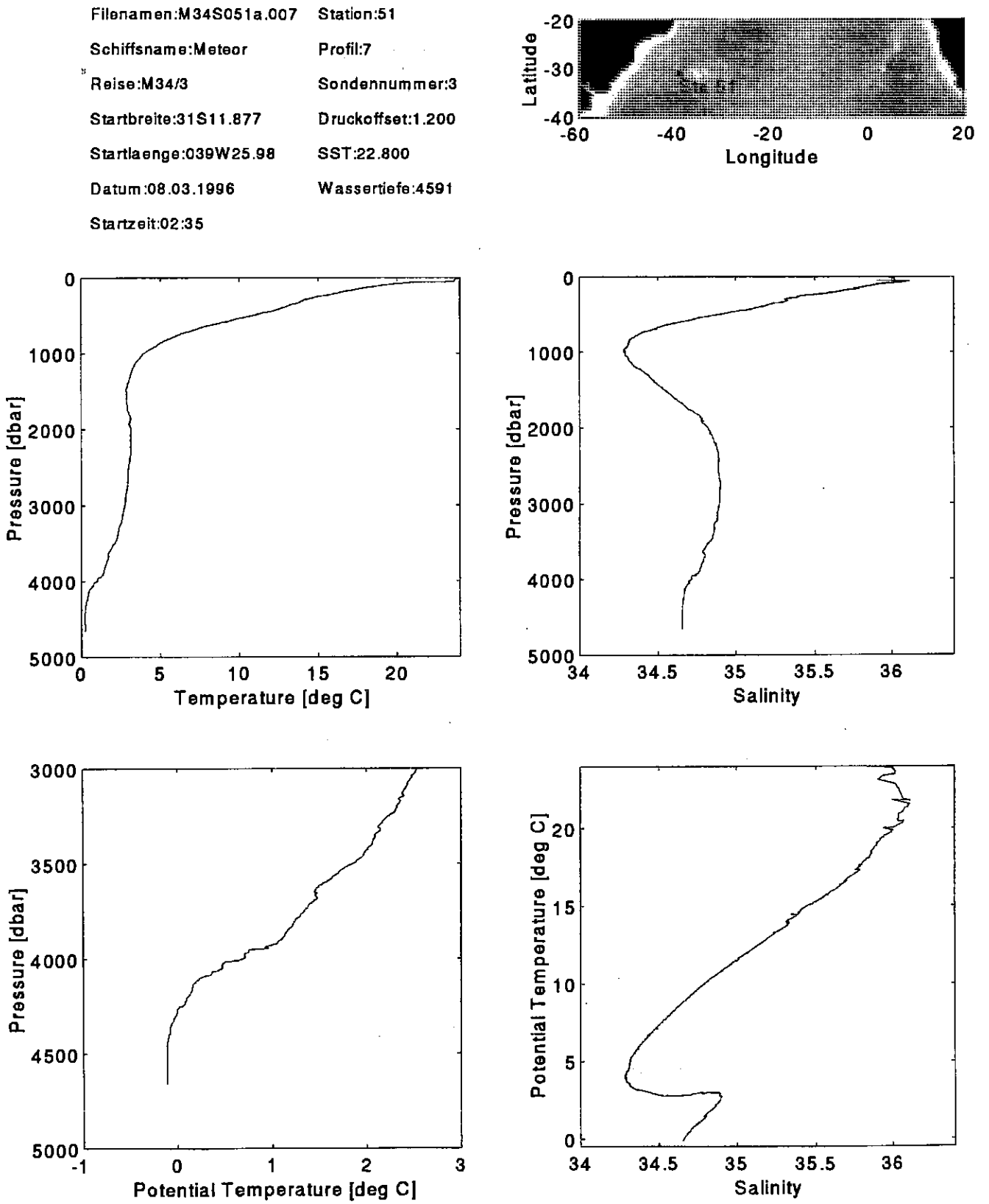

Fig. 133: CTD Station 51, western side of Vema Channel.

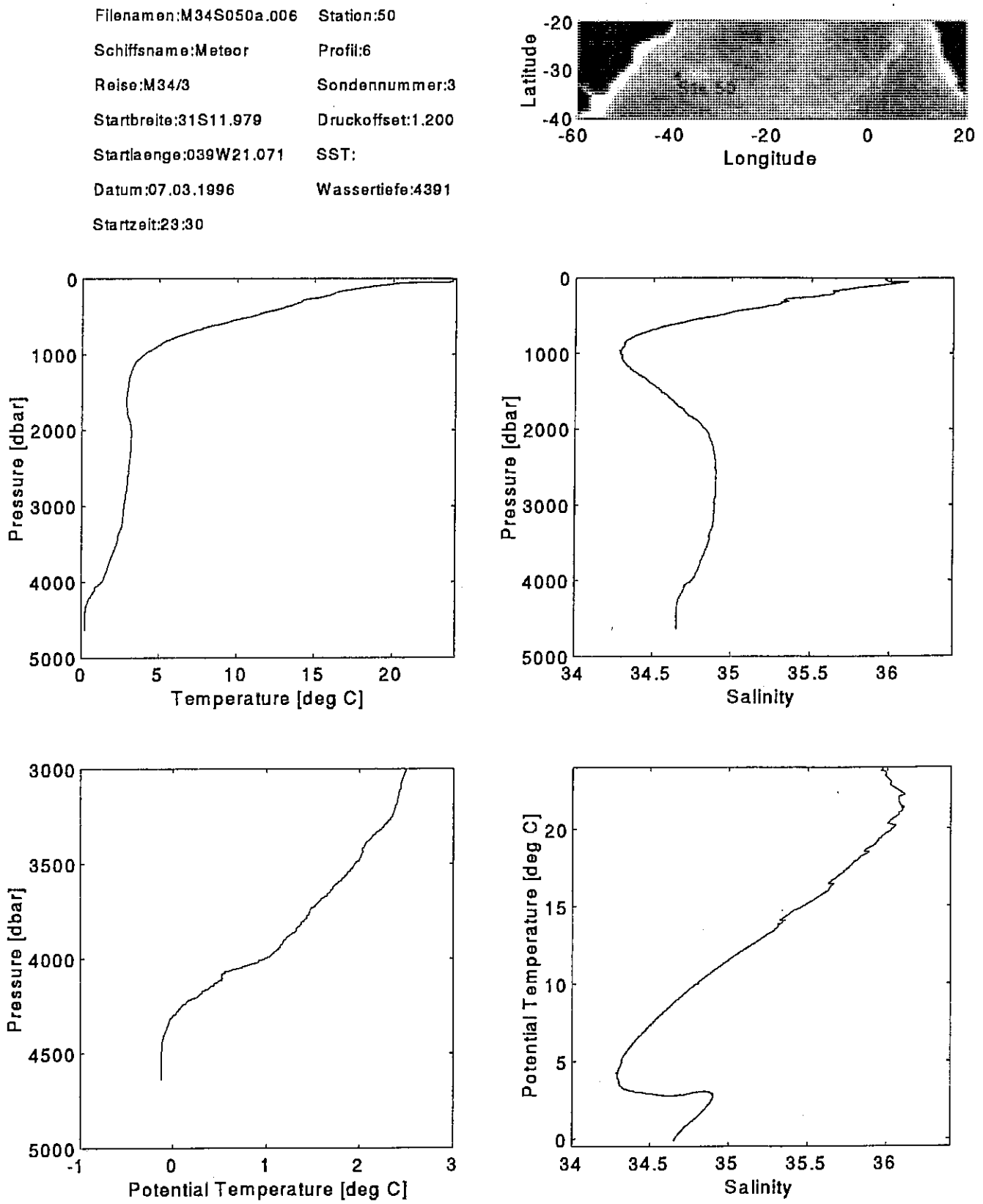

Fig. 134: CTD Station 50, Vema Sill at Vema Channel.

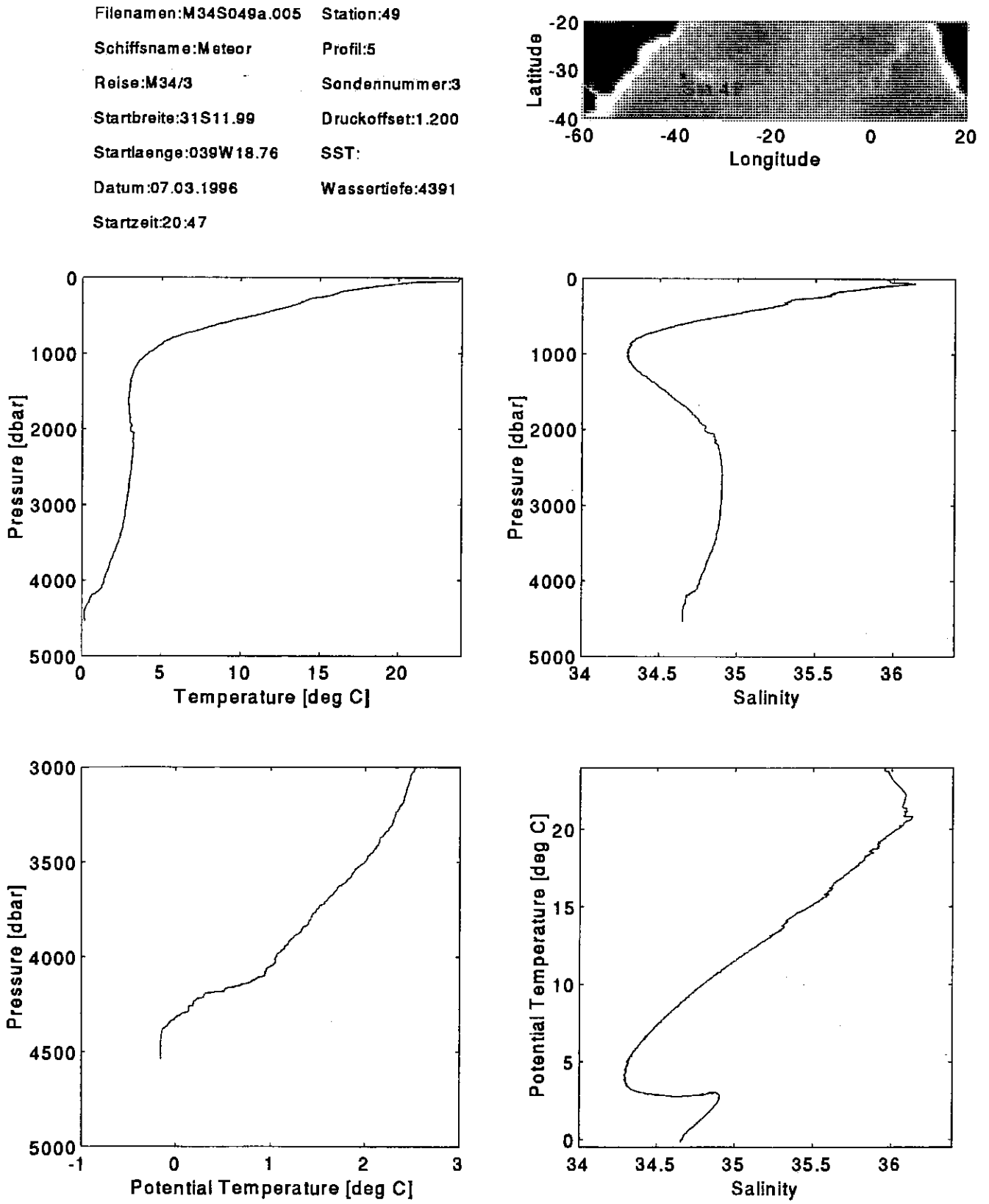

Fig. 135: CTD Station 49, eastern side of Vema Channel.

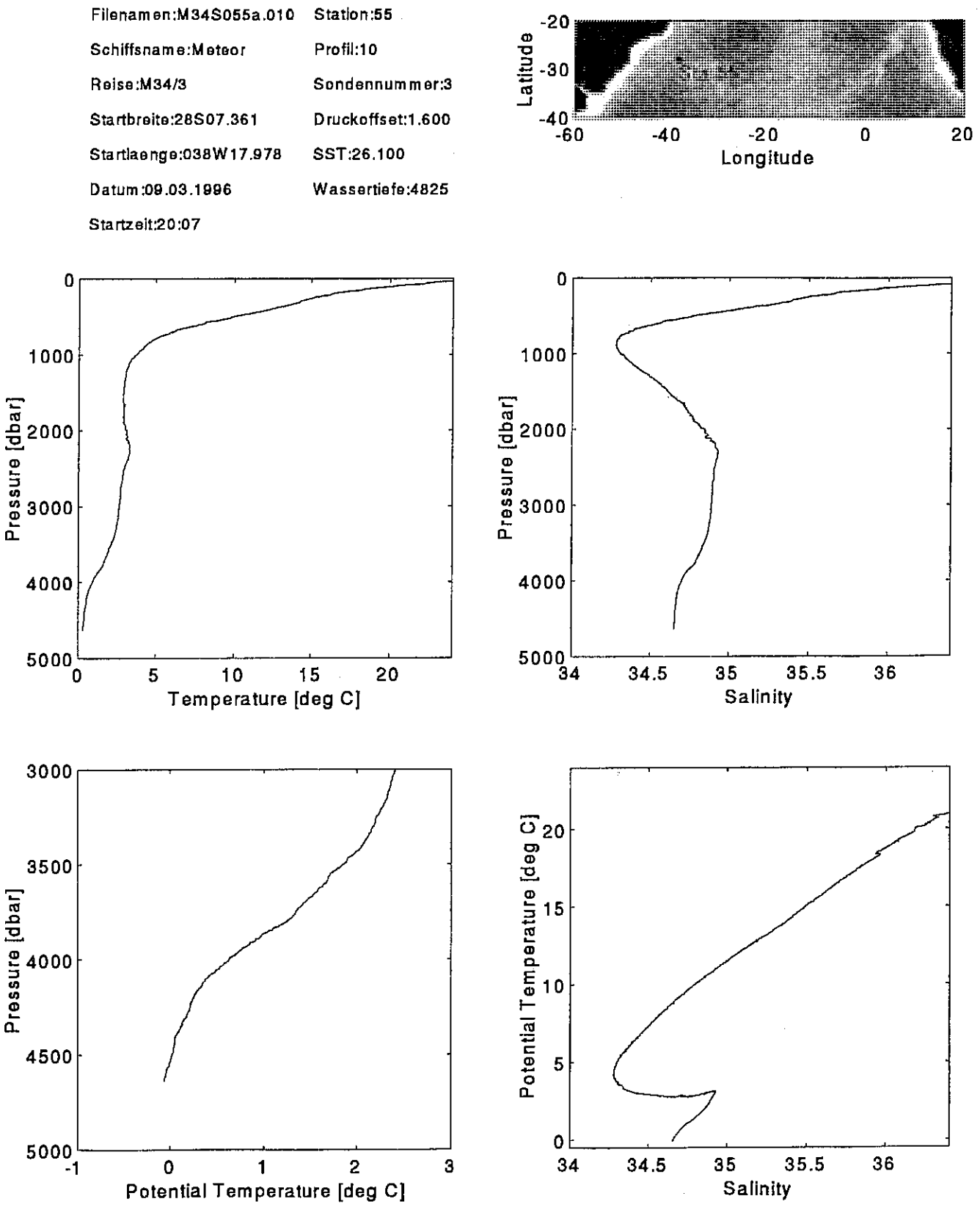

Fig. 136: CTD Station 55, exit of Vema Channel (western side).

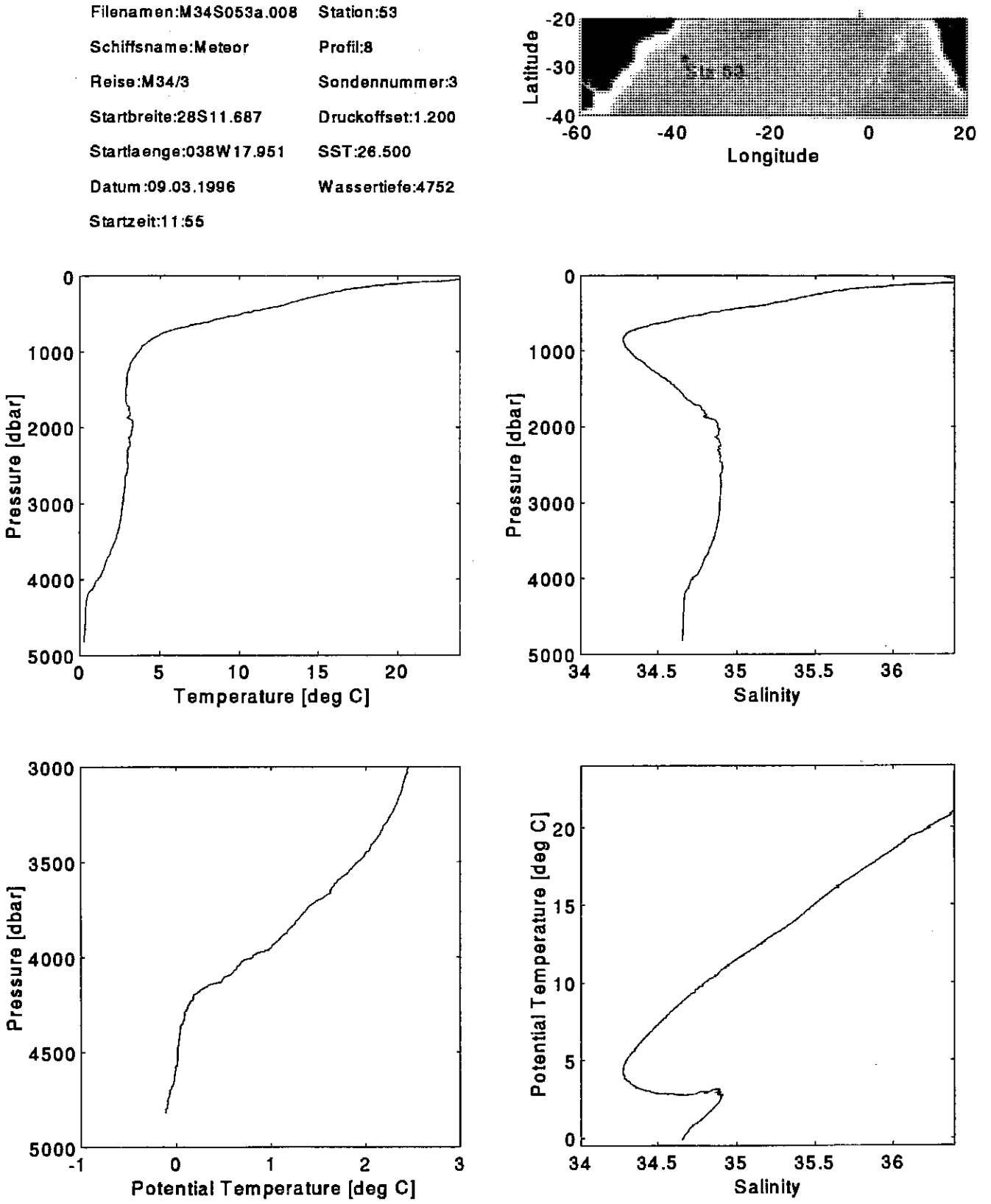

Fig. 137: CTD Station 53, exit of Vema Channel (centre).

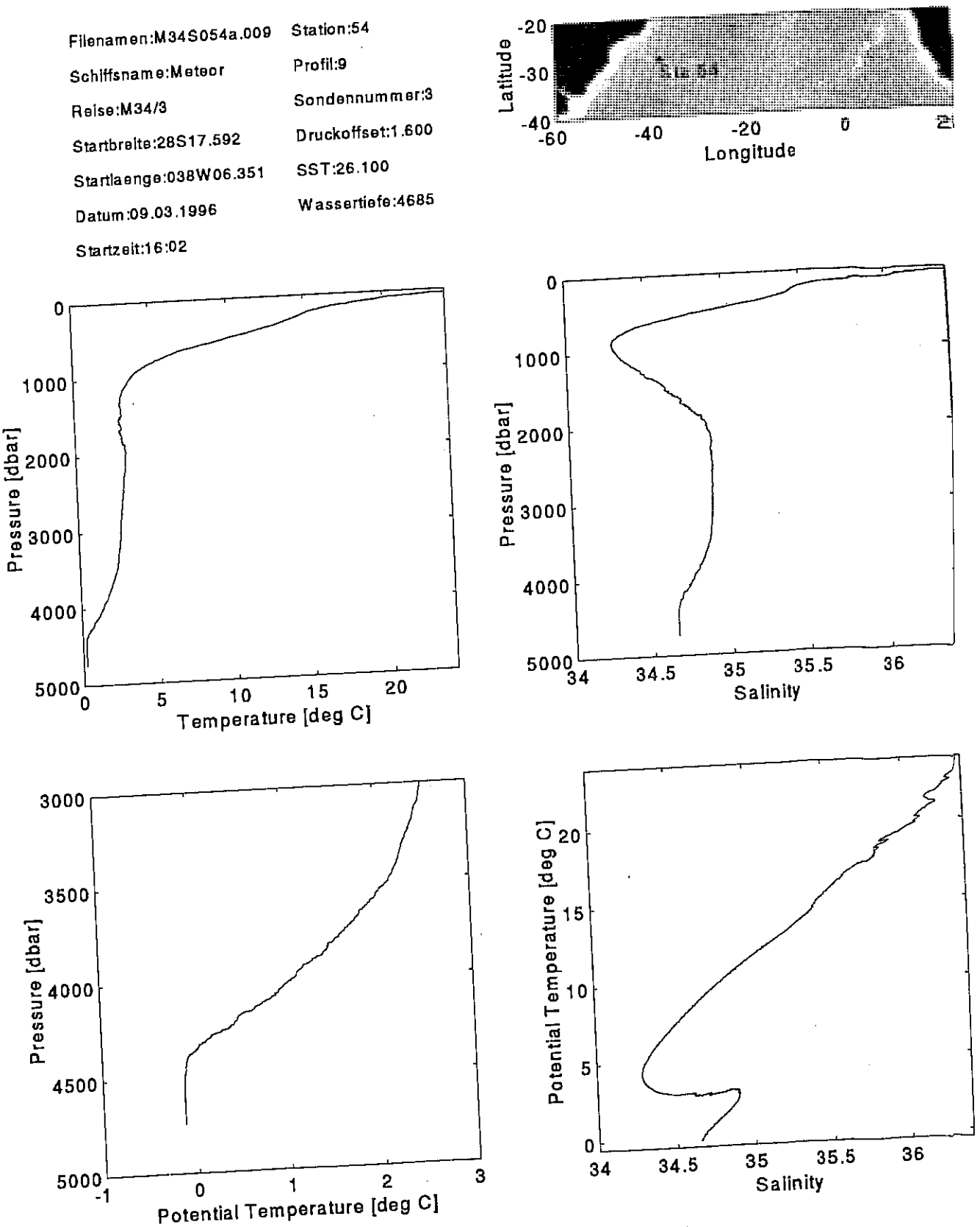

Fig. 138: CTD Station 54, exit of Vema Channel (eastern side).

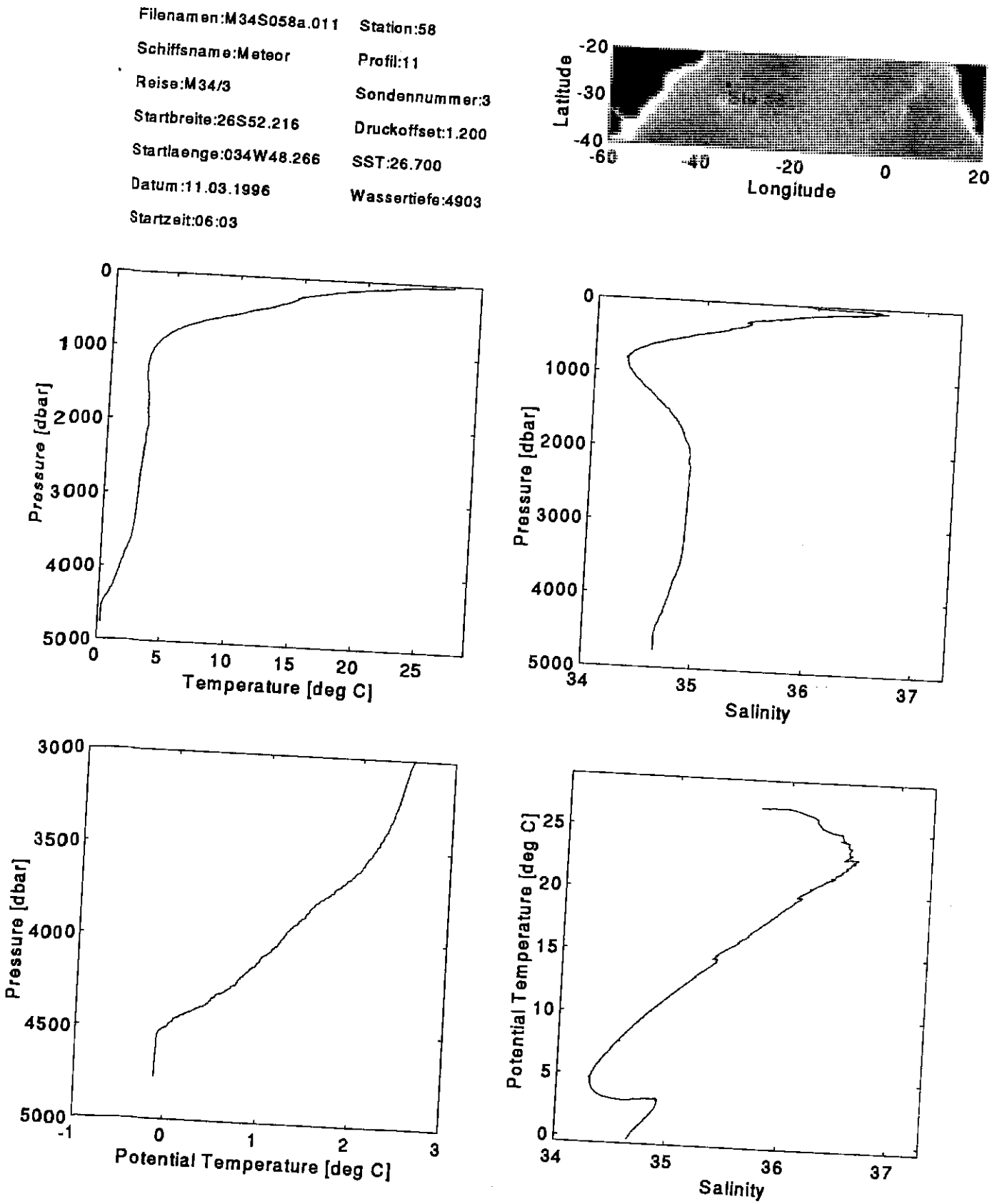

Fig. 139: CTD Station 58, Vema Extension.

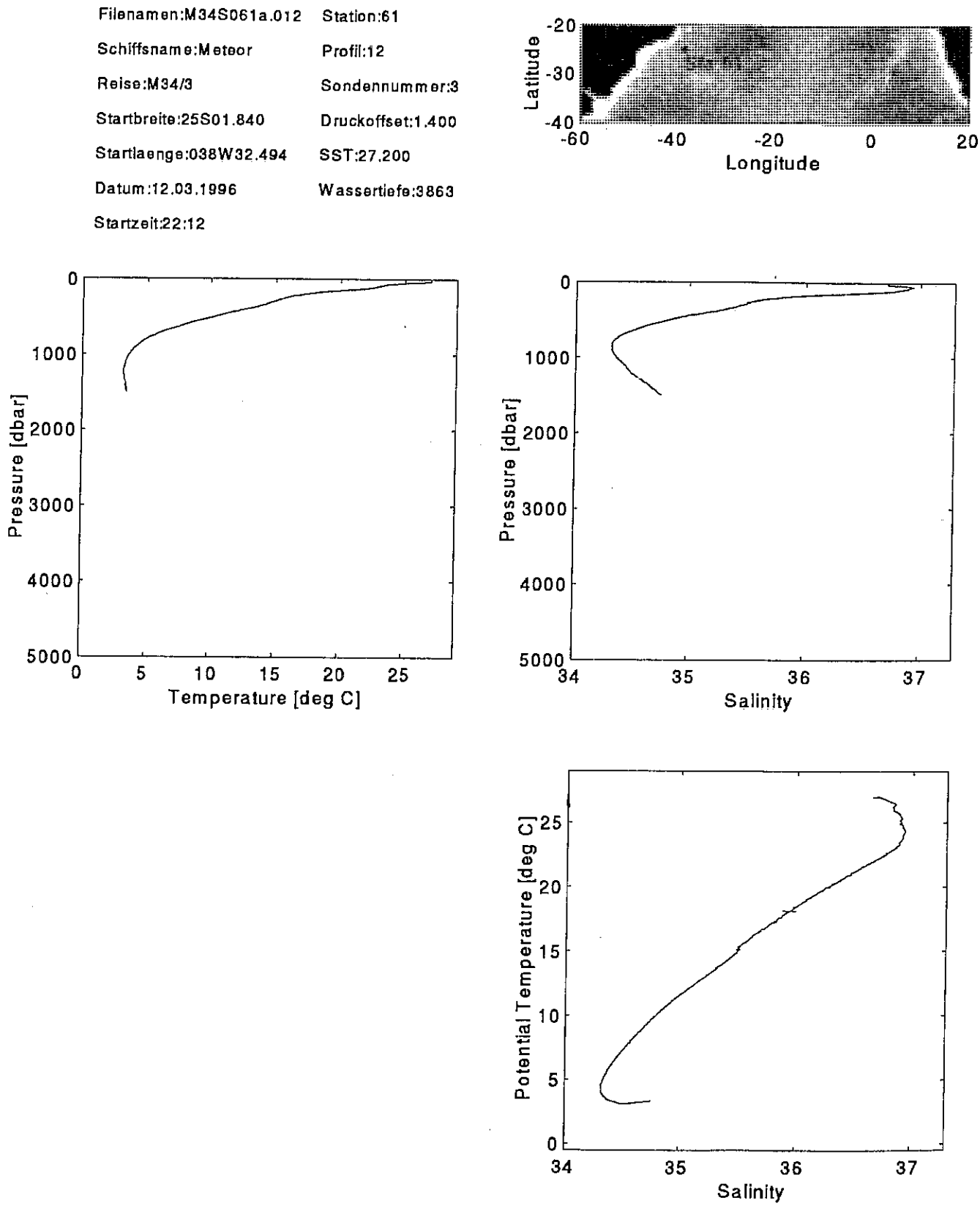

Fig. 140: CTD Station 61.

Filenamen:M34S062a.013 Station:62
Schiffsname:Meteor Profil:13
Reise:M34/3 Sondennummer:3
Startbreite:25S09.771 Druckoffset:1.400
Startlaenge:037W04.627 SST:27.200
Datum:13.03.1996 Wassertiefe:3905
Startzeit:19:00

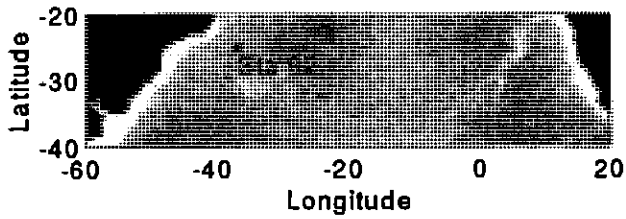

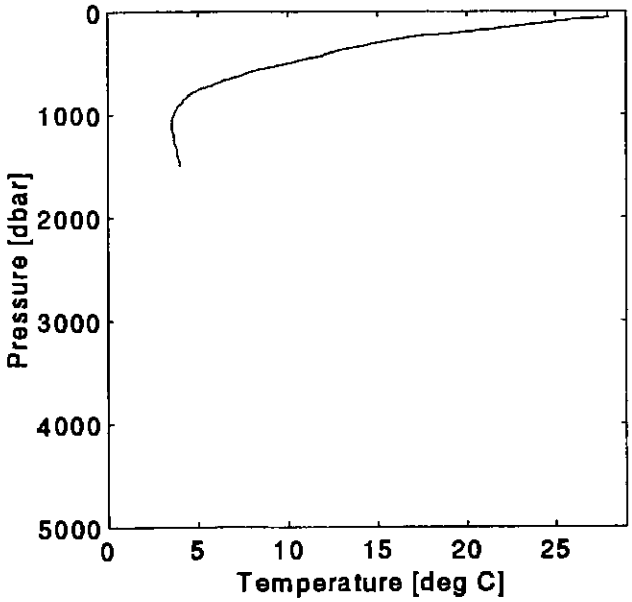

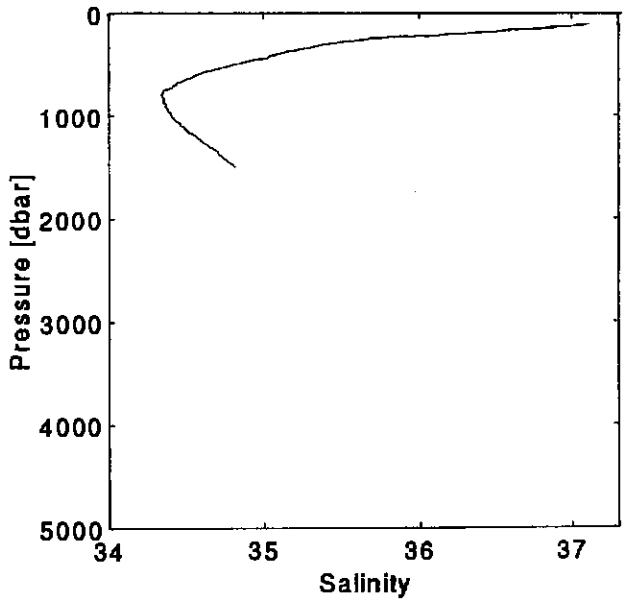

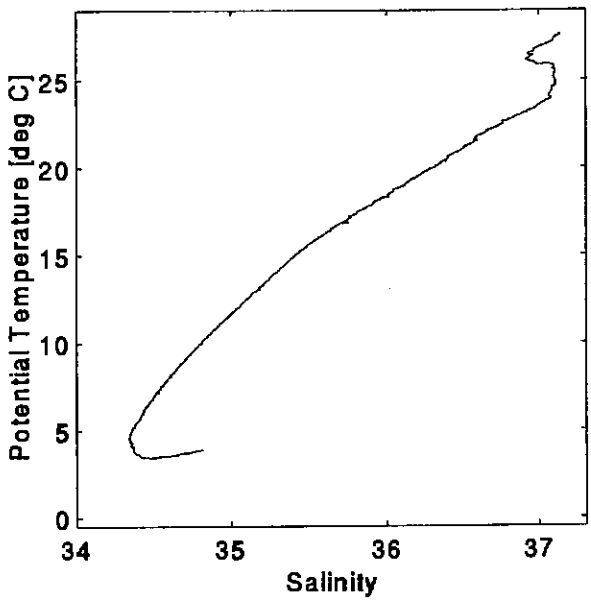

Fig. 141: CTD Station 62.

Filenamen:M34S063a.014 Station:63
Schiffsname:Meteor Profil:14
Reise:M34/3 Sondennummer:3
Startbreite:19S00.706 Druckoffset:1.400
Startlaenge:035W29.996 SST:28.500
Datum:14.03.1996 Wassertiefe:4053
Startzeit:16:01

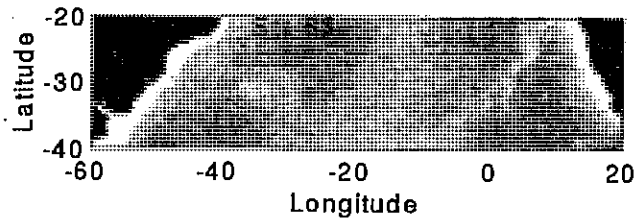

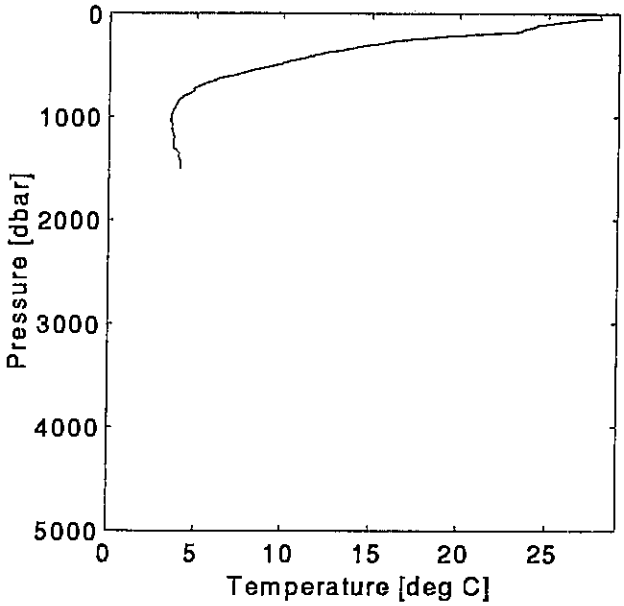

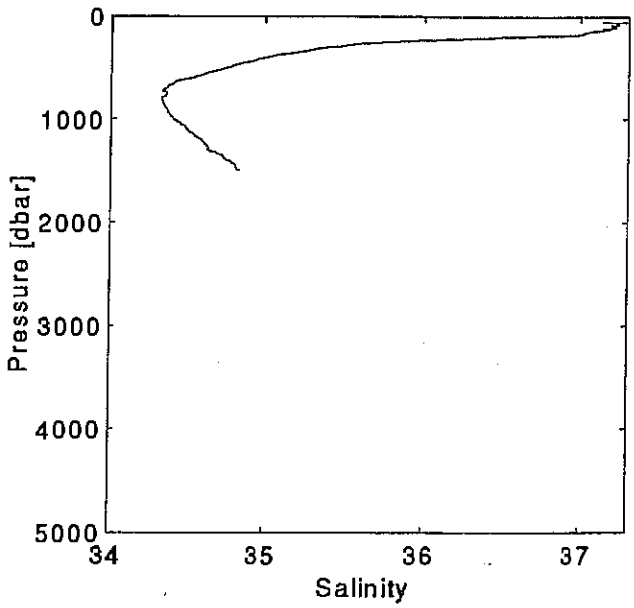

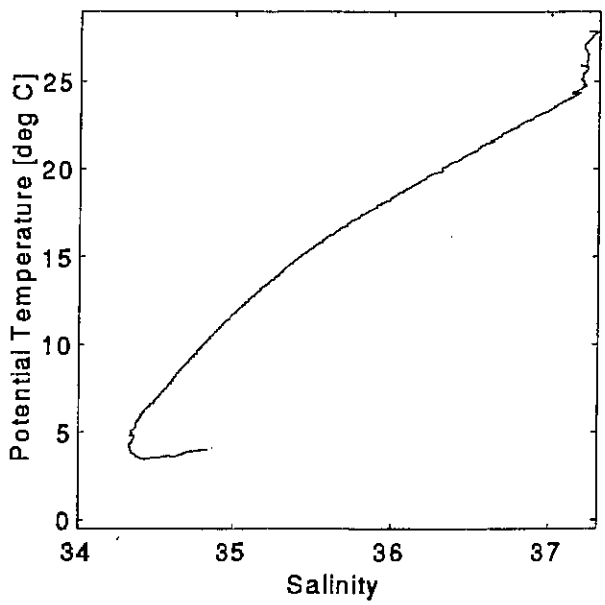

Fig. 142: CTD Station 63.

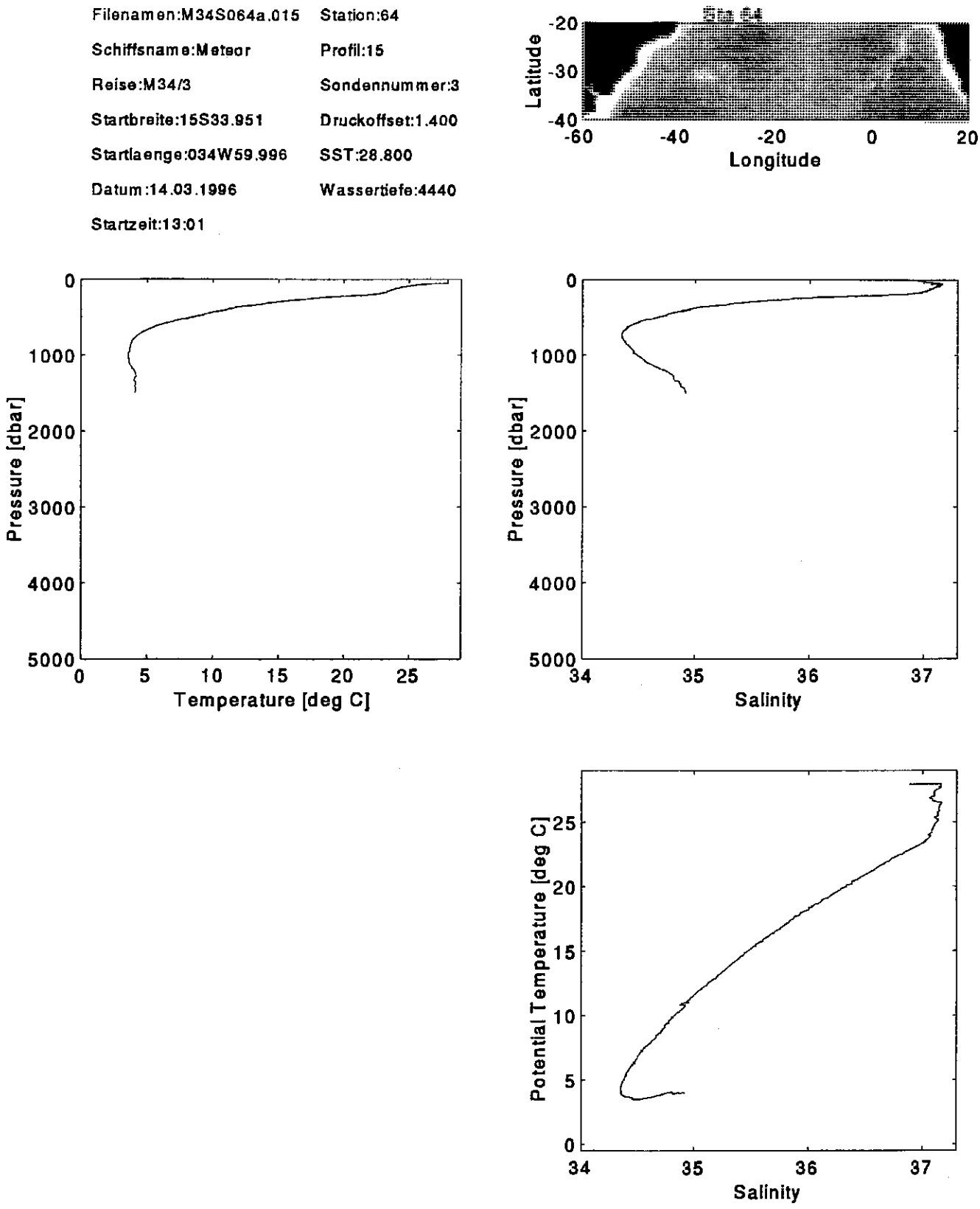

Fig. 143: CTD Station 64.

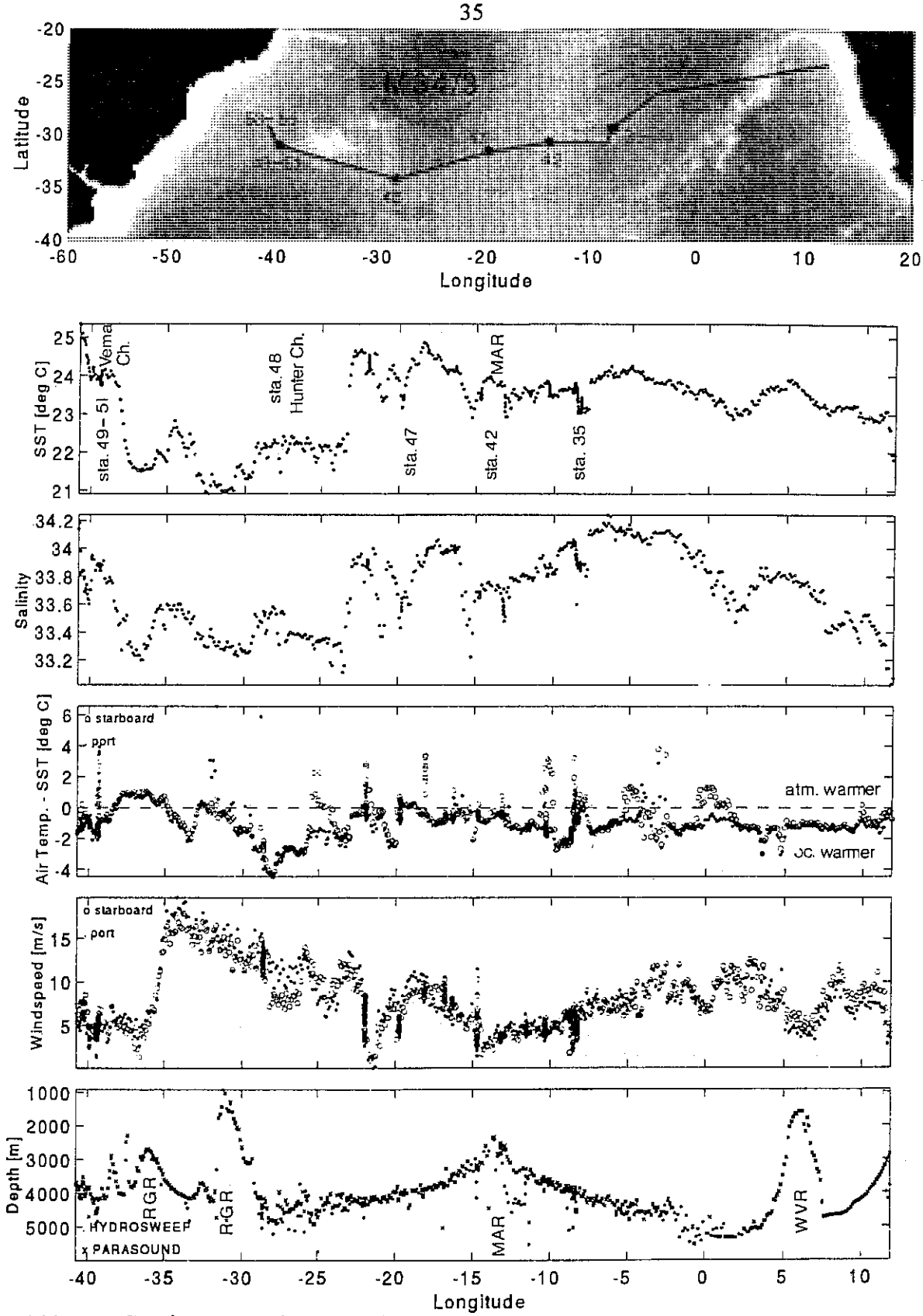

Fig. 144: Continuous environmental parameters (DVS data) sampled between 41° W and 12° E. Data are shown as a function of geographical longitude. Salinity values need to be corrected according to Section 5.3.1. Abbreviations: SST sea surface temperature, MAR Mid-Atlantic Ridge, RGR Rio Grande Rise/Ridge, WVR Walvis Ridge.

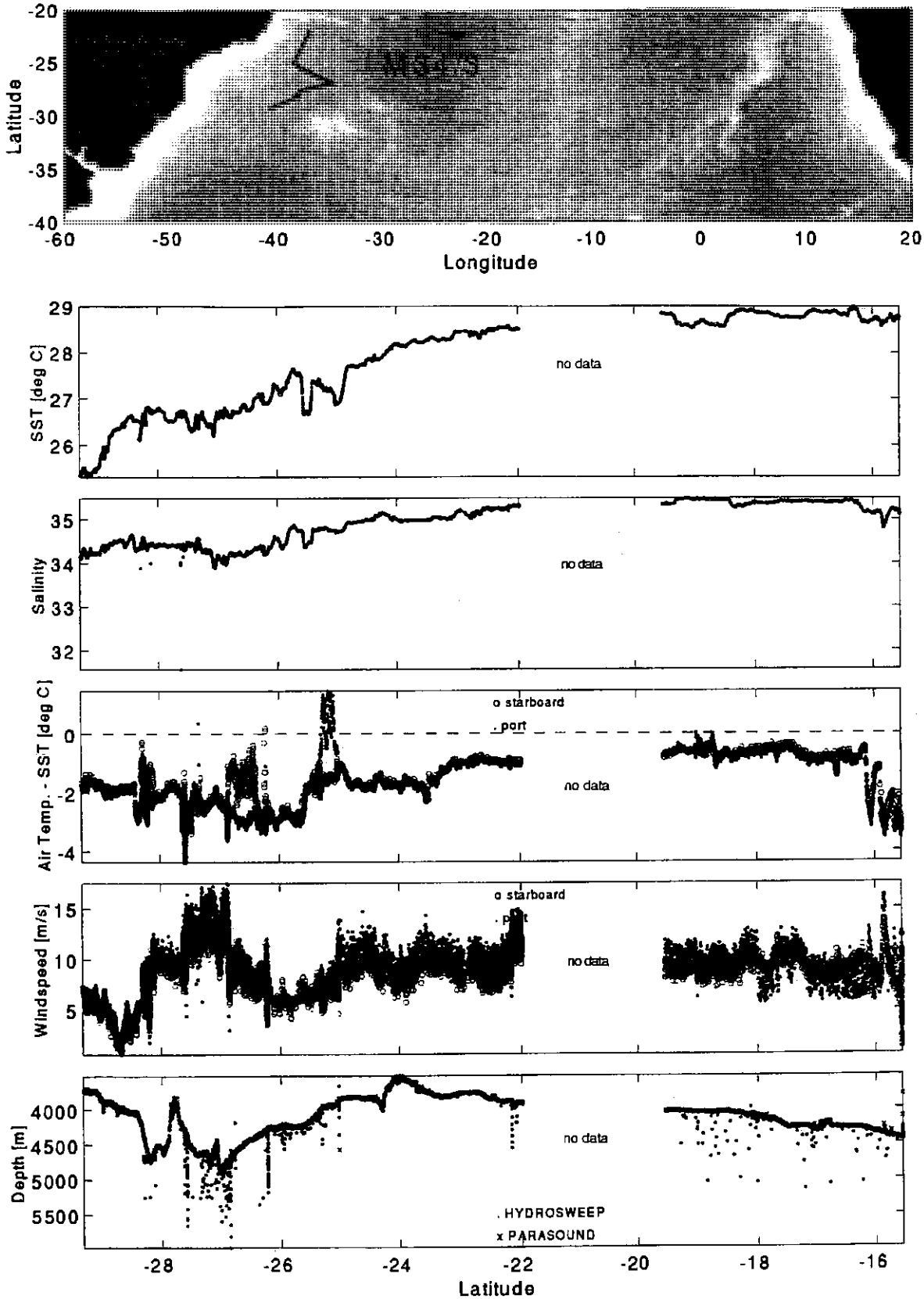

Fig. 145: DVS data north of Vema Extension. Data are shown as a function of geographical latitude.

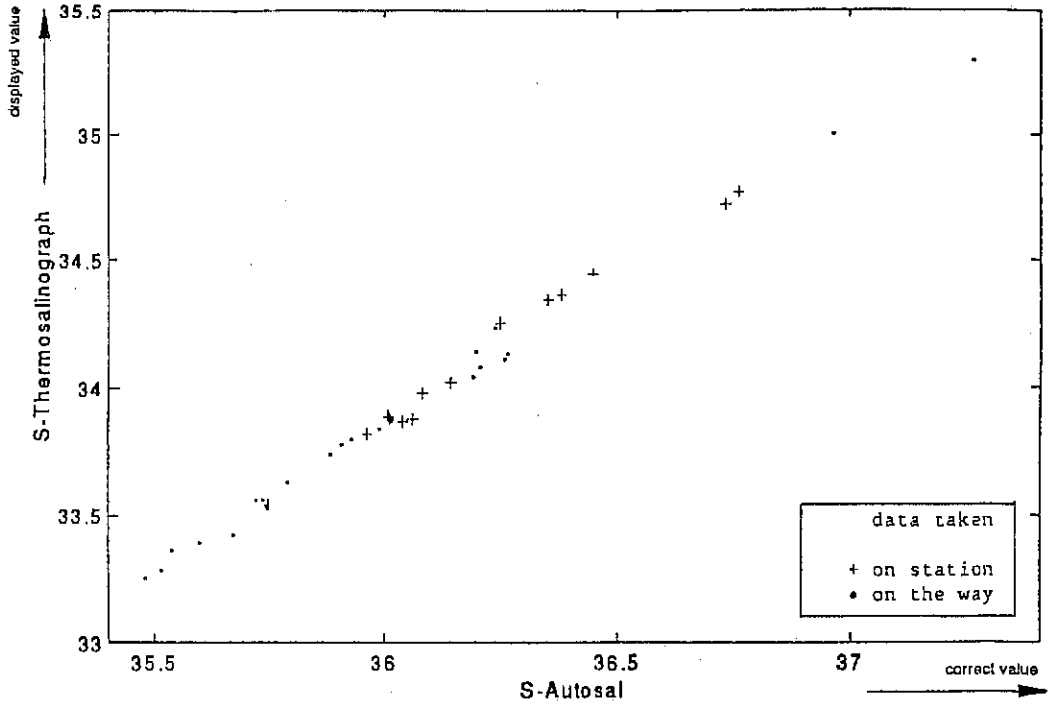

Fig. 146: Correction curve for the thermosalinograph equipment available during METEOR cruise 34/3.

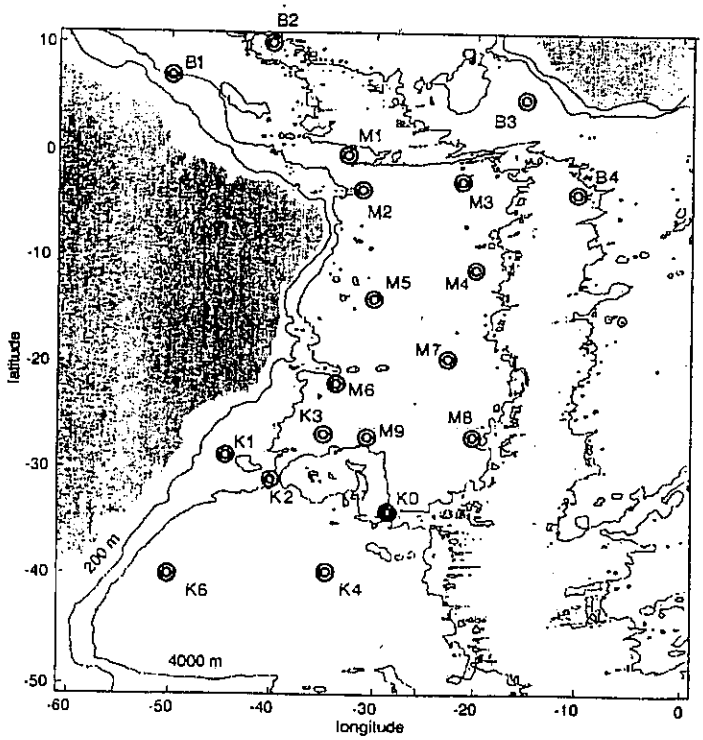

Fig. 147: Distribution of all RAFOS sound sources in the South Atlantic prior to the recovery of K02, K2, and K3. "K" denotes instruments supplied by IfM Kiel, "M" stands for WHOI instruments, and "B" for devices from IFREMER Brest. The insonification network represents the base for all RAFOS float work in the Deep Basin Experiment (DBE) of the World Ocean Circulation Experiment (WOCE).

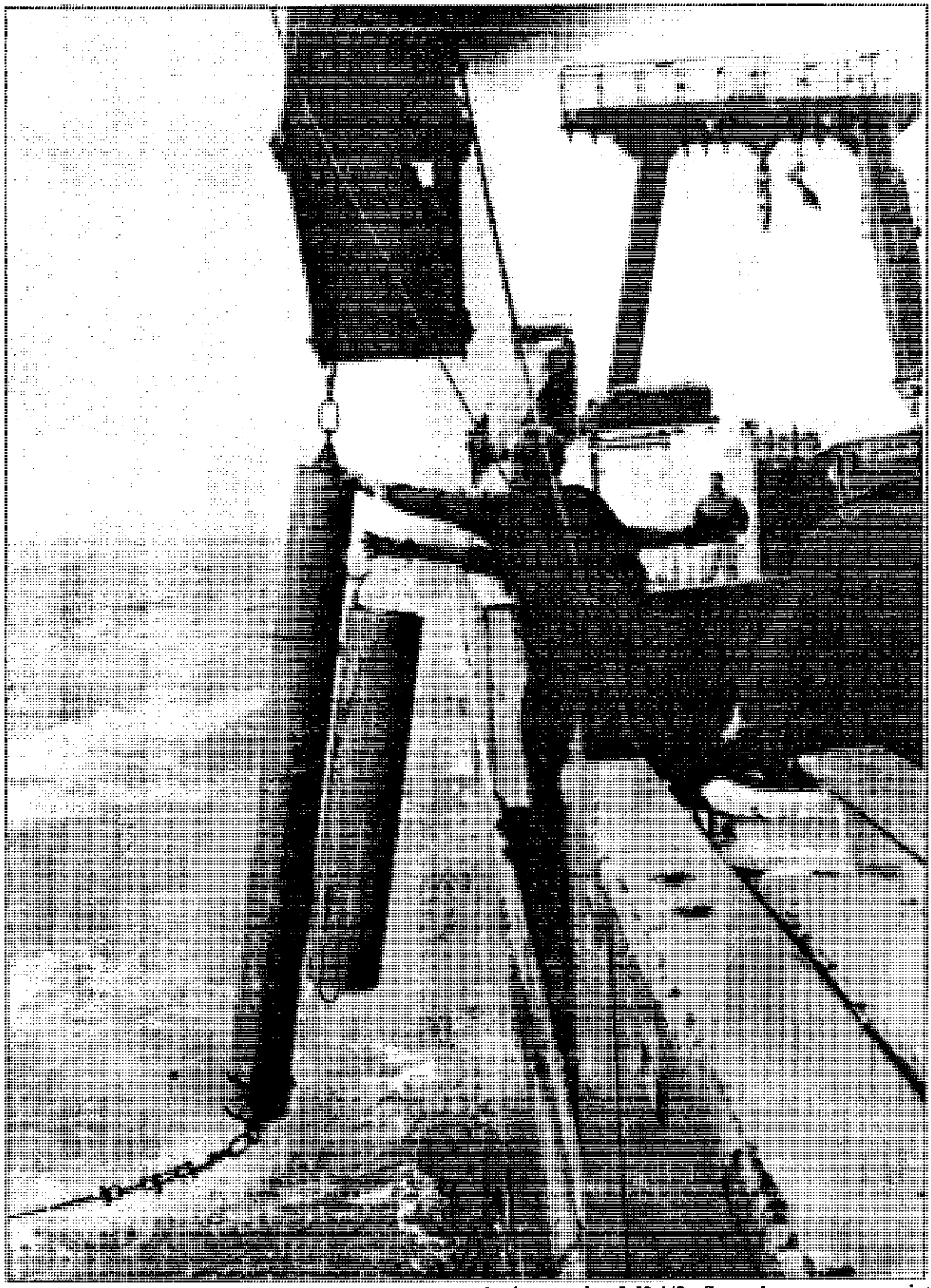

Fig. 148: Recovery of a WRC sound source during cruise M34/3. Sound sources consist of two parallel aluminium tubes. One contains the electronic module and the power package. It is suspended in the mooring line by its end plates. The second tube carries the ceramic transducer at its upper end. The rest of this tube is open and serves as a resonator. The shown instrument (K2) was moored for 3 years and 3 months.

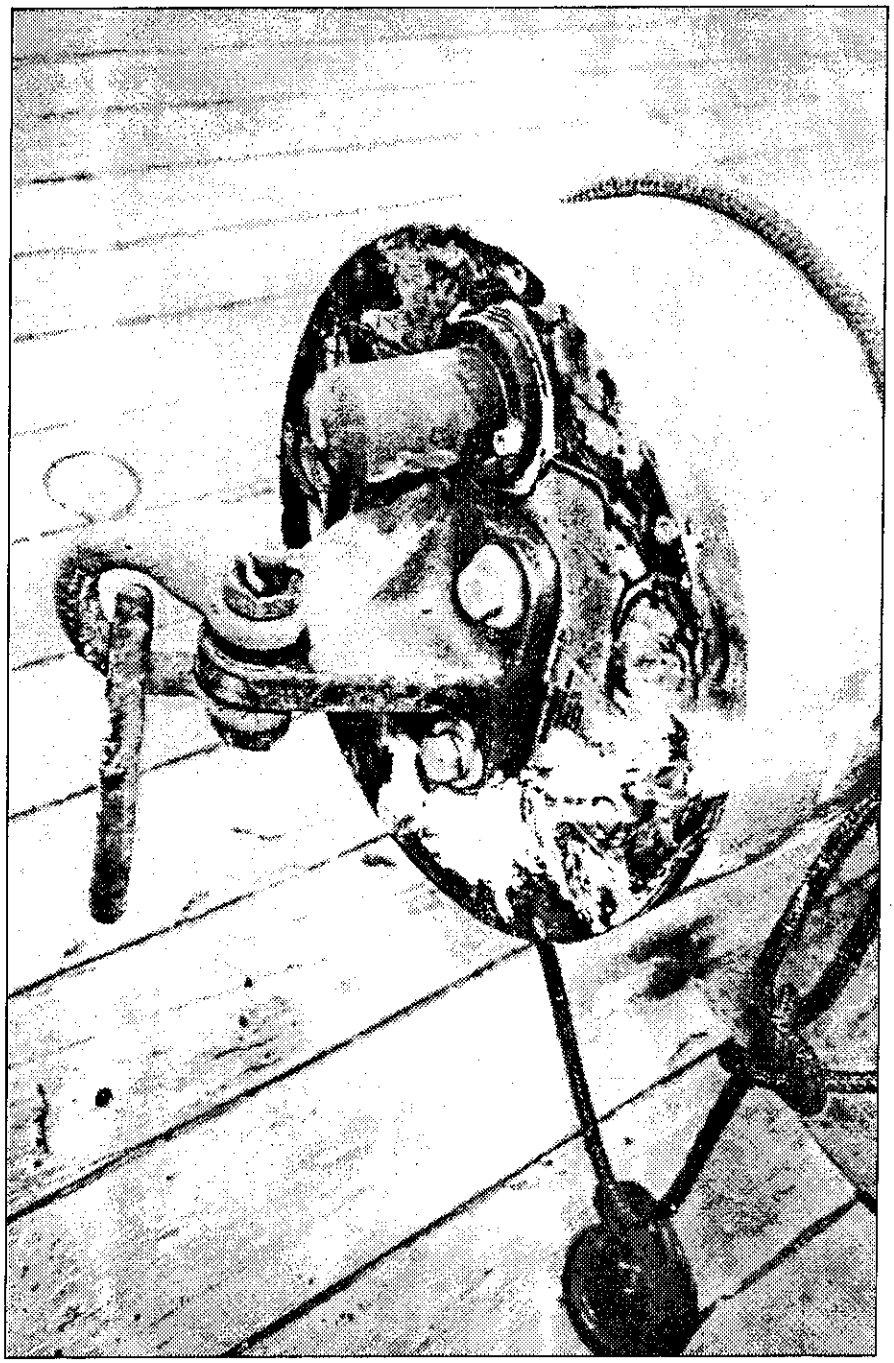

Fig. 149: Endplate of sound source #86 from mooring K2.

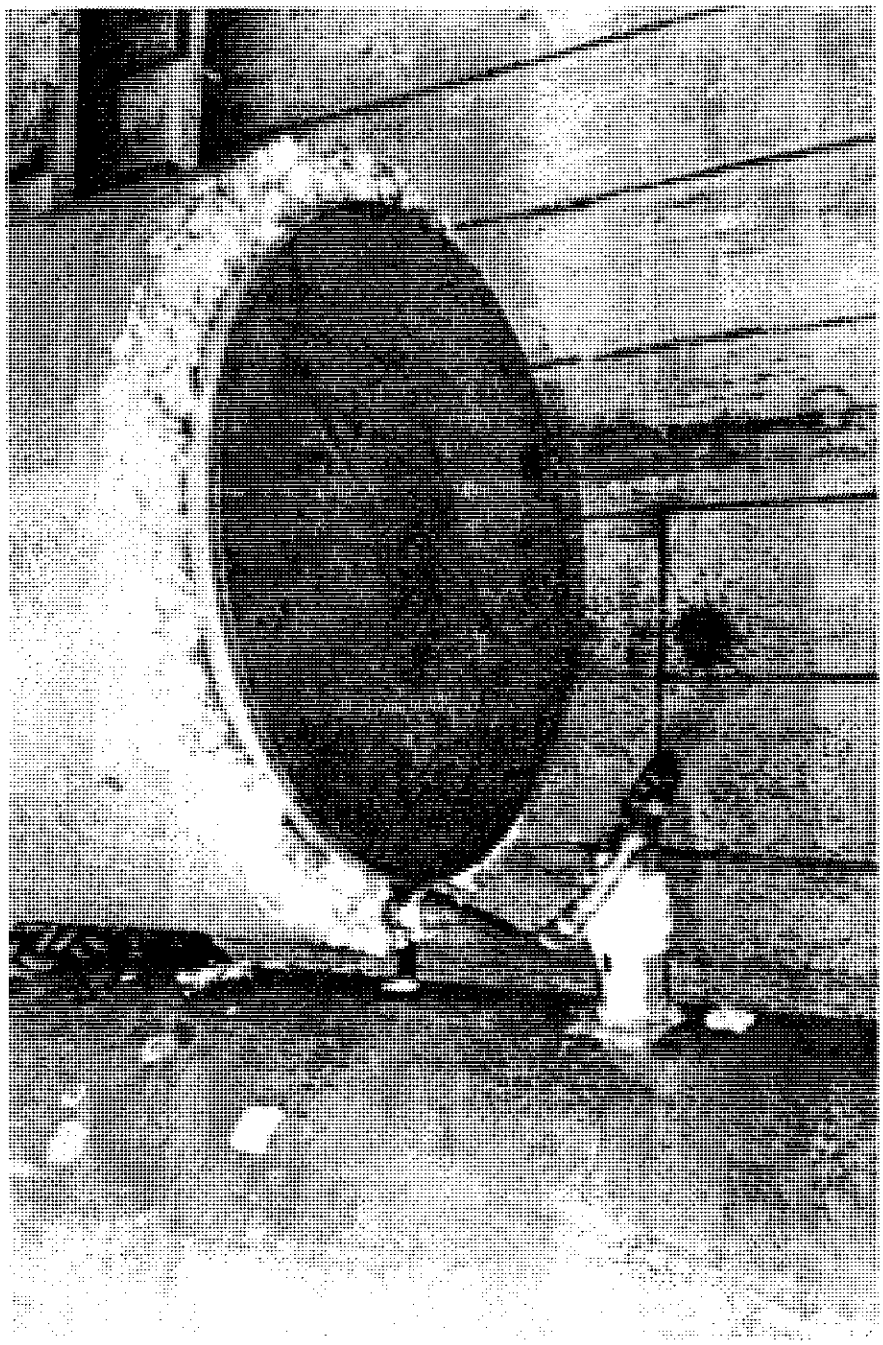

Fig. 150: Transducer face of sound source #68 from mooring K3.

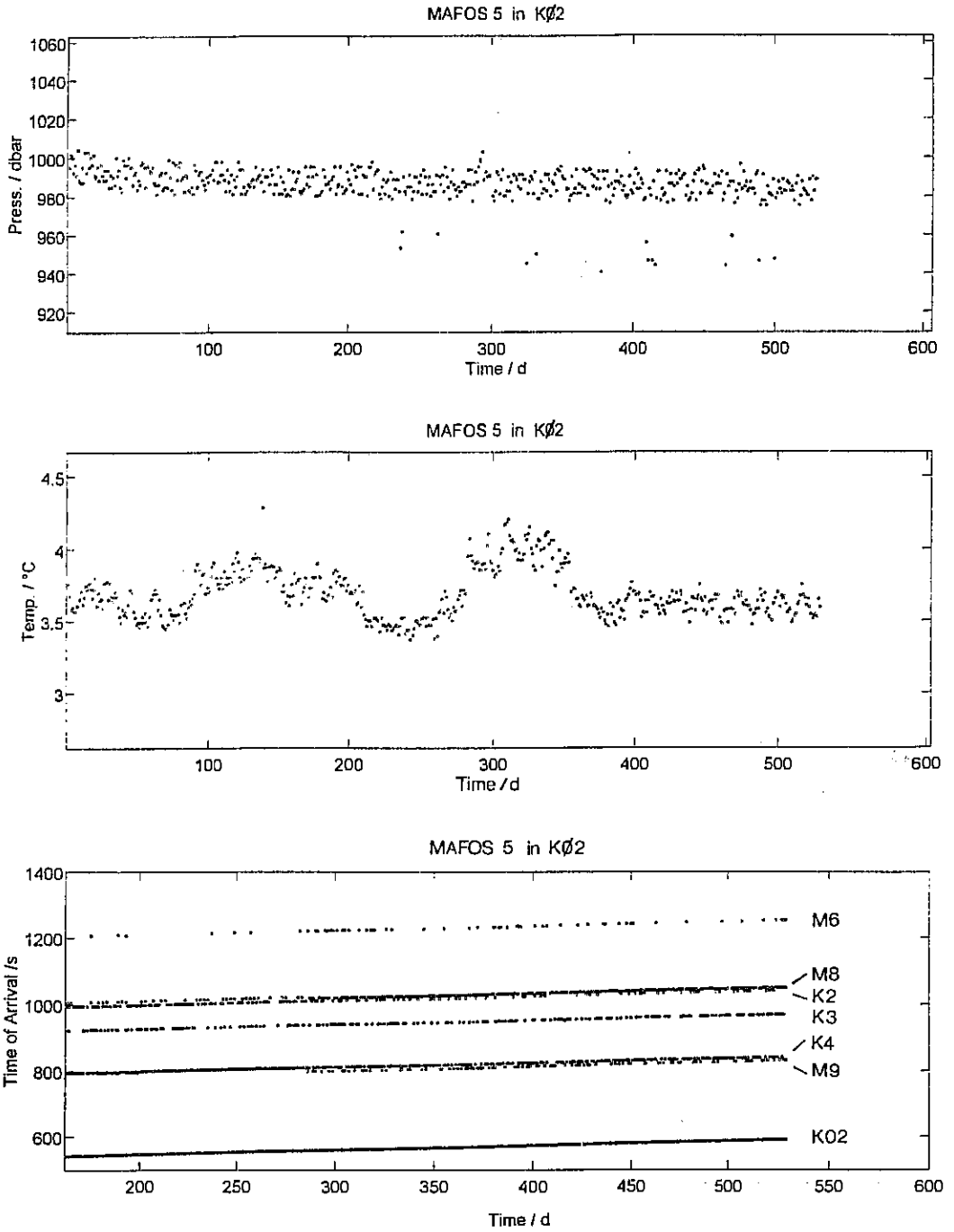

Fig. 151: Time series of MAFOS 5 moored at the Hunter Channel (K02). Record V352202 starts on June 3, 1994, 01:55 UTC. Daily pressure values (a) are shown above corresponding temperatures (b). No filter procedures were applied for these preliminary data. The discrepancy between nominal depth 1100 m and the displayed pressure time series and its mean of 987 dbar in Table 25 remains open. The extremely rough bottom topography at the mooring site may be a first explanation. Subfigure (c) displays RAFOS time of arrival (TOA) series from various sound sources shown in Figure 147. For details see OLLITRAULT (1995) and SIEDLER et al. (1993). "K" denotes signal generators supplied by IfM Kiel, "M" those from the Woods Hole Oceanographic Institution (WHOI). TOA series were processed by IfM ARTOA by MENZEL (1995).

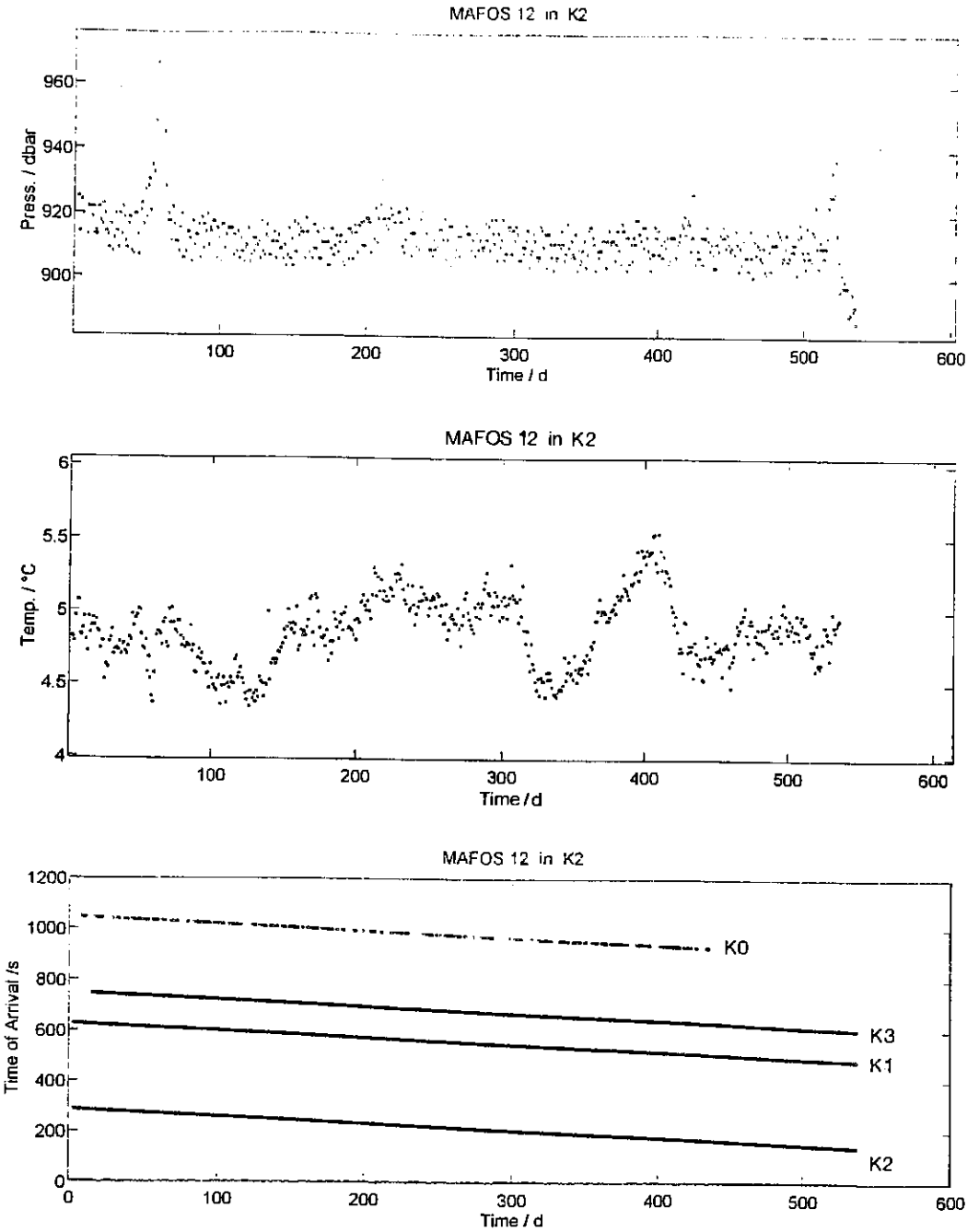

Fig. 152: Time series from MAFOS 12 moored at the Vema Channel (K2). Record V350101 starts on December 7, 1992, 01:55 UTC. Daily pressure (a) values are displayed above corresponding temperatures (b). No filter procedures were applied to these preliminary data. The mean pressure amounts to 906 dbar which is in good agreement with the instrument's nominal depth of 900 m (cf. Table 25). Subfigure (c) shows simultaneous arrival times (TOA) of RAFOS signals from sound sources K0, K1, K2, and K3. For details on insonification see SIEDLER et al. (1993) and Figure 153. Note the meeting signal of K0 after ~440 d. This sound source later was replaced by K02. TOA series were processed by IFM ARTOA by MENZEL (1995).

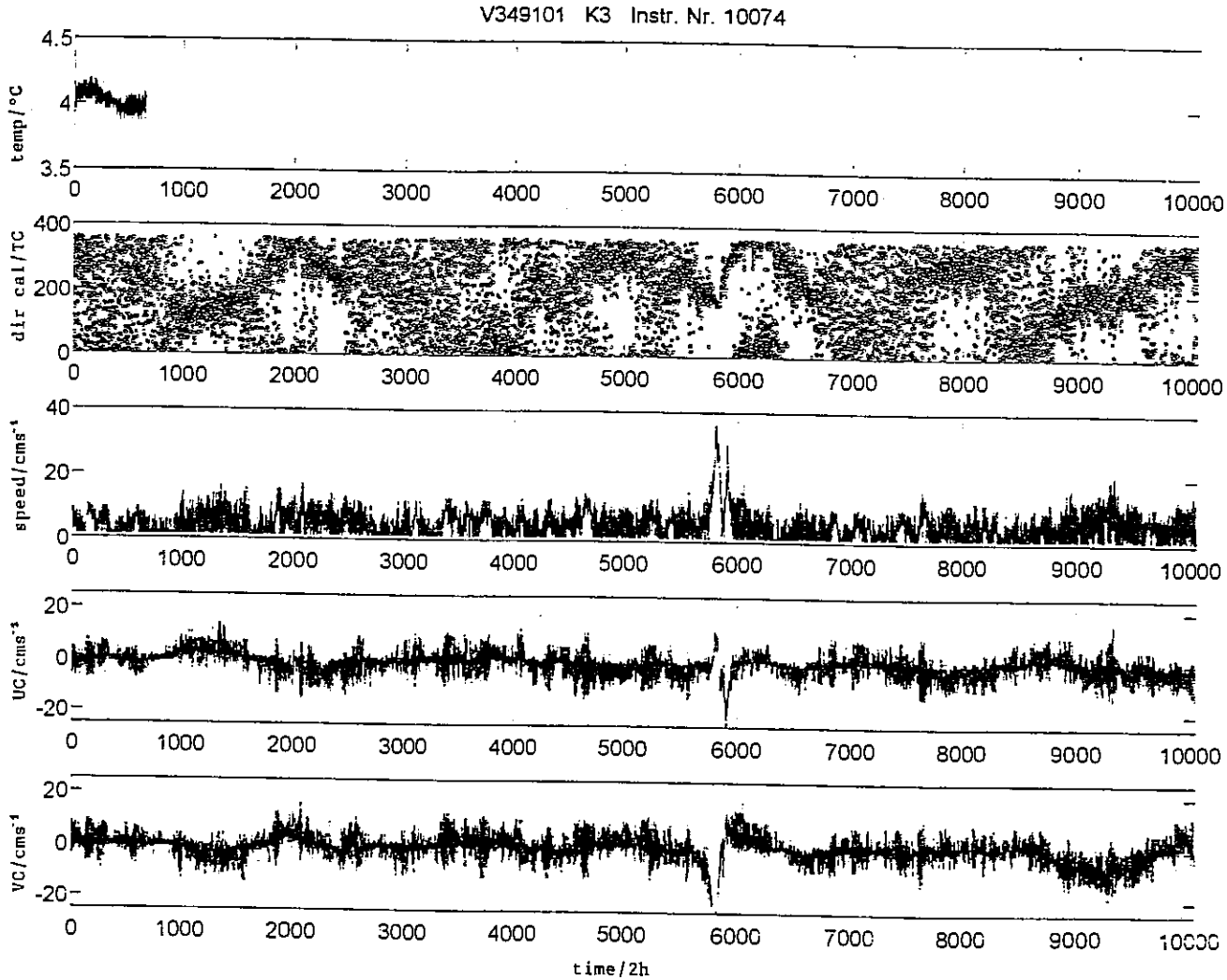

Fig. 153: Time series of V349101 in K3 at 997 m, i.e. the level of the Antarctic Intermediate Water at the Vema Extension. Time series start on December 19, 1992, 00:00 UTC. For location see Figure 125 and 147. The top panel (a) contains preliminary temperature data. This series ends after 55 days due to technical problems. The followingsubfigure (b) shows directions corrected for the magnetic deviation (24° W). Next (c) is recorded vector/averaged speed. The two lowest subfigures (d) and (e) contain zonal and meridional current components (UC, VC).

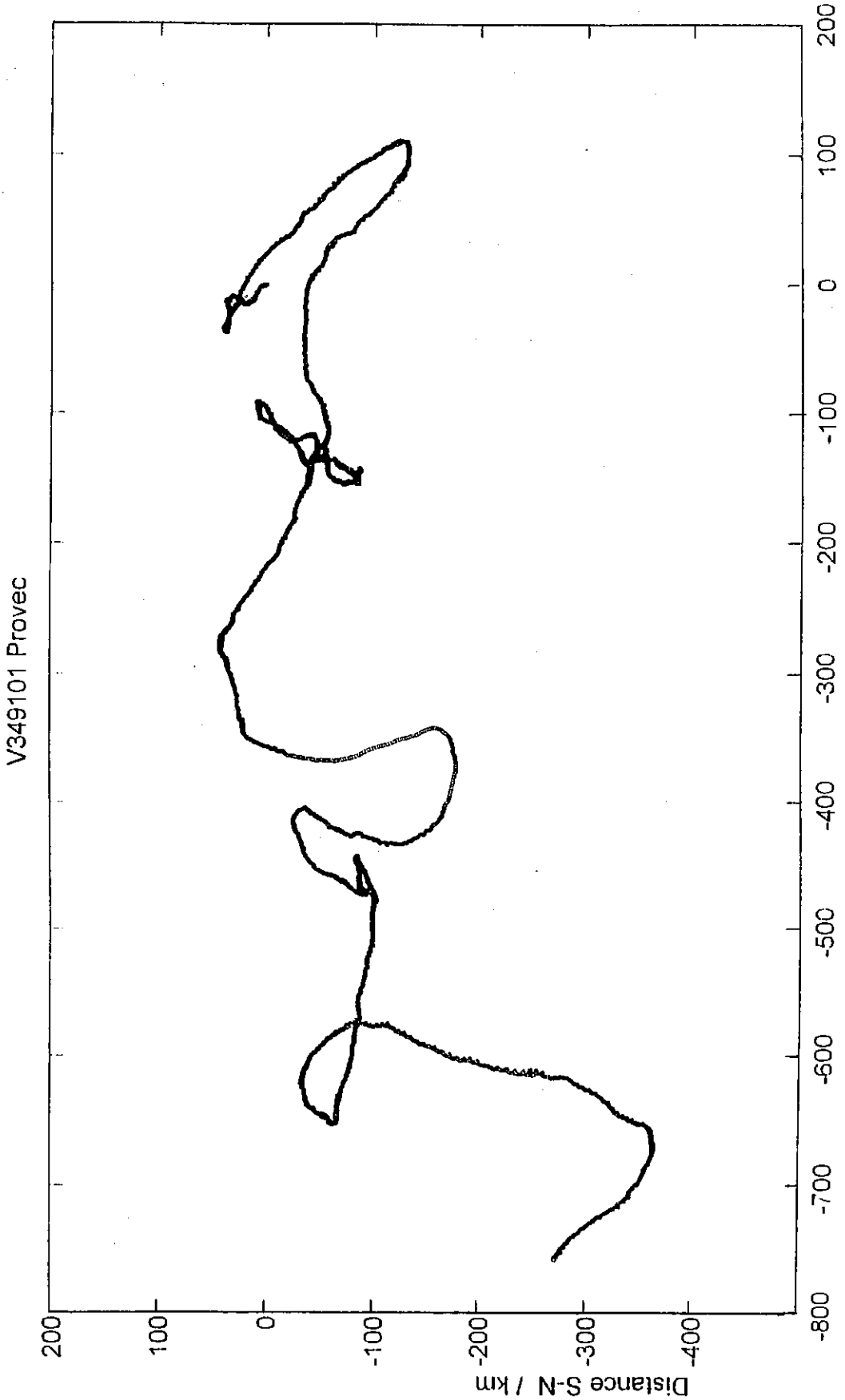

Fig. 154: Progressive vector diagram from V349101 at K3, 997 m representing 27.5 data month (cf. Fig. 153). North is upward. 2-hourly data were not filtered prior to plotting. The general trend towards west coincided with similar findings from Lagrangian observation in the area (BOEBBEL et al., 1996). It is part of the basin-wide anticyclonic circulation of the Intermediate Water in the subtropics of the South Atlantic.

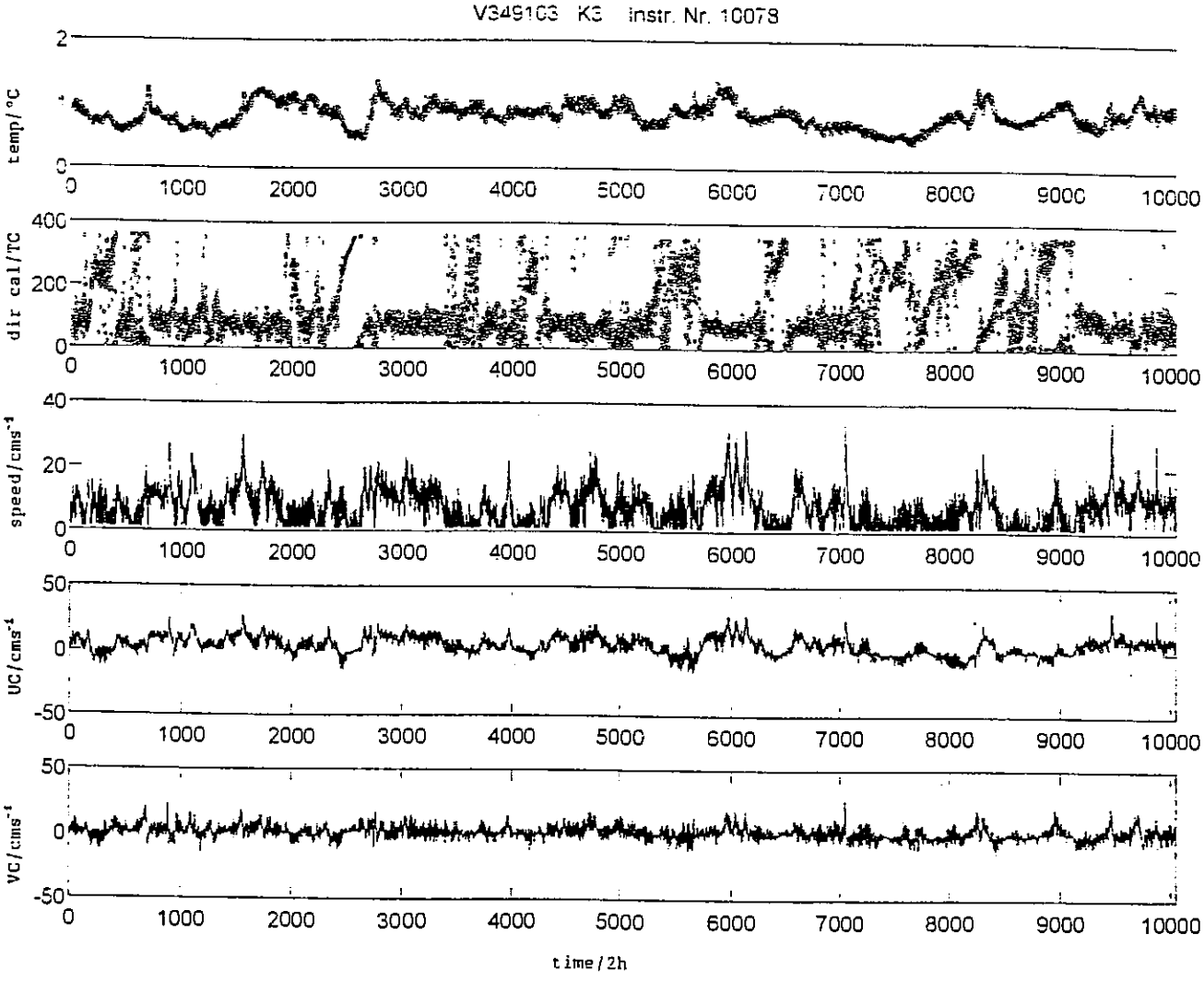

Fig. 155: As Figure 153, but for V349103 in K3 at 4352 m, i.e. the level of Antarctic Bottom Water (θ <2.0°C). Temperature calibration in (a) is not yet final.

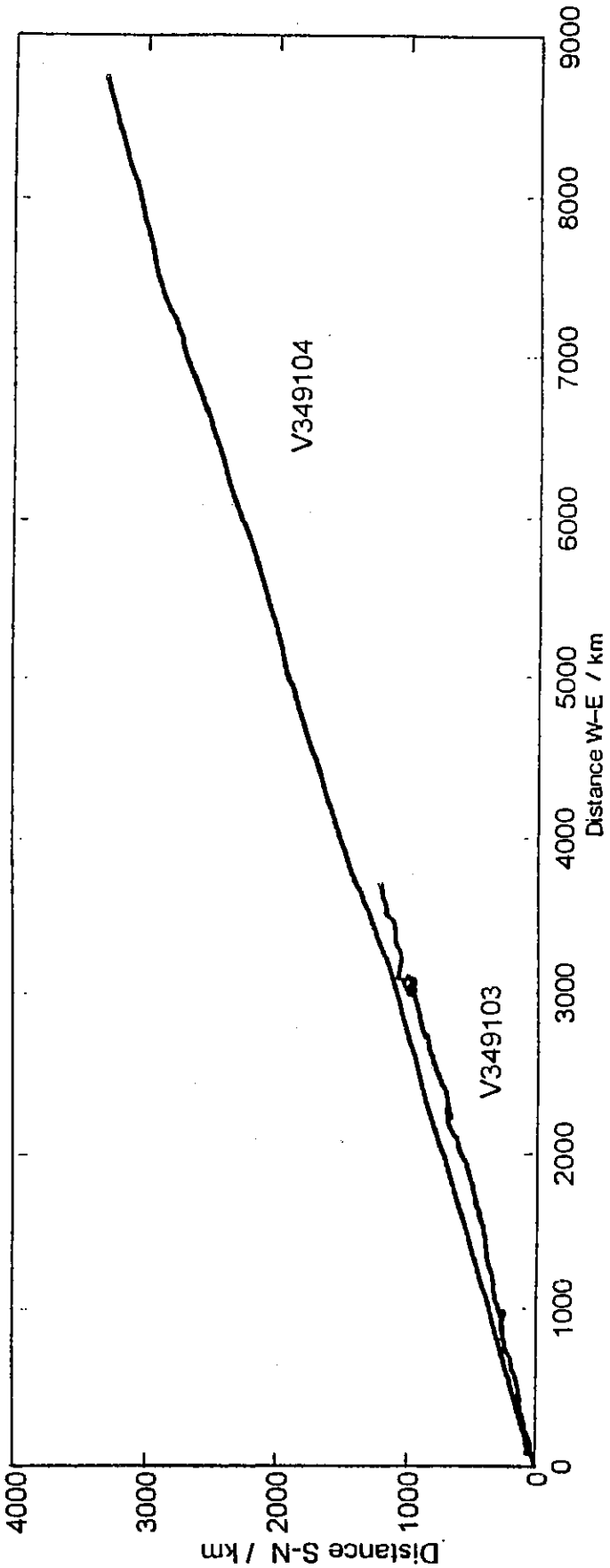

Fig. 156: Progressive vector diagrams from V349104 at K3, 4352 m and 4849 m. Details as in Figure 154. A clearly directed deep flow is controlled by the local bottom topography. The current advects Antarctic Bottom Water (θ <2.0°C) and ist sub-water mass Weddell Sea Deep Water (θ <0.2°C) eastnortheastward into the deep (z > 500 km) Brazil Basin with highest speeds near the bottom contour current). Vertical velocity shear amount to > 14 cm s^{-1}/km.

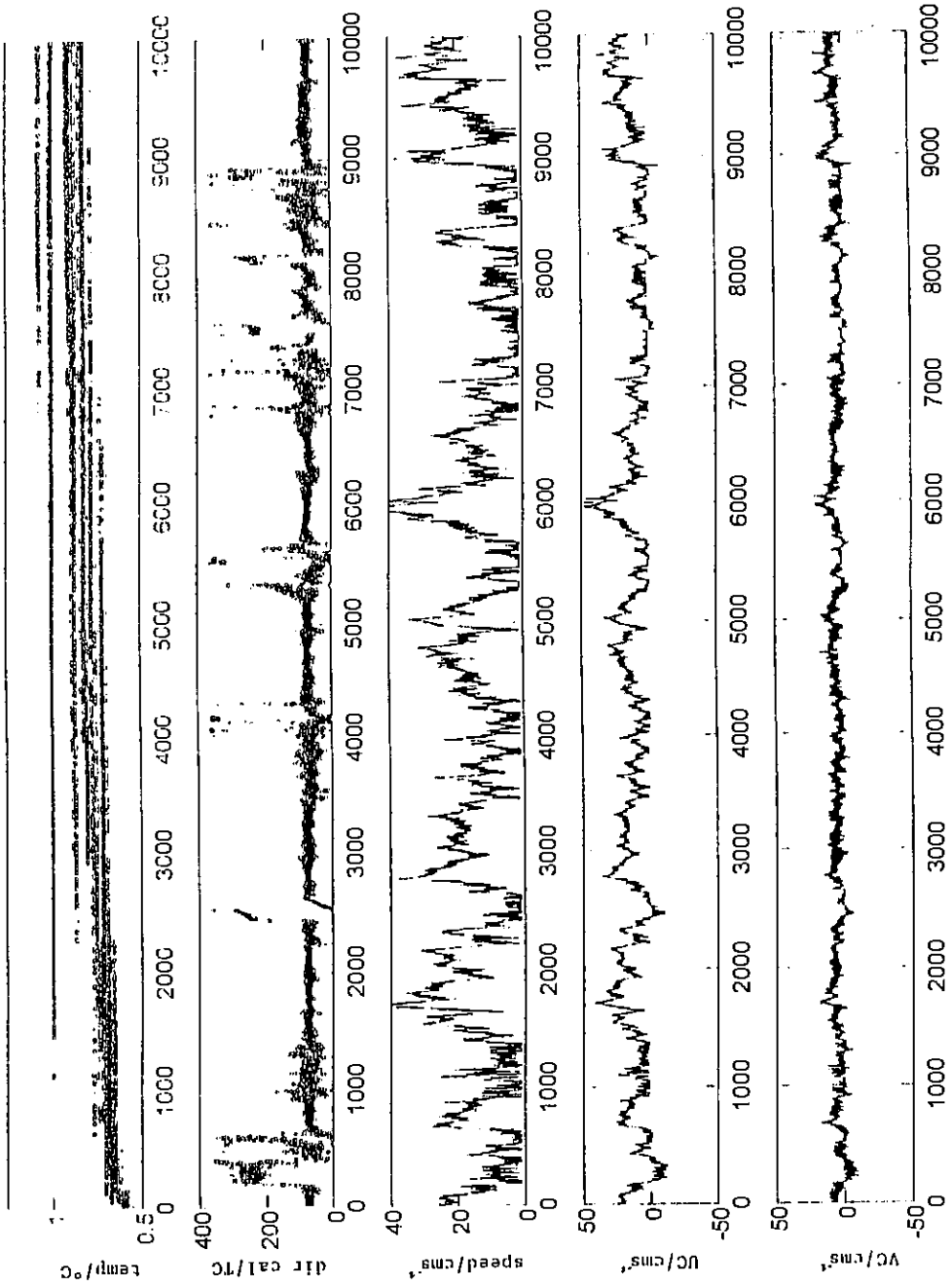

Fig. 157: As Figure 153, but for V349104 in K3 at 4849 m, i.e. in the Weddell Sea Deep Water range. Temperature calibration in (a) is not yet final. Note the strong directional character of the flow also seen in Figure 156. For more information see Table 25.

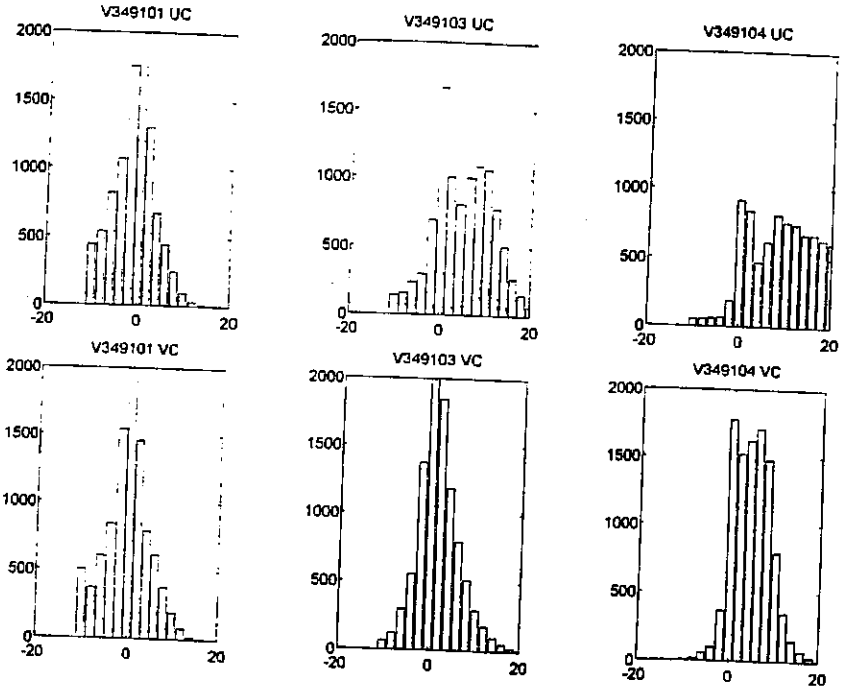

a)

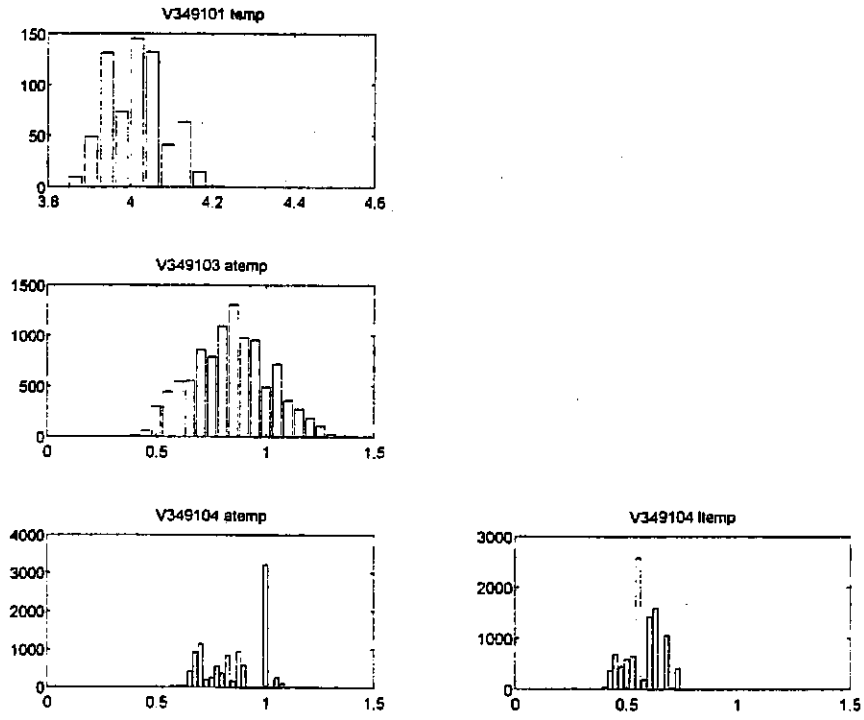

b)

Fig. 158: Histograms of time series V349101, 03, and 04 shown in Figure 153, 155, and 157. The absolute frequency distribution of current components (a) UC and VC (cm s^{-1}) and (b) temperatures (°C) are displayed.

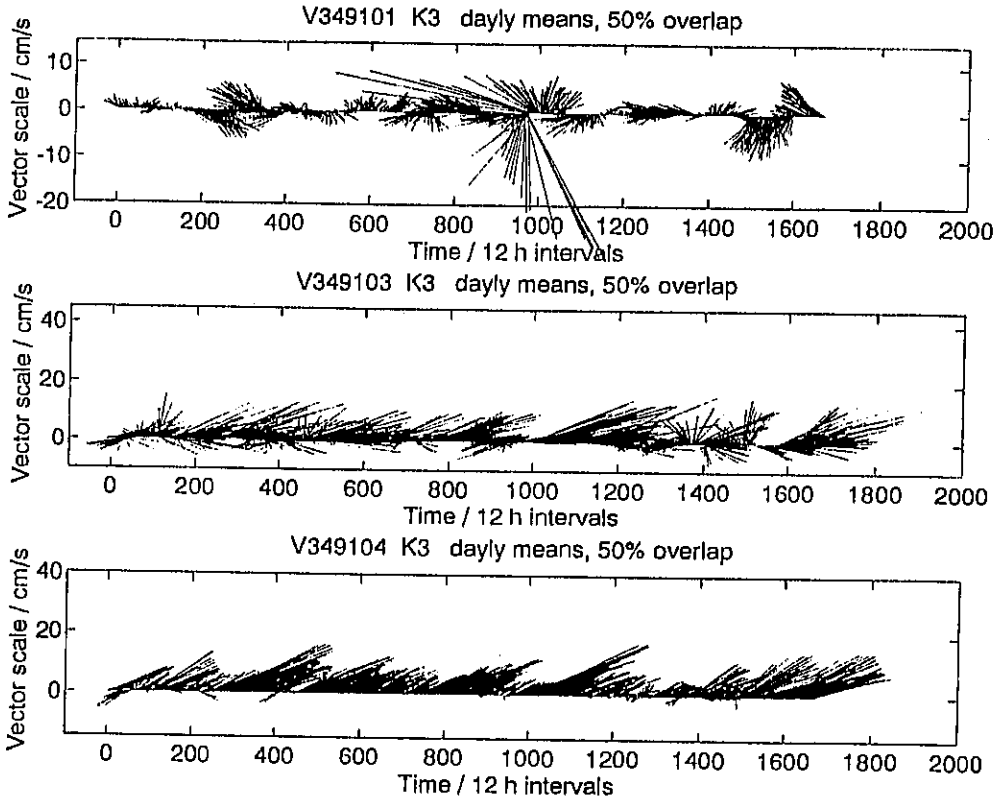

Fig. 159: Stick plot diagram of mooring V349.

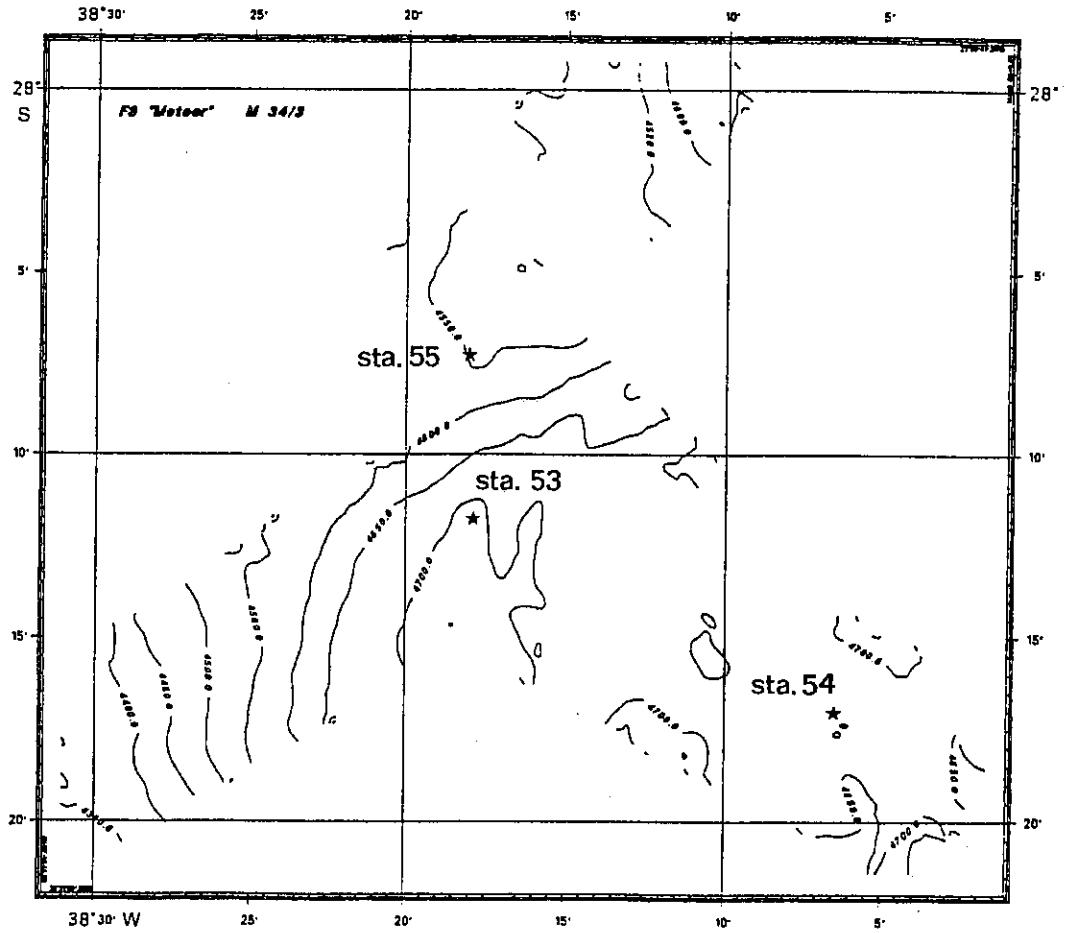

Fig. 160: Topography at Vema Exit. Stars (*) denote CTD stations. Isobath distance 50 m (processed by Steffenhagen).

5.3.2 Continuous Chlorophyll-a Measurements

(H. Buschhoff, M. Giese, M. Scholz,)

For the determination of chlorophyll-a concentrations in the surface waters, 1 l seawater was collected about 3 times a day from a membrane pump (inlet in 3.5 m water depth) and filtered onto glass fibre filters and freezed at -20°C. Chl-a measurements by photometry will be done in the laboratory in Bremen. 61 samples were taken during the cruise. Up to now, Chl-a data are available from several METEOR cruises in the Atlantic Ocean (M6/6, M9/6, M12/1/2, M16/1/2, M20/1/2, M22/1, M23/1/2/3 and M29/1/2/3). 123 water samples were taken from the locations listed in Table 28. The chlorophyll-a data will provide information about the seasonal and regional variations in biomass and will also be used to calibrate satellite-derived chlorophyll data.

Tab. 28: List of water sampling for chlorophyll determinations

Sample No.	Date 1996	Time (UTC)	Latitude	Longitude	Water Depth	Salinity (‰)	Temperature (°C)	Volume (l)
98/99	22.02.	09:58	23°24,0' S	11°20,2' E	3357	33,19	22,8	2*0,5
100/101	22.02.	15:07	23°35,3' S	10°15,0 E	4094	33,52	23,0	2*0,5
102/103	23.02.	06:34	24°110,6' S	06°58,5' E	2994	33,62	23,2	2*0,5
104/105	23.02.	10:29	24°19,7' S	06°07,9' E	1611	33,75	23,5	2*0,5
106/107	23.02.	16:08	24°33,2' S	04°53,5' E	3432	33,8	23,7	2*0,5
108/109	24.02	06:56	25°07,9' S	01°44,3' E	5328	33,5	23,0	2*0,5
110/111	24.02	10:11	25°15,5' S	01°02,6' E	4319	33,66	23,1	2*0,5
112/113	24:02	16:02	25°29,2' S	00°11,8' W	7882	33,88	23,6	2*0,5
114/115	25.02.	07:54	26°02,2'	03°38,8'	4593	34,08	23,9	2*0,5
116/117	25.02	11:10	26°18,9'	04°17,1'	4457	34,05	24,1	2*0,5
118/119	25.02	17:01	37°05,1'	05°15,2'	4443	34,14	24,1	2*0,5
120/121	26.02.	07:57	29°02,3'	07°44,4'	3964	34,11	23,8	2*0,5
122/123	26.02.	11:03	29°25,4'	08°14,2'	4062	33,88	23,1	2*0,5
124/1254	26.02.	17:06	29°30,2'	08°17,4'	4524	33,89	23,4	2*0,5
126/127	27.02.	07:20	30°09,0'	08°30,0'	3970	33,88	23,0	2*0,5
128/129	27.02.	11:23	30°15,0'	08°32,7'	3963	33,93	23,3	2*0,5
130/131	27.03.	17:25	30°25,9'	08°35,9'	3988	33,97	23,6	2*0,5
132/133	28.02.	07:25	30°44'	09°53'	3722	33,81	23,5	2*0,5
134/135	28.02.	14:18	30°44,8'	10°20,8'	3657	33,85	23,7	2*0,5
136/137	28.02.	17:13	30°44,9'	10°26,6	3530	33,84	23,7	2*0,5
138/139	29.02.	07:51	30°45'	12°53,7'	2717	33,8	23,5	2*0,5
140/141	29.02.	11:16	30°45,0'	13°12,1'	2508	33,55	23,1	2*0,5
142/143	29.02.	17:03	30°45,0'	13°30,1'	3206	33,74	23,8	2*0,5
144/145	01.03.	07:53	30°48,8'	14°42,7'	3213	33,65	23,5	2*0,5
146/147	01.03.	17:18	31°03,2'	16°19,6'	3470	33,99	24,2	2*0,5
148/149	02.03.	07:53	31°20,7'	18°05,7'	3887	34,00	24,6	2*0,5
150/151	02.03.	12:17	31°21,3'	18°09,8'	4090	33,98	24,6	2*0,5
152/153	02.03.	18:10	31°31,2'	19°07,9'	4458	33,75	24,4	2*0,5
154/155	03.03.	07:52	32°03,5'	21°15,2'	4175	33,64	23,8	2*0,5
156/157	03.03.	12:15	32°16,4'	21°58,4'	4923	33,86	24,0	2*0,5
158/159	03.03.	18:10	32°16,3'	21°58,2'	4332	33,88	24,4	2*0,5
160/161	04.03.	08:44	32°44,1'	23°32,4'	4079	33,09	22,0	2*0,5
162/163	04.03.	12:26	32°57,0'	24°16,6'	4177	33,16	21,5	2*0,5
164/165	04.03.	18:14	33°18,1'	25°28,5'	4679	33,3	21,8	2*0,5
166/167	05.03.	10:01	34°13,5'	28°38,2'	4330	33,52	22,33	2*0,5
168/169	06.03	10:00	33°18,7'	32°00,6'	4144	33,36	21,2	2*0,5
170/171	06.03.	13:08	33°08,9'	32°40,0'	3714	33,36	21,2	2*0,5
172/173	06.03.	19:08	32°46,1'	34°00,1'	4011	33,53	22,2	2*0,5
174/175	07.03.	10:04	31°54,1'	37°07,6'	3789	33,25	21,6	2*0,5
176/177	07.03.	13:31	31°40'	37°51,5'	4053	33,29	22,4	2*0,5
178/179	07.03.	19:11	34°17,7'	39°01,2'	4033	33,74	23,9	2*0,5
180/181	08.03.	09:59	31°07,7'	39°53,9'	4693	33,95	24,2	2*0,5
182/183	08.03.	13:05	30°54,3'	40°00,4'	3824	33,72	23,8	2*0,5
184/185	08.03.	19:01	29°48,7'	40°31,6'	4044	33,83	25,0	2*0,5
186/187	09.03.	10:58	28°14,6'	38°23,5'	4604	34,35	26,5	2*0,5
188/189	09.03.	14:11	28°12,1'	38°17,3'	4708	34,33	26,7	2*0,5
190/191	09.03.	20:14	28°07,3'	38°17,8'	4565	34,42	26,7	2*0,5
92/193	10.03.	10:49	27°35,2'	37°55,2'	4371	34,36	26,6	2*0,5
194/195	10.03.	22:18	27°12,3'	36°15,6'	4688	34,31	26,5	2*0,5

Sample No.	Date 1996	Time (UTC)	Latitude	Longitude	Water Depth	Salinity (%)	Temperature (°C)	Volume (l)
196/197	11.03.	10:47	26°52,3'	34°48,3'	4780	34,00	26,7	2*0,5
198/199	11.03.	14:39	26°45,6'	35°02,9'	4585	34,17	26,6	2*0,5
200/201	11.03.	20:11	26°19,4'	36°06,7'	4327	34,35	27,1	2*0,5
202/203	12.03.	10:51	25°20,1'	37°59,0'	4009	34,78	27,3	2*0,5
204/205	12.03.	14:14	25°19,0'	38°00,2'	3983	34,78	27,3	2*0,5
206/207	12.03.	20:34	25°01,9'	38°32,8'	3844	34,73	27,0	2*0,5
208/209	13.03.	10:40	23°30,3'	37°45,7'	3772	34,98	28,3	2*0,5
210/211	13.03.	14:09	22°56,1'	37°28,3'	3759	35,17	28,5	2*0,5
212/213	13.03.	20:21	22°07,8'	37°03,8'	3932	35,27	28,5	2*0,5
214/215	14.03.	10:53	19°49,8'	35°54,4'	4000	35,32	28,7	2*0,5
216/217	14.03.	14:33	19°14,1'	35°36,6'	4043	35,44	28,6	2*0,5
218/219	14.03.	20:12	18°30,6'	35°15,2'	4034	35,42	28,6	2*0,5
220/221	15.03.	10:56	15°55,2'	34°59,9'	4362	35,17	28,7	2*0,5

5.3.3 Continuous pCO_2 Determination

(A. Körtzinger, S. Schweinsberg)

During the third leg of cruise no. 34 of RV METEOR the partial pressure of CO_2 (pCO_2) in surface seawater and overlying air was measured by the CO_2 project of Kiel University.

The pCO_2 is one of four measurable parameters (i.e. partial pressure of CO_2, total dissolved inorganic carbon, total alkalinity, pH value) of the marine CO_2 system. The individual chemical species of CO_2 in seawater (CO_2, HCO_3^-, CO_3^{2-}) are not susceptible to direct analysis. However, due to the very precise knowledge of the thermodynamic relationships within the marine CO_2 system these species can be calculated from measurements of at least two parameters. Furthermore the measurement of pCO_2 in surface seawater and overlying air provides valuable information about the degree of saturation of the surface seawater and the CO_2 exchange. Any partial pressure difference (ΔpCO_2) at the interface between the two bulk layers is the thermodynamic driving force of net gas flux. Thus the measured ΔpCO_2 can directly be converted into values of the net flux of CO_2 across the air-sea interface by applying valid exchange coefficients taking into account temperature, salinity and wind speed. The activities of the Kiel CO_2 project during cruise no. 34/3 of RV METEOR only included pCO_2 measurements.

The pCO_2 measurements were carried out in the context of large international efforts to assess the surface pCO_2 and produce a pCO_2 map of the world ocean. This is mainly based on two ideas. First of all a good qualitative and quantitative knowledge of the surface distribution of sources and sinks for atmospheric CO_2 is crucial in understanding the marine and the global carbon cycle. Furthermore a precise and reliable assessment of the surface pCO_2 in the world ocean may serve as an additional tool to estimate the oceanic uptake of anthropogenic CO_2, which has become a key question in the discussion of climate change.

The analytical system used to measure the pCO_2 (KÖRTZINGER et al., 1996) is based on the continuous equilibration of a seawater stream with a carrier gas the CO_2 content of which is monitored and usually logged at 1 or 2 minute intervals. The system includes an open system equilibrator operated at ambient pressure, into which the carrier gas is pumped through a glass frit to equilibrate with the seawater stream. The time constant for the equilibration proc-

ess is about 75 sec. Due to this comparatively short time constant even small-scale features of the surface pCO_2 patterns can be resolved. The CO_2 content of the carrier gas is continuously measured by infrared detection. Parallel measurement of the water vapour content allow the carrier gas to be measured without drying. Thus it can be recycled through the system completely unchanged. The CO_2 readings are automatically corrected for pressure, temperature and water vapour pressure. The measurement of pCO_2 in air in carried out with clean outside air, which is pumped to the system from the compass platform of the vessel.

The measured raw data (CO_2 mole fraction, corrected for dry air at a pressure of 1 atm) are converted into the partial pressure of CO_2 by using data for sea surface temperature and barometric pressure. They are then merged with GPS positions (and other meteorological parameters) to give surface profiles of the *in situ* surface pCO_2 along the ship track. The conversion and merging of raw data as well as the validation process take some time and could not be carried so far. A full evaluation of the data is therefore impossible at this stage. A first inspection of the data sets allows for some qualitative statements, which shall be explained briefly.

The most striking feature of the data is the fact, that during the whole cruise the surface waters were considerably supersaturated with CO_2 with respect to the atmospheric level. While the CO_2 mole fraction was around 360 ppmv throughout the cruise the CO_2 mole fraction in the seawater equilibrated carrier gas ranged between 380 and above 500 ppmv, with the average lying slightly above 400 ppmv. This is equivalent to a range from only slight supersaturation to a marked supersaturation of up to 150 ppmv and more in some spots. Depending on the wind forcing prevailing at the time and place of measurement the resulting CO_2 fluxes are significant. In general the patterns of surface pCO_2 clearly follow the patterns of the sea surface temperature, i.e. higher temperature are associated with higher pCO_2 values. This reflects the temperature dependency of solubility of CO_2 gas, which is decreasing with increasing temperature. However, the observed pCO_2-temperature relationship does rarely reach the thermodynamic value of about 4.1 %/°C. This is due to the superposition of various processes that effect the surface pCO_2, i.e. air-sea exchange, photosynthesis and respiration, and temperature changes.

According to the qualitative inspection of the data there is no firm evidence of marked upwelling. Upwelling processes may have a dramatic impact on the surface pCO_2, as observed in the Arabian Sea during the 1995 south-west monsoon. In a few cases a reversed pCO_2-temperature correlation was observed, which may be indicated of waters affected by upwelling. However, these interesting first findings will have to be analyzed more carefully.

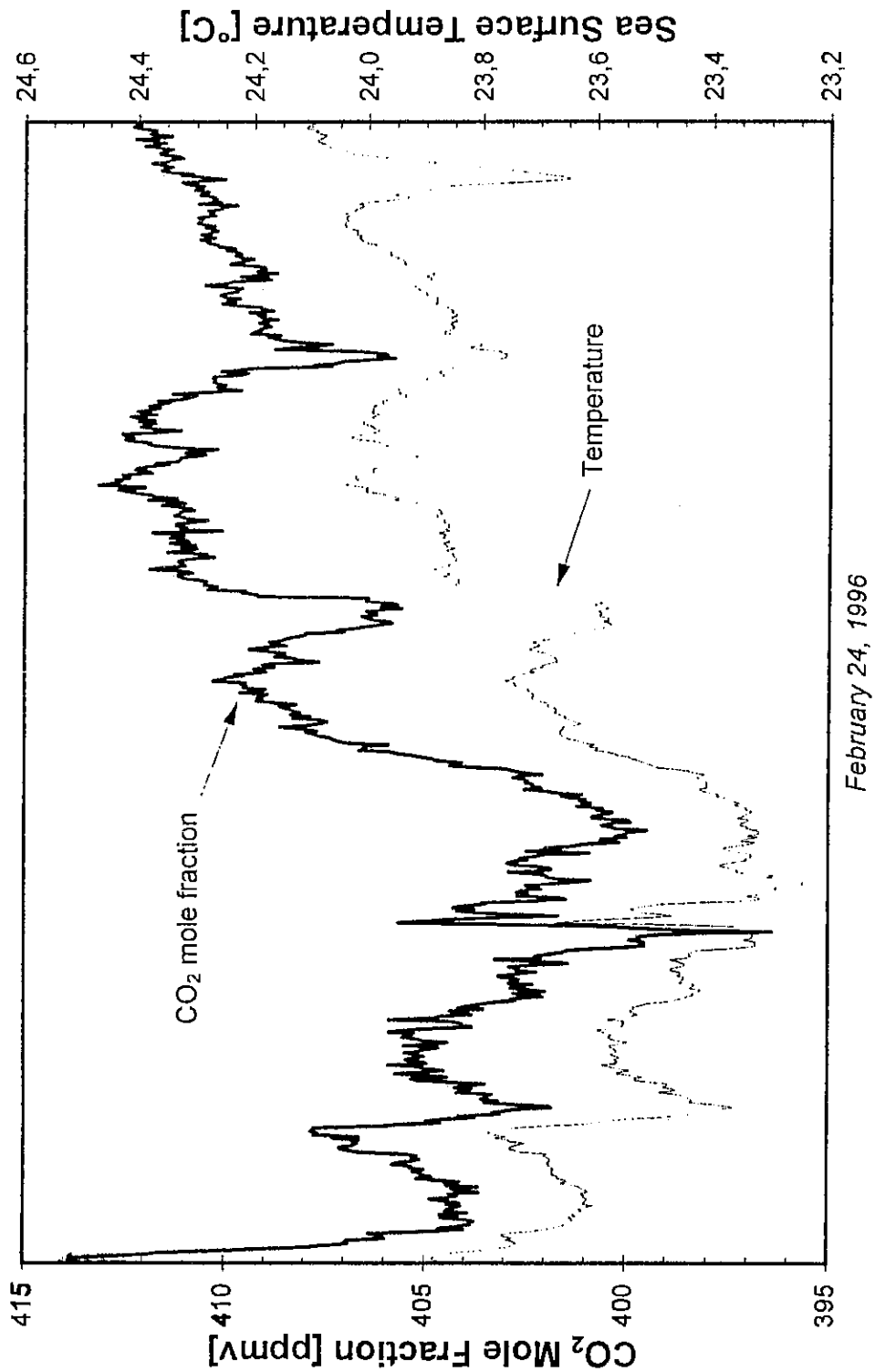

Fig. 161: CO_2 mole fraction and temperature during February 24, 1996.

5.3.4 Phytoplankton Sampling Using Filtration Methods

5.3.4.1 Dinoflagellates

(A. Meyer, H. Willems)

Dinoflagellates are one of the major groups in the marine phytoplankton community. As a result of their life cycle, they occur in two different stages: As a motile cellulose vegetative-thecate stage, among them the only calcareous-walled vegetative-coccoid *Th. heimii*, and as a resting cyst stage which in most cases is organic-walled but which also comprises calcareous tests (•calcispheres"). During the cruise, phytoplankton samples were collected from the water column at different depth ranging from surface waters to 200 m and analyzed on the content of living dinoflagellates. Of special interest was the appearance of calcareous tests, resting cysts as well as the vegetative *Th. heimii*, with regard to their lateral and vertical distribution in the investigated water column. The study aims at a better understanding of the interaction between the species associations and the related environmental parameters (temperature, salinity, light) for a better interpretation of fossil assemblages in the underlying sedimentary record and their applicability as a proxy in paleoceanography.

The plankton was collected by filtering surface water pumped on board with the ship's membrane pump from a depth of 2.5 m three times a day: morning, midday, afternoon (Tab. 29). The zooplankton was separated by passing the water through a 250 µm mesh sieve (DIN 4188). The water was filtered through a 10 µm gauze continuously for a time period of 2 to 4 hours. For the isolation of living specimens of dinoflagellates for culturing experiments, the filtered water was investigated for vegetative-thecate dinoflagellates, their calcareous cysts, and the vegetative-coccoid *Th. heimii*. Individual specimens - mainly calcareous cysts - were isolated and rinsed in polyterene Cell Wells™ with different culture media (f/2 35‰, K 35‰, filtered sea water). An attempt was made to culture calcareous cysts under "on board" conditions, i.e. the local day/night cycle and temperatures between 20°-25°C. Germination experiments and routine culturing of living calcareous cysts-producing dinoflagellates for the investigation of productivity, life cycles, biomineralisation and systematic will be done at the Laboratory at Bremen University.

After the isolation of living forms, the filtered residue together with 250 ml sea water was stored in autoclaved NALGENE polycarbonate flasks and fixed with 2-4 % Formaldehyde. For transportation, the samples were stored in the dark at 4°C. Parallel to this procedure, another 30 litters of sea water were filtered using a 5 µm gauze by a vacuum pump system (Tab. 30), especially to obtain the very small-sized specimens of *Th. heimii*. The phytoplankton concentrated on these polycarbonate filters was first investigated for living dinoflagellates, too, and afterwards stored in the same way like the 10 µm material. In a third step, samples from different depth were collected using a combined CTD/Rosette device with 10 l NISKIN Bottles. At depth of about 20, 50, 100, 150, and 200 m between 8 and 10, occasionally up to 20 liters of sea water have been collected (Tab. 31). The sea water obtained was sieved through a 250 µm sieve, afterwards it was filtered using a 5 µm pore size polycarbonate filter. The filtered residue was scanned for its living dinoflagellate cyst content and afterwards

stored in the same manner in 250 ml NALGENE flasks. All stored water samples and filters will be prepared for Scanning Electron Microscopy (SEM) in the Laboratory for the examination of the composition and regional distribution of dinoflagellate communities in the South Atlantic.

Among the dinofagellates, the motile vegetative-thecate stages have been observed in almost every sample, but only with extremely few specimens in the Central South Atlantic (south of 27° S). They were generally very rare in samples deeper than 20 m. In the eastern part of the South Atlantic, the predominant genera was *Ceratium*, followed by *Ornithocercus*. In the western part the predominant genera were *Protoperidinium* (with highest diversity), *Gonyaulax*, *Ornithocercus*, *Ceratocorys*, and occasionally *Scrippsiella*. Calcareous dinocysts were encountered in almost every sample north of 28° S and in water more than 26°C. They became very frequent in water between 26,5 and 28,5°C. There, they are present in profiles down to 150 m water depth. Predominant forms were *"Sphaerodinella" albatrosiana, "S." tuberosa*, less frequent the coccoid-vegetative *Thoracosphaera heimii*, but only very rare the cysts *Orthopithonella granifera*, and *Scrippsiella trochoidea*. Organic-walled cysts were extremely rare, but were found up to depth of 100 m. - About 250 specimens mainly of calcareous cysts but also of some motile stages mainly of *Scrippsiella* have been isolated in order to culture them on board for further examinations at the University of Bremen. At the end of the cruise the cells were scanned. After a time period of two weeks excystment of some cysts has been identified, with the production of several hundred motile specimens out of one single cyst. None of the isolated motile vegetative-thecate stage reproduced within this time.

Tab. 29: Surface water samples for Dinoflagellate Analyses. Sampling with 10 µm membrane pump filtration

Sample No. 34/3-	Time of Filtration UTC	Station	Latitude S	Longitude E/W	Water Depth (m)	Water Temperature (°C)	Salinity (‰)
2/22a	09.30-		23°23,1'	11°20,2'E	3265	22,6	33,14
	09.40						
2/23a	07.00-		24°11,6'	06°52,3'E	3100	--	--
	09.05		24°16,4'	06°26,3'E	1800	23,5	33,73
2/23b	11.20-		24°21,7'	05°57,3'E	1572	23,6	33,75
	15.45		24°32,4'	04°58,0'E	3489	23,9	33,82
2/23c	17.20-		24°36,0'	04°37,8'E	4067	23,7	33,81
	19.05		24°40,3'	04°15,0'E	4617	23,7	33,81
2/24a	09.00-		25°12,8'	01°17,6'E	4800	23,0	33,58
	12.10		25°20,2'	00°37,5'E	4960	23,4	33,82
2/24b	13.50-		25°24,1'	00°16,0'E	5351	23,3	33,68
	16.20		25°30,6'	00°19,1'W	--	23,6	33,91
2/24c	18.00-		25°33,8'	00°37,2'W	--	23,6	33,97
	20.10		25°38,7'	00°44,5'W	--	23,5	33,93

Sample No. 34/3-	Time of Filtration UTC	Station	Latitude S	Longitude E/W	Water Depth (m)	Water Temperature (°C)	Salinity (‰)
2/25a	07.25-		26°01,2'	03°31,0'W	4505	23,8	34,11
	10.30		26°16,4'	04°14,0'W	4487	24,0	34,04
2/25b	13.10-		26°35,0'	04°37,3'W	4481	24,1	34,08
	14.40		26°58,3'	04°51,8'W	4465	24,1	34,10
2/25c	14.55-		26°48,9'	04°54,7'W	4446	24,1	34,10
	17.10		27°07,1'	05°17,7'W	4564	24,1	34,12
2/26a	07.25-		28°58,6'	07°39,6'W	4208	23,9	34,14
	09.45		29°16,0'	08°02,1'W	3850	23,0	33,88
2/26b	13.00-	3801	29°30,1'	08°17,4'W	4538	23,1	33,86
	14.00	3801	29°30,1'	08°17,4'W	4538	23,1	33,86
2/26c	17.05-	3801	29°30,1'	08°17,6'W	4538	23,3	33,89
	18.45	3801	29°30,7'	08°18,2'W	4540	23,2	33,88
2/27a	07.30-	3802	30°09,8'	08°31,0'W	3988	23,0	33,89
	10.45	3802	30°09,8'	08°30,9'W	3974	23,1	33,89
2/27b	13.15-	3803	30°20,9'	08°34,3'W	4173	23,3	33,95
	16.00		30°21,0'	08°34,4'W	4173	23,5	33,97
2/27c	17.15-		30°24,4'	08°35,4'W	4141	23,6	33,97
	20.00	3804	30°44,6'	08°46,1'W	3880	23,8	34,06
2/28a	07.30-		30°45,0'	09°53,7'W	3721	23,5	33,81
	09.45		30°45,1'	10°16,9'W	3615	23,5	33,86
2/28b	14.05-	3805	30°45,0'	10°20,8'W	3660	23,6	33,81
	15.45	3805	30°44,9'	10°20,9'W	3660	23,5	33,79
2/28c	17.15-		30°44,9'	10°28,7'W	3620	23,8	33,82
	19.40		30°45,0'	10°53,1'W	3667	23,7	33,92
2/29a	07.30-		30°45,0'	12°41,4'W	2972	23,6	33,80
	10.20		30°45,0'	13°06,7'W	2540	23,1	33,64
2/29b	13.30-	3807	30°45,0'	13°11,9'W	2531	23,6	33,57
	15.45	3807	30°45,0'	13°12,0'W	2531	23,6	33,57
2/29c	17.10-		30°45,0'	13°32,3'W	3498	23,8	33,70
	19.45		30°45,0'	14°04,2'W	2841	24,0	33,74
3/01a	07.30-	3808	30°48,8'	14°42,6'W	3210	23,5	33,66
	09.55		30°51,4'	15°00,4'W	2813	23,4	33,61
3/01b	13.30-		30°59,0'	15°51,5'W	3400	23,6	33,66
	15.45		31°03,2'	16°19,7'W	3470	24,1	33,99
3/01c	17.05-	3809	31°03,2'	16°19,8'W	3469	24,2	34,00
	19.30	3809	31°03,3'	16°19,5'W	3469	24,1	34,01
3/02a	08.30-		31°19,9'	18°00,9'W	3850	24,6	34,00
	09.30	3811	31°21,4'	18°09,8'W	4090	24,6	33,98
3/02b	14.10-		31°22,4'	18°15,7'W	3811	24,8	33,92
	16.30		31°27,6'	18°46,6'W	3918	24,3	34,00

Sample No. 34/3-	Time of Filtration UTC	Station	Latitude S	Longitude E/W	Water Depth (m)	Water Tempera-ture (°C)	Salinity (‰)
3/02c	18.10-		31°31,3'	19°08,3'W	4460	24,4	33,73
	21.00		31°37,0'	19°45,5'W	4200	23,5	33,58
3/03a	09.15-		32°05,0'	21°20,3'W	4031	23,7	33,66
	12.00		32°15,5'	21°55,7'W	4250	24,3	33,90
3/03b	14.05-	3813	32°16,1'	21°58,2'W	4306	24,4	33,90
	17.00	3813	32°16,1'	21°58,8'W	44267	24,2	33,96
3/03c	18.30-	3813	32°16,1'	21°58,0'W	4329	24,3	33,89
	21.00	3813	32°16,4'	21°58,1'W	4332	24,2	33,90
3/04b	14.25-		33°04,1'	24°40,5'W	4431	22,1	33,33
	16.00		33°09,1'	24°01,.9'W	4370	22,1	33,34
3/04c	19.00-		33°15,4'	25°00,6'W	4220	22,2	33,34
	21.00		33°27,6'	26°00,6'W	4278	22,3	33,38
3/05a	09.30-		34°11,9'	28°33,4'W	4382	21,8	33,39
	13.00	3814	34°11,1'	28°38,0'W	4336	22,1	33,39
3/05b	15.00-	3814	34°10,2'	28°37,6'W	4371	22,1	33,39
	18.00	3814	34°11,0'	28°38,1'W	4340	22,1	33,39
3/05c	19.15-		34°10,1'	28°50,6'W	4165	22,1	33,47
	22.00		34°00,8'	29°25,0'W	3086	21,7	33,36
3/06a	09.30-		33°20,6'	31°53,8'W	4231	21,1	33,40
	12,35		33°09,9'	32°33,1'W	3703	20,9	33,29
3/06b	15.10-		33°00,5'	33°07,7'W	4074	21,4	33,36
	17.45		32°50,9'	33°42,6'W	4070	22,1	33,50
3/06c	19.05-		32°46,1'	34°00,0'W	4010	22,2	33,54
	22.00		32°36,3'	34°35,7'W	3773	22,6	33,56
3/07a	09.30-		31°55,8'	37°01,5'W	3808	21,5	33,23
	13.00		31°42,2'	37°45,2'W	4022	22,2	33,49
3/07b	15.30-		31°32,3'	38°16,1'W	3234	23,7	33,57
	18.00		31°20,4	38°53,0'W	4087	24,0	33,73
3/07c	19.10-		31°17,5'	39°01,8'W	3851	24,0	33,78
	22.00	3815	31°11,8'	39°18,9'W	4447	23,7	33,84
3/08a	09.25-	(3818)	31°08,4'	39°48,4'W	3443	24,0	33,96
	13.00		30°55,4'	39°59,9'W	3843	23,9	33,72
3/08b	15.10-		30°31,4'	40°11,3'W	3915	24,2	33,69
	18.00		29°40,0'	40°05,0'W	4050	24,8	33,78
3/08c	19.05		29°47,3'	40°32,4'W	3914	24,9	33,83
	21.45		29°17,9'	40°46,4'W	3701	25,3	34,15
3/09a	10.25-		28°17,6'	38°29,1'W	4408	26,5	34,34
	13.35	3819	28°11,9'	38°17,7'W	4703	26,7	34,38
3/09b	16.05-	3820	28°17,6'	38°06,2'W	4663	26,2	34,41
	19.00		28°10,9'	38°14,0'W	4700	26,8	34,31

3/09c	20.15-	3821	28°07,4'	38°17,9'W	4566	26,7	34,42
	23.00		28°02,1'	38°14,4'W	4535	26,7	34,40
3/10a	10.05-	3823	27°35,2'	37°55,2'W	4370	26,6	34,38
	14.00	3823	27°35,1'	37°55,2'W	4370	26,6	34,38
3/10b	16.30-		27°26,9'	37°18,0'W	4624	26,3	34,46
	19.00		27°20,6'	36°53,6'W	4636	26,6	34,55
3/10c	20.05-		27°18,6'	36°43,2'W	4614	26,5	34,40
	22.50		27°10,7'	36°09,2'W	4762	26,4	34,22
3/11a	10.15-	3824	26°52,3'	34°48,3'W	4777	26,6	34,00
	14.00		26°48,4'	34°56,2'W	4657	26,6	34,21
3/11b	16.25-		26°36,6'	35°24,8'W	4467	26,7	34,18
	19.00		26°24,8'	35°53,6'W	4384	26,8	34,29
3/11c	20.10-		26°19,0'	36°07,7'W	4335	27,1	34,37
	23.00		26°14,0'	36°29,9'W	4276	27,0	34,27
3/12a	10.30-		25°21,5'	37°56,5'W	4052	27,3	34,76
	14.00	3826	25°19,2'	38°00,4'W	3989	27,3	34,76
3/12b	16.15-		25°11,5'	38°15,0'W	3927	27,2	34,81
	19.00	3827	25°01,9'	38°32,9'W	3842	27,0	34,73
3/12c	21.00-	3827	25°01,9'	38°32,9'W	3842	27,0	34,73
	22.55	3827	25°01,9'	38°32,2'W	3842	27,0	34,73
3/13a	10.30-		23°31,5'	37°46,3'W	3805	28,2	34,98
	14.00		22°58,3'	37°29,4'W	3761	28,4	35,18
3/13b	16.15-		22°36,0'	37°18,1'W	3826	28,4	35,16
	19.00	3828	22°09,8'	37°04,6'W	3886	28,6	35,26
3/13c	20.15-	(3828)	22°09,6'	37°04,5'W	3887	28,6	35,27
	23.00		21°32,5'	36°46,0'W	4176	28,5	35,18
3/14a	10.30-		19°54,3'	35°56,6'W	3933	28,7	35,32
	14.00		19°14,8'	35°37,0'W	4032	28,6	35,44
3/14b	16.00-	3829	19°00,7'	35°29,9'W	4042	28,6	35,43
	19.00		18°42,2'	35°20,8'W	4039	28,6	35,43
3/14c	20.15-		18°32,2'	35°15,1'W	4042	28,7	35,28
	23.00		18°04,3'	35°02,0'W	4080	28,9	35,33
3/15a	10.20-		16.02,3'	35.00,0'W	4338	28,7	35,13
	13.30	3830	15°33,9'	34°59,6'W	4426	28,8	35,13

Tab. 30: Surface water samples for Dinoflagellate Analyses. Sampling with 5 µm vacuum pump filtration

Sample No.	Volume of fil-	Time	Station	Latitude	Longitude	Water	Water Tem-	Salinity (‰)
2/29a	30	10.00		30°45,1'	13°01,7'	2527	22,8	33,62
2/29b	30	13.30	3807	30°45,0'	13°11,8'	2531	23,6	33,57
2/29c	30	17.15		30°45,0'	13°32,3'	3498	23,8	33,50
3/01a	30	08.00	3808	30°48,7'	14°42,6'	3210	23,5	33,66
3/01b	30	13.30		30°59,0'	15°51,5'	3400	23,6	33,66
3/01c	30	17.15	3809	31°03,2'	16°19,8'	3469	24,2	34,00
3/02a	30	08.30		31°20,8'	18°06,8'	3857	24,6	34,00
3/02b	30	14.20		31°22,4'	18°15,7'	3811	24,8	33,92
3/02c	30	19.10		31°33,5'	19°21,6'	4050	23,9	33,68
3/03a	30	09.20		32°05,1'	21°20,8'	4003	23,7	33,67
3/03b	30	17.00	3813	32°16,1'	21°58,8'	4306	24,2	33,96
3/04a	30	10.00		32°48,5'	23°46,4'	4350	22,2	33,31
3/04b	30	14.35		33°05,1'	24°44,1'	4146	22,2	33,34
3/04c	30	19.35		33°23,1'	25°45,6'	4203	22,2	33,35
3/05a	30	10.00	3814	34°11,4'	28°38,0'	4350	22,2	33,47
3/06a	30	10.20		33°17,3'	32°05,6'	4158	21,3	33,39
3/06b	30	15.15		33°00,5'	33°08,0'	4075	22,4	33,52
3/06c	30	20.00		32°43,1'	34°10,9'	3958	22,3	33,61
3/07a	30	09.30		31°55,8'	37°01,5'	3808	21,5	33,23
3/07b	30	15.35		31°31,7'	38°17,7'	3157	23,7	33,56
3/07c	30	19.30		31°16,3'	39°05,6'	4098	24,2	33,90
3/08a	30	10.00	3818	31°07,0'	39°54,1'	4692	24,2	33,94
3/08b	30	16.30		30°15,0'	40°19,2'	3644	24,4	33,71
3/08c	30	19.15		29°45,7'	40°33,1'	3871	24,9	33,83
3/09a	30	10.15		28°18,8'	38°31,3'	4348	26,5	34,33
3/09b	30	17.20	3820	28°17,6'	38°06,2'	4662	26,2	34,42
3/10a	30	10.05	3823	27°35,1'	37°55,2'	4370	26,6	34,38
3/10b	30	17.00		27°25,9'	37°14,9'	4623	26,3	34,43
3/10c	30	21.30		27°14,3'	36°24,5'	4663	26,6	34,26
3/11b	30	17.40		26°30,4'	35°40,0'	4417	26,7	34,24
3/11c	30	20.20		26°18,2'	36°09,8'	4326	27,1	34,38
3/12a	30	11.30	3826	25°19,2'	38°00,4'	3989	27,3	34,76
3/12b	30	18.05	3827	25°01,9'	38°32,9'	3851	27,0	34,74
3/13a	30	11.45		23°20,6'	37°40,8'	3815	28,2	34,96
3/13b	30	16.45		22°29,2'	37°14,6'	3843	28,5	35,23
3/14a	30	11.00		19°48,1'	35°53,6'	4008	28,8	35,34

Tab. 31: Water samples for Dinoflagellate Analyses from 10 l NISKIN Bottles at about 20, 50, 100, 150, 200 m water depth. Filtration with 5 µm Polycarbonate Filters

Sample No.	Time	Volume of	Latitude	Longitude	Water	Water Tem-	Salinity
Station 3801-1							
3801-1	15.16	7,0	29°30,1'	08°17,4'	20	23,00	36,00
3801-1	15.14	8,0	29°30,1'	08°17,4'	49	19,98	35,80
3801-1	15.10	17,0	29°30,1'	08°17,4'	100	17,52	35,73
3801-1	15.07	8,0	29°30,1'	08°17,4'	149	17,11	35,72
3801-1	15.04	7,0	29°30,1'	08°17,4'	194	17,06	35,71
Station 3808-1							
3808-1	00.47	15,0	30°48,6'	14°42,7'	19	23,21	35,77
3808-1	00.44	9,0	30°48,6'	14°42,7'	50	20,36	35,69
3808-1	00.43	18,3	30°48,6'	14°42,7'	100	17,15	35,60
3808-1	00.40	8,0	30°48,6'	14°42,7'	149	16,04	35,49
3808-1	00.38	8,0	30°48,6'	14°42,7'	199	15,00	35,35
Station 3813-1							
3813-1	14.49	16,0	32°16,2'	21°58,2'	15	23,83	35,99
3813-1	14.46	8,0	32°16,2'	21°58,2'	49	22,47	36,01
3813-1	14.45	18,5	32°16,2'	21°58,2'	93	19,35	35,88
3813-1	14.42	8,5	32°16,2'	21°58,2'	149	17,07	35,66
3813-1	14.40	8,5	32°16,2'	21°58,2'	171	16,63	35,59
Station 3814-5							
3814-5	16.02	15,0	34°09,7'	28°37,6'	19	22,18	35,72
3814-5	16.00	18,5	34°09,7'	28°37,6'	48	19,63	35,78
3814-5	15.57	18,5	34°09,7'	28°37,6'	99	16,08	35,56
3814-5	15.55	20,0	34°09,7'	28°37,6'	148	15,13	35,50
3814-5	15.52	16,5	34°09,7'	28°37,6'	200	14,55	35,46
Station 3817-1							
3817-1	04.55	16,0	31°11,4'	39°26,1'	19	23,74	36,00
3817-1	04.52	8,5	31°11,4'	39°26,1'	50	23,65	36,00
3817-1	04.50	19,0	31°11,4'	39°26,1'	100	19,32	35,93
3817-1	04.46	no sample	31°11,4'	39°26,1'	150	17,61	35,78
3817-1	04.44	9,0	31°11,4'	39°26,1'	206	16,15	35,63

Station 3821-1

3821-1	22.24	18,7	28°07,4'	38°17,9'	19	26,79	36,55
3821-1	22.22	7,8	28°07,4'	38°17,9'	50	22,75	36,63
3821-1	22.20	17,5	28°07,4'	38°17,9'	99	20,42	36,28
3821-1	22.17	7,8	28°07,4'	38°17,9'	149	17,61	35,84
3821-1	22.15	7,5	28°07,4'	38°17,9'	200	16,29	35,65

Station 3824-1

3824-1	08.28	19,0	26°52,2'	34°48,3'	19	26,73	35,97
3824-1	08.25	8,7	26°52,2'	34°48,3'	50	23,09	36,42
3824-1	08.23	18,7	26°52,2'	34°48,3'	100	20,83	36,25
3824-1	08.20	7,7	26°52,2'	34°48,3'	145	18,65	35,92
3824-1	08.18	8,8	26°52,2'	34°48,3'	200	16,51	35,66

Station 3827-3

3827-3	23.07	15,5	25°01,9'	38°32,2'	19	26,99	36,70
3827-3	23.04	17,0	25°01,9'	38°32,2'	49	25,01	36,89
3827-3	23.02	17,5	25°01,9'	38°32,2'	99	22,68	36,79
3827-3	22.59	17,0	25°01,9'	38°32,2'	149	20,40	36,34
3827-3	22.57	17,0	25°01,9'	38°32,2'	200	17,37	35,81

Station 3828-1

3828-1	20.01	15,5	22°09,8'	37°04,6'	22	28,59	37,19
3828-1	19.58	17,0	22°09,8'	37°04,6'	48	28,60	37,19
3828-1	19.56	17,0	22°09,8'	37°04,6'	98	24,93	37,10
3828-1	19.53	17,0	22°09,8'	37°04,6'	150	22,34	36,70
3828-1	19.50	17,0	22°09,8'	37°04,6'	199	19,93	36,26

Station 3829-1

3829-1	16.55	17,0	19°00,7'	35°29,9'	20	28,57	37,38
3829-1	16.52	17,5	19°00,7'	35°29,9'	51	26,88	37,21
3829-1	16.50	17,5	19°00,7'	35°29,9'	99	25,06	37,20
3829-1	16.47	17,5	19°00,7'	35°29,9'	149	23,71	37,03
3829-1	16.45	17,5	19°00,7'	35°29,9'	200	20,69	36,43

Station 3830-1

3830-1	13.51	17,5	15°33,9'	34°59,6'	19	22,18	35,72
3830-1	13.48	17,5	15°33,9'	34°59,6'	48	19,63	35,78
3830-1	13.46	17,0	15°33,9'	34°59,6'	100	16,08	35,56
3830-1	13.44	16,5	15°33,9'	34°59,6'	150	15,13	35,50
3830-1	13.42	17,0	15°33,9'	34°59,6'	198	14,55	35,46

5.3.4.2 Coccolithophorids

(N. Dittert, R. Henning, A. Meyer, H. Willems)

An investigation of the living coccolithophore communities in the South Atlantic was started with regard to their distribution and abundance in the uppermost water column. This is essential for a better understanding of the relationship between these communities and the accumulated assemblages in the sediments catched by multicorer and gravity corer (see chapter "5.3.7 sampling"). At 11 stations 2 l water samples were taken from the rosette with 12 Niskin bottles (10 l) of five different depths (generally at 200 m, 100 m, 50 m, 20 m, and 10 m) (see Tab. 32). In addition, 64 surface water samples from 2.5 m water depth were taken from the vessel's membrane pump system along the whole transect from 23°23,1' S - 11°20,2' E to 15°33,7' S - 34°59,5' W (see Tab. 33), mostly at dawn, high noon, twilight and midnight. Generally, 2 liters of the water samples were filtered through cellulose nitrate filters (25 mm diameter, 0.45 µm pore size) by a vacuum pump immediately on board. Without washing, rinsing or chemical conservation the filters were dried at 45°C for at least 24 h and then kept permanently dry with silica gel in transparent film to protect them from humidity. The filtered material will be used for studies on distribution and composition of the coccoloithophorid communities in the upper 200 m of the water column with Scanning Electron Microscope (SEM). Species composition and abundance will be determined by identification and counting on measured filter transects.

Tab. 32: Phytoplankton water profile sampling (Coccolithophorids)

No.	Date	Time [UTC]	GeoB No.	Water depth [m]	Geographic position Latitude	Longitude	Water depth of sampling [m]	Water temp. [°C]	Salinity [‰]
I) 1	26.02.96	15:17	GeoB 3801-1	4534	29°30,0' S	08°17,6' W	20	23,00	36,00
I) 2		15:14					49	19,99	35,80
I) 3		15:11					100	17,48	35,73
I) 4		15:07					149	17,12	35,72
I) 5		15:04					194	17,06	35,71
II) 1	29.02.96	00:47	GeoB 3808-1	3214	30°48,6' S	14°42,7' W	19	23,21	35,77
II) 2		00:44					50	20,36	35,69
II) 3		00:43					100	17,15	35,62
II) 4		00:40					149	16,04	35,49
II) 5		00:38					199	15,00	35,35
III) 1	03.03.96	14:49	GeoB 3813-1	4320	32°16,1' S	21°58,5' W	15	23,83	35,99
III) 2		14:46					49	22,47	36,01
III) 3		14:43					100	18,88	35,88
III) 4		14:42					149	17,07	35,66
III) 5		14:40					171	16,63	35,59

No.	Date	Time [UTC]	GeoB No.	Water depth [m]	Geographic position Latitude	Longitude	Water depth of sampling [m]	Water temp. [°C]	Salinity [‰]
IV) 1	05.03.96	16:02	GeoB 3814-5	4379	34°09,7' S	28°37,6' W	19	22,18	35,72
IV) 2		15:59					49	19,52	35,78
IV) 3		15:57					99	16,09	35,56
IV) 4		15:55					148	15,13	35,50
IV) 5		15:52					200	14,55	35,46
V) 1	08.03.96	04:55	GeoB 3817-1	4588	31°11,4' S	39°26,1' W	19	23,74	36,00
V) 2		04:52					50	23,65	36,01
V) 3		04:50					100	19,32	35,93
V) 4		04:44					206	16,15	35,63
VI) 1	09.03.96	22:27	GeoB 3821-1	4565	28°07,4' S	38°17,9' W	19	26,79	36,55
VI) 2		22:21					50	22,75	36,63
VI) 3		22:19					100	20,40	36,28
VI) 4		22:17					149	17,61	35,84
VI) 5		22:15					200	16,29	35,65
VII) 1	11.03.96	08:28	GeoB 3824-1	4786	26°52,2' S	34°48,3' W	19	26,73	35,97
VII) 2		08:25					50	23,09	36,42
VII) 3		08:22					100	20,84	36,26
VII) 4		08:20					145	18,37	35,92
VII) 5		08:18					200	16,51	35,67
VIII) 1	12.03.96	23:07	GeoB 3827-3	3846	25°01,9' S	38°32,2' W	19	29,99	36,71
VIII) 2		23:04					50	25,01	36,88
VIII) 3		23:02					99	22,68	36,79
VIII) 4		22:59					149	20,40	36,34
VIII) 5		22:57					200	17,37	35,81
IX) 1	13.03.96	20:01	GeoB 3828-1	3887	22°09,8' S	37°04,5' W	22	28,59	37,19
IX) 2		19:58					48	28,59	37,19
IX) 3		19:55					99	24,93	37,10
IX) 4		19:53					150	22,35	36,70
IX) 5		19:49					200	19,92	36,26
X) 1	14.03.96	16:55	GeoB 3829-1	4043	19°00,7' S	35°29,8' W	20	28,57	37,38
X) 2		16:52					51	26,88	37,21
X) 3		16:50					99	25,06	37,21
X) 4		16:47					149	23,71	37,03
X) 5		16:45					200	20,69	36,43

No.	Date	Time [UTC]	GeoB No.	Water depth [m]	Geographic position Latitude	Longitude	Water depth of sampling [m]	Water temp. [°C]	Salinity [‰]
XI) 1	15.03.96	13:51	GeoB 3830-1	4332	15°33,9' S	34°59,6' W	19	28,77	37,16
XI) 2		13:48					48	28,35	37,19
XI) 3		13:46					100	24,62	37,09
XI) 4		13:44					150	23,59	37,02
XI) 5		13:42					198	22,75	36,85

Tab. 33: Phytoplankton surface water sampling (Coccolithophorids)

No.	Date	Time [UTC]	GeoB No.	Water depth [m]	Geographic position Latitude	Longitude	Water temp. [°C]	Salinity [‰]
1	22.02.1996	09:30	underway	3265	23°23,1' S	11°20,2'E	22,6	33,14
2		15:30	underway	4131	23°36,2' S	10°32,2'E	22,9	33,53
3		21:30	underway	4617	23°50,3' S	08°51,8'E	23,2	33,56
4	23.02.1996	06:27	underway	3013	24°10,5' S	06°59,4'E	23,2	33,62
5		10:35	underway	1668	24°20,1' S	06°06,3'E	23,5	33,75
6		16:42	underway	3886	24°34,6' S	04°45,9'E	23,6	33,81
7		22:30	underway	5081	24°48,4' S	03°30,6'E	23,5	33,78
8	24.02.1996	06:09	underway	5336	25°06,1' S	01°54,3'E	23,0	33,56
9		10:26	underway	5316	25°16,1' S	00°59,5'E	23,2	33,73
10		16:36	underway	5036	25°30,5' S	00°18,8'E	23,6	33,94
11		22:35	underway	4914	25°43,5' S	01°35,9' W	23,6	34,01
12	25.02.1996	07:08	underway	4546	26°00,6' S	03°28,1' W	23,8	34,12
13		11:31	underway	4206	26°21,6' S	04°20,5' W	24,1	34,07
14		17:31	underway	4585	27°09,0' S	05°20,1' W	24,0	34,11
15		23:30	underway	4115	27°56,4' S	06°20,1' W	24,2	34,23
16	26.02.1996	07:03	underway	4287	28°55,6' S	07°35,8' W	23,8	34,11
17		11:30	underway	4520	29°28,6' S	08°18,4' W	23,0	33,86
18		17:20	GeoB 3801	4527	29°30,1' S	08°17,6' W	23,3	33,87
19	27.02.1996	07:00	GeoB 3802	3970	30°09,9' S	08°30,9' W	23,0	33,89
20	28.02.1996	07:10	GeoB 38O5	3679	30°44,9' S	09°51,2' W	23,5	33,82
21		17:25	GeoB 3806	3622	30°44,9' S	10°28,6' W	23,8	33,83
22	29.02.1996	07:20	underway	2856	30°45,0' S	12°37,6' W	23,6	33,78
23		11:30	GeoB 3807	2515	30°45,0' S	13°11,9' W	23,1	33,54
24	01.03.1996	07:12	GeoB 3808	3212	30°48,7' S	14°42,6' W	23,5	33,66
25		14:00	underway	3474	30°00,2' S	15°59,4' W	23,8	33,87
26		20:00	GeoB 3809	3462	31°03,2' S	16°19,5' W	24,1	34,02
27	02.03.1996	08:00	underway	3828	31°18,9' S	17°55,3 ' W	24,5	34,02
28		15:35	underway	3859	31°25,5' S	18°34,1' W	24,7	33,89
29		21:00	underway	4102	31°37,3' S	19°43,8' W	23,6	33,62

No.	Date	Time [UTC]	GeoB No.	Water depth [m]	Geographic position Latitude	Longitude	Water temp. [°C]	Salinity [‰]
30	03.03.1996	08:18	underway	4098	32°01,4' S	21°08,0' W	23,3	33,32
31		16:20	GeoB 3813	4277	32°16,1' S	21°58,7' W	24,3	33,94
32	04.03.1996	08:20	underway	4018	32°42,7' S	23°27,7' W	22,0	33,13
33		12:30	underway	4170	32°57,1' S	24°16,9' W	21,5	33,15
34		19:00	underway	4123	33°20,8' S	25°37,9' W	22,1	33,37
35	05.03.1996	09:00	underway	4235	34°11,3' S	28°31,2' W	21,8	30,38
36		15:20	GeoB 3814	4379	34°09,8' S	28°37,6' W	22,1	30,38
37	06.03.1996	01:35	underway	2095	33°48,1' S	30°12,4' W	21,5	33,28
38		09:10	underway	4220	33°21,3' S	31°51,1' W	21,0	33,29
39		13:20	underway	3662	33°,07,2' S	32°42,7' W	21,1	33,33
40		19:10	underway	4011	32°46,1' S	34°00,1' W	22,2	33,55
41	07.03.1996	02:02	underway	2971	32°22,3' S	35°26,1' W	22,0	33,57
42		09:10	underway	3767	31°57,2' S	36°56,6' W	21,5	33,27
43		13:30	underway	4052	31°40,3' S	37°51,2' W	22,3	33,28
44		19:30	underway	4068	31°16,3' S	39°05,6' W	24,2	33,90
45	08.03.1996	09:00	GeoB 3817	4015	31°08,8' S	39°45,8' W	24,0	33,93
46		19:12	underway	3914	29°46,8' S	40°32,6' W	24,9	33,84
47	09.03.1996	01:48	underway	3930	28°58,2' S	40°01,7' W	25,5	34,23
48		10:10	underway	4255	28°19,3' S	38°32,3' W	26,5	34,34
49		20:15	GeoB 3821	4564	28°07,3' S	38°17,8' W	26,7	34,42
50	10.03.1996	10:20	GeoB 3823	4369	27°35,2' S	37°55,2' W	26,6	34,36
51		19:00	underway	4630	27°20,3' S	36°53,8' W	26,6	34,56
52		02:43	underway	4846	27°00,6' S	35°24,4' W	26,6	34,62
53	11.03.1996	10:15	GeoB 3824	4774	26°52,1' S	34°48,3' W	26,7	34,00
54		14:37	underway	4590	26°45,8' S	35°02,3' W	26,6	34,18
55		20:20	underway	4324	26°18,5' S	36°09,1' W	27,1	34,38
56	12.03.1996	11:05	GeoB 3826	3990	25°19,1' S	38°00,3' W	27,3	34,76
57		21:05	GeoB 3827	3843	25°01,9' S	38°32,9' W	27,0	34,73
58	13.03.1996	10:10	underway	3752	23°24,6' S	37°47,9' W	28,2	34,96
59		20:28	GeoB 3828	3969	22°06,8' S	37°03,3' W	28,5	35,28
60	14.03.1996	10:10	underway	3859	19°56,0' S	35°57,5' W	28,7	35,33
61		17:00	GeoB 3829	4042	19°00,8' S	35°29,6' W	28,6	35,44
62	15.03.1996	02:35	underway	4261	17°26,1' S	35°00,0' W	28,8	35,40
63		10:15	underway	4338	16°02,0' S	34°59,9' W	28,7	35,13
64		13:30	GeoB 3830	4426	15°33,7' S	34°59,5' W	28,8	35,14

5.3.5 Pumped Net Samples

(H. Buschhoff, M. Giese, M. Scholz,)

Marine plankton from surface waters was sampled during the whole cruise (Tab. 34). Each day we filtered 100 to 2000 l with the help of the shipboard-installed pump. The exact amount of water depended of its plankton concentration. The quicker the 10 µm net openings closed, the sooner the water flow was stopped and registered. The concentrated plankton in the net was washed into Kautex bottles and frozen at -20°C. The net was washed and used again.

The material will be used to investigate the composition of biogenic detritus. We are interested in a comparison with the fluxes of biogenic particles caught in sediment traps.

Tab. 34: List of pumped net samples during cruise 34/3

Sample No.	Date 1996	Time (UTC)	Lat.	Long.	Sal. (‰)	Temp. (°C)	Time (UTC)	Lat.	Long.	Sal. (‰)	Temp. (°C)	Vol. (l)
1	23.02	07:01	24°10,6' S	06°54,0' E	33,62	23,2	17:33	24°36,6S	04°34,9' E	33,8	23,7	2267
2	24.002.	07:03	25°08,2' S	01°42,7' W	33,56	23,0	17:24	25°32,3' S	00°29,2' W	33,98	223,6	1949
3	25.02.	08:00	26°02,4'	03°40,1'	34,08	23,9	17:11	27°14,1'	05°26,5'	34,11	24,1	3479
4	26.02.	07:59	29°02,6'	07°44,8'	34,10	23,8	18:12	29°30,7'	08°18,3'	33,89	23,3	3742
5	27.02.	07:13	30°09,8'	08°30,8'	33,88	23,0	18:17	30°33,2'	08°38,0'	33,99	27,3	2445
6	28.02	07:25	30°44,0'	09°53,0'	33,81	23,5	19:33	30°44,9'	10°53,3'	33,94	23,7	4007
7	29.02.	07:59	30°45,0'	12°44,5'	33,79	23,6	17:53	30°45,0'	13°40,6'	33,72	23,7	6507
8	01.03.	07:59	30°48,7'	14°42,7'	33,65	23,5	18:59	31°03,2'	16°19,6'	34,01"	24,1	5513
9	02.03.	07:59	31°20,9'	18°07,3'	34,00	24,6	19:11	31°33,4'	19°20,0'	33,64	24,1	4745
10	03.03.	07:59	32°03,9'	21°16,6'	33,64	23,7	19:31	32°16,6'	21°57,6'	33,89	24,3	2596
11	04.03.	08:54	32°44,7'	23°34,4'	33,13	22,1	19:15	33°21,6'	25°40,7'	33,36	22,1	3899
12	05.03.	10:09	34°13,3'	28°38,1'	33,5	22,1	21:03	34°04,8'	29°10,1'	33,50	22,2	1474
13	06.03.	10:12	33°18,0'	32°03,2'	33,37	22,2	19:14	32°45,7'	34°01,4'	33.57	22,3	731
14	07.03.	10:21	31°53,2'	37°11,1'	33,36	21,6	19:17	31°17,4'	39°02,3'	33,82	24,0	4031
15	08.03.	10:07	31°07,7'	39°53,9'	33,94	24,2	19:15	29°46,1'	40°32,0'	33,84	24,9	1326
16	09.03.	10:03	28°14,1'	38°22,5'	34,35	26,5	22:04	28°07,5'	38°17,9'	34,45	26,7	3569
17	10.03.	10:53	27°35,1'	37°55,1'	34,34	26,6	22:24	27°11,9'	36°14,5'	34,31	26,5	4511
18	11.03.	10:56	26°52,3'	34°48,3'	33.99	26,7	20:16	26°19,0'	36°07,7'	34,37	27,1	2322
19	12.03.	11:09	25°19,2'	38°00,3'	34,77	27,3	23:27	25°01,9'	38°32,1'	34,27	26,9	2388
20	13.03.	10:48	23°28,9'	37°45,0'	34,99	28,3	21:21	21°58,4'	36°59,1'	35,29	28,5	3181
21	14.03.	11:02	19°48,2'	35°53,0'	35,33	28,7	20:20	18°29,4'	35°14,6'	35,42	28,6	3979
22	15.03.	11:07	15°53,1'	35°00,0'	35,15	28,7	13:56	15°33,6'	34°59,5'	35,12	28,7	1073

5.3.6 Plankton Sampling Using a Multiple Closing Net

(M. Giese, M. Scholz)

Plankton was sampled with a multiple closing net (Fa. HYDROBIOS) with 0.25 m^2 opening and 64 micrometer mesh size. It was used for vertical hauls at 5 sites (chapt. 7.3). Each multinet station comprised three hauls:

1. The depth intervals from 500-300, 300-200, 200-100, 100-50 and 50-0 m.

2. The depth intervals from 400-200, 200-100, 100-0, 40-20 and 20-0 m.

3. The depth intervals from 250-00, 100-75, 75-50, 50-25 and 25-0 m.

Haul 1 will be used for studies on planktonic foraminifers, haul 2 for radiolarian and diatom analyses, and haul 3 for geochemical and isotopic analyses The samples containing mostly zooplankton and some phytoplankton and only small amounts of phytoplankton were carefully rinsed with seawater into KAUTEX bottles, fixed with mercury chloride for the reduction of bacterial degradation, and stored at 4°C. At all stations, 2 l Niskin bottles were used during the first and the third haul to obtain water samples from the different water depths for analyses of carbon and oxygen stable isotopes.

5.3.7 Sediment Sampling

(H. Buschhoff, N. Dittert, G. Eggerichs, M. Giese, F. Gingele, R. Henning, J. Klump, H. Kuhnert, F. Lamy, A. Meyer, M. Scholz, T. Wolff)

At 19 stations over the mid Atlantic ridge, in the Vema and Hunter Channel and on the continental slope off Brazil multicorer and gravity corer was used to retrieve sediment samples. Additional to these stations the three moorings K02, K2 and K3 were recovered. Details about core localities, water depth and core recovery are given in chapter 7.3.1 (station list). Parasound profiling along short transects from deeper basins to shallower ridges was used for determination of core localities.

5.3.7.1 Sampling Strategy and Methods

Multicorer

For the sampling of complete and undisturbed sediment surfaces and the overlying bottom water the multicorer equipped with 8 large tubes of 10 cm and 4 smaller tubes of 6 cm diameter was used at 16 stations of the cruise. At all stations core recovery was good. Penetration depths reach from 15 cm in the mid Atlantic ridge sites to 47 cm in the continental margin sides off Brazil.

Bottom water (100 and 250 cm^3) was sampled from 10 cm above the surface sediment for stable oxygen and carbon analysis. The samples for $\delta^{13}C$ analysis were poisoned with mercury chloride. Sample bottles were sealed with wax and stored at 4°C. About 20 ml bottom-water was taken for nutrient analysis and stored at -20°C.

For detailed studies on benthic foraminifera and dissolution of carbonaceous tests three cores (two 10 cm and one 6 cm in diameter) were cut into 1 cm segments. One sample set was stained with rose bengal/ethanol and cooled at 4°C. One core (of 10 cm in diameter), cut into 1 cm segments, was taken for detailed organic geochemical and organic petrological analysis (frozen at -20°C), diatoms, calcareous dinoflagellates and magnetic bacteria. One big-sized core of 10 cm in diameter was used by the geochemistry group for pore water analysis.

Sediment gravity cores

During cruise M34-3 (Walvisbay-Recife) 19 gravity cores from water depths between 2518 m and 4768 m were recovered (see chapter 7.3.1). All cores were subject of preliminary geological analyses on board comprising core descriptions, smear slide and color-scanner analyses, and bulk carbonate measurements (on 2 cores).

5.3.7.2 Core Description and Smear Slide Analysis

(J. Klump, H. Kuhnert, F. Lamy, T. Wolff)

Methods

The most important observations from the core descriptions were obtained by shipboard analysis during Leg 3 of METEOR cruise M34 and are summarized in core description forms following ODP convention. No stratigraphic analysis was performed onboard ship.

Smear slides were taken from all representative lithological units in all cores and from layers of special interest. The slides were then mounted with optical adhesive. A total of 346 smear slides were examined on board ship using a transmitted light microscope at 100 to 400x magnification under plane-polarized and cross-polarized light. Small quantities of the sediment were smeared on a glass slide and fixed with Nordland Optical Adhesive (n = 1.56). The sediment classification is based on ODP nomenclature following the terminology defined by DEAN et al. (1985). The structure column shows features such as intensity of bioturbation, layering, nature of lithological contacts and presence of mega-fossils. The hue and chroma attributes of the sediment color were determined by comparison with the MUNSELL soil color charts as soon as the cores were split. Colors are named and coded according to the MUNSELL color notation.

A color scanner was used to record the color of the fresh sediments at a 3 cm sampling interval (see Spectrophotometry). All core sections were photographed together with a color reference card.

Core description

Core GeoB 3801-6 (position: 29°30.4'S/08°18,3'W, water depth: 4546 m, length: 937 cm, Figures 162a, b):
Nannofossil ooze comprises the major part of core 3801-6 down to a depth of 669 cm and from 790 cm to the bottom of the core. Diatoms form a major component from 669 to 790 cm. There are incursions of diatoms at 519 to 525 cm and 656.5 cm. The core is interrupted by six foram-nannofossil ooze turbidites. The thickness of these turbidites range from 0.5 cm to 5 cm. The foraminifera in these turbidites are notably larger than foraminifera in other sections of the core and are overgrown with secondary inorganic calcite. Bioturbation is generally low and restricted to sections of mainly nannofossil ooze. The color of the core is very pale brown with darker laminae and mottles in sections of nannofossil ooze. The core is white in sections of diatom-nannofossil ooze with a brown layer on top and gray and yellow laminae down the core. The color of the laminae in this section of the core seems to be controlled by the abundance of ferrous hydroxides and pyrite.

Core GeoB 3802-1 (position: 30°09.8'S/08°31.0'W, water depth: 3969 m, length: 416, Figures 163a, b):
The top of this core is composed of foram-nannofossil ooze and foram-bearing nannofossil ooze. The foram content decreases down core to a depth of 260 cm and forams reappear below 370 cm. Clay is present in minor amounts from 180 to 240 cm and around 370 cm, otherwise in accessory amounts only. Nannofossil ooze is the dominant component between 260 and 370 cm. Most of the core is of very pale brown color with pale brown to brown bands around 70 cm, 190 cm, 235 cm, 345 cm and between 85 and 160 cm. The top part of the core was waterlogged. Bioturbation of the sediment is low to moderate.

Core GeoB 3803-2 (position: 30°21.0'S/08°34.3'W, water depth: 4173 m, length: 367 cm, Figures 164a, b):
While nannofossil ooze comprises most of the core, clay, forams and sponge-spicules constitute minor components in varying abundance. Most of the core is bioturbated. The color of the core is characterized by light gray and pale brown in the upper part of the core while the lower part is mostly white.

Core GeoB 3804-1 (position: 30°44.6'S/08°46.1'W, water depth: 3891 m, length: 413 cm, Figures 165a, b):
The dominant sedimentary component in this core is nannofossil ooze. Clay forms a minor component in the upper part of the core and decreases towards a depth of 230 cm. Forams increase in abundance from 100 cm down core until they form a minor component. Below 340 cm no minor components are added to the nannofossil ooze. Bioturbation can be noticed throughout the core, being strongest around 250 cm. Most of the core is light gray in color

with white and light brown bands. The sediments of the first segment of the core were water-saturated and very soft. Due to its high water content, the top 21 cm of the archive-half of the core were lost during splitting of the core.

Core GeoB 3805-3 (position 30°44.9'S/10°20.9'W, water depth: 3659 m, length 309 cm, Figures 166a, b):
Most of the core is composed of foram-bearing nannofossil ooze. Forams a present in major proportions around 150 cm but decrease to accessory amounts below 280 cm. The color of the core is pale brown to very pale brown. Bioturbation is found below 70 cm. It is localized and of low to moderate degree.

Core GeoB 3806-1 (position: 30°45.0'S/14°42.7'W, water depth: 3294 m, length: 366 cm, Figures 167a, b):
This core consists of very pale brown foram-bearing nannofossil ooze and nannofossil ooze over its entire length. Besides nannofossils and forams the amount of other components is negligible. Variations are limited to minor changes in the ratio of these two major components.

Core GeoB 3807-2 (position: 30°45.1'S/13°12.0'W, water depth: 2518 m, length 71 cm, Figures 168a, b):
Most of this core is composed of clay-bearing nannofossil ooze. A thin layer of foram ooze can be found at 52 cm. This layer probably represents a turbidite. The forams in this layer are overgrown with secondary calcite and are filled with an opaque material, probably pyrite. The colour of the sediments is very pale brown, the foram ooze is pale brown in colour. A low degree of bioturbation can be seen in a 20 cm layer just above the foram ooze.

Core GeoB 3808-5 (position 30°48.7'S/14°42.7'W, water depth: 3213 m, length 568 cm, Figures 169a, b):
Most of the core is composed of foram-bearing nannofossil ooze, except a section of foram-nannofossil ooze from 200 to 230 cm and of nannofossil ooze from 360 to 420 cm. The first meter of the core is characterized by a cyclic succession of very pale brown and light yellowish brown beds. These colors are also found in the remainder of the core, except for a section from 245 to 420 cm which is of an even lighter shade of very pale brown. The color change at the base of this unit is very sharp which might identify a scoured contact. Bioturbation is localized and of low degree, but it is not apparent in the very light section from 245 to 420 cm.

Core GeoB 3809-2 (position: 31°03.3'S/16°19.5'W, water depth: 3463 m, length: 234 cm, Figures 170a, b):
Most of this core consist of nannofossil ooze which is very pale brown in color. From 146 to 210 cm the proportion of forams increases above 10 %. Two populations of planktonic forams can be recognized of which one is noticeably larger than planktonic forams in comparable cores from this profile and which all have an overgrowth of secondary calcite. The bottom section of the core, from 210 to 234 cm is almost pure nannofossil ooze and has a color

of a lighter shade than the sections above. Bioturbation, where recognizable, is moderate to low.

Core GeoB 3810-1 (position: 31°07.9'S/16°50.3'W, water depth: 3810 m, length 218 cm, Figures 171a, b):
This core consists of very pale brown foram bearing nannofossil ooze over its entire length. Components other than nannnofossils and forams are present only in trace amounts. Variations are limited to minor changes in the ratio of these two major components. The core is very similar to core GeoB 3806-1.

Core GeoB 3811-2 (position: 31°21.4'S/18°09.8'W, water depth: 4091 m, length: 140 cm, Figures 172a, b):
The core is composed almost entirely of nannofossil ooze of uniform very light brown color. Bioturbation is moderate to low. The very end of the core is composed of diatom-nannofossil ooze and is white in color.

Core GeoB 3812-1 (position: 31°36.9'S/19°45.5'W, water depth: 4205 m, length: 532 cm, Figures 173a, b):
Almost all of this core is composed of nannofossil ooze. A foraminiferal ooze turbidite can be found at 115 to 121 cm with intraclasts of nannofossil ooze. The color of the nannofossil ooze is mostly various shades of very pale brown with darker bands at 95 to 100 cm, 260 to 273 cm and around 360 cm. A light yellowish brown band with sharp top and bottom contacts and with a width of only 1.5 cm can be found at 161 cm. At 310 cm a dark ferrous crust can be found which is not disturbed by bioturbation. Bioturbation in the rest of the core is low to moderate and decreases down core.

Core GeoB 3813-3 (position: 32°16.3'S/21°58.0'W, water depth: 4331 m, length 983 cm, Figures 174a, b):
This core is dominated by pale brown to yellowish brown nannofossil ooze. While forams are present in most layers, they rarely exceed 10% in abundance. However, sections of lighter color normally show a slight increase in the foram to nannofossil ratio.

Two turbidite layers are present: At 402 to 442 cm a multiple turbidite, consisting of large diatom fragments occurs. At about 670 cm a thin layer of foram ooze indicates another turbidite.

Towards the base of the profile the thickness of the different layers decreases to about 10 cm, resulting in a regular interbedding of darker nannofossil ooze and lighter foram bearing nannofossil ooze.

Core GeoB 3814-6 (position: 34°11.0'S/28°38.1'W, water depth: 4340 m, length 795 cm, Figures 175a, b):
The core consists of nannofossile ooze. Some sections are foram- or clay-bearing, but the overall composition is not subject to major changes. The brownish color is caused by a rela-

tively high (ca. 3 %) content of ferric hydroxide micronodules. At 380 to 389 cm a layer of nannofossil-foram ooze probably represents a turbidite. The lack of an erosive base may be due to bioturbation. From 550 cm downwards the stratification was deformed in the process of gravity coring.

Core GeoB 3822-3 (position 27°37,7'S/37°57.0'W, water depth: 4272 m, length 891 cm, Figures 176a, b):
Clayey nannofossil ooze and nannofossil clay comprise most of this core. Minor components are diatoms at 460 cm, 520 cm, 770 cm, quartz around 590 cm and 700 cm, and mica around 620 cm. Opaque minerals are most abundant in dark laminae, especially between 20 and 50 cm and 810 and 850 cm. Cemented ferro-manganese crusts are found throughout the core. A layer of nannofossil-bearing foram ooze from 120 to 150 cm is interpreted to be a turbidite. Drilling deformations are visible below 280 cm. Some of the stratigraphy might be missing in the lowest parts of the core.

Core GeoB 3823-1 (position: 27°35.2'S/37°55.2'W, water depth: 4368, length: 905 cm, Figures 177a, b):
The core is dominated by clay. Minor components are nannofossils, quartz and diatoms. Clayey nannofossil ooze is found between 360 and 410 cm. Ferro-manganese micronodules are abundant in a very dark grayish brown horizon around 20 cm depth. A thin white layer of diatom-bearing nannofossil-bearing foram ooze is found at 140 cm and is interpreted as a turbidite. Several cemented ferrous crusts can be found throughout the core. The top of the core is of grayish brown colors to a depth of 42 cm. Here the color changes abruptly without an accompanying change in lithology to greenish gray colors. Bioturbation is apparent only in the bottom two meters of the core and is only of low degree. From 570 cm downwards drilling deformations can be found. Thus, the stratigraphy might be incomplete.

Core GeoB 3825-2 (position: 26°14,0'S/36°19,9'W, water depth: 4267 m, length: 945 cm, Figures 178a, b):
Clay constitutes most of this core. Nannofossils as a major component are found from 180 to 220 cm and as the dominant component from 220 to 690 cm. Hard clay layers of 0.5 cm thickness can be found at and below 600 cm, sometimes with small concretions. The color of the sediment is brown to gray in clay-rich layers and pale brown to light olive brown in parts where nannofossils are abundant. The top half is rarely bioturbated, especially the top meter which is well laminated. Bioturbation increases towards the bottom of the core and reaches its peak around 750 cm, where it is of moderate degree.

Core GeoB 3826-1 (position: 25°19.2'S 038°00.4'W, water depth: 4012 m, length: 684 cm, Figures 179a, b):
The top 220 cm of the core consist uniformly of nannofossil ooze with minor amounts of clay and coarser terrigenous material. Below 220 cm clay-bearing nannofossil ooze and nannofossil-clay dominate. The amount of silt increases to approximately 20 %. It is composed of Fe-micronodules with varying quantities of quartz, mica and accessory minerals. Turbiditic quartz-foram sands occur at 220, 488 and 633 cm. Below 488 cm the core is deformed due to

the coring procedure. Color ranges from light yellowish brown to greenish gray, where grayish colors indicate the presence of micronodules.

Core GeoB 3827-2 (position: 25°01.9'S/38°32.9'W, water depth: 3845 m, length: 784 cm, Figures 180a, b):
Most of the core is composed of nannofossil ooze with clay, forams, and sponge-spicules as minor components. Nannofossil clay can be found from 90 to 149 cm. At 150 cm a one centimeter layer and at 370 cm a two centimeter thick layer of well sorted quartz sand are found and were interpreted as turbidites. Drilling deformations are found from 500 cm down core. Certain units are deformed to wedge-shaped structures, which suggests that parts of the stratigraphy are disturbed and might be missing. Colors vary between very pale brown, yellowish brown and brownish gray. Bioturbation is moderate to high.

5.3.7.3 Spectrophotometry

The light reflectance of all gravity cores was measured at 31 wavelength channels in the range of visible light (400-700 nm). This method is used to quantify the color of the sediment.

A Minolta CM-2002™ hand-held spectrophotometer was used. The readings were taken immediately after splitting the core. The archive halves of the cores were scraped with a knife to expose a fresh, unsmeared surface for the measurements. The core was then covered with a transparent plastic film to protect the camera. Measurements were taken every 3 cm to resolve small scale color changes. Before measurements were taken, a white calibration of the spectrophotometer was perfomed using a white calibration cap. The calibration surface was covered with the same plastic film as the core to avoid any bias in the readings. The data were stored in the instrument and later transferred to a personal computer using the program "PROCOMM PLUS" ™. They were then further processed using the program COLREAD to be able to import them into a spreadsheet program.

The reflectance profiles at the three wavelengths (450 nm, 550 nm, 700 nm) are shown next to the core diagrams. These three wavelengths give a good overview of sediment color spectrum, since they cover most of the spectrum measured. In addition they represent the colors blue, green and red, respectively.

In most cores a significant negative correlation with magnetic susceptibility can be seen, which can be explained by the dependence of both, high reflectance and low susceptibility on calcite concentration on the one hand and low reflectance and high susceptibility of ferromanganese minerals on the other.

In addition, the calcite content is dependent on paleoceanographic conditions at the time of deposition so that color reflectivity can often be used as a first stratigraphic proxy.

Legend for stratigraphic columns

Lithology

one major component

calcareous

foraminiferal ooze

nannofossil ooze

siliceous

siliceous ooze

diatom ooze

terrigenous

clay

mud

mixtures

calcareous

nannofossil-bearing foram ooze

foram-nannofossil ooze or nannofossil-foram ooze

foram-bearing nannofossil ooze

siliceous

diatomaceous nannof. ooze or diatom-bearing nannof. ooze

terrigenous

clayey nannofossil ooze or clay-bearing nanno ooze

foram-bearing clayey nannofossil ooze

nannofossil clay

admixtures

calcareous

foram-bearing

nannofossil-bearing

siliceous

siliceous

diatom -bearing

terrigenous

clay-bearing

mud-bearing

sand-bearing

Structures

weakly bedded

bedded/laminated

mm
cm dimension of bedding
dm

scoured contact

S bioturbation (<30% of sediment)

SS bioturbation (30-60% of sediment)

SSS bioturbation (>60% of sediment)

fining upwards

coarsening upwards

graded bedding

ww wavy bedding

Fossils

shells

shell fragments

megafossil

Colour

Munsell value

8

7

6

5

4

3

2

GeoB 3801-6

Date: 26.02.96 Pos: 29°30,7' S 8°18,3' W
Water Depth: 4546 m Core Length: 937 cm

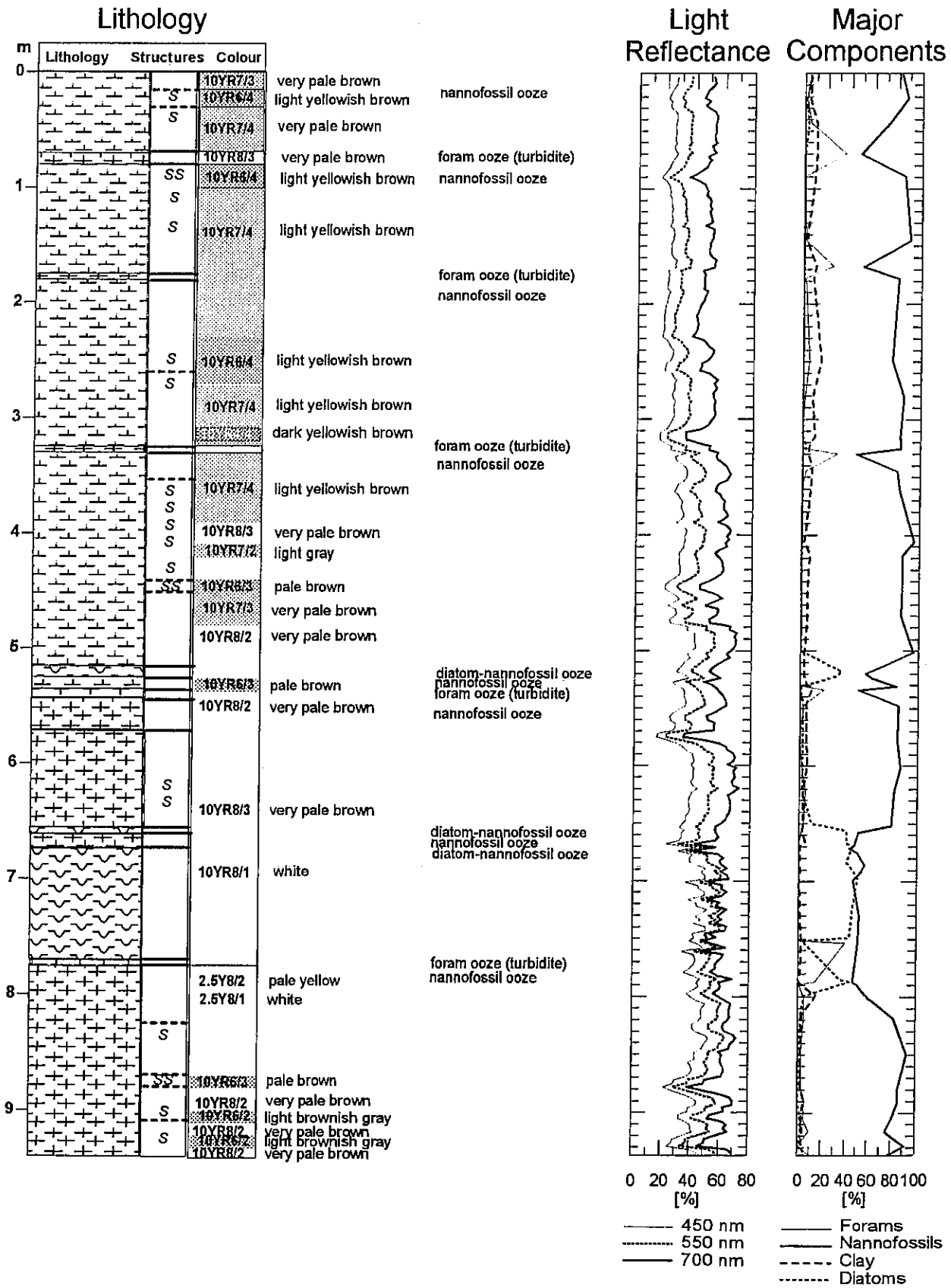

Fig. 162a: Core description gravity core GeoB 3801-6.

Fig. 162b: Physical properties gravity core GeoB 3801-6.

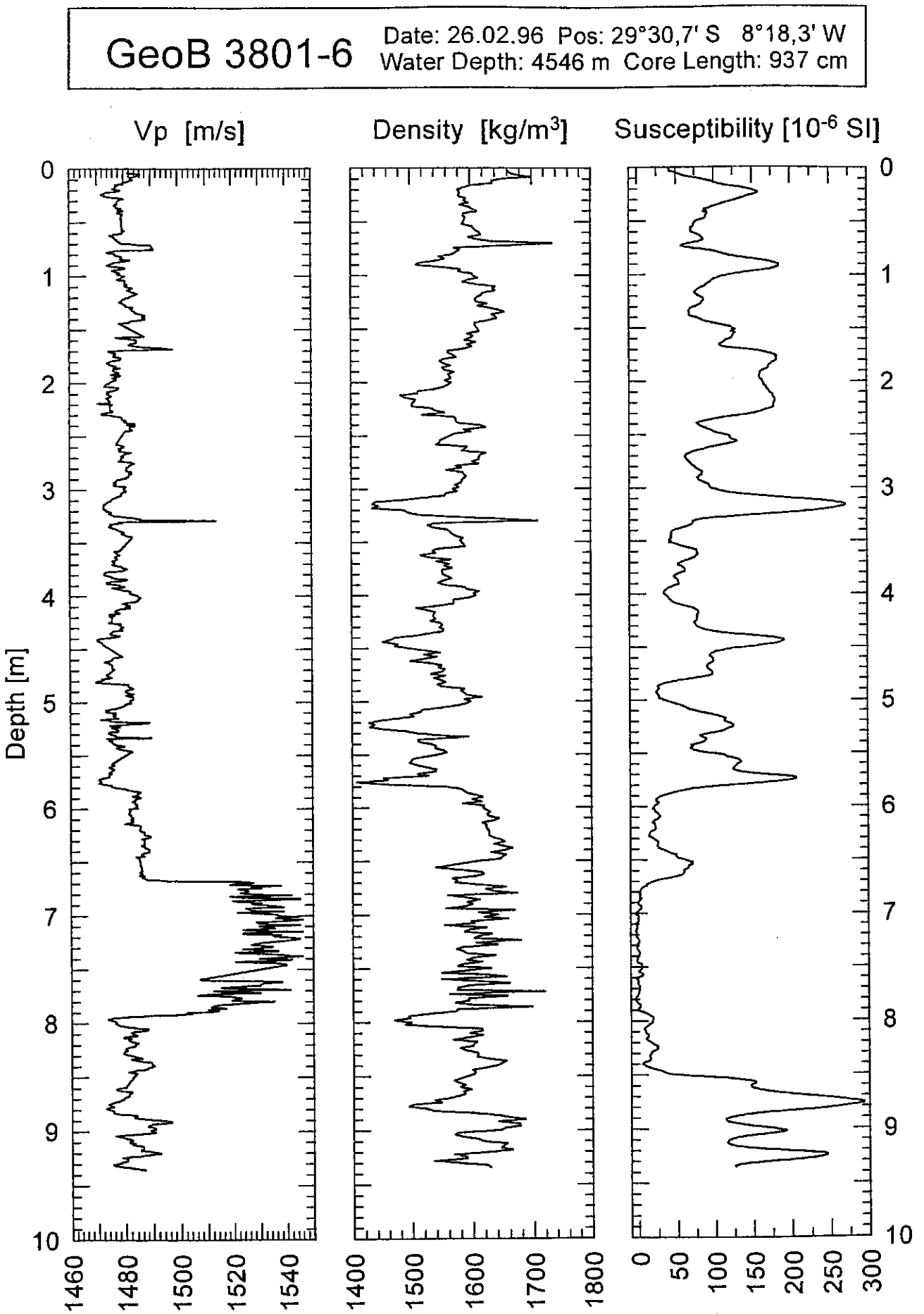
GeoB 3801-6
Date: 26.02.96 Pos: 29°30,7' S 8°18,3' W
Water Depth: 4546 m Core Length: 937 cm
Vp [m/s]
Density [kg/m3]
Susceptibility [10-6 SI]
Depth [m]
0
1
2
3
4
5
6
7
8
9
10
1460
1480
1500
1520
1540
1400
1500
1600
1700
1800
0
50
100
150
200
250
300

GeoB 3802-1

Date: 27.02.96 Pos: 30°09,8' S 8°31,0' W
Water Depth: 3969 m Core Length: 416 cm

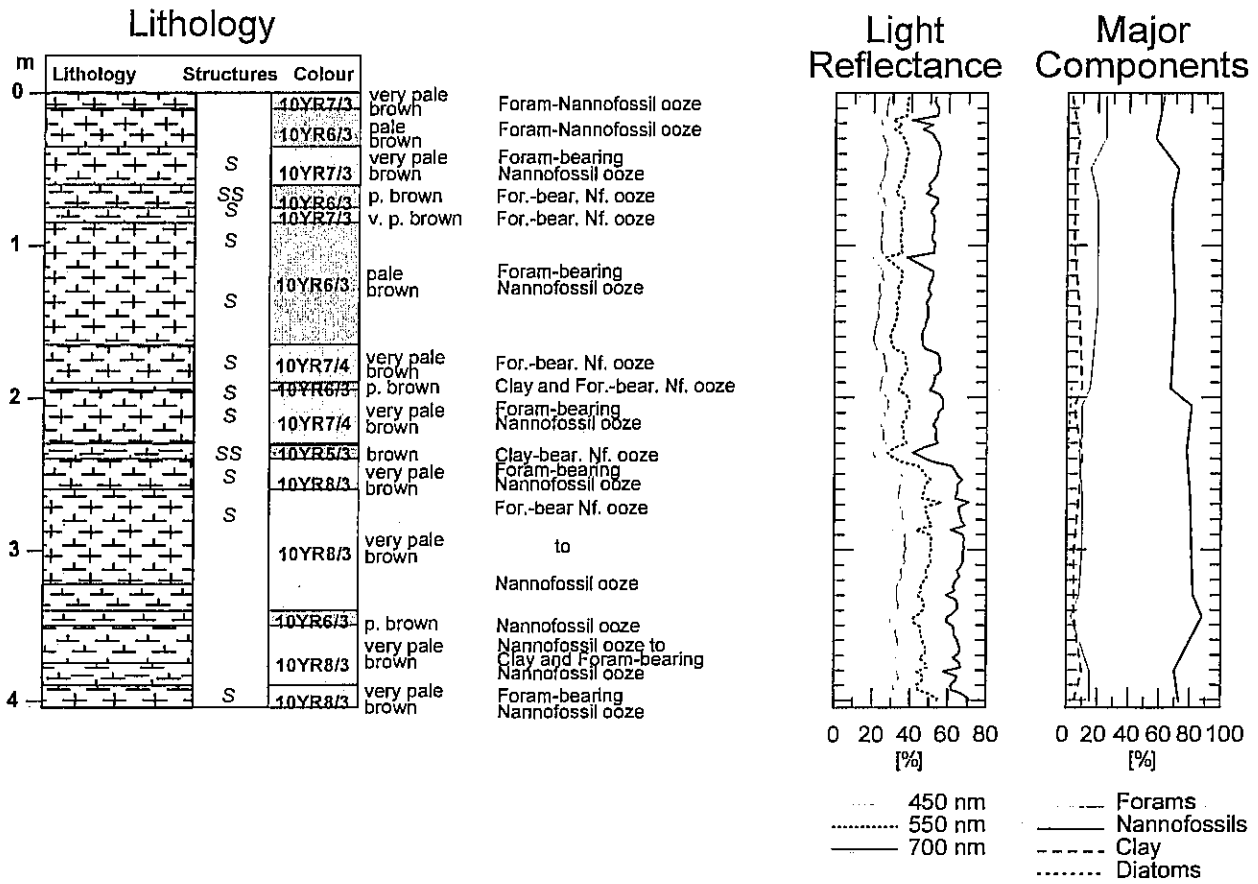

Fig. 163a: Core description gravity core GeoB 3802-1.

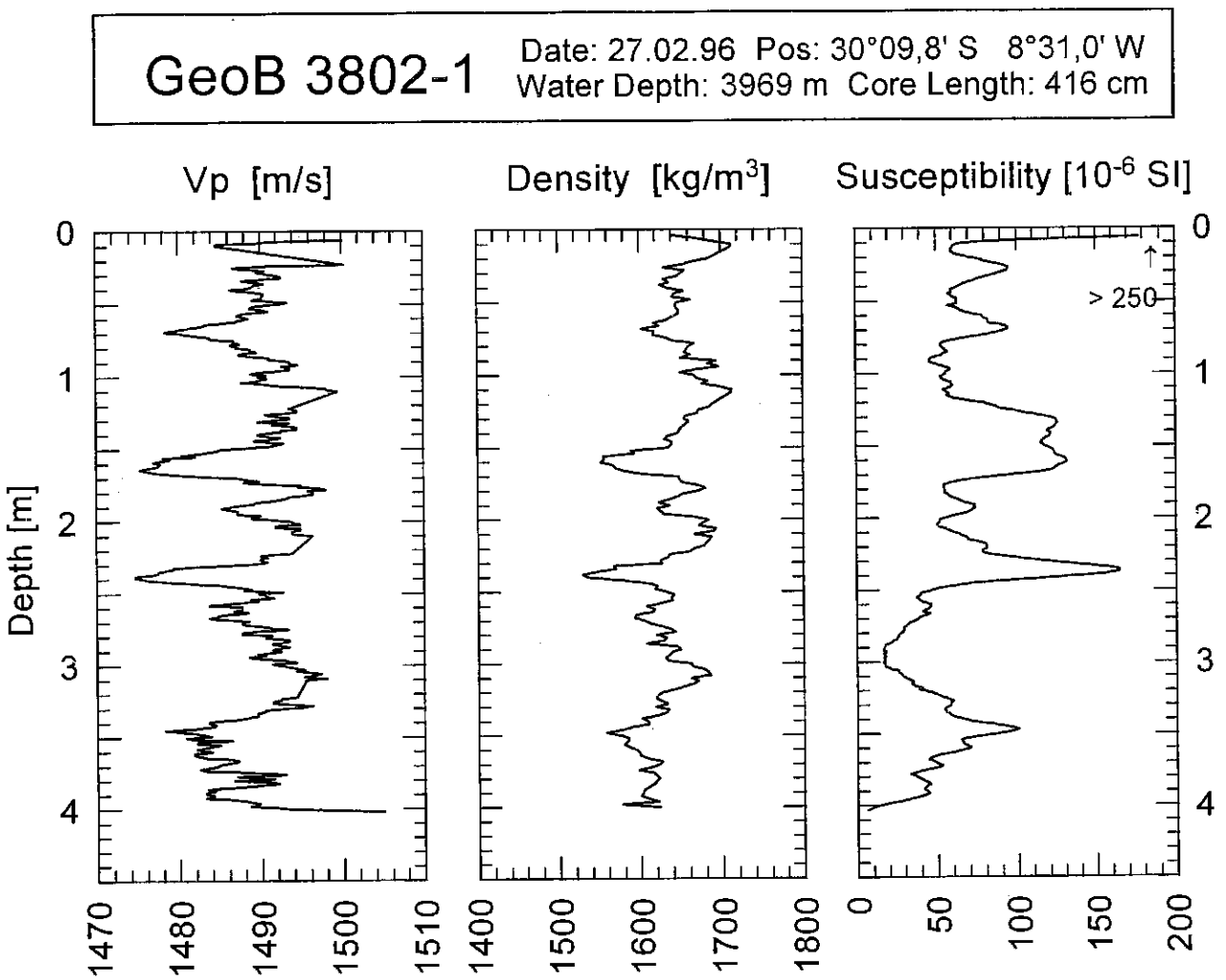

Fig. 163b: Physical properties gravity core GeoB 3802-1.

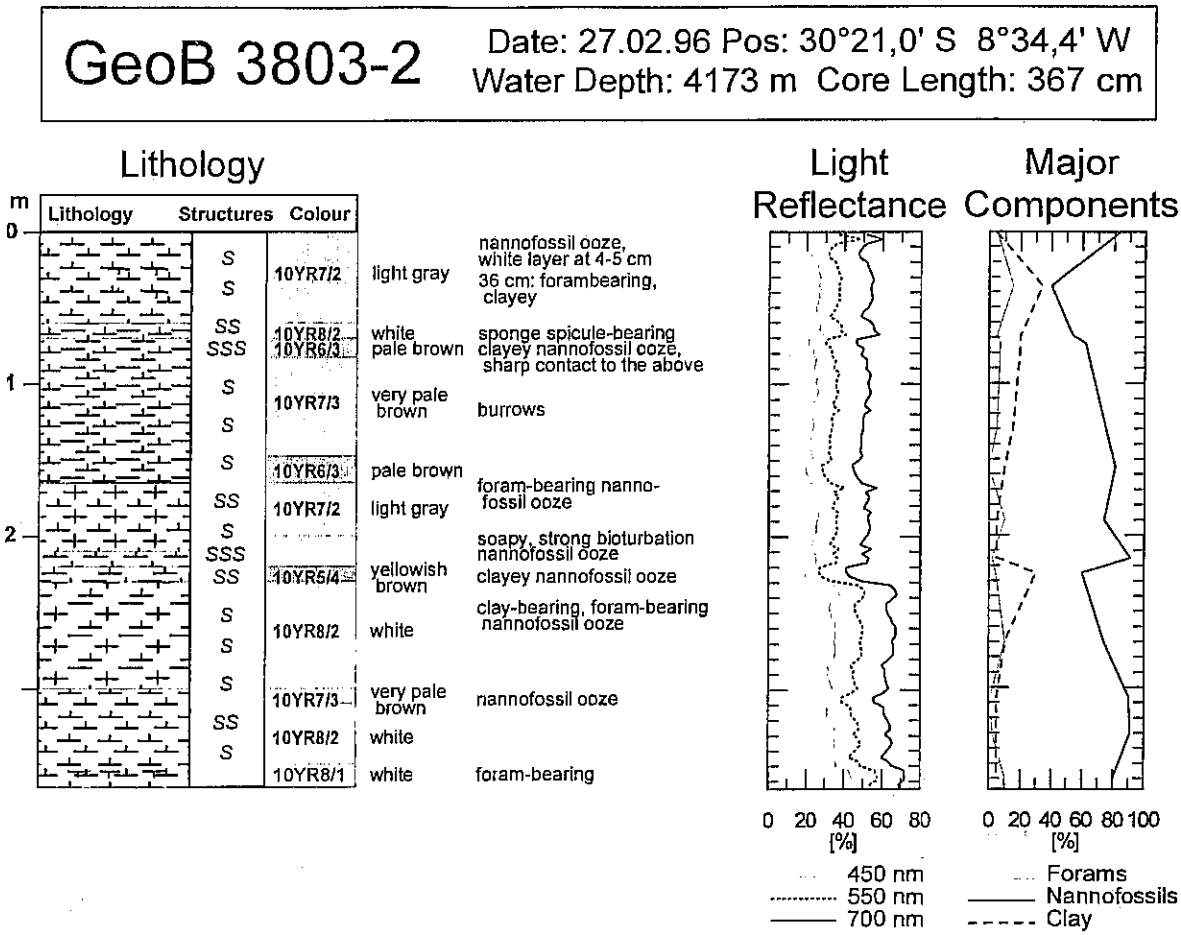

Fig. 164a: Core description gravity core GeoB 3803-2.

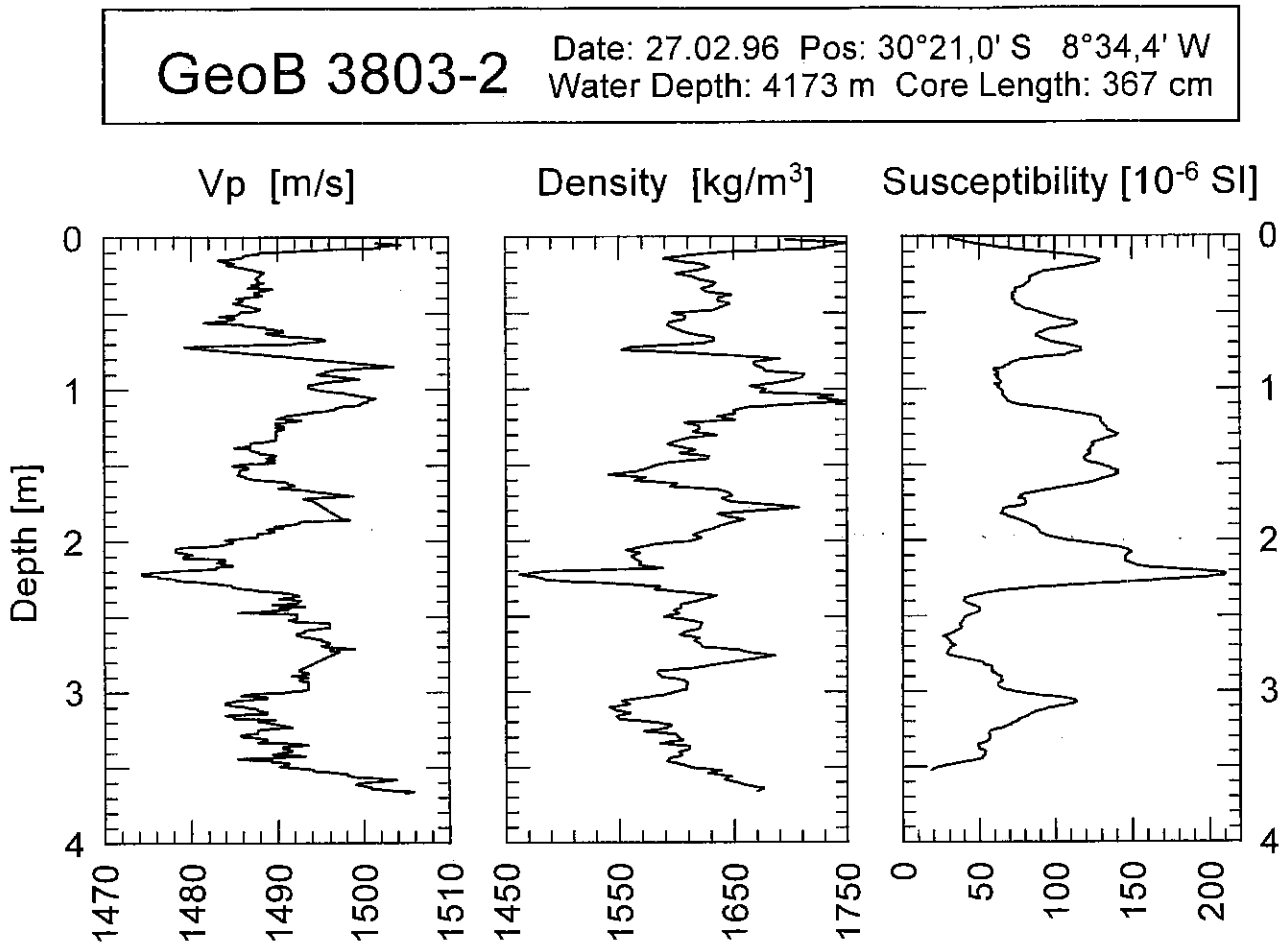

Fig. 164b: Physical properties gravity core GeoB 3803-2.

GeoB 3804-1

Date: 27.02.96 Pos: 30°44,6' S 08°46,1' W
Water Depth: 3891 m Core Length: 423 cm

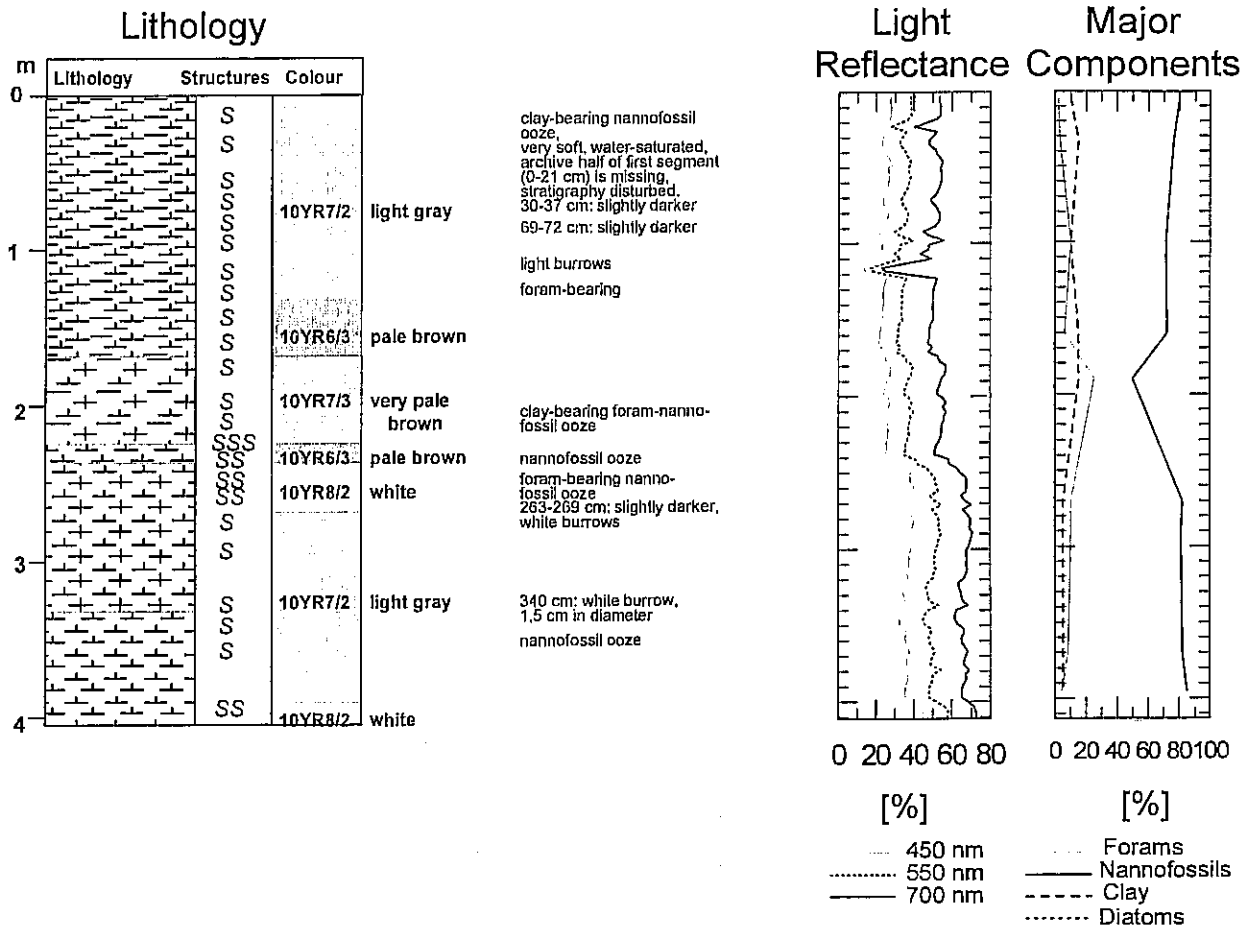

Fig. 165a: Core description gravity core GeoB 3804-1.

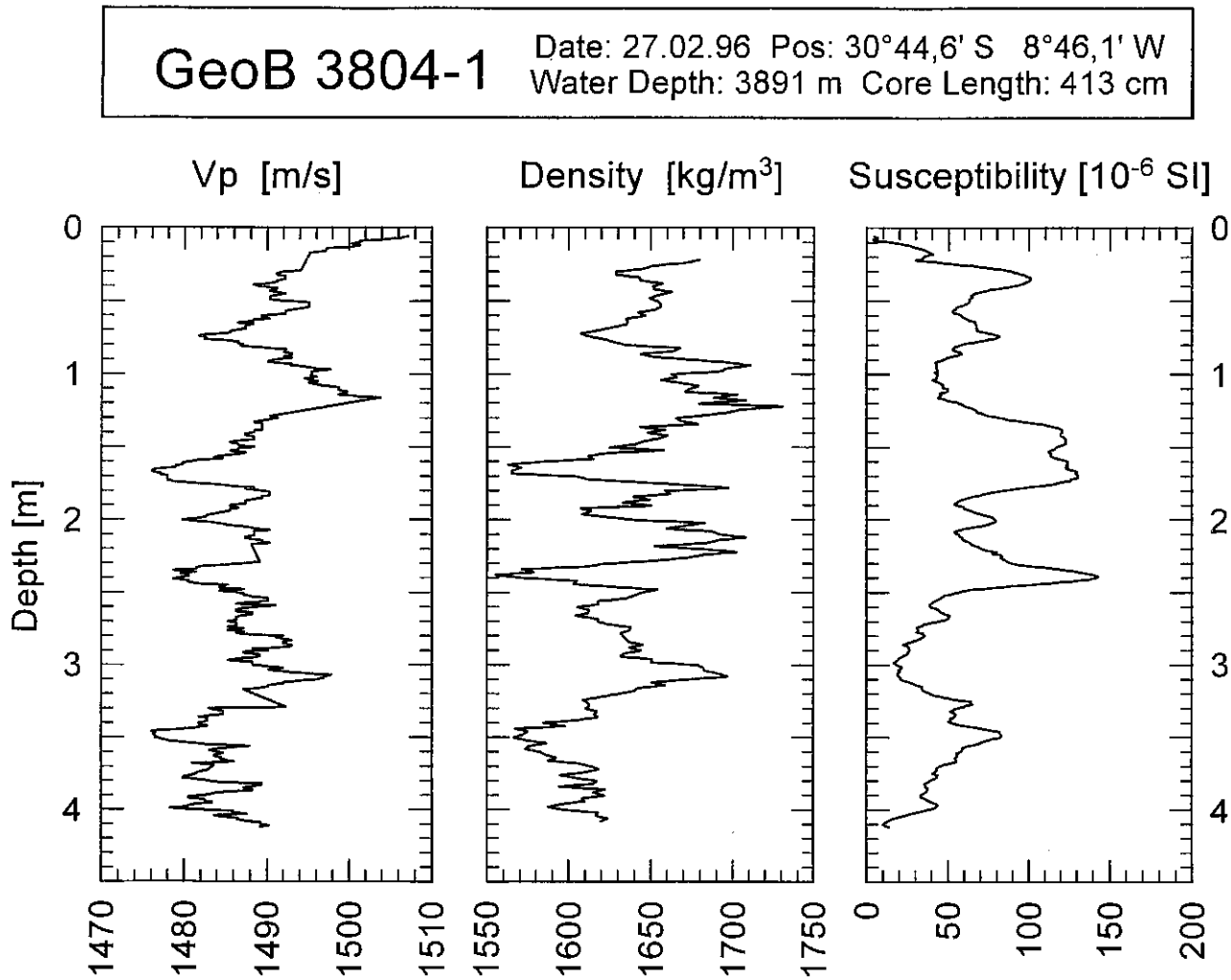

Fig. 165b: Physical properties gravity core GeoB 3804-1.

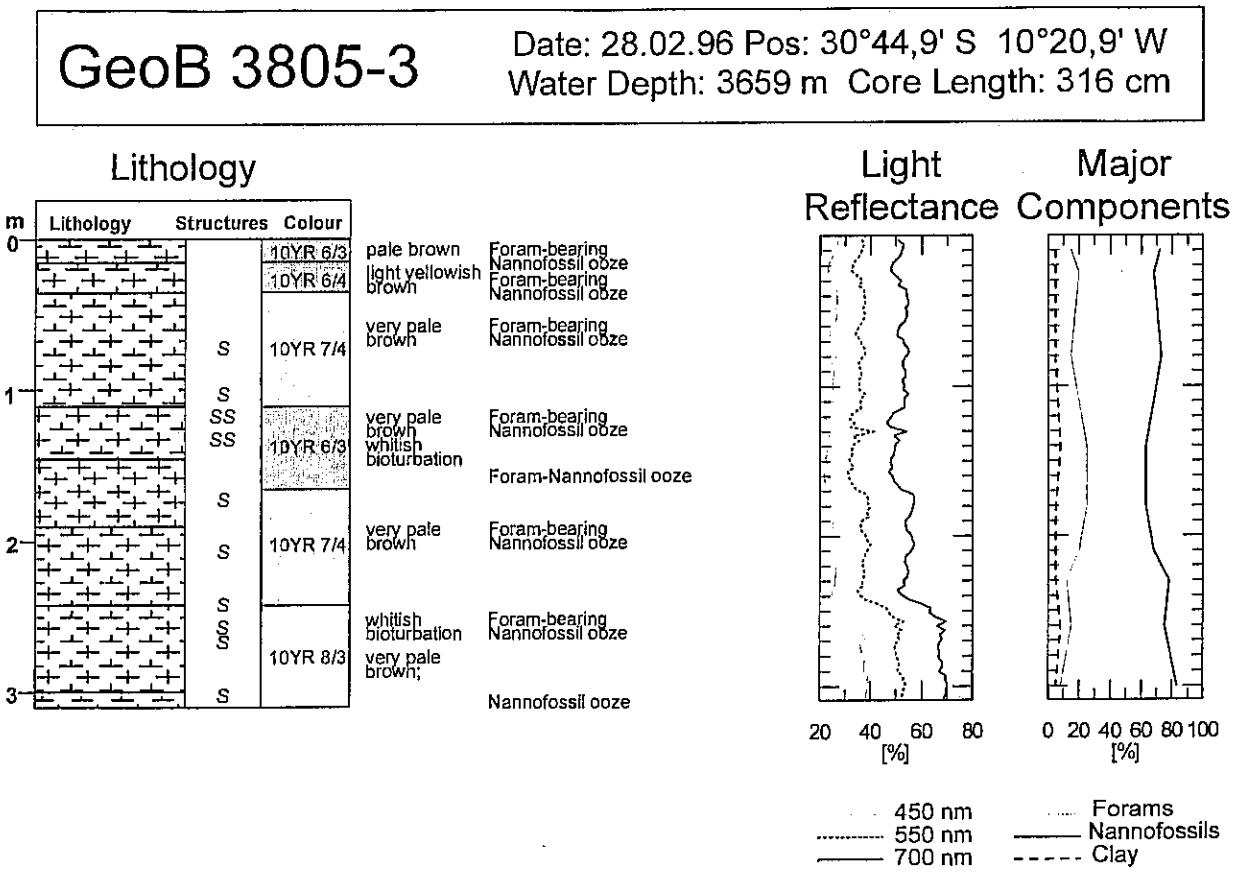

Fig. 166a: Core description gravity core GeoB 3805-3.

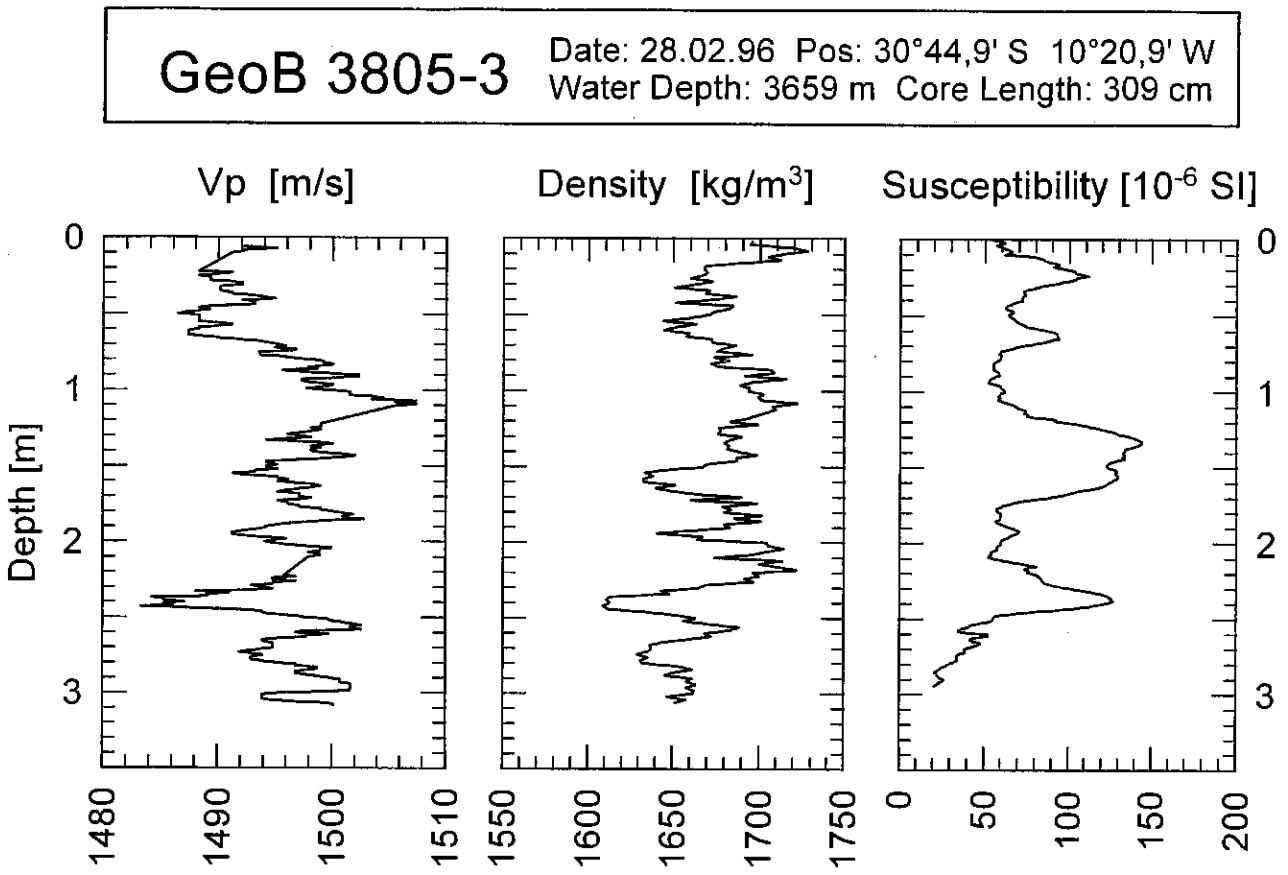

Fig. 166b: Physical properties gravity core GeoB 3805-3.

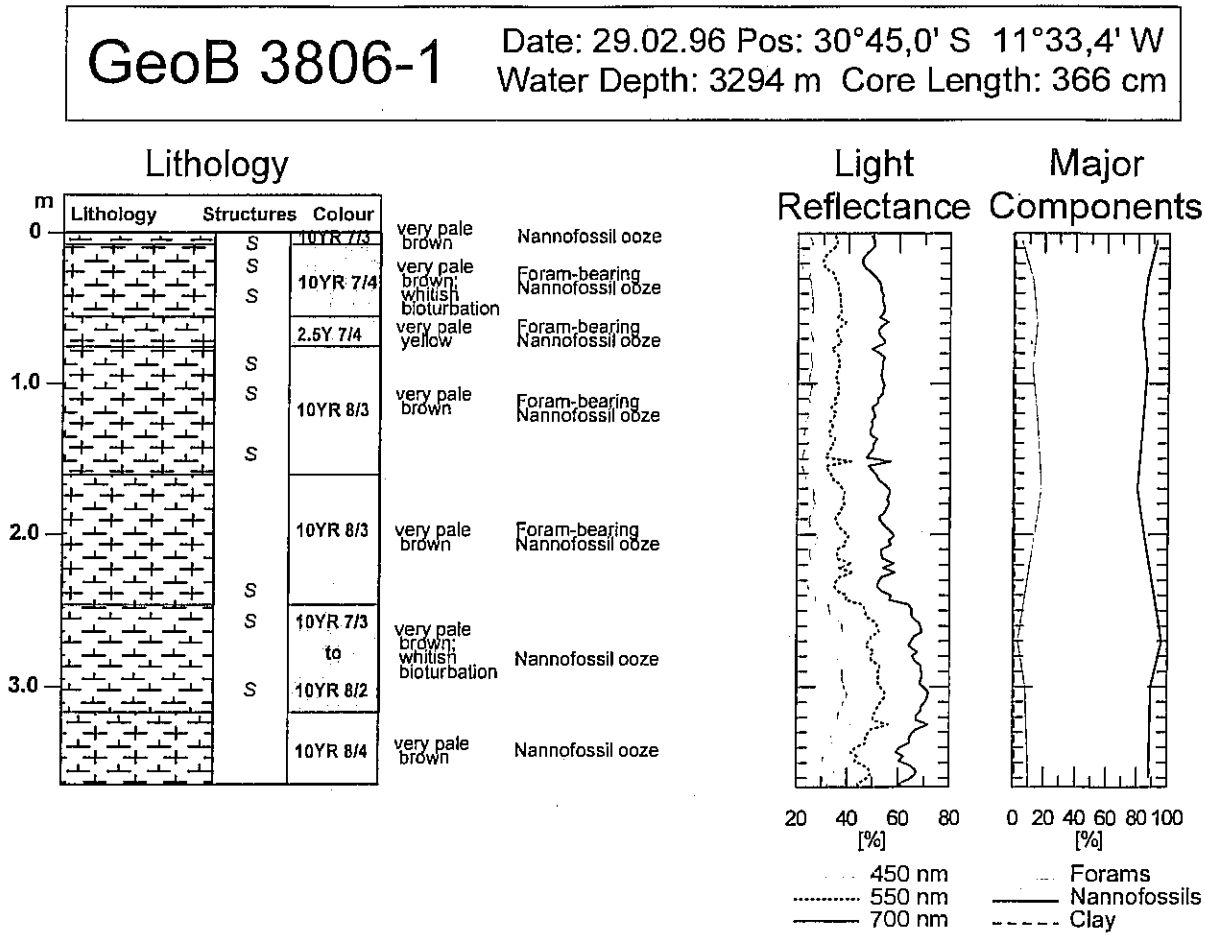

Fig. 167a: Core description gravity core GeoB 3806-1.

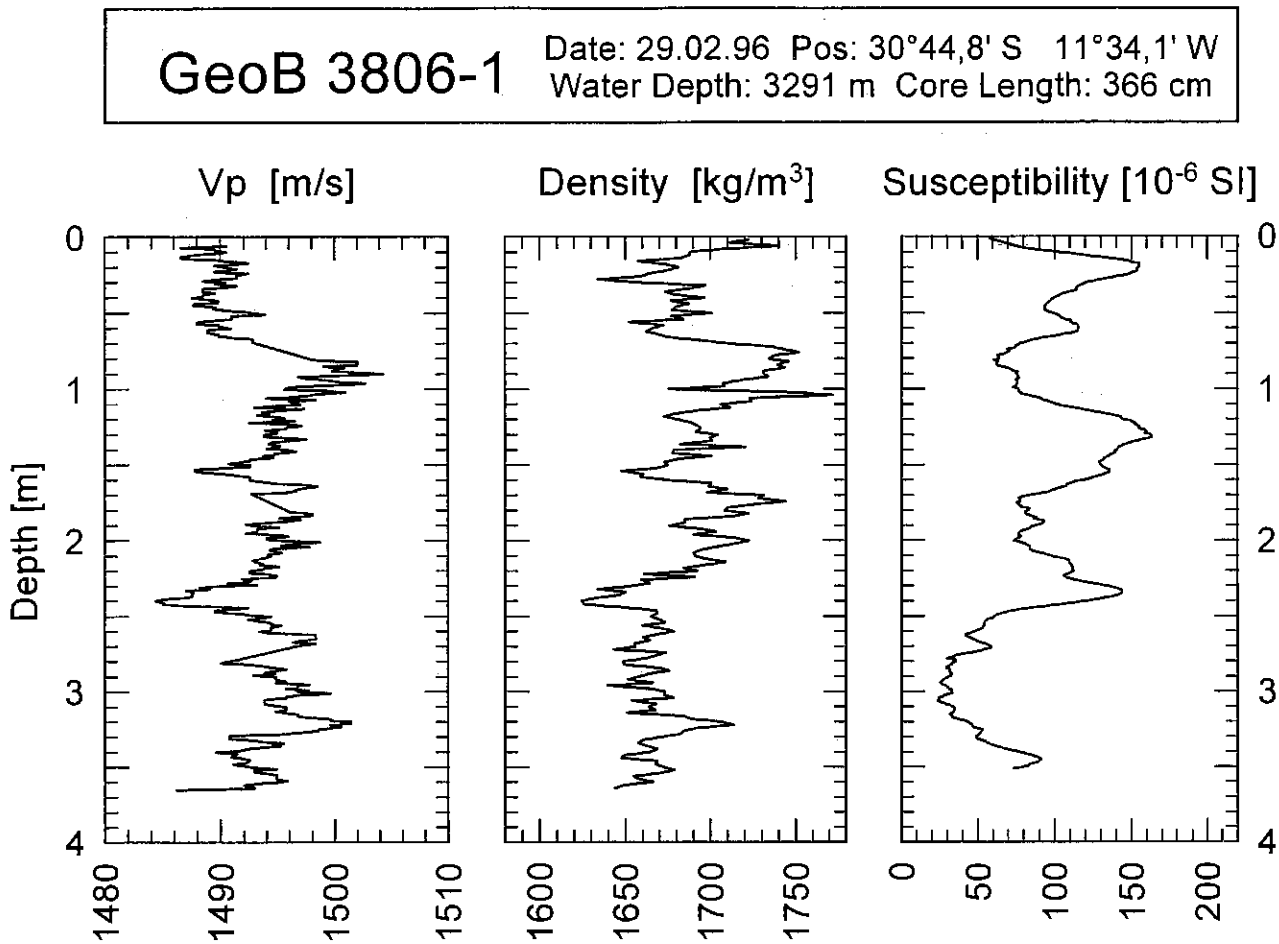

Fig. 167b: Physical properties gravity core GeoB 3806-1.

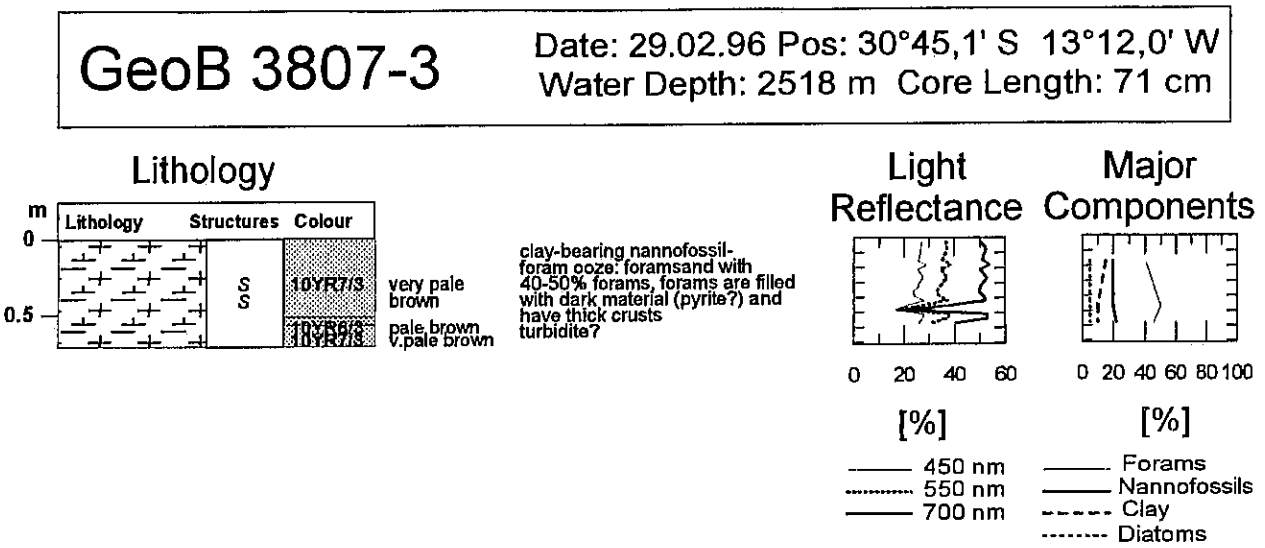

Fig. 168a: Core descrition gravity core GeoB 3807-3.

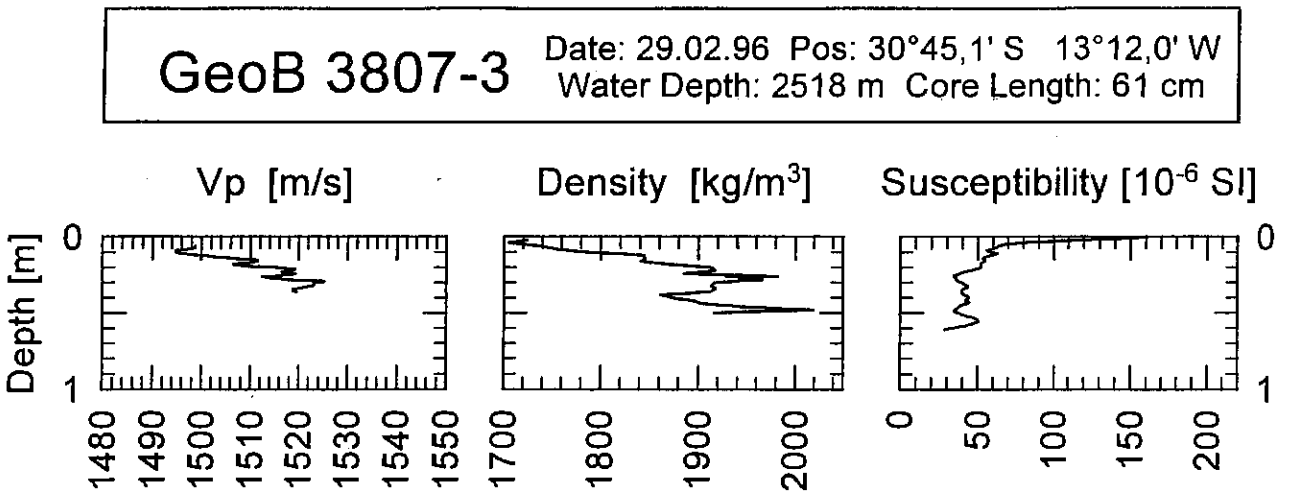

Fig. 168b: Physical properties gravity core GeoB 3807-3.

GeoB 3808-5

Date: 01.03.96 Pos: 30°48,7' S 14°42,7' W
Water Depth: 3213 m Core Length: 580 cm

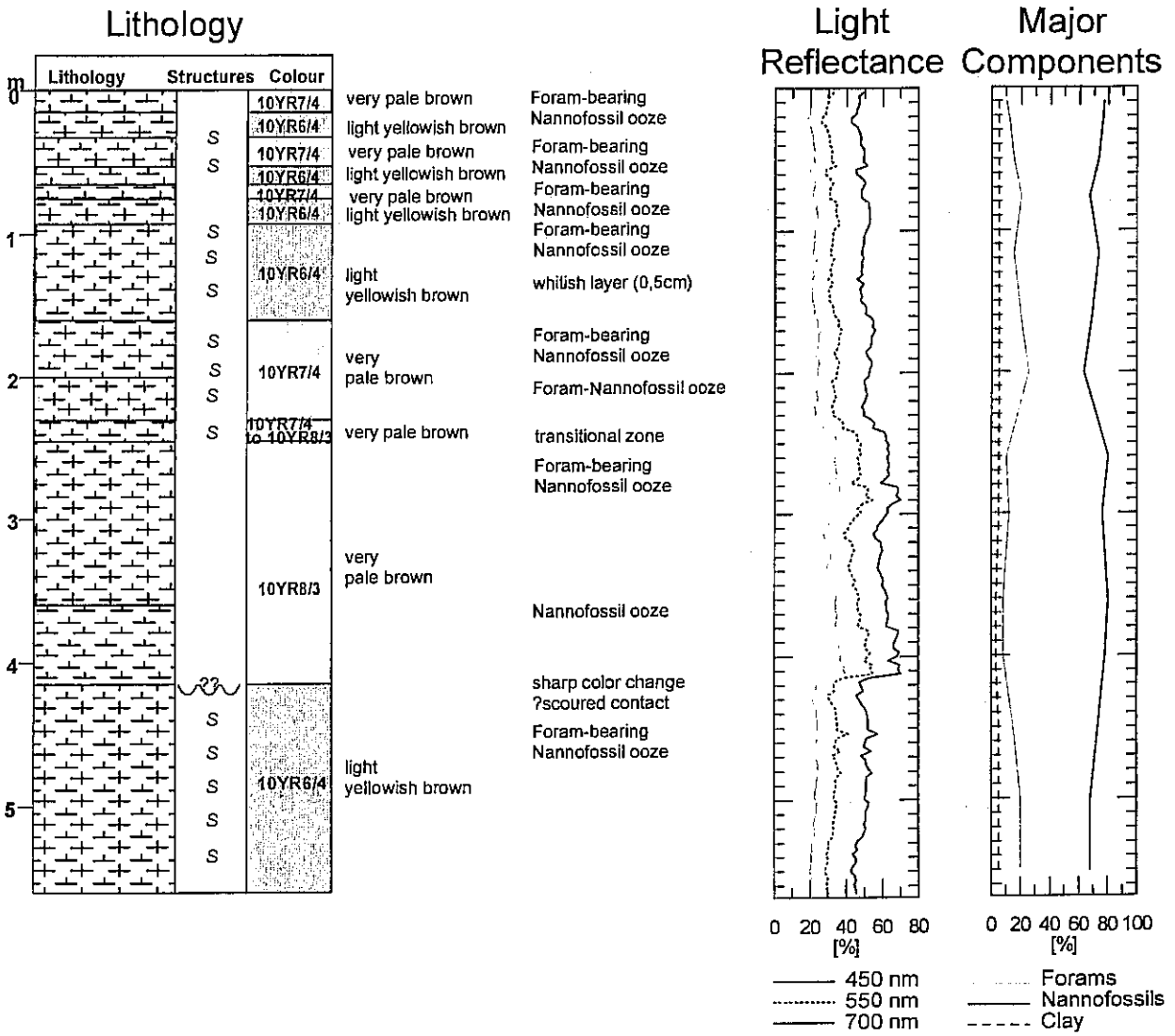

Fig. 169a: Core description gravity core GeoB 3808-5.

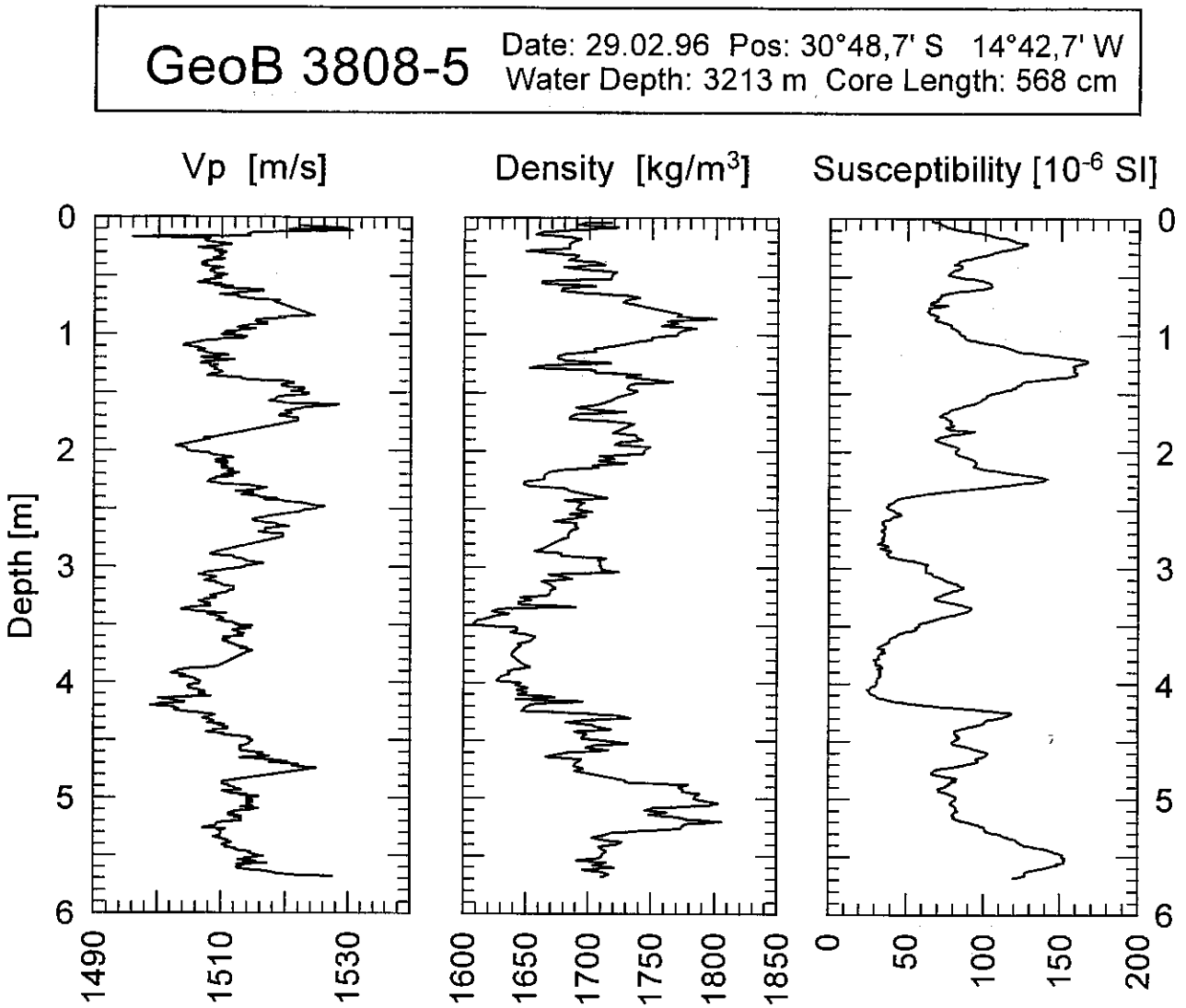

Fig. 169b: Physical properties gravity core GeoB 3808-5.

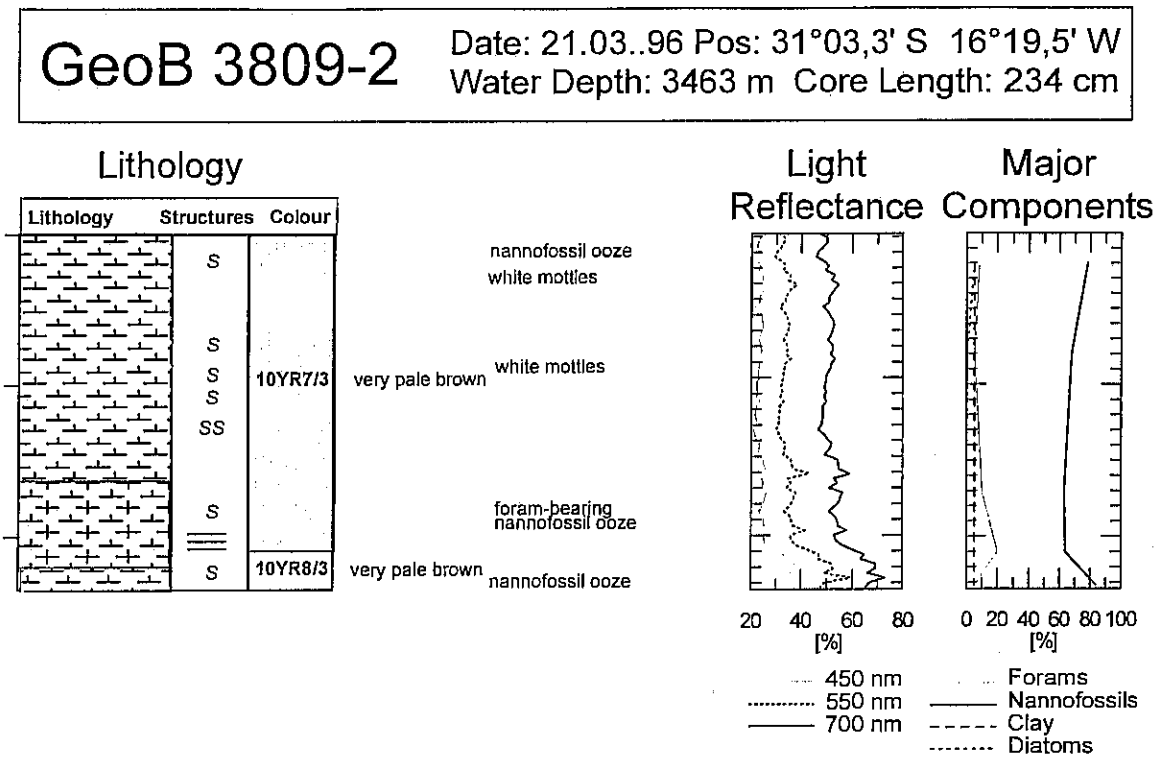

Fig. 170a: Core description gravity core GeoB 3809-2.

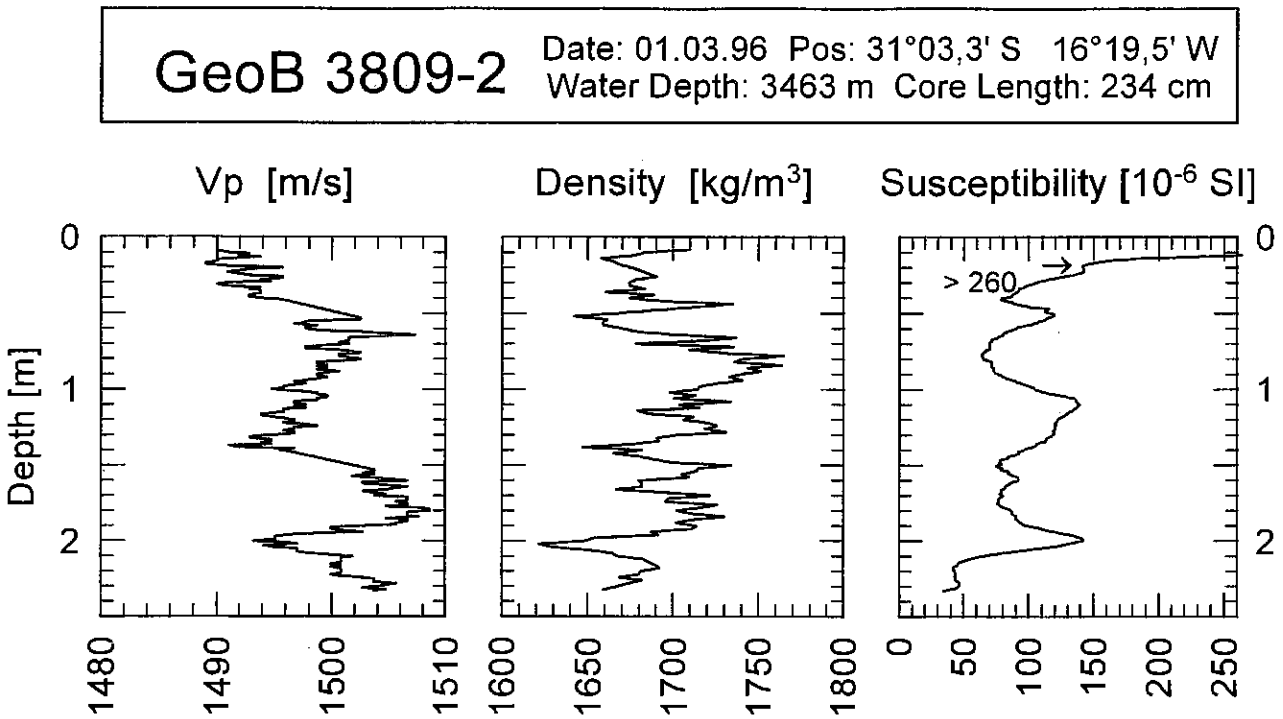

Fig. 170b: Physical properties gravity core GeoB 3809-2.

GeoB 3810-1

Date: 02.03.96 Pos: 31°07,9' S 16°50,3' W
Water Depth: 3810 m Core Length: 218 cm

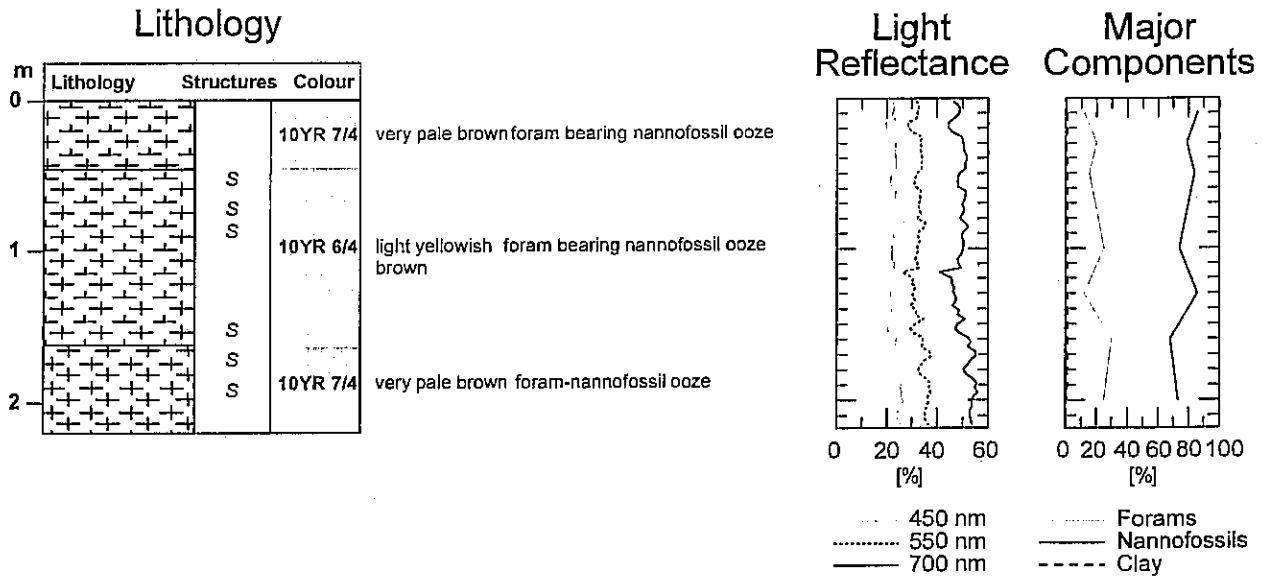

Fig. 171a: Core description gravity core GeoB 3810-1.

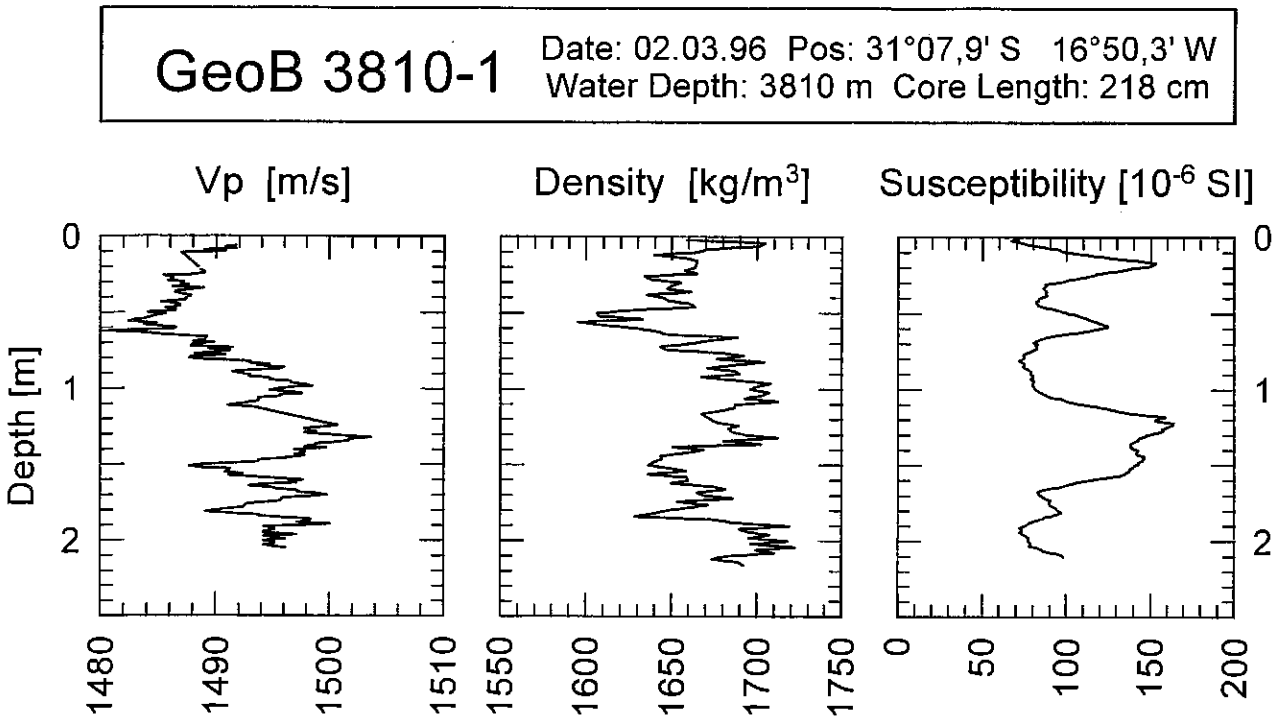

Fig. 171b: Physical properties gravity core GeoB 3810-1.

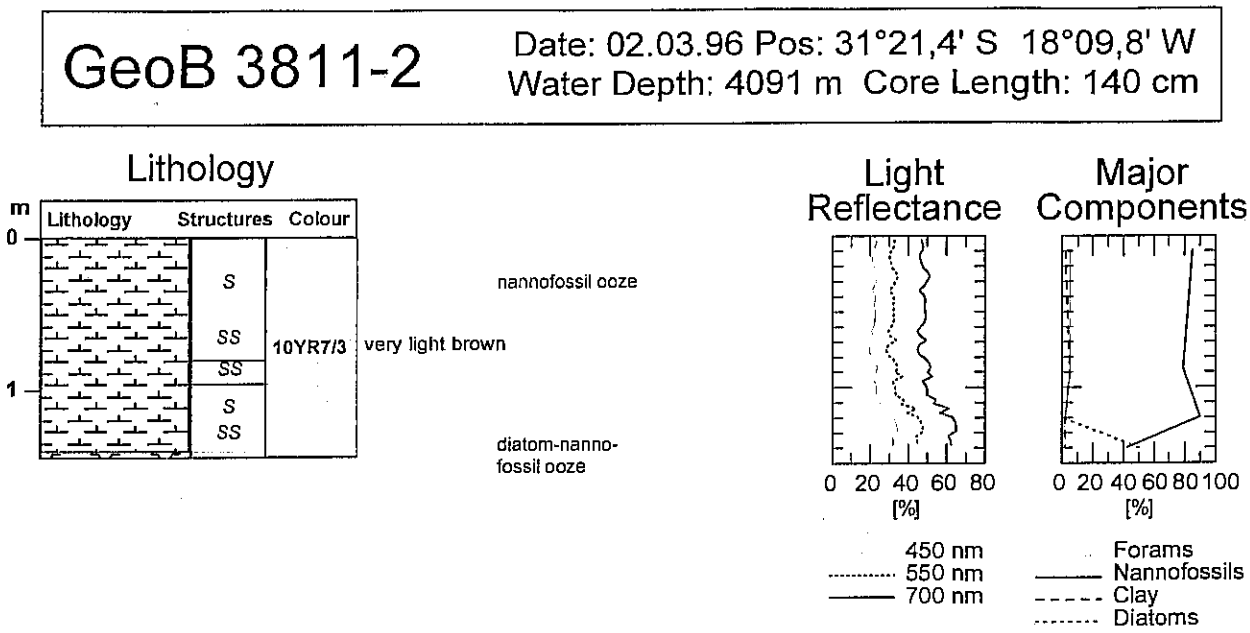

Fig. 172a: Core description gravity core GeoB 3811-2.

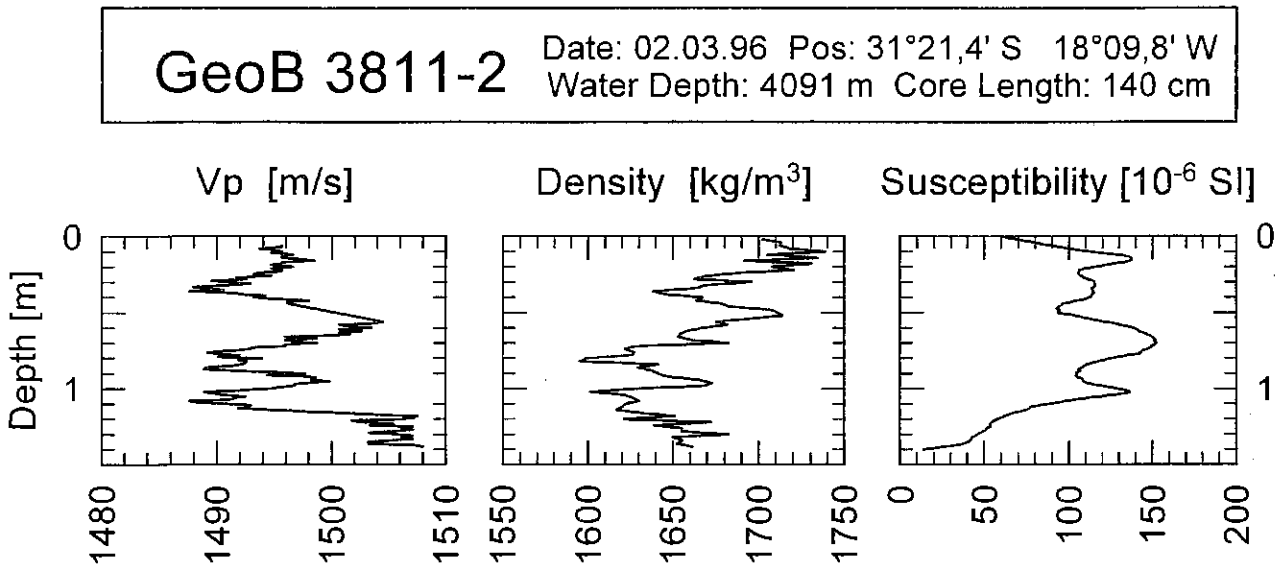

Fig. 172b: Physical properties gravity core GeoB 3811-2.

GeoB 3812-1

Date: 02.03.96 Pos: 31°36,9' S 19°45,5' W
Water Depth: 4205 m Core Length: 532 cm

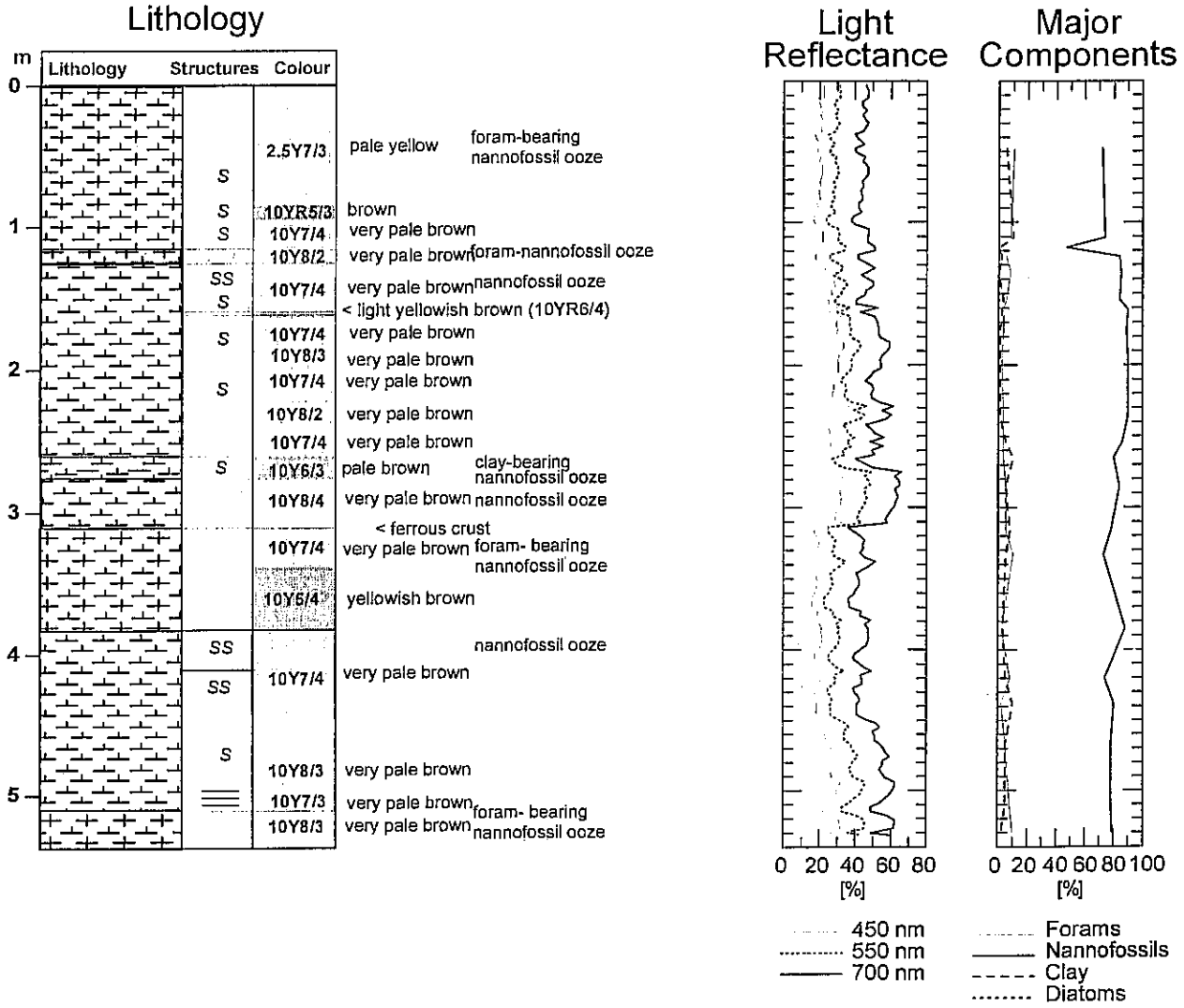

Fig. 173a: Core description gravity core GeoB 3812-1.

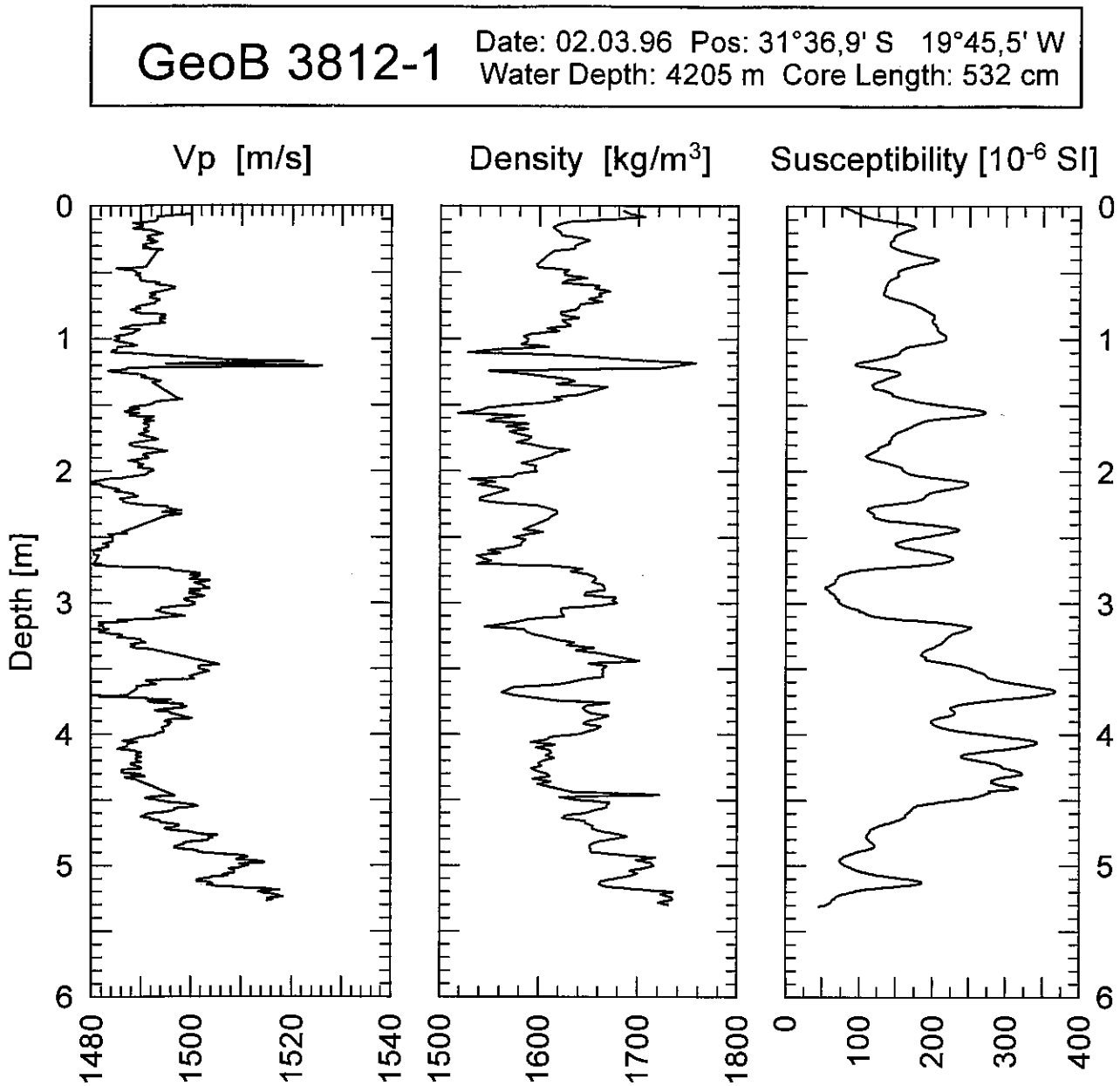

Fig. 173b: Physical properties gravity core GeoB 3812-1.

GeoB 3813-3

Date: 3.03.96 Pos: 32°16,1' S 21°58,0' W
Water Depth: 4331 m Core Length: 983 cm

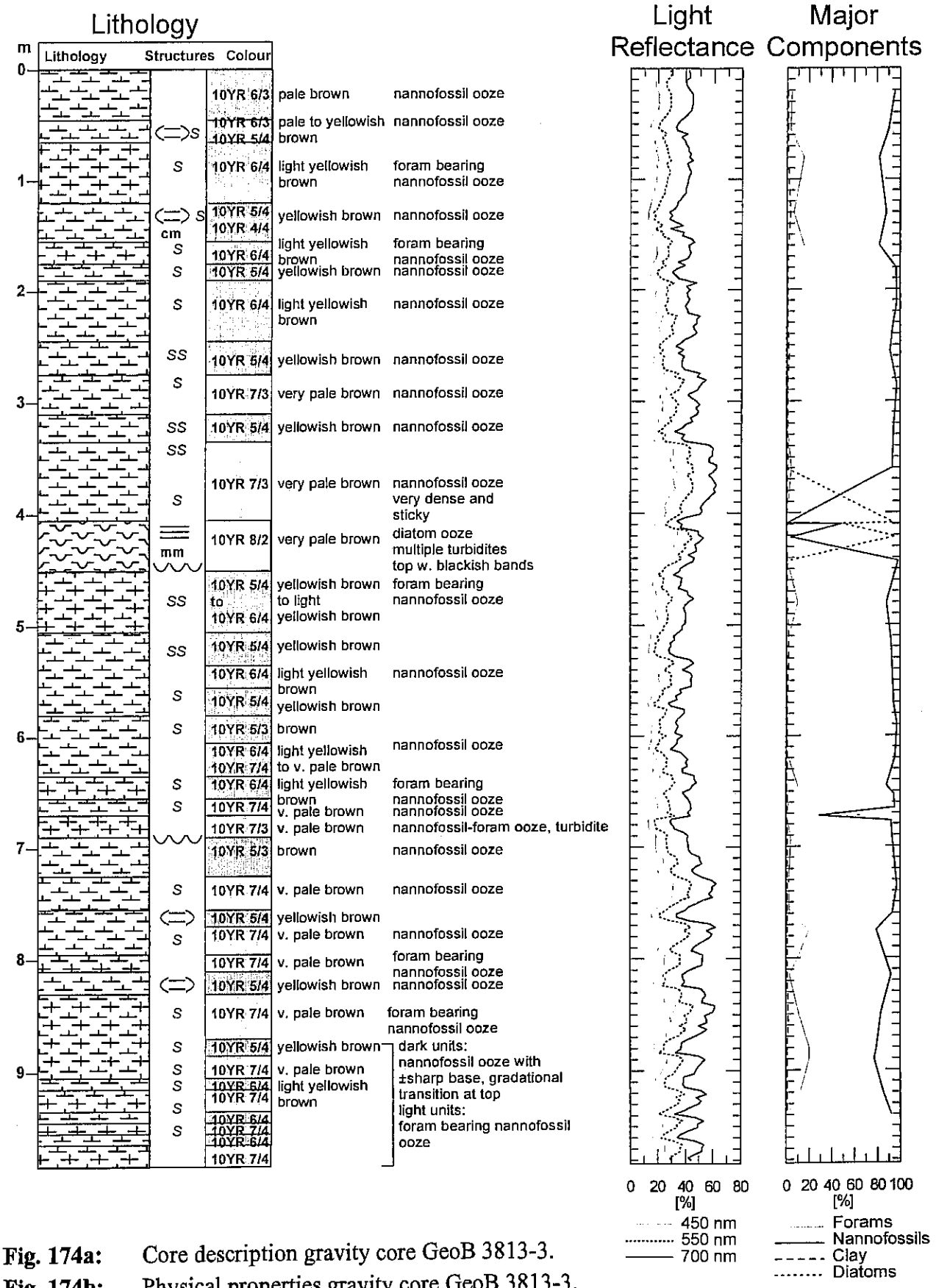

Fig. 174a: Core description gravity core GeoB 3813-3.

Fig. 174b: Physical properties gravity core GeoB 3813-3.

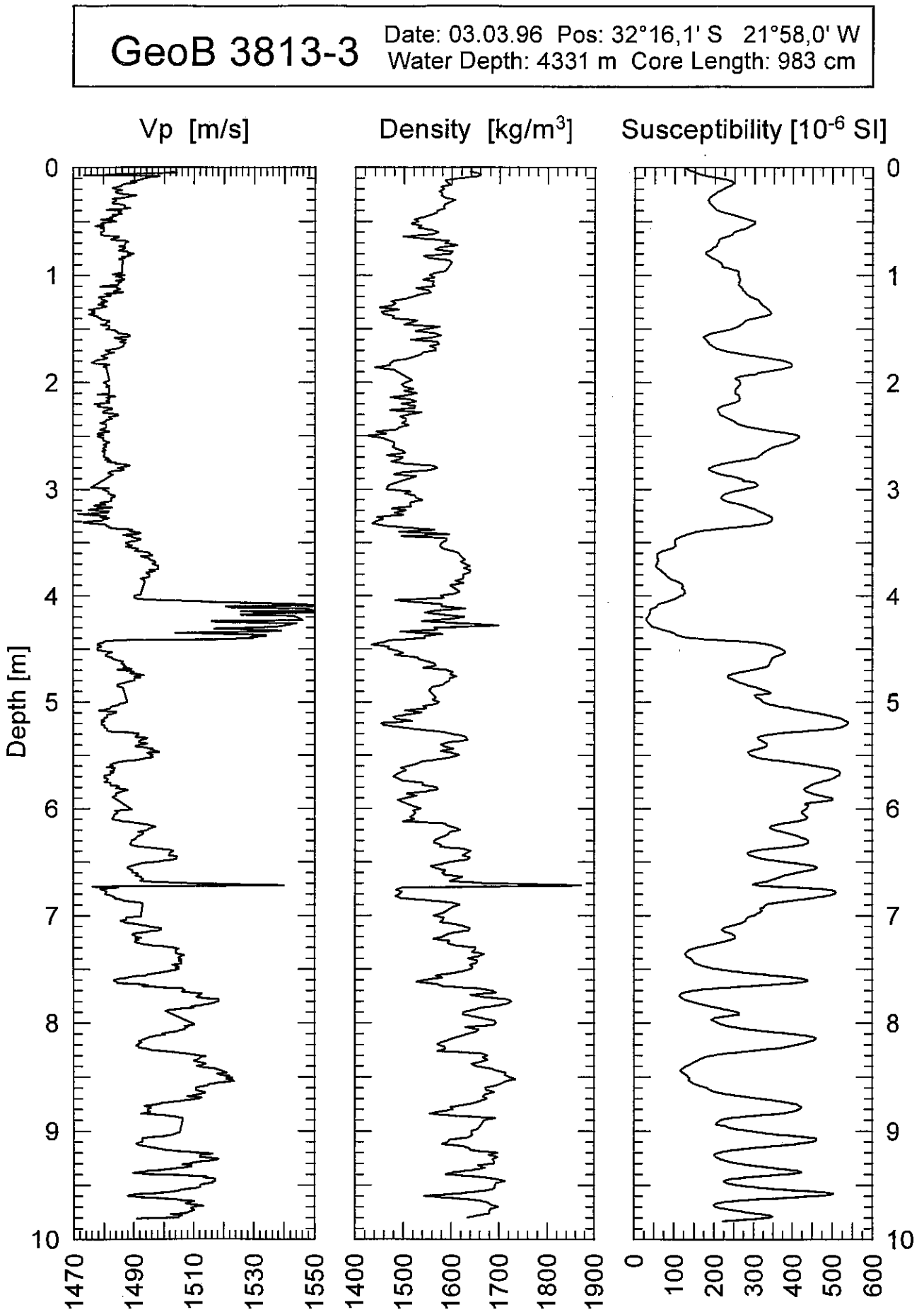
GeoB 3813-3
Date: 03.03.96 Pos: 32°16,1' S 21°58,0' W
Water Depth: 4331 m Core Length: 983 cm
Vp [m/s]
Density [kg/m3]
Susceptibility [10-6 SI]
Depth [m]
0
1
2
3
4
5
6
7
8
9
10
1470
1490
1510
1530
1550
1400
1500
1600
1700
1800
1900
0
100
200
300
400
500
600

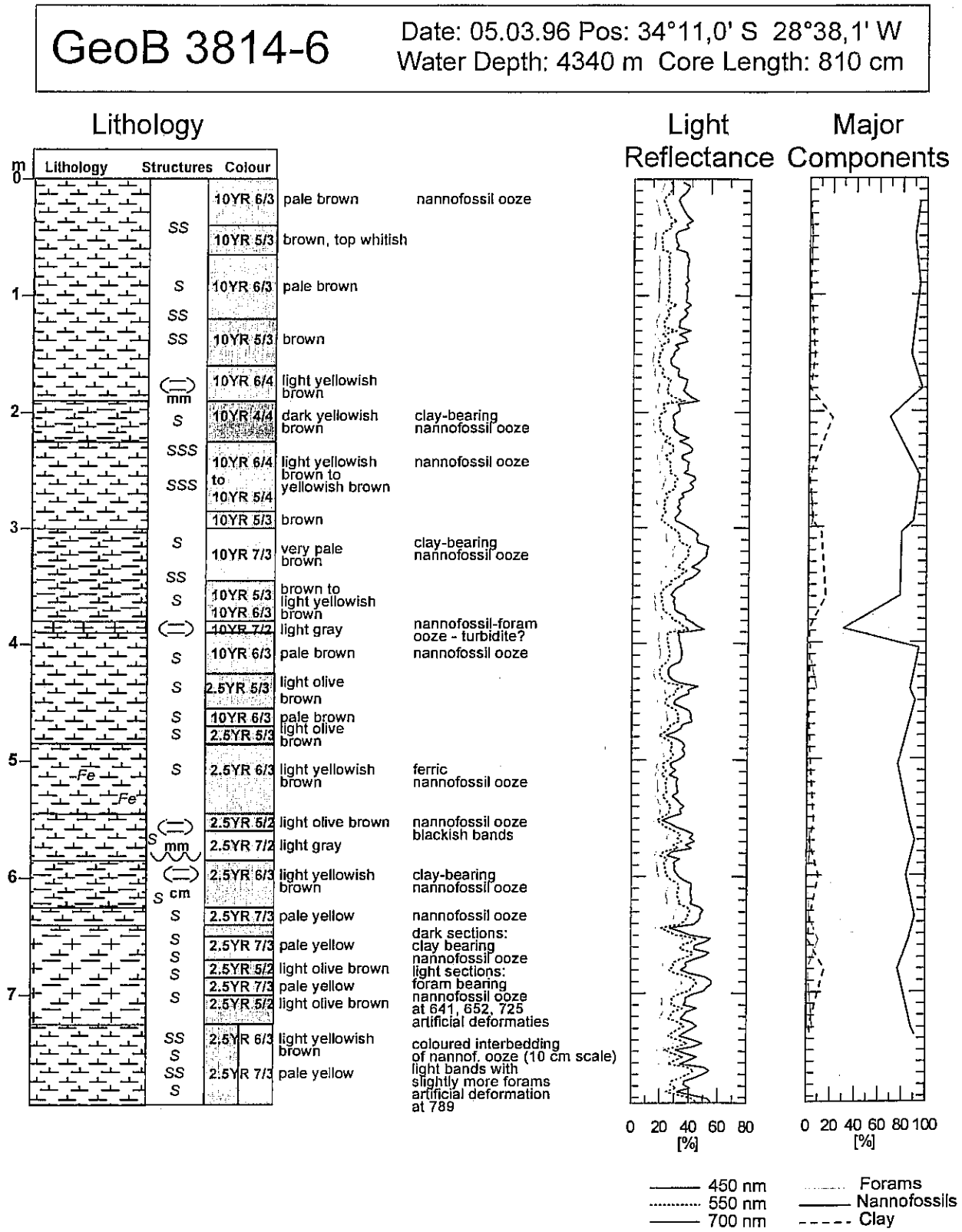

Fig. 175a: Core description gravity core GeoB 3814-6.

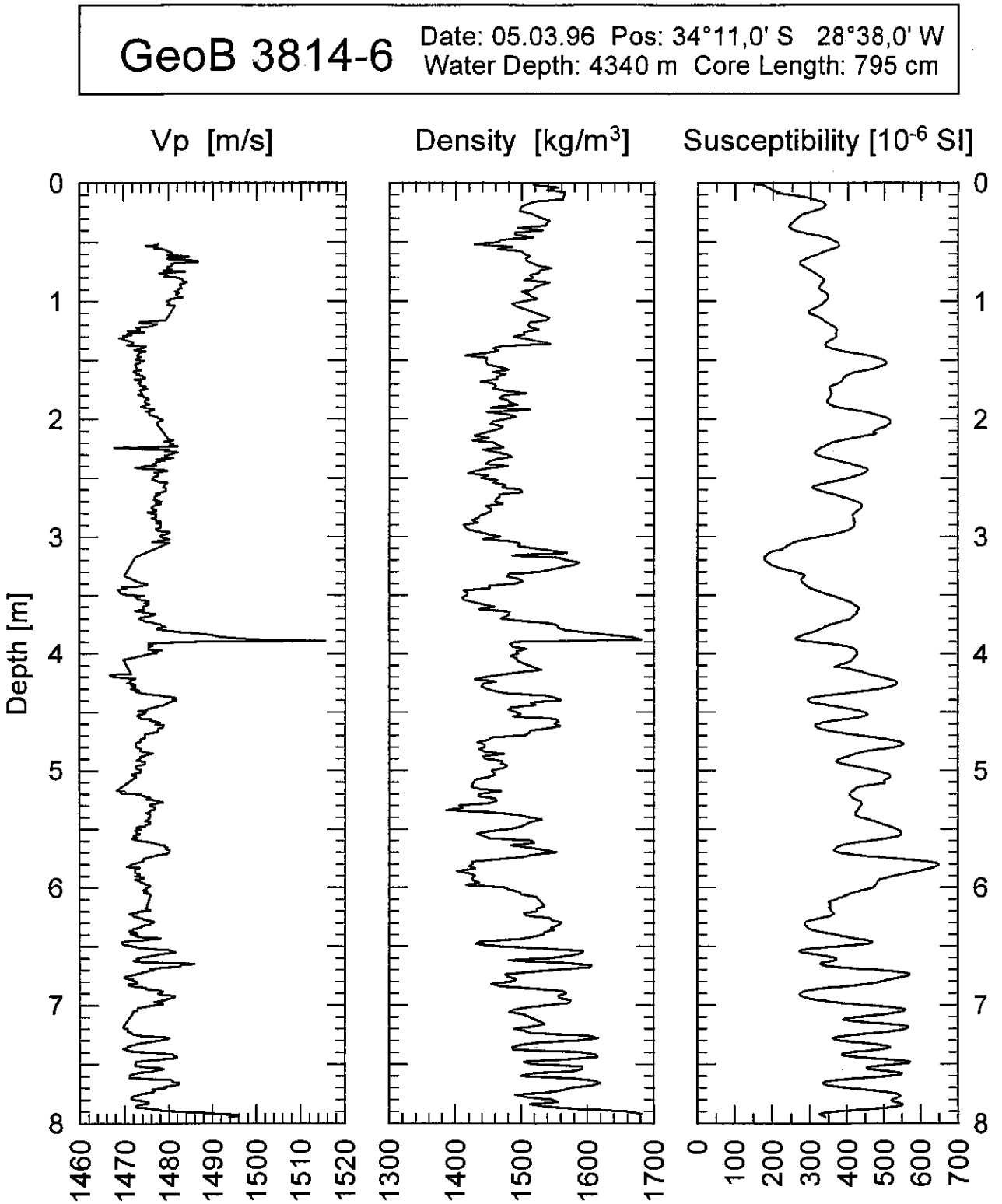

Fig. 175b: Physical properties gravity core GeoB 3814-6.

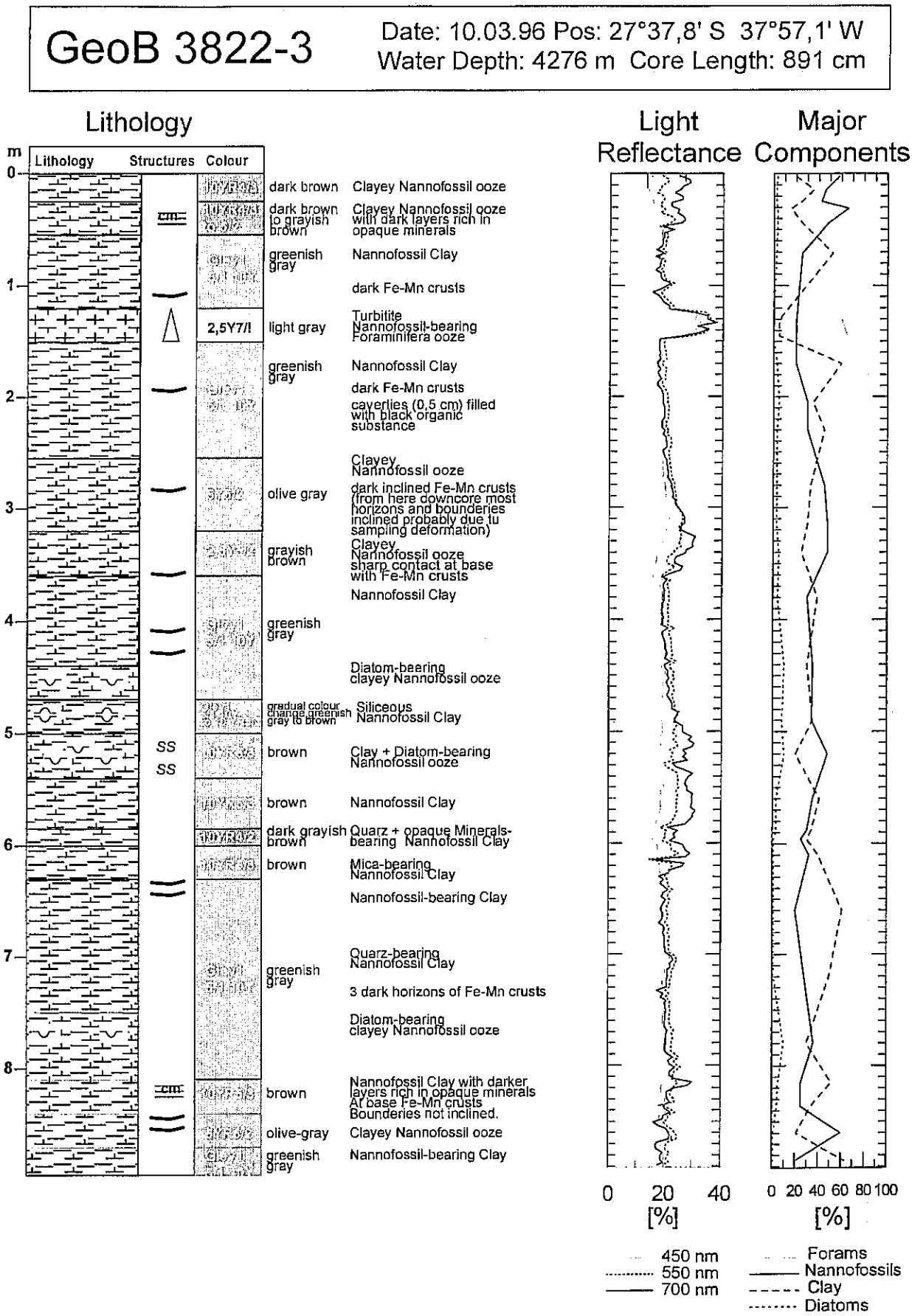

Fig. 176a: Core description gravity core GeoB 3822-3.

Fig. 176b: Physical properties gravity core GeoB 3822-3.

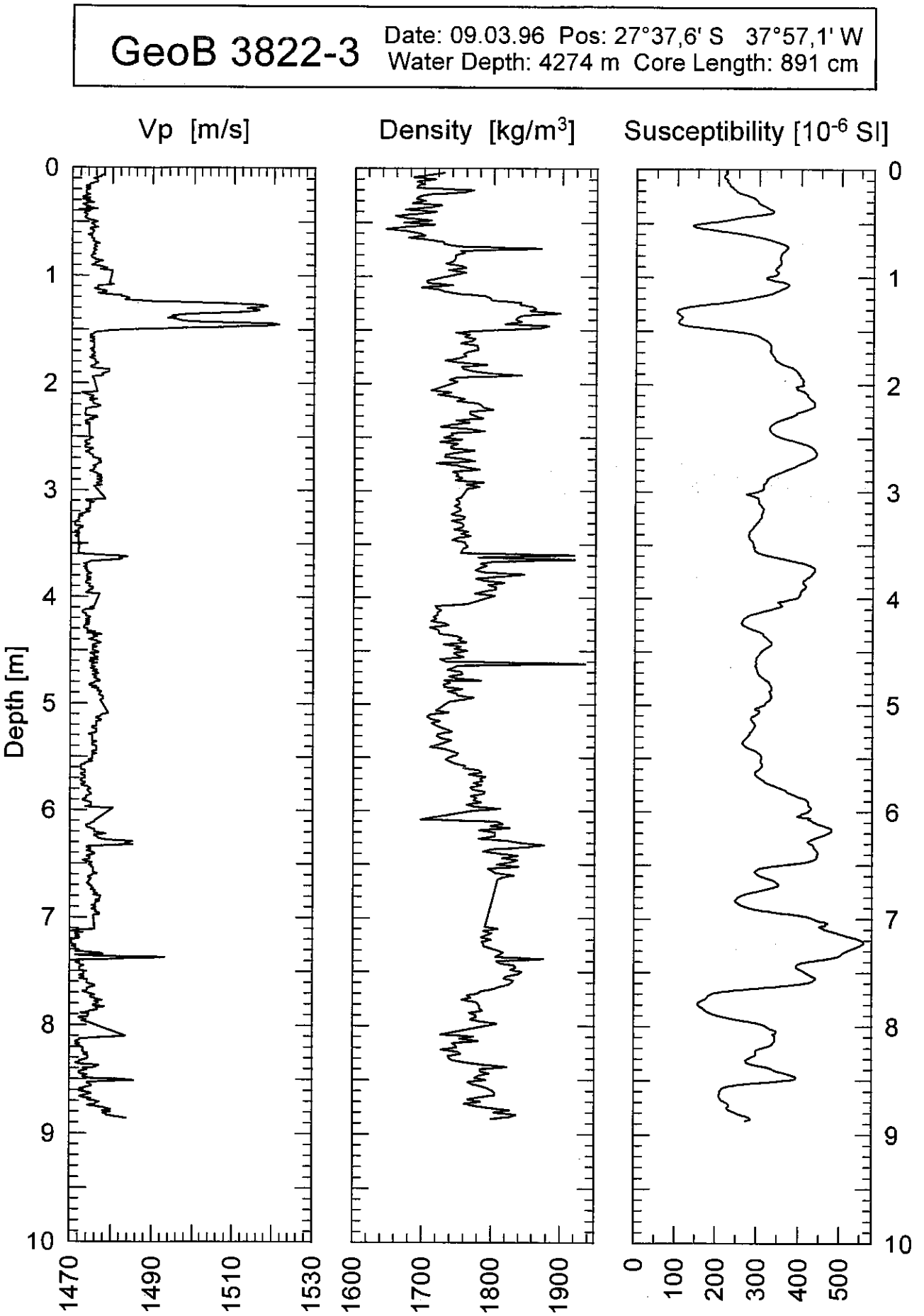
GeoB 3822-3
Date: 09.03.96 Pos: 27°37,6' S 37°57,1' W
Water Depth: 4274 m Core Length: 891 cm
Vp [m/s]
Density [kg/m3]
Susceptibility [10-6 SI]
Depth [m]
0
1
2
3
4
5
6
7
8
9
10
1470
1490
1510
1530
1600
1700
1800
1900
0
100
200
300
400
500

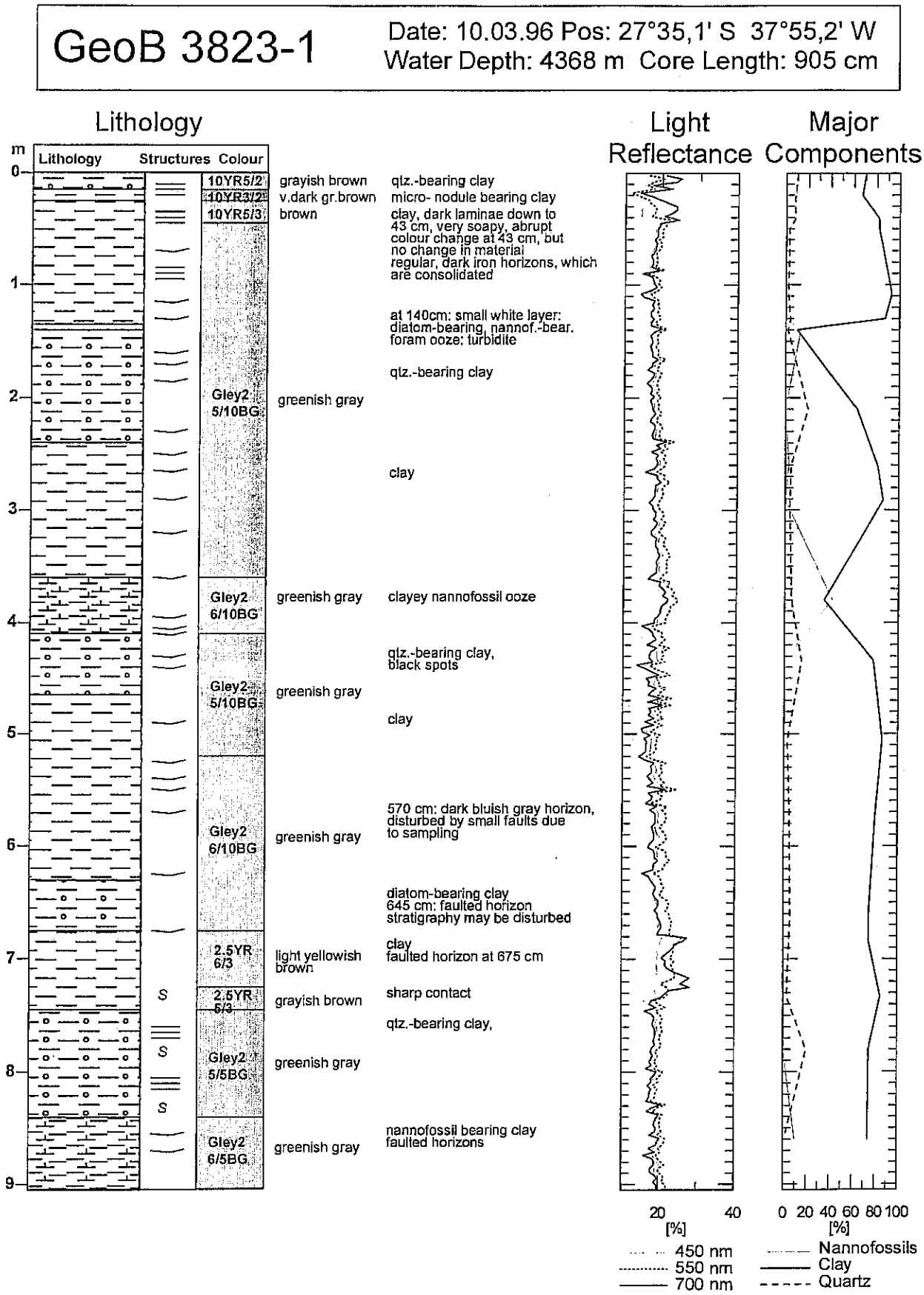

Fig. 177a: Core description gravity core GeoB 3823-1.

Fig. 177b: Physical properties gravity core GeoB 3823-1.

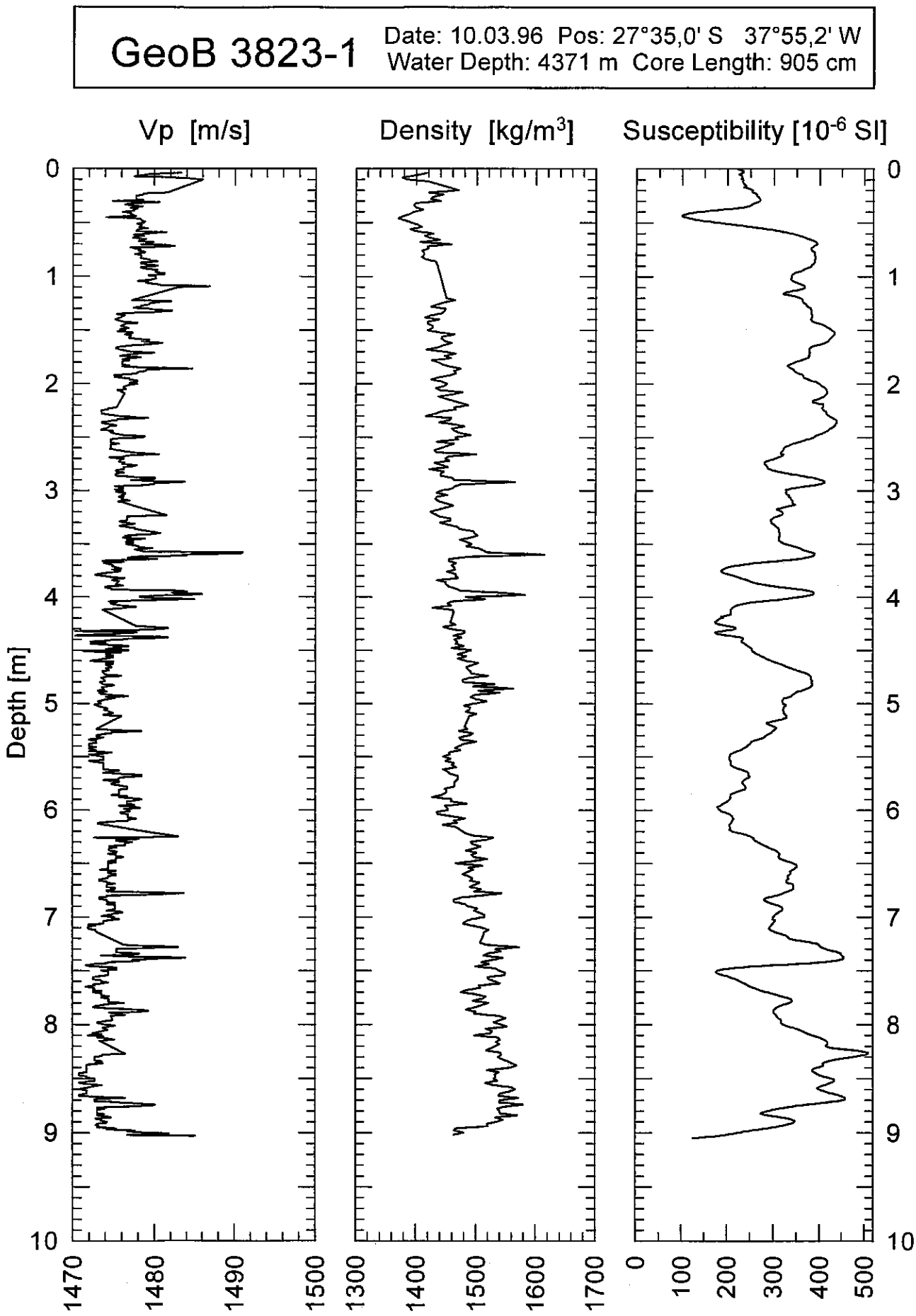
GeoB 3823-1
Date: 10.03.96 Pos: 27°35,0' S 37°55,2' W
Water Depth: 4371 m Core Length: 905 cm
Vp [m/s]
Density [kg/m3]
Susceptibility [10-6 SI]
Depth [m]
0
1
2
3
4
5
6
7
8
9
10
1470
1480
1490
1500
1300
1400
1500
1600
1700
0
100
200
300
400
500

GeoB 3825-2

Date: 12.03.96 Pos: 26°14,0' S 36°19,9' W
Water Depth: 4267 m Core Length: 945 cm

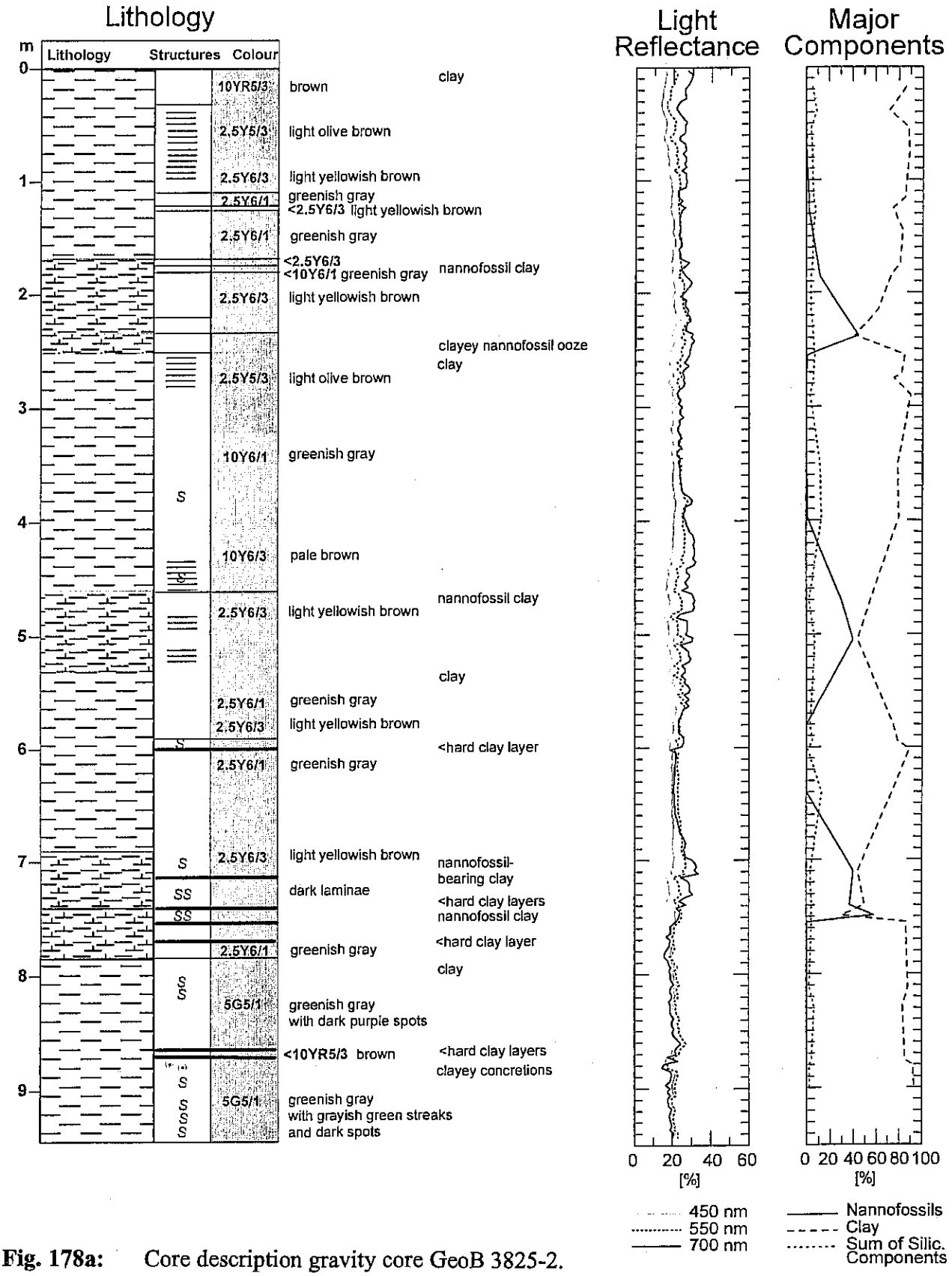

Fig. 178a: Core description gravity core GeoB 3825-2.
Fig. 178b: Physical properties gravity core GeoB 3825-2.

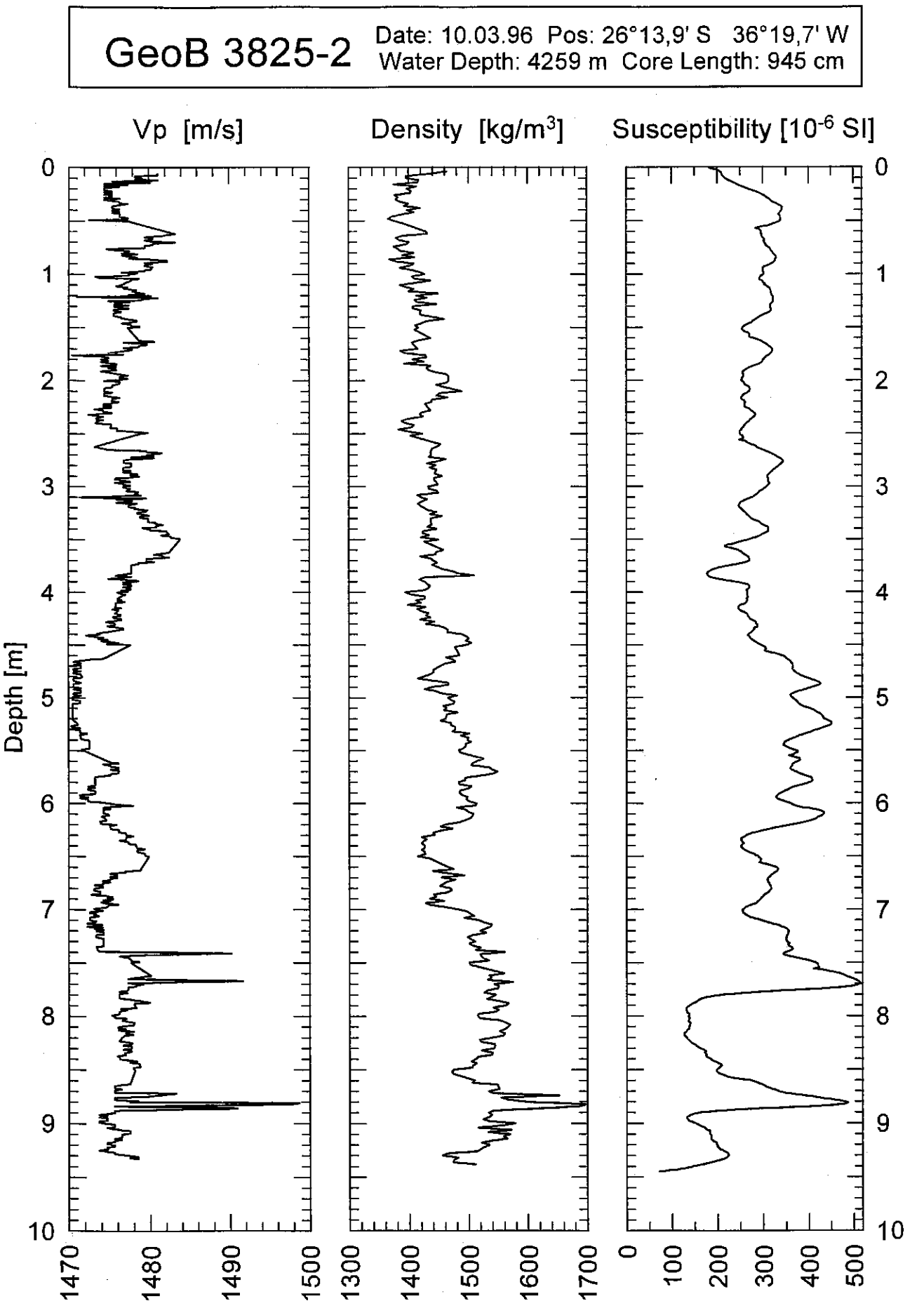
GeoB 3825-2
Date: 10.03.96 Pos: 26°13,9' S 36°19,7' W
Water Depth: 4259 m Core Length: 945 cm
Vp [m/s]
Density [kg/m3]
Susceptibility [10-6 SI]
Depth [m]
0
1
2
3
4
5
6
7
8
9
10
1470
1480
1490
1500
1300
1400
1500
1600
1700
0
100
200
300
400
500

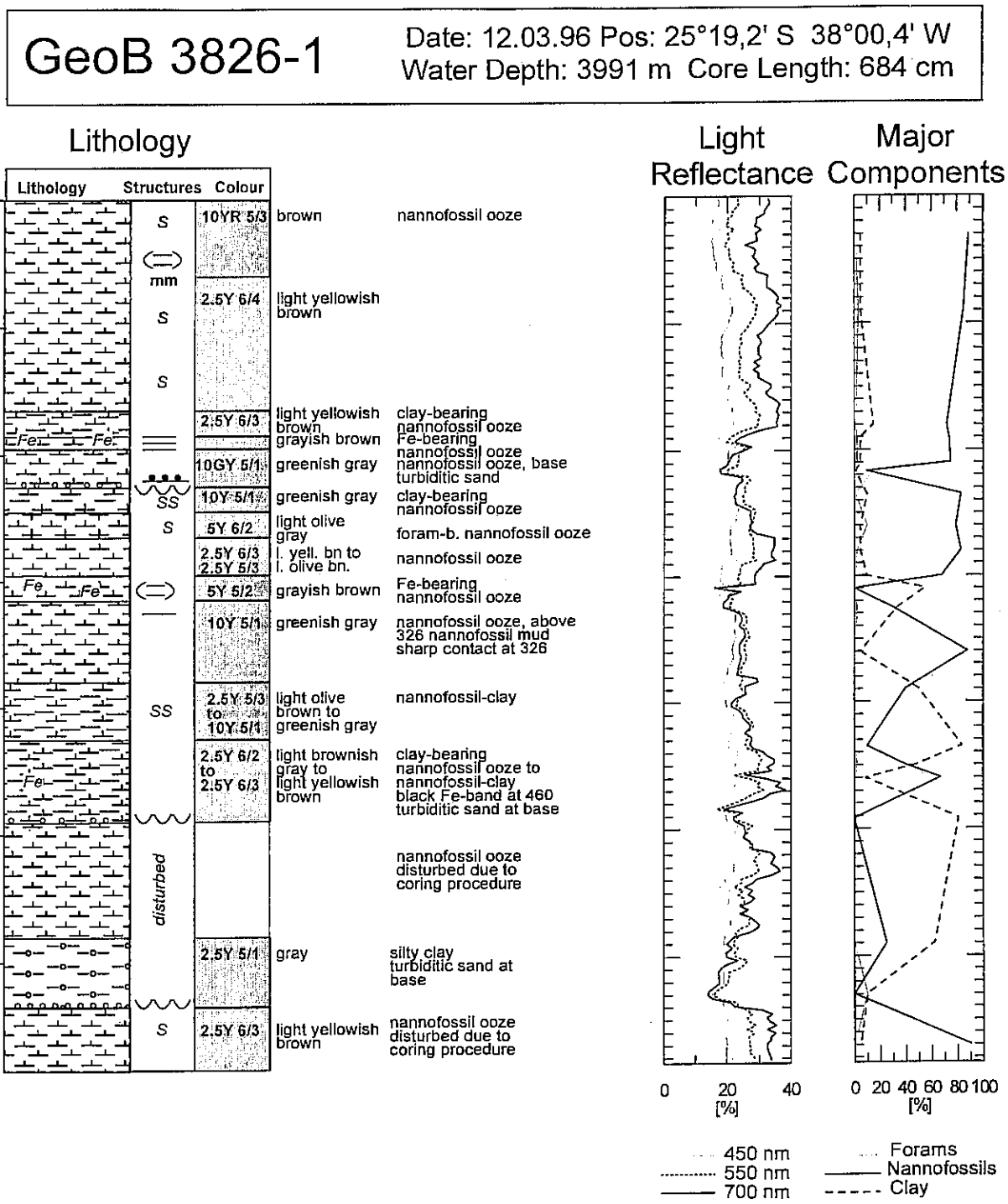

Fig. 179a: Core description gravity core GeoB 3826-1.

Fig. 179b: Physical properties gravity core GeoB 3826-1.

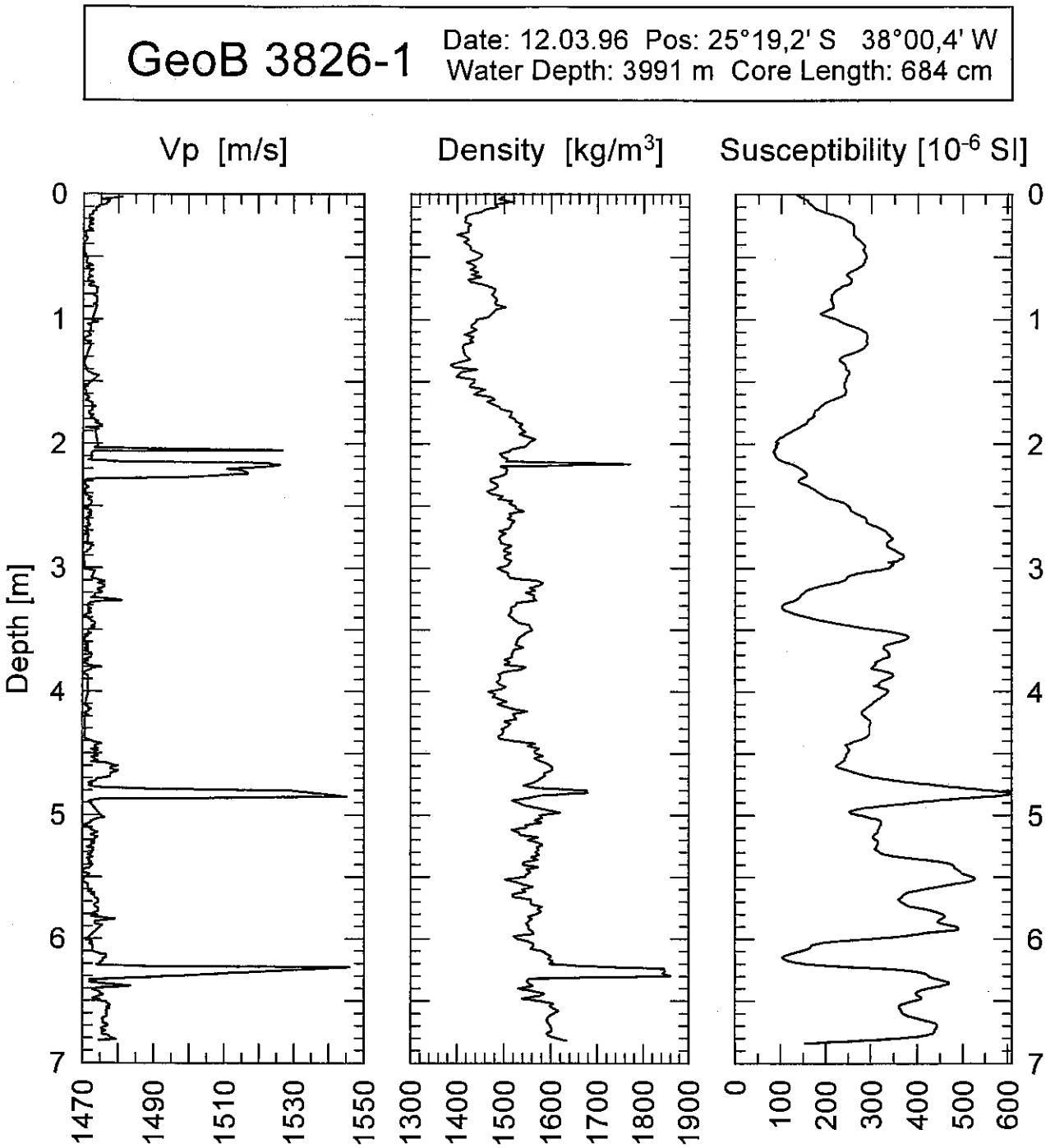
GeoB 3826-1
Date: 12.03.96 Pos: 25°19,2' S 38°00,4' W
Water Depth: 3991 m Core Length: 684 cm
Vp [m/s]
Density [kg/m3]
Susceptibility [10-6 SI]
Depth [m]
0
1
2
3
4
5
6
7
1470
1490
1510
1530
1550
1300
1400
1500
1600
1700
1800
1900
0
100
200
300
400
500
600

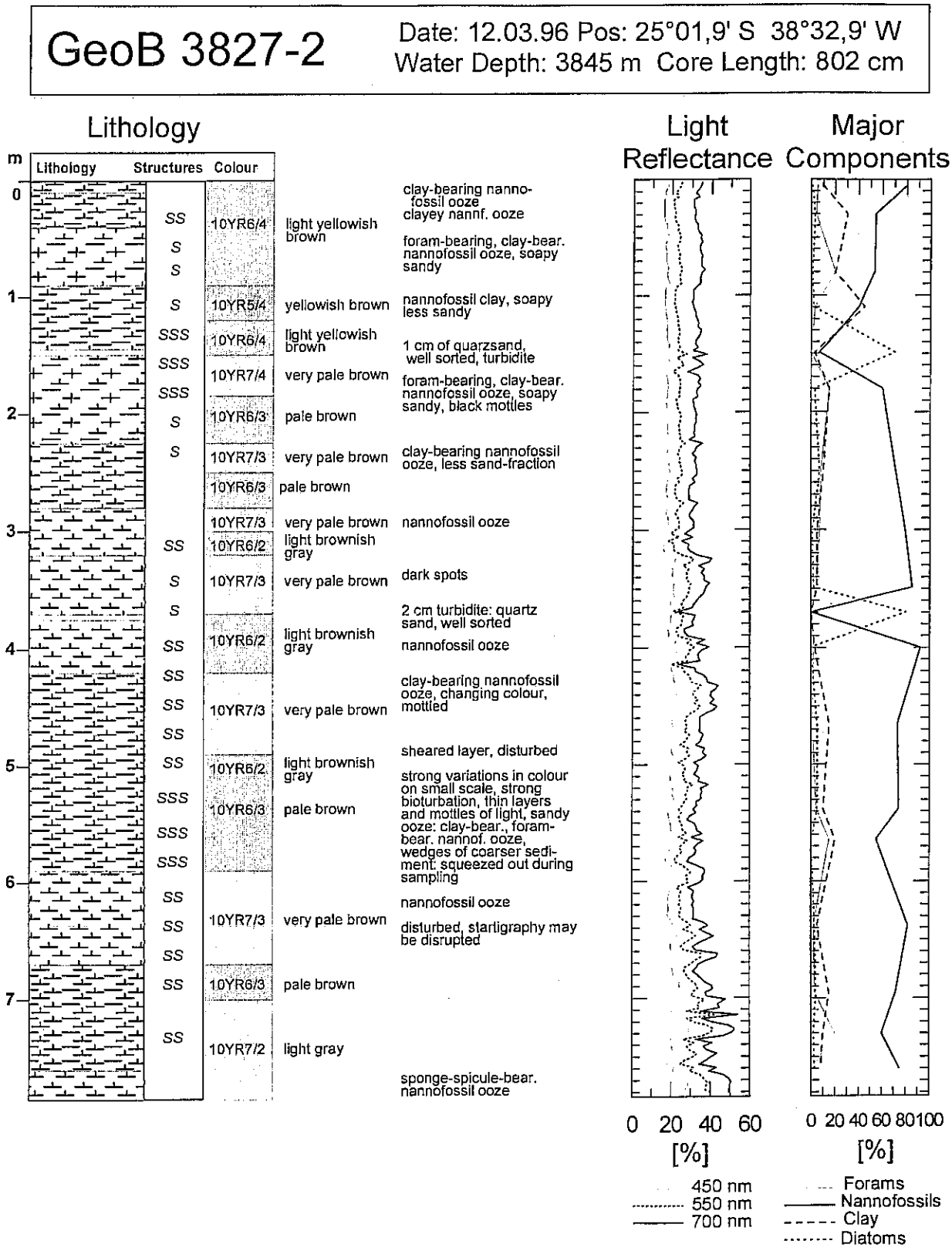

Fig. 180a: Core description gravity core GeoB 3827-2.

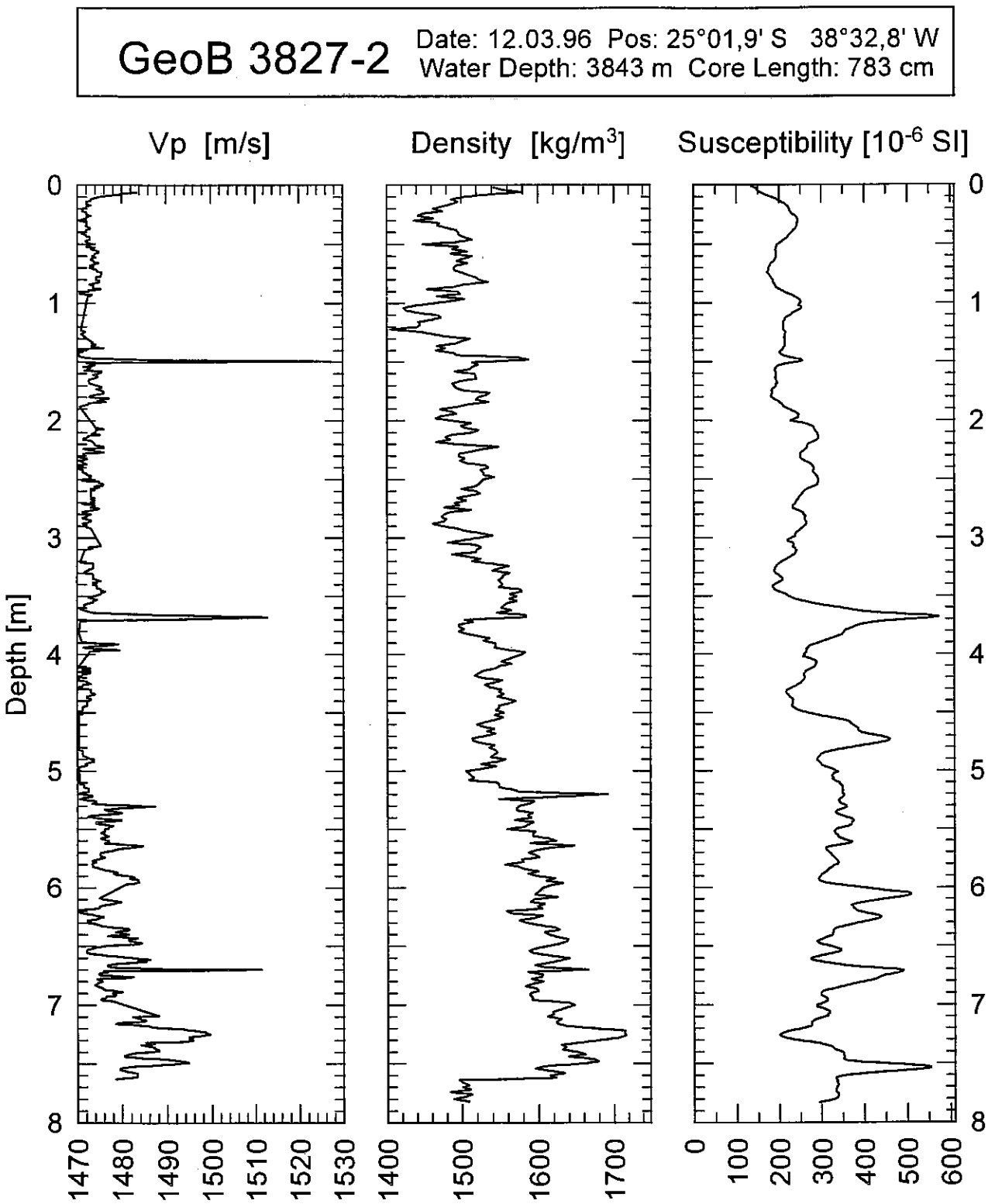

Fig. 180b: Physical properties gravity core GeoB 3827-2.

5.3.7.4 EOF-Analysis of the Spectrophotometry Data

(B. Grieger)

Compared to other methods, e. g. the measurement of magnetic susceptibility, the spectrophotometry yields a considerable amount of data. In each core depth the reflectance is measured at 31 different wavelength values between 400 and 700 nm. For the concise representation of the results the reflectances at the wavelengths 450, 500 and 700 nm have been singled out (see the previous section), which correspond to the colours blue, green and red.

Looking at the reflectances in each of the Figures 162a,b-180a,b, the high correlation of the three curves can be noticed straight away. This implies that mainly the total brightness the value varies, while hue and saturation remain almost constant. However, there are some weak colour variations, but they are difficult to derive from a representation limited to three fixed wavelengths.

This suggests to carry out an EOF-analysis *(Empirical Orthogonal Functions)* of the spectrophotometry data. In the high-dimensional vector space of the observations (31 dimensions in this case), a new set of basis vectors (EOFs) is calculated, where the first EOF points in the direction of the largest variance of the observations, the second EOF is perpendicular to the first EOF and points in the direction of the largest residual variance and so on. The projection of the observations on the EOFs yields a new set of 31 time series, the so called PCs *(Principal Components)*.

In the PCs the information is distributed quite unsymmetrical. The original time series generally all explain about the same amount of variance. On the contrary, the first few PCs i. e. the ones corresponding to the EOFs which point in the directions of the largest variances explain a large fraction of the variance of the observed data. In this way almost the complete information contained in the 31 observed time series can be represented by only a few PCs.

For the five gravity cores investigated preliminary, the first three EOFs explain together more than 99 % of the total variance, see Table 35. For the first three cores the first EOF explains more than 97 %. The reflectance spectrum given by the first EOF comes off relatively flat, compare Figures 162 a,b-180 a,b . This confirms that the observed variances are dominated by changes of the total brightness, which are represented by the first PC.

Tab. 35: The variances explained by the first three *Empirical Orthogonal Functions* for the investigated gravity cores

Gravity core	1. EOF	2. EOF	3. EOF
GeoB 3709-2	98.47 %	1.36 %	0.13 %
GeoB 3801-6	97.13 %	2.78 %	0.06 %
GeoB 3813-3	98.35 %	1.58 %	0.05 %
GeoB 3822-3	81.19 %	18.30 %	0.46 %
GeoB 3825-2	71.27 %	28.04 %	0.57 %

The second PC represents colour variations which correspond to the reflectance spectrum of the first EOF. Considering e. g. the gravity core GeoB 3709-2, see Report M34/2, Figure 86a,b , the spectrum runs from positive values in the blue wavelength range to negative values in the red, i. e. the second PC represents colour variations between red and blue. The third EOF is positive in the blue and red range and negative in the green, i. e. the third PC represents colour variations between magenta and green.

The gravity cores GeoB 3822-3 and GeoB 3825-2, see Figures 176 a,b and 178 a,b, exhibit larger colour variations than the other three cores. The reflectance spectrum of the first EOF has a steeper slope and the second EOF explains a considerable fraction of the variance.

The PC time series which preliminary have been calculated only for five selected gravity cores should be compared with time series of other parameters. It can be assumed that the PCs are correlated with the abundance of certain minerals or organic components in the cores. This would offer an extremely fast and simple possibility to obtain estimations of these parameters.

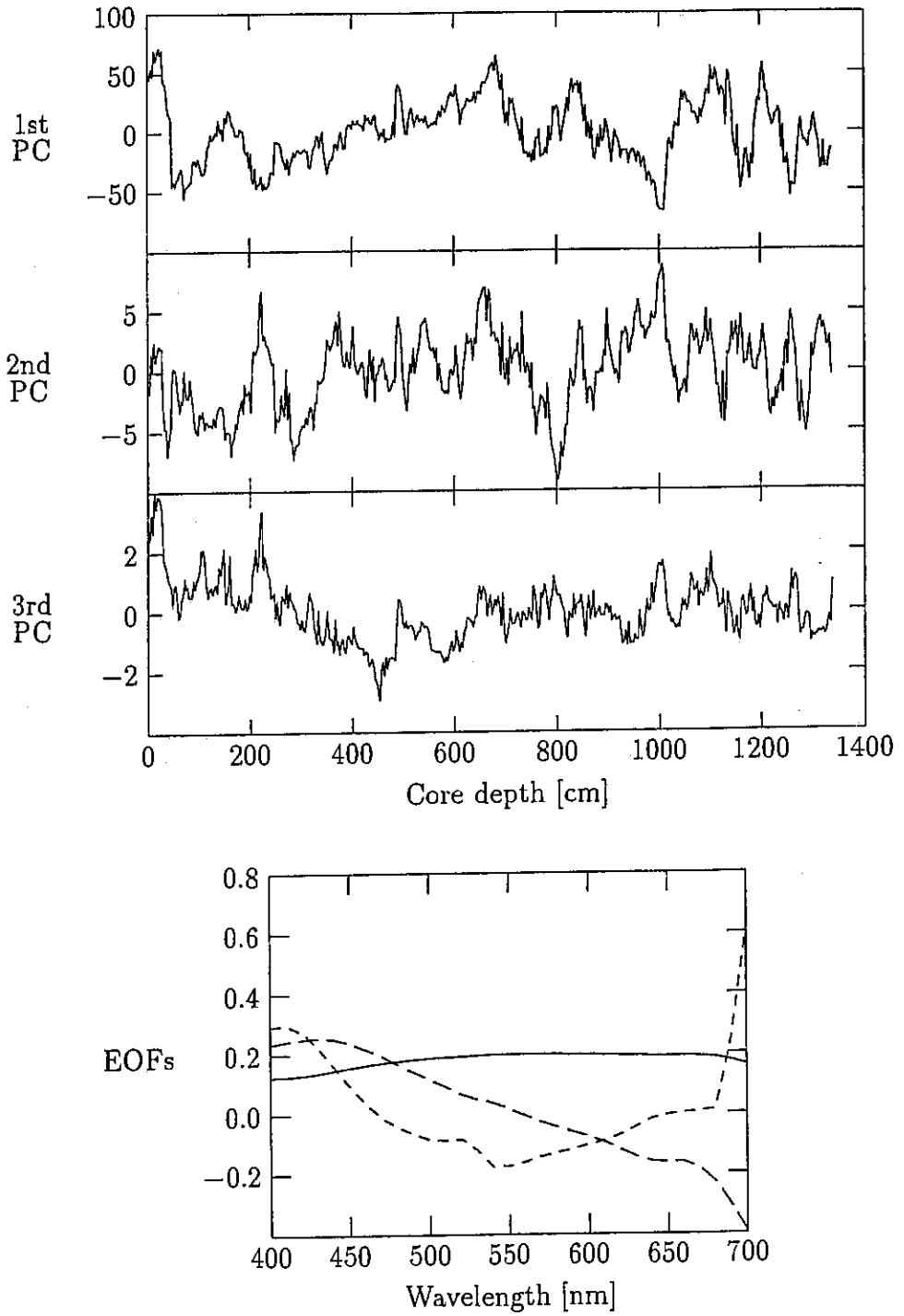

Fig. 181: GeoB 3709-2, results of the EOF-analysis of the spectrophotometry data. *Top:* Time series of the first tree Principle Components. *Bottom:* The first three Empirical Orthogonal Functions (1st solid line, 2nd long dashed, 3rd short dashed).

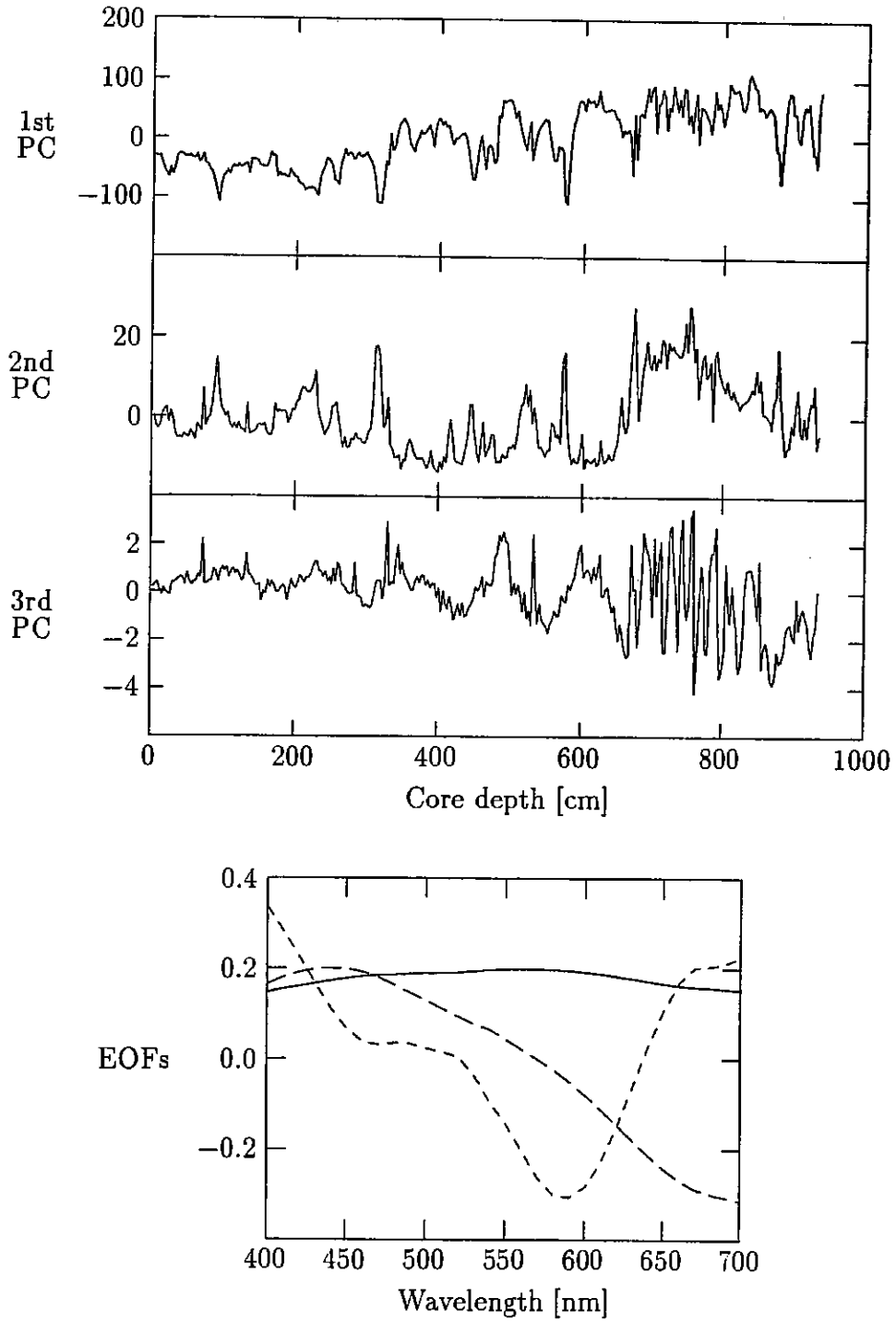

Fig. 182: GeoB 3801-6, results of the EOF-analysis of the spectrophotometry data. *Top:* Time series of the first tree Principle Components. *Bottom:* The first three Empirical Orthogonal Functions (1st solid line, 2nd long dashed, 3rd short dashed).

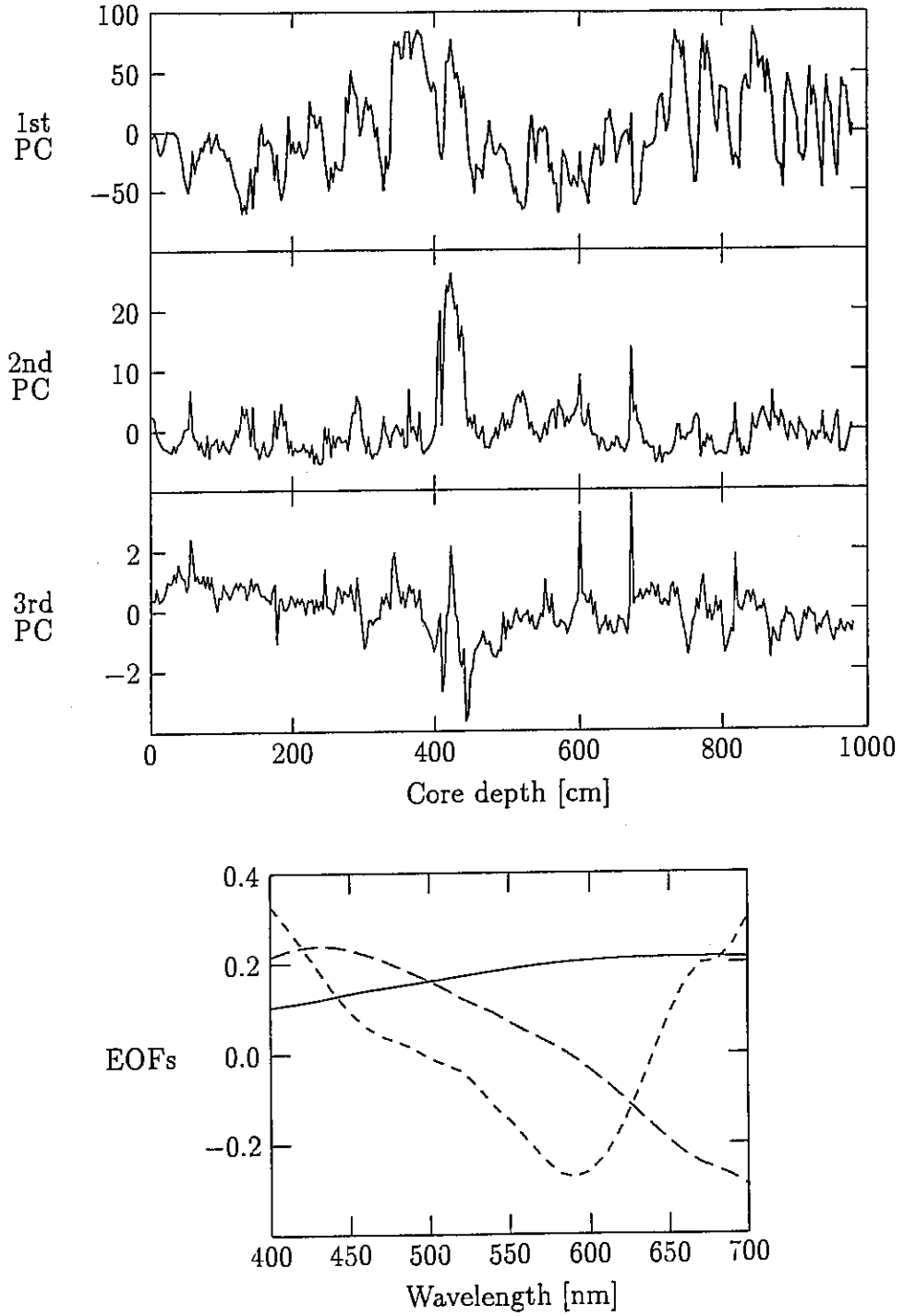

Fig. 183: GeoB 3813-3, results of the EOF-analysis of the spectrophotometry data. *Top:* Time series of the first tree Principle Components. *Bottom:* The first three Empirical Orthogonal Functions (1st solid line, 2nd long dashed, 3rd short dashed).

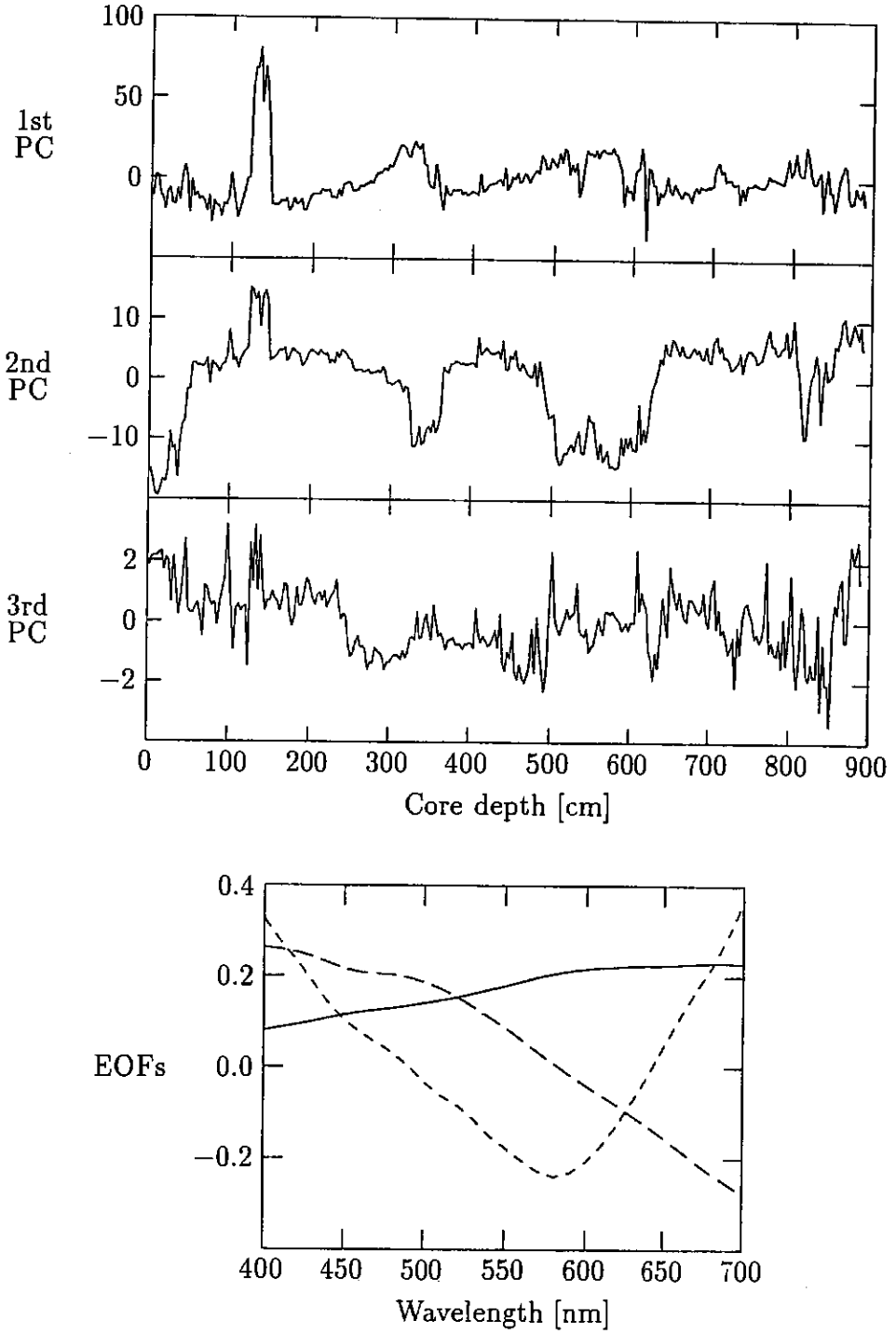

Fig. 184: GeoB 3822-3, results of the EOF-analysis of the spectrophotometry data. *Top:* Time series of the first tree Principle Components. *Bottom:* The first three Empirical Orthogonal Functions (1st solid line, 2nd long dashed, 3rd short dashed).

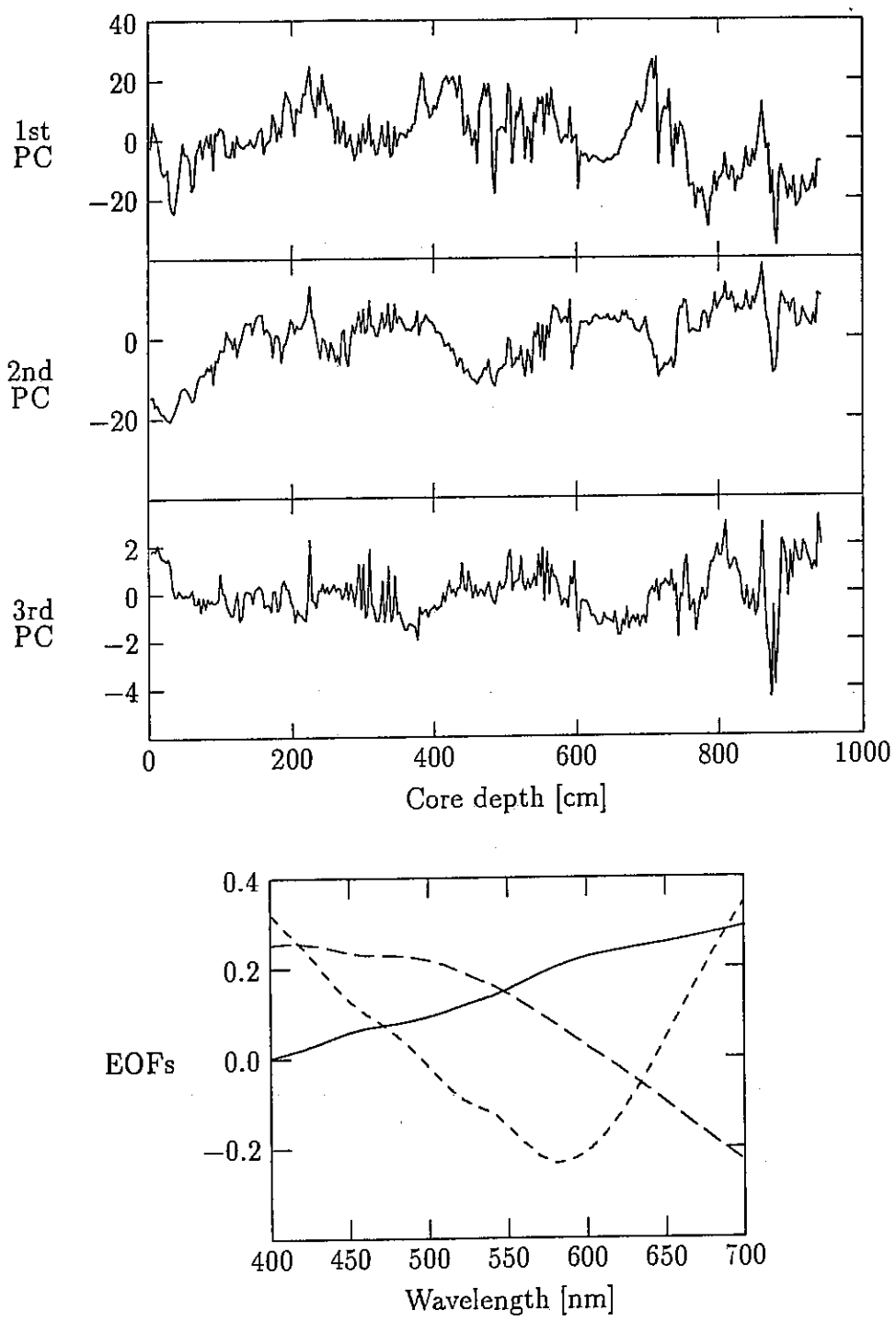

Fig. 185: GeoB 3825-2, results of the EOF-analysis of the spectrophotometry data. *Top:* Time series of the first tree Principle Components. *Bottom:* The first three Empirical Orthogonal Functions (1st solid line, 2nd long dashed, 3rd short dashed).

5.3.7.5 Carbonate Content Measuring

(N. Dittert, R. Henning)

Carbonate contents were measured on board using a "Karbonat-Bombe". The $CaCO_3$ content of a sample was ascertained by the measurement of the CO_2 pressure after the treatment with HCl. The absolute error of a single determination is given as about 1 % calcium carbonate (MÜLLER and GASTNER, 1971).

In total, two cores were measured for their carbonate content in 10 cm intervals:

GeoB No	Core type	Geographic position		Water depth	Recovery
		Latitude	Longitude	[m]	[cm]
GeoB 3722-2	SL15	25°15,0' S	12°01,3' E	3506	1296
GeoB 3813-3	SL12	32°16,3' S	21°58,0' W	4331	995

Generally the sediments are rich in carbonate. Both of the cores were taken at waterdepths which are above the recent carbonate compensation depth (CCD); core 3722-2 from the upwelling area off Namibia, core 3813-3 from the western part of the Mid Atlantic Ridge. In general, carbonate values vary from 0 wt.-% up to more than 95 wt.-% (see chapter "5.3.7.1 sampling"). The sediments mainly consist of calcareous planktonic foraminifera and nannofossils (see chapter "5.3.7.2 Core description" and "smear slides"). The two cores show a similar pattern of alternating high and low carbonate contents, indicating interglacial and glacial variations in productivity. Maximum values exceeding 75 wt.-% to 80 wt.-% are assumed to display interglacial conditions; glacial maxima may be characterized by carbonate values below 75 wt.-%. Core 3722-2 may be influenced by turbidite deposition interpreted by fining upward in the lowest parts.

Reliability of carbonate content measuring can be tested by the correlation of carbonate data with light reflectance data of the color scanner (see chapter "5.3.7.3 Spectrometry") and susceptibility data (see chapter "5.3.8 Physical properties"). The correlation of light reflection and carbonate content shows relatively high correlation coefficient r^2 of 0,82 (700 nm), i. e. the higher (lower) the carbonate content the higher (lower) becomes light reflection. The correlation of susceptibility and carbonate content shows low anticorrelation with a correlation coefficient r^2 of 0,42, i. e. the higher (lower) the carbonate content the lower (higher) becomes susceptibility (Fig. 186).

Tab. 36: Carbonate content proxies

No.	Sample weight [g]	Depth [cm]	GeoB 3722-2 $CaCO_3$ content [%]	GeoB 3813-3 $CaCO_3$ content [%]
1	1,0	3	81,5	77,2
2	1,0	13	78,1	63,6
3	1,0	23	79,4	69,4
4	1,0	33	77,1	72,4
5	1,0	43	69,1	64,4
6	1,0	53	60,1	47,1
7	1,0	63	43,1	53,7
8	1,0	73	47,3	69,1
9	1,0	83	24,2	74,7
10	1,0	93	15,7	64,0
11	1,0	103	36,3	65,5
12	1,0	113	46,8	64,3
13	1,0	123	43,1	52,2
14	1,0	133	50,7	39,2
15	1,0	143	51,1	60,2
16	1,0	153	58,2	69,2
17	1,0	163	49,4	70,3
18	1,0	173	55,1	62,2
19	1,0	183	53,0	37,2
20	1,0	193	58,4	69,6
21	1,0	203	63,1	61,1
22	1,0	213	67,6	62,9
23	1,0	223	60,1	72,0
24	1,0	233	48,7	68,8
25	1,0	243	39,0	64,3
26	1,0	253	38,6	51,7
27	1,0	263	32,3	54,7
28	1,0	273	63,4	62,2
29	1,0	283	66,7	79,5
30	1,0	293	72,4	60,1
31	1,0	303	74,6	72,6
32	1,0	313	68,0	69,8
33	1,0	323	55,7	53,8
34	1,0	333	64,8	51,7
35	1,0	343	58,4	74,0
36	1,0	353	69,7	83,1
37	1,0	363	76,9	90,7
38	1,0	373	66,8	92,0
39	1,0	383	60,8	90,4
40	1,0	393	81,6	84,9
41	1,0	403	77,1	71,8
42	1,0	413	83,0	19,3
43	1,0	423	78,5	49,6
44	1,0	433	75,0	27,2
45	1,0	443	74,6	46,4
46	1,0	453	61,8	41,7
47	1,0	463	57,9	55,8
48	1,0	473	58,9	68,5
49	1,0	483	50,3	66,1
50	1,0	493	53,9	61,5
51	1,0	503	54,1	59,2
52	1,0	513	53,8	35,8
53	1,0	523	63,5	32,7

54	1,0	533	62,3	62,7
55	1,0	543	55,3	68,3
56	1,0	553	56,2	68,0
57	1,0	563	47,5	42,0
58	1,0	573	58,2	37,0
59	1,0	583	47,2	54,3
60	1,0	593	44,7	40,2
61	1,0	603	50,9	50,6
62	1,0	613	61,1	51,5
63	1,0	623	53,5	63,0
64	1,0	633	46,7	55,7
65	1,0	643	35,7	73,1
66	1,0	653	28,3	54,0
67	1,0	663	24,0	65,6
68	1,0	673	9,1	63,4
69	1,0	683	0,0	43,3
70	1,0	693	37,2	65,4
71	1,0	703	56,9	68,6
72	1,0	713	84,5	77,1
73	1,0	723	78,3	73,0
74	1,0	733	44,6	88,5
75	1,0	743	49,5	85,5
76	1,0	753	48,9	73,9
77	1,0	763	76,5	53,1
78	1,0	773	71,0	90,6
79	1,0	783	51,3	87,3
80	1,0	793	32,2	74,0
81	1,0	803	57,5	48,2
82	1,0	813	65,2	55,2
83	1,0	823	49,6	59,7
84	1,0	833	56,5	85,0
85	1,0	843	54,1	86,5
86	1,0	853	31,2	82,7
87	1,0	863	34,5	81,8
88	1,0	873	69,0	68,2
89	1,0	883	84,9	57,5
90	1,0	893	85,5	76,4
91	1,0	903	88,2	68,7
92	1,0	913	78,6	59,2
93	1,0	923	82,2	83,7
94	1,0	933	79,6	73,1
95	1,0	943	74,5	84,1
96	1,0	953	73,1	69,3
97	1,0	963	77,2	70,5
98	1,0	973	84,6	81,2
99	1,0	983	80,0	
100	1,0	993	82,8	
101	1,0	1003	89,2	
102	1,0	1013	85,6	
103	1,0	1023	87,3	
104	1,0	1033	81,9	
105	1,0	1043	71,6	
106	1,0	1053	61,6	
107	1,0	1063	68,9	
108	1,0	1073	68,6	
109	1,0	1083	74,4	
110	1,0	1093	70,0	
111	1,0	1103	68,9	
112	1,0	1113	74,8	

113	1,0	1123	69,6
114	1,0	1133	66,1
115	1,0	1143	74,4
116	1,0	1153	82,0
117	1,0	1163	85,0
118	1,0	1173	73,0
119	1,0	1183	80,6
120	1,0	1193	85,1
121	1,0	1203	82,9
122	1,0	1213	91,5
123	1,0	1223	79,5
124	1,0	1233	91,9
125	1,0	1243	81,9
126	1,0	1253	78,4
127	1,0	1263	81,1
128	1,0	1273	82,3
129	1,0	1283	82,1

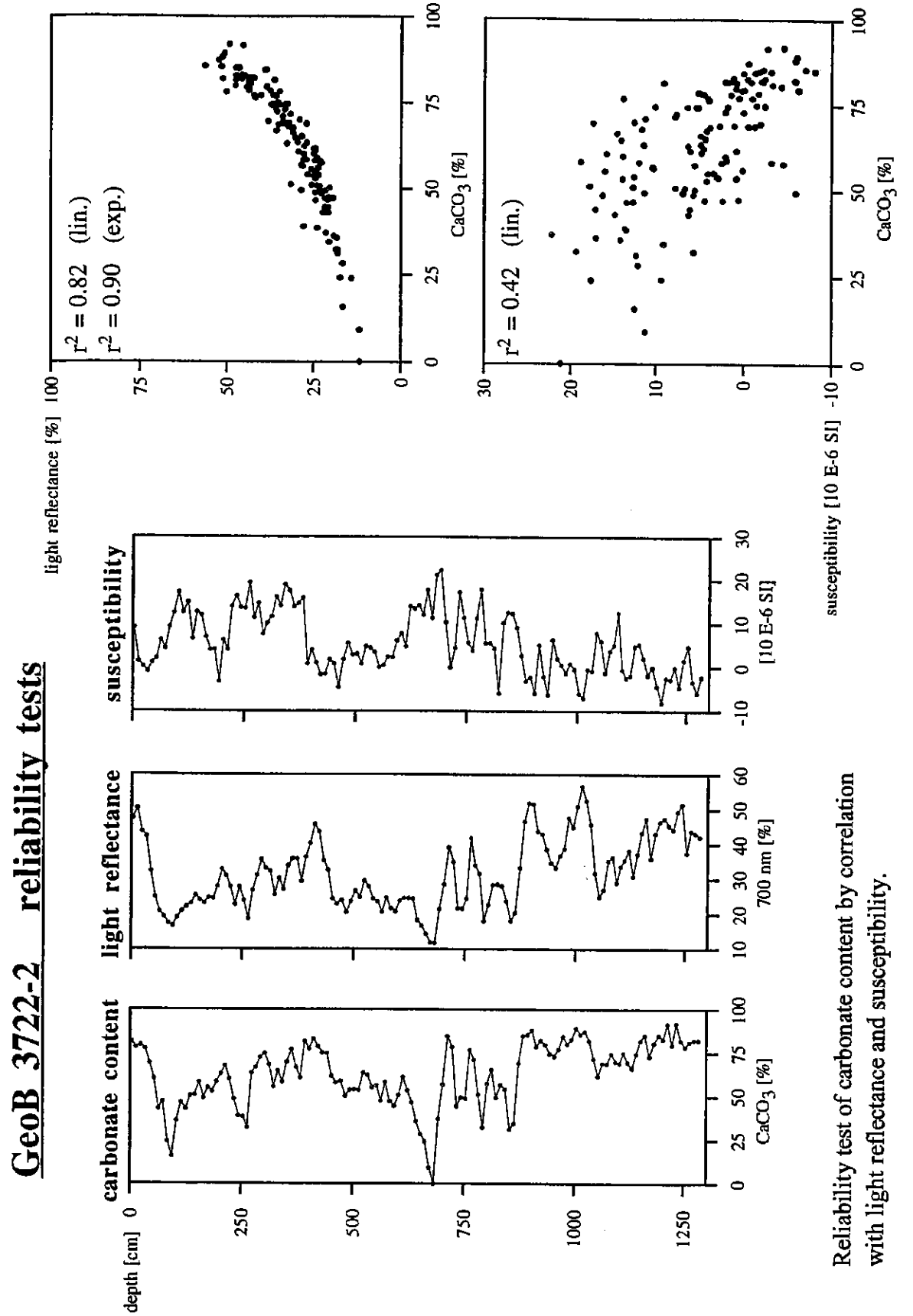

Fig. 186: Reliability test of carbonate content by correlation with light reflectance and susceptibility.

GeoB 3813-3 reliability tests

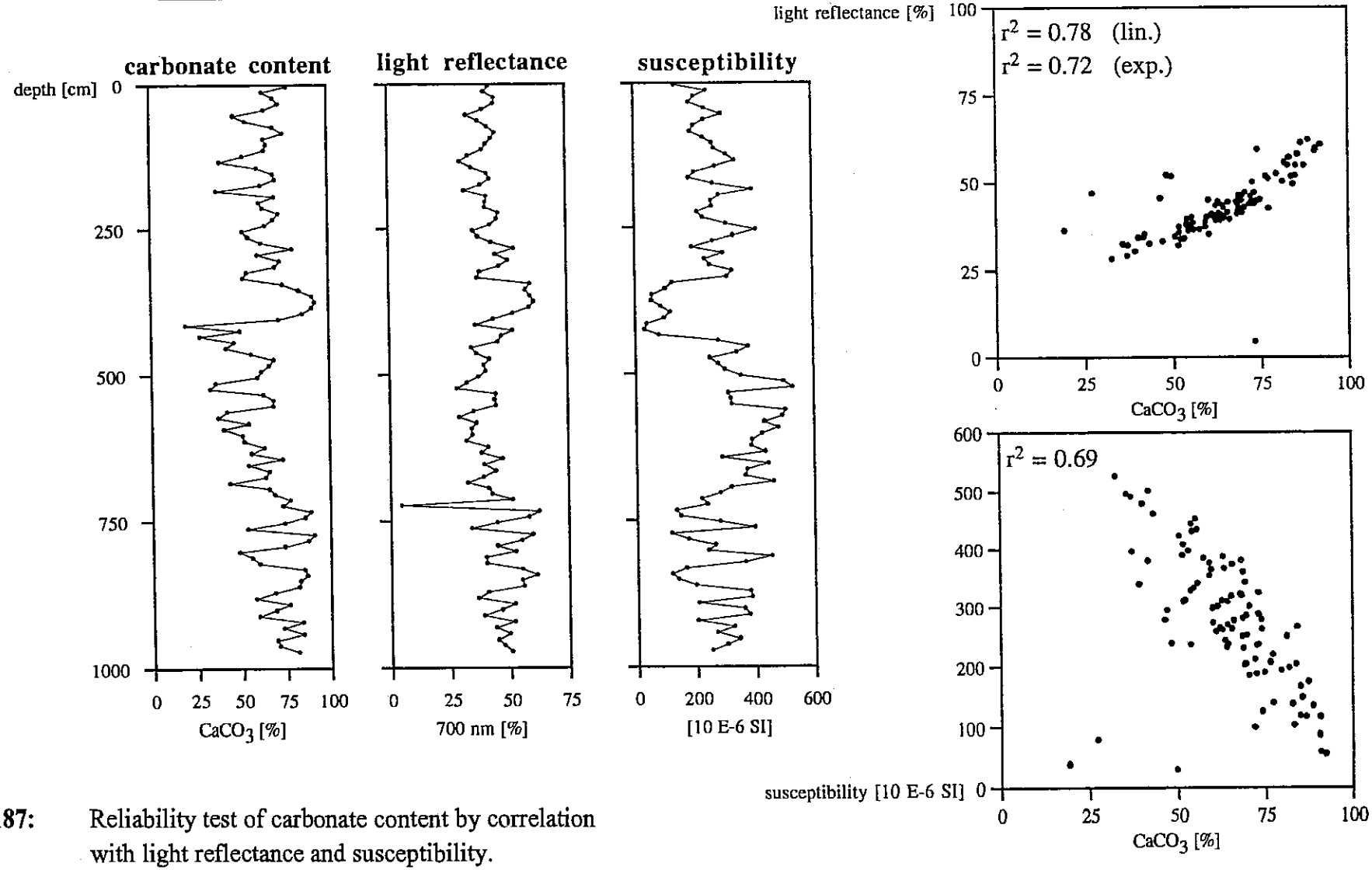

Fig. 187: Reliability test of carbonate content by correlation with light reflectance and susceptibility.

5.3.7.6 Clay Mineral Investigations

(F. Gingele)

Samples for clay mineral investigations were taken from 10 multicorer tubes and 4 gravity cores (chapter 7.3.1). Two main lines of investigations are intended. Clay mineral assemblages, esp. the kaolinite/chlorite ratio have proved to be sensitive proxies for the past fluctuation of water masses (PETSCHICK et al., 1996 DIEKMANN et al., 1996). Kaolinite is injected into the deep ocean at low latitudes and advected south with North Atlantic Deep Water (NADW), while chlorite reaches low latitudes with water masses of southern origin. Investigations in the eastern South Atlantic have shown a glacial/interglacial pattern of kaolinite/chlorite ratios, which is related to fluctuating deep water masses (DIEKMANN et al., 1996) NADW and AABW (Antarctic Bottom Water). However, the main pathway of AABW is through the Argentine and Brazil Basins in the western Atlantic. Gravity cores taken during this cruise will extend the clay mineral records to the area west of the Midatlantic Ridge. They will also stretch the time scale for these records - based on preliminary stratigraphy - beyond the Brunhes-Matuyama boundary.

The second goal is to investigate the influence of the Midatlantic Ridge on the clay mineral suite. Previous workers (e.g. BISCAYE 1965) have shown exceptionally high smectite contents near the Midatlantic Ridge fostering speculations of authigenic formation of this mineral. Cores from the equatorial sector of the Ridge reveal an absolute smectite minima in the upper 0.5 m of the sediment (GINGELE, 1992), indicating neoformation deeper in the sedimentary column.

Sediment core 3808-5 near the crest of the Midatlantic Ridge was taken for early diagenetic investigations. With the help of the geochemistry group pore water was extracted and partly analyzed on board. Cations will be analysed later at Bremen University. This data will allow the calculation of saturation indices and give information on the possible formation of alumosilicates. Solid-phase analyses will include standard X-ray measurements of the clay fraction, the separation and analysis of an ultrafine fraction (<0,2µm) and TEM-scans. Multicorer material will be treated accordingly. The results will hopefully contribute towards a better evaluation of the clay mineral signal as a paleoceanographic proxy.

Tab. 37: Gravity core sampling, METEOR cruise 34/3

GeoB No.	Water depth (m)	Recovery (cm)	Sedimentology Corg	Foraminifera	Paleomagnetics	Pore water	Smearslides	Carbonate sedimentology
3801-6	4546	950	190	190	95	190	50	190
3802-1	3969	416	82	82	41	82	16	-
3803-2	4173	379	75	75	37	75	12	-
3804-1	3891	423	84	84	42	84	9	-
3805-3	3659	316	63	63	31	63	9	-

3806-1	3294	375	75	75	37	75	9	-
3807-3	2518	71	14	14	7	14	3	-
3808-5	3213	580	116	116	58	116	14	-
3808-6	3213	426	85	85	42	-	7	-
3809-2	3463	247	49	49	24	49	5	-
3810-1	3810	218	43	43	21	43	7	-
3811-2	4091	150	30	30	15	30		-
3812-1	4205	580	116	116	58	116	29	-
3813-3	4331	995	199	199	109	199	37	199
3814-6	4340	810	162	162	81	162	23	-
3822-3	4276	900	180	180	90	180	29	-
3823-1	4368	916	183	183	91	183	20	-
3825-2	4267	956	191	191	95	191	33	
3826-1	3991	684	136	136	68	136	21	-
3827-2	3845	802	160	160	80	160	18	-

5.3.8 Physical Properties Studies

(A. Schmidt, F. Schmieder, B. Laser, Th. Frederichs)

During METEOR cruise 34/3 the recovered gravity cores were subject to laboratory geophysical studies. A routine shipboard measurement of three physical parameters was carried out on the segmented sediment cores, comprising the determination of

- the compressional (P-) wave velocity v_p,
- the electric resistivity R_s, and
- the magnetic volume susceptibility κ.

These properties are closely related to the grain size, porosity and lithology of the sediments and provide high-resolution core logs (spacing 1 cm for P-wave velocity and magnetic volume susceptibility, 2 cm for electric resistivity) available prior to all other detailed investigations. In addition, oriented samples for later shore based paleo- and rockmagnetic studies were taken at intervals of 10 cm.

Physical Background and Experimental Techniques

The experimental setup for the shipboard measurements was basically identical to that of previous cruises. Therefore, the descriptions given here are kept brief. For a more detailed treatment of the experimental procedures we refer to WEFER et al. (1991) for R_s and to SCHULZ et al. (1991) for v_p.

P-wave velocity

The P-wave velocity v_p was derived from digitally processed ultrasonic transmission seismograms, which were recorded perpendicular to the core axis with a fully automated logging system. First arrivals are picked using a cross-correlation algorithm based on the 'zero-offset' signal of the piezoelectric wheel probes. In combination with a measure of the core diameter d the travel time of the first arrivals t lead to a P-wave velocity profile with an accuracy of 1 to 2 m/s.

$$v_p = (d - d_L) / (t - t_L)$$

where d_L is the thickness of the liner walls, t_L the travel time through the liner walls.

Following SCHULTHEISS and McPHAIL (1989), a temperature calibration of v_p is effected using the equation

$$v_{20} = v_T + 3 \cdot (20 - T)$$

where v_{20} is the P-wave velocity at 20°C and T the temperature (in °C) of the core segment when logged. Simultaneously, the maximum peak-to-peak amplitudes of the transmission seis

mograms are evaluated to estimate attenuation variations along the sediment core. P-wave profiles can be used for locating strong as well as fine-scale lithological changes, e.g. turbidite layers or gradual changes in the sand, silt or clay content.

Electric resistivity, porosity and density

The electric sediment resistivity R_s was determined using a handheld sensor with a miniaturized four-electrodes-in-line ('Wenner') configuration (electrode spacing: 4mm). A rectangular alternating current signal is fed to the sediment about 1 cm below the split core surface by the two outer electrodes. Assuming a homogeneously conducting medium, the potential difference at the inner two electrodes is directly proportional to the sediment resistivity R_s. A newly integrated fast resistance thermometer simultaneously provides data for a temperature correction.

According to the empirical ARCHIE's equation, the ratio of sediment resistivity R_s and pore water resistivity R_w may be approximated by a power function of porosity ϕ

$$R_S / R_W = k \cdot \phi^{-m}$$

Following a recommendation by BOYCE (1968), suitable for seawater saturated, clay rich sediments, values of 1.30 and 1.45 were used for the constants k and m. The calculated porosity ϕ is subsequently converted to wet bulk density ρ_{wet} using the equation (BOYCE, 1976)

$$\rho_{wet} = \phi \cdot \rho_f + (1 - \phi) \cdot \rho_m$$

with a pore water density ρ_f of 1030 kg/m^3 and a matrix density ρ_m of 2670 kg/m^3. For the sake of an unbiased uniform treatment of all cores, these empiric coefficients were not adapted to individual sediment lithologies at this stage. Nevertheless, at least relative density changes should be well documented.

Magnetic volume susceptibility

The magnetic volume susceptibility κ is defined by the equations

$$B = \mu_0 \cdot \mu_r \cdot H = \mu_0 \cdot (1 + \kappa) \cdot H = \mu_0 \cdot H + \mu_0 \cdot \kappa \cdot H = B_0 + M$$

with the magnetic induction B, the absolute/relative permeability $\mu_{0/r}$, the magnetising field H, the magnetic volume susceptibility κ and the volume magnetisation M. As can be seen from the third term, κ is a dimensionless physical quantity. It describes the amount to which a material is magnetised by an external magnetic field.

For marine sediments the magnetic susceptibility may vary from an absolute minimum value of around $-15 \cdot 10^{-6}$ (diamagnetic minerals such as pure calcite or quartz) to a maximum of

some $10.000 \cdot 10^{-6}$ for basaltic debris rich in (titano-) magnetite. In most cases κ is primarily determined by the concentration of ferrimagnetic minerals while paramagnetic minerals such as clays are of minor importance. High magnetic susceptibilities indicate a high lithogenic input/high iron (bio-) mineralisation or low carbonate/opal productivity and vice versa. This relation may serve for the mutual correlation of sedimentary sequences which were deposited under similar global or regional conditions.

The measuring equipment consists of a commercial Bartington M.S.2 susceptibility meter with a 125 mm loop sensor and a non-magnetic core conveyor system. Due to the sensor's size, its sensitive volume covers a core interval of about 8 cm. Consequently, sharp susceptibility changes in the sediment column will appear smoother in the κ core log and, e.g., thin layers such as ashes cannot appropriately be resolved by whole-core susceptibility measurement.

Shipboard Results

Sampling Sites and Recovery

During METEOR cruise 34/3 gravity coring was performed in four working areas. Profile A crossed the Mid Atlantic Ridge near 30° S. It startet at 8° W at the edge of the Angola Basin, and ended at 22° W. On this transect the Cores GeoB 3801-6 to GeoB 3813-3 were taken from water depths between 3200 and 4500 m. Core GeoB 3814-6 was recovered in the Hunter Channel at 4340 m, Cores GeoB 3822-3 and GeoB 3823-1 at the northern outlet of the Vema Channel at about 4300 m. Profile B, the fourth working area, started at DSDP Site 515 with station GeoB 3825 at 4259 m water depth. Two more stations, GeoB 3826 and GeoB 3827, at 3843 and 2624 m were located at the continental slope north of the Santos Plateau.

The core recovery was generally good, even under the difficult conditions on the Mid Atlantic Ridge core lengths from to 3 to 10 m were reached. A total of 20 sediment cores with a cumulative length of 110 m was investigated (upper part of Fig. 188). Additionally p-wave velocity and magnetic susceptibility of four cores from cruise M34/2 (GeoB 3721-3, GeoB 3722-3, GeoB 3723-1 and GeoB 3724-4) and electric resistivity of these and 14 more cores (cumulative length: ~120 m) from cruise M34/2, which were opened during M34/3, were measured. The results of these cores are presented in the cruise report of M34/2.

Initial Results

A compilation of the characteristic physical properties of all cores is given in the lower part of Figure 188. The dots mark the median values of compressional wave velocity, density and magnetic susceptibility for each core, the vertical bars denote their standard deviations. Each diagram is divided into four parts corresponding to the different working areas described above.

The average p-wave velocities and densities of the cores from the Mid Atlantic Ridge show an obvious connection with water depth. Both parameters increase steadily with decreasing water depth. The v_p values range from 1490 to 1510 m/s, while density values from 1575 to 1875 kg/m^3 were found. The extremely high density of GeoB 3817-3, which ranges from 1700 to 2020 kg/m^3, may be responsible for the small core recovery of only 61 cm at this site on the center of the ridge. For the other three working areas the p-wave velocity takes values around 1475 m/s, density values range between 1500 and 1550 kg/m^3.

In the western part of profile A the magnetic susceptibility shows a markable postive E-W trend. While the values in the eastern part stay on a constant level of approximately $80 \cdot 10^{-6}$ SI they increase west of 16° W, beginning with GeoB 3809-2 and reach $275 \cdot 10^{-6}$ SI in Core GeoB 3813-3. West of profile A the susceptibility values are generally higher ($300\text{-}400 \cdot 10^{-6}$ SI).

Physical property logs for the cores are shown in Figures 162 to 180 together with the core descriptions.

Mid Atlantic Ridge (Cores GeoB 3801-6 to 3813-3)

The cores of profile A consist mainly of nannofossil foraminiferal ooze. Core GeoB 3801-6 contains five foraminiferal ooze turbidite layers at 0.7, 1.65, 3.30, 5.20 and 5.35 m, which cause high v_p and ρ_{wet} values. Between 6.70 and 7.52 m a thick diatom ooze layer causes the highest v_p values (~1550 m/s) measured during cruise M34/3. A corresponding layer was detected in Core GeoB 3813-3 between 4.00 and 4.40 m. In Core GeoB 3801-6 this sediment type goes along with a very low magnetic susceptibility. In GeoB 3812-1 at 1.20 m and in GeoB 3813-3 at 6.70 m a foraminiferal sand produces typical high p-wave velocities and densities.

The magnetic susceptibility signals of all cores can be clearly correlated. Their variations show obvious similarities with climatic cycles. Chronostratigraphies can be obtained by correlating the susceptibility patterns to the high-resolution $\delta^{13}C$ record of ODP Site 806 (BICKERT et al., 1996). The results are presented in chapter 'Susceptibility stratigraphy'. The Milankovitch patterns are also reflected in the v_p and density records, which are positively correlated with each other and inversely with magnetic susceptibility.

Hunter Channel (Core GeoB 3814-6)

Nannofossil ooze containing some foraminifera is the main component of Core GeoB 3814-6. While the average p-wave velocity lies within the range of the cores from the Vema Channel and the continental slope, the susceptibility of this core delivered the highest values of all cores investigated during the cruise. This could be an effect of the corrosive Antarctic Bottom Water which strongly influences the sedimentation in this water depth (4340 m) and decreases the carbonate content. Between 3.80 and 3.89 m a foraminiferal ooze turbidite causes a distinct peak in p-wave velocity and density. Similar to the cores from the Mid Atlantic

Ridge the susceptibility signal of GeoB 3814-6 shows characteristic Milankovitch patterns which have been used for dating purposes (see chapter 'Susceptibility stratigraphy').

Northern outlet of Vema Channel (Cores GeoB 3822-3 and GeoB 3823-1)

Core GeoB 3822-3 consists mainly of diatom bearing nannofossil ooze. In a depth of 1.22 to 1.47 m a foraminiferal ooze turbidite is connected with extremely high v_p values. The same layer shows a strong minimum in the magnetic susceptibility signal. Various smaller peaks in p-wave velocity seem to be caused by thin layers of hard greenish concretions.

Continental slope north of the Santos Plateau (Cores GeoB 3825-2 up to GeoB 3827-2)

The principal constituents of all cores taken on this profile are nannofossile oozes. The peaks in the p-wave velocities of Core GeoB 3825-2 at 7.40, 8.75 and 8.80 m go along with hard layers and clayey concretions. In Core GeoB 3826-1 three turbidite layers at 2.14-2.22, 4.85 and 6.23-6.33 m cause peaks in the v_p and ρ_{wet} signal.

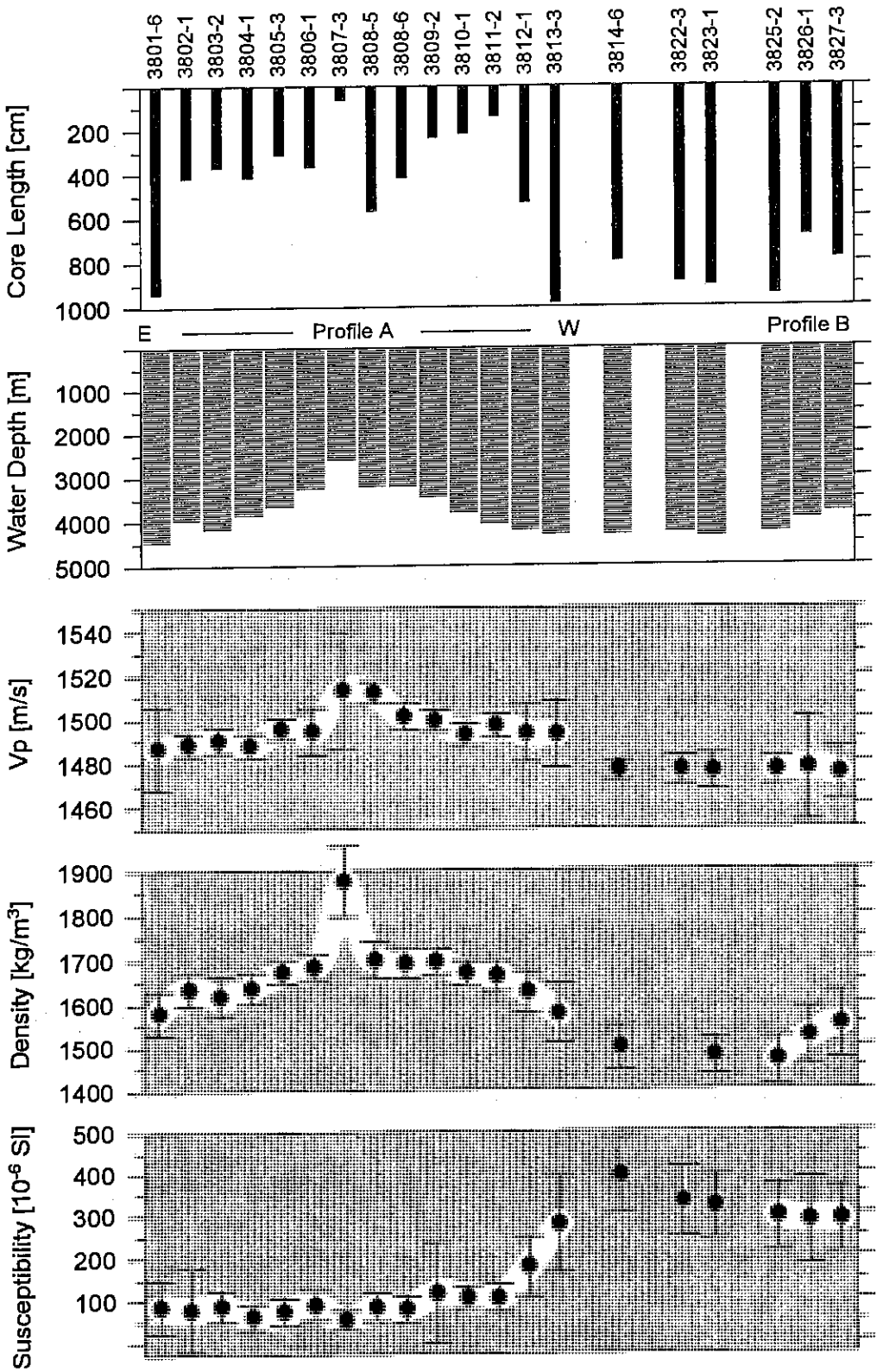

Fig. 188: Mean compressional wave velocity, density and magnetic susceptibility of gravity Cores GeoB 3801-6 up to GeoB 3827-2 as compared to variations in water depth at the sampling stations and core recovery. The vertical bars denote the standard deviations.

5.3.8.1 Susceptibiliy Stratigraphy

(F. Schmieder)

Method

Magnetic susceptibility records are often used to correlate sediment cores to other already dated cores. BICKERT and VON DOBENECK (1994) successfully used this method to establish on board chronostratigraphies for three cores of METEOR cruise 23/1.

The magnetic susceptibility of marine sediments premarily reflects the (titano-) magnetite content, which is mainly due to terrigenous input, volcanism and erosion of deep sea basalts (an important exception is bacterial magnetite). The susceptibility record often represents paleoclimatic variations of biogenic and lithogenic sediment accumulation rates (e.g. BLOEMENDAL and DE MENOCAL, 1989, PARK et al., 1993). This relation could be used to date several cores of METEOR cruise 34/3 on board by correlating their magnetic susceptibility data to the well dated $\delta^{13}C$ record of ODP Site 806 (BICKERT et al., 1996). The ages were determined without taking possible phase differences between $\delta^{13}C$ and magnetic susceptibility into account.

Results

The magnetic susceptibility signals of all cores of profile A can be clearly correlated. Their variations show obvious similarities with climatic cycles. In Core GeoB 3813-3, the longest of the cores from profile A, even the so-called Mid Pleistocene Revolution with its change in the dominant period from 41 to 100 ky is very well documented at about 5-6 m. This distinct paleoclimatic link made it possible to correlate the susceptibilty data to the high resolution $\delta^{13}C$ record of ODP Site 806 (BICKERT et al., 1996) to obtain a first chronostratigraphies for the cores. The correlation and the resulting age model for GeoB 3813-3 are shown in Figure 189. The correlation is strikingly good and yields for the diatom ooze layer between 6.70 and 7.90 m an age of 510-530 ka. The sedimentation rate of approximately 0.7 cm/ky is nearly constant over the whole core except for the diatom ooze layer, where it increases to 2 cm/ky.

Table 38 shows the ages of the core ends and average sedimentation rates for all cores from profile A and Core GeoB 3814-6 from the Hunter Channel based on a correlation of the susceptibility variations to the $\delta^{13}C$ record of ODP Site 806. The record of GeoB 3801-6 was correlated only down to a depth of 6.70 m (Fig. 190). The diatom ooze layer shows no characteristic susceptibility variations and the age of the sediments underlying this layer seems much higher than expected from a constant sedimentation rate. The distinct, nearly sinusoidal patterns which can be seen in Figure 162 b from 8.50 m to the core end are typical for sediments which are older than 1.2 Ma. Similar patterns are visible in Core GeoB 3813-3 below 8.80 m. For GeoB 3812-1 the correlation results in an age of about 800 ka in a depth of 4.45 m. In this core depth a peak in density seems to be related to a hiatus, because below 4.45 m correlation of the susceptibilty pattern yields an age of 930 to 1060 ka. Core GeoB 3807-3, which is only 61 cm long, is not represented in this Table.

Tab. 38: Age of the oldest sediments and average sedimentation rate for the cores of profile A (except GeoB 3807-3) and GeoB 3814-6 from the Hunter Channel based on a correlation of susceptibility variations with the high resolution $\delta^{13}C$ record of ODP Site 806 (BICKERT et al., 1996).*: see text for explanation

Core	Age of core ends [ka]	Average sedimentation rate [cm/ky]	Core	Age of core ends [ka]	Average sedimentation rate [cm/ky]
GeoB 3801-6	520*	1.3	GeoB 3808-6	380	1.0
GeoB 3802-1	400	1.0	GeoB 3809-2	280	0.8
GeoB 3803-2	400	1.0	GeoB 3810-1	240	0.9
GeoB 3804-1	400	1.0	GeoB 3811-2	200	0.7
GeoB 3805-3	320	0.9	GeoB 3812-1	1060*	0.6
GeoB 3806-1	380	0.9	GeoB 3813-3	1400	0.7
GeoB 3808-5	560	1.0	GeoB 3814-6	1500	0.5

Similar to the cores from profile A the susceptibility signal of GeoB 3814-6 from the Hunter Channel shows characteristic Milankovitch patterns. With an average sedimentation rate of only 0.5 cm/ky this core contains sediments over the past 1.5 Ma.

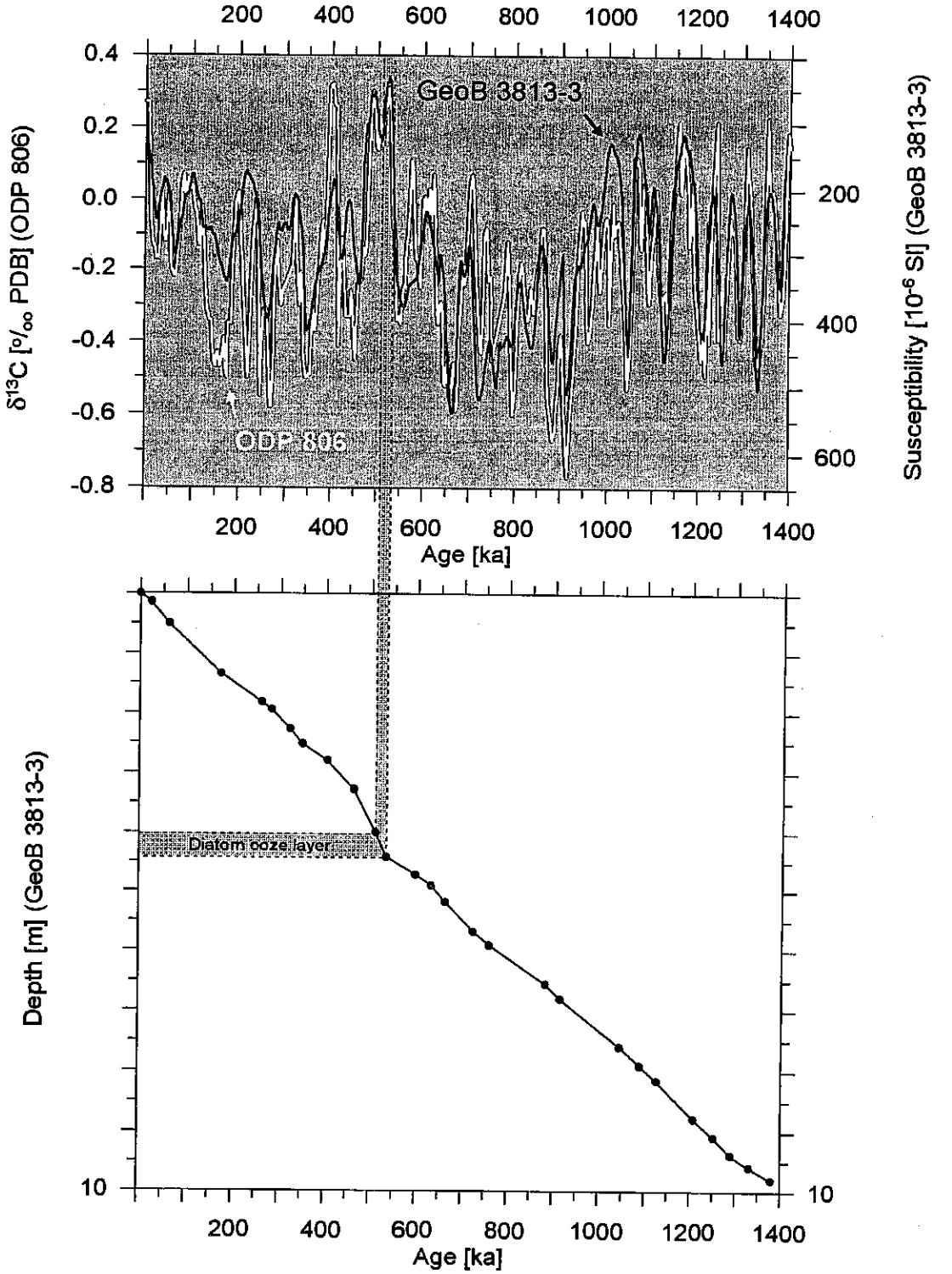

Fig. 189: The susceptibility variations of GeoB 3813-3 were correlated to the high resolution $\delta^{13}C$ record of ODP Site 806 (BICKERT et al., 1996). The resulting age model reveals a nearly constant sedimentation rate of approximately 0.7 cm/ky.

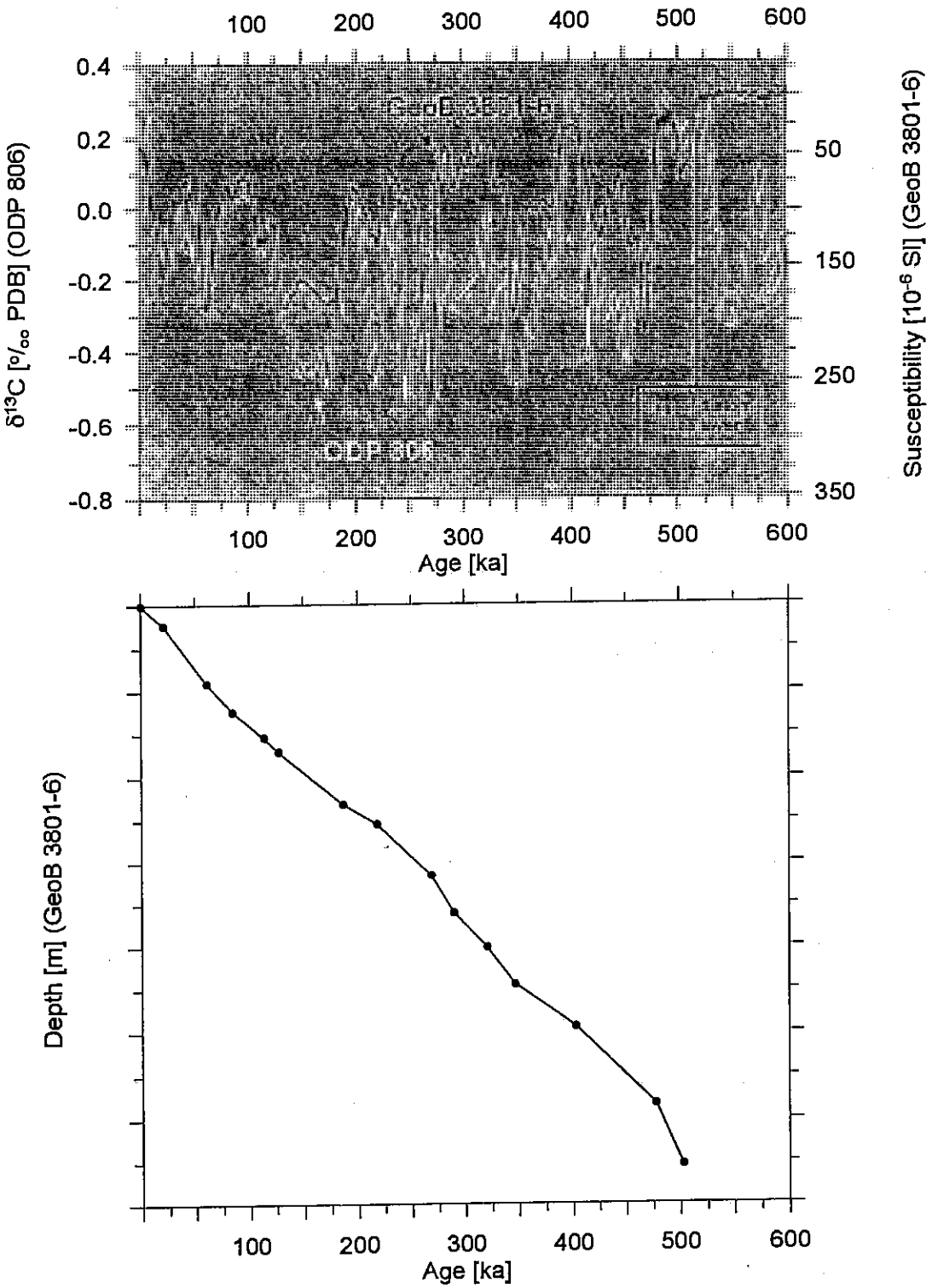

Fig. 190: The susceptibility variations of GeoB 3801-6 were correlated to the high resolution $\delta^{13}C$ record of ODP Site 806 (BICKERT et al., 1996). The resulting age model reveals a nearly constant sedimentation rate of approximately 1.3 cm/ky.

5.3.9 Pore Water Chemistry

(C. Niewöhner, E. Steinmetz)

The research studies of the marine geochemistry group focused mainly on two aspects during this cruise:

- Determination of the diffusive pore water fluxes and the geochemical processes at the sediment/water-interface in order to characterize and quantify the regional distribution patterns of the reaction products
- Determination of pore water concentration profiles for the investigation of early diagenetic mineralization processes

The main interest hereby is to gather geochemical data of the oxic sediments from multicorer-cores at the sampling sites along the profile across the Mid-Atlantic Ridge in order to enlarge the existing data point net. From these data calculations and modeling of the diffusive nutrients fluxes at the sediment/water-interface in regional dimensions will be carried out later on at the University of Bremen within the framework of the German JGOFS program. A gravity core from the Mid-Atlantic Ridge was examined to supplement the work of Franz Gingele (chapter 5.3.7.6) with pore water concentration profiles. Additionally, three multicorer-cores at sampling sites north of the Vema channel were geochemically analysed.

Experimental Methods

To prevent a warming of the sediments on board the MUC-cores were immediately placed in a cooling room after recovery and maintained at a temperature of 4-6°C. They were processed within a few hours. The gravity core was first cut into segments of 1 m length and processed during the following days. All work on opened cores was carried out in a glove box under argon atmosphere.

Immediately after recovery two samples of the overstanding bottom water were taken for oxygen determination by Winkler titration and two more samples for nutrients determination. The remaining bottom water was carefully removed with help of a siphon to avoid destruction of the sediment surface. During the subsequent cutting of the core into slices for pressure filtration, pH and Eh measurements were performed with a minimum resolution depth of 0.5 cm. On a second, parallel multicorer conductivity and temperature were measured to calculate sediment density and porosity. The gravity cores were cut lengthwise. On the working halves pH and Eh were determined and sediment samples were taken every 25 cm for pressure filtration. Conductivity and temperature were measured on the archive halves by the geophysical group. Samples for sequential extractions of the solid phase were taken every 20 cm and kept in gas-tight glass bottles under argon atmosphere. The storage temperature for all sediment samples was -20°C to avoid dissimilatory oxidation.

For pressure filtration Teflon- and PE-squeezers were used. The squeezers were operated with argon at a pressure gradually increasing up to 5 bar. Depending on the porosity and compressibility of the sediments, varying amounts of pore water volume could be gained. From the MUC-cores, consisting out of nannofossil oozes, could only poor volumes of approxi-

mately 5 ml be retrieved. From the gravity core up to 20 ml could be gained. The pore water was filtered through 0.2 µm cellulose acetate membrane filters.

The following parameters were measured within one day after sampling on this cruise:
pH, Eh, conductivity, temperature, O_2, NO_3^-, NH_4^+, PO_4^{3-}, alkalinity, Fe^{2+} (in some cases).

Bottom water O_2 concentration was determined by Winkler titration. pH, Eh, conductivity and temperature values were determined with electrodes before the sediment structure was disturbed by sampling for pressure filtration. Nitrate, ammonia and phosphate were measured photometrically by means of an autoanalyser using standard methods. Alkalinity was calculated from a volumetric analysis by titration of 1 ml sample with 0.01 M HCl. For the analysis of iron concentrations subsamples of 1 ml were taken within the glove box and immediately complexed with 50 µl of Ferrospectral and afterwards determined photometrically.

The remaining pore water samples were acidified with HNO_3 (suprapure) down to a pH value of 2 for storing and subsequent determination of cations by ICP-AES and AAS. All pore water samples will be maintained at 4°C until further treatment in Bremen.

Shipboard Results

At 8 out of 13 sampling sites along the E-W-profile across the Mid-Atlantic Ridge surface sediments could be recovered by the multicorer, which showed undisturbed surface and sediment layers for adequate geochemical determination. In addition a gravity core with a length of 5,80 m was taken at GeoB 3808. The results of the MUC-cores are shown in Figure 192-196 and the ones of the gravity core are displayed in Figure 197. At most sampling sites the oxygen concentrations of the bottom water were determined. The results show variations around 250 µmol/l O_2.

Three multicorer-cores were taken north of the Vema channel and also examined geochemically. The analysis results from one multicorer are displayed in Figure 198 as an example since their pore water concentration profiles are very similar. At the station GeoB 3822 north of the Vema Channel a gravity core with a length of 8,84 m was recovered out of a water depth of 4300 m. This core however was not processed for pore water profiles, but instead immediately frozen for investigations of the solid phase later on at the University of Bremen.

Along the E-W-profile across the Mid-Atlantic Ridge the eight multicorers have been recovered out of water depths between 4500 m (GeoB 3801, 3812) and 3200 m (GeoB 3808) on both sides of the center of the Ridge. The sediments at all locations were dominated by carbonate (nannofossil/foraminiferal) oozes and showed pale brownish colors. The pore water profiles of these fine grained sediments are typical for environments with very little input of organic matter and very low microbiological degradation (Fig. 192-196). The concentration profiles of mineralisations products (PO_4^{3-}, NH_4^+, alkalinity) show no increase along the sediment depth and the nutrients concentrations are very low compared to those of areas with high biological activities (see chapter 5.2). The phosphate, ammonia and alkalinity profiles

agree well with the results from the cruise M29/3 where a similar profile across the Mid-Atlantic Ridge (an equatorial transect) had been examined. The nitrate profiles (Fig. 195) display no distinctive maxima within the analysed 6 to 20 cm. This observation leads to the conclusion that the oxygen penetration depth is not reached in these surface sediments which fits well with the postulated low degradable organic matter input.

The pore water concentrations profiles of the gravity core GeoB 3808-5 (Fig. 197) support the interpretation derived from the above mentioned multicorer samples of the same profile. The Eh-profile shows increasing values along the whole sediment depth which points at a great oxygen penetration and denitrification depth, since usually decreasing values occur when oxygen and nitrate are consumed through the degradation of organic matter. The nitrate profile reveals that the zone of denitrification is not reached within the first 5,5 m of the sediment due to the very low microbiological activity. Moreover the phosphate and alkalinity profiles display no increase of the concentrations along the sediment depth and Fe^{2+}, which was measured in selected depths, could not be determined (ammonia was not analysed).

The MUC-core at the station GeoB 3825 north of the Vema channel was recovered out of a water depth of 4270 m. The sediment contained less carbonate oozes and more terrigenous material than on the sampling sites across the Mid-Atlantic Ridge. However the pore water profiles are similar concerning the concentration levels and the represented geochemical processes (Fig. 198). A nitrate maxima was not determined in the first 35 cm and the values show no increase along the depth. The phosphate and ammonia pore water profiles display a release of nutrients in the bottom water and a slight increase of their concentrations with increasing sediment depth. Diffusive fluxes from greater depths are indicated by these small concentration gradients. The concentration levels of phosphate and ammonia however are very low, so that the rates of organic matter input and microbiological degradation at this sampling site have to be small.

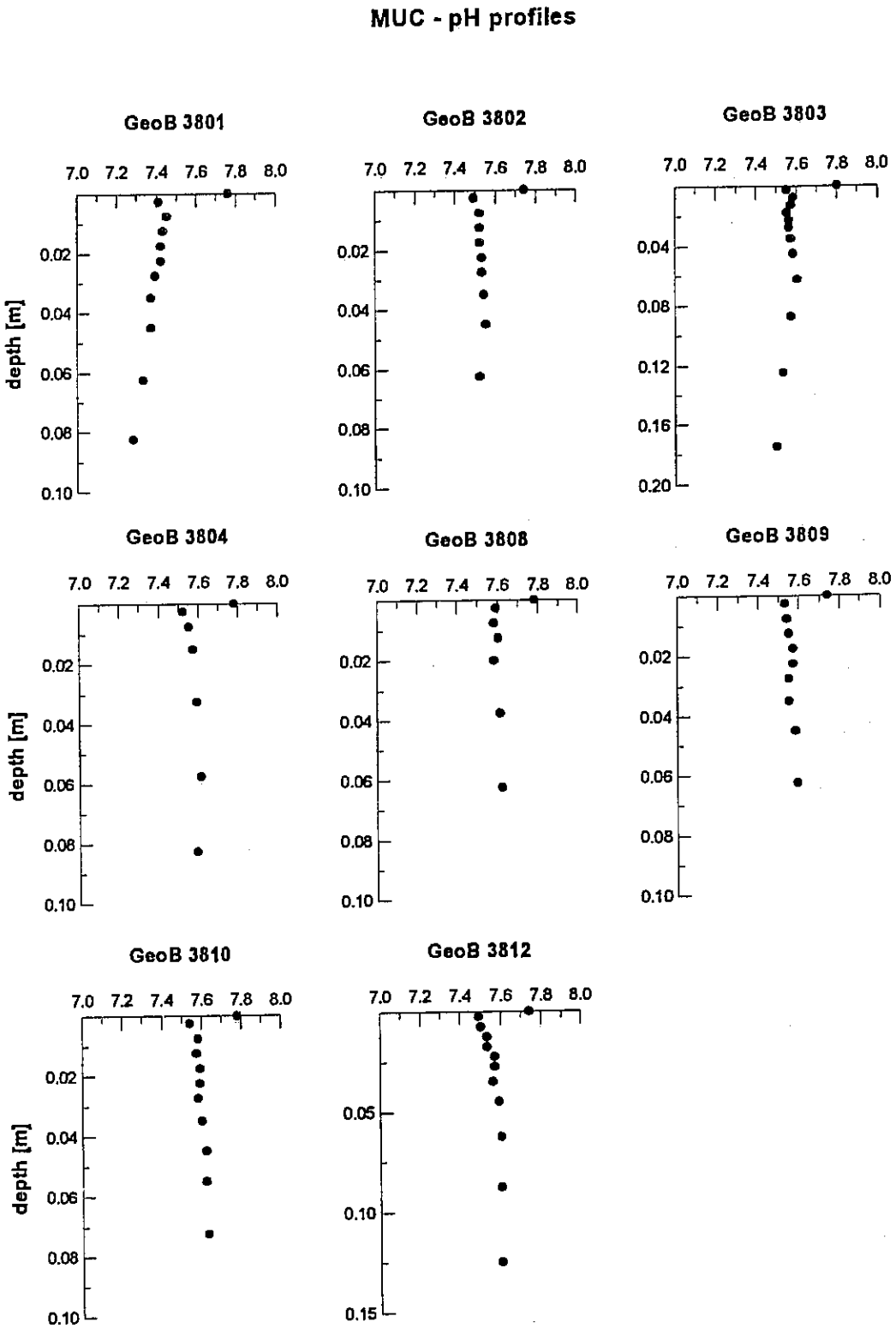

Fig. 191: ph profiles across the Mid-Atlantic Ridge (MUC).

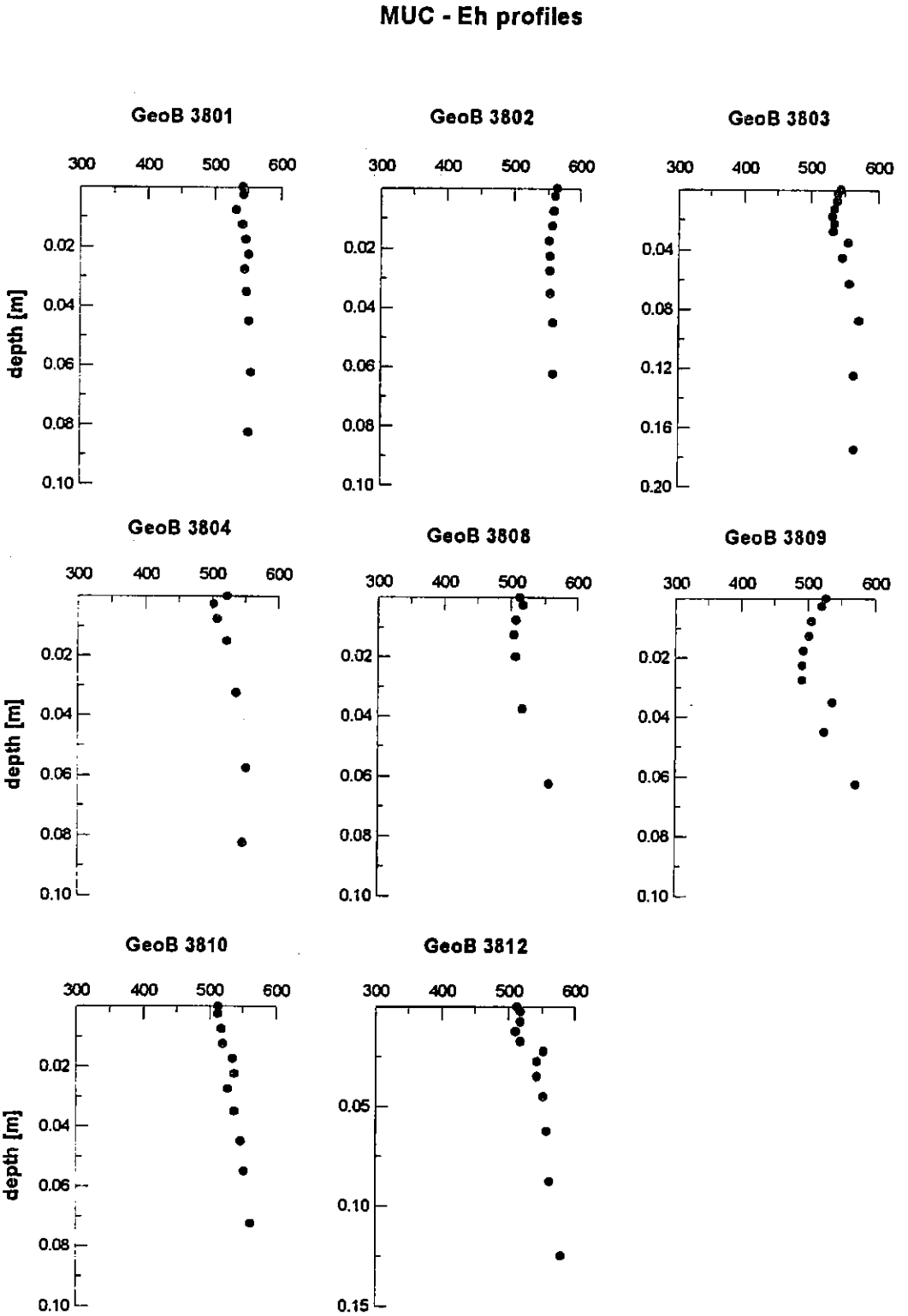

Fig. 192: Eh profiles across the Mid-Atlantic Ridge (MUC).

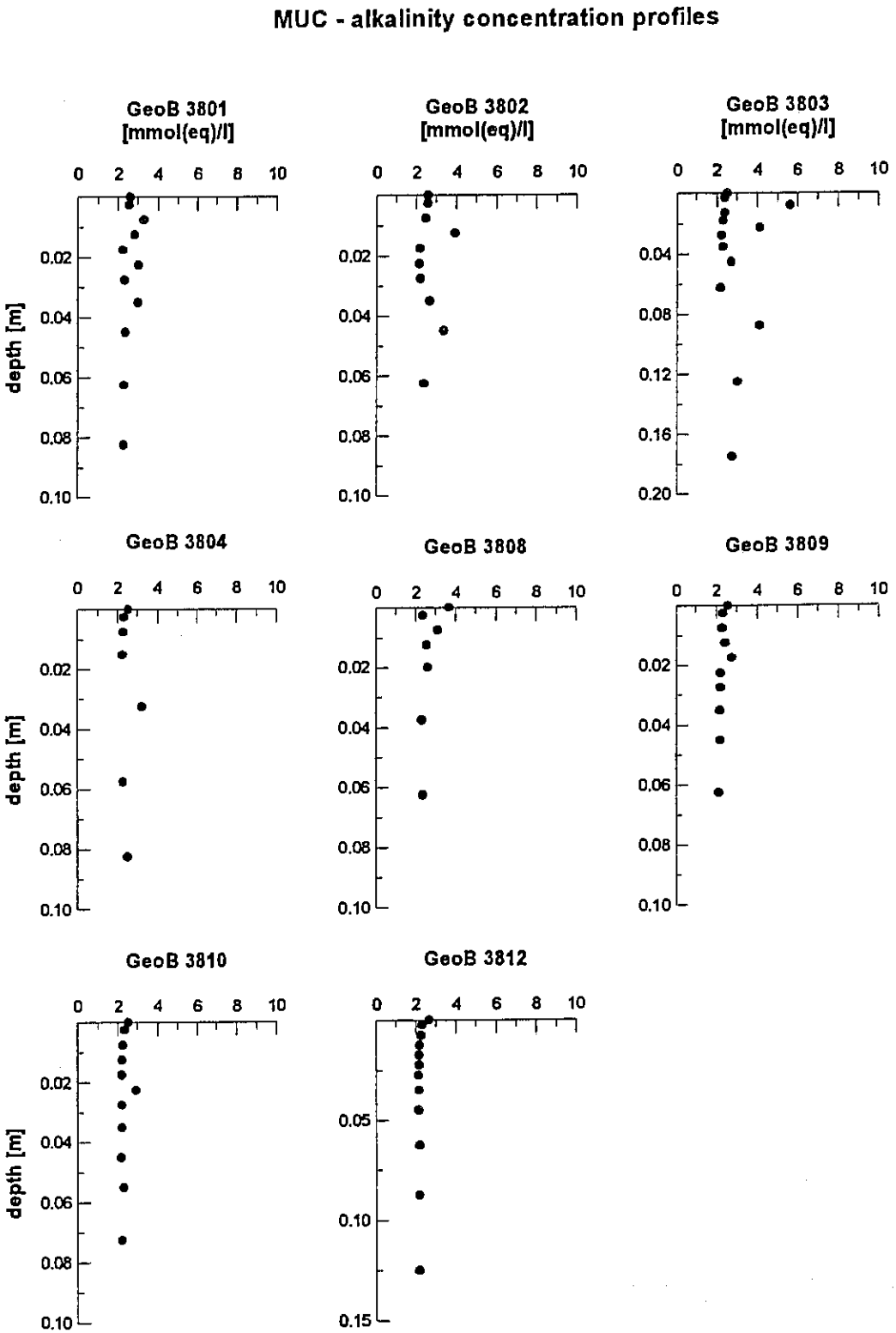

Fig. 193: Concentration profiles of alkalinity across the Mid-Atlantic Ridge (MUC).

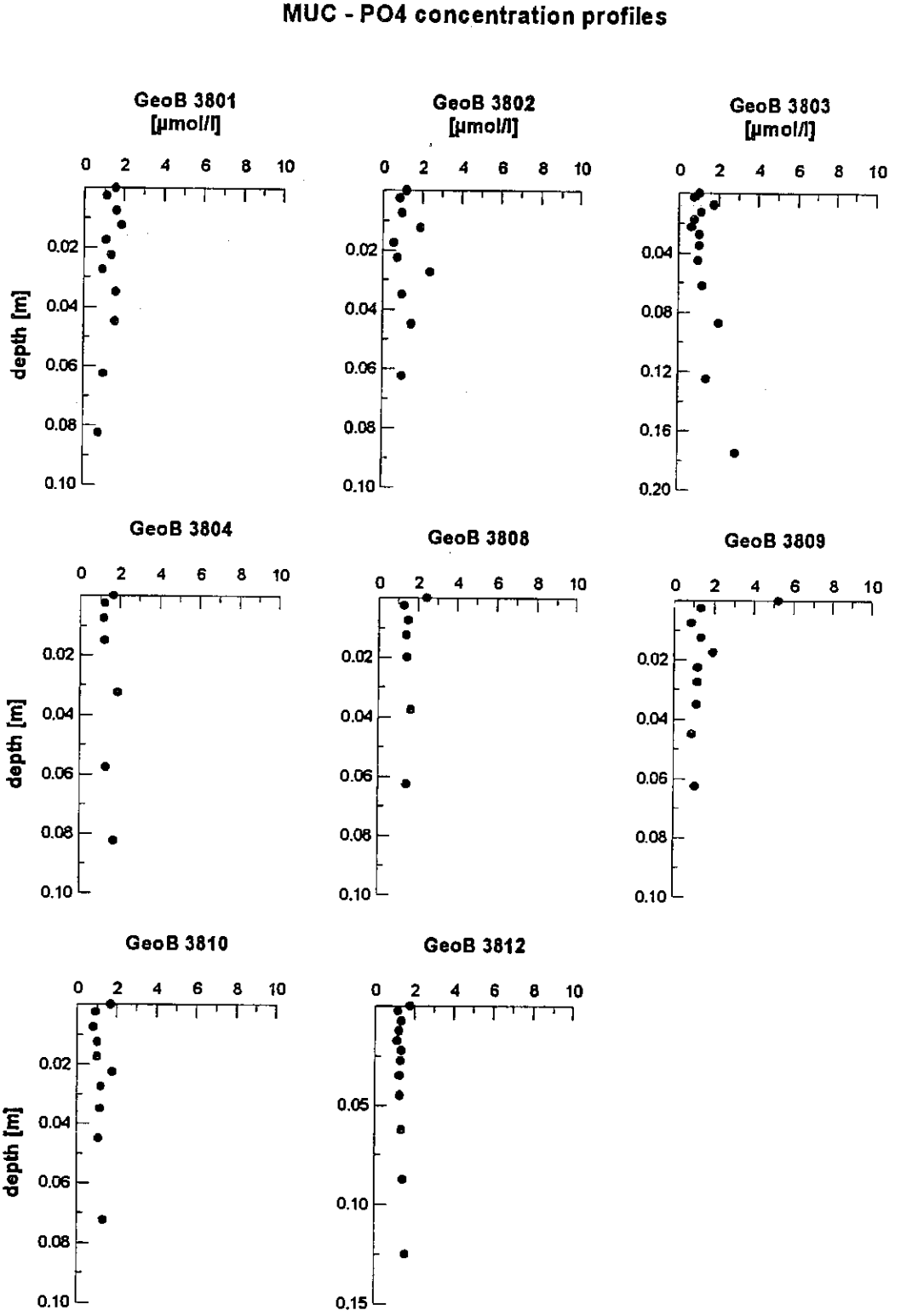

Fig. 194: Concentration profiles of PO_4 across the Mid-Atlantic Ridge (MUC).

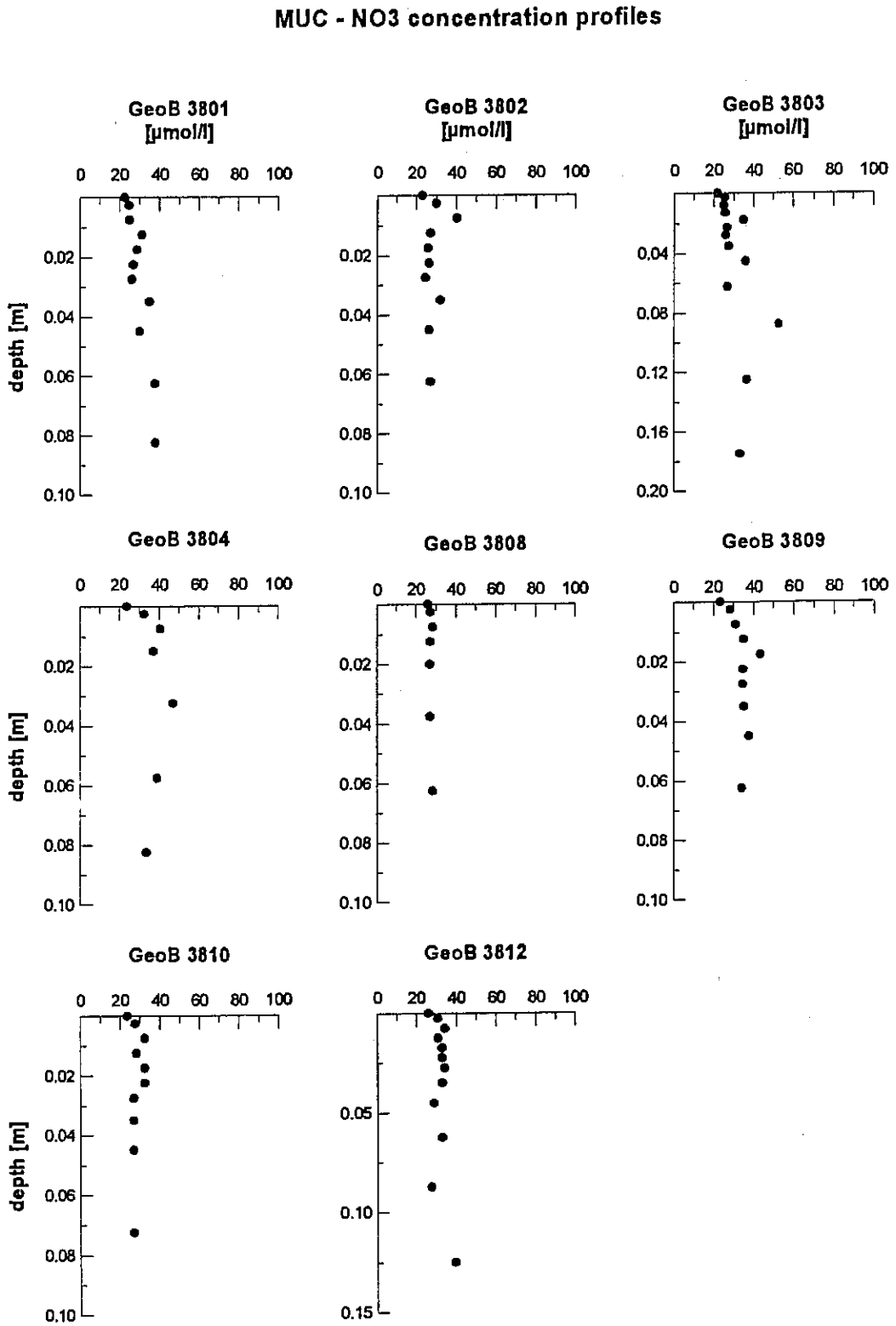

Fig. 195: Concentration profiles of NO_3 across the Mid-Atlantic Ridge (MUC).

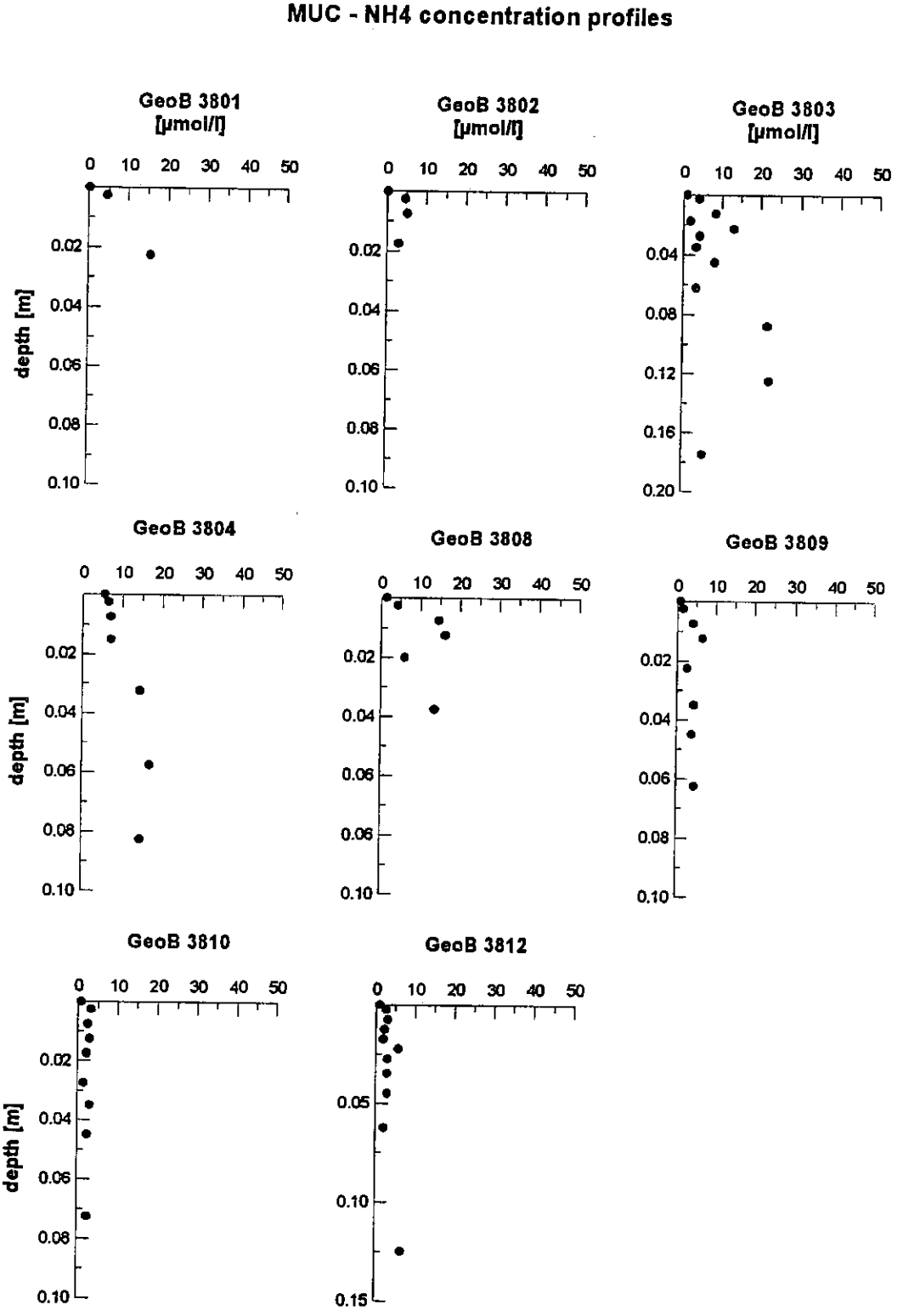

Fig. 196: Concentration profiles of NH_4 across the Mid-Atlantic Ridge (MUC).

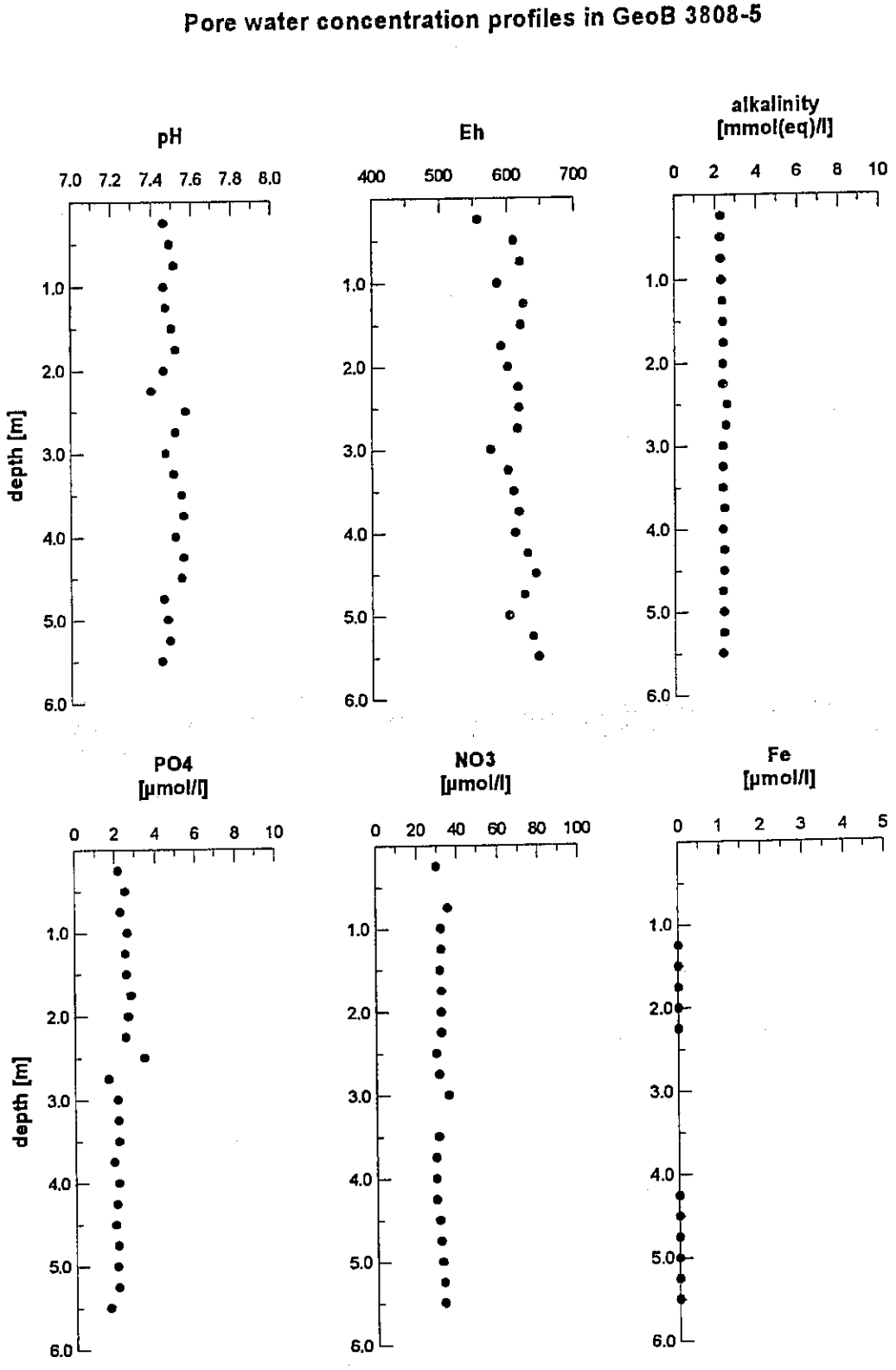

Fig. 197: Pore water concentration profiles in gravity core GeoB 3808-5.

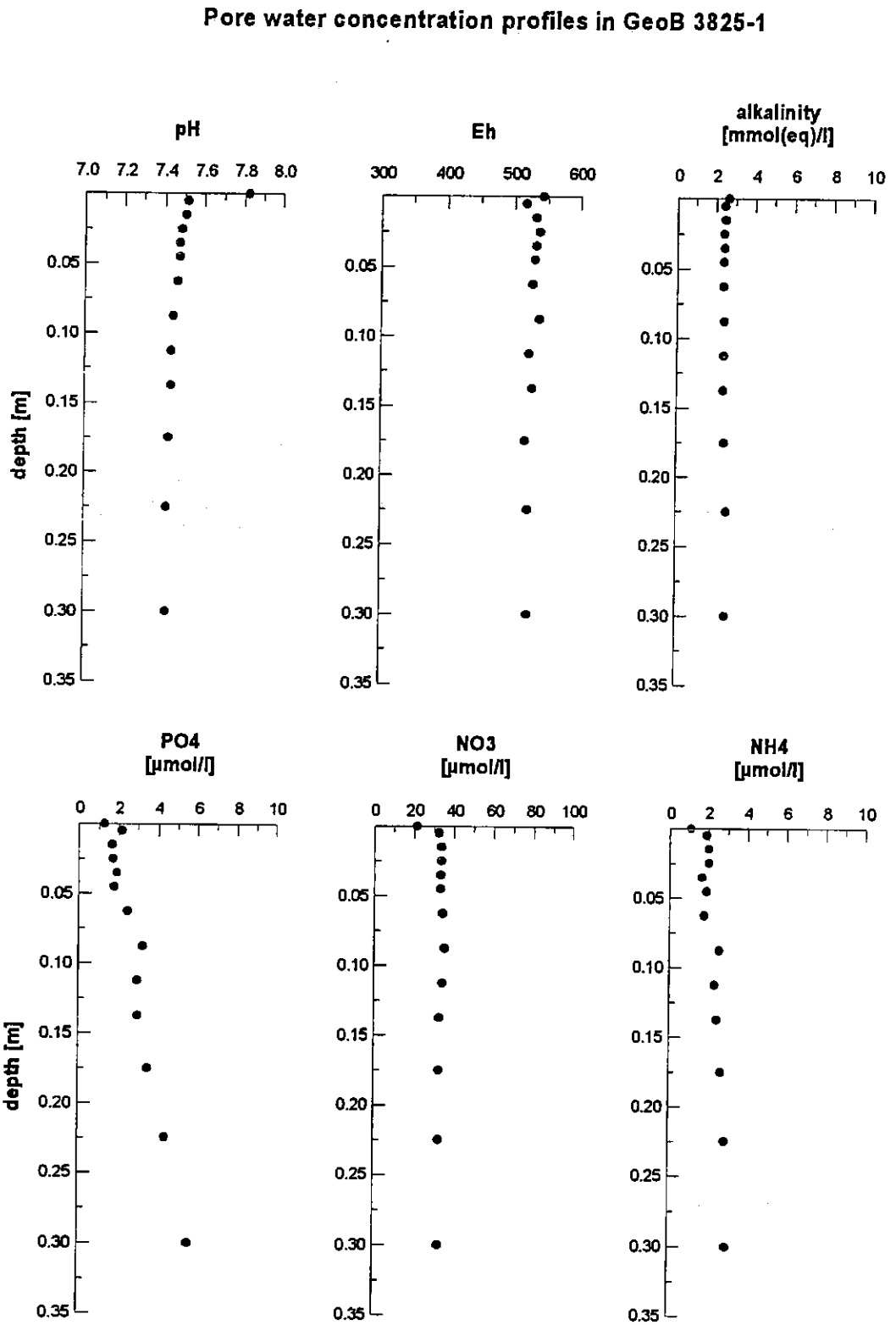

Fig. 198: Pore water concentration profiles in core GeoB 3825-1 (MUC).

5.3.10 Underway Geophysics

(B.Laser, A. Schmidt, F. Schmieder and Shipboard Scientific Party)

Introduction

During METEOR cruise M34/3 the shipboard acoustical systems HYDROSWEEP and PARASOUND were used on a 24 hour schedule to record continuous high resolution bathymetric and sediment echosounding profiles. The digitization and storage of the echosounding seismograms were realized by usage of the software package PARADIGMA (SPIEß, 1992).

The underway geophysical program along several profiles on the Namibian continental margin, the Namibia Abyssal Plain, Walvis Ridge, the Mid-Atlantic Ridge, Hunter Channel, Rio Grande Rise, Vema Channel and finally the continental margin off Brazil serves the long term research program Sonderforschungsbereich 261, the complete coverage of the South Atlantic Ocean with a net of sampling stations and geophysical profiles. Along the profiles the recorded data provided valuable information for finding suitable coring stations from different sedimental environments of the Mid-Atlantic Ridge, Hunter and Vema channel and the south american continental margin, which can be well discriminated by their different echotypes.

Recording Parameters and Preliminary Data Processing

The shipboard sediment echosounder PARASOUND and the multibeam echosounder HYDROSWEEP were operated by the scientific crew during a 24 hour watch. Both systems worked without severe technical problems.

The new registration and recording system HYDROMAP ONLINE (STN-Atlas-Elektronik,1994) which was installed on RV METEOR in December, 1996, allowed an increased online control of the swath-data quality by permitting the display of several different survey datasets at time in a windowed screen layout. Rough sea bottom topography, like found at the Mid-Atlantic Ridge, caused problems to the system. Some profiles in such areas suffer from a poor coverage of the bottom topography. The raw data recording was continuously performed.

The multibeam sounder provides bathymetric data with a swath width of twice the water depth and, in combination with the sediment echosounder PARASOUND, proved to be a very efficent aid for the selection of suitable coring stations. The precise knowledge of the local topography is essential to select suitable sites and to evaluate the impact of morphology, slope angles and sediment instabilities on the continuity of sedimentation.

The sediment echosounding data were routinely registered as analogue paper recordings with the DESO 25 device and in parallel digitally by means of the PARADIGMA 4.01 system (SPIEß, 1992). The data were stored directly on 6250 bpi, 1/2" magnetic tapes using the standard, industry-compatible SEGY-format.

The seismograms were sampled at 40 kHz with a typical registration length of 266 ms for a depth window of ~200 m. The source signal was a non bandlimited sinusoidal wavelet of 4 kHz dominant frequency with a duration of 2 periods.

A preprocessed profile plot plot was produced online with a vertical depth scale of several hundred meters to eliminate most of the changes in window depth. To improve the signal to noise ratio the seismogram sections were filterd with a wide bandpass filter of 1.5-10.0 kHz and with a secondary bandpass filter of 2.5-5.5 kHz. In addition the data were normalized to a constant value much smaller than the maximum average amplitude. In particular deeper and often weaker reflections could thereby be amplified. These plots provided a first impression of variations in sea floor morphology, sediment coverage and sediment patterns along the ships track.

To study the influence of frequency and length of source signal, these parameters were varied systematically at core sampling stations ('Source signal testi). The dominant signal frequency was increased in 0.5 kHz steps over the available range from 2.5-5.5 kHz while setting the number of sinusoidal pulses to 1, 2 and 4. Every setting was kept for about 2 minutes to enable later signal stacking. To quantify interference phenomena, seismograms recorded with different frequencies will be studied later in more detailed analyses. Furtheron the data of these tests will be compared with synthetic seismograms, which are calculated from the p-wave velocity and density measurements of the corresponding sediment cores.

Shipboard Results

During cruise METEOR M34/3 a profile of sediment cores was taken across the Mid-Atlantic Ridge at 30° S. Other cores were taken at the Hunter channel, north of the Vema channel and at the continental margin of South America following a profile from the DSDP drill site 515 upslope. These coring locations were found by the aid of the PARASOUND and HYDROSWEEP systems. The PARASOUND data provided information about the the physical state of the sea bottom as well as about sediment structures up to a depth of 50m below sea floor on this cruise. The penetration of the PARASOUND signal depends on the density of the uppermost sediment layers and the impedance contrasts between these layers and at the sea floor. Thus the penetration was used as a first hint for the quality of a coring location.

Since the limitation of the PARASOUND system to sea bottom slopes less than 6° profiles in ridge areas and fracture zones show a generally lesser quality. At the Mid-Atlantic Ridge signal penetration varied between a few meters and maximal ~30 meters. It was possible though to identify well-layered sediments in more even areas or in relatively small basins. In the eastmost part of the Rio Grande fracture zone, after crossing of the Walvis Ridge, we found sediment filled basins showing a signal penetration of up to ~80 m. These were parted by basement highs.

The sediments in the western work area, at Hunter and Vema channels, showed the influence of relatively strong currents. In the deep channels the reflection patterns of PARASOUND

indicate almost none or in a high degree sorted sediments. Mostly only a strong, elongated sea bottom reflector could be observed. On the eastern flank of Rio Grande Rise sediment waves were found in a water depth of ~4100 m.

The cruise M34/3 led the ship to extremly different sedimentary environments including ridges and fracture zones, deep sea basins and the strongly current influenced areas of Hunter and Vema channels. More than 12 Gbyte of data were recorded during the long steaming times between the work areas and during the search of suitable coring locations. The following examples are intended to give a short overwiew of the sediment structures which were found.

The first example was recorded at the Namibian continental rise from 23°35' S / 10° 16' E to 23°38' S / 9°59' E at a water depth of 4100 m (Fig. 199). The signal penetration varies heavily between ~10 m and 35 - 40 m. The lateral changes in penetration occur quite abrupt. These jumps are probably caused by a high free gas content in the sediment, which produces a high reflection coefficient on top and prevents further penetration of sound waves.

The sediments appear well layered though, in the void parts of the profile some of the stronger reflectors are still observable. Over the larger part of the profile the gas seems to be trapped by a sediment layer in ~10m. The lower continental slope in greater water depths off the Namibian coast and south of the Wavis Ridge is characterized by a smooth topography and parallel, well stratified sediment layers, indicating undisturbed sedimentation. The appearance of gas indicates a high content of organic matter and characterizes the source of the sediments as part of the high-production zone in the Namibian upwelling area.

On top of the Walvis Ridge are comparably hard and rich in carbon. Thus the penetration of the PARASOUND signal is limited to ~20m. Figure 200 shows an example of this sedimentation pattern from 24°20' S / 6°3' E to 24°25' S / 5°38' E. The water depth ranges from 1530 m to 1710 m. A layered structure of the sediments is observable, the density of the material must be comparatively high and prevents a higher penetration of the sound waves. The first five kilometers of the profile show a sequence of steps with a height of ~10m. These structures may be interpreted as faulted sediment blocks at the steeper slope.

The data recorded on the transit across the eastern part of the Rio Grande fracture zone suffer significantly from the very steep slopes observed in this area. However, north of the Walvis Ridge some small deep basins could be observed where well-layered sediments allowing a signal penetration of up to ~80 m. The sediments are draping the deeper topography and these basins are parted by steep, sudden basement highs. Figure 201 shows a part of the largest basin observed, the transect of the basin is ~70 km. At ~8 km through ~15 km profile length it can be observed how the sediment patern is spreded where basement throughs are filled. This leads to the generation of sediment lenses, here in ~10 m sub-bottom depth. The dominant comparatively transparent layer in 3m to 10m depth is observed in all profiles of this area and exceeds basin boundaries. At some spots it onlaps the deeper refections indicating a major

change in sedimentation with intermediate erosion. The profile shown is situated between 25°6' S / 1°48'E and 25°9'S / 1°35' E in a water depth of 5320 m.

The sediments found in the Mid-Atlantic Ridge area vary mainly with water depth. In greater depth the softer sediments are found and the signal penetration is higher. An example of a less steep topography is shown in Figure 202 between 30°26'S / 8°36'W and 30°45' S / 12°44'W ranging from 3780 m to 3940 m water depth. The less steep parts of the profile show layered sediments with a signal penetration of up to 30 m. A very distinct reflector can be seen in ~5m sub-bottom depth. The topography along this profile is parially masked by reflection hypebolae, caused by structures which are small against the footprint of the echosounder. This profile is taken from the vicinity of core site GeoB 3808.

Figure 203 shows a profile east of the Rio Grande Rise in a water depth of 4800 m between 33°56'S / 27°38'W and 34°2'S / 27°56'W. Well-layered sediments draping an erosional surface of older sediments can be seen. The layer thickness of the sediments varies intensively with the lower topography along the profile. An almost transparent layer between 5-10 and 8-16 m sub-bottom depth marks the change in sedimentation.

Sediment patterns at the western flank of the Hunter channel show a great variation in penetration and structure.

A part of the steep slope of Rio Grande Rise in this Area is given in Figure 204. It starts in ~2000 m water depth at 33°45'S / 30°20'W and rises until 1250m water depth at 33°40'S / 30°40'W. We observe less steep parts of the slope parted by abrupt steps of ~75 and ~125 m height. The sediment pattern and signal penetration vary intensively with water depth and slope angle. In the lowest part of the profile a strong elongated sea bottom reflector indicates hard, coarse grained sediments. This part is followed by an increase in slope angle and we observe possibly two small slumps of ~1 km size each. Further upslope the sediment pattern changes abruptly to a layered sediment wit a penetration of ~30 m. After the first step of ~75m height reflectors seem to be cut by erosion, followed by another change in patter. After the second step of ~125 m height the signal penetration reaches ~75 m with a still high slope angle. The thickness of the sediment layers observed here decreases quickly with decreasing water depth and increasing slope angle along the profile.

Mud waves are a prominent feature of the current controlled sedimentation around the Rio Grande Rise and north of Vema and Hunter channels. The first occurence of mud waves during cruise M34/3 was at the south-eastern flank of Rio Grande Rise at 33°1'S / 33°5'W. The profile shown in Figure 205 ranges from 4175 m water depth to 4050m water depth between 32°55'S / 33°25'W and 32°49'S / 33°47'W. The mud waves are symmetrical and vary in length and amplitude along the profile. Within the wave field even sections of the sea floor can be observed. In the upper part of the profile the mud waves seem to be superimposed on an also wavy underlying topography.

An example of migrating, non-symmetrical, mud waves is given in Figure 206. The profile is situated north of the Vema channel in ~4050 m water depth between 28°30'S / 38°51'W and 28°23'S / 38°40'W. Partially the migration of the waves crest is easily observable. The waves are irregular in length and height, seemingly they superimpose each other and grow together. The profile was taken at a slightly lower ship speed than the other examples while searching a coring site.

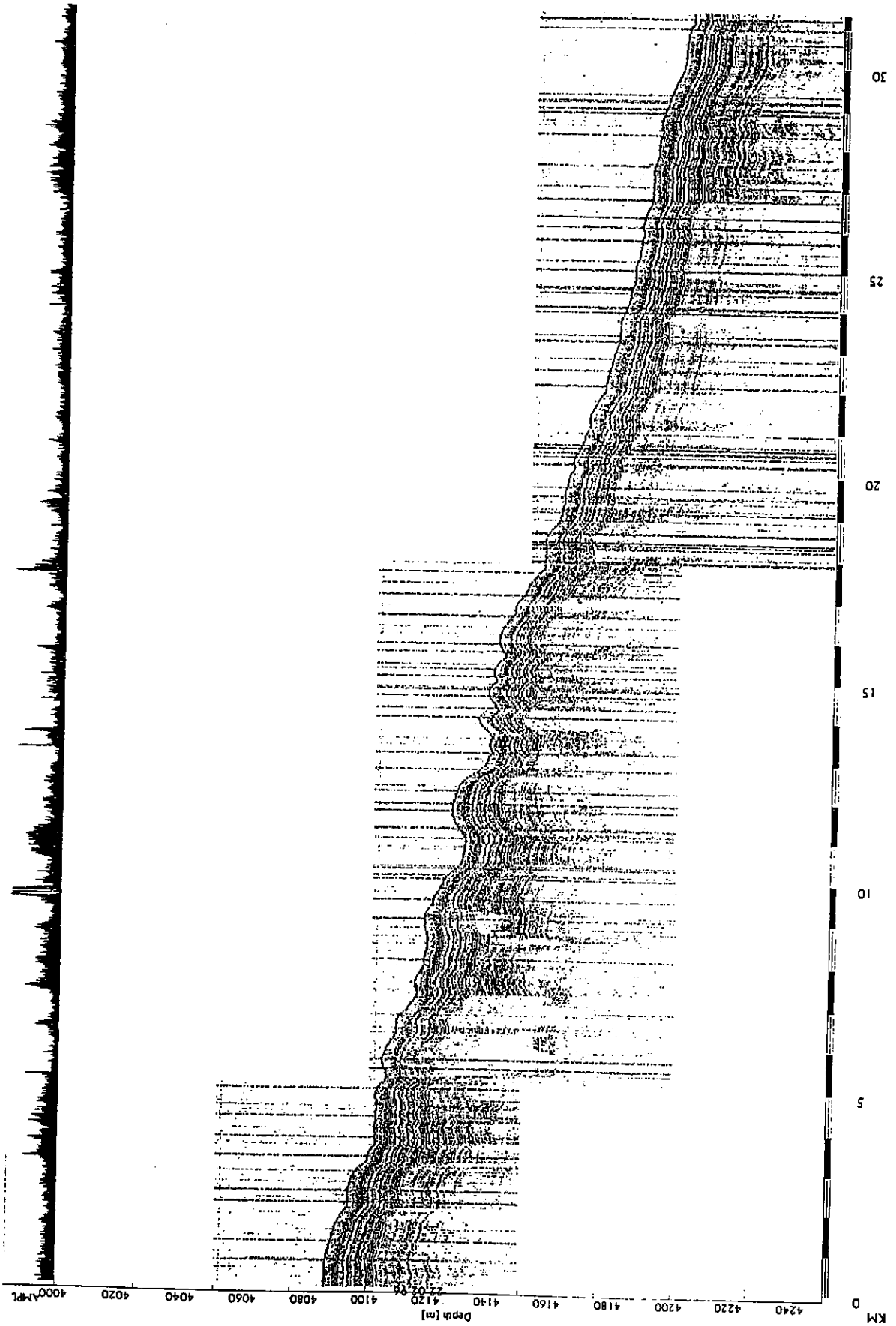

Fig. 199: Digital PARASOUND profile of the lower continental slope off Namibia. Profile length and geographical coordinates are annotated. For further details see text.

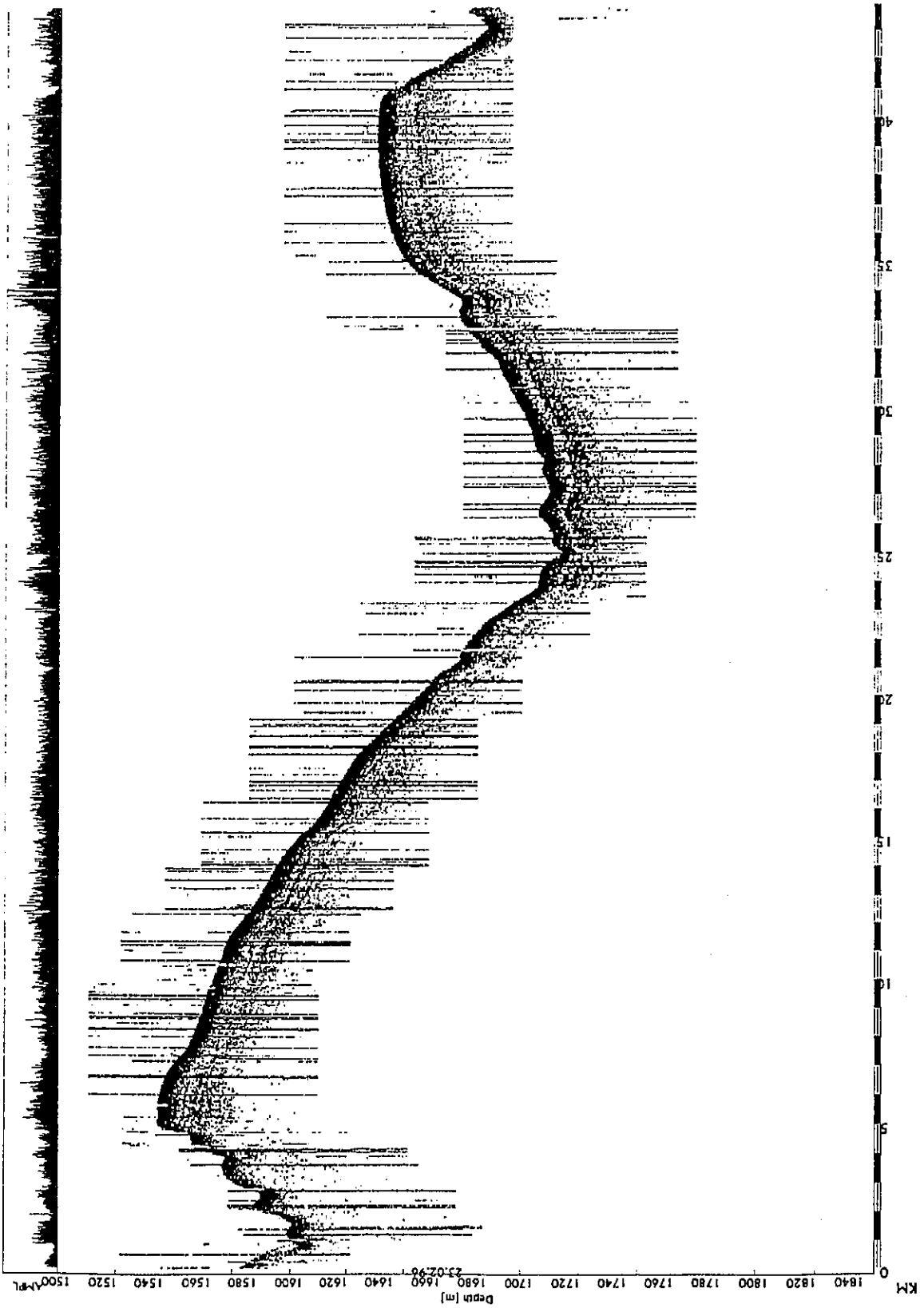

Fig. 200: Digital PARASOUND profile of the top of the Walvis Ridge. Profile length and geographical coordinates are annotated. For further details see text.

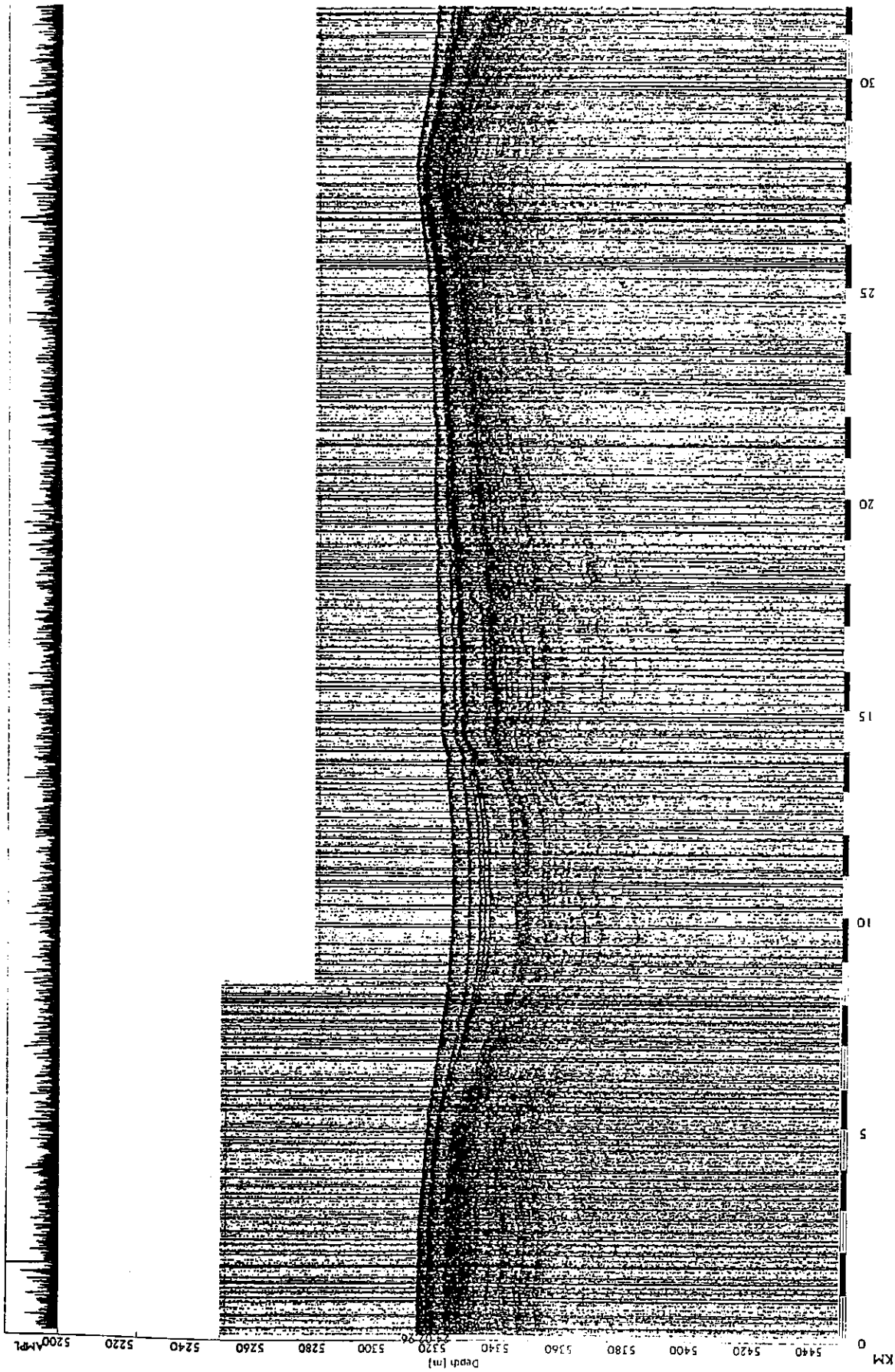

Fig. 201: Digital PARASOUND profile showing a sediment basin in the eastern Rio Grandefracture zone. Profile length and geographical co-ordinates are annotated. For further details see text.

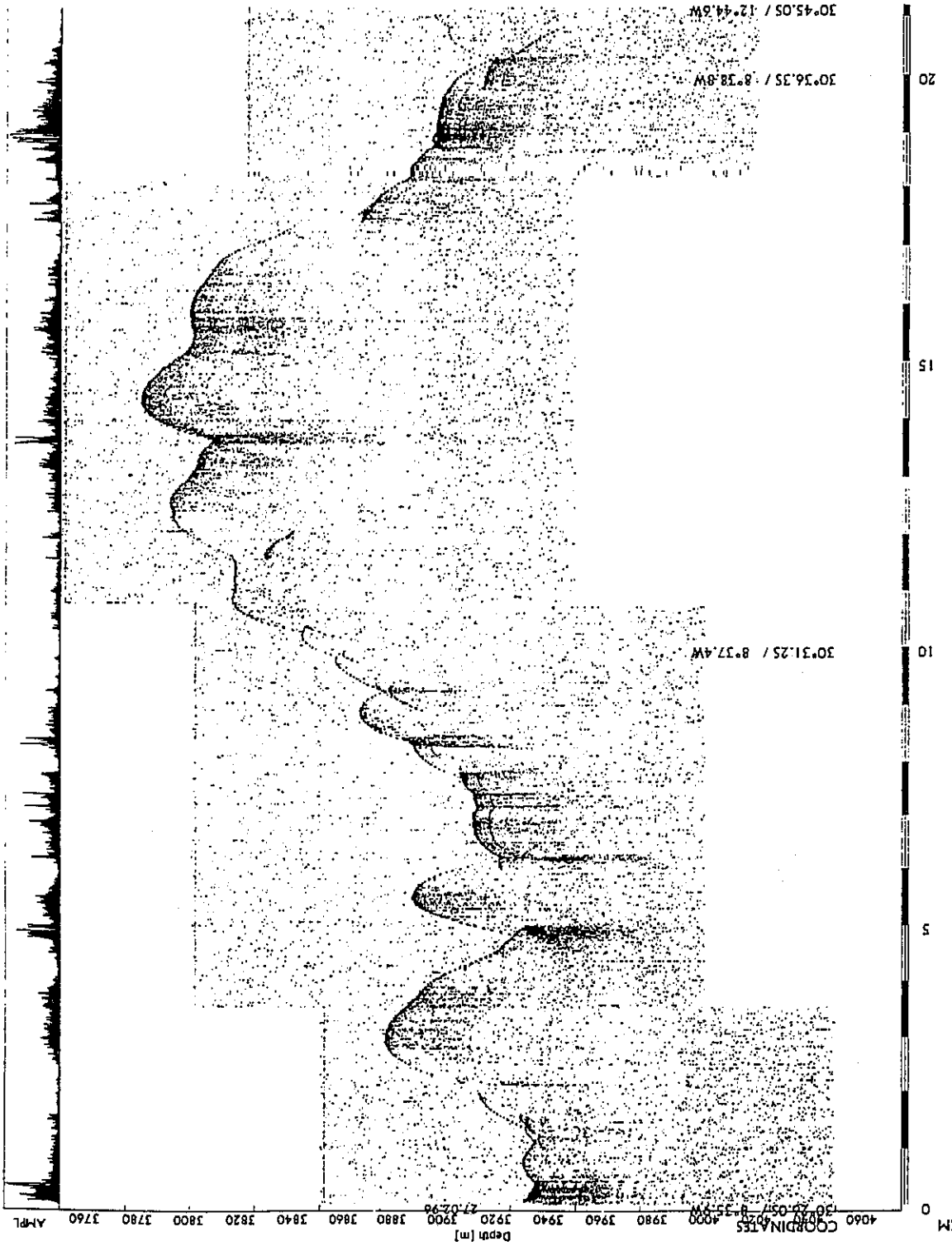

Fig. 202: Digital PARASOUND profile of the lower eastern flank of the mid-Atlantik Ridge. Profile length and geographical coordinates are annotated. For further details see text.

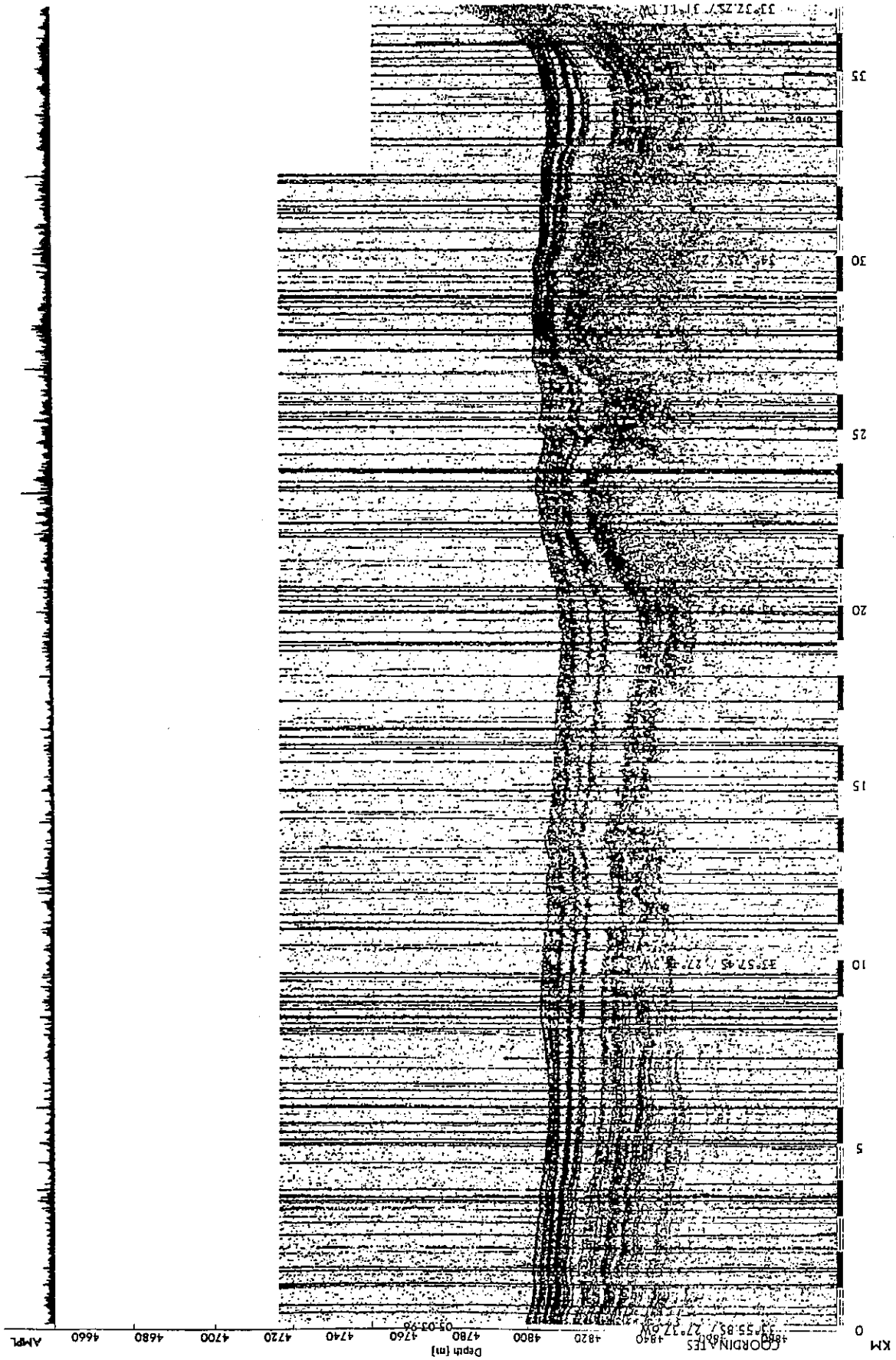

Fig. 203: Digital PARASOUND profile of deep-sea sediments at the eastern flank of Rio Grande Rise. Profile length and geographical coordinates are annotated. For further details see text.

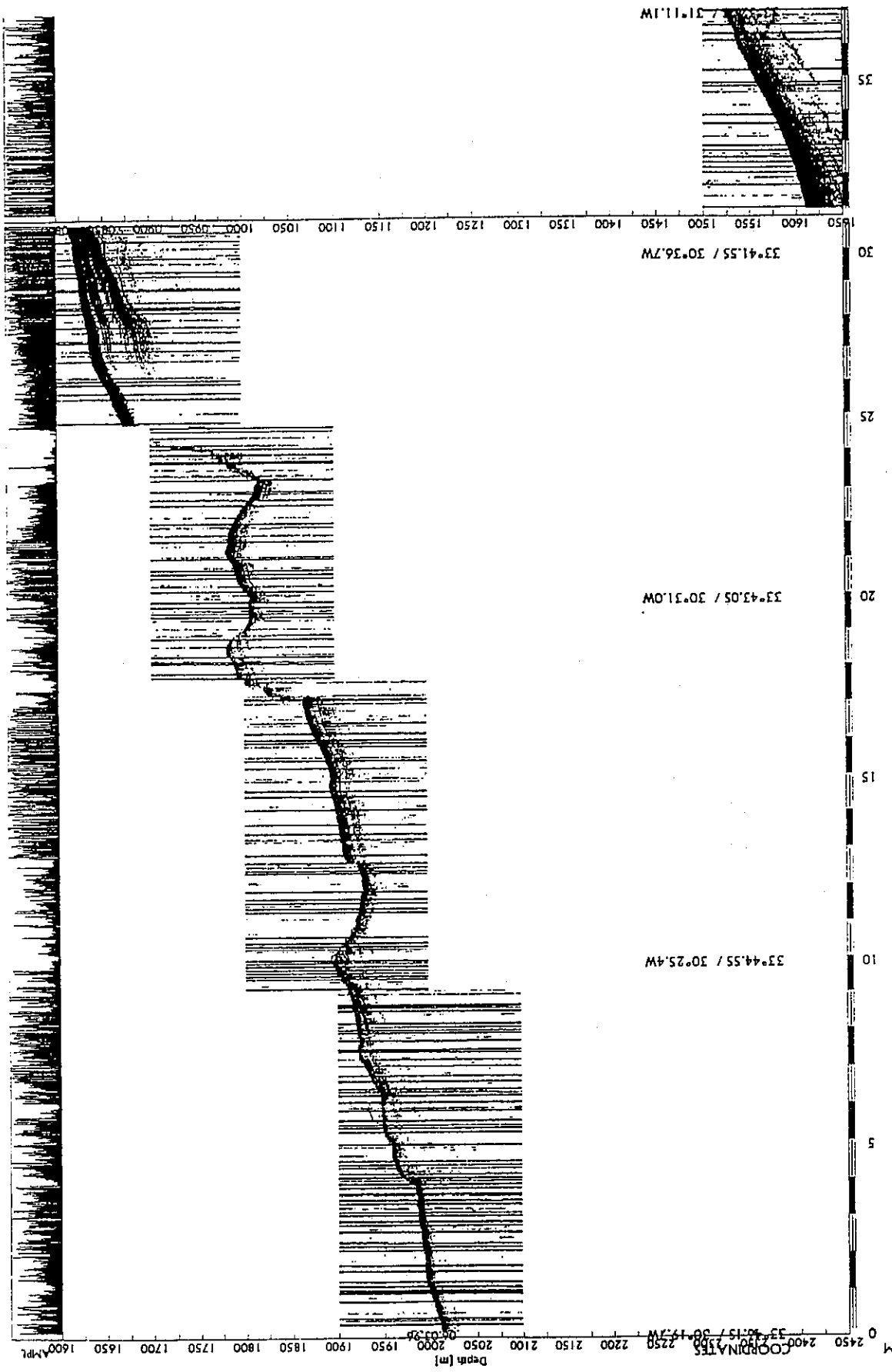

Fig. 204: Digital PARASOUND profile of the intermediate south-eastern flank of Rio Grande Rise. Profile length and geographical coordinates are annotated. For further details see text.

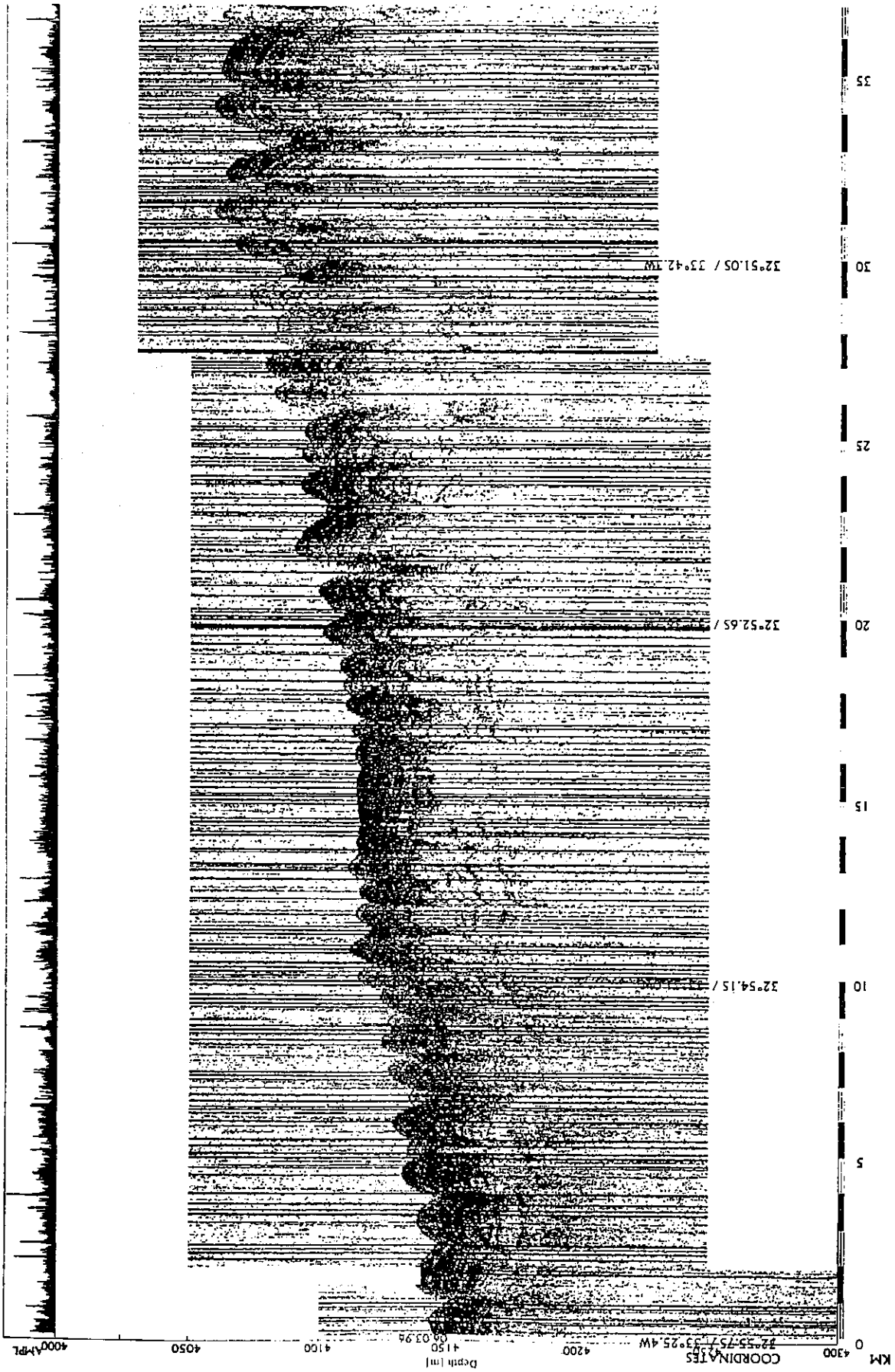

Fig. 205: Digital PARASOUND profile of mud waves at the western boundary of Hunter channel. Profile length and geographical coordinates are annotated. For further details see text.

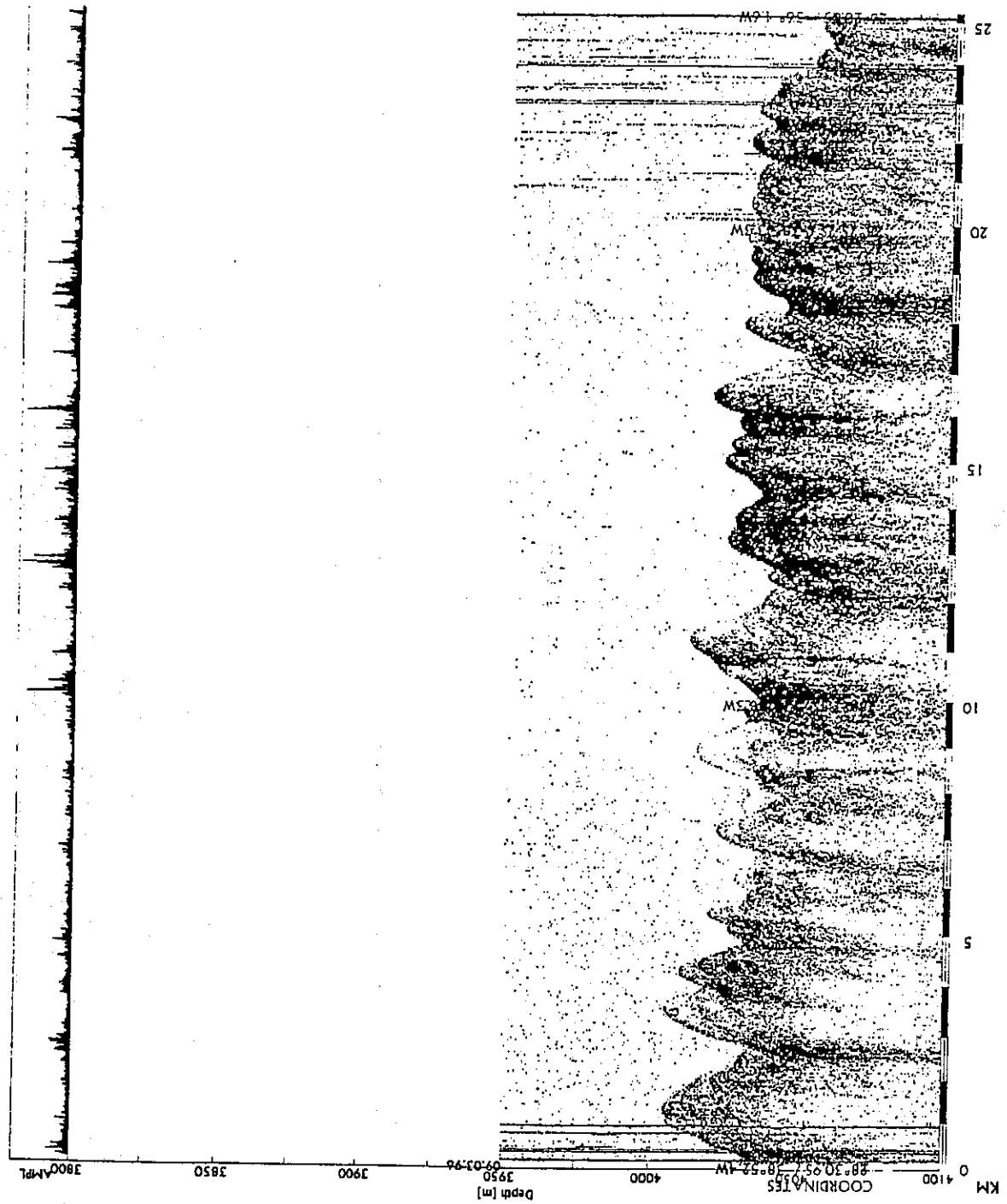

Fig. 206: Digital PARASOUND profile of mud waves north of Vema channel. Profile length and geographical coordinates are annotated. For further details see text.

5.4 Marine Geoscience M 34/4

5.4.1 Shipboard ADCP-Measurements and CTD-O_2-Transparency Probe

(U. Garternicht, B. Baschek)

5.4.1.1. Methods

A vessel-mounted acoustic Doppler current profiler (VM-ADCP) has been used to measure open ocean currents in the western tropical Atlantic. The good performance of the ADCP and the associated Ashtech-GPS lead to an almost complete data set with a vertical resolution of 8 m, beginning at 21 m depth, and a horizontal resolution of about 1.5 km.

33 CTD/O_2-profiles (with a conductivity-temperature-depth sonde plus oxygen sensor and transmissiometer) were taken with a self-contained SBE 19 sonde at a sampling rate of 1-2 samples/dbar. At about half of the stations, the CTD was attached to the wire 50 m above a bottom reaching multicorer. Profiles with CTD were only down to 1000–1200 m water depth. The CTD/O_2-sensors have been calibrated prior to the cruise by the manufacturer. The calibration coefficients from this calibration have been used to process the down-cast data on board shortly after reading them out of the memory of the CTD. A new oxygen sensor has been installed in place of one damaged during the preceeding cruise. Comparison with chemically analyzed water samples (Winkler titration) show the values of the new oxygen sensor as being to low (approx. 0.4 ± 0.4 ml/l). There were too few analyzed samples to perform another calibration. At some of stations the down-cast profiles of beam attenuation measured with the transmissiometer show a broad peak over several 100 m centered around 400–500 m, which had no equivalent in the upcast profiles. In such cases, the upcast profile of beam attenuation coefficient was taken.

The ships data recording system (DVS) has collected hull temperature and salinity, shipsdrift, depth and meteorological data. A linear correction scheme from Autosal-analyzed surface water samples was used to calibrate salinity values (courtesy of M. Vanicek and W. Zenk, M34/3).

5.4.1.2 Preliminary Scientific Results

In the upper western tropical Atlantic warm water of the South Atlantic crosses the equator to the north within the North Brazil Current (NBC), compensating much of the southward flow of North Atlantic Deep Water (NADW) confined to depth below 1200 m. The NBUC and the South Equatorial Current (SEC) have been shown to feed the

NBC in its source region located at the northeastern tip of Brazil (SCHOTT et al., 1994). These three currents have been crossed during the cruise, the latter several times.

Figure 207 shows the geostrophic velocities of the NBUC (relative to the deepest available CTD-data at about 1150 m) as derived from the hydrographic section at 8° S. The current core was very close to the shelf and was not covered by this survey. The geostrophic transport of the NBUC was about 25 Sv (1 Sv=10^6 m^3s^{-1}) to the north, whereas the additional wind-driven Ekman transport to the south was negligible. The horizontal current fields along the cruise track can be seen in Figure 208 as measured by the ADCP. In the upper 300 m the NBC transported about 18 Sv along the South American coast to the northwest. Maximum velocities wee above 1 m/s in 100 m depth. Between 36° and 38° W, an anticyclonic recirculation cell was found to flank the NBC to the south below 75 m depth. The CTD/ADCP-transect at roughly 5° N exhibited northwestward flow off the South American shelf west of 48° W. The upper-layer velocity field along the equator was dominated by the Equatorial Undercurrent (EUC) with eastward velocities up to 80 cm/s. The section along the equator (Fig. 209) marks the source region of the EUC which was between 42°–43° W. The depth of its current core rapidly decreased to the east; it was 250 m at 43° W, 100 m at 38° W and 50 m at 24° W.

The two sections offshore of Guayana and Barbados have been completed successfully. They have not been processed during the cruise due to the ending of the survey in Barbados. It is intended to combine these direct ADCP and indirect geostrophic current measurements with water mass characteristics from the CTD/O_2 to find the pathways along which warm waters of the South Atlantic flow into the Caribbean Sea.

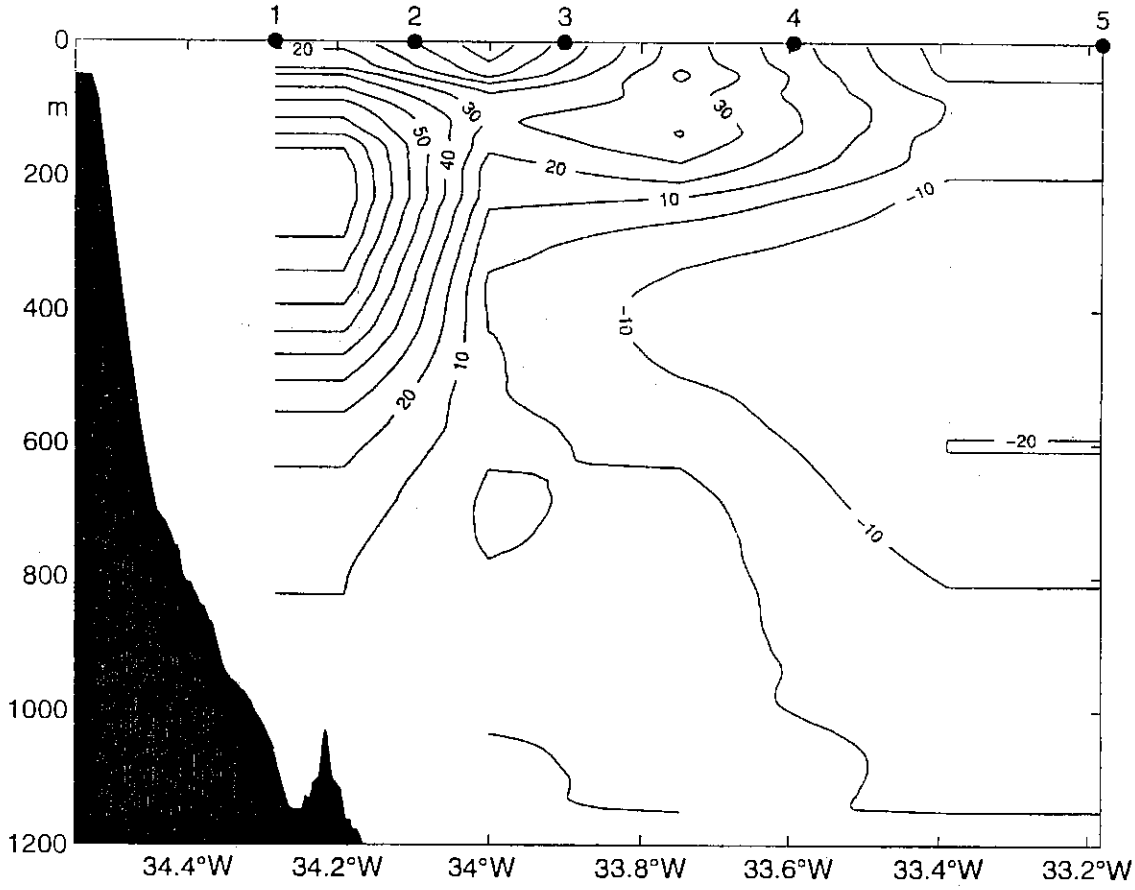

Fig. 207: Geostrophic velocities of the NBUC from a hydrographic section at 8° S. The reference level is about 1150 m. Northward velocities are shaded and the contour interval is 10 cm s^{-1}.

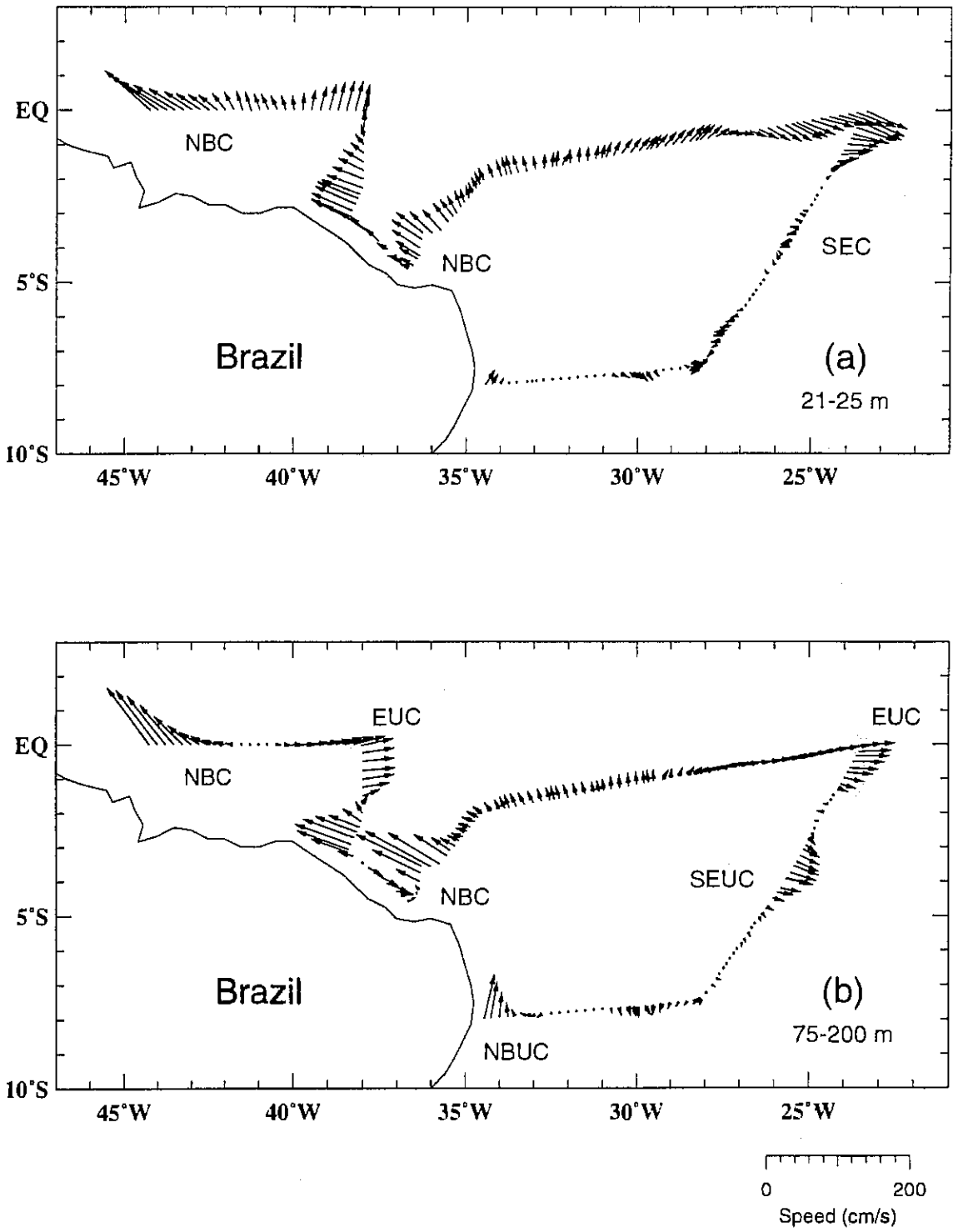

Fig. 208: The horizontal current field along the cruise track as derived from VM-ADCP (a) within the surface layer (21-25 m) and (b) within the subsurface layer at 75-200 m depth.

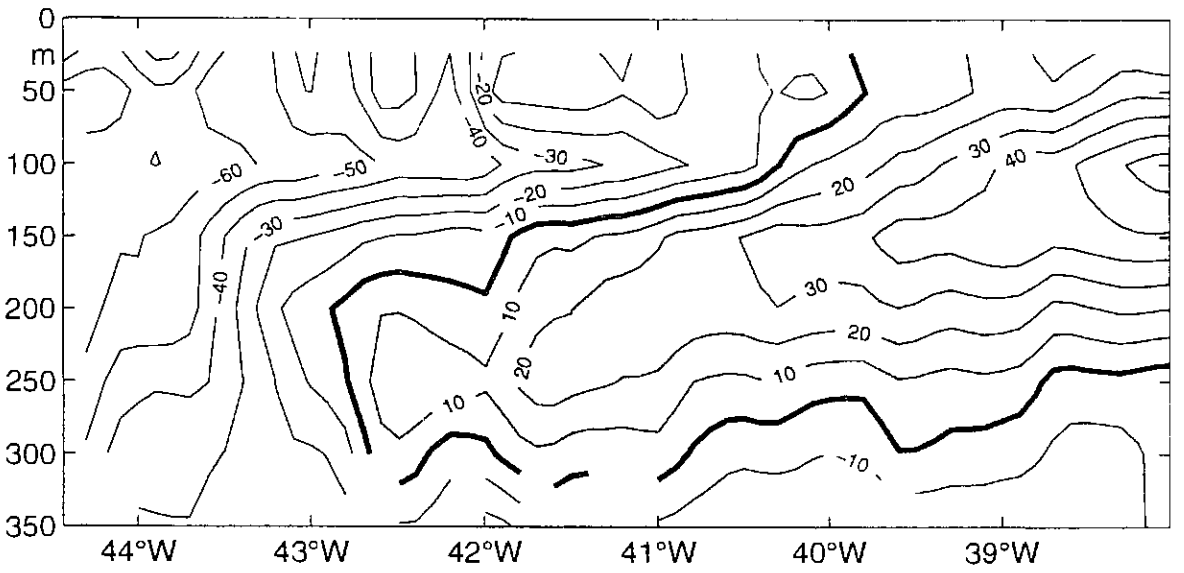

Fig. 209: Zonal velocities from the VM-ADCP-section along the equator at the source region of the EUC. The EUC's eastward velocities are shaded. The contour interval is 10 cm s^{-1}.

5.4.2 Marine Chemistry

(A. Deeken, H. Dierssen)

A major key for understanding the biogeochemical cycling of chemical elements in the ocean are particle-water interaction processes. The main objectives during this cruise were to increase our knowledge about the control of trace element distribution in the water column which interact with biogenic and abiotic particles and to investigate how particle sedimentation in a high productivity region effects the vertical trace element distribution. The sampling strategy was to collect water samples, samples of suspended particulate material (SPM) and subsamples from three sites with multi-sample sediment traps; the latter were deployed on a SW-NE-transect during METEOR cruise 29/3 (see cruise track of M34/4, Fig. 4).

5.4.2.1 Water Sampling

At all three stations where sediment traps were recovered/redeployed (see cruise track of M34/4, Fig. 4) and one station from the Amazon Fan, 12 GoFlo-bottles from GENERAL OCEANICS were taken to analyze the vertical distribution of trace elements in the water column. To minimize contamination, GoFlo-bottles with pressure valves were employed, enabling the bottles to remain closed while passing through the surface layer. At a depth of 10-15 m, these bottles will open. For lowering through the water column, the GoFlo-water-sampler and the *in situ* pumps were attached to a metal-free and non-greased KEVLAR® wire. All samples from the water column were collected rigorously applying clean sampling techniques to avoid contamination. A laboratory container proved to be a valuable facility for this purpose. All manipulations after subsampling were performed under a clean bench in the lab-container. A total of 48 water samples were collected for nutrients, oxygen and trace element analysis. Part of the collected water samples were provided for other studies (AG Wefer (GeoB), AG Lochte (IOW) and AG U. Fischer (UBBC)). The nutrients phosphate and nitrate were kindly analyzed by AG Schulz with an air-segmented Autoanalyser. Silicate was analyzed according to a standard photometric procedure. Immediately after collecting, oxygen content was determined by conventional Winkler titration. The resulting values show a similar depth profile than the oxygen sensor of the CTD-sonde. The absolute values, however, deviate somewhat from each other (see chapter 5.4.1).

The only trace element which was determined on board was Al, which was determined spectrophotometrically (fluorescence) with lumogallione (after HYDES and LISS, 1976). The data quality control will be carried out onshore. All other trace elements (primarily Cd, Co, Cr, Cu, Mn, Ni and Pb) will be analyzed onshore with anodic stripping voltammetry (ASV) or graphite furnance atomic absorption spectrometry (GF-AAS). After the water samples for trace elements were filtered through a polycarbonate filter (0,4 µm pore size, NUCLEPORE) in a plastic container, they were acidified with subboiled HNO_3 for storage.

5.4.2.2 *In situ* Filtration of Suspended Particles

At the same stations where sediment traps were recovered/redeployed and one station from the Amazon Fan, suspended particulate material (SPM) was filtered using *in situ* pumps at different depths (stations GeoB 3906 (100 m, 400 m, 700 m and 1200m), GeoB 3907 (100 m, 400 m, 700 m, 1200 m, 2000 m, 3000 m, 4000 m and 5000 m), GeoB 3908 (100 m, 400 m, 700 m and 1200 m) and GeoB 3925 (100 m, 400 m, 700 m and 1200 m)) (Tab. 39).

The filtered suspended particulate material is supposed to consist of slowly sinking biogenic and terrestrial detritus exhibiting a large surface area for sorptive processes. Due to the low concentration of SPM, larger volumes of sea water have to be filtered, if trace elements are to be analyzed in SPM. Between 300 l and 600 l sea water from depths down to 5000 m were filtered through acid cleaned polycarbonate filter (∅ 293 mm; 0,4 µm pore size, NUCLEPORE) using an *in situ* pump from CHALLENGER. To reduce contamination, a metal-free and non-greased KEVLAR® wire was used and all handling of the filters was performed under a clean bench. From pump deployments, a total of 20 filters was obtained. The filters with the retained particles will be examined for trace elements later in the laboratory in Bremen. Part of the particulate material collected by the *in situ* pumps were provided for microbiological studies (AG U. Fischer). Aliquots of the material caught at the three mooring stations with intercepting sediment traps consists of larger, faster sinking particles which incorporated trace elements during their formation and by scavening of SPM; they will be analyzed in Bremen for trace and major components after digestion with nitric and hydrofluoric acid.

Tab. 39: Location and depth of sampling with the *in situ* pumps (*pump failed, **filter teared)

Meteor-No./ GeoB-No.	Date	Location	Water depth (m)	Depth of pump (m)	Pumping time (min)	Pumping volume (l)
70/3906	21.03.96	07°25.6S	5581	100	60	826**
		28°09.2W		400	60	541
				700	60	598**
				1200	60	475
71/3907	23.03.96	03°56.4S	5553	100	60	864**
		25°41.2W		400	60	551
				700	60	482
				1200	60	540
				2000	60	509
				3000	60	571
				4000	60	561
				5000	60	576
72/3908	25.03.96	00°01.3S	3620	100	60	387
		23°28.3W		400	60	533
				700	*	*
				1200	60	545
89/3925	07.04.96	05°08,4N	3150	100	60	307
		47°31,8W		400	60	532
				700	60	535
				1200	60	586

5.4.3 Plankton Samples

5.4.3.1 Dinoflagellate Investigations

(A. Freesemann, B. Karwath)

Dinoflagellates are unicellular, biflagellated organisms, representing one of the major groups in the marine phytoplankton. During their life-cycle, dinoflagellates undergo certain stages: a motile vegetative-thecate stage and a resting cyst stage. Dinoflagellates in the motile vegetative-thecate stage usually consist of cellulose, the only exception being the calcareous-walled vegetative-coccoid *Thoracosphaera heimii*. The resting-cyst stage is in most cases organic-walled, but calcareous tests are also known ("calcispheres"). During this cruise, phytoplankton samples were collected from surface waters to 100 m depth. They were analysed for the content of living dinoflagellates, especially calcareous resting cysts and the vegetative *Th. heimii*. Of special interest are the interaction between the species associations and the related environmental parameters (temperature, salinity, light). Knowledge of these may allow a better interpretation of fossil assemblages in the sedimentary record.

Surface water was sampled with the ship's membrane pump three times per day (morning, mid-day, afternoon). The water was passed through a 100 µm mesh-sieve (DIN 4188) to separate the zooplankton. It was then filtered through 5 µm gauze (polycarbonate filters) using a vacuum pump system (Tab. 40). The samples were scanned for vegetative-thecate dinoflagellates, calcareous cysts and the vegetative-coccoid *Th. heimii*. Individual specimens were isolated and rinsed in polyterene Cell Wells™ with different culture media (f/2 35 ‰, K 35 ‰, filtered seawater), attempting to culture calcareous cysts under "on board" conditions using the local day/night cycle and temperatures between 20° and 25°C. Germination experiments and routine culturing of living calcareous cyst producing dinoflagellates will be done at the Laboratory at Bremen for the investigation of productivity, life-cycles, biomineralisation and systematics. The remaining 100 ml of seawater were stored together with the polycarbonate filters in 250 ml NALGENE polycarbonate flasks and fixed with 3-4 % Formaldehyde. For transportation, the samples were stored in the dark at 4°C.

In addition, about 10 l of seawater were collected with a Rosette using 30 l Niskin-bottles (Tab. 41). Samples were taken at depths of about 20, 50 and 100 m. The obtained sea water was treated in the same manner than the samples from the ship's membrane pump. All stored samples and filters will be prepared for Scanning Electron Microscopy (SEM) at the Laboratory for the examination of the composition and regional distribution of dinoflagellate communities in the equatorial South Atlantic.

Motile vegetative-thecate stages have been observed in every sample (calcareaus resting cysts in almost every) except those taken from the Amazon Delta. Here, salinities dropped from 34 ‰ to 12 ‰ and even further below. In marine environments, dinoflagellates were abundant to about 20 m depth, becoming rarer towards 100 m. Predominant forms of cacareous dinoflagellates were *"Sphaerodinella" albatrosiana*, *"S." tuberosa* and the vegetative-coccoid *Th. heimii*. The cysts *Orthopithonella granifera* and *Rhabdothorax* sp. were rarely observed. Organic-walled cysts were extremely rare. About 270 specimens of mainly calcareous dinoflagellates and some motile stages have been isolated for cultivation on board for further examination at Bremen University. The cells were scanned at regular intervalls. After a time period of four weeks excystment has been observed in a number of cells, only some resulting in the production of a sufficient number of motile specimens.

Tab. 40: Surface water samples for dinoflagellate analyses. Sampling with 5 µm vacuum pump filtration

Sample No.	Time of filtration UTC	Station	Latitude S/N	Longitude W	Water depth (m)	Water temperature (°C)	Salinity (•)	Volume of filtered water (l)
3/20a	10.30		07°52.9′ S	33° 00.2′	3399	28.6	34.52	40
3/20b	16.30		07°47.1′ S	31°51.4′	4982	28.9	34.51	40
3/20c	21.30		07°42.4′ S	30°54.6′	-	-	34.6	30
3/21a	10.30		07°30.3′ S	28°31.2′	5000	28.4	34.44	30
3/21b	16.30	3906	07°25.5′ S	28°08.0′	5411	28.9	34.41	30
3/21c	21.30	3906	07°25.9′ S	28°08.2′	5280	28.6	34.45	30
3/22a	13.30		07°27.7′ S	28°06.9′	4868	28.6	34.48	30
3/22c	21.45		06°18.9′ S	27°18.3′	5650	28.8	34.31	13
3/23a	11.40		04°10.6′ S	25°47.8′	5376	28.6	34.15	30
3/23b	16.30	3907	03°56.9′ S	25°41.0′	5555	29.0	34.24	30
3/24a	11.30		03°54.7′ S	25°41.7′	5554	28.6	34.22	30
3/24b	18.00		03°54.7′ S	25°32.7′	5558	28.7	34.04	30
3/24c	22.00		03°30.1′ S	25°23.4′	5609	28.6	33.93	30
3/25a	11.00		01°11.2′ S	24°07.0′	4751	28.6	33.95	30
3/25b	17.00		00°14.6′ S	23°35.7′	3780	28.1	34.12	30
3/25c	21.00		00°01.3′ S	23°28.1′	3609	28.0	34.07	30
3/26a	11.00		00°00.4′ N	23°26.4′	3710	28.0	34.12	30
3/26b	16.30	3908	00°00.4′ S	23°25.6′	3690	28.3	34.14	30
3/26c	22.00		00°08.1′ S	24°10.3′	2884	28.1	34.08	30
3/27a	11.00		00°34.1′ S	26°35.1′	3674	28.4	33.93	30
3/27b	17.00		00°47.8′ S	27°52.2′	3755	28.7	34.02	30
3/27c	21.00		00°55.1′ S	28°32.8′	4089	28.6	33.87	30
3/28a	12.00		01°25.7′ S	31°22.5′	4903	28.5	34.01	30
3/28b	16.30		01°34.4′ S	32°10.0′	4679	28.5	34.09	30
3/28c	21.30		01°45.1′ S	33°08.5′	4485	28.7	34.26	30
3/29a	13.30		03°21.6′ S	35°36.7′	3594	-	34.16	30
3/29b	16.30		03°33.9′ S	36°02.5′	3289	28.9	34.33	30
3/29c	20.30	3909	03°32.6′ S	36°12.6′	3173	29.0	34.26	30
3/31b	16.30		02°43.3′ S	38°13.6′	2465	29.0	34.29	30
3/31c	21.00		02°43.3′ S	38°13.7	1010	28.9	34.43	50
4/1a	11.00		01°26.3′ S	38°00.0′	4141	28.9	34.37	50
4/1b	16.30		00°34.1′ S	27°59.9′	4380	29.1	34.37	50
4/2a	11.00		00°00.0′	41°03.1′	3795	28.1	34.3	50
4/2b	16.30		00°00.0′	42°05.2′	3859	28.5	34.36	50
4/2c	20.15		00°00.0′	42°49.7′	3630	28.4	34.36	50
4/3a	13.00		00°27.2′ N	46°22.0′	44.2	28.4	32.78	30
4/3b	16.30		00°34.6′ N	46°52.9′	30.9	28.4	30.75	30
4/3c	20.15		00°46.7′ N	47°42.7′	42.1	28.2	12.2	3.0
4/4a	10.50		01°54.0′ N	48°15.2′	48.1	28.1	29.11	30
4/4b	16.30		02°17.7′ N	48°09.6′	75.9	28.3	32.91	30
4/4c	21.00		02°37.1′ N	48°43.5′	92.9	28.1	32.13	30
4/5a	10.50		03°11.6′ N	49°23.4′	78.8	28.0	30.1	30
4/5b	17.00		03°41.1′ N	49°23.4′	50.1	28.1	19.16	3.5
4/5c	20.15		03°42.2′ N	50°24.3′	49.3	27.8	19.34	3.0
4/6a	12.00		04°36.0′ N	49°42.1′	1937	27.7	33.79	50
4/6c	20.30		05°00.4′ N	48°46.4′	2659	27.6	34.20	50
4/7a	12.00		05°08.6′ N	47°31.7′	3197	27.5	34.3	50
4/7b	16.00	3925	05°07.9′ N	47°30.8′	3167	27.6	34.29	50
4/7c	20.00		05°08.1′ N	47°30.5′	3187	27.5	34.29	50
4/10b	17.30		08°22.6′ N	58°04.7′	1282	27.4	33.36	50
4/11b	18.00		10°26.6′ N	56°50.0′	4089	27.1	-	50
4/12a	12.00		11°54.2′ N	57°48.9′	3047	27.2	33.63	40
4/12b	18.00		12°15.8′ N	58°20.2′	1955	27.1	33.46	40

Tab. 41: Water samples for dinoflagellate analyses taken from 30 l Niskin-bottles at about 20, 50, 100 m water depth (filtration with 5 µm polycarbonate filters)

Sample No.	Time UTC	Water depth (m)	Volume of filtered water (l)	Latitude S/N	Longitude W	SST (°C)	Salinity in surface water (‰)
Station 3906							
20 m	18.10	5215	13	07°25.4′ S	28°07.9′	28.8	34.47
50 m			13				
100 m			13				
Station 3907							
20 m	18.45	5555	13	03°55.7′ S	25°40.9′	29.6	34.38
50 m			13				
100 m			13				
Station 3908							
20 m	15.00	4234	13	00°00.2′ S	23°23.8′	28.3	34.12
50 m			13				
100 m			13				
Station 3925							
20 m	18.30	4808	13	05°07.8′ N	47°30.6′	27.6	34.29
50 m			13				
100 m			13				
Station 3932							
20 m	23.30	4239	13	10°59.9′ N	56°30.0′	-	-
50 m			13				
100 m			13				

5.4.3.2 Coccolithophore Communities

(M. v. Herz, H. Kinkel)

Coccolithophorids are a diverse group of marine phytoplankton belonging to the algal class Prymnesiophyceae. They produce external plates of carbonate, named coccoliths. Coccoliths are a major component in almost all ocean sediments. Their distribution in the sediments is relatively well known, but information on their abundance, ecology and physiology in the surface waters is rare. The water samples taken during that cruise will allow us to better understand the relationship between living communities and the assemblages in the sediments. At 4 stations, water samples of 2 l were taken from the rosette with 6 Niskin bottles (30 l) or from the small Niskin-bottles (1.2 l) attached to the multinet (depths generally at 200 m, 100 m, 75 m, 50 m and 20 m). In addition, 37 surface water samples from about 3.5 m water depth were taken from the vessel's membrane pump system along the cruise (see cruise track plot), mostly at dawn, high noon, twylight and midnight. Generally, 2 of the water samples were filtered through cellulose nitrate filters (25 m in diameter, 0.45 m pore size) by a vacuum pump immediately. Without washing, rinsing or chemical conservation, the filters were dried at 45° C for at least 24 and then kept permanently dry with silica gel in transparent film to protect them from humidity. The filtered material will be used for studies on distribution and composition of the coccoloithophorid communities with Scanning Electron Microscope (SEM). Species composition and abundances will be determined by identification and counting on measured filter transects.

5.4.3.3 Chlorophyll-a Measurements

(V. Diekamp. I. Engelbrecht)

For the determination of chlorophyll-a concentrations in the surface waters, 0.5 of seawater was collected 3 times a day from the ship´s seawater pump (inlet in about 3.5 m water depth). The water was filtered onto glass fibre filters and frozen to -20° C. Chlorophyll-a measurements by means of photometry will be carried out in the laboratory in Bremen. The chlorophyll-a data should give information on seasonal and regional variability in biomass distribution; satellite-derived chlorophyll-a concentrations may also calibrated against these mesurements. For sampling locations see Table 42.

Tab. 42: Sampling locations for chlorophyll-a measurements

No.	Date	Time UTC	location	Water-depth (m)	Salinity (‰)	Water-temp. (C)	Sample-volume (l)
222	20.03.96	11:30	07°52.0S,	4698	34.52	28.7	2x0.5
224	20.03.96	14:58	07°48.7S,	5035	34.55	29.0	2x0.5
226	20.03.96	21:16	07°42.7S,	5344	34.59	28.8	2x0.5
228	21.03.96	11:10	07°29.5S,	5562	34.42	28.4	2x0.5
230	21.03.96	15:09	07°27.5S,	5052	34.40	28.8	2x0.5
232	21.03.96	21:57	07°25.8S,	5275	34.46	28.6	2x0.5
234	22.03.96	11:54	07°27.8S,	4854	34.47	28.5	2x0.5
236	22.03.96	14:14	07°26.9S,	4878	34.48	28.7	2x0.5
238	22.03.96	21:11	06°24.1S,	5645	34.30	28.7	2x0.5
240	23.03.96	11:30	04°12.5S,	5421	34.12	28.6	2x0.5
242	23.03.96	14:52	03°58.7S,	5554	34.26	28.7	2x0.5
244	23.03.96	21:51	03°54.8S,	5559	34.26	28.9	2x0.5
246	24.03.96	11:24	03°54.6S,	5552	34.22	28.6	2x0.5
248	24.03.96	15:18	03°54.9S,	5558	34.21	28.6	2x0.5
250	24.03.96	21:41	03°34.4S,	5327	33.95	28.8	2x0.5
252	25.03.96	11:29	01°12.8S,	4297	33.97	28.6	2x0.5
254	25.03.96	14:11	00°48.2S,	3880	34.00	28.9	2x0.5
256	25.03.96	21:32	00°01.3S,	3624	34.06	28.0	2x0.5
258	26.03.96	11:22	00°00.5S,	3706	34.12	28.0	2x0.5
260	26.03.96	14:27	00°00.1S,	3859	34.12	28.3	2x0.5
262	26.03.96	21:13	00°06.7N,	2910	34.08	28.2	2x0.5
264	27.03.96	11:35	00°35.0S,	3812	34.01	28.4	2x0.5
266	27.03.96	14:29	00°40.9S,	3739	34.03	28.6	2x0.5
268	27.03.96	21:15	00°54.6S,	3877	33.91	28.6	2x0.5
270	28.03.96	11:47	01°24.2S,	4863	33.83	28.5	2x0.5
272	28.03.96	14:14	01°29.3S,	4777	34.06	28.4	2x0.5
274	28.03.96	21:34	01°44.5S,	4494	34.25	28.6	2x0.5
276	29.03.96	11:12	02°56.3S,	3766	34.13	28.7	2x0.5
278	29.03.96	14:31	03°26.0S,	3553	34.15	29.0	2x0.5
280	29.03.96	22:03	03°33.4S,	3160	34.31	29.1	2x0.5
282	31.03.96	14:14	02°47.5S,	2482	34.27	29.0	2x0.5

Table 42 continued

No.	Date	Time UTC	location	Water-depth (m)	Salinity (‰)	Water-temp. (C)	Sample-volume (l)
284	31.03.96	21:39	02°43.2S,	2455	34.43	28.9	2x0.5
286	01.04.96	11:25	02°56.0S,	3847	34.39	28.4	2x0.5
288	01.04.96	14:05	02°07.8S,	4289	34.34	29.0	2x0.5
290	01.04.96	21:19	00°00.5S,	4387	34.38	28.7	2x0.5
292	02.04.96	11:30	00°00.0 ,	3799	34.34	28.2	2x0.5
294	02.04.96	14:10	00°00.1S,	3889	34.34	28.3	2x0.5
296	02.04.96	21:11	00°00.01N,	2754	34.37	28.4	2x0.5
298	03.04.96	11:11	00°21.1N,	53	32.69	28.3	2x0.5
300	03.04.96	15:06	00°31.3N,	39	31.85	28.3	2x0.5
302	03.04.96	20:20	00°45.1N,	44	12.61	28.2	2x0.5
304	04.04.96	11:26	01°56.8N,	55	30.05	28.0	2x0.5
306	04.04.96	14:56	02°11.1N,	69	32.99	28.2	2x0.5
308	04.04.96	21:27	02°39.9N,	87	32.02	28.1	2x0.5
310	05.04.96	11:20	03°14.0S,	74	29.82	27.9	2x0.5
312	05.04.96	14:25	03°30.8N,	78	27.30	28.1	2x0.5
314	05.04.96	21:16	03°46.4N,	55	21.49	28.1	2x0.5
316	06.04.96	11:34	04°45.9N,	1849	33.76	27.7	2x0.5
318	06.04.96	15:53	04°46.6N,	2451	34.26	27.7	2x0.5
320	06.04.96	21:36	05°04.7N,	2836	34.34	27.6	2x0.5
321	07.04.96	11:21	05°08.6N,	3198	34.29	27.4	2x0.5
323	07.04.96	14:10	05°08.6N,	3195	34.30	27.5	2x0.5
325	07.04.96	21:41	05°.08.3N,	3198	34.29	27.5	2x0.5
327	08:04.96	11:19	05°44.5N,	3651	34.26	27.6	2x0.5
329	10.04.96	15:33	08°28.5N,	1620	33.53	27.4	2x0.5
331	10.04.96	22:12	08°39.3N,	2080	33.57	27.4	2x0.5
333	11.04.96	13:28	09°54.2N,	3677	30.84	27.4	2x0.5
335	11.04.96	14:59	09°59.3N,	3465	---	27.5	2x0.5
337	11.04.96	22:39	10°55.3N,	4167	33.39	27.2	2x0.5
339	12.04.96	12:22	11°51.0N,	3128	33.64	27.3	2x0.5
341	12.04.96	15:21	12°03.0N,	2334	33.47	27.2	2x0.5
343	12.04.96	22:13	12°32.3N,	1623	33.28	27.2	2x0.5

5.4.3.4 Pumped Plankton Samples

(R. Schneider)

Marine plankton from surface waters was sampled during the whole cruise (Tab. 43). The shipboard installed sea-water pump was used to filter about 2000 to 6000 l each day, mostly during daylight. The amount of water filtered, depended on the plankton mass caught in the net. The sea-water was pumped through a net with a mesh size of 10 µm. When the water flow was stopped by the material closing the net openings, the plankton was washed into plastic bottles and the sampling was continued with the cleaned net. For each day the wet plankton samples were concentrated into one bottle and frozen at -20°C.

The plankton material will be investigated for the bulk composition of the biogenic detritus in order to determine the ratios between bulk opal, organic carbon and carbonate produced by near surface water plankton communities. In particular, the marine organic material will be investigated in more detail. It is planned to analyse the composition of stable carbon and nitrogen isotopes as well as organic compounds which can be related to specific phytoplankton organisms. This type of data is needed to compare the marine plankton production in the surface waters of different high productivity systems with fluxes of biogenic particles caught in sediment traps and found in the surface sediments beneath high productivity areas.

Tab. 43: Plankton Pump Samples

Nr.	Date	Start filtration: time	Position Latitude	Longitude	Salinity	Temp.	Water-clock	Stop filtration: time	Position Latitude	Longitude	Salinity	Temp.	Water-clock	Liters pumped
1	24.04.96	08:05	03°55.4S	25°42.2W	36.39	28.6	509290	19:35	03°25.4S	25°20.8W	36.00	28.7	511947	2659
2	25.03.96	08:05	01°17.1S	24°10.2W	36.05	28.7	511967	21:15	00°01.4S	23°28.2W	36.21	28.0	518397	6430
3	26.03.96	10:00	00°00.7S	23°25.9W	36.21	28.1	518397	19:55	00°10.1S	24°21.7W	36.21	28.2	523375	4978
4	27.03.96	09:45	00°37.3S	26°53.4W	36.12	28.5	523375	20:31	00°59.2S	28°25.7W	35.95	28.5	530202	6827
5	28.03.96	08:00	01°22.7S	31°05.2W	35.95	28.0	530202	18:35	01°44.5S	33°05.1W	36.33	28.6	535877	5675
6	29.03.96	08:05	02°55.6S	35°15.5W	36.01	28.8	535877	20:20	03°41.5S	36°17.1W	36.38	29.0	542020	6143
7	31.03.96	11:20	02°55.2S	38°19.1W	---	28.9	542022	19:30	02°39.4S	38°11.8W	36.48	29.0	546307	4285
8	01.04.96	06:10	01°55.3S	38°00.1W	36.31	28.8	546307	18:50	0°00.02S	38°24.3W	36.44	28.7	552220	5913
9	02.03.96	08:20	0°00.02S	41°38.2W	36.40	28.2	552220	00:51	00°00.1S	44°29.6W	36.44	28.6	560241	8021
10	03.04.96	09:00	00°23.2S	46°05.6W	35.85	28.3	560259	13:40	00°35.8S	46°57.9W	31.36	28.5	562400	2141
11	03.04.96	13:40	00°35.8S	46°57.9W	31.36	28.5	562400	20:20	00°53.9S	48°12.3W	14.10	28.6	565735	3335
12	04.04.96	06:25	01°45.6S	48°22.3W	29.96	28.2	565735	18:45	02°37.3S	48°43.4W	34.44	28.2	571261	5526
13	05.04.96	08:30	03°15.2N	49°29.6W	32.38	27.9	571261	14:00	03°43.6S	50°19.2W	25.19	28.2	573834	2573
14	05.04.96	15:30	03°43.5N	50°20.7W	24.74	28.1	573834	20:35	04°04.3N	50°23.0W	27.29	28.1	575014	1180
15	06.04.96	12:25	04°44.9N	49°21.6W	36.31	27.6	575014	19:45	05°06.1N	48°34.3W	36.41	27.5	578908	3894
16	07.04.96	09:50	05°08.6N	47°31.8W	36.36	27.5	578908	19:55	05°08.2N	47°30.7W	36.36	27.5	583162	4254
17	10.04.96	14:45	08°24.3N	58°03.4W	35.91	27.5	583218	20:45	08°54.7N	57°45.3W	35.76	27.4	586202	2984
18	11.04.96	08:20	09°45.2N	57°14.9W	35.88	27.4	586202	00:15	11°13.9N	56°50.4W	35.63	27.1	594007	7805
19	12.04.96	08:35	11°51.9N	57°14.9W	35.83	27.3	594029	20:00	12°39.8N	58°55.4W	35.55	27.1	599836	5807

Salinity values from ships salinometer were corrected for instrument deviation by $S_{corr}=S_{value} \times 0.8411+7.515$

5.4.3.5 Plankton Sampling using a Multiple Closing Net

(H. Kinkel, M. v. Herz, V. Diekamp, I. Engelbrecht)

Plankton was sampled with a multiple closing net (Fa. HYDROBIOS) with 0.25 m^2 opening and 64 µm mesh size. It was used for vertical hawls at 4 sites (Tab. 44). Each multinet station comprised three hawls with:

1. depth intervals from 500-300, 300-200, 200-100, 100-50 and 50-0 m.
2. depth intervals from 400-200, 200-100, 100-0, 40-20 and 20-0 m.
3. depth intervals from 250-00, 100-75, 75-50, 50-25 and 25-0 m.

Hawl 1 will be used for studies on planktonic foraminifera, hawl 2 for radiolarian and diatom analyses, and hawl 3 for geochemical and isotopic analyses. The samples containing mostly zooplankton and some phytoplankton were carefully rinsed with seawater into KAUTEX bottles, fixed with mercury chloride for the reduction of bacterial degradation, and stored at 4°C. At all stations, 1.2 l Niskin-bottles were used during the first and the third hawl to obtain water samples from the different water depths for analyses of carbon and oxygen stable isotopes and phytoplankton investigations (see chapter 5.4.3).

Tab. 44: Water samples for $\delta^{13}C$ and $\delta^{18}O$ analyses (multinet- and GoFlo-bottles)

Station GeoB	depth (m)	$\delta^{13}C$ (‰ PDB)	$\delta^{18}O$	corr. depth (m)	Position Latitude Longitude
3906-5(MN)	50	x	x	100	7°26,1S 28°08,3W
	100	x	x	200	
	200	x	x	300	
	300	x	x	500	
	500	x	x	50	
3906-7(MN)	25	x	x	50	7°25,8S 28,08,1W
	50	x	x	75	
	75	x	x	100	
	100	x	x	250	
	250	x	x	25	
3906-8(GF)	700	x	x		7°25,0S 28°07,9W
	1200	x	x		
	2000	x	x		
	3000	x	x		
	4000	x	x		
	5000	x	x		
3907-5(MN)	50	x	x	100	3°55,1S 25°40,1W
	100	x	x	200	
	200	x	x	300	
	300	x	x	500	
	500	x	x	50	
3907-6(MN)	25	x	x	50	3°54,8S 25°40,4W
	50	x	x	75	
	75	x	x	100	
	100	x	x	250	
	250	x	x	25	
3907-10(GF)	700	x	x		3°54,9S 25°36,6W
	1200	x	x		
	2000	x	x		
	3000	x	x		
	3950	x	x		
	4950	x	x		
3908-3(GF)	675	x	x		0°00,2S 23°27,9W
	1150	x	x		
	2000	x	x		
	2500	x	x		
	3000	x	x		
3908-4(MN)	50	x	x		0°00,2S 23^27,9w
	100	x	x		
	200	x	x		
	300	x	x		
	500	x	x		
3908-5(MN)	25	x	x		0°00,24S 23°27,9W
	50	x	x		
	75	x	x		
	100	x	x		
	250	x	x		
3925-1(GF)	650	x	x		5°08,6N 47°31,7W
	1150	x	x		
	2000	x	x		
	2500	x	x		
	3000	x	x		
3925-7(MN)	50	x	x		5°08,3N 47°30,9W
	100	x	x		
3925-8(MN)	200	x	x		
3925-7(MN)	300	x	x		
	500	x	x		
3925-9(MN)	25	x	x		5°08,3N 47°31,4W
	50	x	x		
	75	x	x		
	100	x	x		
	250	x	x		

5.4.4 Stable Carbon and Nitrogen Isotope Investigations and Experiments

(C. Eichner)

In all biological (enzymatic) reactions fractionation of stable N and C isotopes occurs. The resulting isotope values in suspended particulate matter, sedimenting particles and also in sediments are used to infer enviromental conditions during particle formation. The aim of this investigation was to examine the fractionation during degredation of organic matter, especially at the water/sediment boundary layer. There, the influence of nutrient concentrations, oxygen contents or water depth for the fractionation has to be known. For this, *in situ* measurements as well as experiments were carried out.

At different stations samples were taken from the water column (Niskin-, Goflo-bottles (AG Balzer), overlying water from the multicorer)) and from the upper sediment layers (multicorer); at other sites, bottom water and surface sediment was taken (multicorer) (see Tab. 45). Oxygen in the water from different depth was measured by conventional titration (GRASSHOFF et al., 1983). A defined volume of water from Niskin- or Goflo-bottles was filtered (GF/F-filters), filters were frozen for later measurement of $\delta^{15}N$, $\delta^{13}C$ and C/N-ratios in the particulate fraction and for chlorophyll determination. Nitrite, nitrate and ammonium in the filtrate was determined either by autoanalyser (AG Schulz) or was frozen for later measurement. Unfiltered water has been fixed with formaldehyde (end concentation 0.4 %) for later dying with the fluorescent dye DAPI to count bacteria and measure their volume under the fluorescence-microscope and for microscopic identification of particles (algae etc.).

The sediments sampled with the multicorer were cut into 1 cm slices. These were partly frozen (-18°C) for later determination of $\delta^{15}N$, $\delta^{13}C$ and C/N-ratios. 1 cm^3 was fixed with formaldehyde for counting and measuring bacteria (see above). The remaining sediment was centrifugated for pore water recovery. It was frozen for later determination of $\delta^{15}N$ in the dissolved nitrogen fraction.

Aging experiments were carried out with suspended particles from stations 3906 and 3907, and with sediments from station 3908. Water from the euphotic zone (50 m, Niskin-bottle), below the euphotic zone (250 m, Niskin-bottle) and bottom water (multicorer) has been incubated at *in situ* temperature for 20 days. Organic matter from both upper layers was concentrated through a 10 mm gaze. At certain intervals, an aliquot was taken for filtration and nutrient measurement. In another experiment, surface water was single-fold, double- and four-fold enriched. Subsamples were taken at certain time intervals and treated as described above.

To investigate the influence of oxygen on the fractionation of C- and N-isotopes in bottom water, another experiment was done. Bottom water from station 3908 was filled into glas bottles and one half was bubbled with argon to get oxygen free water. The rest was shaken every day to keep the samples oxic. At certain time intervals, an oxic and anoxic bottle was subsampled for $\delta^{15}N$, $\delta^{13}C$, C/N-ratios and nutrient measurement and for number and volume of bacteria. The same set of experiments was carried out with sediments. Surface sediment was homogenized, diluted with bottom water and filled into glas bottles. One half was bubbled with argon. After certain intervals, an oxic and an anoxic bottle was subsampled. The sediment was partly preserved with formaldehyde and partly frozen (see below). The overlying water was analysed for nitrite, nitrate and ammonium.

Tab. 45: Sampling and preparation for stable C- and N-isotope analyses

Station no.	Position	Water depth (m)	Sampling equipment and depth	Treatment of sample	Measurement
3906	07°27,7′S 28°06,9′W	5581m	Niskin-bottles: 20m, 50m, 100m, 250m Goflo-bottles:	O_2 concentration (Winkler) filtration	$\delta^{15}N$, $\delta^{13}C$, C/N, Chl -a NO_3, NO_2, NH_4 in filtered sea water
3907	03°55,8′S 25°40,9′W	5551m	Niskin-bottles: 20m, 50m, 100m, 250m Goflo-bottles:	same as 3906	see above
3908	00°00,5′N 23°26,5′W	3635m	Niskin-bottles: 20m, 50m, 100m, 250m Goflo-bottles: 10m, 25m, 50m, 100m, 150m, 200m, 400m, 670m, 1150m, 2000m, 2500m, 3000m multicorer	same as 3906	see above
3909	03°32,9′ S 36°16,2′W	3165m	multicorer	same as 3906	see above
3914	02°43,5′S 38°13,6′W	2472m	multicorer	same as 3906	see above
3915	02° 16,8′S 38° 01,1′W	3256m	multicorer	same as 3906	see above
3916	01° 49,9'N 48°26,9'W		multicorer	same as 3906	see above
3925	05°08,4′N 47°31,8′S	3190m	Niskin-bottles: 20m, 50m, 75m, 100m, 200m, 250m, 400m, 700m, 1200m, 2000m, 3000m multicorer	same as 3906	see above

5.4.5 Microbial Colonisation of "Marine Snow"

(I. Miesner)

Rapidly sinking particles in the water column, so called "Marine Snow", consist of dissolved and colloidal organic matter which aggregates together, i.e. phytoplankton aggregates, fecal pellets and detritus. Bacteria and protozoa seem to play an important role in decomposition of "Marine Snow"; the main decomposition takes place in the mesopelagic zone (LOCHTE, 1991, LOCHTE, 1993 and AUSTIN, 1988). During this cruise, samples were taken from different depths as well as material from long-term placed sediment traps (poisoned with $HgCl_2$). Enrichments of the bacteria attached to "Marine Snow" and the free living bacteria in the surrounding seawater were made by use of different culturing techniques, as well as preparations for light and electron microscopy. In this case, both seasonal and regional differences have to be recorded.

For the sampling of living material different sampling methods were used. At four stations sea water was taken at different depths from 20 to 3000 m with a Niskin-bottle. It was possible to obtain samples with a GoFlo-water sampler and *in situ* pumps (AG Balzer) from different depths between 10 to 5000 m. When sampling with the multicorer was carried out, samples from the overlying sea water were taken. As the samples turned out to be poor in containing macroaggregates, about 300 l water from the surface (3.5 m water depth) were taken daily by the ship's membrane pump and passed through a 55 µm gaze from which the aggregates were collected with a sterile pasteur pipette and transferred into sterilized seawater (for detailed list of all samples see Tab. 46). All samples were transferred directly to sterile vessels. From each water sample and diluted filtrate of the *in situ* pumps, 2 ml were transferred immediately into 50 % glycerine and stored at -20°C. 10 ml of each sample were fixed with formalin (2 % v/v) and stored at 4°C. Preparations for electron microscopy and direct counting by epifluorescence techniques will be done at the laboratory at Bremen University. The remainder of each sample was stored in sterile screw cap tubes at 4°C.

For the determination of aerobic heterotrophic bacteria 200 ml of each Niskin-bottle water sample were filtered through 0,45 µm cellulose acetate filters. The filters were pressed on agar plates containing ASN_{III}-medium with 0.05 % yeast extract added. Then the filters were transferred to liquid cultures in ERLENMEYER flasks containing ASN_{III}-medium and 0.05 % yeast extract. Streaks on agar plates containing ASN_{III}-medium, 0.05 % yeast extract and 1.6% agar were made from a number of samples. The cultures were incubated aerobically under night/day cycle-light conditions at room temperature (20-25°C). Liquid cultures from the GoFlo-water samples were made in ERLENMEYER flasks containing ASN_{III}-medium and 0.05 % yeast extract, inoculated with 1 ml sample. The cultures from water depths > 400 m were incubated aerobically in the dark at 4°C. Complementary, various samples were streaked on agar plates with ASN_{III} and 0.05 % yeast extract and were incubated under anaerobic conditions in an anaerobic jar under day/night-light conditions at 20-25°C. The filtrates of the *in situ* pumps, diluted in sterilized seawater, were used to inoculate agar plates containing ASN_{III}-medium and 0.05 % yeast extract. 1 ml of each sample was used for liquid cultures under aerobic conditions in sterile-filtrated seawater. Simplified enrichment cultures

for the recovery of autotrophic bacteria (i.e. cyanobacteria, purple/green sulphur bacteria) were tested. Liquid and solid ASN_{III}-medium without yeast extract was used for the enrichment of cyanobacteria. 1mM Na_2S was added to liquid ASN_{III}-medium as an electron donor for the enrichment of sulfur bacteria. The cultures were incubated anaerobically in screw cap bottles. Separate colonies which grew on the agar plates, were picked and streaked on fresh agar plates to obtain pure strains.

All cultures were scanned using light microscopy with phase contrast in regular intervals. The highest abundance was shown by various greenish rod-shaped, motile or nonmotile forms, 0.5-1 x 3-5 µm in size. Cocci, spirilla and budding forms were also observed. In several cultures, filamentous cyanobacteria were observed. The isolated strains showed various types of heterotrophic bacteria. Greenish and reddish colony forming rods, 1 x 5-7 µm in size, able to decompose agar were isolated, as well as various shorter rods which form colourless and yellowish colonies on agar. The isolates are to be examined at the laboratory at Bremen University for further identification and characterization.

The samples taken by the ship's membrane pump included aggregates (< 2 mm), which consisted of phyto- and zooplankton detritus (copepods, algae debris, empty diatoms, etc.). In the area around these aggregates and attached to them, a much greater number of bacteria than in the surrounding seawater appeared, but it seems to be the same or similar bacteria. Preparations for light microscopy were made, the coverslips were sealed with nail varnish. The preparations were stored at 4°C.

Three moorings with two multi-sample sediment traps each were installed during METEOR cruise 29/3. The sediment traps consisted of 20 bottles which sampled over a period of about 4 weeks each. 1 ml of poisoned material was transferred from each bottle to sterile 1.5 ml EPPENDORF caps and stored at 4°C (WA6/upper 1-20, WA6/lower 1-20, WA7/upper 1-20, WA7/lower 1-20, WA8/upper 1-20 and WA8/lower 1-20). Attached bacteria, possible seasonal and regional differences are to be determined using scanning electron microscopy techniques.

Tab. 46: Water samples for microbiological investigations

Sample No.*	Station	Latitude S/N	Longitude W	Water depth (m)
MP 1	3904	07°53.0′ S	33°00.3′	2,5
MP 2	3906	07°25.6′ S	28°08.0′	2,5
MP 3	3906	07°25.3′ S	28°08.1′	2,5
MP 4	3906	07°27.7′ S	28°06.9′	2,5
MP 5	-	07°47.2′ S	31°51.4′	2,5
MP 6	-	06°15.2′ S	27°15.7′	2,5
MP 7	-	04°10.6′ S	25°47.9′	2,5
MP 8	3907	03°55.8′ S	25°40.9′	2,5

Table 46 continued

Sample No.*	Station	Latitude S/N	Longitude W	Water depth (m)
MP 9	-	01°01.5′ S	24°01.6′	2,5
MP 10	-	00°54.8′ S	28°31.2′	2,5
MP 11	-	01°32.5′ S	31°59.2′	2,5
MP 12	-	03°24.7′ S	35°39.2′	2,5
MP 13	-	02°42.7′ S	38°13.2′	2,5
MP 14	-	00°00.0′ S	38°31.0′	2,5
MP 15	-	00°46.7′ S	47°42.8′	2,5
MP 16	-	02°37.1′ N	48°43.6′	2,5
MP 17	-	04°42.7′ N	49°26.4′	2,5
MP 18	3925	05°08.6′ N	47°31.8′	2,5
MP 19	-	09°55.7′ N	57°08.7′	2,5
WS 1	3906-3	07°24.8′ S	28°08.0′	250
WS 2	3906-3	07°24.8′ S	28°08.0′	100
WS 3	3906-3	07°24.8′ S	28°08.0′	50
WS 4	3906-3	07°24.8′ S	28°08.0′	20
WS 5	3907-3	03°55.8′ S	25°41.0′	250
WS 6	3907-3	03°55.8′ S	25°41.0′	100
WS 7	3907-3	03°55.8′ S	25°41.0′	50
WS 8	3907-3	03°55.8′ S	25°41.0′	20
WS 9	3908-8	00°00.4′ S	23°26.4′	250
WS 10	3908-8	00°00.4′ S	23°26.4′	100
WS 11	3908-8	00°00.4′ S	23°26.4′	20
WS 12	3925-6	05°08.3′ N	47°30.7′	3000
WS 13	3925-6	05°08.3′ N	47°30.7′	2000
WS 14	3925-6	05°08.3′ N	47°30.7′	1200
WS 15	3925-6	05°08.3′ N	47°30.7′	700
WS 16	3925-6	05°08.3′ N	47°30.7′	400
WS 17	3925-6	05°08.3′ N	47°30.7′	250
WS 18	3925-6	05°08.3′ N	47°30.7′	200
WS 19	3925-6	05°08.3′ N	47°30.7′	100
WS 20	3925-6	05°08.3′ N	47°30.7′	75
WS 21	3925-6	05°08.3′ N	47°30.7′	50
WS 22	3925-6	05°08.3′ N	47°30.7′	20
WS 23	3932-1	11°00.0′ N	56°29.8′	3000
WS 24	3932-1	11°00.0′ N	56°29.8′	400
WS 25	3932-1	11°00.0′ N	56°29.8′	100
WS 26	3932-1	11°00.0′ N	56°29.8′	50
WS 27	3932-1	11°00.0′ N	56°29.8′	20

Table 46 continued

Sample No.[a]	Station	Latitude S/N	Longitude W	Water depth (m)
GF 1	3906-8	07°25.0′ S	28°07.9′	10
GF 2	3906-8	07°25.0′ S	28°07.9′	25
GF 3	3906-8	07°25.0′ S	28°07.9′	50
GF 4	3906-8	07°25.0′ S	28°07.9′	700
GF 5	3906-8	07°25.0′ S	28°07.9′	1200
GF 6	3906-8	07°25.0′ S	28°07.9′	2000
GF 7	3906-8	07°25.0′ S	28°07.9′	3000
GF 8	3906-8	07°25.0′ S	28°07.9′	4000
GF 9	3906-8	07°25.0′ S	28°07.9′	5000
GF 10	3907-10	03°54.9′ S	25°36.6′	10
GF 11	3907-10	03°54.9′ S	25°36.6′	25
GF 12	3907-10	03°54.9′ S	25°36.6′	50
GF 13	3907-10	03°54.9′ S	25°36.6′	100
GF 14	3907-10	03°54.9′ S	25°36.6′	200
GF 15	3907-10	03°54.9′ S	25°36.6′	700
GF 16	3907-10	03°54.9′ S	25°36.6′	1200
GF 17	3907-10	03°54.9′ S	25°36.6′	3000
GF 18	3907-10	03°54.9′ S	25°36.6′	3950
GF 19	3907-10	03°54.9′ S	25°36.6′	4950
GF 20	3908-3	00°02.7′ S	23°27.9′	25
GF 21	3908-3	00°02.7′ S	23°27.9′	50
GF 22	3908-3	00°02.6′ S	23°27.9′	100
GF 23	3908-3	00°02.7′ S	23°27.9′	200
GF 24	3908-3	00°02.7′ S	23°27.9′	400
GF 25	3908-3	00°02.7′ S	23°27.9′	675
GF 26	3908-3	00°02.7′ S	23°27.9′	1150
GF 27	3908-3	00°02.7′ S	23°27.9′	3000
MUC 1	3906-9	07°28.0′ S	28°06.4′	4886
MUC 2[b]	3906-9	07°28.0′ S	28°06.4′	4886
MUC 3	3908-11	00°00.4′ S	23°25.7′	3693
MUC 4	3909-1	03°32.9′ S	36°16.2′	3174
MUC 4[b]	3909-1	03°32.9′ S	36°16.2′	3174
MUC 5	3910-3	04°14.7′ S	36°20.8′	2361
MUC 6	3911-1	04°36.8′ S	36°38.1′	826
MUC 7	3912-2	03°40.0′ S	37°43.1′	772
MUC 8	3913-2	02°53.8′ S	38°18.6′	2289
MUC 9	3915-1	02°16.8′ S	38°00.9′	3127
MUC 10	3916-1	01°41.9′ N	48°26.0′	37

Table 46 continued

Sample No.[a]	Station	Latitude S/N	Longitude W	Water depth (m)
MUC 11	3918-1	03°42.3` N	50°24.3´	52
MUC 12	3925-2	05°08.6´ N	47°31.8´	3198
ISP 1	3925-5	05°07.9´ N	47°30.4´	100
ISP 2	3925-5	05°07.9´ N	47°30.4´	400
ISP 3	3925-1	05°08.6´ N	47°31.7´	700
ISP 4	3925-1	05°08.6´ N	47°31.7´	1200
WA 6/upper 1-20	3906-1	07°27.4´ S	28°08.4´	544
WA 6/lower 1-20	3906-1	07°27.4´ S	28°08.4´	4410
WA 7/upper 1-20	3907-1	03°58.6´ S	25°40.6´	854
WA 7/lower 1-20	3907-1	03°58.6´ S	25°40.6´	4630
WA 8/upper 1-20	3908-7	00°00.5´ N	23°26.5´	718
WA 8/lower 1-20	3908-7	00°00.5´ N	23°26.5´	3204

[a] abbreviations in Table 46:

MP, membrane pump; WS, Niskin-bottle sampler, GF, GoFlo-water sampler; MUC, multicorer; ISP, *In situ* pumps; WA, West Atlantic mooring.

[b] sediment sample, uppermost layer.

5.4.6 *In situ* Particle Camera System, PARCA

(V. Ratmeyer)

For measuring the vertical particle concentration, size distribution and aggregate composition in the water column a high-resolution fotographic camera system was used (RATMEYER and WEFER, 1996). It was designed and improved in consideration of similar systems used by HONJO et al. (1984), ASPER (1987) and LAMPITT (1985). This method provides *in situ* information on the origin and abundance of particles and aggregates ("Marine Snow"). In addition to the use of sediment traps, particle flux can be measured even in areas or depths with high lateral transport.

The aim of deployment to different depths between 1000 and 3000 m was to observe the deep-sea particle population and possible lateral advection of particle clouds from the continental shelf towards the open ocean. Abundance profiles were made on two of the mooring stations as well at three different sites close to the continental shelf of Guyana. (Tab. 47). The pictures show variable particle and plankton concentrations, with maximal concentrations in the upper 100 m. This correlates to previous measurements with particle camera and chlorophyll sensors in the Brazil Basin (RATMEYER and WEFER, 1996). Various known species of plankton and macroplankton can be identified on the images, including foraminifera, radiolaria, copepods and medusa. Particle and aggregate sizes vary

from 80 µm to > 20 cm. Largest aggregates were found on profile 4 (site GeoB 3926-1), above the continental slope off Guyana, with fractal shapes of marine snow and stringers. Also, highest particle concentrations were found at this site. Quantitative analysis of concentration, shape and size of particles will be performed using a PC-based image analysis system.

The ParCa system consists of the following components:

For best optical resolution we used a 70 mm deep-sea camera (model PHOTOSEA 70) with max. 45.7 m film capacity. Two 150 Ws (model PHOTOSEA 1500S/1500SD) strobelights were installed as light sources. The illuminating beam was collimated by a combination of highly refractive fresnel-lenses mounted inside a steelframe at the focal distance in front of the strobes. Camera and light source consisting of two flashlights plus collimator were installed in orthogonal position, thus avoiding backscatter of water molecules and highly hydrated particles. Power source is a 24V/38Ah rechargeable lead battery designed for the use to full ocean depth. Maximum operation depth is 6000 m for the complete system. The system is fixed inside a frame of the dimension 200 x 200 x 120 cm, which is made of 48 mm hot galvanized steel pipe. Pipes mounted close to the probe volume are painted black to avoid backscatter. The complete system weight is approximately 300 kg in air. Camera and the strobe-collimator units can be slided to any position inside the frame for correct justification. The camera was triggered by a computer on deck of the ship. Communication with the ship is performed by two micro-computers inside the ParCa system, allowing different exposure programs to be run during profiling and moored deployment. Pictures were exposed while lowering the system with a speed of 0.3 m s^{-1}. The flash duration of < 1/2.000 second was short enough to get sharp pictures of particles down to a size of 80 µm using Kodak Tri X Pan Film.

Tab. 47: Deployment data of the ParCa system

Station GeoB	Water depth (m)	Profile depth (m)	Trigger (m)
3907-8	5558	2000	10
3908-2	3609	3000	10
3925-10	3186	1000	5
3926-1	1116	1000	10
3929-1	3195	2000	10

5.4.7 Particle Collection with Sediment Traps

(G. Ruhland, V. Ratmeyer, G. Fischer)

Table 48 lists deployment and recovery data for all moorings as well as the sampling data of the traps. During cruise M34/4, three moorings were recovered and deployed afterwards at the same position (see cruise track, Fig. 4). The moorings were located in the oligotrophic northern Brazil Basin and in the higher productive western eqatorial upwelling region. The arrays were equipped each with two multisample traps and one current meter. All moorings are planned to be recovered by RV METEOR (M38/1) in February, 1997.

On March 21th, the mooring WA6 was recovered successfully at a site located in the lower productive subtropical gyre. This mooring array was equipped with two multisample traps in 544 and 4410 m water depth and one current meter in 569 m. All instruments had worked perfectly. Both traps had been programed for a 28 day sampling interval for each bottle starting at August 18, 1994. The traps provided two complete sample series showing flux maxima in summer and fall with clearly lower fluxes to the deeper waters (Fig. 210a). On March 22th, the mooring array was deployed again as WA9 at the same position. The traps have been scheduled for a 17 day sampling interval starting March 23, 1996.

The mooring WA7 has been recovered on March 23th. This mooring array was deployed during M29/3 in an area between the oligotrophic site represented by WA6 and the western equatorial upwelling area where WA8 was deployed. Both traps (854 m, 4630 m) worked fine as well as the moored current meter. Fluxes again peaked in late summer (Fig. 210b). On March 24th, the mooring WA10 was redeployed with similar equipment. Additionally, an inclinometer has been installed on the upper trap.

Tab. 48: Mooring data for recoveries and redeployments

Mooring	Position	Water depth (m)	Interval	Instr.	Depth (m)	Intervals (no x days)
Mooring recoveries during M34-4:						
BRAZIL BASIN / WESTERN EQUTORIAL ATLANTIC						
WA6	07°28.3'S 28°07,4'W	4950	18.08.94 29.02.96	S/MT 234 S/MT 234 RCM 8 569	544 4410	20x28 20x28
WA7	03°58.0'S 25°39.0'W	5601	20.08.94 29.02.96	S/MT 230 S/MT 230 RCM 8 879	854 4630	19x28 (+1x26) 19x28 (+1x26)
WA8	00°01.4'N 23°27.1'W	3744	25.08.94 29.02.96	S/MT 230 S/MT 230 RCM 8 743	718 3204	19x28 (+1x21) 19x28 (+1x21)
Mooring deployments during M34-4:						

BRAZIL BASIN / WESTERN EQUATORIAL ATLANTIC

WA9	07°28.0'S 28°08.5'W	4996	23.03.96 26.02.97	S/MT 234 S/MT 230 RCM 8	591 4456 615	20x17 20x17
WA10	03°54.7'S 25°41.0'W	5555	25.03.96 26.02.97	S/MT 234 S/MT 234 RCM 8 S/MT 105	800 4585 824 800	19x17 (+1x15) 19x17 (+1x15)
WA11	00°00.1'S 23°24.7'W	3860	27.03.96 26.02.97	S/MT 230 S/MT 230 RCM 8	834 3319 858	19x17 (+1x13) 19x17 (+1x13)

Instruments used:

S/MT 230	= Sediment trap S/MT 230 Aquatec Meerestechnik, Kiel
S/MT 234	= Sediment trap S/MT 234 Aquatec Meerestechnik, Kiel
S/MT 105	= Inclinometer S/MT 105 Aquatec Meerestechnik, Kiel
RCM 8	= current meter Aanderaa, RCM 8

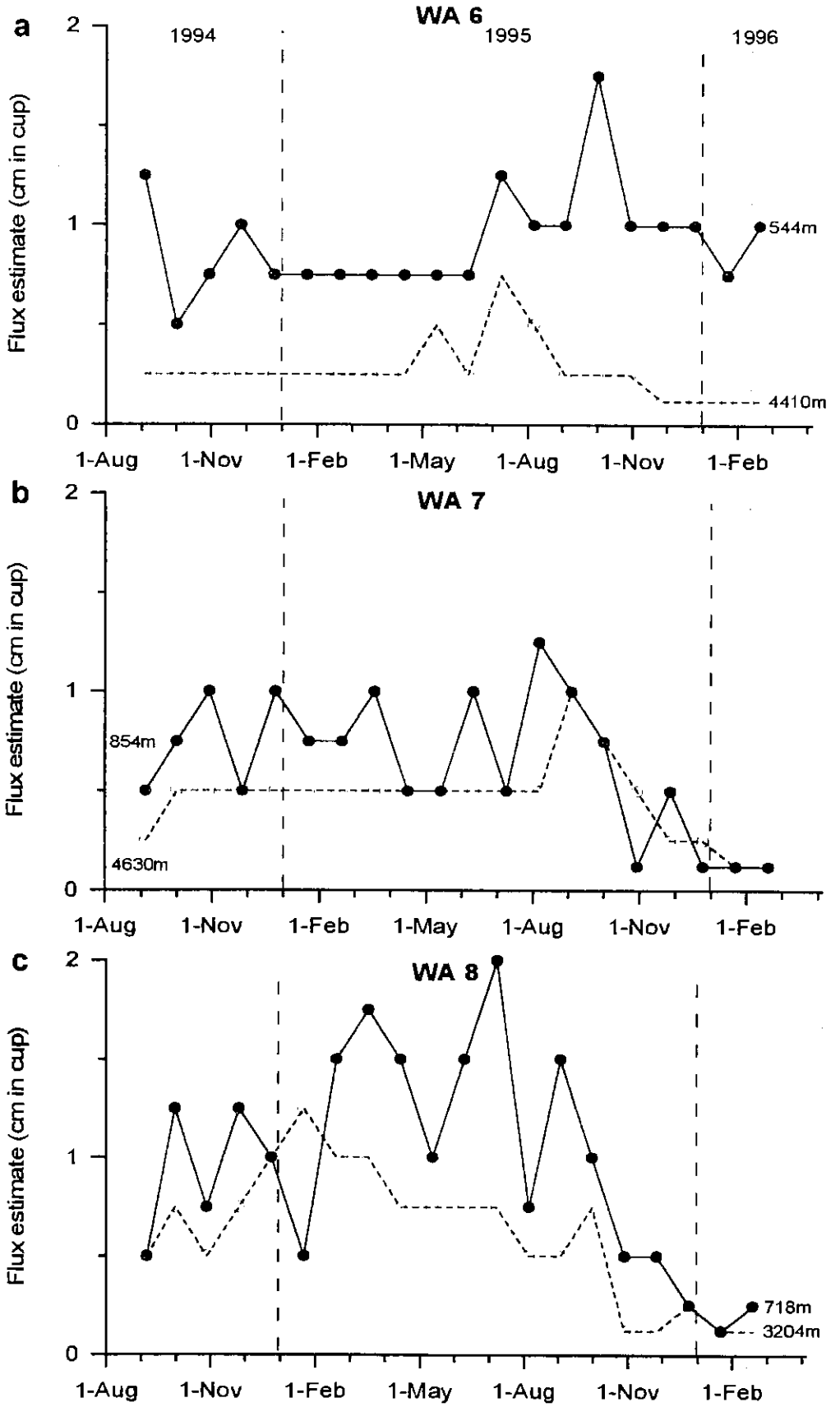

Fig. 210: Flux estimates (cm sediment in trap cup) at the mooring sites WA6 (a), WA7 (b) and WA8 (c). For locations see Fig. 4.

On March 26th, the mooring WA8 was completely recovered. This mooring was located in the western equatorial upwelling area. The two moored traps worked well and provided two sample sets of 20 samples each. Seasonality and absolute fluxes were highest at this site which is located in the more eutrophic equatorial upwelling band; highest fluxes were observed in spring and summer (Fig. 210c). The current meter did not register data due to a malfunction. At the same day a similar mooring named WA11 was deployed at the same position.

5.4.8 Marine Geology, Sediment Cores

(R. Schneider, H. Arz, E. Costa, V. Diekamp, I. Engelbrecht, A. Figueiredo, M. v. Herz, H. Kinkel, G. Ruhland, B. Schlünz)

During this cruise we used box corer (2x), multicorer (20x) and gravity corer (22x) in order to recover surface and late Quaternary sediments (between 35 and 3300 m) from the continental slope off Northeast Brasil, from the Amazon estuary and fan, and from the Caribbean continental slope off Barbados. The coring locations and related water depths are given in the station list (chapter 7.4.1). This table also shows the devices used for our program at all stations and the core lengths recovered.

5.4.8.1 Multicorer and Box Corer Samples

The multicorer is designed to recover undisturbed surface sediment sections and the overlying bottom water. The model used on M34/4 was equipped with 4 small plastic tubes and 8 larger tubes (6 and 10 cm in diameter). At most of the stations 10 to 12 tubes were filled with the uppermost 15 to 35 cm of sediment and the superimposed bottom water (Tab. 49). Only at station GeoB 3917 the multicorer failed three times due to a hardground (pieces of beachrock recovered with the gravity corer) at the sediment surface. Depending on recovery the tubes were sampled as follows:

- 1 large tube, cut into 1 cm thick slices for the investigations of dinoflagellates,
- 1 large and 1 small tube, cut into 1 cm slices and frozen for organic carbon (TOC) geochemistry and microscopy, respectively,
- 2 large tubes, cut in 1 cm slices for investigation of foraminiferal composition,
- 2 large tubes for pore water analysis, oxygen consumption and mineralogy,
- 1 large tube for nitrogen isotopes on porewater and sedimentary organic carbon,
- 1 small tube, cut in 1 cm slices for paleomagnetic studies,
- 1 small tube for clay mineralogy,
- 1 large and 1 small tube as frozen archive cores,

- 50 ml bottom water samples for stable carbon and oxygen isotopes were taken at all stations, while at selected sites several liters of bottom water were sampled for investigations of bacteria and nitrogen isotopes.

The box corer was used at two stations off the Amazon (GeoB 3919-1 and 3920-1) in order to sample expected oolithes and coarse sands. From the retrieved sediments surface photos were taken. The sediment at Station GeoB 3919-1 was subsampled with 3 multicorer tubes, which afterwards were cutted into 2 cm slices for stratigraphic, mineralogical and geochemical analysis (A. Figueiredo). Two extra bulk samples from this box corer were sealed in plastic bags. The box corer from Station GeoB 3920-1, containing a ferromanganese hardground at the sediment surface, was subsampled with four core-liner tubes which will be sampled according to the gravity corer sampling scheme onshore.

Tab. 49: Multicorer Samples

Station GeoB	Water depth (m)	Core length (cm)	TOC & Water (ml)	Dino-flagell.	Foram.	Clay miner.	Magn. facies	Archive frozen	N-Isot.	Bottom water, N-Isot. & Bact.	Pore water Chem.
3906-9	4886	30	2, 2x50	1	2	---	---	2	1	x	2
3908-11	3693	16	2, 2x50	1	2	1	1	2	1	x	2
3909-1	3174	34	2, 2x50	1	2	1	1	2	1	x	2
3910-3	2361	32	2, 2x50	1	2	1	1	2	---	x, only	2
3911-1	826	33	2, 2x50	1	2	1	1	1	---	x, only	2
3912-2	772	12	2, 2x50	1	2	1	1	2	---	x, only	---
3913-2	2264	13	2x50	1	2	---	---	1	---	x, only	---
3914-	2461	25	2, 2x50	1	1	---	---	1	1	x	1
3915-1	3127	34	2, 2x50	1	2	---	1	2	1	x	2
3916-1	37	34	2+C14	1	2	1	1	2	1	x	---
3918-1	52	25	1	1	1	1	1	1	---	x, only	2
3925-2	3198	25	2, 2x50	1	1	1	1	1	1	x	2
3935-1	1554	37	2, 2x50	1	2	1	1	2	---	---	---
3936-2	1854	35	2, 2x50	1	2	1	1	3	---	---	---
3937-1	1654	32	2, 2x50	1	2	1	1	1	---	---	---
3938-2	1972	33	2, 2x50	1	2	1	1	2	---	---	---
3939-1	2467	31	2, 2x50	1	2	1	1	2	---	---	---

5.4.8.2 Gravity Cores

5.4.8.2.1 Sampling

With the gravity corer sediment cores between 4.00 and 8.80 m core length were taken at 22 stations (chapter 7.4.1). During M34/4 altogether 136 m of sediments were recovered with this device. Before using the coring tools, the liners were marked with a straight line lengthwise, in order to be able to sample the core segments afterwards in the same orientation, in particular for paleomagnetic purposes. When the core was retrieved on deck, the core liners were cut into 1-m segments, closed with caps at both ends and inscribed (Fig. 211).

All cores were cut along-core in two half pieces: one Archive and one Work half. The sediments were described, smear-slide samples were taken from distinctive layers and spectrophotometric measurements were carried out on the Archive half, which was stored in a cool room at +4°C after taking a photo. For color scanning a Minolta CM - 2002 hand-held spectrophotometer was used to measure percent reflectance values of sediment colour at 31 wavelength channels over the visible light range (400-700 nm). The digital reflectance data of the spectrophotometer readings were routinely obtained from the surfaces of split archive halfs immediately after core opening to provide a continous record of the sediment color variation. The surfaces of all core segments were scraped with a knife to expose a fresh, unsmeared surface for measurements at 2 cm intervals. A thin, transparent plastic film (Hostaphan) was used to cover the wet surface of the sediment to protect the photometer from being soiled. Before measuring each core the spectrophotometer was calibrated for white color reflectance by attaching a white calibration cap. The spectrophotometer readings were transfered to a personal computer and a graphic representation for selected wave band reflection (450, 550, and 700 nm) in each core is given in the following section.

From the Work-Half three parallel series of syringe samples (10 ccm) and 1 cm thick half-round samples were taken at a depth interval of 5 cm. These samples were taken for the measurements and determination of physical properties, stable isotopes, foraminiferal and dinoflagellate assemblages, as well as for mineralogy and organic geochemistry. One additional syringe sample series was taken in 20 cm intervals in order to get a first impression about the composition of planktonic foraminifera and changes in sand content for each core, whilst onboard. On selected cores the carbonate content was determined at 5 cm intervals.

Cores obtained for pore water analysis are indicated as geochemistry cores in chapter 7.4.1. They were sampled as described in section 5.4.9 and frozen afterwards.

Inscription:

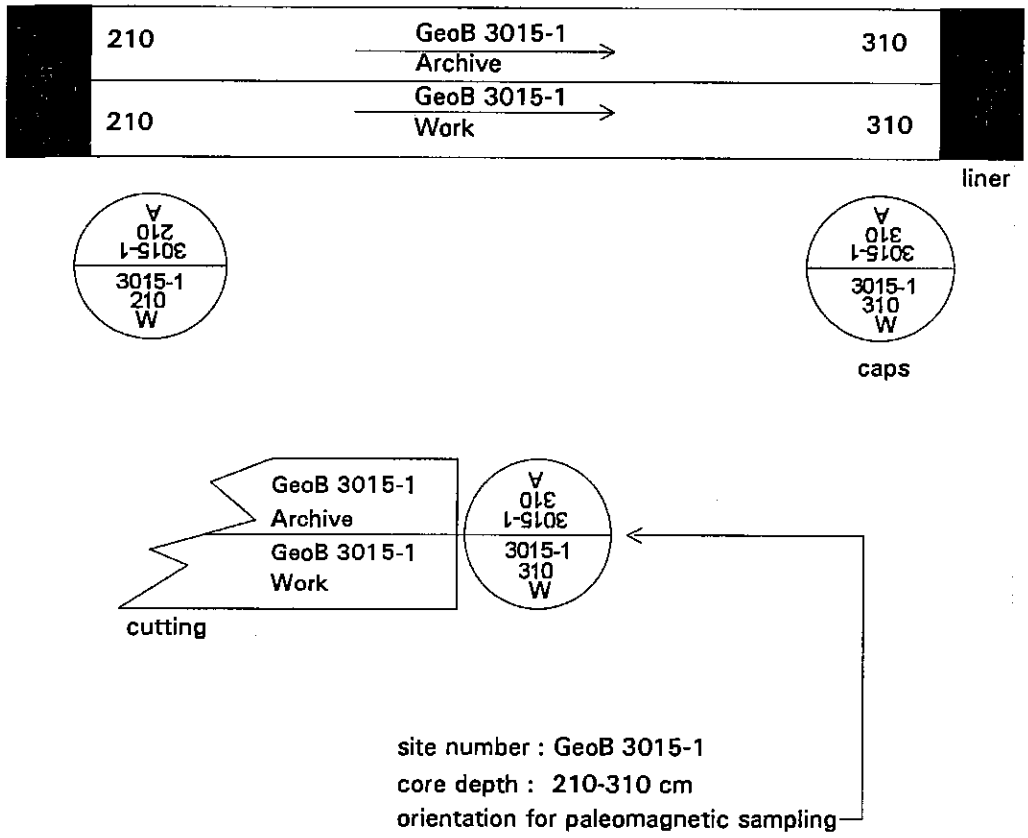

Fig. 211: Scheme of the inscription of gravity core segments.

5.4.8.2.2 Lithologic Core Summary

(H. Arz, H. Kinkel, B. Schlünz, R. Schneider)

This preliminary lithologic summary of the sediments retrieved with the gravity corer is based on visual description, and colour scanner readings, as well as microscopic inspection of stratigraphy samples and smear slides taken from distinctive sediment horizons. Core descriptions are shown in Figures 212 to 221 (legend for stratigraphic columns is shown in Fig. 222), presenting main lithologies, their colour according to the MUNSELL soil colour chart, sedimentary structures, and if already determined the carbonate content. Stratigraphic information was obtained from the foraminiferal assemblages, using the *Globorotalia menardii* and *Pulleniatina obliqueloculata* as biostratigraphic markers according to ERICSON and WOLLIN (1968) and to DAMUTH (1975), respectively. For correlation colour scanner readings of distinctive wave length bands (450, 550, 700 nm) are also shown. It is likely, that these colour changes result from variations in the sediment composition - particularly the ratio of carbonate or silicate (light and high reflection values) to organic residue and clay mineral (dark or low reflection values) content. The lithological data are primarily based on smear slide analysis. The main purpose was to describe all representative lithologies and special or unique layers of particular interest.

A first measure of sediment grain size variation is provided by the sand content reported in Figures for each core (Figs. 223-228). Cores GeoB 3935-2, 3936-1, 3937-2, 3938-1, 3939-2 were not opened onboard and are thus, not included in this summary.

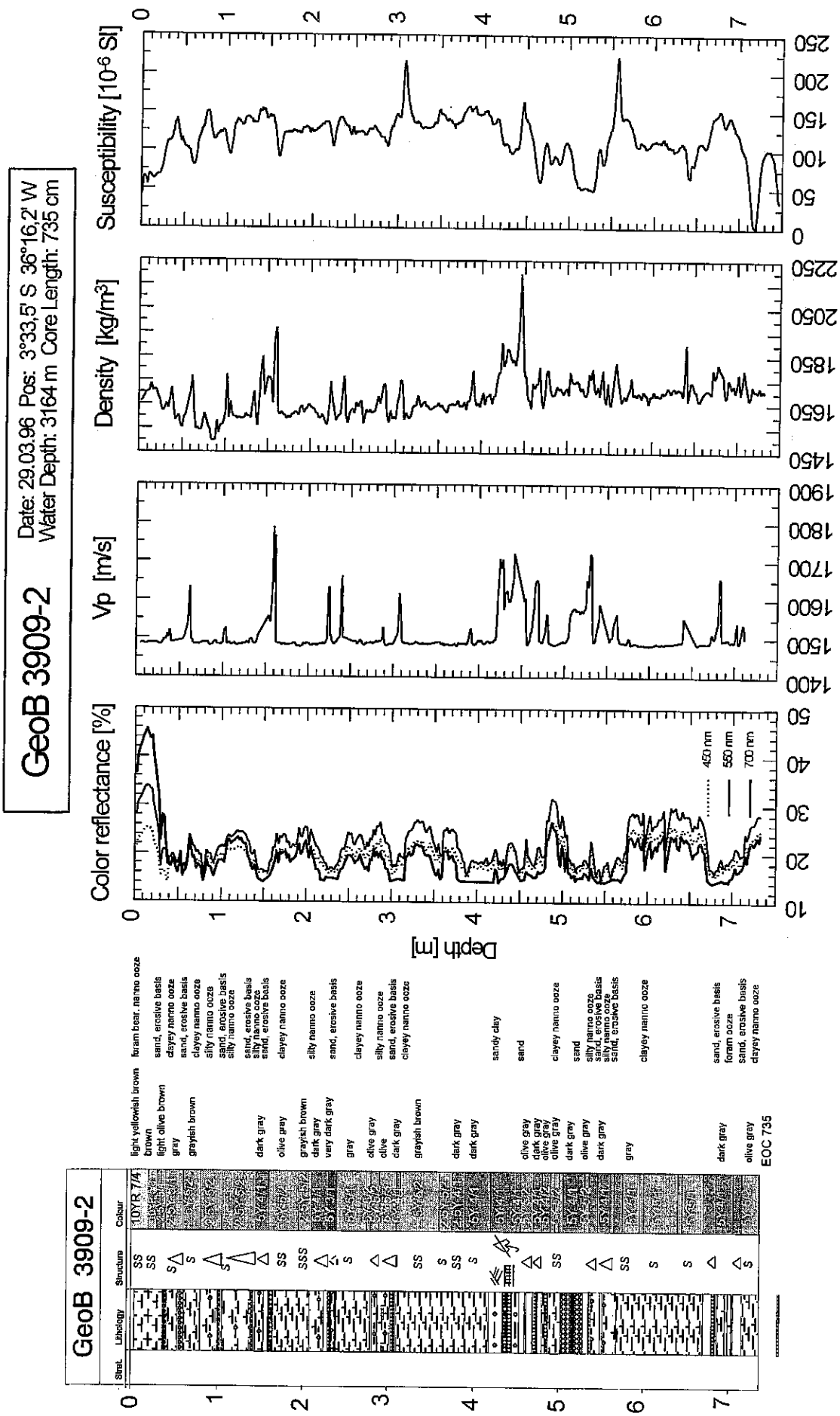

Fig. 212: Sediment descriptions, colour reflectance, and physical properties studies (Vp, density, susceptibility) for the gravity core GeoB 3909-2.

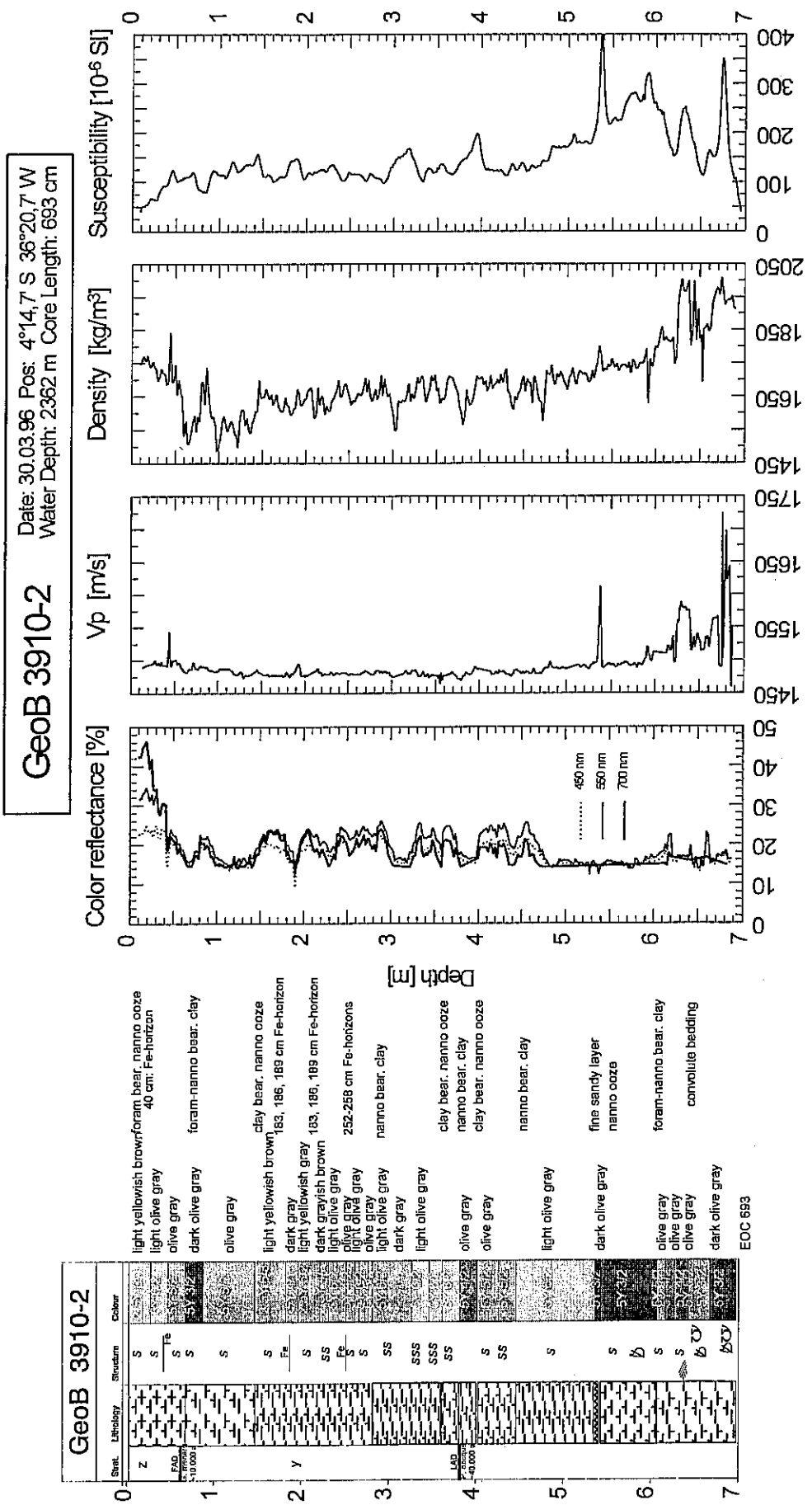

Fig. 213: Sediment descriptions, colour reflectance, and physical properties studies (Vp, density, susceptibility) for the gravity core GeoB 3910-2.

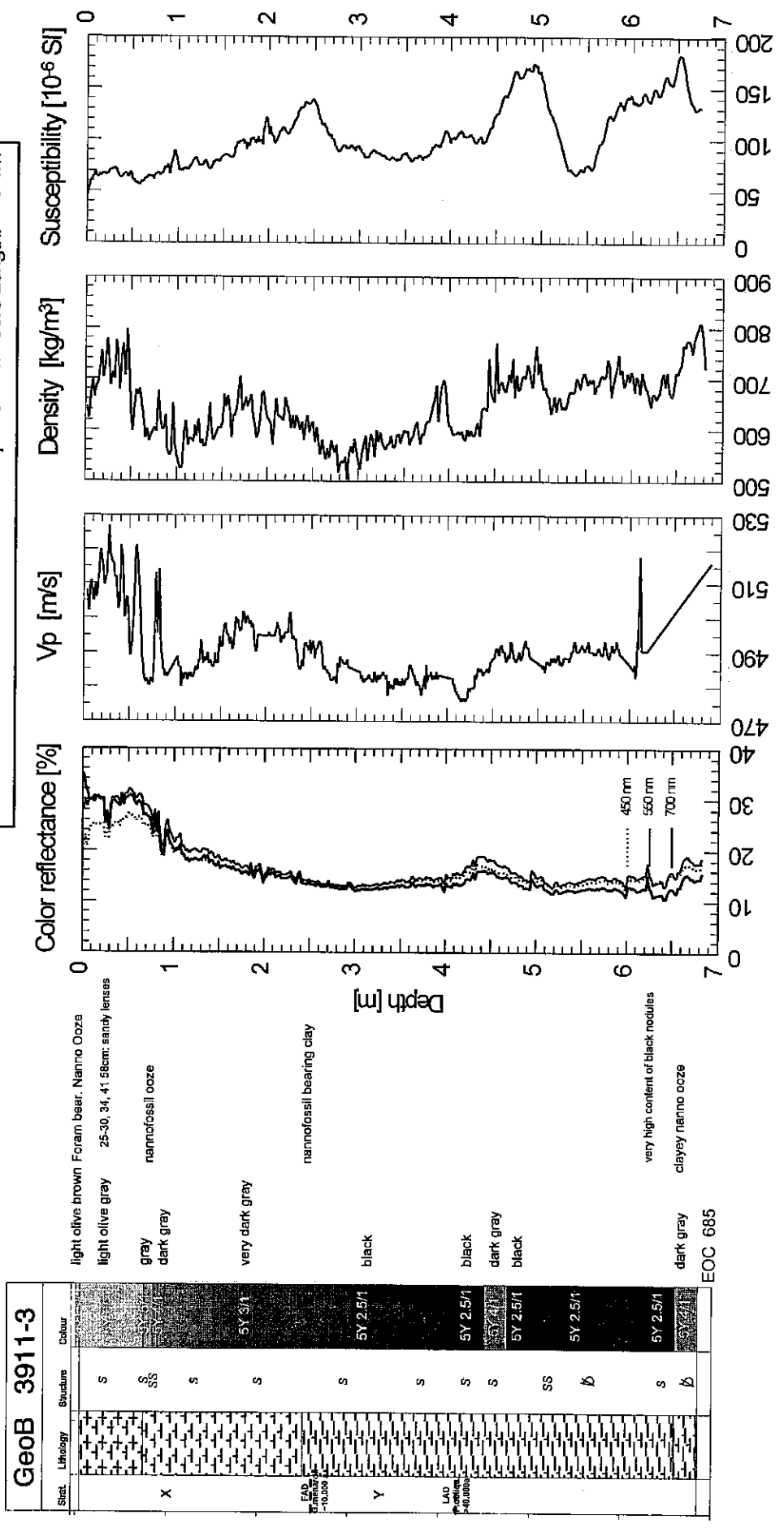

Fig. 214: Sediment descriptions, colour reflectance, and physical properties studies (Vp, density, susceptibility) for the gravity core GeoB 3911-3.

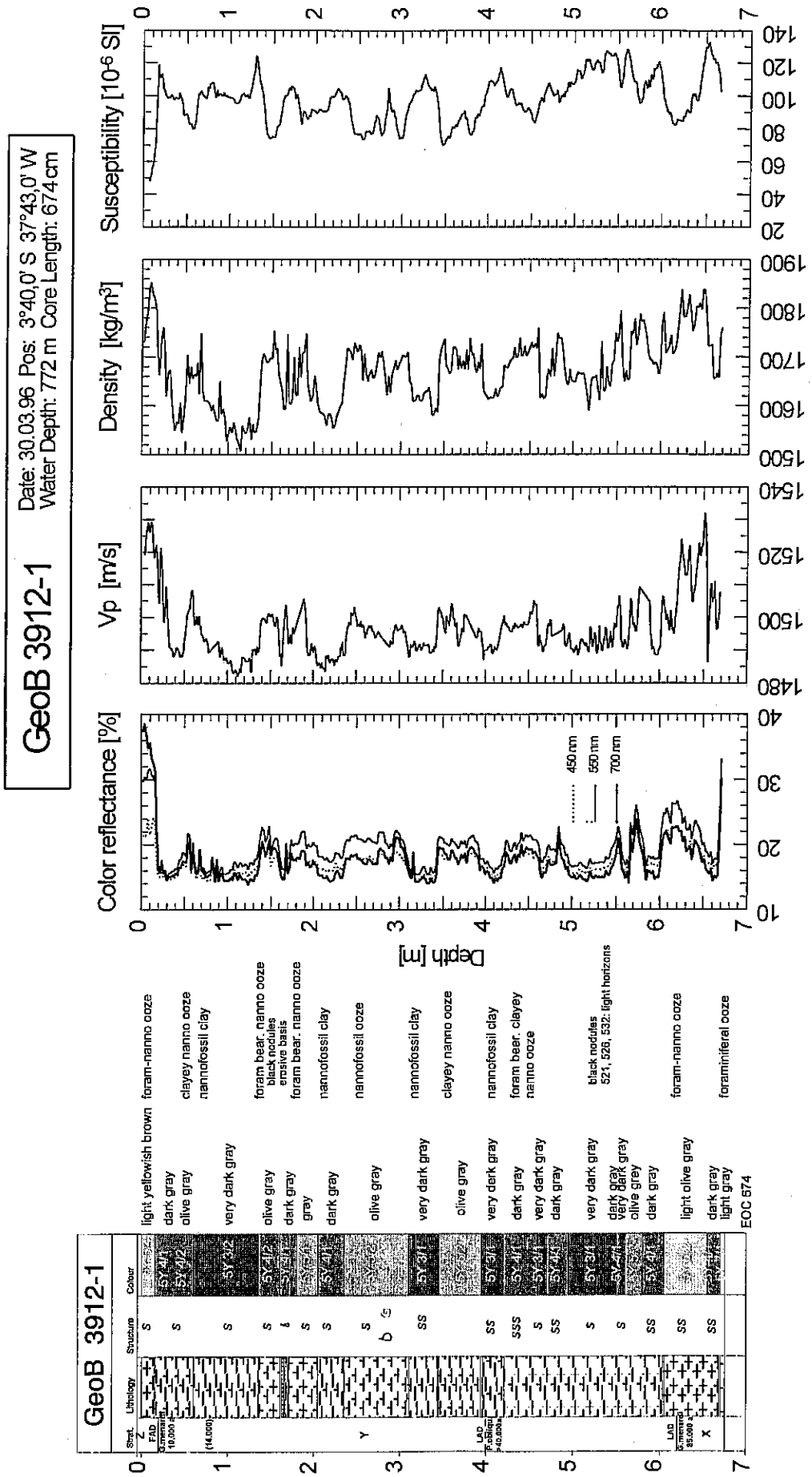

Fig. 215: Sediment descriptions, colour reflectance, and physical properties studies (Vp, density, susceptibility) for the gravity core GeoB 3912-1.

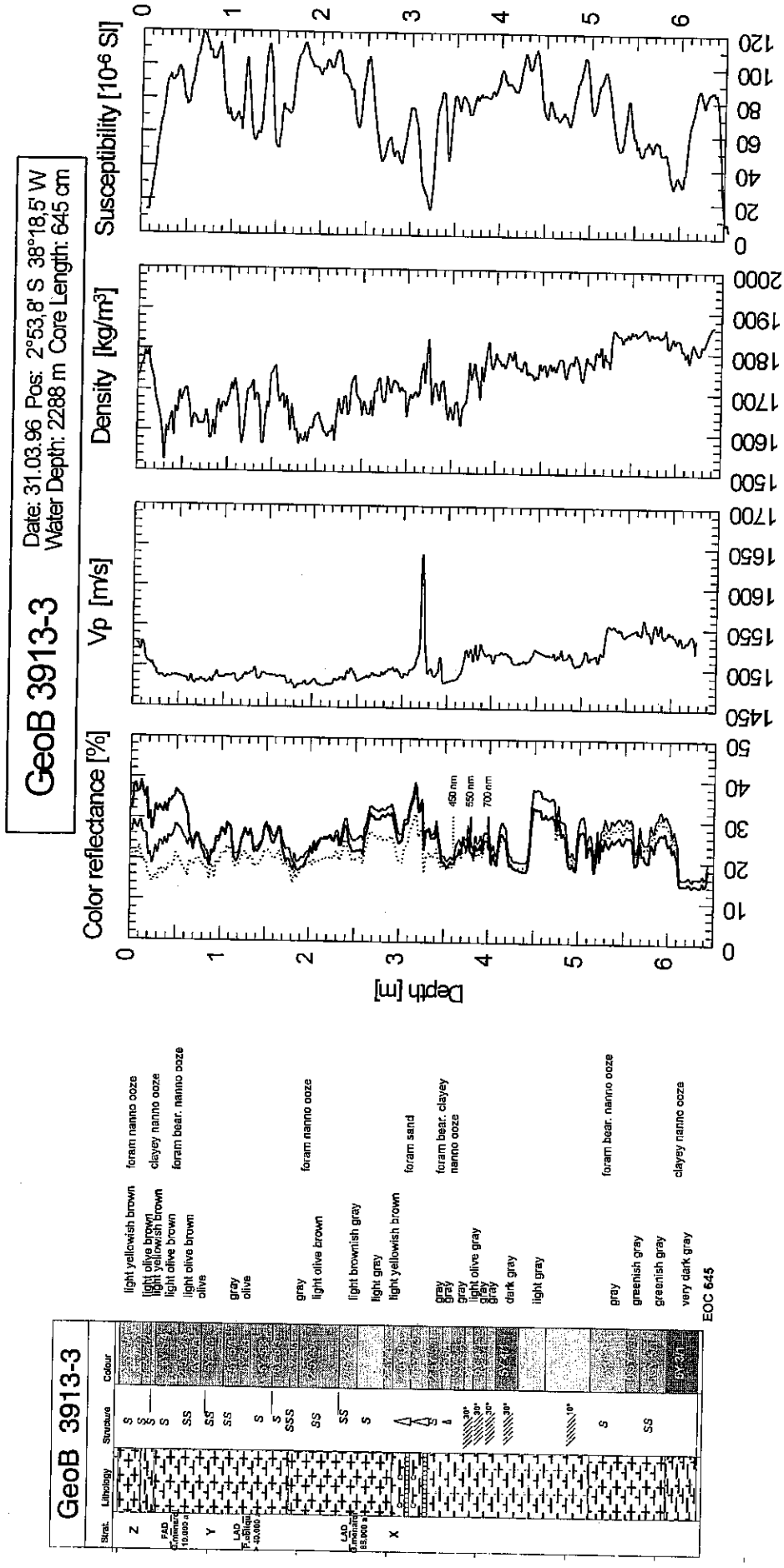

Fig. 216: Sediment descriptions, colour reflectance, and physical properties studies (Vp, density, susceptibility) for the gravity core GeoB 3913-3.

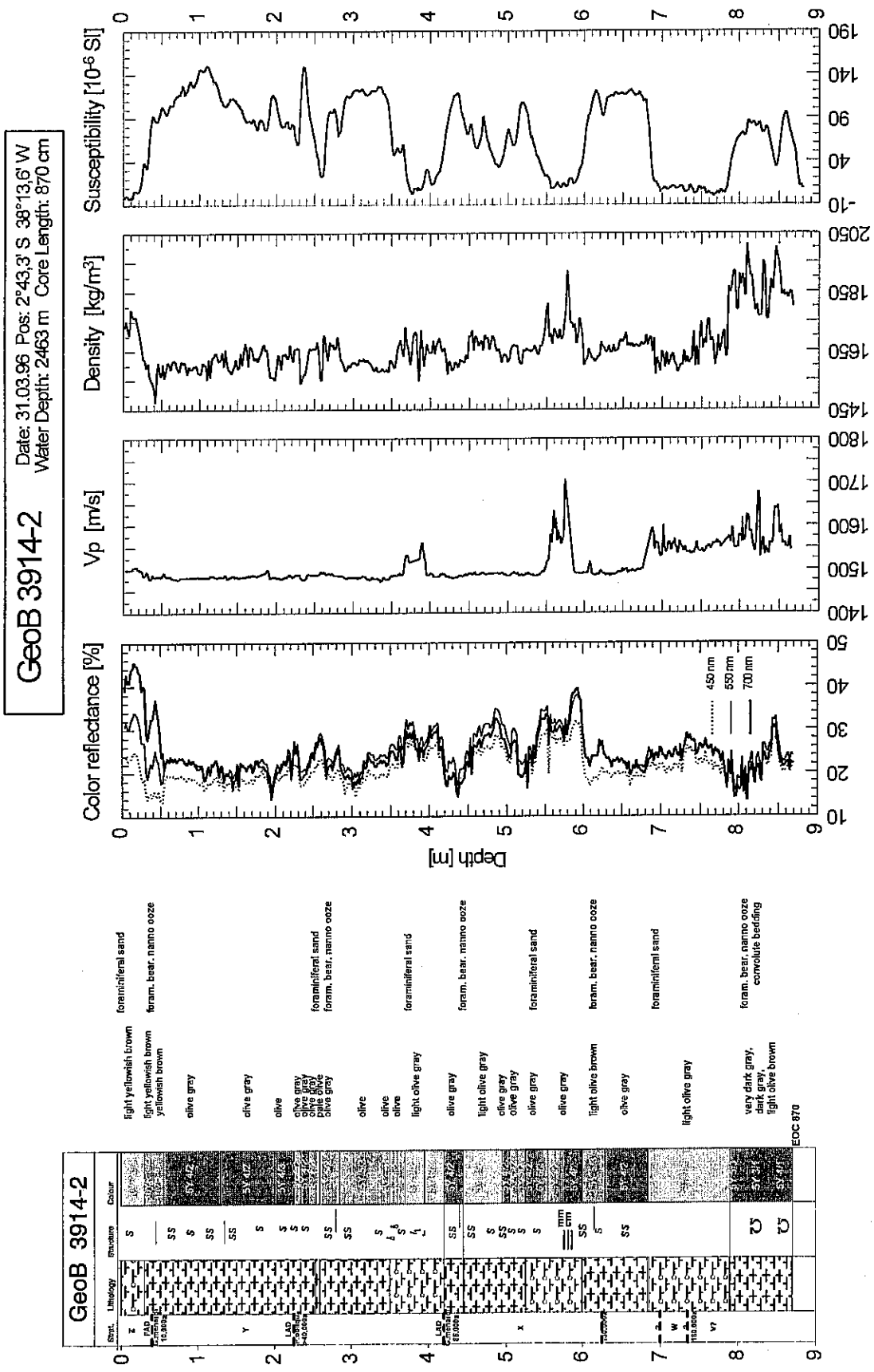

Fig. 217: Sediment descriptions, colour reflectance, and physical properties studies (Vp, density, susceptibility) for the gravity core GeoB 3914-2.

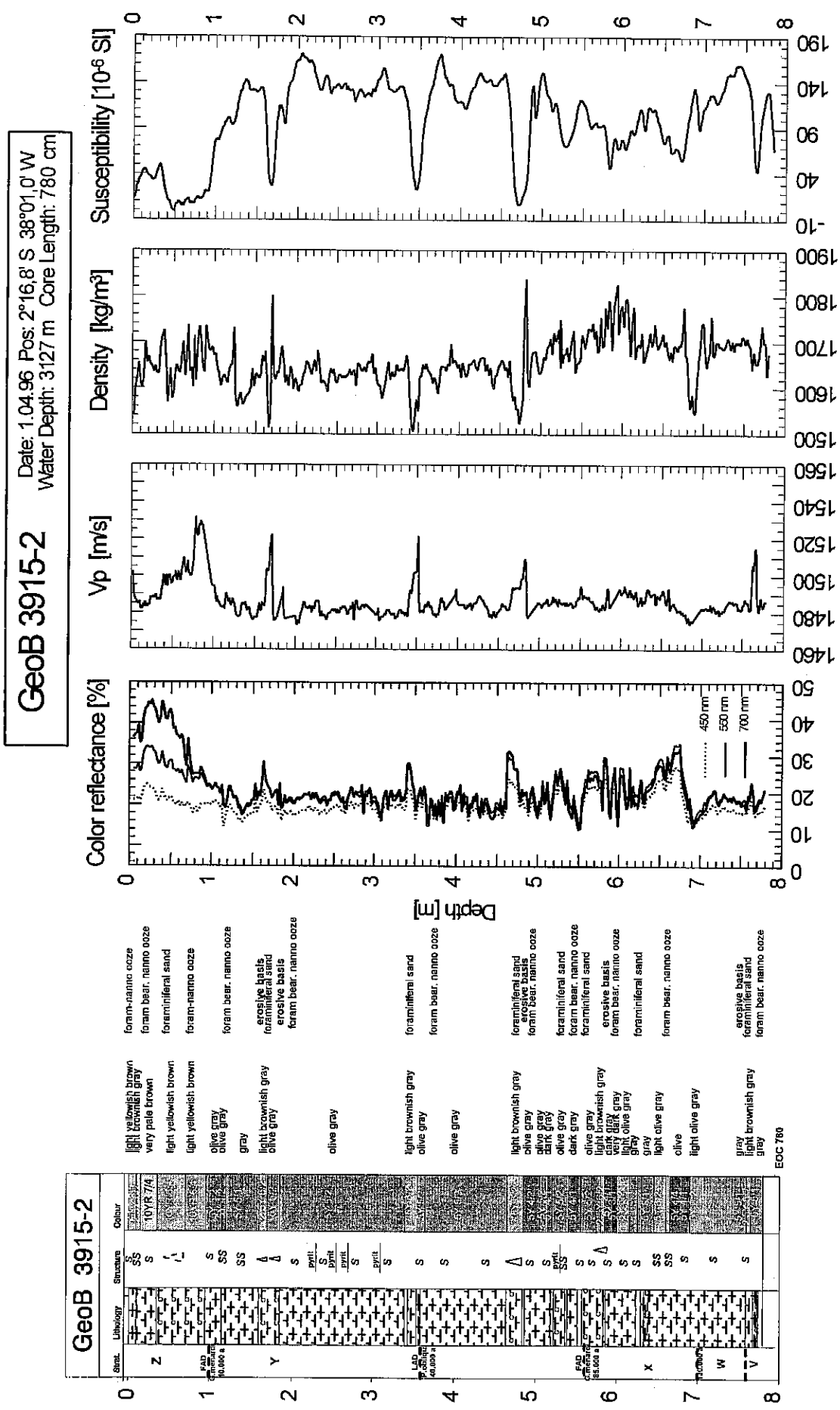

Fig. 218: Sediment descriptions, colour reflectance, and physical properties studies (Vp, density, susceptibility) for the gravity core GeoB 3915-2.

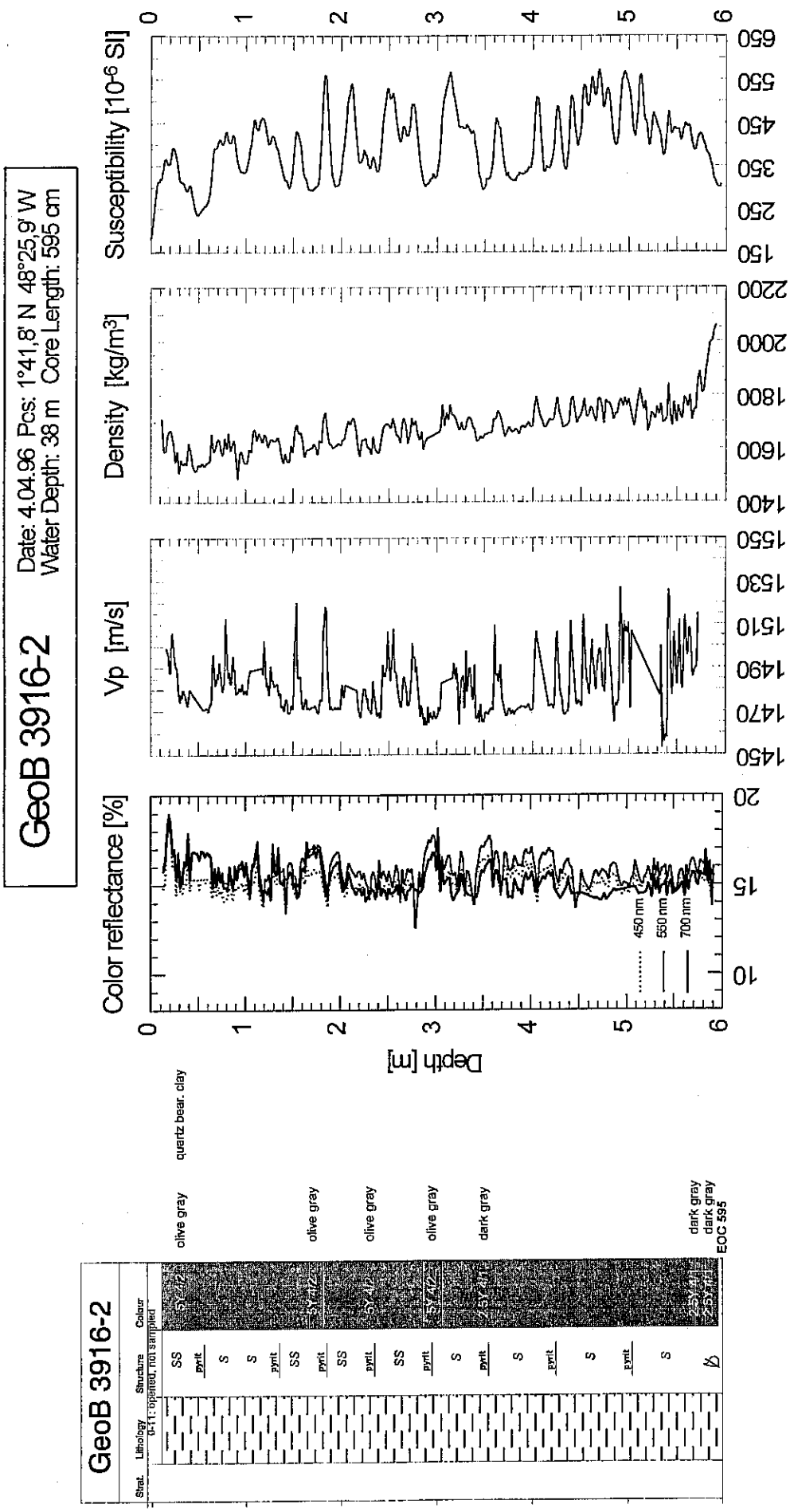

Fig. 219: Sediment descriptions, colour reflectance, and physical properties studies (Vp, density, susceptibility) for the gravity core GeoB 3916-2.

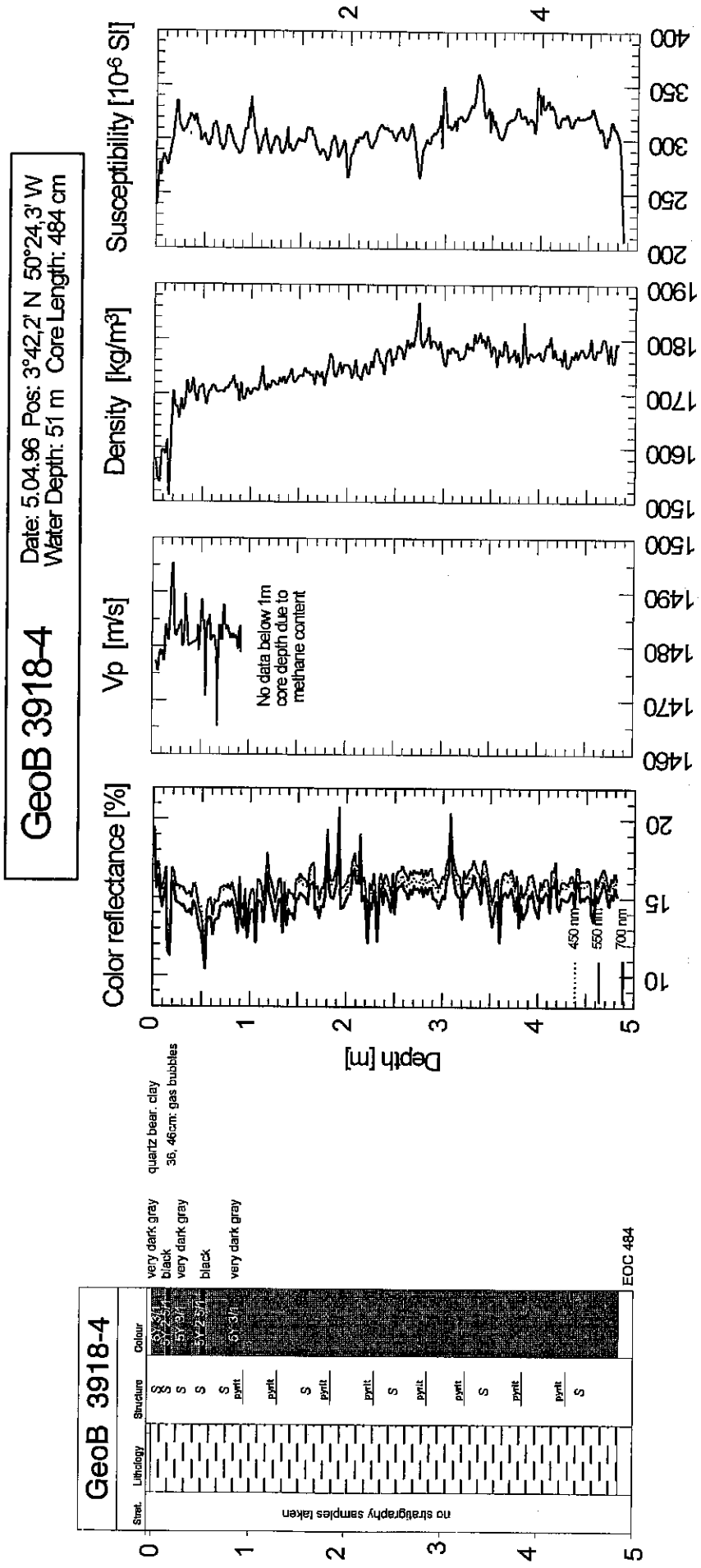

Fig. 220: Sediment descriptions, colour reflectance, and physical properties studies (Vp, density, susceptibility) for the gravity core GeoB 3918-4.

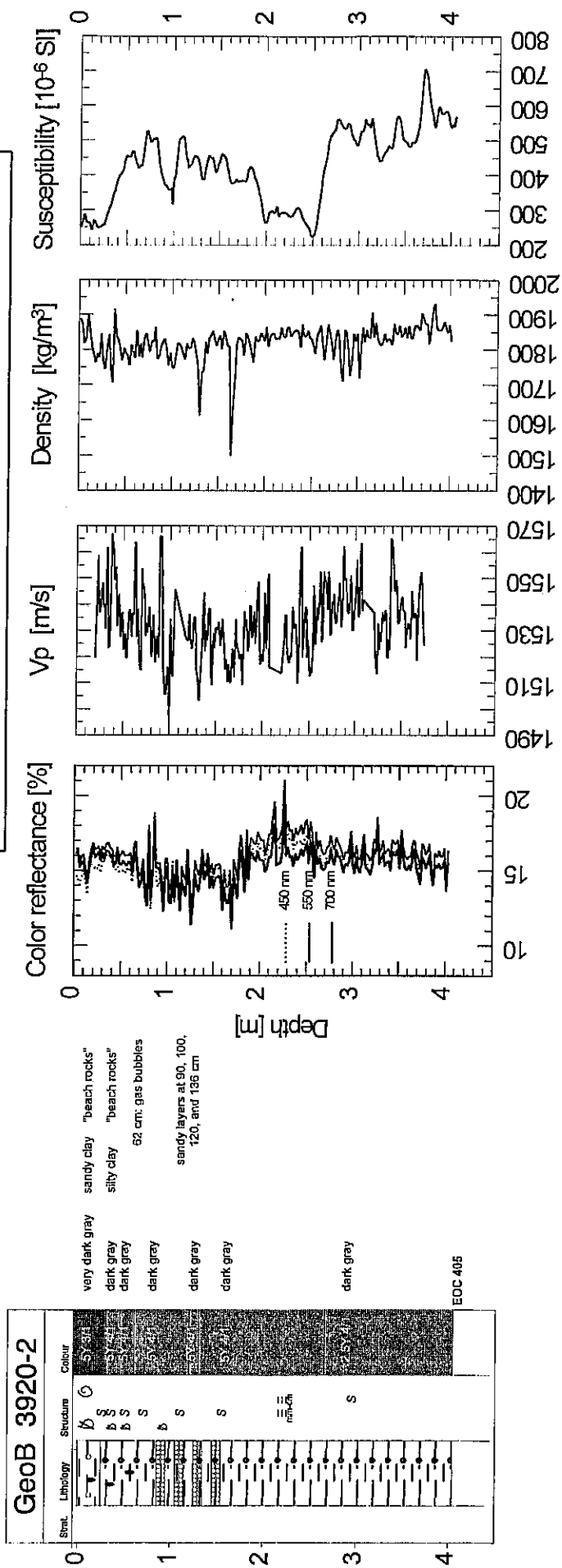

Fig. 221: Sediment descriptions, colour reflectance, and physical properties studies (Vp, density, susceptibility) for the gravity core GeoB 3920-2.

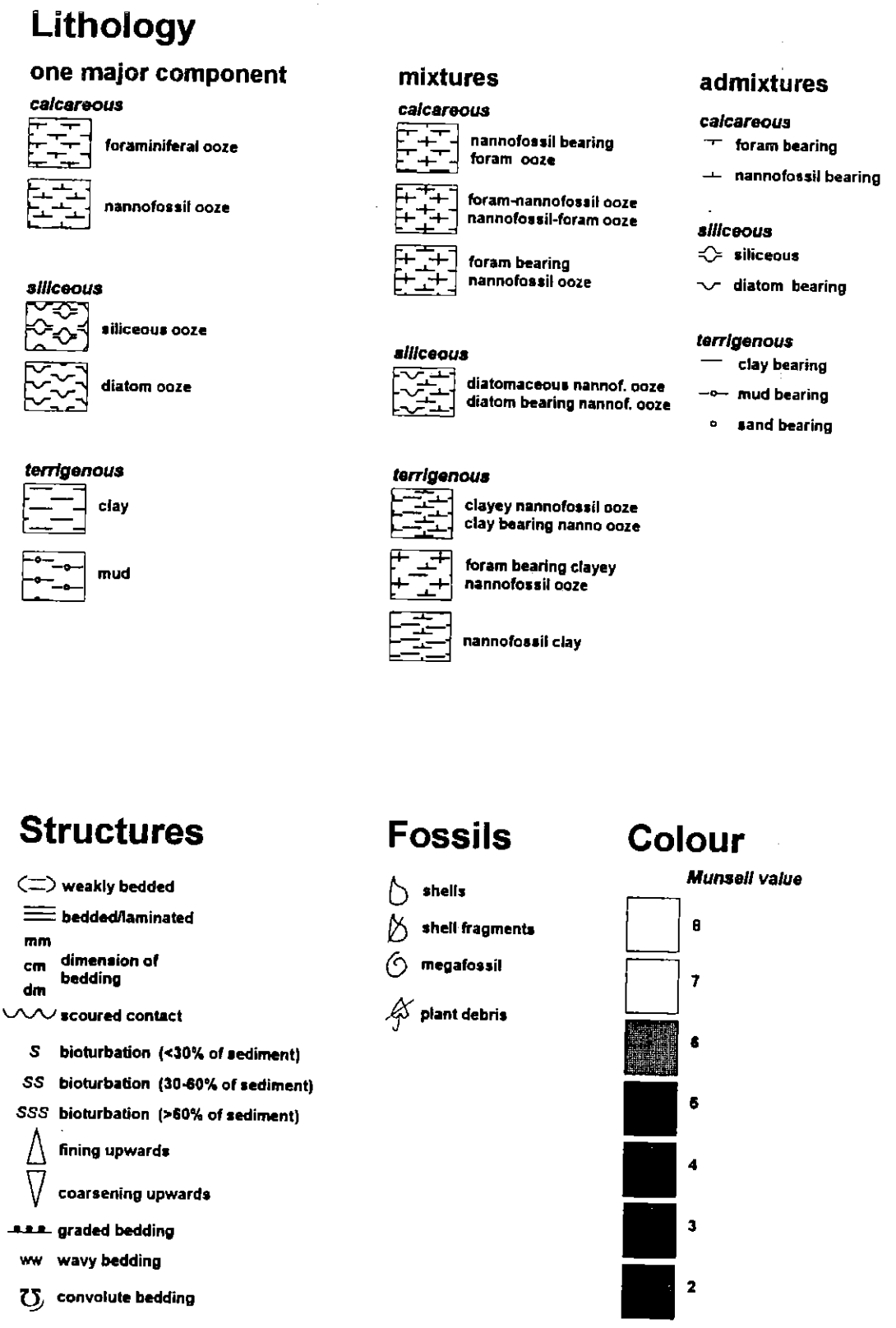

Fig. 222: Legend for stratigraphic columns of Figures 212-221.

Northeast Brasilian Margin: Profile A

Three gravity cores, core GeoB 3909-2, 3910-2 , and 3911-3 where taken at water depth of 3164, 2362, and 828 m respectively. The average core recovery was about 700 cm (chapter 7.4.1). According to the smear slide analysis, core GeoB 3909-2 consists predominantely of olive gray to dark gray nannofossil ooze with variable clay content (Fig. 212). Throughout the core erosive turbidity sequences of terrigenous sediments (quartz sands) with an average thickness of 10-20 cm are interbedded. At about 420 cm depth in the core, cross bedded and laminated sandy layers with plant debris occur.

The uppermost 30 cm of core GeoB 3910-2 are composed of yellowish brown coloured foraminiferal nannofossil ooze (Fig. 213). Below, the sediment turns to more grayish coloures consisting of clayey nannofossil ooze. In the upper part of the core several layers rich in Fe-oxyhydroxides (2-3 mm thick) were found. The sediment is sligthly bioturbated, with burrow density reaching a maximum between 3-4 m. The last 50 cm of the core are showing disturbed sediments, which are cross bedded and convoluted. Within this bottom end, shell fragments were observed.

The top 50 cm of the shallowest core GeoB 3911-3 consists, like in GeoB 3910-2, of light brownish foraminiferal nannofossil ooze (Fig. 214). The following two meters are characterized by increasing content of terrigenous silt and clay with the sediment colour turning to almost black. At about 460 cm and at the bottom end of the core layers with slightly increased content of nannofossils occure. The core is overall sligthly bioturbated.

Northeast Brasilian Margin: Profile B

Four gravity cores (GeoB 3915-2, 3914-2, 3913-3, and 3912-1) where taken at water depths of 3127, 2463, 2288, and 772 m, respectively. The core recovery varies between 645 and 870 cm (chapter 7.4.1). Cores GeoB 3915-2 and 3914-2 in the uppermost part consist of foraminiferal sand (Figs. 217, 218). Similar layers, partly graded, especially in core GeoB 3915-2, were observed over the whole length of the core. In between, olive to olive gray foraminifera bearing nannofossil ooze occur. The lowermost meter of the core GeoB 3914-2 shows convoluted sediments.

In the upper half of core GeoB 3913-3 the sediment is composed predominatly of strongly bioturbated, light olive brown to gray foraminiferal nannofossil ooze (Fig. 216). From 300 to 350 cm two graded beds with foraminiferal sands at the base were observed. Below, down to 525 cm the layers are tilted by 30° and are marked by nannofossil ooze with slightley enhanced clay content. From 525 cm to the end of the core the sediment consists of gray to greenish gray nannofossil ooze with varying content of foraminiferas and clay.

Like in the shallower cores of the profile A, the uppermost part of GeoB 3912-1 consists of yellowish brown foraminiferal nannofossil ooze (Fig. 215). Below, alterating sections of olive gray and very dark gray sediment occur, indicating fluctuations in terrigenous and marine (nannofossils) components. Over the whole core length, and especially the lower part, the sediment is bioturbated.

Amazon shelf

Three gravity cores, core GeoB 3916-2, 3918-4, and 3920-2 where taken at shallow water depths (< 130 m) on the Amazon shelf area. An environmental summary of the Amazon shelf area based on these cores is given in chapter 5.4.11.4 GeoB 3916-2 and 3918-4 are characterized by olive gray to very dark gray terrigenous clays (Figs. 219, 220). Only small variations in sediment composition are recognized. Remarkable features are black lenses and layers rich in pyrite and organic matter. The uppermost 10 cm of GeoB 3916-2 are enriched in 2-4 cm large oyster shells. Generally, core GeoB 3920-2, retrieved from a water depth of 128 m, consists of dark gray silty clay (Fig. 221). In the uppermost 200 cm sandy layers and lenses are interbedded. The top sediment of the core contains fossil beach rocks up to 10 cm in size. Between 220-264 cm a weak lamination of the sediment occures. According to the preliminary stratigraphic investigations mentioned above, all the cores of profile A and B are probably older then 40 ka. In the cores GeoB 3912-1 and 3913-3 the biostratigraphic *Globorotalia menardii* - zone X was detectet, and an age > 85 ka can be expected (Figs. 215, 216). Cores GeoB 3914-2 and 3915-2, however, are showing an age of more than 180 ka (Zone V) (Figs. 217, 218). Due to frequent turbidity (erosional ?) interbeddings in some of these cores, the preliminary stratigraphic results are to handle with care. For detailed stratigraphic information concerning the cores taken on the Amazon shelf refer to Figueiredo et al. (this volume).

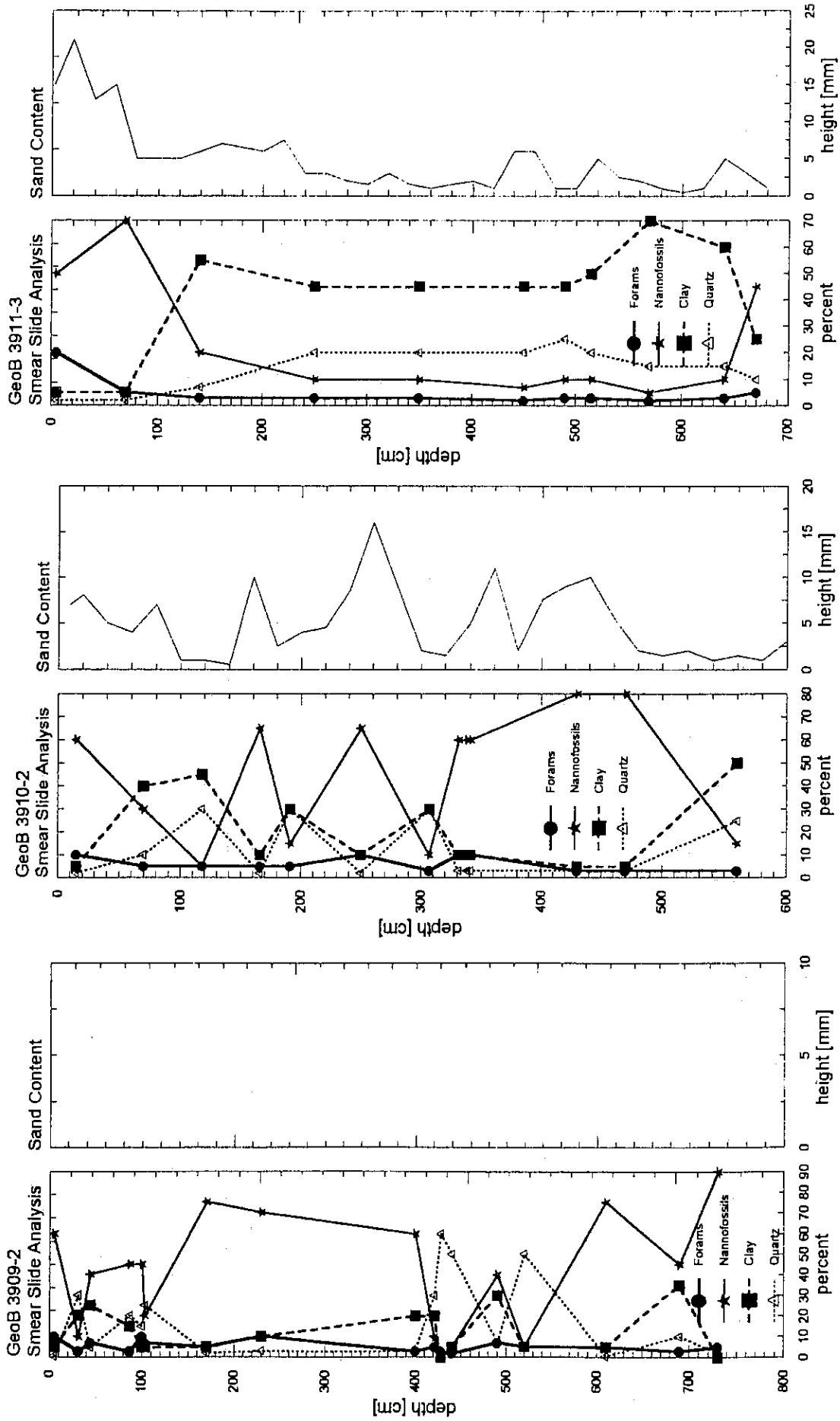

Figs. 223-225: Smear slide results and sand contents for cores 3909-2, 3910-2 and 3911-3.

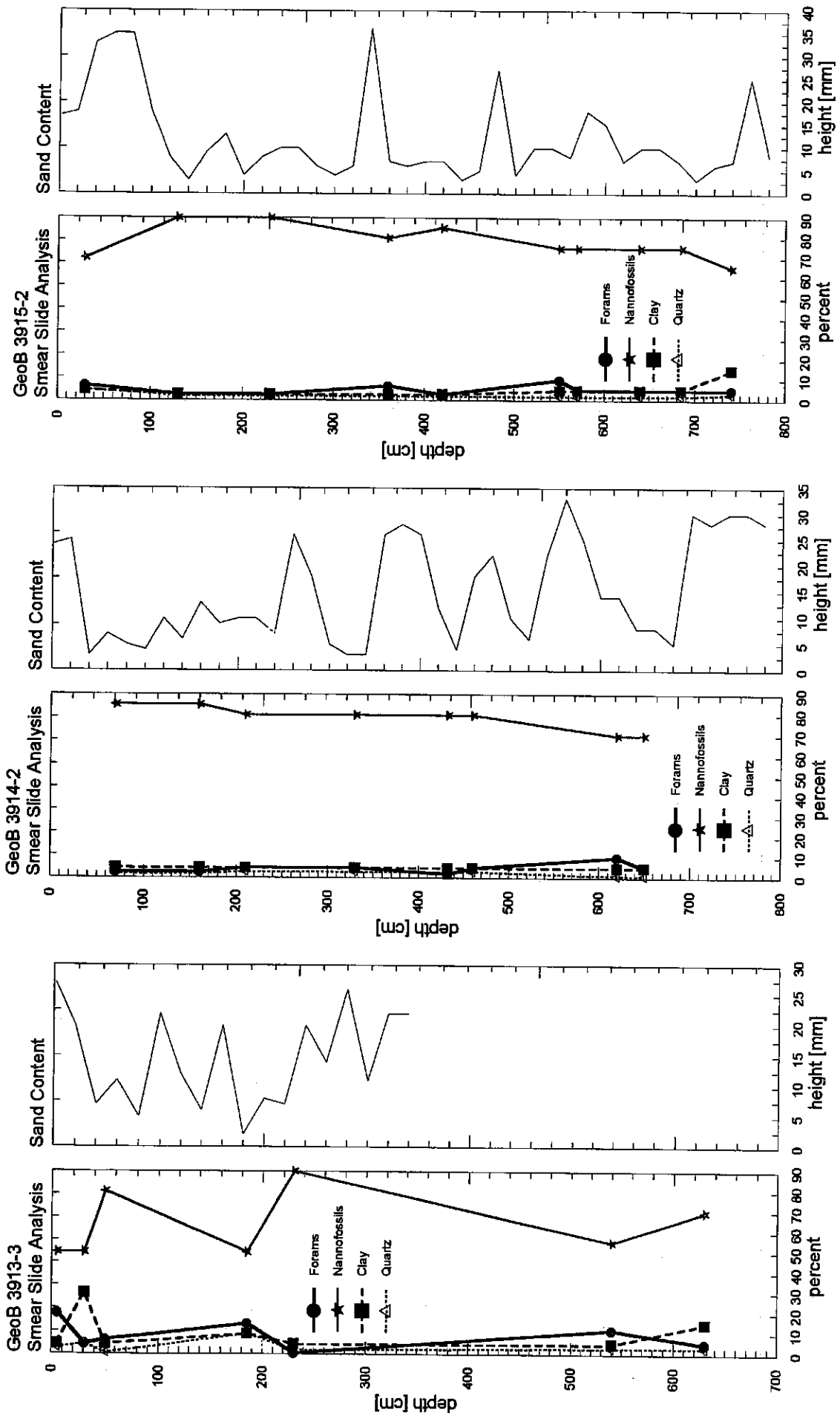

Figs. 226-228: Smear slide results and sand contents for cores 3913-3 , 3914-2 and 3915-2.

5.4.8.2.3 Carbonate Records

(H. Kinkel, M. v. Herz)

Carbonate contents were measured on board with a "carbonate-bomb". The $CaCO_3$ content of a sample was ascertained by the measurement of the CO_2 pressure after the treatment with HCl. The absolute error of a single determination is about 1 % (MÜLLER and GASTNER, 1971). In total, two cores were measured for their carbonate content in 10 cm intervals. The lower parts of both cores were not analyzed, as they obviously show disturbed sedimentation patterns (turbidites, slumping).

Both cores analysed for their carbonate content were retrieved from the northeast Brazilian margin. They are located at water depths above the recent carbonate compensation depth (CCD). Even during glacial shallowing of the CCD, these sites were not affected by carbonate dissolution. Relatively high content of aragonitic pteropods in both cores indicates that the deposition occurred above the aragonite compensation depths (ACD) (Fig. 229). Variations in the carbonate content mainly reflect changes between marine, carbonate-dominated sedimentation during sea-level highstands (interglacials) and terrigenous sedimentation during sea-level lowstands (glacials). These results are confirmed by the preliminary biostratigraphy established on board. The carbonate mainly origins from skeletons of planktonic organisms (foraminiferas, pteropods and coccoliths).

Moderate high carbonate contents (66 %) in the uppermost part of the cores (Holocene, Z-Zone, Fig. 229) suggest that there is still a relatively large amount of terrigenous dilution. The input of terrigenous material in core 3910-2 is much higher during glacials, with carbonate-contents dropping close to zero, whereas in core 3913-3 the carbonate content never drops below 15 %. Moreover, in core 3910-2 the carbonate content undergoes strong fluctuations during the Y-Zone indicating very instable conditions shifting from terrigenous to marine sedimentation patterns, with several pteropod layers indicated by distinct peaks in the carbonate content record (Fig. 229). This observation is consistent with earlier studies (e.g. DAMUTH, 1975). In core 3910-2, numerous iron-rich hardgrounds occur, indicating oxidation of organic matter.

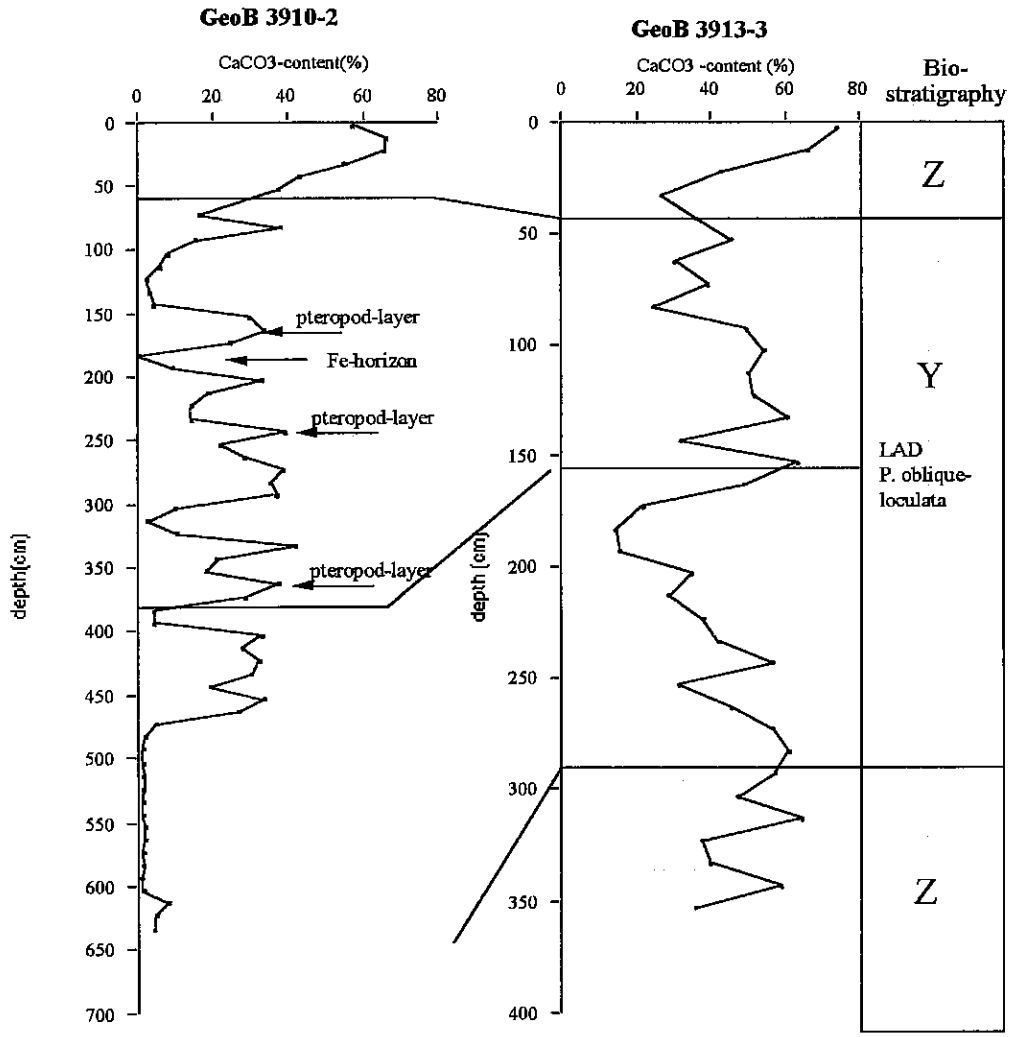

Fig. 229: Carbonate contents (%) and biostratigraphy of the gravity cores GeoB 3910-2 and GeoB 3913-3; pteropod layers are indicated by an arrow. For core location see Fig. 4 and chapter 7.4.1.

5.4.9 Pore Water Chemistry

(K. Enneking, S. Kasten, M. Kölling, M. Zabel)

The main objectives of geochemical investigations carried out during this cruise are:

• to study the processes of early diagenetic mineralization of organic matter in marine sediments through determination and quantification of diffusive pore water fluxes. A further aim was to extent the pore water database for sediments from the western equatorial Atlantic Ocean in order to calculate and model the diffusive nutrient fluxes across the sediment/water interface on a regional scale. This will be carried out in detail at the University of Bremen within the framework of the German JGOFS program. Besides the standard sampling and analyses of multicorer samples, incubation experiments were performed on selected multicorer cores. The aim was to determine the differences in pore water concentration profiles between cores sampled immediately after retrieval and those incubated for several days at *in situ* temperature. In addition, the variation of nutrient concentrations in the incubated bottom water with time was monitored.

• to examine mineralization processes at a shallow sampling site off the Amazon River mouth which has been studied e.g. by BLAIR and ALLER (1995). In contrast to the hemipelagic sediments from the western Atlantic Ocean which are generally low in reactivity, this sampling location on the Brazilian shelf is characterized by high mineralization rates and therefore allows a comparison with the organic-rich deposits from the eastern South Atlantic mainly focussing on the importance of anaerobic methane oxidation and the sedimentary sulphur cycle. Additional solid phase examinations will be performed at the University of Bremen.

• to recover a sediment core from the Amazon Deep-Sea Fan that shows the typical stratigraphy with terrigenous glacial deposits overlain by Holocene calcareous sediments. It was intended to analyse methane in the deeper core section and to sample the sediment solid phase under argon atmosphere as these data and kind of samples are lacking for the gravity cores taken on the Amazon Fan during a former METEOR cruise in 1991. The main focus in studying these deep-sea fan sediments is to evaluate the potential of climatically induced non-steady-state conditions to modify the sedimentary record. The Amazon Fan experienced such a distinct change in depositional conditions during the Pleistocene/Holocene transition. Detailed solid phase examinations including acid digestion, mineralogical and geophysical studies are to be carried out at the University of Bremen. Although it was originally intended to reoccupy station GeoB 1514 it was finally decided to recover a gravity core at ODP site 940 for cooperation with the Marine Geology group. This location which is close to the active Amazon Channel experienced strong differences in sediment type and accumulation rates between the Last Glacial and the Holocene and was therefore assumed to be suitable for the exmination of non-steady-state early diagenetic processes induced by strong changes in depositional conditions.

5.4.9.1 Methods

To prevent a warming of the sediments on board all cores were transferred into a cooling room immediately after recovery and maintained at a temperature of 4°-6°C. The multicorer cores were processed within a few hours. Two samples of the associated bottom water were taken for oxygen determination and two samples for nutrient analysis. The remaining bottom water was carefully removed from the multicorer tube by means of a siphon in order to avoid destruction of the sediment surface. During subsequent cutting of the core into slices for pressure filtration, pH and Eh measurements were performed with a minimum resolution depth of 0.5 cm. Conductivity and temperature were measured on a second, parallel core to calculate sediment density and porosity. At some stations this second core was stored under in situ temperature within an incubation box for two or three days. Therefore the tubes were captured with 1.8 l-plexiglas cells ("Dittert cells") which are combined with a pumping system to simulate the bottom water current. During the experiments the overlying waters were analysed continously. After incubation the cores were processed like described before.

The gravity cores were cut into 1 m segments on deck. At sampling locations where methane was expected to be present, syringe samples were taken on deck from every cut segment surface. Higher resolution sampling for methane analysis was carried out in the cooling laboratory immediately after storing by sawing 2-4 cm rectangles into the PVC liner. In this way, syringe samples of 5 ml sediment were taken every 10-20 cm and injected into 50 ml septum vials containing 20 ml of a concentrated (1.2 M) NaCl-solution. $HgCl_2$ was added to the solution to prevent additional production of methane by microbial activity. After closing and subsequent shaking methane becomes enriched in the headspace of the vial. Within a few days after recovery, gravity cores were cut lengthwise into two halves and processed. On the working halves pH and Eh were determined and sediment samples were taken every 20 cm for pressure filtration. Conductivity and temperature were measured on the archive halves. Solid phase samples were taken at same intervals and kept in gas-tight glass bottles under argon atmosphere. The storage temperature for all sediments was -20°C to avoid dissimilatory oxidation.

All work done on opened cores was carried out in a glove box under argon atmosphere. For pressure filtration Teflon- and PE-squeezers were used. The squeezers were operated with argon at a pressure gradually increasing up to 5 bar. The pore water was retrieved through 0.2 µm cellulose acetate membrane filters. Depending on the porosity and compressibility of the sediments, the amount of pore water recovered ranged between 5 and 20 ml.

The following parameters were determined on this cruise:
Eh, pH, conductivity (porosity), O_2, NO_3^-, NH_4^+, PO_4^{3-}, alkalinity, Fe^{2+}, SO_4^{2-}, Cl^- and CH_4.

H_2S was not analysed because the sediments in the study area are mainly dominated by iron reduction. The high amounts of dissolved iron result in an immediate precipitation of iron sulphides as soon as any sulphide is produced - in this way preventing the buildup of significant amounts of H_2S in the pore waters. Bottom water O_2 concentrations were analysed in duplicate

by Winkler titration. Eh, pH, conductivity and temperature values were determined by means of electrodes before the sediment structure was disturbed by sampling for pressure filtration. Nitrate, ammonium and phosphate were measured photometrically with an autoanalyser using standard methods. Alkalinity was calculated from a volumetric analysis by tritration of 1 ml sample with 0.01 or 0.05 M HCl, respectively. For the analysis of iron subsamples of 1 ml were taken within the glove box and immediately complexed with 50 µl of Ferrospectral and determined photometrically afterwards. SO_4^{2-} and Cl^- were analysed by ion chromatography from pore water diluted 1:20 with deionized water. For the detection of methane 25 µl of the headspace gas was injected into a gas-chromatograph. The concentrations of methane measured have to be related to the sediment porosity. Since corrected porosity data were not available we assumed a uniform porosity of 0.6 in all gravity cores for the calculation of preliminary methane contents. These concentrations will be recalculated with the corrected porosity values at the University of Bremen. The remaining pore water samples were acidified with $HNO_{3\,(suprapure)}^-$ down to a pH value of 2 for storing and subsequent determination of cations by ICP-AES and AAS. All pore water samples will be maintained at 4°C until further treatment in Bremen.

5.4.9.2 Shipboard Results

During this cruise a total of 10 stations was examined geochemically including 5 gravity cores and 9 multicorer cores. In addition, multicorer cores from five stations were incubated. The locations of the sampling sites are illustrated in Figure 230.

Most of the sampling sites examined on this cruise are characterized by low mineralization rates of organic matter. Furthermore the sedimentary sequences of three of the investigated gravity cores (GeoB 3910, 3911, 3914) are disturbed by abundant turbidites. Although being of overall low reactivity, the multicorer cores taken along Profile A on the northeast Brazilian Margin (GeoB 3909, 3910 and 3911) show a characteristic increase in mineralization activity with decreasing water depth. This is demonstrated by the NO_3 pore water concentration profiles illustrated in Figure 231. For PO_4 the same trend is observed with no concentration gradient detectable within the upper centimeters at the deepest station GeoB 3909 (3174 m). At stations GeoB 3910 and 3911 pore water concentrations indicate a flux of PO_4 across the sediment/water interface. The steepest PO_4 concentration gradient was determined for the shallowest sampling location GeoB 3911 at a water depth of 826 m. Pore water iron and NO_3 at this station show characteristic profiles (Fig. 232a) . Both are consumed at around 13-15 cm sediment depth accompanied by a pronounced shift in redox potential.

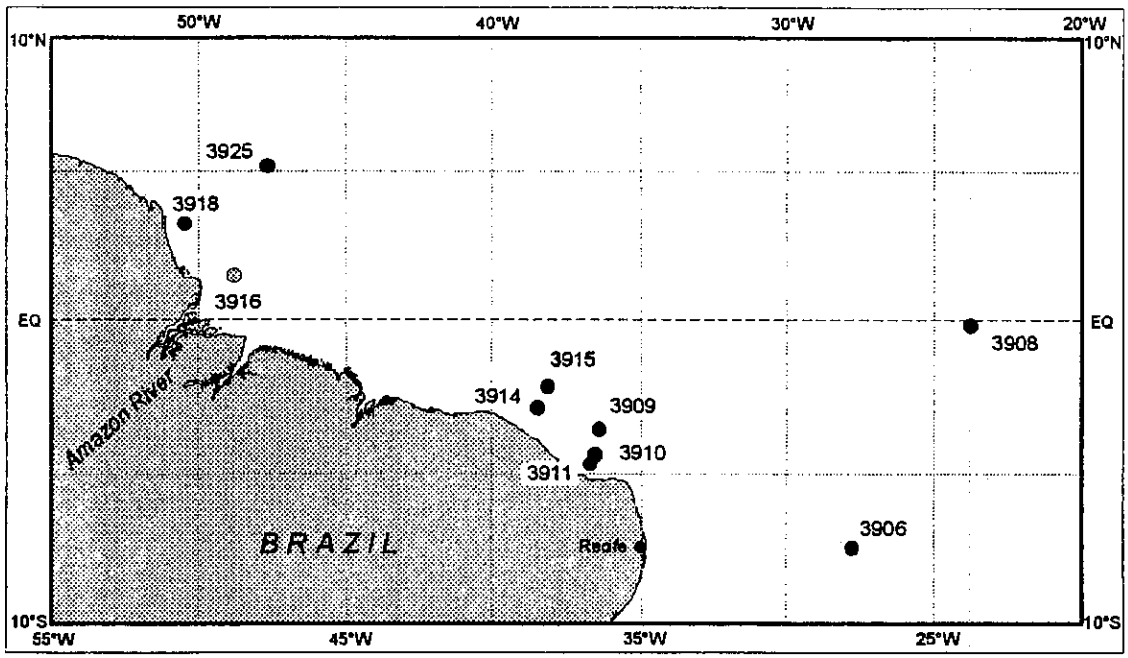

Fig. 230: Stations where geochemical investigations were carried out.

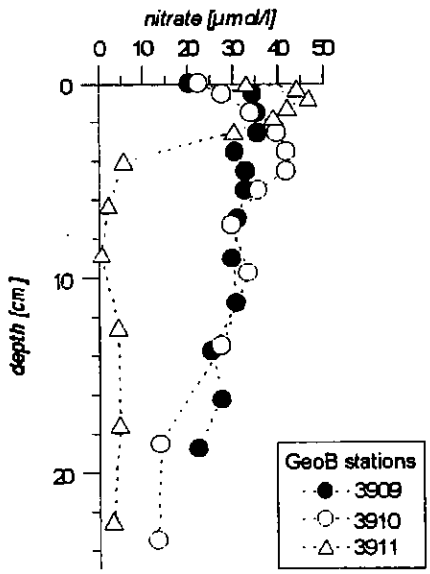

Fig. 231: Nitrate pore water profiles from multicorer sediments sampled on profile A.

Station GeoB 3918 is located on the Amazon River shelf close to the site examined by BLAIR and ALLER (1995) as part of the AmasSeds project (NITTROUER et al., 1991) and has been subject to an erosional event about 5-10 years ago. The pore water profiles for the multicorer core displayed in Fig. 232b illustrate the higher reactivity of the sediments at this location compared to those from site GeoB 3911 (Fig. 232a). The determined concentration profiles for alkalinity, sulphate (Fig. 233) and methane for the gravity core are comparable to those reported by BLAIR and ALLER (1995). They demonstrate that the rate of methane oxidation can be increased when methane-charged buried sediments are reexposed to sulphate-rich seawater by a physical non-steady-state process, such as erosion. The highest methane concentrations detected in this core amount to 4.5 mmol (CH_4)/l (wet sed). The methane contents determined in the samples immediately taken on deck from the cut sediment segments were generally higher than those measured from the higher resolution samples taken subsequently in the cooling laboratory. The methane contents detected in gravity core GeoB 3925-3 below 1 m sediment depth are a tenfold higher than those measured in geology core GeoB 3916-2 below 3 m. The latter core is located directly in front of the Amazon River mouth.

At station GeoB 3925 - which corresponds to ODP-site 940 - the examined multicorer core consists of the characteristic Holocene carbonate ooze and shows a gradual increase in alkalinity and PO_4 with depth. Nitrification is completed at about 1 cm sediment depth from whereon NO_3 concentrations decrease to values around 10 µmol/l at the base of the core in 20 cm depth. At this level iron was detected in pore water. Due to a slight shift in the position of the ship before recovering the gravity core, the multicorer core and gravity core taken at this station do not fit into a sequence. A top pelagic unit is absent in the gravity core and pore water concentration profiles of alkalinity and NH_4 (Fig. 234) indicate that several meters of the upper sedimentary sequence are missing. Furthermore, sulphate reduction is not completed so that, unfortunately, the early diagenetic zone of interest has not been reached in this gravity core.

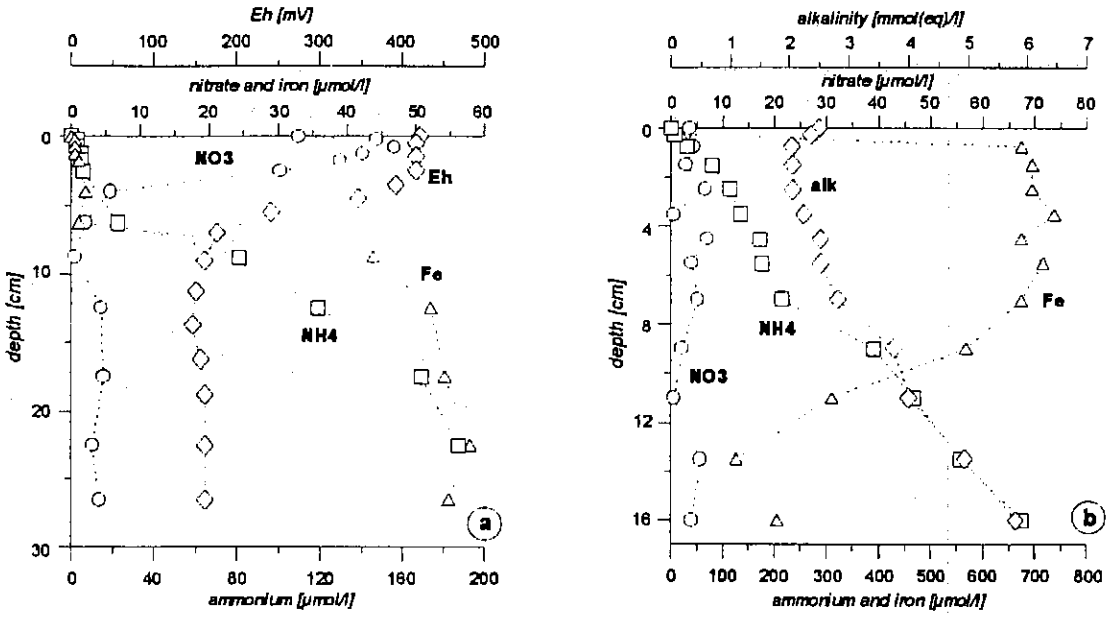

Fig. 232: Pore water profiles from multicorer sediments sampled at GeoB sites 3911 (a) and 3918 (b). While concentrations profiles at station GeoB 3911 show the common sequence, the very high mineralization rates at GeoB 3918 lead to the compression of nitrification and denitrification directly at the sediment surface and the overlying water, respectively.

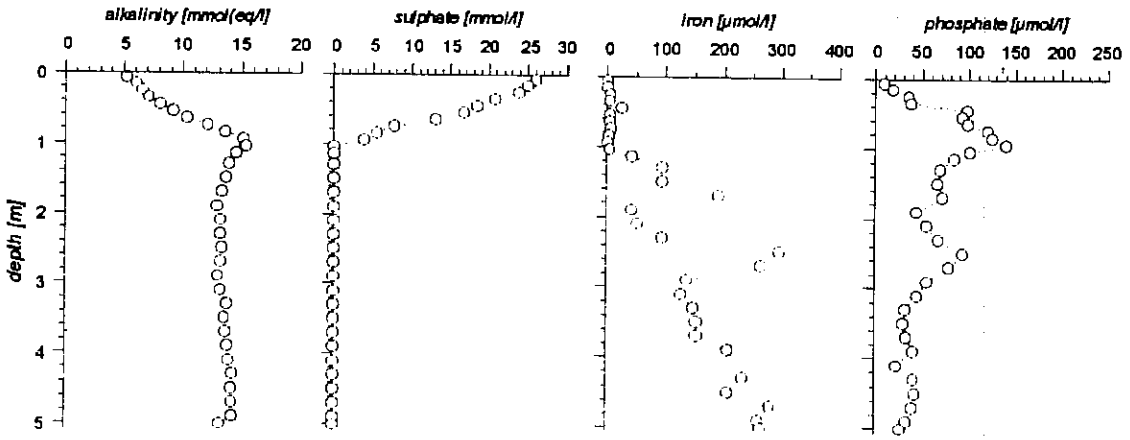

Fig. 233: Pore water concentration profiles at station GeoB 3918. Sulphate reduction is completed at about 1m depth, where the released sulphide precipitates with iron as authigenic iron sulphides. Sulphate reduction seems to be controlled by the anaerobic oxidation of upward diffusing methane.

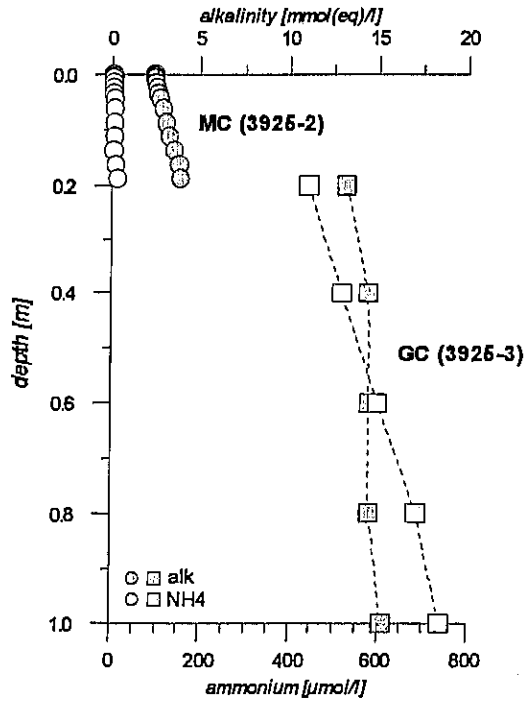

Fig. 234: Pore water concentration profiles from multicorer and gravity core samples at station GeoB 3925. Obviously the top layers of the gravity cores have been eroded.

5.4.10 Physical Properties -Studies

(T. Frederichs, F. Schmieder, C. Hübscher, A.Figueiredo, E. Costa)

During METEOR cruise 34/4 the recovered gravity cores were subject to laboratory geophysical studies. A routine shipboard measurement of three physical parameters was carried out on the segmented sediment cores, comprising the determination of:

- the compressional (P-) wave velocity v_p,
- the electric resistivity R_S, and
- the magnetic volume susceptibility κ.

These properties are closely related to the grain size, porosity and lithology of the sediments and provide high-resolution core logs (spacing 1 cm for P-wave velocity and magnetic volume susceptibility, 2 cm for electric resistivity) available prior to all other detailed investigations. In addition, oriented samples for later shore based paleo- and rockmagnetic studies were taken at intervals of 10 cm.

5.4.10.1 Physical Background and Experimental Techniques

The experimental setup for the shipboard measurements was basically identical to that of previous cruises. Therefore, the descriptions given here are kept brief. For a more detailed treatment of the experimental procedures we refer to WEFER et al. (1991) for R_s and to SCHULZ et al. (1991) for v_p.

P-wave velocity
The P-wave velocity v_p was derived from digitally processed ultrasonic transmission seismograms, which were recorded perpendicular to the core axis with a fully automated logging system. First arrivals are picked using a cross-correlation algorithm based on the 'zero-offset' signal of the piezoelectric wheel probes. In combination with a measure of the core diameter d the travel time of the first arrivals t lead to a P-wave velocity profile with an accuracy of 1 to 2 m/s.

$$v_p = (d - d_L) / (t - t_0 - t_L)$$

where d_L is the thickness of the liner walls, t_L the travel time through the liner walls and t_0 the 'zero-offset' travel time.

Following Schultheiss and McPhail (1989), a temperature calibration of v_p is effected using the equation

$$v_{20} = v_T + 3 \cdot (20 - T)$$

where v_{20} is the P-wave velocity at 20°C and T the temperature (in °C) of the core segment when logged. Simultaneously, the maximum peak-to-peak amplitudes of the transmission seismograms are evaluated to estimate attenuation variations along the sediment core. P-wave profiles can be used for locating strong as well as fine-scale lithological changes, e.g. turbidite layers or gradual changes in the sand, silt or clay content.

Electric resistivity, porosity and density
The electric sediment resistivity R_s was determined using a handheld sensor with a miniaturized four-electrodes-in-line ('Wenner') configuration (electrode spacing: 4 mm). A rectangular alternating current signal is fed to the sediment about 1 cm below the split core surface by the two outer electrodes. Assuming a homogeneously conducting medium, the potential difference at the inner two electrodes is directly proportional to the sediment resistivity R_s. A newly integrated fast resistance thermometer simultaneously provides data for a temperature correction.

According to the empirical ARCHIE's equation, the ratio of sediment resistivity R_s and pore water resistivity R_w may be approximated by a power function of porosity d

$$R_S/R_W = k \cdot d^{-m}$$

Following a recommendation by BOYCE (1968), suitable for seawater saturated, clay-rich sediments, values of 1.30 and 1.45 were used for the constants k and m. The calculated porosity d is subsequently converted to wet bulk density σ_{wet} using the equation (BOYCE, 1976)

$$\sigma_{wet} = d \cdot \sigma_f + (1 - d) \cdot \sigma_m$$

with a pore water density σ_f of 1030 kg/m^3 and a matrix density σ_m of 2670 kg/m^3. For the sake of an unbiased uniform treatment of all cores, these empiric coefficients were not adapted to individual sediment lithologies at this stage. Nevertheless, at least relative density changes should be well documented.

Magnetic volume susceptibility
The magnetic volume susceptibility κ is defined by the equations:

$$B = \mu_0 \cdot \mu_r \cdot H = \mu_0 \cdot (1 + \kappa) \cdot H = \mu_0 \cdot H + \mu_0 \cdot \kappa \cdot H = B_0 + M$$

with the magnetic induction B, the absolute/relative permeability $\mu_{0/r}$, the magnetising field H, the magnetic volume susceptibility κ and the volume magnetisation M. As can be seen from the third term, κ is a dimensionless physical quantity. It describes the amount to which a material is magnetised by an external magnetic field.

For marine sediments, the magnetic susceptibility may vary from an absolute minimum value of around $-15 \cdot 10^{-6}$ (diamagnetic minerals such as pure calcite or quartz) to a maximum of some $10.000 \cdot 10^{-6}$ for basaltic debris rich in (titano-) magnetite. In most cases κ is primarily determined by the concentration of ferrimagnetic minerals while paramagnetic minerals such as clays are of minor importance. High magnetic susceptibilities indicate a high lithogenic input/high iron (bio-) mineralisation or low carbonate/opal productivity and vice versa. This relation may serve for the mutual correlation of sedimentary sequences which were deposited under similar global or regional conditions.

The measuring equipment consists of a commercial Bartington M.S.2 susceptibility meter with a 125 mm loop sensor and a non-magnetic core conveyor system. Due to the sensor's size, its sensitive volume covers a core interval of about 8 cm. Consequently, sharp susceptibility changes in the sediment column will appear smoother in the κ core log and, e.g., thin layers such as ashes cannot appropriately be resolved by whole-core susceptibility measurement.

5.4.10.2 Shipboard Results

Sampling Sites and Recovery

The gravity coring program of cruise 34/4 was performed in two working areas. Profiles A and B were located northeast of Brazil, between 2° and 5° S and 36° and 39° W, respectively (Fig. 4). The cores GeoB 3909-2 to 3915-2 were taken from water depths between 772 and 4061 m. Cores GeoB 3916-2, 3918-4, 3920-2 were recovered on the Amazon shelf, between 1° and 5° N and 48° and 51° W, respectively, in waterdepths of 38, 51 and 128 m.

The core recovery varies between 405 (GeoB 3920-2) and 880 cm (GeoB 3914-2). A total of 10 sediment cores with a cumulative length of 67 m was investigated (upper part of Fig. 235).

General Results

A compilation of the characteristic physical properties of all cores is given in the lower part of Figure 235. The dots mark the median values of compressional wave velocity, density and magnetic susceptibility for each core, the vertical bars denote their standard deviations. Each diagram is divided into three parts corresponding to profiles A and B and the Amazon shelf.

On the northeast Brazilian Margin (profiles A and B) the average p-wave velocities range from 1489 to 1509 m/s, while mean densities from 1647 to 1724 kg/m^3 were found. The average magnetic susceptibility shows constant values of about $100 \cdot 10^{-6}$ SI on both profiles A and B. Significant higher intensities up to $427 \cdot 10^{-6}$ SI (GeoB 3920-2) were determined in the cores from the Amazon shelf. P-wave velocity and density ranging from 1476 to 1534 m/s and 1677 to 1821 kg/m^3, respectively, differ only slightly from those of the cores of profiles A and B.

Physical property logs for the cores together with the core descriptions are shown in Figs. 212-221 (chapter 5.4.8.2.2).

Special Features

Northeast Brazilian Margin (profiles A and B)

In general, there is no obvious core to core correlation based on physical properties, except for the magnetic susceptibility in the upper 340 cm of core GeoB 3914-2 (Fig. 217) which correlates with that of the upper 220 cm of core GeoB 3913-3 (Fig. 216). A preliminary interpretation of these characteristic, probably climatically driven patterns revealed that these core intervals recorded a time period up to oxygen isotope stage 4. Dating of the older sediments is not possible, while in GeoB 3913-3 age may be estimated at least down to 320 cm depth which corresponds to oxygen isotope stage 5.5. These tentative age models are supported by biostratigraphy.

In all cores, except for GeoB 3911-3 (Fig. 214) and GeoB 3912-1 (Fig. 215), turbidites cause distinct maxima in p-wave velocities and density values. In GeoB 3909-2 (Fig. 212) ,these charactistic peaks are associated with minima in the magnetic susceptibility due to foraminiferal

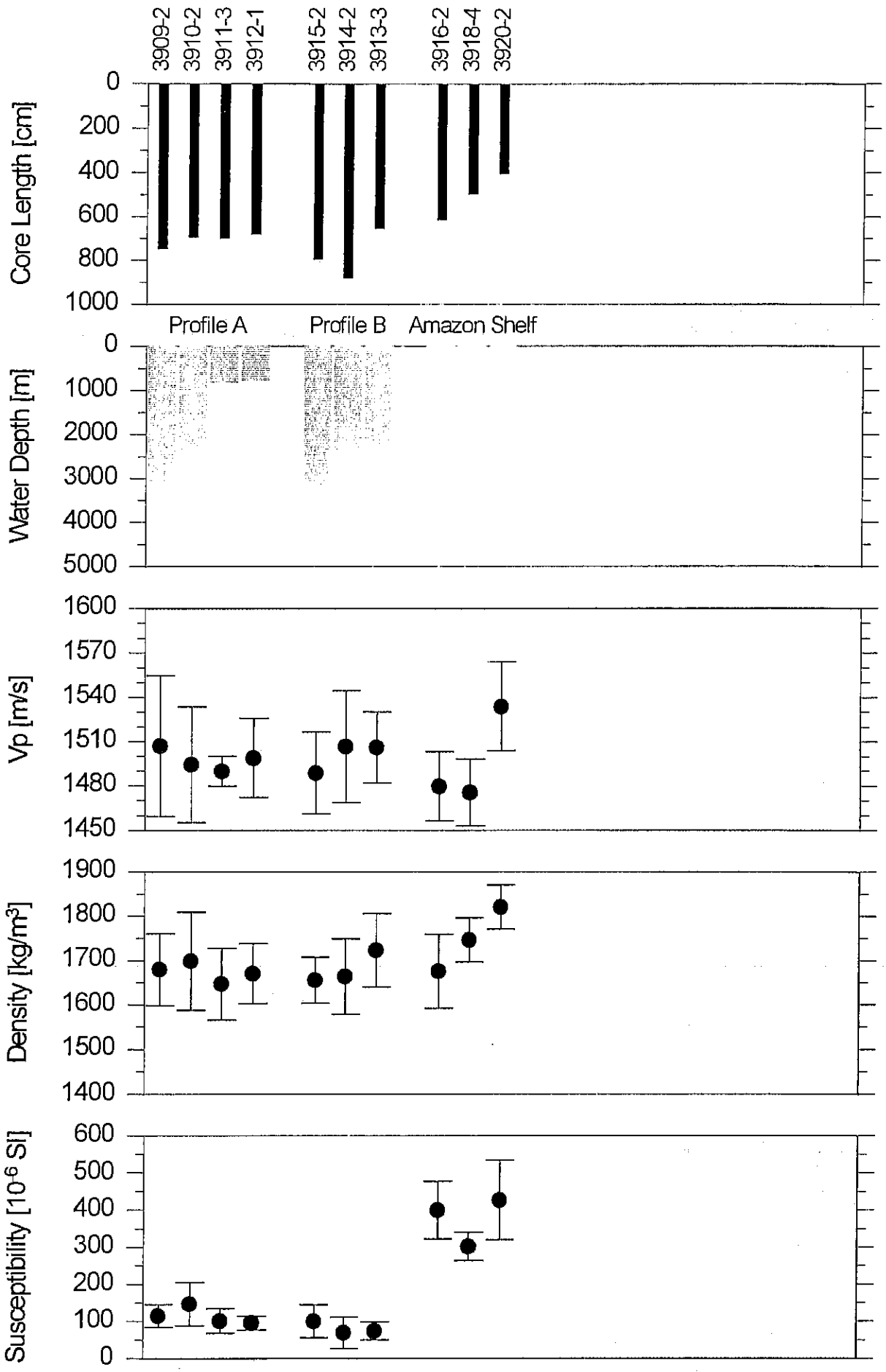

Fig. 235: Mean compressional wave velocity, density and magnetic susceptibility of gravity cores GeoB 3909-2 through 3920-2 compared to water depth and core length. The bars denote the standard deviations.

sands. The graded bedding of these sediments is reflected particularly in the down-core variations of v_p, for example in 160 cm core depth. In core GeoB 3915-2 (Fig. 218), core depth 170 and 480 cm, layers of pteropod-rich sediments produce maxima in p-wave velocities but minima in density values while the underlaying foraminiferal sands show a typical positive correlation of both parameters. In core GeoB 3910-2 (Fig. 213), p-wave velocity and susceptibility are positively correlated in a layer of fine sandy mica bearing sediments (540 cm core depth).

Amazon shelf
The variations of magnetic susceptibility in core GeoB 3916-2 (Fig. 219), in particular in the lower 250 cm, may correspond to Milankovitch cycles with a characteristic change of frequency at 400 cm core depth. Core GeoB 3918-4 (Fig. 220) is not acoustically measurable below a core depth of about 100 cm due to insufficient signal strength. The reason for this problem seems to be the degassing of methane gas due to preasure release. Gas bubbles in the sediment greatly attenuate sound transmission.

5.4.11 Profiling Hydroacoustic Systems

(C. Hübscher, T. Frederichs, F. Schmieder)

During the entire cruise M34/4 the Hydrographic Multi-Beam Deep-Sea Sweeping Echosounder HYDROSWEEP and the Parametric NBS Deep-Sea Echosounder and Sub-Bottom Profiling System PARASOUND were operated 24 hours a day outside the 12 nm zone of Brazil and the territorial waters of Surinam and French Guayana.

5.4.11.1 HYDROSWEEP

The general purpose of the HYDROSWEEP system is to survey topographic features of the seafloor. A sector of 90° is covered by a fan of 59 pre-formed beams. Thus, a stripe with the width of twice the water depth is mapped perpendicular to the ship track. A shiprelative bottom map is plotted online. Data are stored on DAT cartridges in a sensor undependent format. Since HYDROSWEEP is not longer a rack mounted system, a workstation is installed directly beside the ParaDigMa PC, enabeling the PARASOUND operator to check the topographic map and cross- and ahead profiles on the HYDROSWEEP screen for optimized PARASOUND control. Beside the production of bathymetric maps HYDROSWEEP data are an important tool for the determination of gravity core and MUC sites. Also, the gained 3D information of the seafloor topography represents an important contribution to the interpretation of the 2D-PARASOUND cross sections.

5.4.11.2 PARASOUND

The PARASOUND system surveys the uppermost sedimentary layers of the seafloor. Due to the high signal frequency of 4 kHz, the short signal length of two sinoid pulses and the narrow beam angle of 4.5° a very high vertical resolution is achieved. Sedimentary layers along the ship track on a scale of less than one meter can be resolved. An optimized succession of generated signals allows the resolution of small horizontal variations. Most of the data reveal no diffraction hyperbolas. The data quality can be compared with stacked and partly migrated MCS data. The ParaDigMa system (SPIEß, 1993) converts the analog to digital data and stores them on 9-track tapes or hard disks in a SEG-Y like format. Lateron the data are copied on DAT-cartridges. Therewith, they are available for further processing. The preprocessed analog and digital data are plotted online with the DESO 25 and a HP PaintJet, respectively. Navigation data from the DVS are plotted and stored to disk simultanously.

Besides the usage of the PARASOUND system as a tool for localization of core positions (gravity core, MUC), the main objectives of the PARASOUND survey were

- to image and describe the dominating sedimentation process at the continental slope,
- to study the development and internal structures of channel-levee complexes of the Amazon Deep-Sea Fan,
- to investigate the prograding subaquaeous Amazon Delta with its top-, fore- and bottom set,
- to interprete the structural context of the gravity cores.

5.4.11.3 Selected PARASOUND Data - First Results

The quality of PARASOUND data will be illustrated by four examples in this chapter. Data from the Amazon shelf are presented by Figueiredo et al. (this volume, chapter 5.4.11.4). An example from the continental slope off Guyana is shown in Figure 235. The 24 km long profile strikes perpendicular to the coast and is located at 9.5° N, 57.5° W. The water depth is around 3000 m. The signal penetration reaches 40 m. No or little distinct reflectors can be observed beneath the wavy seafloor, diffuse reflectivity dominates the resolved sediments. Diffuse diffraction hyperbolae contribute to the blurred internal layers. However, no distinct layers can be resolved beneath the plateau at the center of the profile. Therewith it is assumed that disturbed deposited sediments are present. The observed sediment structures are representative for the entire slope between 1900 and 4200 m water depth. The seafloor itself is mainly characterized by sediment waves with a wavelength of around 2 km. The observed reflection characteristic is typical for slumps or contourites and winnowed sediments, respectively. If slumping caused the wavy sediments, changing wavelength and slide plains would have been expected. Therefore, it is more likely that a strong current caused the disturbed layering or a reworking of already deposited sediments. The North Atlantic Depth Water (NADW) forms a strong countour current at the north-west continental slope of South-America (REID, 1989). The current is reported for water depths between 1800 and 4200 m like it is observed in the data. Therewith, the NADW current is regarded as the causative process for the sediment waves.

Another example for current influenced vs. gravity transported sediments is shown in Figure 237. The 54 km long profile has been gained in a depth of almost 5000 m close to the Mid-Ocean Ridge, which is located directly in the northeastern prolongation of the profile. Two canyons incise into well layered sediments, which are covered by a 4 m thick semi-transparent layer, presumably consisting of (hemi-)pelagic sediments. The 14 km wide basin in the east is located at the base of a steep slope towards the MOR, its shape is typical of current triggered moats. The origin of the western canyon is less clear. If the sediment block between the canyon represents a sediment slide - internal structures are still seen - the smaller canyon is a slide scarp. The absence of hemipelagic sediments indicates, however, the impact of bottom currents. In this case, both canyons represent erosional channels.

The next section shows a channel-levee complex (CLC) from the Amazon fan. The modern channel has been crossed in a water depth of 3700 m (CLC A, Fig. 238). Sediment waves can be observed at the outer flanks of the levees. East of the active channel, older and abandoned channels have been crossed (CLC B, C, Fig. 238). The eastern levee of CLC B strikes out against the western levee of CLC C as an onlap. All three channels reveal a very high sinuosity, why the meandering channels are crossed several times. e.g., the channel of CLC A itself has been crossed three times.

A typical example for submarine channels outside of fan systems is presented in Figure 239. An up to 2 km wide mixed depositional-erosional CLC is seen at the western side. The depositional levees exhibit parallel reflectors with no sediment waves at the outer flanks. It is remarkable that no divergent reflectors or inwards thickening of the layers can be observed within the levees. The well layered eastern levees are truncated by a meandering erosional channel. The channel is crossed two times due to the high sinuosity (B, C). No depositions can be observed at the channel shoulders.

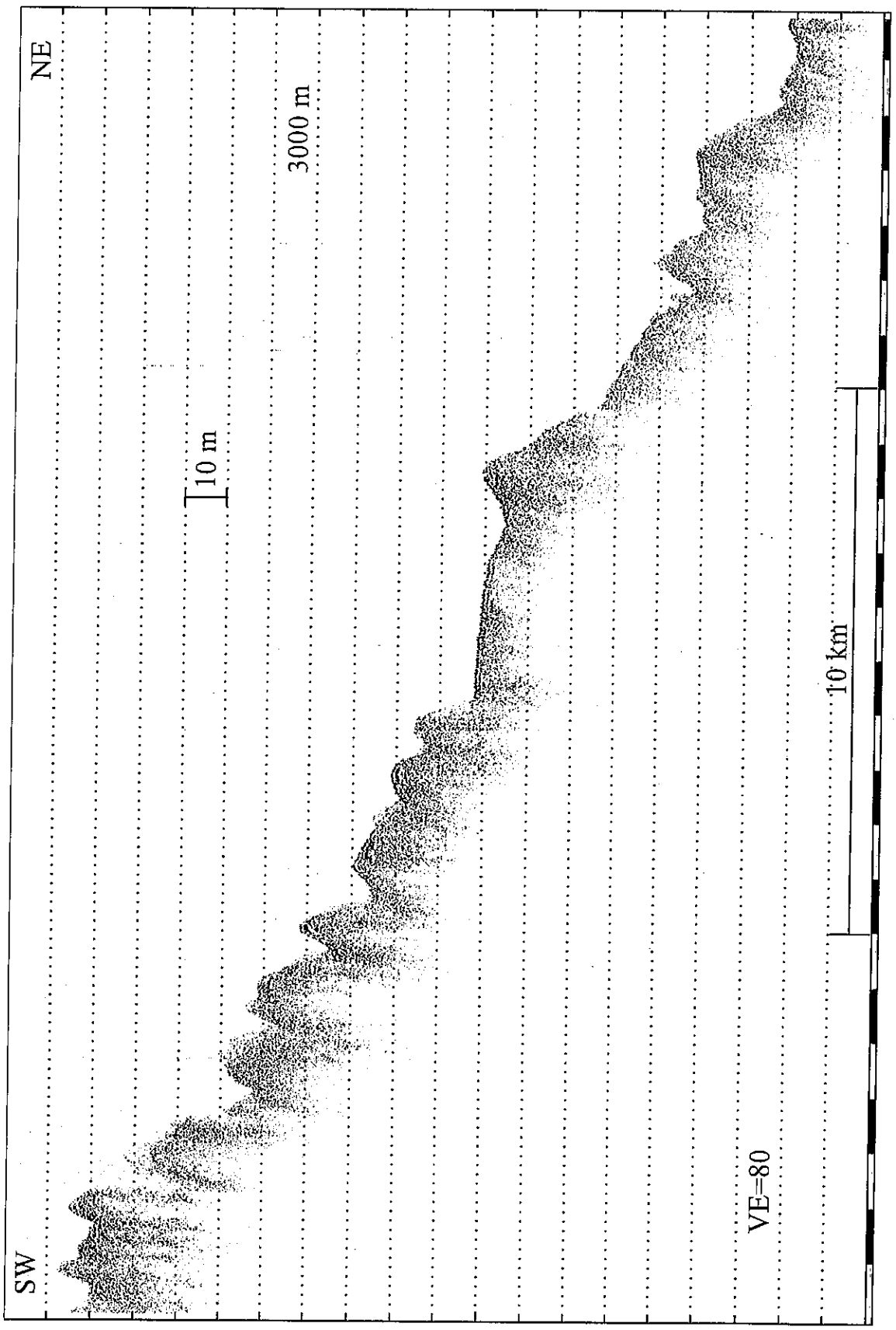

Fig. 236: PARASOUND profile showing diffuse reflecting sediment waves at the continental slope off Guyana, caused by the NADW current.

Fig. 237: PARASOUND profile from the western foot of the MOR in the central Atlantic. Two canyons are observed. The western canyon represents a moat, the western canyon a slide scarp or erosive channel.

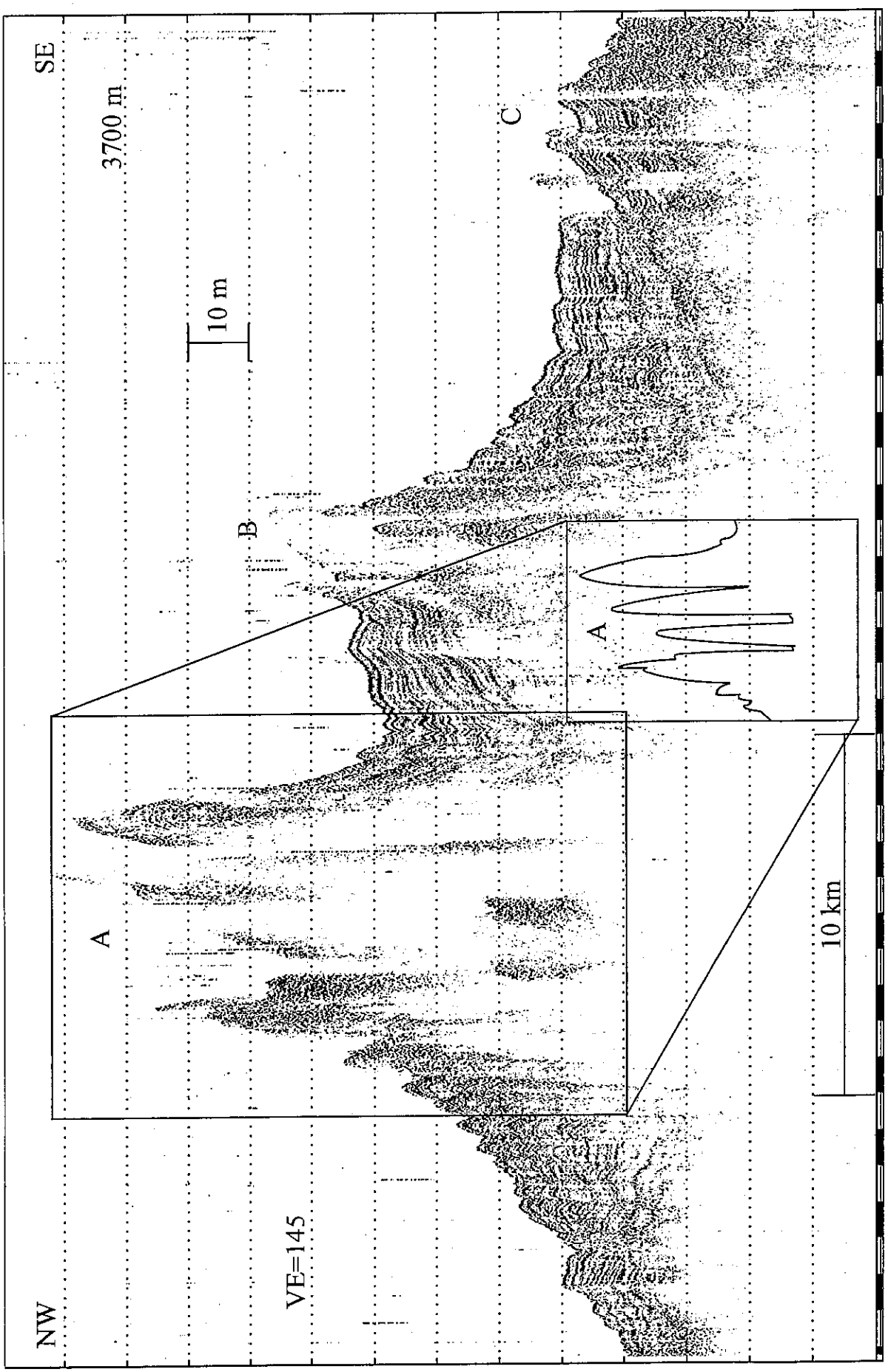

Fig. 238: PARASOUND profile crossing the modern channel-levee complex (CLC A) and older complexes at the lower Amazon Fan. Due to the high sinuosity the meandering channels are crossed more than once.

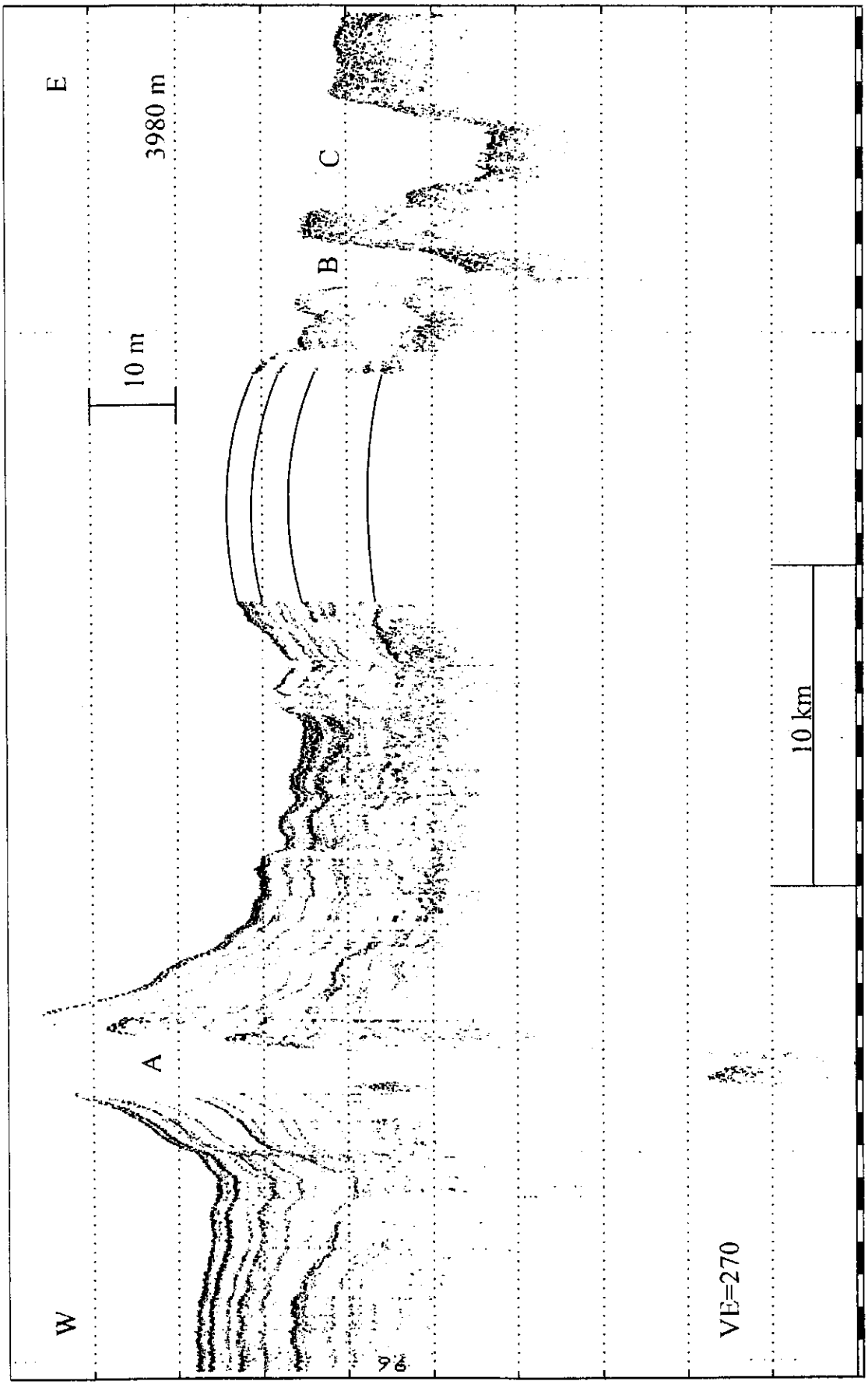

Fig. 239: PARASOUND profile exhibiting a mixed erosional-depositional channel-levee complex (A) with an erosional meandering channel (B, C) in the juxtaposition.

5.4.11.4 Amazon Shelf Research

(A.G. Figueiredo, E.A. Costa, C. Hübscher, T. Frederichs, F. Schmieder)

The Amazon shelf is a scenario for interaction of strong nature forces, including river discharge, the North Brazilian Current (NBC), tide currents and the trade winds. The Amazon river is the largest river in the world and its discharge corresponds to 18 % of all rivers going to the oceans (CURTIN, 1986). During peak discharge, volume can reach 354,793 $m^3 s^{-1}$ (FIGUEIREDO et al., 1993) and sediment load carried by the river is estimated to be 11-13 x 10^8 ton/yr. (De MEADE et al., 1985). As river sediment enters the shelf, it is deposited accordingly to interaction with tide currents, the NBC and the trade winds. As a result of this interactions, the most prominent feature on the shelf is a submarine delta being constructed over relict sands, since last sea-level lowstand (FIGUEIREDO et al., 1972, FIGUEIREDO and NITTROUER, 1995). Together with sediments, it is also included organic matter, which with time generates methane gas and it can be easily detected on the seismic (FIGUEIREDO et al., 1996). Extensive research have been performed in this area by the AMASEDS research group (NITTROUER et al., 1990). However, new seismic techniques and physical property measurements in the cores, performed during METEOR cruise M34/4, are important contribution to further understanding interaction of processes during the last 30 thousand years. Collection of cores for geochemical analysis were also performed (see K. Enneking et al., chapter 5.4.9).

Work in the area involved 486 nautical miles of profiling with PARASOUND and HYDROSWEEP, on 10 profiles, in water depth ranging between 20 and 130 m (see C. Hübscher et al., chapter 5.4.11), 5 stations with collection of 5 gravity cores, 2 multicorers and 2 box corers (see R. Schneider et al., chapter 5.4.8, Fig. 4). Results of PARASOUND and geological data are presented for every profile shown in Figure 240. On profile 1-2, PARASOUND records show a sand wave field with waves of 4 to 8 m height with none to small echo penetration. On the second half of the profile, with approaching Amazon river mouth, sand waves become covered by muddy sediments from the Amazon delta. Penetration increases up to 12 m and internal reflectors are characterized by a plan-parallel arrangement. The base of the mud unit become undefined and irregular with typical characteristics of gas charged sediments. In this case, since there is no stratigraphic traps, the depth of the gas is controled by the sulphate reduction zone above as stated by BLAIR and ALLER (1995) and reported by K. Enneking et al. (chapter 5.4.9). On profile 2-3, records also have the plan-parallel reflectors and penetration can reach 25 m. Underlying boundary of the records also reflects gas-charged sediments. Profile 3-4 is perpendicular to the delta foreset and is characterized by prograding sigmoidal reflectors over a sand wave field. Sand waves disappear under the foreset, where the gas concentration do not allow for sound penetration. Core GeoB 3916, collected on the foreset, shows several spikes on the p-wave velocity measurements and on the magnetic susceptibility measurements, height frequency peaks at the base, passing to lower frequency peaks at the top (see T. Frederichs et al., chapter 5.4.10). After opening the core, it was possible to correlate the spikes and peaks with groups of fine sand and silt laminations in a muddier core. At the base of the core, well preserved shells were found in a coarse sand sediment. The shells were saved for C-14 dating. The last portion of profile 3-4 is covered by the sand wave field with no sound penetration.

Further seaward, bottom drops from 50 to 70 m and the sand waves disappear. At the end of profile 3-4, there was a tentative coring, resulting in a collection of carbonate crusts (GeoB 3917). The strike oriented profile 4-5 presents a gentle undulating bottom with no echo penetration. Profile 5-6 is perpendicular to the foreset and again shows a downlaping of sigmoidal reflectors over an undulating sand bottom (Fig. 241). Profile 6-7 is parallel to the coast next to the "Cabo Norte" area. The bottom is flat with small echo penetration, except for some places with 10 m echo penetration. Profile 7-8 is perpendicular to the foreset, showing the typical progradation of the sigmoids over an undulating sandy bottom. At end of profile there is no echo penetration. Profile 8-9 is characterized at the first third by a gentle undulating bottom with depressions being filled up with seismically transparent mud. The last two thirds, has an irregular surface being covered by muddier sediments. Next to point 9, the irregular surface disappears and a strong reflector can be seen near the surface. Cored at Station GeoB 3918, this reflector prove to be a gas charged mud. In this case the gas is stratigraphycally traped the concentration is higher (see K. Enneking et al., chapter 5.4.9) and consequently the seismic reflector is strong. One of the cores was specifically collected and sampled for measuring concentration of methane. On profile 9-10, the gas-charged unit disappears and a sub-bottom irregular surface can be traced till half way to point 10. Echo penetration decreases and sediment become more sandier and the ocean bottom have small sand waves over larger undulations. Station GeoB 3919 was done with the objective of collecting relict ooliths, previously described by MILLIMAN and BARRETO (1975). At first look, the sample appears to indicate presence of ooliths mixed with carbonate sands. Profile 10-11 has small echo penetration and increasing up to 45 m next to station GeoB 3920. Reflectors are parallel and gentle seaward dipping with erosional surface at sea bottom. Underlying this unit there is an irregular reflector and few meters (500) seaward of this station, a carbonate like platform lies at the shelf break (Fig. 242). This station had also the objective of collecting oolithic sand as indicated in the literature. However, the sediment was mainly mud and only a laboratory analysis could indicate about the presence or not of ooliths.

Major results

These findings are based on an expedite data analysis on board of RV METEOR and further studies at the laboratories will provide more information to elucidate these findings.

1) PARASOUND system allowed for observation that the submarine delta is migrating over a field of sand waves.

2) On station GeoB 3917, unexpected carbonate crusts were collected.

3) Gas charged sediments can be seen on the PARASOUND records, observed on the p-waves velocity measurements and detected by geochemical methods. Further studies on this topic might lead to estimation of gas concentration using seismic methods.

4) Cores from the active delta foreset (GeoB 3916), presents a peculiar profile of magnetic susceptibility, varying from high frequency peaks at the base to lower frequency at top.

Application of this technique to other cores collected in the area, can lead to an alternative dating method.

5) Collection of shells at the base of core GeoB 3916 will serve as a good reference for dating the events above.

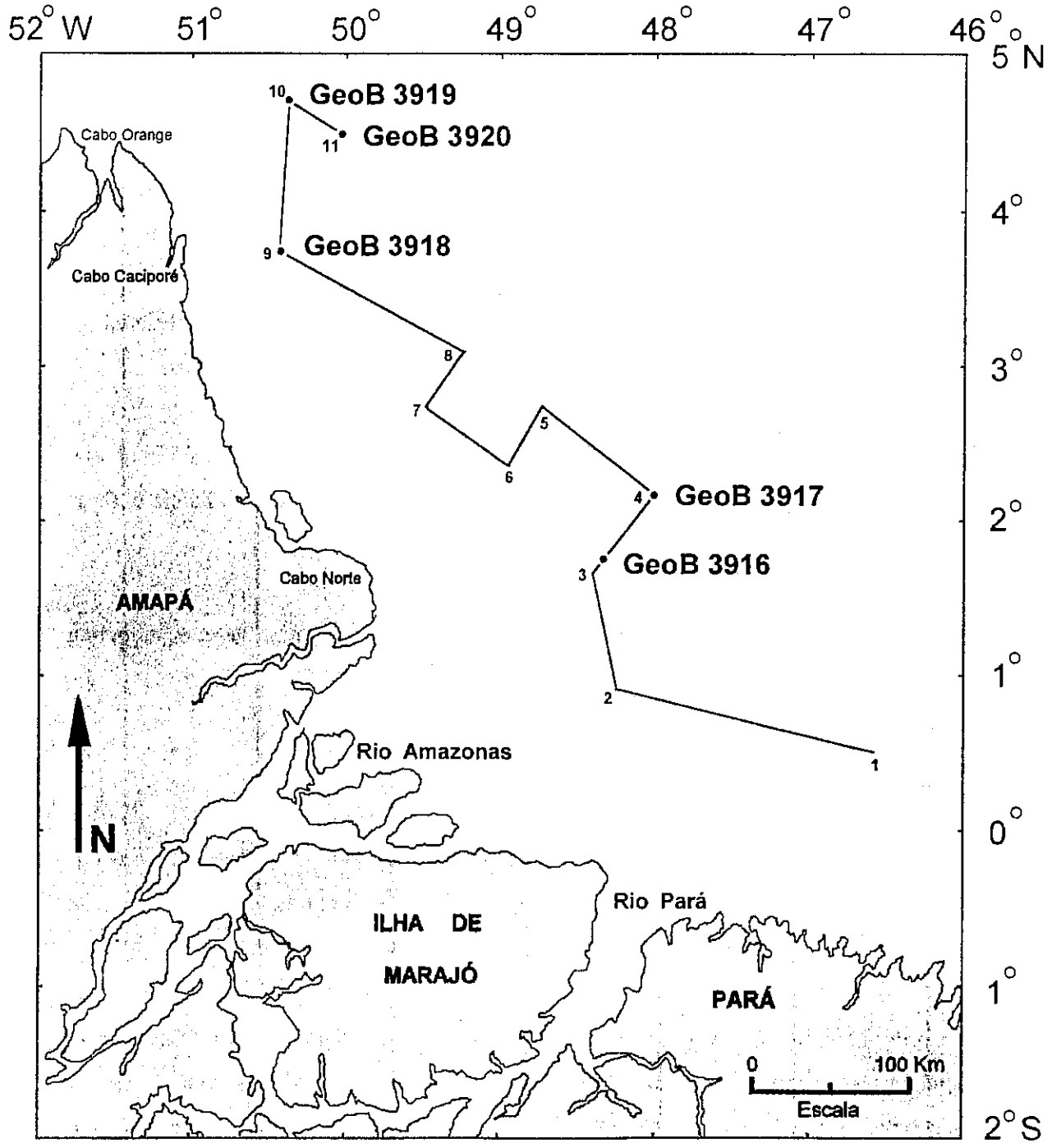

Fig. 240: Amazon shelf research area. Lines indicate location of PARASOUND profiles. GeoB indicates location of geological stations.

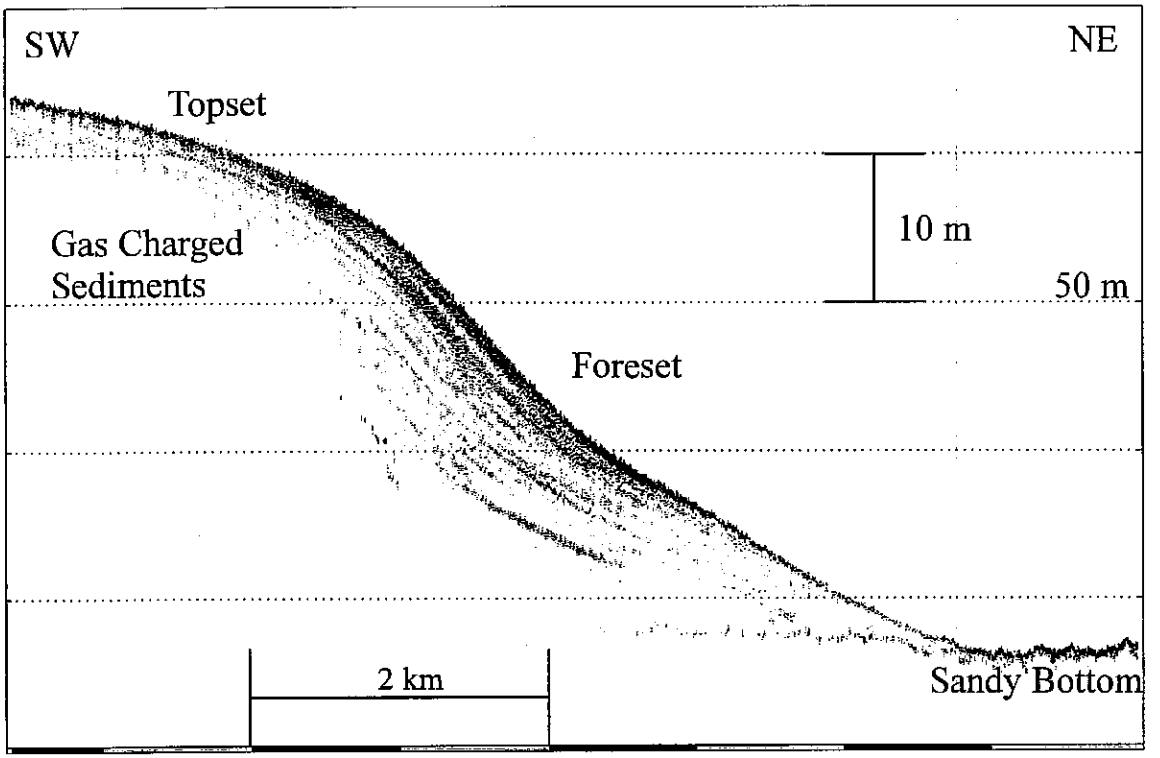

Fig. 241: Foreset beds of the Amazon submarine delta on profile 5-6, migrating over an irregular topography. Gas charged sediments on the right, do not allow for echo penetration.

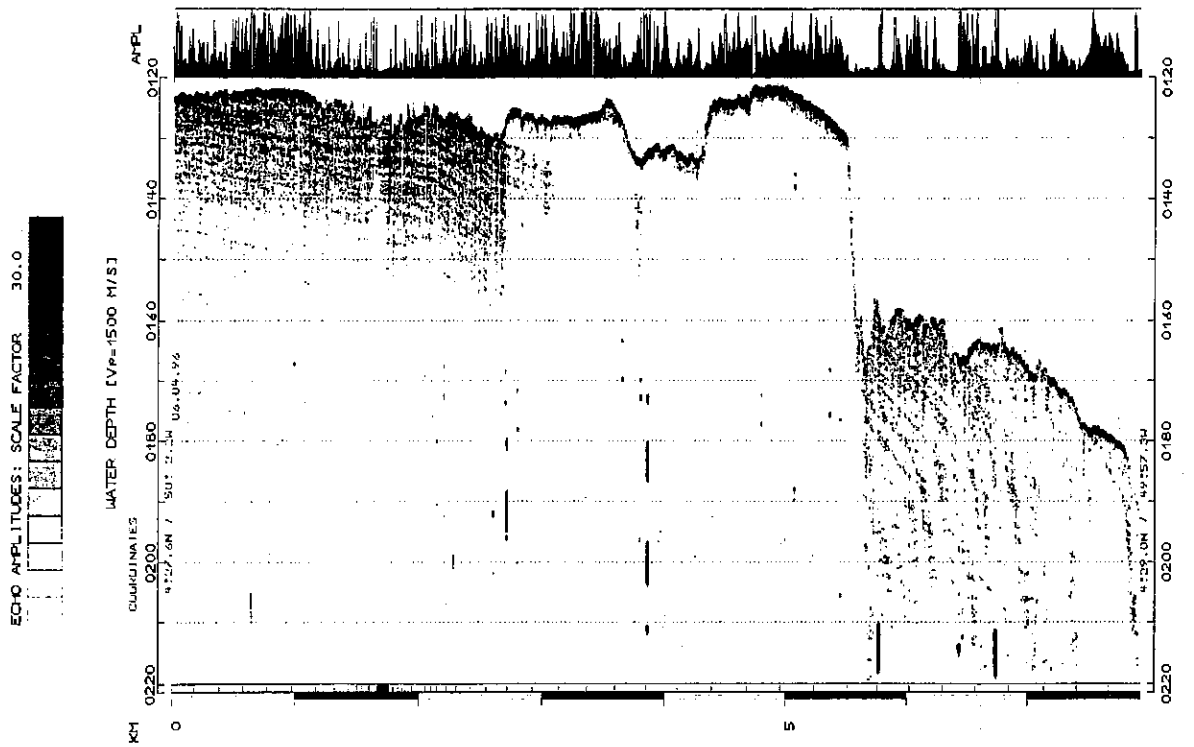

Fig. 242: Carbonate like platform next to station GeoB 3920. On the left, sediments are well layered with erosional surface at the top.

6 Ship´s Meteorological Station

No meterological report exists for cruise M34/1 and M34/2 due to the absence of the sick ship´s meteorologist.

6.1 Weather and Meterological Conditions during M 34/3

(K. Flechsenhar, W.-T. Ochsenhirt)

RV METEOR left the port of Walvis Bay, Namibia in the evening of February 21st, 1996, and steered on a westerly course to her first working station at approximately 29° S / 08° W, which was reached in the afternoon of February 26th. The Zero-Meridian was passed on February 24th at approximately 25° S. During this transit course the eastern part of a stable South-atlantic subtropic high was crossed and the weather was mainly fair with SE'ly to E'ly winds of 4 to 6 Beaufort, which were favourable for the speed of the ship. From south a long to intermediate wavelength swell of 2 to 3 m height was coming in, which caused some pitching and rolling of the ship, but did not seriously disturb the station works.

From 27th February on the cruise proceeded, interrupted by station works, slowly to the west, crossing the meridian 10° W on February 28th at the latitude 31° S and passing 20° W in the night from 2nd to 3rd March at about 32° S.

Until 1st March the ship encountered mainly E'ly to NE'ly winds of 2 to 4 Bft. Sometimes the remnants of dissipating fronts, belonging to the so called "Roaring Forties" gale centers far in the south, went through. So the weather continued to be mainly fair and RV METEOR continued in a smooth rolling and pitching motion, caused by the 2 to 3 m high swell, coming in continuously from the south.

On March 2nd and 3rd the ship entered a low pressure trough, which approached from the west rapidly and the wind turned towards to the north, increasing up to 16 to 20 knots for a while. On March 4th the cold front of a low with center at 37° S / 22° W was passed with wind NW 6 Bft., sea and swell 3 m, decreasing during the day. In the morning of March 5th, position approximately 34° S / 22° W, a mooring system with an acoustic signal generator, which had been moored in the deep sea for more than two years, was taken on board. At the time of this maneuver RV METEOR was at the edge of a high pressure cell, centered near 42° S / 38° W, and the wind was ESE 6 Bft, sea 3 m high.

On March 6th the ship passed the meridian 30° W at approximately 34° S and the E'ly wind increased to 7 to 8 Bft., sea 4 m high.

As RV METEOR just at this time had to sail a longer distance on a westerly course, this bad weather did not cause any thing negative and the stormy shoving wind was seen as benevolent by most of the participants, but it caused some lack of appetite to some others.

On March 7th the wind decreased and the sea became smooth, so that on March 8th the deep sea mooring system of the second acoustic sound generator could be taken on board at a position of approximately 31° S / 40° W under good weather conditions.

On March 9th weather was still fair. On March 10th RV METEOR did some station works near 28° S / 38° W an the wind increased S to SE 6 to 7 Bft., sea 2 to 3 m high. This strong wind was caused by a high pressure system with center off the Rio de la Plata mouth and a low pressure trough, which extended from Cape Frio to southeast.

On March 11th the wind decreased to SE 5 Bft., swell 3 m. So the third of the acoustic signal generators, which had been moored in the deep sea for more than three years, could be taken on board at approximately 27° S / 35° W without any difficulties.

On March 12th RV METEOR proceeded on a northwesterly course and changed to a northnortheasterly course on 13th, with some more station work, staying well clear of the Brazilian 200 Nautical Miles economic zone. During this part of the voyage SE'ly to E'ly wind of 5 Bft. was observed and the still incoming 3 m high swell made nobody forget that they were on board of a ship. On March 14th the latitude 20° S was crossed at the longitude 36° W, course eastnortheast. From then wind, sea and swell decreased bit by bit. On March 15th all research activities were suspended and RV METEOR changed course heading for the Brazilian port of Recife, where they moored at the quay under smooth, but hot and humid tropical weather conditions in the morning of March 17th.

Activities of the ship's weather watch

a.) Day by day a weather report was compiled and published, so that the ship's command, chief scientist and participants received a general weather forecast. The necessary charts and data were received from wireless stations (Pretoria, Rio de Janeiro), as satellite pictures (METEOSAT, GOES and NOAA satellites) and by fax or e-mail from Deutscher Wetterdienst, Hamburg. Special warning advice or a five days forecast were given in some cases.
b.) Meteorological parameters have been measured and recorded continuously and were put into the ship's data delivery system. So every participant could retrieve the necessary data into his PC. Sensors and equipment were maintained regularly.
c.) Every day 8 WMO standard weather observations were practiced and transmitted into the WMO Global Telecommunication System (GTS). Six of them included eye observations by meteorological staff.
d.) Everyday two rawinsondes were launched with the ASAP-System, determining a vertical profile of pressure, temperature, moisture and wind up to an altitude of 20 to 25 km. The evaluated data (temps) were transmitted into the GTS of WMO.

6.2 Weather and Meteorological Conditions during M 34/4

(K. Flechsenhaar)

RV METEOR left the port of Recife in the afternoon of Thursday, March 19th, 1996 steered on Eïly courses and started a few hours later with the station works. Also on March 20th and 21st the ship moved slowly to the E and dwelled on March, 22nd for a while at approximately 7.5 S 28 W. Here a mooring system with sediment traps was recovered and a new one was set out. After that METEOR steered N to NE and dwelled on March 23nd/24th at approximately 4° S 26° W and on March 25th/26th at approximately 0° N 23° W to take another two mooring systems with sediment traps on board, put new ones out and get an extensive number of samples.

Then the ship proceeded W to SW and reached on March 29th a position at approximately 4°S 36° W. From now on further station works were done over the coastal shelf of northern Brazil, and the vessel moved , sometimes in sight of the shore, sometimes far out over the deep sea, slowly to NW.

Until to this day the ship operated partly at the edge of a South Atlantic subtropic high and partly within the equatorial low pressure trough. The Intertropical Convergence Zone (ITCZ) varied between 5° S and 5° N, sometimes two ITCZ had been analysed. Accordingly was the weather: Mainly weak to moderate Eïly winds occurred, sometimes the wind was weak and variable. The sky was partly sunny, partly overcast, sometimes a shower came down, which was, due to the tropical temperatures, seen as a welcome refreshing by most of the participants. RV METEOR rolled and pitched smoothly in an Eïly swell of 1 to 1.5 m hight, temporarily the ship was tranquil. The station works had never been disturbed by unfavourable weather conditions.

On April 1st the ship reached the equator at the longitude 38° W and steered now, leaving the spring on starboard and the autumn on her port side, exactly olong the equator to the W, until the region off the Amazonas estuary was reached at approximately 45° W on April 3rd. Here further station works were done, sometimes in shallow water of about 30 m. The weather was influenced by the ITCZ: Sometimes showers with heavy rain, wind partly variable, but mainly E to NE 3 and 4, hight of swell 1 to 2 m.

On April 6th the station works concerning the Amazonas estuary were finished at approximately 5°N 50°W and also the ITCZ was passed through and left behind. From now on the weather was dominated by the NE trade-wind, which blow out of a Northatlantic subtropic high with its axis at about 28° N. So the wind was NE 5 on April 6th, increasing 6 to 7 on April 7th, hight of sea and swell about 3 m.

On April 8th the 200 nautical miles economic zone of French Guiana was reached at the position approximately 6° N 48° W. No research activities in the waters of French Guiana and Surinam were performed. RV METEOR steered now along the coast line W to NW, wind NE 5 or 6, swell 2 to 3 m.

An April 10th, meanwhile in the waters off Guyana, the activities started again at the position approximately 8°N 58°W. A strong NE trade-wind was blowing continuously and some rolling and pitching was caused by a 2 to 3 m high swell. From April 11th to 14th the ship operated in waters between Guyana and Barbados with high pressure influence, Wind E to NE 3 to 5, sea 1.5 to 2 m, swell between 2 and 3 m. East of the Lesser Antilles a contamination of the air with dust sometimes was observed. Dust originates from the Sahara and is transported via the trade-winds to the Caribbean Sea. In the morning of April 15th METEOR moored under moderate Eily winds at the quay of the port of Bridgetown, Barbados.

Activities of the Ship's Weather Watch

a.) Day by day a weather report was compiled and published, so that the shipïs command, chief scientist and participants received a general weather forecast. The necessary charts and data were received from wireless stations (Rio de Janeiro and Bracknell), as satellite pictures (METEOSAT, GOES and NOAA satellites) and by fax (ECMF forecast charts) or e-mail from Deutscher Wetterdienst, Hamburg and Offenbach.

Special advice or a five days forecast were given in some cases. The forecast of weather conditions and hight of sea and swell based mainly on surface analyses charts of the Central Atlantic Ocean between 40° N and 40° S. These charts, containing surface observations of South American stations and voluntary observing merchant ships, had been drawn by hand every day.

b.) Meteorological parameters have been measured and recorded continuously and were put into the ship's data delivery system. So every participant could retrieve the necessary data into his PC. Sensors and equipment were maintained regularly, some repairs were done.

c.) Every day 8 WMO standard weather observations were practiced and transmitted into the WMO Global Telecommunicating System (GTS). Six of them included eye observations by meteorological staff.

d.) Everyday two rawin sondes were launched with the ASAP-System, determining a vertical profile of pressure, temperature, moisture and wind up to an altitude of 20 to 25 km. The evaluated data (temps) were transmitted into the GTS of WMO.

7 Lists

7.1 Leg M 34/1

7.1.1 List of Sampling Stations

GeoB No.	Date 1996	Equipment	Bottom Contact (UTC)	Location Latitude [S]	Location Longitude [E]	Water Depth [m]	Core Length [cm]	Remarks
Southern Cape Basin								
3601-1	03.01.	MC	14:37	34°38.3'	17°51.7'	945	35	foraminiferal sand, olive green
3601-2		SL12	16:04	34°38.4'	17°51.3'	1039	---	core washed out, very sandy
3601-3		SL12	15:03	34°38.2'	17°52.5'	965	---	core washed out, very sandy
3602-1	03.01	SL12	20:39	34°47.9'	17°45.3'	1885	984	CC: carbonate ooze, olive green, foraminifera
3602-2		MC	22:20	34°47.8'	17°45.3'	1880	26	carbonate ooze, olive green, foraminifera
3603-1	04.01	MC	02:57	35°07.3'	17°32.0'	2851	30	carbonate ooze, grayish to white
3603-2		SL12	05:07	35°07.5'	17°32.6'	2840	1130	CC: carbonate ooze, upper 5 cm lost
3604-1	10.01	MC	02:13	31°47.1'	15°30.0'	1508	---	no sediment, early release
3604-2		MC	03:17	31°47.1'	15°29.6'	1512	---	no sediment, early release
3604-3		SL12	04:32	31°47.1'	15°30.0'	1514	942	CC: carbonate ooze, light olive green
3604-4		MC	06:03	31°47.1'	15°30.0'	1510	25	carbonate ooze, grayish white
3605-1	10.01	MC	09:15	31°26.8'	15°17.8'	1373	21	carbonate ooze, olive green
3605-2		SL12	10:27	31°26.7'	15°17.8'	1375	898	co CC sample, carbonate ooze
3605-3		HN50	9:55	31°26.7'	15°17.8'	1374		plankton, foraminifera
Northern Cape Basin								
3606-1	15.01	SL12	07:14	25°28.0'	13°05.0'	1785	1074	CC: olive green mud, foraminifera, pellets
3606-2		MC	08:44	25°28.0'	13°05.0'	1793	35	soft olive green mud, pellets
3606-3		HN50	08:00	25°28.0'	13°05.0'	1784		plankton, foraminifera

GeoB No.	Date 1996	Equipment	Bottom Contact (UTC)	Location Latitude [S]	Location Longitude [E]	Water Depth [m]	Core Length [cm]	Remarks
3607-1	15.01	MC	20:27	23°53.3'	14°19.9'	97	58	very soft diatomaceous mud, olive
3607-2		SL6	21:10	23°53.3'	14°20.0'	97	525	CC: sandy mud, olive green, mollusk shells
3607-3		HN30	20:45	23°53.3'	14°20.0'	97		plankton, foraminifera
3608-1	16.01	MC	18:16	22°21.7'	12°12.1'	1972	21	carbonate ooze, light olive
3608-2		SL12	19:48	22°21.5'	12°12.0'	1972	846	CC: carbonate ooze, olive green

Equipment:		
	MC	Multicorer (10 tubes)
	SL6	Gravity Corer (Schwerelot), 6 m
	SL12	Gravity Corer (Schwerelot), 12 m
	HN30	Handnet, 30 m line
	HN30	Handnet, 50 m line

7.1.2 Multicorer Sampling Scheme

GeoB No.	Water Depth [m]	Recovery [cm]	C_{org} Water Sample	C_{org} Surface Sample	Dinoflagellates	Foraminifera	Radiolaria Surface Sample	Archive (frozen)	Magnetics	Geochemistry
3601-1	945	35	x	x	x	2	x	2	x	-
3602-2	1880	26	x	x	x	2	x	2	x	-
3603-1	2851	30	x	x	x	2	x	2	x	-
3604-4	1510	25	x	x	x	2	-	2	x	-
3605-1	1373	21	x	x	x	2	-	2	x	x
3606-2	1793	35	x	x	x	2	x	2	x	-
3607-1	97	58	x	x	x	2	x	3	x	x
3608-1	1972	21	x	x	x	2	x	2	x	2

7.2 Leg M 34/2

7.2.1 List of Sampling Stations

GeoB No	Date 1996	Coring device	Time seafloor (UTC)	Latitude (°S)	Longitude (°E)	Water depth (m)	Core length (cm)	Remarks
TRANSECT A		**NORTHERN CAPE BASIN**						
3701-1	31.01	MUC +CTD	00:28	27°57,1	14°00,3	1488	25	8/4 tubes filled all sensors worked
3701-2		MUC	01:56	27°57,1	14°00,2	1488	28	7/4 tubes filled
3701-3		SL12	03:35	27°57,1	14°00,2	1488	966	Geology, CC in plastic bag
3702-1	31.01	SL12	11:20	26°47,5	13°27,2	1315	777	eology, CC in plastic bag
3702-2		MUC +CTD	12:51	26°47,5	13°27,3	1319	28	8/4 tubes filled all sensors worked
3702-3		MUC	14:06	26°47,5	13°27,3	1311	28	8/4 tubes filled
3703-1	31.01	Profilur	21:20 22:40	25°31,4	13°11,4	1379		deployed; defect, no sampling recovered
3703-2		Elinor	21:40 21:04	25°31,4	14°08,1	1370		deployed, defect: corer lid did not close recovered
3703-3	01.02.	MN + WS	23:53	25°30,9	13°13,8	1376		500-300, 300-200, 200-100, 100-50, 50-0 500, 300, 200, 100, 50
3703-4		MUC +CTD	02:02	25°31,0	13°14,0	1376	42	8/4 tubes filled all sensors worked
3703-5		MUC	03:17	25°31,0	13°14,0	1372	36	8/4 tubes filled
3703-6		MUC	04:31	25°31,0	13°13,9	1376	37	8/4 tubes filled
3703-7		SL18	05:44	25°31,1	13°13,8	1373	950	Biogeochemistry
3703-8		SL18	07:14	25°31,1	13°13,8	1369	1136	Geochemistry
3703-9		SL18	08:41	25°30,9	13°14,0	1373	933	Geology
3703-10		SL18	10:02	25°30,9	13°13,9	1369	1029	Sedimentology, frozen at -20°C
3704-1	01.02.	SL18	12:00	25°28,1	13°04,8	1794	1093	Sedimentology, frozen at -20°C
3704-2		MUC +CTD	14:00	25°28,0	13°05,0	1780	38	8/4 tubes filled O2 sensor clogged in greater depths
3705-1	02.02.	Profilur	04:11 10:43	24°18,7	12°59,9			deployed recovered
3705-2		MUC +CTD	05:01	24°18,1	12°59,9	1305	35	8/4 tubes filled O_2 sensor clogged in greater depths
3705-3		MUC	06:11	24°18,2	12°59,8	1308	31	8/4 tubes filled
3705-4		SL18	07:21	24°18,1	12°59,9	1305	1409	Geology, CC in plastic bag
3706-1		Profilur	19:30 19:50 00:45	22°43,5	12°36,3	1323		defect: weights lost deployed recovered
3706-2		SL18	20:26	22°43,0	12°36,0	1315	928	banana, Geology, CC in plastic bag
3706-3		MUC +CTD	22:01	22°43,0	12°36,1	1313	26	8/4 tubes filled O_2 sensor clogged in greater depths
3706-4		MUC	23:15	22°43,2	12°36,1	1313	28	8/4 tubes filled

GeoB No	Date 1996	Coring device	Time seafloor (UTC)	Latitude (°S)	Longitude (°E)	Water depth (m)	Core length (cm)	Remarks
3707-1	03.02.	Elinor	06:52	21°37,8	12°11,8	1355		deployed
	04.02.		07:45					recovered
3707-2	03.02.	MN +WS	07:24	21°37,5	12°11,7	1350		500-300, 300-200, 200-100, 100-50, 50-0 m
								500, 300, 200, 100, 50m
3707-3		MUC +CTD	08:53	21°38,0	12°11,6	1350	38	7/4 tubes filled
								O2 sensor worked
3707-4		MUC	10:04	21°37,5	12°11,6	1352	34	4/4 tubes filled
3707-5		MUC	11:22	21°37,5	12°11,6	1347	34	7/4 tubes filled
3707-6		MUC	12:35	21°37,4	12°11,7	1345	36	7/4 tubes filled
3707-7		SL12	13:58	21°37,4	12°11,6	1351	1110	Sedimentology, frozen at -20°C
3707-8		SL14	15:49	21°37,4	12°11,5	1353		Geochemistry, disturbed
3707-9		SL14	17:32	21°37,4	12°11,7	1350		Geochemistry
3707-10		SL14	19:01	21°37,5	12°11,6	1352	1378	Geology, CC in plastic bag
3707-11		Profilur	19:40	21°37,9	12°11,6			deployed and lost until
	(10.2.)		03:20	21°27,1	12°08,6			
Profiling			21:40	21°37,9	12°11,6			start of profile 1
			22:48	21°45,5	12°03,3			end of profile 1
			22:48	21°45,5	12°03,3			start of profile 2
			23:05	21°34,6	11°52,8			end of profile 2
			23:27	21°32,8	11°54,5			start of profile 3
	04.02.		01:50	21°43,8	12°05,0			end of profile 3
			02:00	21°38,2	12°01,7			start of profile 4
			04:20	21°31,8	11°55,8			end of profile 4
			04:31	21°30,9	11°56,9			start of profile 5
			06:43	21°42,0	12°07,1			end of profile 5
			06:43	21°42,0	12°07,1			start of profile 6
			07:17	21°37,7	12°11,4			end of profile 6
ODP-PRESITE SURVEY			**NORTHERN CAPE BASIN**					
3708-1	04.02.	MUC +CTD	20:04	21°05,4	11°49,5	1283	32	8/4 tubes filled
								O_2 sensor clogged in greater depths
3708-2		SL14	21:12	21°05,4	11°49,5	1284	804	Geology, CC in plastic bag
3709-1	05.02.	MUC +CTD	03:00	21°29,0	11°15,3	2709	23	8/4 tubes filled
								O_2 sensor clogged at 800 dbars
3709-2		SL14	04:54	21°29,0	11°15,5	2707	1355	Geology, CC in plastic bag
TRANSECT A (continued)			**NORTHERN CAPE BASIN, WALVIS RIDGE, SOUTHERN ANGOLA BASIN**					
3710-1		MUC +CTD	11:39	20°39,7	11°24,0	1313	30	8/4 tubes filled
								O_2 sensor clogged at 1000 dbars
3710-2		MUC	12:50	20°39,7	11°24,2	1312	30	8/4 tubes filled
3710-3		SL14	14:00	20°39,7	11°24,2	1313	1357	Geology, CC in plastic bag
3711-1		MUC +CTD	22:23	19°50,1	10°46,3	1214	33	8/4 tubes filled
								O_2 sensor clogged in greater depths
3711-2		MUC	23:30	19°50,1	10°46,1	1214	28	8/4 tubes filled
3711-3	06.02.	SL14	00:36	19°50,1	10°46,1	1215	1148	Geology, CC in plastic bag

GeoB No	Date 1996	Coring device	Time seafloor (UTC)	Latitude (°S)	Longitude (°E)	Water depth (m)	Core length (cm)	Remarks
3712-1		MUC +CTD	18:45	17°11,2	11°07,5	1242	26	8/4 tubes filled O_2 sensor clogged in greater depths
3712-2		MUC	19:47	17°11,2	11°07,5	1243	30	8/4 tubes filled
3712-3		SL14	22:48	17°11,1	11°07,6	1248	591	banana, geology, CC in pastic bag
3713-1	07.02.	MUC +CTD	07:56	15°37,7	11°34,8	1330	20	7/2 tubes filled O_2 sensor clogged in greater depths
3713-2		MUC	09:06	15°37,6	11°34,9	1322	19	8/2 tubes filled
3714-1	07.02.	Elinor	18:27	17°09,9	10°59,8			deployed
	08.02.		20:32					recovered
Profiling	07.02.		18:43	17°09,3	10°59,9			start of profile 7
			19:03	17°08,6	10°57,3			end of profile 7
			19:14	17°07,4	10°57,4			start of profile 8
			21:10	17°10,8	11°11,1			end of profile 8
			21:21	17°09,8	11°11,8			start of profile 9
			23:01	17°06,1	10°57,9			end of profile 9
			23:21	17°05,0	10°58,0			start of profile 10
	08.02.		00:53	17°07,3	11°08,2			end of profile 10
			00:53	17°07,3	11°08,2			start of profile 11
			01:40	17°13,2	11°06,8			end of profile 11
			01:40	17°13,2	11°06,8			start of profile 12
			03:05	17°11,0	10°56,3			end of profile 12
			03:17	17°09,8	10°56,7			start of profile 13
			05:16	17°13,4	11°10,9			end of profile 13
			05:27	17°12,1	11°11,2			start of profile 14
			06:58	17°09,3	11°00,0			end of profile 14
3714-2		MN	07:41	17°09,7	10°59,8	2061		500-300, 300-200, 200-100
		+						100-50, 50-0
		WS						500, 300, 200, 100, 50
3714-3		MUC +CTD	09:25	17°09,6	10°59,9	2060	36	8/4 tubes filled O_2 sensor clogged in greater depths
3714-4		MUC	11:00	17°09,6	10°59,9	2062	32	8/4 tubes filled
3714-5		MUC	12:32	17°09,6	10°59,9	2062	35	8/2 tubes filled
3714-6		MUC	14:12	17°09,6	10°59,8	2072	34	8/2 tubes filled
3714-7		MUC	15:52	17°09,5	10°59,9	2060	35	8/4 tubes filled
3714-8		SL14	17:22	17°09,5	10°59,9	2062	1209	Geology, CC & 0-2 cm plastic bag
3714-9		SL14	19:06	17°09,6	10°59,9	2060	1241	Geochemistry
3714-10		SL14	21:21	17°09,6	10°59,8	2065	1297	Biogeochemistry
3714-11		SL14	23:05	17°09,6	10°59,9	2066	1241	Sedimentology, frozen at -20°C
3715-1	09.02.	MUC +CTD	09:40	18°57,3	11°03,4	1204	32	8/4 tubes filled
3715-2		MUC	10:44	18°57,3	11°03,4	1203	32	8/4 tubes filled
3715-3		SL14	11:48	18°57,2	11°03,4	1200	819	Geology, CC in plastic bag
3716-1	10.02.	MUC	21:36	23°53,3	14°20,1	92		looking for Thioploca
3716-2		MUC	22:02	23°53,3	14°19,9	96		dto.
3716-3		MUC	22:24	23°53,3	14°19,7	98		dto.
3716-4		MUC	22:59	23°53,3	14°18,5	107		dto.
3716-5		MUC	23:32	23°53,4	14°17,5	113		dto.
3716-6	11.02.	MUC	00:02	23°53,4	14°16,4	116		dto.
3716-7		MUC	00:37	23°53,4	14°15,2	121		dto.

GeoB No	Date 1996	Coring device	Time seafloor (UTC)	Latitude (°S)	Longitude (°E)	Water depth (m)	Core length (cm)	Remarks
3716-8	11.02	MUC	01:12	23°53,4	14°14,0	123		dto.
3716-9		MUC	01:49	23°53,5	14°12,8	132		dto.
3716-10		MUC	02:29	23°53,4	14°10,6	140		dto.
3716-11		MUC	03:18	23°53,3	14°07,2	160		did not close
3716-12		MUC	03:34	23°53,3	14°07,1	160		did not close
3716-13		MUC	03:55	23°53,4	14°07,1	162		looking for Thioploca
3716-14		MUC	04:42	23°53,4	14°03,7	184		dto.
Profiling			09:15	24°32,5	14°17,8			start of profile 13
			13:20	24°46,0	13°33,0			turning point
			14:30	24°49,9	13°22,0			end of profile 13
TRANSECT B		**FROM SHELF TO DEEP SEA BASIN**						
3717-1		MUC +CTD	15:32	24°50,0	13°21,0	855	33	8/4 tubes filed O_2 sensor worked
3717-2		MUC	16:20	24°50,0	13°21,8	858	38	8/4 tubes filled
3717-3		SL12	17:10	24°50,2	13°21,9	857	800	Geology, CC in plastic bag
3718-1	11.02.	Profilur	19:19	24°53,9	13°10,0	1313		deployed, sampling
	12.02.		09:37					recovered
3718-2	11.02.	Elinor	19:25	24°53,9	13°10,0	1308		deployed, sampling
	12.02.		22:06					recovered
Profiling	11.02.		19:41	24°54,5	13°19,4			start of profile 14
			19:54	24°53,9	13°12,1			end of profile 14
			20:09	24°52,0	13°11,2			start of profile 15
			23:05	24°57,2	12°49,8			end of profile 15
			23:25	24°59,2	12°50,4			start of profile 16
	12.02.		02:11	24°52,9	13°11,7			end of profile 16
			02:20	24°54,9	13°12,5			start of profile 17
			05:36	25°03,3	12°52,0			end of profile 17
			05:50	25°01,3	12°51,2			start of profile 18
			08:35	24°54,5	13°10,4			end of profile 18
3718-3	12.02.	MN	10:21	24°53,7	13°09,7	1316		500-300, 300-200, 200-100
								100-50, 50-0 m
		+WS						500, 300, 200, 100, 50 m
3718-4		MUC +CTD	12:09	24°53,7	13°09,6	1316	33	8/4 tubes filled O_2 sensor clogged in greater depths
3718-5		MUC	13:18	24°53,7	13°09,6	1317	36	8/2 tubes filled
3718-6		MUC	14:22	24°53,7	13°09,7	1313	34	recovery undisturbed only in 3 tubes
3718-7		MUC	15:29	24°53,7	13°09,7	1310	33	8/4 tubes filled
3718-8		MUC	16:32	24°53,7	13°09,7	1313	33	8/2 tubes filled
3718-9		SL14	17:36	24°53,6	13°09,8	1312	1371	Geochemistry
3718-10		SL14	18:54	24°53,7	13°09,7	1350	1374	Geology, CC in plastic bag
3719-0	12.02.	Profilur	23:55	24°59,9	12°52,0			deployed
	13.03.		05:08	24°59,7	12°52,3			
recovered								
3719-1	13.02.	SL14	00:40	24°59,7	12°52,3	1995	1366	Geology, CC in plastic bag
3719-2		MUC +CTD	02:43	24°59,7	12°52,3	1995	23	8/4 tubes filled O2 sensor clogged
3719-3		MUC	04:14	24°59,8	12°52,4	1995	20	8/4 tubes filled

GeoB No	Date 1996	Coring device	Time seafloor (UTC)	Latitude (°S)	Longitude (°E)	Water depth (m)	Core length (cm)	Remarks
3720-1		MUC +CTD	07:22	25°04,1	12°40,1	2516	21	4/4 tubes filled O2 sensor defect
3720-2		MUC	09:08	25°04,1	12°40,0	2518	21	4/4 tubes filled
3720-3		SL14	10:54	25°04,1	12°40,0	2517	1361	Geology, CC in plastic bag
3721-1	13.02.	Profilur	13:22	28°08,8	12°24,2	3007		deployed
	14.02.		00:07	25°29,1	12°24,0	3010		recovered
3721-2	13.02.	MN	13:48	25°08,9	12°24,1	3007		500-300, 300-200, 200-100, 100-50, 50-0
		+ WS						500, 300, 200, 100, 50
3721-3		SL14	15:22	25°09,1	12°24,0	3013	1384	Geology, CC in plastic bag
3721-4		MUC +CTD	17:38	25°09,1	12°24,0	3014	20	8/4 tubes filled O2 sensor defect
3721-5		MUC	19:46	25°09,1	12°23,9	3017	19	8/4 tubes filled
3721-6	13.02.	Elinor	21:05	25°09,1	12°24,1	3017		deployed
	16.02.		15:03	25°09,5	12°19,2			recovered
3722-1	14.02.	MUC +CTD	03:34	25°15,0	12°01,4	3505	22	8/4 tubes filled O2 sensor defect
3722-2		SL15	05:54	25°15,0	12°01,3	3506	1296	Geology, CC in plastic bag
3723-1		SL15	10:36	25°23,6	11°31,6	4003	1253	Geology, CC in plastic bag
3723-2		MUC +CTD	12:58	25°23,7	11°31,6	4004	11	6/1 tubes filled O2 sensor defect
3723-3		MUC	15:42	25°23,6	11°31,7	4002	11	7/4 tubes filled
3724-1	15.02.	MUC +CTD	07:13	26°08,3	08°55,6	4766	40	7/4 tubes filled O2 sensor defect
3724-2		MUC	11:20	26°08,3	08°55,7	4763	40	7/4 tubes filled
3724-3		MUC	14:28	26°08,2	08°55,6	4766	22	2/3 tubes filled
3724-4		SL15	17:26	26°08,2	08°55,6	4763	1141	Geology, CC in plastic bag
Profiling	16.02.		16:00	25°03,9	12°15,1			start of profile 19
	17.02.		03:11	23°53,6	11°26,3			end of profile 19
			03:11	23°53,6	11°26,3			start of profile 20
			11:34	23°19,0	11°26,3			end of profile 20
3725-1	17.02.	MUC +CTD	12:12	23°19,0	12°22,3	1980	24	7/4 tubes filled O2 sensor defect
Profiling			12:56	23°19,0	12°22,5			start of profile 21
			17:13	23°11,1	13°04,2			end of profile 21
3726-1		MUC	17:24	23°11,2	13°04,9	496		looking for Thioploca
3726-2		MUC	18:08	23°10,8	13°05,8	453		dto.
3726-3		MUC	18:59	23°10,1	13°08,6	403		dto.
3726-4		MUC	20:41	23°07,5	13°19,9	353		dto.
3726-5		MUC	21:47	23°06,2	13°24,5	302		dto.
3726-6		MUC	23:04	23°00,2	13°23,6	325		dto.

Equipment:

MUC	Multicorer	MN	Multinet
SL12, 14	Gravity corer 12, 14 m length	WS	Water sampler
CTD	Seacat Profiler		

GeoB No (cm)	MICROPALEONTOLOGY Recovery	Forami-nifera	Radiol. surface	Diatoms	Dinoflag. Bacteria	Magnetic	GEOCHEMISTRY Corg water	Pore-	O2 tivity	Conduc- Reduction	Sulfate	Density Nitrat	Fe/ duction	Fe-Re- 18O	13C/	Archives
3701-1	25	2 lg	1 sm	-	1 lg	2 lg /1 sm	-	1 lg	1 lg	-	-	1 sm	-	x	1 lg / 2 sm
3701-2	28	-	-	-	-	-	1 lg	-	-	3 lg	1 lg	-	-	-	1 sm
3702-2	28	2 lg	-	-	-	2 lg / 1 sm	-	1 lg	1 lg	-	-	1 sm	-	x	1 lg / 2 sm
3702-3	28	-	1 sm	-	1 lg	-	1 lg	-	-	3 lg	2 lg	-	-	-	-
3703-4	42	2 lg	1 sm	-	-	2 lg/ 1 sm	-	-	-	3 lg	-	-	-	x	1 lg / 1 sm
3703-5	36	-	-	-	-	-	-	-	-	-	-	4 sm	8 lg	-	-
3703-6	37	-	-	-	1 lg	-	-	1 lg	1 lg	-	2 lg	-	2 lg	-	-
3704-2	38	2 lg	1 sm	-	1 lg	2 lg / 1 sm	-	1 lg	1 lg	-	-	-	-	x	1 lg / 1 sm
3705-2	35	2 lg	1 sm	-	-	3 lg	-	1 lg	1lg	-	-	-	-	x	1 lg / 3 sm
3705-3	31	-	-	-	1 lg	-	1 lg	-	-	2 lg	2 lg	-	-	-	-
3706-3	26	2 lg	1sm	-	-	3 lg	-	1 lg	1 lg	-	-	-	-	x	1 lg / 3 sm
3706-4	28	-	-	-	2 lg	-	1 lg	-	-	3 lg	2 lg	-	-	-	4 sm
3707-3	38	2 lg	1 sm	-	-	3 lg	1 lg	-	-	-	-	-	-	x	1 lg / 2 sm
3707-4	34	-	-	-	-	-	-	1 lg	1 lg	-	2 lg	-	-	-	-
3707-5	34	-	-	-	-	-	-	-	-	3 lg	-	-	4 lg	-	1 sm
3707-6	36	-	-	-	1 lg	-	-	-	-	-	-	1 lg /4 sm	5 lg	-	-
3708-1	32	2 lg	1 sm	-	1 lg	3 lg	-	1 lg	-	-	-	-	-	x	1 lg / 2 sm
3709-1	23	2 lg	1 sm	-	1 lg	3 lg	-	1 lg	-	-	-	-	-	x	1 lg / 2 sm
3710-1	30	2 lg	1 sm	-	-	3 lg	-	1 lg	-	-	-	-	-	x	1 lg / 2 sm
3710-2	30	-	-	-	1 lg	-	1 lg	-	-	3 lg	2 lg	-	-	-	-
3711-2	33	2 lg	1 sm	-	1 lg	3 lg	-	1 lg	-	-	-	-	-	x	1 lg / 3 sm
3711-2	28	-	-	-	-	-	1 lg	-	-	3 lg	2 lg	-	-	-	-
3712-1	26	2 lg	1 sm	-	1 lg	3 lg	-	1 lg	-	-	-	-	-	x	1 lg / 3 sm
3712-2	30	-	-	-	-	-	1 lg	-	-	3 lg	2 lg	-	-	-	-
3713-1	20	2 lg	-	-	-	3 lg	-	1 lg	1 lg	-	-	-	-	x	2 sm
3713-2	19	-	1 sm	-	1 lg	-	1 lg	-	-	3 lg	2 lg	-	-	-	1 lg / 1 sm
3714-3	36	2 lg	1 sm	-	-	3 lg	-	1 lg	1 lg	-	-	1 sm	-	x	1 lg / 2 sm
3714-4	32	-	-	-	1 lg	-	1 lg	-	-	2 lg	2 lg	2 lg	-	-	1 sm
3714-5	35	-	-	1 lg	-	-	-	2 lg	-	-	-	-	4 lg	-	-
3714-6	34	-	-	-	-	-	-	-	-	-	-	-	8 lg	-	-
3714-7	35	-	-	-	-	-	-	3 lg	1 lg	-	-	-	-	-	1 sm
3715-1	32	2 lg	1 sm	1 lg	-	3 lg	-	-	-	-	-	-	-	x	1 lg / 2 sm
3715-2	32	-	-	-	1 lg	-	1 lg	1 lg	1 lg	2 lg	2 lg	-	-	-	1 sm

GeoB No (cm)	MICROPALEONTOLOGY Recovery	Forami-nifera	Radiol. surface	Diatoms	Dinoflag. Bacteria	Magnetic	Corg water	GEOCHEMISTRY Pore-	O2 tivity	Conduc- Reduction	Sulfate	Density Nitrat	Fe/ duction	Fe-Re- 18O	13C/	Archives
3716-1 to 3716-13	looking for Thioploca in 100 m water depth															
3717-1	33	2 lg	1 sm	1 lg	-	3 lg	-	-	-	-	-	-	-	x	1 lg / 2 sm
3717-2	38	-	-	-	1 lg	-	1 lg	1 lg	1 lg	3 lg	1 lg	-	-	-	1 sm
3718-4	33	2 lg	1 sm	-	-	2 lg	-	1 lg	1 lg	-	-	-	-	x	2 lg / 2 sm
3718-5	28	-	-	-	1 lg	-	1 lg	-	-	3 lg	1 lg	-	2 lg	-	-
3718-6	32	-	-	-	-	-	-	-	-	-	-	-	3 lg	-	-
3718-7	33	-	-	-	-	-	-	-	-	-	-	1 lg / 2 sm	5 lg	-	-
3718-8	30	-	-	1 lg	-	-	-	3 lg / 1sm	-	-	-	1 lg	-	-	-
3719-2	23	2 lg	1 sm	1 lg	-	2 lg	-	1 lg	1 lg	-	-	-	-	x	1 lg / 2 sm
3719-3	20	-	-	-	1 lg	-	1 lg	-	-	3 lg	1 lg	-	-	-	1 lg / 1 sm
3720-1	21	2 lg	1 sm	-	-	1 lg	-	-	-	-	-	-	-	x	1 lg / 2 sm
3720-2	21	-	-	1 lg	1 lg	-	--	-	-	-	-	-	-	-	1 lg
3721-4	20	2 lg	1 sm	1 lg	-	2 lg	-	1 lg	1 lg	-	-	-	-	x	1 lg / 3 sm
3721-5	19	-	-	-	1 lg	-	1 lg	2 lg / 1 sm	-	3 lg	1 lg	-	-	-	1 sm
3722-1	22	2 lg	1 sm	1 lg	1 lg	2 lg	-	-	-	-	-	-	-	x	2 lg / 3 sm
3723-2	11	2 lg	-	1 lg	-	1 lg	-	1 lg	-	-	-	-	-	x	1 lg / 1 sm
3723-3	11	-	-	-	1 lg	1 lg	-	-	-	-	-	-	-	-	1 lg / 1 sm
3724-1	40	2 lg	1 sm	1 lg	-	2 lg	-	-	-	-	-	-	-	x	2 lg / 2 sm
3724-2	22	-	-	-	-	-	-	2 sm	-	-	-	-	-	-	-
3724-3	38	-	-	-	1 lg	-	-	1 lg	1 lg	1 lg / 1 sm	-	-	-	-	1 sm
3725-1	22	2 lg	1 sm	-	1 lg	2 lg	-	-	-	-	-	-	-	x	2 lg / 3 sm
3726-1 to 3726-6	looking for Thioploca in 300-400 m water depth, no success														

7.2.3 Gravity Core Sampling

GEOLOGY / SEDIMENTOLOGY

GeoB No	Water depth (m)	Recovery (cm)	Physical Properties	Foramini-fera	Pore-water	Sedimen-tology	Paleo-Magnetics	Smear-Slides	Color Scan/ Corephoto
3701-3	1494	966	x	x	x	x	x	x	x
3702-1	1320	777	x	x	x	x	x	x	x
3703-9	1371	933	Geology, opened on M34/3						
3703-10	1369	1029	Sedimentology, frozen in m-segments						
3704-1	1798	1093	Sedimentology, frozen in m-segments						
3705-4	1309	1409	x	x	x	x	x	x	x
3706-2	1304	928	Geology, opened on M34/3						
3707-7	1356	1110	Sedimentology, frozen in m-segments						
3707-10	1361	1378	x	x	x	x	x	x	x
3708-2	1289	804	x	x	x	x	x	x	x
3709-2	2717	1355	Geology, opened on M34/3						
3710-3	1314	1357	x	x	x	x	x	x	x
3711-3	1214	1148	Geology, opened on M34/3						
3712-3	1248	591	Geology, opened on M34/3						
3714-8	2070	1209	x	x	x	x	x	x	x
3714-11	2060	1241	Sedimentology, frozen in m-segments						
3715-3	1204	819	Geology, opened on M34/3						
3717-3	861	800	Geology, opened on M34/3						
3718-10	1321	1374	Geology, opened on M34/3						
3719-1	1993	1366	Geology, opened on M34/3						
3720-3	2513	1361	Geology, opened on M34/3						
3721-3	3013	1384	Geology, opened on M34/3						
3722-2	3505	1296	Geology, opened on M34/3						
3723-1	4001	1253	Geology, opened on M34/3						
3724-4	4792	1141	Geology, opened on M34/3						

BIOGEOCHEMISTRY

GeoB No	Water depth (m)	Recovery (cm)	Sulfate-reduction rate	Sulfur-compounds	Methan / Methan isotope	Molecular ecological techniques
3703-7	1373	950	x	x	x	x
3714-10	2067	1297	x	x	x	x

GEOCHEMISTRY

GeoB No	Water depth (m)	Recovery (cm)	Methan / Sulfid	SO_4^{2-}/ Cl^-	NH_4^+/ NO_3^-	PO_4^{3-}/ Fe	pH/ Eh	Alka-linity	Conduc-tivity	F^-
3703-8	1377	1136	x	x	x	x	x	x	x	x
3707-9	1360	1105	x	x	x	x	x	x	x	x
3707-8	1357	800	torn apart, in m-segments stored, unsampled							
3714-9	2071	1241	x	x	x	x	x	x	x	x
3718-9	1321	1371	x	x	x	x	x	x	x	x

7.3 Leg M 34/3

7.3.1 List of Sampling Stations

Station No.	Date 1996	Equipment	Bottom Contact (UTC)	Latitude S	Longitude W	Water Depth (m)	Core recovery (cm)	Remarks
Profil A	**Mid**	**Atlantic**	**Ridge**					
3801-1	26.02.	CTD	14:06	29°30,1'	08°17,4'	4545		Niskin Bottles at 4604, 3800, 2199, 919, 194, 149, 100, 49, 20
3801-2		MN	15:41	29°29,9'	08°17,8'	4545		Nets at 500, 300, 200, 100, 50m water depth Niskin Bottles at the same depths
3801-3		MN	16:49	29°30,3'	08°17,3'	4545		Nets at 400, 200, 100, 40, 20m water depth Niskin Bottles at the same depths
3801-4		MN	17:38	29°30,1'	08°17,6'	4545		Nets at 250, 100, 75, 50, 25m water depth Niskin Bottles at the same depths
3801-5		MUC	19:16	29°30,7'	08°18,2'	4545	8	2 tubes empty (1/6cm, 1/10cm)
3801-6		SL 12	21:35	29°30,7'	08°18,3'	4546	937	Geology
3802-1	27.02.	SL 12	5:19	30°09,8'	08°31,0'	3969	416	Geology, core damaged at 5m
3802-2		MUC+CTD	7:23	30°09,8'	08°30,9'	3970	7	7 tubes empty (2/6cm, 5/10cm)
3802-3		MUC	9:28	30°09,8'	08°30,8'	3974	14	4 tubes empty (2/6cm, 2/10cm)
3803-1		MUC+CTD	13:34	30°20,9'	08°34,3'	4173	23	
3803-2		SL 9	15:41	30°21,0'	08°34,4'	4173	367	Geology
3804-1		SL 9	21:12	30°44,6'	08°46,1'	3891	413	Geology
3804-2		MUC+CTD	23:10	30°44,6'	08°46,2'	3882	14	all tubes filled
3805-1	28.02.	MUC+CTD	11:47	30°45,0'	10°20,9'	3661	9	6 tubes empty (6/10cm)
3805-2		MUC	13:52	30°45,0'	10°20,8'	3669	7	10 tubes empty (2/6cm, 8/10cm)
3805-3		SL 9	15:38	30°44,9'	10°20,9'	3659	309	Geology
3806-1	29.02.	SL 9	00:09	30°45,0'	11°33,4'	3294	366	Geology
3806-2		MUC+CTD	2:37	30°44,9'	11°33,4'	3294	8	4 tubes empty (1/6cm, 3/10cm)
3807-1		MUC+CTD	11:58	30°45,0'	13°11,9'	2515	8	9 tubes empty (1/6cm, 8/10cm)
3807-2		MUC	13:22	30°45,0'	13°11,8'	2534	3	
3807-3		SL 9	14:57	30°45,1'	13°12,0'	2518	61	Geology, core damaged after 2m
3808-1		CTD/RO+ CTD	23:57	30°48,6'	14°42,7'	3214		
3808-2	01.03.	MN	01:11	30°48,5'	14°43'	3213		Nets at 500, 300, 200, 100, 50m water depth Niskin Bottles at the same depths

3808-3		MN	02:15	30°48,5'	14°42,7'	3214		Nets at 400, 200, 100, 40, 20m water depth Niskin Bottles at the same depths
3808-4		MN	03:01	30°48,6'	14°42,6'	3213		Nets at 250, 100, 74, 50, 25m water depth Niskin Bottles at the same depths
3808-5		SL 6	04:04	30°48,7'	14°42,7	3213	568	Geochemistry
3808-6		SL 9	06:01	30°48,7	14°42,7	3213	415	Geology
3808-7		MUC	07:43	30°48,7'	14°42,6'	3213	7	1 tube empty (1/10cm)
3809-1		MUC+CTD	15:49	31°03,2'	16°19,8'	3470	8	2 tubes empty (2/10cm)
3809-2		SL 9	19:25	31°03,3'	16°19,5'	3463	234	Geology, core damaged at 3m
3810-1	02.03.	SL 6	00:18	31°07,9'	16°50,3'	3810	218	Geology
3810-2		MUC+CTD	02:07	31°08,0'	16°50,3'	3810	11	2 tubes empty (2/10cm)
3811-1		MUC+CTD	10:34	31°21,4'	18°09,8'	4091		Multicorer damaged
3811-2		SL 6	12:46	31°21,4'	18°09,8'	4091	140	Geology
3812-1		SL 6	22:24	31°36,9'	19°45,5'	4205	532	Geology
3812-2	03.03.	MUC+CTD	0:29	31°36,9'	19°45,6'	4204	10	2 tubes empty (2/10cm)
3813-1		CTD/RO+ CTD	12:35	32°16,2'	21°58,2'	4320		Niskin Bottles at 4383, 3799, 2110, 951, 171, 149, 100, 12
3813-2		MUC	15:52	32°16,1'	21°58,8'	4267		all tubes empty
3813-3		SL 12	18:21	32°16,1	21°58,0	4331	983	Geology
3813-4		MUC	20:43	32°16,4'	21°58,1'	4332		all tubes empty
3813-5		MN	22:21	32°16,9'	21°57,0'	4332		Nets at 500, 300, 200, 100, 50m water depth Niskin Bottles at the same depths
3813-6		MN	23:15	32°17,2'	21°56,3'	4332		Nets at 400, 200, 100, 40, 20m water depth Niskin Bottles at the same depths
3813-7	04.03.	MN	00:01	32°17,8'	21°55,8'	4332		Nets at 250, 100, 75, 50, 25m water depth Niskin Bottles at the same depths
	Hunter	**Channel**						
3814-1	05.03.	mooring K02	12:25	34°11,4'	28°38,0'	4379		Recovery of the mooring
3814-2		MN	12:55	34°11,1'	28°38,0'	4379		Nets at 500, 300, 200, 100, 50m water depth Niskin Bottles at the same water depths
3814-3		MN	13:50	34°10,8'	28°37,6'	4370		Nets at 400, 200, 100, 40, 20m water depth Niskin Bottles at the same water depths
3814-4		MN	14:31	34°10,2'	28°37,6'	4369		Nets at 250, 100, 75, 50, 25m water depth Niskin Bottles at the same water depths

3814-5		CTD/RO+ CTD	15:22	34°09,7'	28°37,6'	4379		Niskin Bottles at 1501, 892, 200, 148, 99, 49, 20m water depth
3814-6		SL 12	17:32	34°11,0'	28°38,1'	4340	795	Geology
	Vema	**Channel**						
3815-1	07.03.	CTD/RO	21:56	31°11,8'	39°18,9'	4448		
3816-1	08.03.	CTD/RO	00:37	31°11,8'	39°21,0	4542		
3817-1	08.03.	CTD/RO+ CTD	03:41	31°11,4'	39°26,1'	4588		Niskin Bottles at 2228, 1035, 206, 150, 100, 50, 19m water depth
3817-2	08.03.	MN	05:21	31°11,4'	39°25,9'	4595		Nets at 500, 300, 200, 100, 50m water depth Niskin Bottles at the same water depths
3817-3	08.03.	MN	06:20	31°11,9'	39°25,9'	4578		Nets at 400, 200, 100, 40, 20m water depth Niskin Bottles at the same water depths
3817-4	08.03.	MN	07:09	31°12,0'	39°25,9'	4574		Nets at 250, 100, 75, 50, 25m water depth Niskin Bottles at the same water depths
3818-1	08.03.	mooring K2	11:43	31°07,0'	39°54,1'			Recovery of the mooring
3819-1	09.03.	CTD/RO	13:11	28°11,9'	38°17,7	4736		
3820-1	09.03.	CTD/RO	17:15	28°17,6'	38°06,2'	4663		
3821-1	09.03.	CTD/RO	21:18	28°07,4'	38°17,9'	4565		
3822-1	10.03.	MUC+CTD	03:08	27°37,6'	37°57,0'	4273	40	
3822-2	10.03.	SL12	05:26	27°37,7'	37°57,0'	4272	884	Geochemistry
3822-3	10.03.	SL12	07:48	27°37,8'	37°57,1'	4276	891	Geology
3823-1	10.03.	SL12	10:33	27°35,1'	37°55,2'	4368	905	Geology
3823-2	10.03	MUC	12:40	27°35,2'	37°55,2	4368		all tubes not closed
3824-1	11.03	CTD/RO	07:17	26°52,2'	34°48,3'	4786		Niskin Bottles at 4830, 3799, 2201, 879, 200, 145, 100, 50, 19m water depth
3824-2	11.03	MN	08:53	26°52,2'	34°48,3'	4783		Nets at 500, 300, 200, 100, 50m water depth Niskin Bottles at the same depths
3824-3	11.03.	MN	09:56	26°52,3'	34°48,2'	4776		Nets at 400, 200, 100, 40, 20m water depth Niskin Bottles at the same depths
3824-4	11.03.	MN	10:41	26°52,3'	34°48,3'	4773		Nets at 250, 100, 75, 50, 25m water depth Niskin Bottles at the same depths
3824-5	11.03.	mooring K3	13:12	26°51,2'	34°19,8'			Recovery of the mooring

	Profile B	Continental	Slope	off Brazil				
3825-1	11.03.	MUC+CTD	22:48	26°14,0'	36°19,8	4279	47	2 tubes empty (2/6 cm)
3825-2	12.03.	SL12	00:55	26°14,0'	36°19,9'	4267	945	Geology
3826-1	12.03.	SL12	11:52	25°19,2'	38°00,4'	3991	684	Geology
3826-2	12.03.	MUC+CTD	13:49	25°19,2'	38°00,4'	3988	30	5 tubes empty (5/10 cm)
3827-1	12.03.	MUC+CTD	18:55	25°01,9'	38°32,9'	3842	37	
3827-2	12.03.	SL12	20:57	25°01,9'	38°32,9'	3845	784	Geology
3827-3	12.03.	CTD/RO	22:38	25°01,9'	38°32,2'	3846		Niskin Bottles at 907, 201, 149, 99, 50, 19m water depth
3827-4	12.03.	MN	23:30	25°01,9'	38°32,1'	3846		Nets at 500, 300, 200, 100, 50m water depth Niskin Bottles at the same depths
3827-5	13.03.	MN	00:25	25°01,9'	38°32,0'	3846		Nets at 400, 200, 100, 40, 20m water depth Niskin Bottles at the same depths
3827-6	13.03.	MN	01:00	25°01,8'	38°31,9'	3846		Nets at 250, 100, 75, 50, 25m water depth Niskin Bottles at the same depths
3828-1	13.03.	CTD/RO	19:30	22°09,8'	37°04,6'	3887		Niskin Bottles at 860, 200, 150, 99, 48, 22m water depth
3829-1	14.03.	CTD/RO	16:26	19°00,7'	35°29,9'	4043		Niskin Bottles at 860, 200, 150, 99, 48, 22m water depth
3830-1	15.03.	CTD/RO	14:24	15°33,9'	34°59,6'	4332		Niskin Bottles at 1506, 200, 149, 100, 51, 20m water depth

7.4 Leg M 34/4

7.4.1 List of Sampling Stations

GeoB #	Date 1996	Coring device	Time seafloor (UTC)	Latitude	Longitude	Water depth (m)	Sample (XX)	Remarks
Brazil Basin								
3901-1	19.03	CTD	23:12	07°59.2S	34°17.0W	1057	---	Profile depth 980m
3902-1	20.03	CTD	01:18	07°58.5S	34°06.0W	1506	---	Profile depth 1180m
3903-1	20.03	CTD	03:25	07°57.6S	33°54.2W	3560	---	Profile depth 1180m
3904-1	20.03	CTD	05:59	07°55.7S	33°35.8W	4419	---	Profile depth 1180m
3905-1	20.03.	CTD	09:11	07°53.7S	33°10.9W	4290	---	Profile depth 1180m
3906-1	21.03	WA6	12:32	07°28.4S	28°08.5W	5580	2	Release, start recovery
		WA6	15:28	07°27.4S	28°08.4W	4950	traps	Stop recovery, 40 cups with sediment
3906-2		ISP	15:55	07°25.3S	28°08.1W	5394	60 min	Trace metals, 100 and 400m water depth
3906-3		ROS	17:46	07°24.8S	28°08.0W	5467	6x30l	2x250m, 1x100m, 2x50m, 1x20m
3906-4		ISP	19:00	07°26.5S	28°07.9W	4895	60 min	Trace metals, 700 and 1200m water depth
3906-5		MN	20:55	07°26.1S	28.08.3W	5300	5 cups	Forams, water isot., 500, 300, 200, 100, 50m
3906-6		MN	21:37	07°25.9S	28°08.2W	5297	5 cups	Radiolaria, 400, 200, 100, 40, 20m
3906-7		MN	22:09	07°25.8S	28°08.1W	5284	5 cups	Corg, water isotopes, 250, 100, 75, 50, 25m
3906-8	22.03	GFW	01:37	07°25.0S	28°07.9W	5441	11x12l	Trace metals, Ox, nutrients, 10 to 5000m
3906-9		MUC & CTD	06:46	07°28.0S	28°06.4W	4886	33 cm	Deep sea clay, manganese nodules Profile depth 4776 m
3906-10		WA9	09:07	07°29.1S	28°04.8W	4988	2	start deployment
		WA9	13:08	07°27.5S	28°08.1W	5085	traps	weight over board, stop deployment
3907-1	23.03	WA7	13:07	03°58.7S	25°39.6W	5554	2	Release, start recovery
		WA7	16:08	03°58.6S	25°40.6W		traps	Stop recovery, 40 cups with sediment
3907-2		ISP	16:58	03°56.3S	25°41.3W	5555	60min	Trace metals, 100 and 400m water depth
3907-3		ROS	18:25	03°55.8S	25°41.0W	5552	6x30l	2x250m,1x100m, 2x50m, 1x20m
3907-4		ISP	19:23	03°55.2S	25°41.0W	5557	60min	Trace metals, 700 and 1200m water depth
3907-5		MN	21:17	03°55.1S	25°40.1W	5556	5 cups	Forams, water isot., 500, 300, 200, 100, 50m
3907-6		MN	21:56	03°54.8S	25°40.4W	5559	5 cups	Corg, water isotopes, 250, 100, 75, 50, 25m
3907-7	24.03	ISP	00:37	03°54.5S	25°39.8W	5555	60min	Trace metals, 2000 and 3000m water depth
3907-8		ParCa & CTD	06:50	03°53.5S	25°38.6W	5558	Photos	to 2000m waterdepth Profile depth 1980m
3907-9		WA10	09:04	03°54.0S	25°39.0W	5554	2	Start deployment
		WA10	11:08	03°55.4S	25°42.3W	5554	traps	weight over board, stop deployment
3907-10		ISP & GFW	15:30	03°54.9S	25°36.6W	5562	60min 12x12l	Trace metals, 4000 and 5000m water depth Trace metals, Ox, nutrients, 10 to 5000m

GeoB #	Date 1996	Coring device	Time seafloor (UTC)	Latitude	Longitude	Water depth (m)	Sample (XX)	Remarks
Equatorial Atlantic								
3908-1	25.03	ISP	19:30	00°01.3S	23°28.2W	3605	60min	Trace metals, 100 and 400m water depth
3908-2		ParCa	23:45	00°01.3S	23°28.2W	3609	Photos	to 3000m water depth, every 10m
3908-3	26.03	ISP &	03:08	00°02.7S	23°27.9W	3542	60min	Trace metals, 700 and 1200m water depth
		GFW					12x12l	Trace metals, Ox, nutrients, 10 to 3000m
3908-4		MN	06:18	00°02.6S	23°27.9W	3546	5 cups	Forams, water isot., 500, 300, 200, 100, 50m
3908-5		MN	06:57	00°02.4S	23°27.9W	3554	5 cups	Corg, water isotopes, 250, 100, 75, 50, 25m
3908-6		MN	07:30	00°02.6S	23°27.9W	3550	5 cups	Radiolaria, 400, 200, 100, 40, 20m
3908-7		WA8	08:43	00°00.5N	23°26.5W	3635	2	Release, start recovery
		WA8	11:18	00°00.5N	23°26.5W		traps	Stop recovery, 40 cups with sediments
3908-8		ROS	11:35	00°00.4N	23°26.4W	3707	1x30l	Only 1 sample from 250 m
3908-9		WA11	12:08	00°01.8N	23°26.8W	3722	2	Start deployment
		WA11	13:46	00°00.1S	23°25.9W		traps	Weight over board, stop deployment
3908-10		ROS	14:44	00°00.2S	23°23.9W	4061	6x30l	2x250m,1x100m, 2x50m, 1x20m
3908-11		MUC &	16:27	00°00.4S	23°25.7W	3693	16cm	Clayey carbonate ooze, pale brown
		CTD						Profile depth ≈ 3600 m
Northeast Brazilian Margin: Profile A								
3909-1	29.03.	MUC &	19:10	03°32,9S	36°16.2W	3174	33cm	Clayey carbonate ooze, forams, pterop. at surf.
		CTD						Profile depth ≈ 3100 m
3909-2		GC12	21:31	03°33.5S	36°16.2W	3164	747cm	CC: stiff gray clay, mica, forams
3910-1	30:03	GC12	03:16	04°14.7S	36°20.7W	2364	650cm	Geochem., cc: Sandy mud, gray, mica, forams
3910-2		GC12	05:07	04°14.7S	36°20.7W	2362	694cm	CC: stiff gray clay, mica, forams
3910-3		MUC &	07:17	04°14.7S	36°20.8W	2361	32cm	Carbonate ooze, forams, pteropods at surf.
		CTD						Profile depth ≈ 2300m
3911-1	30:03	MUC &	11:57	04°36.8S	36°38.1W	826	33cm	Carbonate ooze, forams, pteropods at surf.
		CTD						Profile depth ≈ 2300m
3911-2		GC12	12:45	04°36.8S	36°38.2W	825	650cm	Geochemistry, cc: gray clay, forams
3911-3		GC12	13:43	04°36.8S	36°38.4W	828	700cm	CC: gray clay, forams
3912-1	30:03	GC12	22:03	03°40.0S	37°43.0W	772	680cm	CC: light gray carbonate mud, sandy, forams
3912-2		MUC &	11:57	03°40.0S	37°43.1W	772	12cm	Carbonate ooze, forams, pteropods
		CTD						Profile depth ≈ 720m

GeoB #	Date 1996	Coring device	Time seafloor (UTC)	Latitude	Longitude	Water depth (m)	Sample (XX)	Remarks
Northeast Brazilian Margin: Profile B								
3913-1	31:03	MUC & CTD	08:52	02°53.8S	38°19.0W	2264	---	No bottom contact, strong surface current Profile depth ≈ 2200m
3913-2		MUC	10:53	02°53.8S	38°18.6W	2289	13cm	All big tubes washed out, small t. foram sand
3913-3		GC12	12:32	02°53.8S	38°18.5W	2288	655cm	CC: stiff gray clay clay, forams, pteropods
3914-1	31:03	GC12	16:56	02°43.3S	38°13.6W	2464	820cm	Geochemistry, cc: carbonate mud, gray, forams
3914-1		GC12	18:50	02°43.3S	38°13.6W	2463	880cm	CC: carbonate mud, gray, forams
3914-3		MUC & CTD	20:57	02°43.5S	38°13.7W	2461	25cm	5 big t. washed out, others foram sand, l. brown Profile depth ≈ 2400m
3915-1	01.04.	MUC & CTD	04:04	02°16.8S	38°00.9W	3127	33cm	Carbonate ooze, sandy, forams, pteropods Profile depth ≈ 3050m
3915-2		GC12	06:06	02°16.8S	38.01.0W	3127	794cm	CC: carbonate ooze, light gray to brown
Amazon Shelf and Fan								
3916-1	04.04	MUC	07:37	01°41.9N	48°26.0W	37	34cm	Terrigenous mud, light brown to gray
3916-2		GC12	08:10	01°41.8N	48°25.9W	38	615cm	CC: terrigenous gray mud, sandy
3917-1	04.04	MUC	14:01	02°11.0N	48°00.0W	68	---	All tubes empty, foraminiferal sand, washed out
3917-2		MUC	14:12	02°11.0N	48°00.0W	68	---	All tubes empty, foraminiferal sand, washed out
3917-3		MUC	14:25	02°11.0N	48°00.0W	68	---	All tubes empty, foraminiferal sand, washed out
3917-4		GC6	14:42	02°11.0N	48°00.0W	68	5cm	Beach rock fragments, foram sand, washed out
3918-1	05.04	MUC	18:26	03°42.3N	50°24.3W	52	25cm	4 big tubes washed out, Clayey mud with moll.
3918-2		GC6	18:50	03°42.3N	50°24.3W	50	525cm	Geochemistry, cc: gray clay
3918-3		GC12	19:24	03°42.3N	50.24.3W	50	---	Tube cracked at 2.50 m
3918-4		GC6	20:30	03°42.2N	50°24.3W	51	498cm	CC: gray clay
3919-1	06.04	BC	04:05	04°35.4N	50°20.9W	97	12cm	Brown sand, benthic forams, carbonate ooliths
3920-1	06.04	BC	07:50	04°27.3N	50°01.4W	130	18cm	Brown mud, Fe-Concretions at the surface
3920-2		GC6	08:20	04°27.3N	50.01.3W	128	405cm	CC: gray mud
3921-1	06.04	CTD	10:06	04°30.5N	49°54.4W	1077		Profile depth ≈ 980m
9322-1	06.04	CTD	12:25	04°35.8N	49°43.1W	1893		Profile depth ≈ 1000m
3923-1	06.04	CTD	16:38	04°47.9N	49°15.4W	2519		Profile depth ≈ 1000m

GeoB #	Date 1996	Coring device	Time seafloor (UTC)	Latitude	Longitude	Water depth (m)	Sample (XX)	Remarks
3924-1	06.04	CTD	22:24	05°05.9N	48°34.2W	2882		Profile depth ≈ 1000m
3925-1	07.04	ISP & GFW	10:11	05°08.6N	47°31.7W	3199	60min	Trace metals, 700 and 1200m water depth
							12x12l	Trace metals, Ox, nutrients, 10 to 3000m
3925-2		MUC & CTD	13:56	05°08.6N	47°31.8W	3198	25cm	Carbonate ooze, pteropods, forams
								Profile depth ≈ 3150m
3925-3		GC12	16:41	05°08.0N	47°30.9W	3170	610cm	Geochemistry, cc: stiff gray mud
3925-4		ROS	18:19	05°08.0N	47°31.0W	3167	6x30l	250, 200, 100, 75, 50, 20m
3925-5		ISP	19:15	05°07.9N	47°30.4W	3171	60min	Trace metals, 100 and 400m water depth
3925-6		ROS	21:42	05°08.3N	47°30.7W	3198	6x30l	2x3000, 2000,1200, 700, 400m
3925-7		MN	23:21	05°08.3N	47°30.9W	3194	5 cups	Forams, water isot., 500, 300, 200, 100, 50m
3925-8	08.04	MN	00:06	05°08.4N	47°31.3W	3192	5 cups	Radiolaria, 400, 200, 100, 40, 20m
3925-9		MN	00:43	05°08.3N	47°31.4W	3183	5 cups	Corg, water isotopes, 250, 100, 75, 50, 25m
3925-10		ParCa	02:00	05°08.6N	47°31.5W	3186	Photos	Profile depth 1000 m
Profile Guyana Margin								
3926-1	10.04	ParCa & CTD	18:01	08°22.6N	58°04.7W	1116	Photos	Profile depth 1000 m, 1 photo every 10m
								Profile depth ≈ 950m
3927-1	10.04	CTD	21:13	08°35.6N	57°56.9W	1952		Profile depth ≈ 1030m
3928-1	11.04	CTD	02:27	09°02.5N	57°41.0W	2752		Profile depth ≈ 1030m
3929-1	11.04	ParCa & CTD	09:23	09°28.0N	57°25.5W	3195	Photos	Profile depth 2000 m, 1 photo every 10m
								Profile depth ≈ 1950m
3930-1	11.04	CTD	14:23	09°58.1N	57°07.6W	3453		Profile depth ≈ 1030m
3931-1	11.04	CTD	19:10	10°28.3N	56°49.1W	3881		Profile depth ≈ 1030m
3932-1	12.04	CTD & ROS	00:34	11°00.0N	56°29.8W	4227		Profile depth ≈ 2950m
							6x30l	2x3000m (Standard Water Isotopes)
								400, 100, 50, 20m, N-Isotopes (POC)
3933-1	12.04	CTD	07:26	11°29.0N	57°11.9W	4249		Profile depth ≈ 1050m

Profile Barbados, Atlantic Caribbean Margin

3934-1	13.04	CTD	02:59	12°50.1N	59°10.1W	1616		Profile depth ≈ 1050m
3935-1	13.04	MUC & CTD	07:41	12°36.8N	59°23.3W	1554	37cm	Carbonate ooze, light brown to gray Profile depth ≈ 1500m
3935-2		GC12	09:01	12°36.8N	59°23.2W	1558	518cm	CC: gray carbonate ooze, forams, pteropods
3936-1	13.04	GC12	14:02	12°43.1N	59°00.1W	1843	745cm	CC: gray carbonate ooze, forams, pteropods
3936-2		MUC & CTD	15:41	12°43.1N	58°59.9W	1853	35cm	Carbonate ooze, light brown to gray Profile depth ≈ 1800m
3937-1	13.04	MUC & CTD	18:53	12°33.5N	58°45.9W	1638	32cm	Carbonate ooze, light brown to gray Profile depth ≈ 1600m
3937-2		GC12	20:07	12°33.5N	58°45.9W	1652	653cm	CC: gray carbonate ooze, forams, pteropods
3938-1	14.04	GC12	00:32	12°15.5N	58°19.8W	1972	649cm	CC: gray carbonate ooze, forams, pteropods
3938-2		MUC & CTD	02:12	12°15.4N	58°19.8W	1972	33cm	Carbonate ooze, light brown to gray Profile depth ≈ 1920m
3939-1	14.04	MUC & CTD	10:46	12°35.3N	58°05.9W	2466	31cm	Carbonate ooze, light brown to gray Profile depth ≈ 2400m
3939-2		GC12	12:26	12°35.3N	58°05.9W	2467	723cm	CC: gray carbonate ooze, forams, pteropods

Abbreviations used in station list:

(xx)	Number of water or plankton samples, pumping time, core length, etc.
BC	Box corer
CTD	Conductivity, Temperatur, Density Sensor, profile depth after wire length
GFW	GoFlow -water samplers
ISP	*In situ* Pumps
MUC	Multicorer
ParCa	Particle Camera
ROS	Rosette with 6 Niskin-bottles
GC	Gravity corer, length
WA	Western Atlantic moorings

8 Concluding Remarks

The goals of the research program of cruise M34 were fully achieved. The scientific party gratefully acknowledges the outstanding cooperation and technical assistance of Captain Bruns and his crew, who substantially contributed to the remarkable scientific success of the cruise.

We also appreciate the most valuable help of the Leitstelle METEOR, Hamburg, in planning and realization of the cruise and in receiving the research permission for Brazil, Guyana and Barbados.

The work was funded by the Deutsche Forschungsgemeinschaft within the scope of the Sonderforschungsbereich 261 at Bremen University, grant BI 154/22-2 and by the Bundesministerium für Bildung, Wissenschaft, Forschung und Technologie (FKZ: 03f0157A, WOCE IV).

9 References

ASPER, V. L., (1987): Measuring the flux and sinking speed of marine snow aggregates. Deep-Sea Res., **34**, 1-17.

AUSTIN, B., (1988): Fluorometric method for the determination of low cocnetrations of dissolved aluminum in natural waters. Marine Microbiology. Cambridge University Press, Cambridge.

AUSTIN, Jr., J.A. and E. UCHUPI, (1982): Continental - oceanic crustal transition off Southwest Africa. Am. Ass. Petr. Geol. Bull., **66**, 1328-1347.

BICKERT, T., W. H. BERGER and G. WEFER. The deep western equatorial Pacific in Plio-Pleistocene times: Results from ODP Leg 130 (Ontong Java Plateau), Earth Planet. Sci. Lett. (submitted).

BICKERT, T. and T. v. DOBENECK, (1994): Susceptibility stratigraphy. In: SPIESS et al.:, Bericht und erste Ergebnisse der METEOR-Fahrt M23/1. Berichte, Fachbereich Geowissenschaften, Universität Bremen, **42**, 139 p.

BLAIR, N.E. and R.C. ALLER, (1995): Anaerobic oxidation on the Amazon shelf. Geochim. Cosmochim. Acta, **59**, 3707-3715.

BLEIL, U. et al. (1994): Report and Preliminary Results of SONNE-Cruise SO 86.- Berichte, Fachbereich Geowissenschaften, Universität Bremen, **51**, 116 p.

BLEIL, U. et al. (1996): Report and Preliminary Results of METEOR-Cruise M34/1.- Berichte, Fachbereich Geowissenschaften, Univ. Bremen, 77, 129 p.

BLOEMENDAL, J. and P. DE MENOCAL, (1989): Evidence for a change in the periodicity of tropical climate cycles at 2.4 Myr from whole-core magnetic susceptibility measurements. Nature, **342**, 897-900.

BOCK, E., SCHMIDT, I., STÜVEN, R. and D. ZART (1995): Nitrogen loss caused by denitrifying *Nitrosomonas* cells using ammonium or hydrogen as electron donors and nitrite as electron acceptor.- Arch. Microbiol., **163**, 16-20.

BOEBEL, O. and C. SCHMID (1995): RAFOS floats in the South Atlantic. Ber. Polarforschg., Bremerhaven, 168, 6-11.

BOEBEL, O., C. SCHMID & W. ZENK (1996): Flow and recirculation of Antarctic Intermediate Water across the Rio Grande Rise. J. Geophys. Res. (submitted).

BOYLE, R.E. (1968): Electrical resistivity of modern marine sediments from the Bering Sea.- J. Geophys. Res., **73**, 4759-4766.

BOYCE, R.E. (1976): Sound velocity - density parameters of sediment and rock from DSDP Drill Sites 315 - 318 on the Line Islands Chain, Manihiki Plateau, and Tuamotu Ridge in the Pacific Ocean. In: SCHLANGER, S.O., E.D. JACKSON et al., Init. Repts. DSDP, **33**, 695-728.

BOLLI, H.M., W.B.F. RYAN, J.B. FORESMAN, W. HOTTMAN, H. KAGAMI, J.F. LONGORIA, B.K. McKNIGHT, M. MELGUEN, J. NATLAND, F. PROTO-DECIMA and W.G. SIESSER, (1978): Cape Basin continental rise - Sites 360 and 361. In: BOLLI, H.M. and RYAN, W.B.F. et al. (eds.), Init. Repts. DSDP **40**, US Govt. Printing Office, Washington, 29-182.

CURTIN, T.B., (1986): Physical observation in the plume region of the Amazon river during peak discharge-II. Water masses. Continental Shelf Research, **6**, 53-71.

DAMUTH, J.E., (1975): Quaternary climate change as revealed by calcium carbonate fluctuations in western Equatorial Atlantic sediments. Deep-Sea Res., **22**, 725-743.

DINGLE, R.V., (1980): Large allochtonous sediment masses and their role in the contruction of the continental slope and rise off southwestern Africa. Mar. Geol. **37**, 333-354.

DINGLE, R.V., (1992): Structural and sedimentary development of the continental margin off southwestern Africa. Com. Geol. Surv. Namibia **8**, 35-43.

DINGLE, R.V. and S.H. ROBSON, (1992): Southwestern Africa continental rise: structural and sedimentary evolution. In: POAG C.W. and GRACIANSKY, P.C. (eds.), Geologic Evolution of Atlantic Continental Rises. Van Ostrand, New York, 62-76.

DINGLE, R.V., G.F. BIRCH, J.M. BREMNER, R.H. DE DECKER, A. DU PLESSIS, J.C. ENGELBRECHT, M.J. FINCHAM, T. FITTON, B.W. FLEMMING, R.I. GENTLE, S.W. GOODLAD, A.K. MARTIN, E.G. MILLS, G.J. MOIR, R.J. PARKER, S.H. ROBSON, J. ROGERS, D.A. SALMON, W.G. SIESSER, E.S.W. SIMPSON, C.P. SUMMERHAYES, F. WESTALL and A. WINTER, (1987): Deep-sea sedimentary environments around southern Africa (South-East Atlantic and South-West Indian Oceans). Ann. South African Museum, **98**, 1-27.

EMERY, K.O. and E. UCHUPI, (1984): The Geology of the Atlantic Ocean. Springer, New York, 925 p.

EMERY, K.O., E. UCHUPI, C. BOWIN, J. PHILLIPS and E.S.W. SIMPSON, (1975): Continental margin off western Africa: Cape St. Fracis (South Africa) to Walvis Ridge (South-West Africa). Am. Ass. Petr. Geol. Bull., **59**, 3-59.

ERICSON, D.B: and G. WOLLIN, (1968): Pleistocene climates and chronology in deep-sea sediments. Science, **162**, 1227-1234.

FIGUEIREDO, A.G., L.A.P GAMBOA, M.A. Gorini and E.C. Alves, (1972): Natureza da sedimentacao atual do Rio Amazonas. In Anais do XXVI Congr. Bras. de Geologia, **2**, 51-56.

FIGUEIREDO, A.G., C.A. NITTROUER and E.A. Costa, (1993): Gassy sediment in the Amazon submarine delta. In Anais do 3° Congr. Intern. da Soc. Bras. de Geofisica, **2**, 1243-1247.

FIGUEIREDO, A.G. and C.A. Nittrouer, (1995): New insights to high-resolution stratigraphy on the Amazon continental shelf. Mar. Geol., **125**, 393-399.

FIGUEIREDO, A.G., C.A. Nittrouer and E.A. Costa, (1996): Gas charged sediment in the Amazon submarine delta. Geo-Marine Letters, **16**, 31-35.

GERRARD, I. and G.C. SMITH, (1984): Post-Paleozoic succession and structures of the southwestern African continental margin. In: WATKINS J.S. and DRAKE C.L. (eds.), Studies in Continental Margin Geology. AAPG Memoir **34**, 49-74.

GRAHAM, G. and J. MAZZULLO (1988): Handbook for Shipboard Sedimentologists.- ODP Technical Note No. 8.

HOEHLER, T.M., M.J. ALPERIN, D.B. ALBERT, and C.S. MARTENS (1994): Field and laboratory studies of methane in an anoxic marine sediment: Evidence for a methanogen-sulfate reducer consortium.- Glob. Biogeochem. Cycl., **8,** 451-463.

HOGG, N.G., W.B. OWENS, G. SIEDLER and W. ZENK (1996): Circulation in the Deep Brazil Basin. In: WEFER, G., W.H. BERGER, G. SIEDLER and D. WEBB (eds.): The South Atlantic: Present and Past Circulation. Springer Verlag, 249-260.

HONJO S., K. W. DOHERTY, Y. C. AGRAWAL and V. L. ASPER (1984): Direct optical assessment of large amorphous aggregates (marine snow) in the deep ocean. Deep-Sea Res., **31**, 67-76.

HYDES, D. and H. LISS, (1976): Analyst, **101**, 922-931.

JØRGENSEN, B.B., H. FOSSING, C.O. WIRSEN and H.W. JANNASCH (1991): Sulfide oxidation in the anoxic Black Sea chemocline.- Deep-Sea Res., **38,** 1083-1103.

KÖNIG, H., K. SCHULTZ TOKOS and W. ZENK (1991): MAFOS - a simple tool for monitoring the performance of RAFOS sound sources in the ocean. Journ. Atm. Oc. Techn., **8**, 669-676.

KÖNIG, H. and W. ZENK (1992): Principles of RAFOS technology at the Institut für Meereskunde Kiel. Ber. Inst. f. Meereskunde Kiel, Nr. **222**, 99 p.

KÖRTZINGER, A., H. THOMAS, B. SCHNEIDER, N. GRONAU, L. MINTROP and J.C. DUINKER (1996): At-sea intercomparison of two newly designed underway $pCO2$ systems - encouraging results.

LAMPITT, R.S. (1985): Evidence for the seasonal deposition of dtritus to the deep-sea floor and ist subsequent resuspension. Deep-Sea Res., **32,** 885-897.

LITTLE, M., D. KROON, N.B. PRICE, R. SCHNEIDER, P.J. MÜLLER and G. WEFER, (1996): Foraminiferal record of the palaeoceanographic variations in the Benguela upwelling system for the last 160,000 years. Palaeogeogr., Palaeoclimat., Palaeoecol. (submitted).

LOCHTE, K., (1991): Protozoa as markers and breakers of marine aggregates. In: REID P.C., C.M. TURLEY and P.H. BURKELL (eds.): Protozoa and their role in marine processes. NATO ASI Series, Vol. G25, Springer Verlag, Berlin-Heidelberg, New York, 327-346.

LOCHTE, K. (1993): Mikrobiologie von Tiefseesedimenten. In: MEYER-REIL L.-A. and M. Köster (eds.): Mikrobiologie des Meeresbodens. Gustav Fischer Verlag, Jena, Stuttgart, New York. 258-282.

MEADE, R.H., T. DUNNE, J.E. Richey, U.M. Santos and E. Salati, (1985): Storage and remobilization of suspended sediment in the lower Amazon River of Brazil. Science, **228**, 488-490.

MENZEL, M. (1995): Entwicklung eines Programmpaketes zur Datenaufbereitung, Berechnung und Visualisierung von Floattrajektorien. Diplomarbeit, FH Kiel, 274 p.

MILLIMAN, J.D. and H.T. BARRETO, (1975): Relict magnesian calcite oolithe and subsidnece of the Amazon shelf. Sedimentology, **22**, 137-145.

MÜLLER, G. and M. GASTNER (1971): The "Karbonat-Bombe", a single device for the determination of the carbonate content in sediments, soils and other materials. Neues Jahrb. Min., Monatsh., **10**, 466-469.

NITTROUER, C.A. and Amaseds Research Group (1990): A multidisciplinairy Amazon shelf sediment study. EOS, **71**, 1776-1777.

NITTROUER, C.A., D.J. DeMASTER, A.G. FIGUEIREDO, and J.M. RINE, (1991): AmasSeds: An interdisciplinary investigation of a complex coastal environment. Oceanography, **4**, 3-7.

OLLITRAULT, M., N. CORTÈS, G. LOAEC and J.-P. RANNOU (1994): MARVOR float present results from the SAMBA experiment. OCEANS 94 proceedings, III, 17-22.

PARK, J., S.L. D'HONDT, J. W. KING and C. GIBSON, (1993): Late Cretaceous Precessional Cycles in Double Time: A Warm-Earth Milankovitch Response. Science, **261**, 1431-1434.

PETERMANN, H. and U. BLEIL, (1993): Detection of live magnetotactic bacteria in South Atlantic deep-sea sediments. Earth Planet. Sci. Lett., **117**, 223-228.

PETERMANN, H., (1994): Magnetotaktische Bakterien und ihre Magnetosome in den Oberflächensedimenten des Südatlantiks. Berichte, Fachbereich Geowissenschaften, Universität Bremen, **56**, 135 p.

PETERSEN, N., T. v. DOBENECK and H. VALI, 1986. Fossil bacterial magnetite in deep-sea sediments from the South Atlantic Ocean. Nature, **320**, 611-615.

RATMEYER V. and G. WEFER, (1996): A high resolution camera system (ParCa) for imaging particles in the ocean: System design and results from profiles and a three-month deployment. J. Mar. Res., **54**, 589-603.

REID, J. L. (1989): On the total geostrophic circulation of the South Atlantic Ocean: Flow patterns, tracers and transports. Progr. Oceanogr., **23**, 149-244.

SCHLEGEL, H.G. (1992): Allgemeine Mikrobiologie.- 7.Aufl., Thieme, Stuttgart.

SCHOTT, F.A., L. STRAMMA and J. FISCHER, (1994): The warm water inflow into the western tropical Atlantic boundary regime, spring 1994. J. Geophys. Res., **100**, 24745–24760.

SCHULTHEISS, P.J. and S.D. McPHAIL (1989): An automated p-wave logger for recording fine-scale compressional wave velocity structures in sediments.- In: W. RUDDIMAN, M. SARNTHEIN et al., Proc. ODP, Sci. Results, **108**, 407-413.

SCHULZ, H.D. et al. (1991): Bericht und erste Ergebnisse der METEOR-Fahrt M16/2.- Berichte, Fachbereich Geowissenschaften, Universität Bremen, **19**, 149 p.

SCHULZ H.D. et al., (1992): Bericht und erste Ergebnisse der METEOR-Fahrt M 20/2. Berichte, Fachbereich Geowissenschaften, Universität Bremen, **25**, 173 p.

SCHULZ, H.D., DAHMKE, A., SCHINZEL, U. WALLMANN, K. and M. ZABEL (1994): Early diadenetic processes, fluxes, and reaction rates in sediments of the South Atlantic.- Geochim. Cosmochim. Acta, **58**, 2041-2060.

SIEDLER, G., W. BALZER, T.J. MÜLLER, R. ONKEN, M. RHEIN and W. ZENK (1993): WOCE South Atlantic 1992, Cruise No. 22, 22 September 1992 - 31 January 1993. METEOR-Berichte, Universität Hamburg, **93-5**, 131 p.

SIEDLER, G. and W. ZENK (1992): WOCE Südatlantik 1991, Reise Nr. 15, 30. Dezember 1990 - 23. März 1991. METEOR-Berichte, Universität Hamburg, **92-1**, 126 p.

SPEER, K.G. W. ZENK, G. SIEDLER, J. PÄTZOLD and C. HEIDLAND (1992): First resolution of flow through the Hunter Channel in the South Atlantic. Earth Planet. Sci. Lett., **113**, 287-292.

SPEER, K.G. and W. ZENK (1993): The flow of Antarctic Bottom Water into the Brazil Basin. J. Phys. Oceanogr., **23**, 2667-2682.

SPIEß, V. (1993): Digitale Sedimentechographie - Neue Wege zu einer hochauflösenden Akustostratigraphie.- Berichte, Fachbereich Geowissenschaften, Universität Bremen, **35**, 199 p.

STRAUB, K., BENZ, M., SCHINK, B. and F. WIDDEL (1996):. Anaerobic, nitrate-dependent microbial oxidation of ferrous iron.- Appl. Environ. Microbiol. (in press).

TARBELL, S., R. MEYER, N. HOGG and W. ZENK (1994): A moored array along the southern boundary of the Brazil Basin for the Deep Basin Experiment - Report on a joint experiment 1991-1992. Ber. Inst. f. Meereskunde Kiel, Nr. **243**, 97 p.

THAMDRUP, B. and D. CANFIELD (1996): ...., (in press).

THIESSEN, W. (1993): Magnetische Eigenschaften von Sedimenten des östlichen Südatlantiks und ihre paläozeanographische Relevanz (Dissertation).- Berichte, Fachbereich Geowissenschaften, Universität Bremen, **41**, 170 p.

WEFER, G. et al., (1991): Bericht und erste Ergebnisse über die METEOR-Fahrt M16/1. Berichte, Fachbereich Geowissenschaften, Universität Bremen, **18**, 120 p.

WEFER, G., W.H. BERGER, U. BLEIL, M. BREITZKE, L. DIESTER-HAASS, C. GOHL, W.W. HAY, P. MEYERS, H. OBERHÄNSLI, R. SCHNEIDER, V. SPIEß and G. UENZELMANN-NEBEN, (1995): Neogene history of the Bengueal Current and Angola / Namibia upwelling system. ODP Proposal 354, Rev. 4.

VAN DE GRAAF, A., A. MULDER, P. DE BRUIJN, M.S.M. JETTEN, L.A. ROBERTSON, and J.G. KUENEN (1995): Anaerobic oxidation of ammonium is a biologically mediated process.- Appl. Environ. Microbiol., **61,** 1246-1251.

ZENK, W., K.G. SPEER and N.G. HOGG (1993): Bathymetry at the Vema Sill. Deep-Sea Res., **40** (9), 1925-1933.

ZENK, W. and T.J. MÜLLER (1995) WOCE Studies in the South Atlantic, Cruise No. 28, 9 March - 14 June 1994. METEOR-Berichte, Universität Hamburg, **95-1**, 193 p.

Publications from METEOR expeditions
in other reports

Gerlach, S.A., J. Thiede, G. Graf und F. Werner (1986): Forschungsschiff Meteor, Reise 2 vom 19. Juni bis 16. Juli 1986. Forschungsschiff Poseidon, Reise 128 vom 7. Mai bis 8. Juni 1986. Ber. Sonderforschungsbereich 313, Univ. Kiel, 4, 140 S.

Siedler, G., H. Schmickler, T.J. Müller, H.-W. Schenke und W. Zenk (1987): Forschungsschiff Meteor, Reise Nr. 4, Kapverden - Expedition, Oktober - Dezember 1986. Ber. Inst. f. Meeresk., 173, Kiel, 123 S.

Wefer, G., G.F. Lutze, T.J. Müller, O. Pfannkuche, W. Schenke, G. Siedler und W. Zenk (1988): Kurzbericht über die Meteor - Expedition Nr. 6, Hamburg - Hamburg, 28. Oktober 1987 - 19. Mai 1988. Berichte, Fachbereich Geowissenschaften, Universität Bremen, 4, 29 S.

Müller T.J., G. Siedler und W. Zenk (1988): Forschungsschiff Meteor, Reise Nr. 6, Atlantik 87/88, Fahrtabschnitte Nr. 1 - 3, Oktober - Dezember 1987. Ber. Inst. f. Meeresk., 184, Kiel, 77 S.

Lutze, G.F., C.O.C. Agwu, A. Altenbach, U. Henken-Mellies, C. Kothe, N. Mühlhan, U. Pflaumann, C. Samtleben, M. Sarnthein, M. Segl, Th. Soltwedel, U. Stute, R. Tiedemann und P. Weinholz (1988): Bericht über die "Meteor" -Fahrt 6-5, Dakar - Libreville, 15.1.-16.2.1988.Berichte - Reports, Geol. Paläont. Inst., Univ. Kiel, 22, 60 S.

Wefer, G., U. Bleil, P.J. Müller, H.D. Schulz, W.H.Berger, U. Brathauer, L. Brück, A. Dahmke, K. Dehning, M.L. Durate-Morais, F. Fürsich, S. Hinrichs, K. Klockgeter, A. Kölling, C. Kothe, J.F. Makaya, H. Oberhänsli, W. Oschmann, J. Posny, F. Rostek, H. Schmidt, R. Schneider, M. Segl, M. Sobiesiak, T. Soltwedel und V. Spieß (1988): Bericht über die Meteor - Fahrt M 6-6, Libreville - Las Palmas, 18.2.1988 - 23.2.1988. Berichte, Fachbereich Geowissenschaften, Universität Bremen, 3, 97 S.

Hirschleber, H., F. Theilen, W. Balzer, B. v. Bodungen und J. Thiede (1988): Forschungsschiff Meteor, Reise 7, vom 1. Juni bis 28. September 1988, Ber. Sonderforschungsbereich 313, Univ. Kiel, 10, 358 S.

METEOR-Berichte
List of publications

89-1	(1989) Meincke, J., Quadfasel, D.	GRÖNLANDSEE 1988-Expedition, Reise Nr. 8, 27. Oktober 1988 - 18. Dezember 1988. Universität Hamburg, 40 S.
89-2	(1989) Zenk, W., Müller, T.J., Wefer, G.	BARLAVENTO-Expedition, Reise Nr. 9, 29. Dezember 1988 - 17. März 1989. Universität Hamburg, 238 S.
90-1	(1990) Zeitschel, B., Lenz, J., Thiel, H., Boje, R., Stuhr, A., Passow, U.	PLANKTON'89 - BENTHOS'89, Reise Nr. 10, 19. März - 31. August 1989. Universität Hamburg, 216 S.
90-2	(1990) Roether, W., Sarnthein, M., Müller, T.J., Nellen, W., Sahrhage, D.	SÜDATLANTIK-ZIRKUMPOLARSTROM, Reise Nr. 11, 3. Oktober 1989 - 11. März 1990. Universität Hamburg, 169 S.
91-1	(1991) Wefer, G., Weigel, W., Pfannkuche	OSTATLANTIK 90 - EXPEDITION, Reise Nr. 12, 13. März - 30. Juni 1990. Universität Hamburg, 166 S.
91-2	(1991) Gerlach, S.A., Graf, G.	EUROPÄISCHES NORDMEER, Reise Nr. 13, 6. Juli - 24. August 1990. Universität Hamburg, 217 S.
91-3	(1991) Hinz, K., Hasse, L., Schott, F.	SUBTROPISCHER & TROPISCHER ATLANTIK, Reise Nr. 14/1-3, Maritime Meteorologie und Physikalische Ozeanographie, 17. September - 30. Dezember 1990. Universität Hamburg, 58 S.
91-4	(1991) Hinz, K.	SUBTROPISCHER & TROPISCHER ATLANTIK, Reise Nr. 14/3, Geophysik, 31. Oktober - 30. Dezember 1990. Universität Hamburg, 94 S.
92-1	(1992) Siedler, G., Zenk, W.	WOCE Südatlantik 1991, Reise Nr. 15, 30. Dezember 1990 - 23. März 1991. Universität Hamburg, 126 S.
92-2	(1992) Wefer, G., Schulz, H.D., Schott, F., Hirschleber, H. B.	ATLANTIK 91 - EXPEDITION, Reise Nr. 16, 27. März - 8. Juli 1991. Universität Hamburg, 288 S.

92-3	(1992) Suess, E., Altenbach, A.V.	EUROPÄISCHES NORDMEER, Reise Nr. 17, 15. Juli - 29. August 1991. Universität Hamburg, 164 S.
93-1	(1993) Meincke, J., Becker, G.	WOCE-NORD, Cruise No. 18, 2. September - 26. September 1991. NORDSEE, Cruise No. 19, 30 September - 12 October 1991. Universität Hamburg, 105 pp.
93-2	(1993) Wefer, G., Schulz, H.D.	OSTATLANTIK 91/92 - EXPEDITION, Reise Nr. 20, M 20/1 und M 20/2, 18. November 1991 - 3. Februar 1992. Universität Hamburg, 248 S.
93-3	(1993) Wefer, G., Hinz, K., Roeser, H.A.	OSTATLANTIK 91/92 - EXPEDITION, Reise Nr. 20, M 20/3, 4. Februar - 13. März 1992. Universität Hamburg, 145 S.
93-4	(1993) Pfannkuche, O., Duinker, J.C., Graf, G., Henrich, R., Thiel, H., Zeitschel, B.	NORDATLANTIK 92, Reise Nr. 21, 16. März - 31. August 1992. Universität Hamburg, 281 S.
93-5	(1993) Siedler, G., Balzer, W., Müller, T.J., Rhein, M., Onken, R., Zenk, W.	WOCE South Atlantic 1992, Cruise No. 22, 22 September 1992 - 31 January 1993. Universität Hamburg, 131 pp.
94-1	(1994) Bleil, U., Spieß, V., Wefer, G.	Geo Bremen SOUTH ATLANTIC 1993, Cruise No. 23, 4 February - 12 April 1993. Universität Hamburg, 261 pp.
94-2	(1994) Schmincke, H.-U., Rihm, O.	OZEANVULKAN 1993, Cruise No. 24, 15 April - 9 May 1993. Universität Hamburg, 88 pp.
94-3	(1994) Hieke, W., Halbach, P., Türkay, M., Weikert, H.	MITTELMEER 1993, Cruise No. 25, 12 May - 20 August 1993. Universität Hamburg, 243 pp.
94-4	(1994) Suess, E., Kremling, K., Mienert, J.	NORDATLANTIK 1993, Cruise No. 26, 24 August - 26 November 1993. Universität Hamburg, 256 pp.

94-5	(1994) Bröckel, K. von, Thiel, H., Krause, G.	ÜBERFÜHRUNGSFAHRT, Reise Nr. 0, 15. März - 15. Mai 1986. ERPROBUNGSFAHRT, Reise Nr. 1, 16. Mai - 14. Juni 1986. BIOTRANS IV, Skagerrak 86, Reise Nr. 3, 21. Juli - 28. August 1986. Universität Hamburg, 126 S.
94-6	(1994) Pfannkuche, O., Balzer, W., Schott, F.	CARBON CYCLE AND TRANSPORT OF WATER MASSES IN THE NORTH ATLANTIC - THE WINTER SITUATION, Cruise No. 27, 29 December - 26 March 1994. Universität Hamburg, 134 pp.
95-1	(1995) Zenk, W., Müller, T.J.	WOCE Studies in the South Atlantic, Cruise No. 28, 29 March - 14 June 1994. Universität Hamburg, 193 pp.
95-2	(1995) Schulz, H., Bleil, U., Henrich, R., Segl, M.	Geo Bremen SOUTH ATLANTIC 1994, Cruise No. 29, 17 June - 5 September 1994. Universität Hamburg, 323 pp.
96-1	(1996) Nellen, W., Bettac, W., Roether, W., Schnack, D., Thiel, H., Weikert, H., Zeitschel, B.	MINDIK (Band I), Reise Nr. 5, 2. Januar - 24. September 1987. Universität Hamburg, 275 S.
96-2	(1996) Nellen, W., Bettac, W., Roether, W., Schnack, D., Thiel, H., Weikert, H., Zeitschel, B.	MINDIK (Band II), Reise Nr. 5, 2. Januar - 24. September 1987. Universität Hamburg, 179 S.
96-3	(1996) Koltermann, K.P., Pfannkuche, O., Meincke, J.	JGOFS, OMEX and WOCE in the North Atlantic 1994, Cruise No. 30, 7 September - 22 December 1994. Universität Hamburg, 148 pp.
96-4	(1996) Hemleben, Ch., Roether, W., Stoffers, P.	Östliches Mittelmeer, Rotes Meer, Arabisches Meer, Cruise No. 31, 30 December 1994 - 22 March 1995. Universität Hamburg, 282 pp.

96-5	(1996)	Lochte, K., Halbach, P., Flemming, B.W.	Biogeochemical Fluxes in the Deep-Sea and Investigations of Geological Structures in the Indian Ocean, Cruise No. 33, 22 September - 30 December 1995. Universität Hamburg, 160 pp.
96-6	(1996)	Schott, F., Pollehne, F., Quadfasel, D., Stramma, L., Wiesner, M., Zeitzschel, B.	ARABIAN SEA 1995, Cruise No. 32, 23 March - 19 September 1995. Universität Hamburg, 163 pp.
97-1	(1997)	Wefer, G. Bleil, U. Schulz, H. Fischer, G.	Geo Bremen SOUTH ATLANTIC 1996 (Volume I), Cruise No. 34, 3 January - 18 February 1996. Universität Hamburg, 254 pp.
97-2	(1997)	Wefer, G. Bleil, U. Schulz, H. Fischer, G.	Geo Bremen SOUTH ATLANTIC 1996 (Volume II), Cruise No. 34, 21 February - 15 April 1996. Universität Hamburg, 268 pp.